

Resin Transfer Moulding for Aerospace Structures

Resin Transfer Moulding for Aerospace Structures

Edited by

Teresa M. Kruckenberg

Cooperative Research Centre for Advanced Composite Structures
Bankstown, New South Wales,
Australia

and

Rowan Paton

Cooperative Research Centre for Advanced Composite Structures
Fishermans Bend, Victoria,
Australia



SPRINGER SCIENCE+BUSINESS MEDIA, B.V.

Library of Congress Cataloging-in-Publication Data is available.

ISBN 978-94-010-5906-0 ISBN 978-94-011-4437-7 (eBook)
DOI 10.1007/978-94-011-4437-7

Printed on acid-free paper

All rights reserved

© 1998 Springer Science+Business Media Dordrecht

Originally published by Kluwer Academic Publishers in 1998

Softcover reprint of the hardcover 1st edition 1998

No part of the material protected by this copyright notice may be reproduced or utilized in any form or by any means, electronic or mechanical, including photocopying, recording or by any information storage and retrieval system, without prior permission from the copyright owners.

Contents

<i>List of contributors</i>	xv
<i>Preface</i>	xix
<i>Acknowledgements</i>	xxi
Chapter 1 Introduction to resin transfer moulding	1
Bernd Räckers	
1.1 Introduction	1
1.1.1 Is resin transfer moulding a new process?	2
1.1.2 Reasons for resin transfer moulding	3
1.1.3 Basic principles and requirements for resin transfer moulding	5
1.1.4 Outline of resin transfer moulding development work	12
1.1.5 Resin transfer moulding and resin film infusion: common and different aspects	14
1.2 Current and future applications for resin transfer moulding and resin film infusion	15
1.2.1 Examples for applications and development	16
1.2.2 Outlook for resin transfer moulding in aerospace applications	22
References	24
Chapter 2 Injection equipment	25
Mitch Petervary	
2.1 Introduction	25
2.2 Selection considerations	26
2.2.1 Selection of a manufacturer	26
2.2.2 Application-specific considerations	26
2.3 Basic principles of resin delivery for resin transfer moulding	28
2.3.1 Basic elements	28
2.3.2 Additional features and variations	32

2.3.3 Constant pressure versus constant flow rate	36
2.4 Conclusions	39
References	40
List of manufacturers	41
Chapter 3 Materials	42
Mac Puckett and Mitch Petervary	
3.1 Introduction	42
3.1.1 Background: thermoplastic and thermoset materials	43
3.1.2 Engineering the resin transfer moulding process: the interaction of chemistry and physics in a reactive process	47
3.1.3 Tough composites: tough resins and composite architecture	53
3.1.4 Epoxy systems	55
3.1.5 Phenolic thermoset materials	61
3.1.6 Cyanate resins	62
3.1.7 Bismaleimides	64
3.2 Fibre reinforcements	65
3.2.1 Materials for fibre reinforcements	67
3.2.2 Bundling fibres: tows, yarns and woven fabrics	74
3.2.3 Finishes, sizings and coatings	74
3.3 Conclusions	76
References	78
List of manufacturers	81
Chapter 4 Advanced reinforcements	83
Michael Bannister and Israel Herszberg	
4.1 Introduction	83
4.2 Stitching	84
4.3 Weaving	91
4.4 Braiding	96
4.5 Knitting	102
4.6 Non-crimp fabric	105
4.7 Conclusions	108
References	109
Chapter 5 Fabric drape modelling and preform design	112
Andrew C. Long and Chris D. Rudd	
5.1 Introduction	112
5.2 Fundamentals of fabric deformation	114
5.2.1 Deformation mechanisms	114
5.2.2 Experimental characterisation	116
5.3 Kinematic drape modelling	121

5.3.1	Assumptions	121
5.3.2	Fundamental equations	121
5.3.3	Draping algorithm	124
5.3.4	Examples	124
5.4	Drape model validation	130
5.4.1	Fibre volume fraction variation	130
5.4.2	Automated strain analysis	131
5.5	Effects on processing and performance characteristics	135
5.5.1	Impregnation properties	136
5.5.2	Mechanical properties	141
5.6	Discussion	144
	References	146
Chapter 6 Overview of fibre preforming		148
Vivek Rohatgi, L. James Lee and Adrian Melton		
6.1	Fibre preforming – why is it needed?	148
6.2	Use of binders and tackifiers for fibre preforming	151
6.3	Fibre preforming techniques	152
6.3.1	Simultaneous preforming processes	152
6.3.2	Sequential preforming processes	153
6.4	Net-shape preforming of woven fibre mats by means of tackifiers	161
6.5	Design of preform tools	170
6.6	Design of preforming equipment	171
6.7	Preform storage	172
6.8	Conclusions	173
	References	174
Chapter 7 Preform permeability		177
Richard Parnas		
7.1	Introduction	177
7.1.1	Flow through porous media	177
7.1.2	The importance of permeability in liquid composite moulding	179
7.2	Experimental methods	181
7.2.1	Unidirectional flow method	181
7.2.2	Radial flow method	198
7.3	The general three-dimensional case	206
7.3.1	Analysis of unidirectional flow data	207
7.3.2	Numerical tests	213
7.3.3	Three-dimensional flow experiments	218
7.4	Summary	219
	References	222

Chapter 8 Modelling and simulation of flow, heat transfer and cure	225
Suresh G. Advani and Pavel Simácek	
8.1 Introduction	225
8.1.1 The resin transfer mould filling process	225
8.1.2 The need for a process model of resin impregnation	225
8.1.3 Microscopic and macroscopic flow	228
8.2 Flow and preform architecture	228
8.2.1 Flow in random fabrics	230
8.2.2 Flow in woven or stitched fabrics	231
8.2.3 Unsaturated flow	233
8.2.4 Transverse flow in multilayer preforms	233
8.3 Deformation of fabrics and its impact on flow	234
8.3.1 In-plane deformation	235
8.3.2 Transverse compaction	236
8.3.3 Racetracking	237
8.4 Analytical and numerical models for the preforming stage	238
8.4.1 Preform deformation	238
8.4.2 Permeability	242
8.5 Governing equations	245
8.5.1 Isothermal flow modelling	245
8.5.2 The two-dimensional problem	246
8.5.3 Formulation using a fill factor	247
8.5.4 The energy equation	248
8.5.5 Boundary conditions for energy transfer	249
8.5.6 Cure kinetics coupling	250
8.5.7 Temperature-dependent viscosity	251
8.5.8 The heat dispersion effect	252
8.5.9 Non-Newtonian fluids	253
8.6 Numerical formulations and simulations	253
8.6.1 Complexity of geometry	254
8.6.2 The finite element/control volume approach in two dimensions	254
8.6.3 Coupling with heat transfer and cure – the two-dimensional model	259
8.6.4 The pure finite element approach to mould filling	260
8.6.5 Other numerical approaches	260
8.7 Critical issues	261
8.7.1 Levels of sophistication to build these models	263
8.7.2 Inputs	264
8.8 Case study	267
8.8.1 The permeability model	268
8.8.2 Draping of the mould	269
8.8.3 Filling simulation	272

8.8.4	Conclusions	274
8.9	The use of simulations as a design tool	275
	References	277
Chapter 9 Tooling fundamentals for resin transfer moulding		282
Mark Wadsworth		
9.1	Introduction to resin transfer moulding tooling	282
9.2	Resin transfer moulding tooling materials and processes	284
9.2.1	Selecting mould materials	284
9.2.2	The effects of tolerances on tooling process selection	286
9.2.3	Methods of creating the mould shape	287
9.2.4	Fabricated tooling	288
9.2.5	Replicated tooling	290
9.3	Tooling cost considerations	299
9.3.1	Manufacturing rate and volume capacity	299
9.3.2	Prototype moulds	299
9.3.3	Rigid versus semi-rigid tooling	300
9.3.4	The effect of precision on tooling costs	300
9.3.5	Estimating the durability of moulds	300
9.4	Geometric considerations for moulds for use in resin transfer moulding	302
9.4.1	Net versus excess moulding	302
9.4.2	Mould gap design	303
9.4.3	Parting line considerations	303
9.4.4	Designing the tool flange geometry	304
9.4.5	Accomodating undercuts and zero draft situations	308
9.4.6	Guidance of tool inserts	309
9.4.7	Designing preform control and debulk features	309
9.4.8	Free-floating inserts	311
9.4.9	Part demoulding considerations	312
9.5	Thermal considerations in mould design in resin transfer moulding	314
9.5.1	Mould heating	314
9.5.2	Thermal expansion of the mould	317
9.6	Physical requirements of tooling in resin transfer moulding	318
9.6.1	Surface characteristics	318
9.6.2	Pressure forces on the mould	320
9.6.3	Selecting a mould clamping system	323
9.7	Process considerations for resin transfer moulding tooling	326
9.7.1	Resin injection port	326
9.7.2	Locating injection ports and vents	327
9.7.3	Plumbing requirements for sequential injection	328
9.7.4	Designing resin distribution manifolds	329
9.7.5	Air vent features	330

x Contents

9.7.6	Designing preform tooling	330
9.8	Examples of resin transfer moulding tooling	331
9.8.1	Example 1	332
9.8.2	Example 2	332
9.8.3	Example 3	333
9.8.4	Example 4	335
Reference		337
Further reading		337
Chapter 10 Tooling inserts for resin transfer moulding		338
Mark Thiede-Smet and Mark Wadsworth		
10.1	Introduction	338
10.2	Foam cores	339
10.2.1	Foam selection	341
10.2.2	Method for foaming core shapes	346
10.2.3	Methods for machining core shapes	349
10.2.4	Processing considerations when using foam cores	349
10.2.5	Lessons learned from using foam cores	351
10.3	Honeycomb and other open-cell cores	352
10.3.1	Methods of preventing resin from filling the honeycomb cells	353
10.3.2	Honeycomb selection for resin transfer moulding	356
10.3.3	Special considerations	357
10.4	Balsa wood cures	359
10.4.1	Balsa selection	359
10.4.2	Processing considerations	360
10.5	Bladders	360
10.5.1	Types of bladders	361
10.5.2	Processing considerations when using bladders	365
10.5.3	Bladder material selection	367
10.5.4	Making internal bladders	367
10.6	Phase change tooling inserts	370
10.6.1	Selecting melt-out and soluble mandrel materials	370
10.6.2	Eutectic salts	371
10.6.3	Melt-out metal alloys	373
10.6.4	Waxes	373
10.6.5	Soluble plasters and conglomerates	374
10.6.6	Break-out mandrels	374
10.6.7	Creating the mandrel shape	375
10.6.8	Sealing the mandrel surface	377
10.6.9	Processing considerations for melt-out mandrels	378
10.6.10	Thermal considerations for melt-out mandrels	379
10.7	Extractable tooling inserts	380
10.7.1	Material selection	380

10.7.2 Design and processing considerations	382
References	386
Chapter 11 Manufacturing and tooling cost factors	388
Teresa Kruckenbergs	
11.1 Introduction	388
11.2 Recurring cost factors	389
11.2.1 Effect of manufacturing quantity	389
11.2.2 Material cost factors	390
11.2.3 Manufacturing cost factors	392
11.3 Non-recurring cost factors	400
11.3.1 Injection equipment	400
11.3.2 Heat source	402
11.3.3 Mould costs	403
11.3.4 Certification cost factors	405
11.4 Applications	406
11.5 Case studies	406
11.5.1 Concept 1: flat panel	407
11.5.2 Concept 2: curved panel	408
11.5.3 Concept 3: stiffened panel	408
11.5.4 Concept 4: flap	408
11.5.5 Summary	408
References	411
Chapter 12 Data acquisition: monitoring resin position, reaction advancement and processing properties	412
David E. Kranbuehl and Al Loos	
12.1 Introduction	412
12.2 Instrumentation	415
12.3 Theory	415
12.4 Calibration: monitoring cure in multiple time-temperature processing cycles	417
12.5 Monitoring resin infiltration in conventional resin transfer moulding, and model verification	420
12.6 In situ real time flow sensing in resin film infusion and process monitoring	425
12.7 Smart automated control	428
12.8 Conclusions	429
Acknowledgements	430
References	431
List of manufacturers	433

Chapter 13 Quality and process control	434
Bernd Räckers, Chris Howe and Teresa Kruckenberg	
13.1 Introduction	434
13.2 Defects	434
13.2.1 Void characterisation	435
13.2.2 Void detection	437
13.2.3 Defect formation	438
13.2.4 Structural effects	443
13.2.5 Defect prevention	444
13.3 Process control	445
13.3.1 A comparison between the autoclave-cured prepreg process and resin transfer moulding	445
13.3.2 Resin transfer moulding process control requirements	446
13.3.3 Influence of materials	446
13.3.4 Effect of equipment	447
13.3.5 Process limits and controls	448
13.3.6 Process control coupons	450
13.4 Quality control	450
13.4.1 Material specifications	450
13.4.2 Manufacturing specification	451
13.4.3 Process quality control	451
13.4.4 Tooling	452
13.4.5 Non-destructive testing	453
13.5 Conclusions	453
References	454
 Chapter 14 Qualification of resin transfer moulding for aerospace applications	 456
Robert William Stratton	
14.1 Introduction	456
14.2 What is the qualification process?	457
14.2.1 Variables for qualification	457
14.2.2 Allowables	458
14.2.3 Fibre volume fraction	458
14.2.4 Destructive testing	460
14.2.5 Fibre orientation	462
14.2.6 Property translation	464
14.2.7 Classification of candidate parts	464
14.3 Methods of mechanical property qualification (structural testing)	466
14.3.1 Equivalency technique	467
14.3.2 Structural testing	470
14.4 Proof-of-concept parts	471
14.5 Specifications	474

14.5.1 Material specifications	474
14.5.2 Process specifications	475
14.5.3 Non-destructive inspection and acceptance specifications	476
14.6 Qualification audits	476
14.7 Risk reduction	477
14.8 First-article qualification	478
14.9 Braided and three-dimensional woven structures	479
14.10 Conclusions	479
F-22 programme: equivalence tests	480
Method 1	480
Method 1(a)	481
<i>Appendix A Glossary</i>	482
<i>Appendix B Conversion factors</i>	508
<i>Index</i>	511

Contributors

Suresh G. Advani
Department of Mechanical
Engineering
University of Delaware
126 Spencer Laboratory
Newark
DE 19716-3140
USA

Michael Bannister
Cooperative Research Centre
for Advanced Composite
Structures Ltd
226 Lorimer Street
Fishermens Bend
Vic. 3207
Australia

Israel Herszberg
Sir Lawrence Wackett Centre for
Aerospace Design and Technology
Department of Aerospace
Engineering
Royal Melbourne Institute
of Technology
PO Box 2476V
Melbourne
Vic. 3001
Australia

Chris Howe
Cooperative Research Centre
for Advanced Composite
Structures Ltd
506 Lorimer Street
Fishermens Bend
Vic. 3207
Australia

David E. Kranbuehl
Chemistry Department
College of William and Mary
PO Box 8795
Williamsburg
VA 23187-8795
USA

Teresa Kruckenburg
Cooperative Research Centre
for Advanced Composite
Structures Ltd
361 Milperra Road
Bankstown
NSW 2200
Australia

L. James Lee
Department of Chemical
Engineering

Ohio State University Columbus OH 43210-1180 USA	Vic. 3207 Australia
<i>Andrew C. Long</i> Department of Mechanical Engineering University of Nottingham University Park Nottingham NG7 2RD UK	<i>Boeing Rocket Dyne</i> 6633 Canoga Ave M.S. IB17 P.O. Box 7922 Canoga Park, CA 910309 USA
<i>Al Loos</i> Department of Engineering Science and Mechanics Virginia Polytechnic and State University Blacksburg VA 24061-0219 USA	<i>Mitch Petervary</i> Department of Material Science and Engineering Penn State University 1514 Blue Course Drive State College, PA 16801 USA
<i>Adrian Melton</i> Aerospace Technologies of Australia 226 Lorimer Street Fishermens Bend Vic. 3207 Australia	<i>Mac Puckett</i> Dow Chemical Company 2301 North Brazosport Boulevard, B-1603 Freeport TX 77541-3257 USA
<i>Richard Parnas</i> National Institute of Standards and Technology Gaithersburg MD 20899-0001 USA	<i>Bernd Räckers</i> Daimler-Benz Aerospace Airbus GmbH 28183 Bremen Germany
<i>Rowan Paton</i> Cooperative Research Centre for Advanced Composite Structures Ltd 226 Lorimer Street Fishermens Bend	<i>Vivek Rohatgi</i> Department of Chemical Engineering Ohio State University Columbus OH 43210-1180 USA
	<i>Chris D. Rudd</i> Department of Mechanical Engineering

University of Nottingham University Park Nottingham NG7 2RD UK	Marietta GA 30063 USA
<i>Pavel Simácek</i> Department of Mechanical Engineering University of Delaware 126 Spencer Laboratory Newark DE 19716-3140 USA	<i>Mark Thiede-Smet</i> Hexcel Structures Division 19819 84th Avenue South Hexcel Corporation Kent WA 98032 USA
<i>Robert William Stratton</i> Lockheed Martin Aeronautical Systems 86 South Cobb Drive 73-HH zone 0986	<i>Mark Wadsworth</i> Wadsworth Development Company 749 South Poplar Wichita KS 67211 USA

Preface

The editors would like to commence by stating that we do not claim to be the leading world authorities on all aspects of resin transfer moulding (RTM)! Therefore, the approach we have chosen is to gather together such experts in the various aspects of RTM to produce a book which we believe will become a prominent reference on RTM. This book is intended to be the largest and most comprehensive book on RTM, particularly for high-performance applications, with 15 chapters written by experts in industry and academia. We hope that you will find this book useful, whether you are a student new to the area or an experienced professional seeking different perspectives on your specialty. In our experience, one good idea alone is often worth the purchase price.

Applications of the various types of RTM are growing more diverse by the day, and now range from biomedical components through architectural items to sporting equipment, automotive and aerospace structures and marine and civil engineering. Although the fundamental processing science is largely the same for RTM in all applications there are many differences in the economic justification for RTM in these applications and therefore in the optimum materials, part design and manufacturing approach.

Since this project was started, the editors have become aware of several other excellent newly published books on RTM. Those of which we are aware are either excellent introductions to the subject or are concerned largely with high-volume automotive applications. The experience and interest of the editors has so far been largely in RTM for aerospace applications. As we believe that a comprehensive book on this aspect of RTM is not currently available we have focused this book primarily on RTM for aerospace applications. However, we believe that this volume will be a useful reference for all persons interested in RTM, particularly for high-performance applications.

The reader may find that in this book, where each chapter is written by a different author, the subject matter of some chapters may overlap to some extent. The editors have attempted to reduce such overlap to a minimum but, in order to allow chapter authors to develop their argument logically, some overlap inevitably remains. We trust that any annoyance this may cause will be more than offset by the advantages of being able to view the subject from the different perspectives of each author's specialty. The editors found that these alternative perspectives stimulated thought and discussion on aspects of RTM which we though we knew well, and we hope that the reader will likewise find the different points of view helpful in providing fresh approaches to a problem or application.

In some books, liquid moulding is the more common term used to describe several resin infusion methods such as resin transfer moulding. In this book the term RTM has been used as a shortcut for liquid moulding.

Teresa M. Kruckenberg
Editor

Cooperative Research Centre for Advanced Composite Structures
361 Milperra Road, Bankstown, NSW 2200, Australia

Rowan Paton
Associate Editor

Cooperative Research Centre for Advanced Composite Structures
506 Lorimer Street, Fishermens Bend, Vic 3207, Australia

29 August 1997

Acknowledgements

In 1992 I was asked to edit a book on resin transfer moulding (RTM). At that time I was too busy with part-time graduate studies to accept. However, the seed was planted and later I succumbed to the excitement of putting together a reference book on RTM. As the project evolved, the work seemed to grow exponentially so I am very grateful that Mr Rowan Paton agreed to be associate editor. Without his contribution this book would not be of the quality that it is and it would have been severely delayed.

The glossary involved intensive collaboration between some of the authors and other sources to define and agree on new terminology specifically related to RTM. Dr John Curiskis, Senior Lecturer from The University of New South Wales Department of Textile Technology and Dr Michael Bannister from the Cooperative Research Centre For Advanced Composite Studies (CRC-ACS) helped contribute textile definitions to the glossary. Other sources used for definitions were the ninth edition of Terms and Definitions, edited by M. Tubbs (The Textile Institute, Manchester, 1991), and the Engineered Materials Handbook, Volume. 1: Composites. (ASM International, Metals Park, OH, 1987). We would like to thank everyone who contributed to the glossary.

We would also like to thank the CRC-ACS, its Director, Dr Gordon Long, for his support of the book and the Deputy Director, Stuart Dutton, for his assistance in editing chapters.

Introduction to resin transfer moulding

1

Bernd Räckers

1.1 INTRODUCTION

The aerospace community and especially the advanced composite family is traditionally very much in the forefront of technology. Yet in the past number of years, after composites having been successfully introduced to primary structures of military and civil aircraft, a break was observed. Manufacturing and material costs for composite parts decreased less than expected. Because of extremely low fuel prices weight saving became a less important factor and therefore composites were not used in more applications. So cost became the most important driver for technology development, even in military aviation.

In many companies composites have been faced with strong competition from metals. Comparison was done on the basis of part cost only. The raw material price for carbon fibre epoxy prepreg is still some 5–10 times higher than that of aluminium. Also, the manufacturing costs are higher. This may surprise those who remember the quite optimistic figures from the early days of composites. A reduction of parts by a higher level of integration using one shot co-curing techniques was promised. Unfortunately, experience has shown that the manufacture of highly integrated parts such as the shell of the Airbus fin box resulted in high recurring and non-recurring costs. Cleaning of the various tool parts, the tools themselves and especially tool modifications has been extremely expensive.

Additionally, the standard autoclave cured prepreg technology is not the right approach for every application. At first different types of

2 Introduction to resin transfer moulding

components were fabricated in composites, some of them not suitable for this process. The advantages of composites were realised when applied to the right components such as shells, ribs and spars. Other parts of a more complex shape and with high load concentrations were tried and, after a costly experience, a redesign was done in metal.

In total, manufacturing costs for composite parts were approximately 20%–50% higher per kilogramme than those designed in aluminium. The advantage of 20%–25% weight gain was still of certain interest in the civil airline market. Yet no airline would now spend an extra dollar for it. In the military market, cost consciousness has increased as well. Here also the application of composites is subject to cost comparison.

As a result the growth of the composite share on aircraft structures stopped. In some programmes metals regained new applications. It became obvious that composites could get a higher share only by the application of new cost-effective technologies, especially new processes offering advantages. Resin transfer moulding (RTM) is one amongst many new developments, but it is one of the most promising. The cost advantage will then enable the aircraft industry to use the specific features of advanced composites:

- high weight-saving potential;
- corrosion resistance;
- no fatigue.

These advantages together with material price reduction will form a very competitive package for future developments.

1.1.1 IS RESIN TRANSFER MOULDING A NEW PROCESS?

In the aerospace industry, processes other than autoclave cured prepreg have been used only in a very few minor applications. Early descriptions of the RTM process [1] presented applications for non-aerospace use such as small boat hulls and other simple parts with a low fibre content. Even in the late 1980s RTM was considered only for mechanical engineering, automotive [2] or consumer products purposes. Some water tanks [3] (Figure 1.1), radomes, etc. were the only aerospace examples built in RTM up to the late 1980s. All of these parts have been manufactured with low fibre volume content and mainly with glass reinforcement. The available resins had low viscosity, low glass transition temperature and low toughness as well. These applications could hardly be designated as advanced composites. Yet the principles of the RTM process were incorporated.

Recent developments in textile and resin technology have allowed the switch to more advanced designs, higher loads and finally to the use in primary structure. These new resin systems provided low-viscosity,



Figure 1.1 Freshwater tank for Airbus A310. Reproduced courtesy of AlK Faserverbundtechnik GmbH.

higher toughness and sufficient hot/wet performance. Fibre volume fraction increased to 55%–60%. This led to the use of carbon fibres as well because now their high costs could be paid off for high-performance parts. Advanced textile technology has also helped to increase wettability of the preforms. Higher toughness can be achieved by using three-dimensional (3D) weaving and stitching technology (a feature which cannot be obtained efficiently with prepreg technology).

RTM technology developed from niche applications to a very competitive process, supplementing or replacing prepreg technology.

1.1.2 REASONS FOR RESIN TRANSFER MOULDING

As already mentioned in the introduction, many attempts have been made to use composites on greater numbers of parts. The main deficiency of many of these parts was the application of the well-known autoclave cured prepreg technique even though it was not the most suitable. No adequate process existed which gave reasonable performance without the cost disadvantage of prepreg technology. Other

4 Introduction to resin transfer moulding

processes, such as filament winding, wet resin lay-up and compression moulding were not able to provide equivalent performance and therefore not used for most advanced composites.

Most advanced composite applications were done in prepreg, with variable success. Some components were state of the art and competitive; others failed to meet economic targets. Analysis of these components showed some very interesting reasons.

Big, flat parts such as shells, stiffened or non-stiffened, may be quite competitive in spite of the high costs for prepreg. Nevertheless, the trend is towards a more simple shell-stiffening concept with a multi-step process instead of the one-shot design. A high level of integration was pursued in the beginning of the composite's age, with the intention being to reduce parts and therefore manufacturing time and costs. More than 10 years of manufacturing experience and many modifications have proved that excessive integration is inefficient. High tooling costs, many necessary tool-cleaning operations and especially extremely high non-recurring costs for part modifications were the greatest disadvantages of this concept.

Other parts such as thick and/or more complex-shaped parts were possible in prepreg but required many manual operations to give the correct shape to the numerous small plies. Tooling was difficult; it had to provide sufficient thickness for consolidation, and pressure had to be uniform throughout the complete part to get good quality. Many debulking operations were necessary to reduce voids. Net shape manufacture was impossible because of poor tolerance and thickness control.

The use of an advanced textile preform was also very difficult to achieve with prepreg; no process existed which allowed the use of three-dimensional weave patterns, advanced braiding or multiaxial fabrics.

Despite these problems, the very-high-quality level of parts manufactured by prepreg technology restrained the introduction of other techniques. Nevertheless, the industry looked for other processes that would allow the manufacture of parts that are not really suitable for the autoclave cured prepreg technique at the same quality level. In the meantime work on RTM continued and the breakthrough was achieved by the development of new high-performance resin systems.

A very important issue for RTM is the materials price, which is much lower than that of prepreg. A price difference of 30%–50% per unit mass can be observed. This is to be expected because the process of making prepreg is very expensive owing to high capital investment, slow processing speeds and high costs for auxiliary materials such as release papers and films. The RTM price depends very much on the resin systems (one or two components) and on the preforms used. The most competitive preforms today are multiaxial fabrics (non-crimp fabrics)

which add only 5%–20% to the carbon fibre raw material price. The materials price significantly contributes to the final part price. For some applications this difference alone justifies use of RTM.

1.1.3 BASIC PRINCIPALS AND REQUIREMENTS FOR RESIN TRANSFER MOULDING

The main characteristic of RTM is the separate handling of the reinforcement material and the matrix. Until they meet each other in the mould during the RTM process the components have had a completely different history as in the early days of wet laminate and current boat-hull processing techniques.

Resin systems

The resin is made like any other epoxy resin system but has to have low viscosity to allow easy impregnation. Resin systems are available as one-component (resin premixed with hardener) or two-component systems.

On the one hand, one-component systems allow easy handling and do not require resin mix equipment but have the disadvantage of limited shelf-life. On the other hand, two-component systems require certain mixing knowledge and equipment. For many aerospace companies this is not the preferred solution, as the trend is towards one-component systems mixed by the resin manufacturers. The advantage is that those people are familiar with mixing and it can be done in bigger quantities and with higher reliability. Quality assurance on the mixing is done by the resin specialists who have experience in this area. The part manufacturer does not need to check the correct mixing ratio for any part.

Preforms

Resin systems may be very important for this technology, but for RTM the ‘art and the heart’ is the preform [4]! Preforms may consist of various reinforcements such as fabric, braids, etc. Preforms ideally give the final shape of the component and the reinforcement. Most of today’s RTM users require the preform to have the final shape and thickness before the mould is closed. Correct preforming therefore is the most important step in the RTM process and only this gives very high reliability when done correctly. The preform can be controlled before resin injection and a high fibre volume fraction preform will not change its shape during injection because it is fixed by the closed mould. Preforms can be easily prepared using a binder resin applied to the fabric directly after weaving. The binder allows the compaction of the layers to the final thickness by the application of heat and consolidation pressure.

6 Introduction to resin transfer moulding

Another aspect of the preform itself is the fibre architecture. Reinforcements can be made by a large variety of existing or new textile processes. These may have the task of giving the shape of the part and/or providing additional toughness if necessary.

Today, weaving technology is very well advanced; many different forms such as 3D fabrics (Figure 1.2), T-shape fabrics, and even stiffened skin fabrics have been developed. Stitching technology led to the development of advanced non-crimp fabric (NCF) with multiaxial fibres (Figure 1.3) [5] and to the ability to make multi-layer preforms without using binder, which avoids possible resin compatibility problems. Another advantage of NCF is increased drapability, especially when knitted with the Tricot style or with low tension in the knitting yarns.

Braiding is used as well, and now 3D braids exist in different variants (Figure 1.4). Profiles of different shape can be realised containing $\pm x^\circ$ and 0° fibres, suitable for stringers and stiffeners.

An interesting new process is the stitching of yarns by means of embroidery machines (Figure 1.5) developed by the Institut für Polymerforschung, Dresden [6]. This technique, which is referred to as tailored fibre placement (TFP), allows handling of tows or yarns, which can be aligned according to the stress field requirements (Figure 1.6). The process is fully automated and provides excellent cost-efficiency.

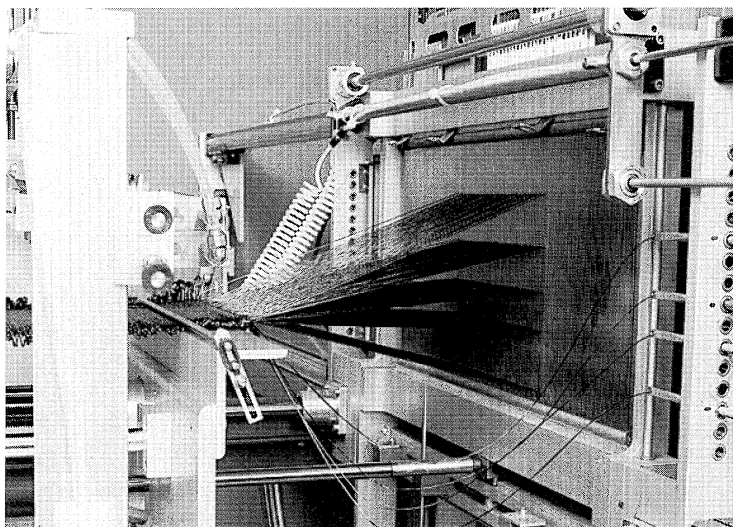


Figure 1.2 Three-dimensional weaving machine. Reproduced courtesy of Daimler-Benz Forschung und Technik.

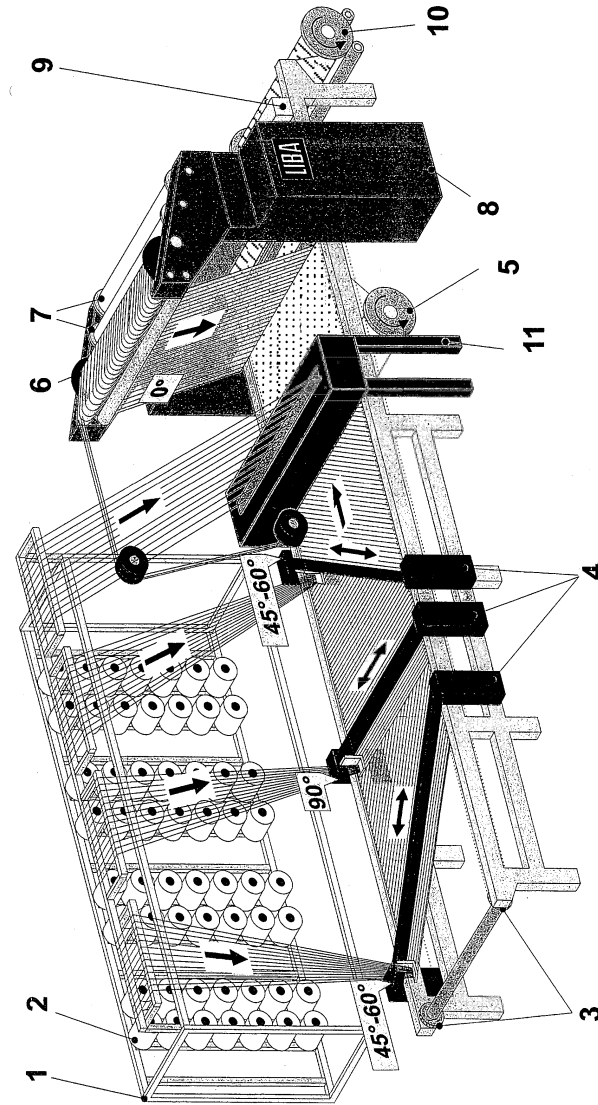


Figure 1.3 Non-crimp fabric machine. 1 = bobbin creel; 2 = overhead bobbin draw-off; 3 = knitting beam; 4 = needle transport chain; 5 = non-woven feeding system carriers; 6 = 0° yarn beam; 7 = carriers; 8 = warp knitting machine; 9 = edge trimming; 10 = chopper head; 11 = fabric take-up roller. Reproduced courtesy of LiBA.

8 Introduction to resin transfer moulding

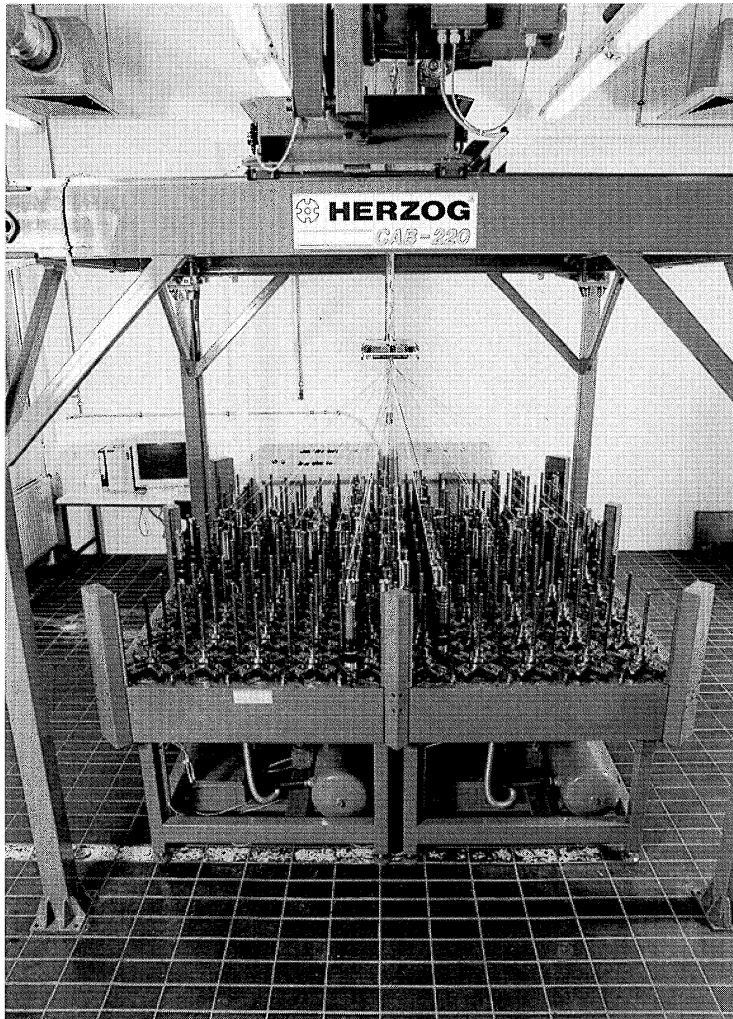


Figure 1.4 Three-dimensional braiding equipment. Reproduced courtesy of Daimler-Benz Forschung und Technik.

By combining some of these technologies preforms of very complex shape can be made at low cost. On the shop floor there is no need for labour-intensive stacking and forming of many single plies.

Cutting of dry fibre preforms may be achieved by different approaches. Ultrasonic knives provide efficient and exact cutting. The use of a binder may assist cutting by other machines such as Gerber cutters.

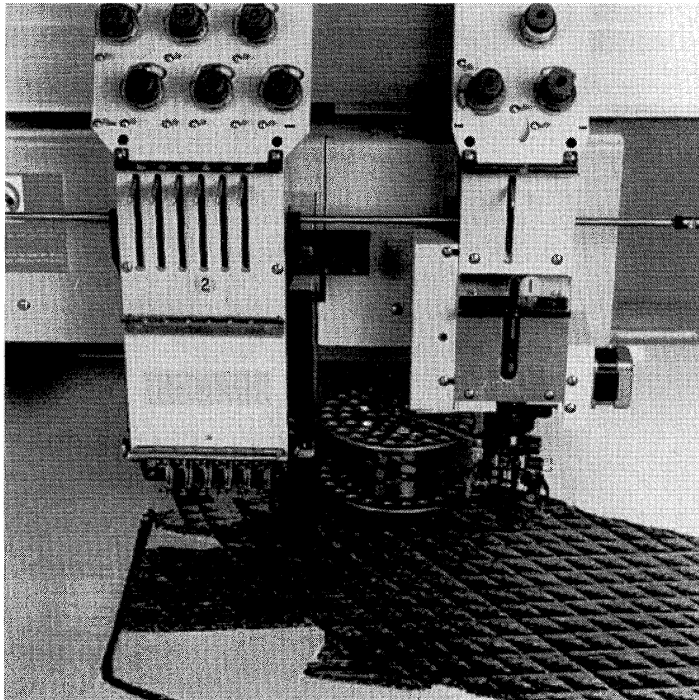


Figure 1.5 Tailored fibre placement unit. Reproduced courtesy of Institut für Polymerforschung.

Supplementary to fibre reinforcements, closed-cell foam can be used for sandwich-type applications. This allows the design of lightweight parts having high thickness that may be necessary for design or stiffness reasons. Nomex honeycomb can be used if the cells are closed, for example by an adhesive, but this may not be a competitive alternative. When using foam core specific care has to be taken because of its hygroscopic behaviour and the possibility of crushing at high pressure and high temperature.

The resin transfer moulding process

The RTM process itself is characterised by a closed mould and ideally the preform has its final shape before the mould is closed. Resin transfer may be carried out by vacuum and additional pressure from a transfer pot or a resin pump. The resin usually flows in-plane through the preform (Figure 1.7). The maximum injection length is limited by the advancing polymerisation of the resin, because usually injection takes place at an elevated temperature to decrease viscosity. This naturally leads to a re-

10 Introduction to resin transfer moulding

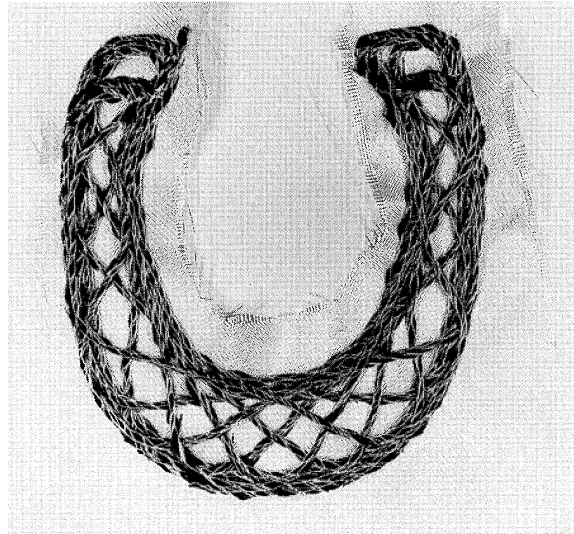


Figure 1.6 Example of a tailored preform. Reproduced courtesy of Institut für Polymerforschung.

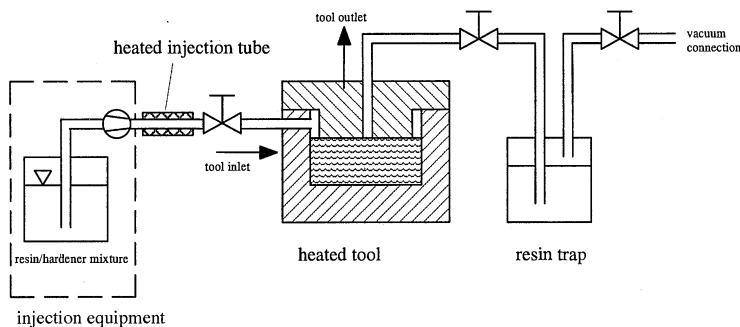


Figure 1.7 Resin transfer moulding flow process. Reproduced courtesy of Daimler-Benz Aerospace Airbus.

duced injection time because the resin cross-links earlier and faster. Another limitation is given by preform permeability. Typical injection times and lengths are 5–120 min and up to 2 m, respectively. Injection lengths can be increased by multi-port or linear injection, so the size of the part can be bigger than the maximum injection length. Another option may be the use of specific fabrics having resin canals applied by a special weaving technique.

Specific care has to be taken for the design of the injection port(s) and the vacuum outlet(s). In the beginning of RTM the selection of these

locations and forms was done empirically using many trials and experience. Nowadays, progress has been achieved in simulation and modelling of the resin penetration. These tools are not yet perfect for complex-shaped parts but give a good first guess. The results of the simulation will become even more reliable because many research programmes are ongoing and understanding of RTM is improving. However, RTM is a quite tolerant process and allows some variations in the tool design.

A special feature of RTM compared with other wet resin techniques is the low risk of operators contacting the resin. Health and safety measures are not a concern, especially if one-component resin systems are used. The only measures to be taken are those to avoid contact with binder during stacking of preforms. Binder quantities are low and give off few volatiles. Ventilation is not necessary.

Curing equipment

The curing of the RTM part takes place in the mould for the time and temperature required by the resin system. The internal mould pressure during curing depends on tooling, preforms, part shape and many other items. Occasionally vacuum pressure only is sufficient, but usually application of pressure after injection helps to shrink voids.

Many methods of heat transfer are possible; the decision over which one to use depends more on available equipment than on technological items. Overall, a concept for an RTM manufacturing plant is necessary and this will determine the means of heat transfer. Possible options are oven, press, integrally heated moulds (by oil or electric) and the autoclave. Of course, by using an oven the heat transfer achieved is the worst obtained of all the options and a long heat-up time is the consequence.

Open-mould process

The closed-mould process is not the only one used. RTM can also be done by using the vacuum-bag technique and autoclave pressure. The advantage is easier mould design. No mould-closing force is required, giving the opportunity to increase part size without having big metal tools weighing several tons.

Differential Pressure RTM (DP-RTM) developed by DLR, Braunschweig, Germany [7] provides an efficient means of applying RTM technology on bigger parts using conventional autoclave tooling. The resin flow is controlled by the difference in pressure in the vacuum bag and the autoclave. Injection is done at a low differential pressure, and compaction is carried out by increasing the autoclave pressure after the

12 Introduction to resin transfer moulding

part is fully impregnated. Another interesting part of the DP-RTM concept is the use of multiple line injection and vacuum lines. Silicone profiles of triangular shape with a round resin channel, which is open to the baseline, are placed on the dry preforms (Figure 1.8). The resin will fill the channels first and then flow into the preform to the vacuum lines. By placing several lines across the width of the part the flow length can be limited to the capability of the resin. This concept allows an increase in the part size comparable to the autoclave-cured prepreg technology.

1.1.4 OUTLINE OF RESIN TRANSFER MOULDING DEVELOPMENT WORK

To start with, the development of a new process requires much information from a variety of sources. Research institutes, corporate research groups, material suppliers or even competitors may be those sources. Different quality levels for this information have to be kept in mind. The closer the relationship between the sources and those who are responsible

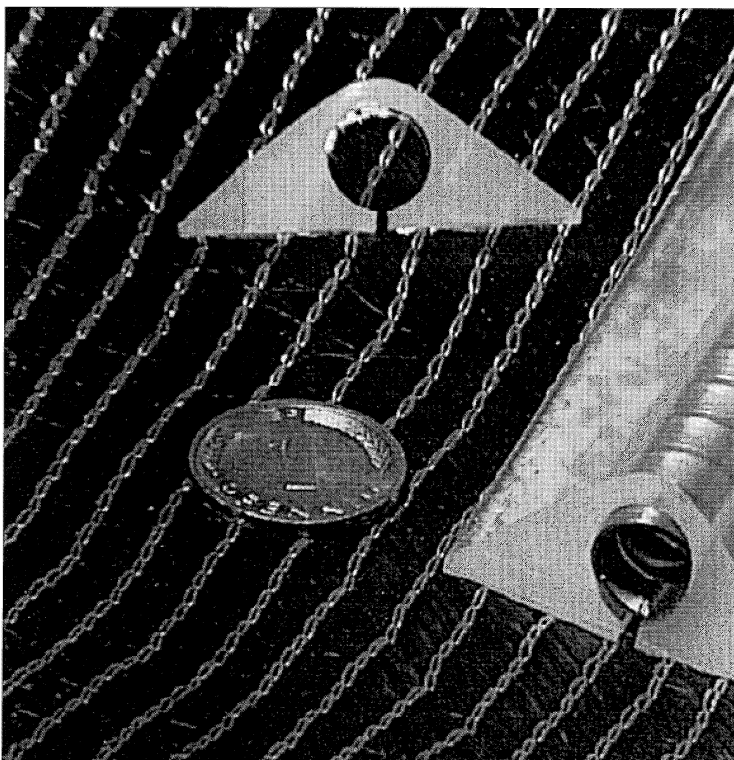


Figure 1.8 Injection line for a differential pressure resin transfer moulding process placed on non-crimp fabric. Reproduced courtesy of DLR.

for development the better the information can be relied upon. Normally a mix of available information leads to the decision to go ahead.

When a new technology is ready for the start of development it is usually still about five years before it is introduced into service. Even if the information comes from a very good source, only an estimate of the success of such a development can be made. Of course, only new processes that are very promising will be continued.

The first things to do are to check whether potential parts are available and whether a transfer into the environment of the company will be successful, gaining either technical or financial benefits (or both, of course).

For a new process in particular, effective screening has to be done to get all the information to justify the spending of the huge amount of money necessary to introduce it. Basic figures must be obtained to estimate technical performance and cost savings. These are highly influenced by the specific part(s) intended to be manufactured by this process. Therefore, representative demonstrator parts have to be chosen to prove the idea and the results of the screening. A wrong choice can lead to an underestimation of the capability of such a new process; conversely, a certain danger exists in taking a very suitable part where the results may be too promising. The chance of convincing the management to invest in a new technology is improved by a thorough evaluation of the results. A good screening programme therefore should involve most of the decision-making people. Manufacturing people especially should be included in the early stages of such a programme. By doing this, introduction is much easier and the economic figures obtained are much more reliable.

Evaluation of structural performance must also be part of the screening and development procedure, either because it is influenced by the process or because the properties are affected by the necessity to select new materials.

Careful screening enables rapid development with a low risk of failure. Realisation of the parts, including certification, will be done in a smooth process. Nevertheless, introduction involves significant detail work and proof that the process is reproducible. Even qualification work has to be done, which finally leads to certification of the parts manufactured by a new process.

A new approach or philosophy is required for RTM; some aspects are known from prepreg, others will be new. RTM-specific topics are the separate handling of fibre and matrix and occasionally the use of a binder on the preforms. In particular the specification system will require a new approach for RTM, although it might be essential that resin, fibre preform and binder be treated as a combination for qualification. This applies to the quality assurance concept as well, which has to be established

14 Introduction to resin transfer moulding

before the start of series production and includes all necessary aspects. Knowledge of the process and possible variations is essential. Quality assurance starts at the manufacture of resins and preforms, includes batch-release testing, incoming inspection and process control and ends with non-destructive testing of the finished parts. It is obvious that this has to be done very carefully because of its importance for the success of a new technology. It should work from the very beginning without failure.

Certification authorities have to be convinced that the new RTM process is as safe as the well-established autoclave-cured prepreg process. A good quality assurance concept is a perfect means of overcoming problems that may arise during introduction. Therefore it is obvious that the development of a new process also includes quality assurance and requirements.

1.1.5 RESIN TRANSFER MOULDING AND RESIN FILM INFUSION: COMMON AND DIFFERENT ASPECTS

The idea of handling the resin and the reinforcing fibres separately is not unique to the RTM process. Whereas the RTM process is characterised by in-plane resin flow, the more recent resin film infusion (RFI) process implies resin flow in the through-thickness direction (Figure 1.9). The resin is sucked into the fibre preform by capillary effects and by carefully selecting the position of the vacuum outlet.

Another difference is the use of a resin film, which is put into the mould together with the preforms. The advantage is that well-known prepreg resin systems can be used and mechanical properties are almost identical to those made by prepreg. Because RFI is very close to the prepreg process the same tools and equipment can be used. This allows manufacture of basically the same components made with prepreg. There is particular interest in parts of the stiffened skin type, which can

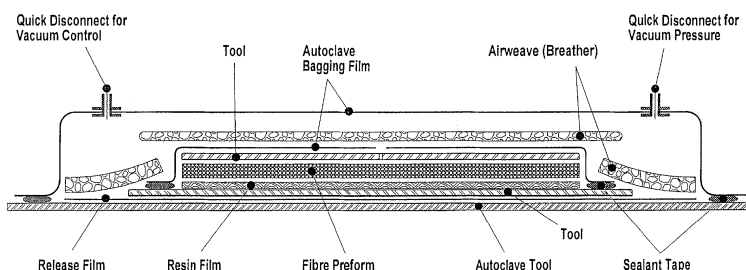


Figure 1.9 Resin film infusion flow process. Reproduced courtesy of Daimler-Benz Aerospace Airbus.

be ribs, spars and shells. These big parts are possible because in RFI the resin flows through the thickness. There is no size limitation stemming from injection length concerns as in RTM. The only possible limitation may be the thickness of the component, including integrated (e.g. stitched) stiffeners.

The use of resin film is a disadvantage for this process because the manufacture of a resin film is quite costly and therefore the price for such a film is about twice that of the pure resin. Another disadvantage is the difficult handling of such a film having no carrier as in the case of, for example, adhesive films. Owing to the low aerial weight of the film, the stacking of many plies may be necessary and labour costs will increase.

The RFI process also gives the opportunity to incorporate advanced textile preforms as in the RTM process. Sometimes this might be essential, because most of the suitable resin films have low toughness. Normally the required low viscosity can only be achieved by omitting thermoplastic modifiers which increase toughness. Fortunately, the use of 3D stitched preforms may provide sufficient toughness even for impact-critical areas.

RTM and RFI will play their specific role in future applications and will match different requirements. The combination of both processes will play an important role in many future aerospace programmes because their specific advantages will create structures with specific solutions, for example RTM for smaller, complex parts, and RFI and DP-RTM for large, flat stiffened panels.

1.2 CURRENT AND FUTURE APPLICATIONS FOR RESIN TRANSFER MOULDING AND RESIN FILM INFUSION

As mentioned before, some minor applications, most of them non-structural, have been used in aerospace parts for a long time. Today, with the appearance of new resins and advanced fibre preforms a boom for RTM parts can be observed. Many new parts have been developed in the USA for programmes such as the V22 Osprey and the F22 fighter project. In Europe some applications can be found in the Airbus programme, the Aerospatial Consortium ATR, and missile projects. Another very interesting area for RTM is the jet engine. Especially here RTM can prove its ability to allow the creation of complex-shaped parts at an unbeatable low cost with sufficient performance.

In this section an overview on some RTM projects will be given. Of course, this overview cannot be complete because many projects are confidential or classified.

16 Introduction to resin transfer moulding

1.2.1 EXAMPLES FOR APPLICATIONS AND DEVELOPMENT

In the aerospace industry RTM first appeared on some semi-structural or secondary structural parts such as small fairings and fittings. Very early in the development it became clear that RTM had a potential for more. At the same time, material suppliers produced samples of new resin systems fulfilling nearly all the requirements for structural applications. This gave a boost to RTM development worldwide. Many companies then started RTM research programmes. Some of these programmes were successful and some applications have been introduced to series production. Many demonstrator parts have been made in order to demonstrate the potential of RTM.

Typical examples for the first development parts that resulted in series production are the ATR flaptrack fairing and the rear pylon fairing of the Airbus A321 (Figure 1.10) developed by Aerospatiale and Brochier SA [8]. Although these parts are relatively simple they show some of the specific RTM advantages such as the use of textile preforms.

Other interesting applications have appeared in the engine industry. Good examples are the thrust reverser blocker doors for P&W 4000 engines designed by BP Advanced Materials [9]. These doors demonstrated cost efficiency and lightweight design. The geometry can be complex but is repeatable at high quality. This is possible by good design and ingenious use of preforming techniques. Even more complex is the vane-shaped component [10] of the RB 211-Trent/A330 thrust reverser. In this example RTM clearly outperformed aluminium and offered a 36% weight saving. A comparable part is the Trent engine kicker plate (Figure 1.11).

All these examples can be considered as secondary structure components. To develop primary structure components and introduce them into service was an even more challenging effort. Early RTM parts fulfilling structural requirements were the propeller blades (Figure 1.12) for the SAAB 340 and Fokker 50 turboprops developed by Dowty Rotol [11]. These parts are manufactured by using braids and fabric and represent an early application for the new approach combining RTM processing technology and textile preforming (braiding).

An important programme that set the pace for RTM primary structures was the F22 prototype development. On this aircraft, RTM is used to produce some 325 components throughout. Sinewave spars are produced by subcontractor Dow-UT [12]. Spars up to 4.5 m long are produced by stacking dry fibres in a preform die and then injecting the resin. Two advantages of the process are cited – dimensional control and recurring costs. Although non-recurring expense is high it will be paid off within a short time during series production. RTM provides excellent dimensional control, critical for this stealthy aircraft, at a comparable price.

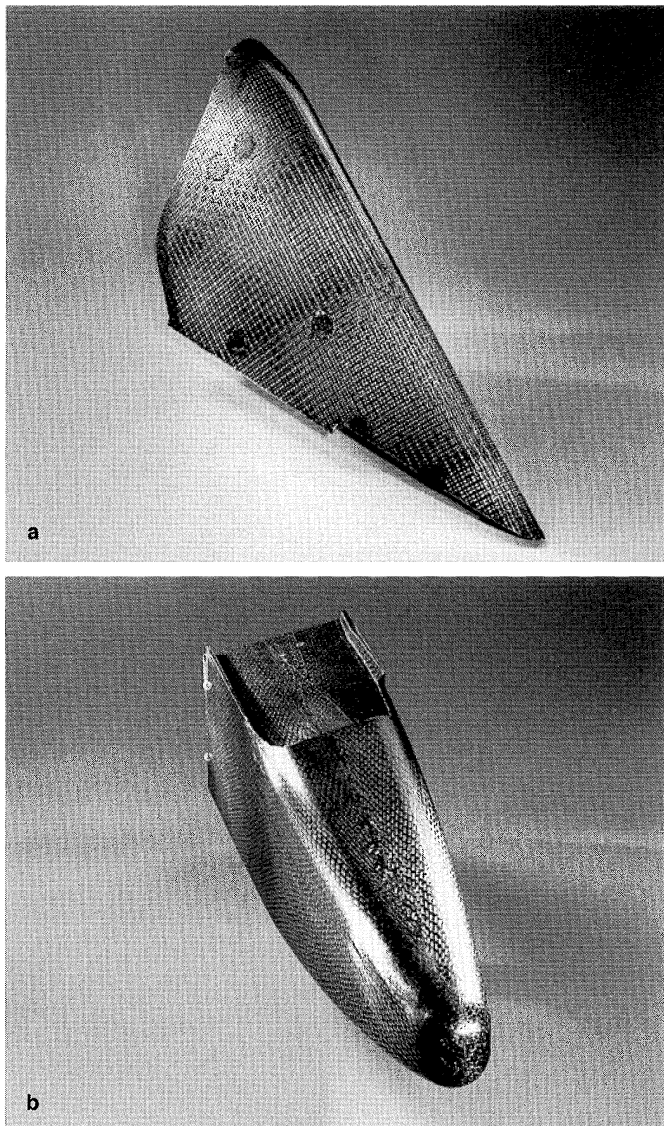


Figure 1.10 (a) Aerospatial Consortium ATR flaptrack fairing; (b) Airbus A321 rear pylon fairing. Reproduced courtesy of Hexcel.

In the engine industry primary structure RTM parts are being developed. A good example of growing use and confidence is the fan exit case (Figure 1.13) produced by Dow-UT for the advanced ducted prop high-bypass turbofan. The 2.8 m component is designed as the structural attachment between the engine core and the fan case. It has to withstand

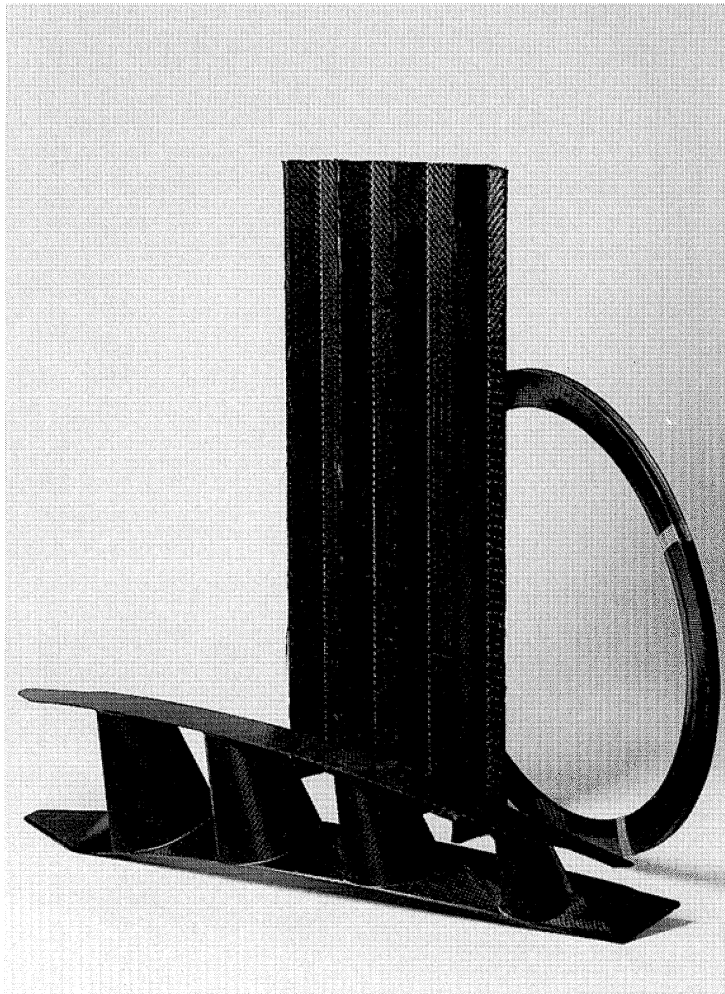


Figure 1.11 Trent engine kicker plate (front), self-stiffened preform (middle) and bicycle rim (rear). Reproduced courtesy of Hexcel.

birdstrike and rotor-imbalance loads resulting from the loss of a fan blade [13].

Another breakthrough for RTM was achieved by Daimler-Benz Aerospace Airbus for the Airbus programme. Two structural components which are very important for survival of the aircraft have been developed using RTM. The first ones are the fin-box attachment lugs for the Airbus wide-body family, A330/340. The fin box was the first composite primary structure on a civil aircraft, introduced in 1985 on the



Figure 1.12 Propeller blades, in use, for the SAAB 2000. Reproduced courtesy of Dowty Rotol.

A310-300. It is an all-carbon-fibre design using a high level of integration [Figure 1.14(a)]. The lateral attachment to the fuselage is by six bolts. The load is transferred from the shell to the bolts via thick lugs [Figure 1.14(b)]. In order to achieve the thickness required, the six lugs are pre-manufactured in two halves each and then cured together with the skin of the shells. Bonding between skin and the pre-cured lugs is done in a co-bonding process. The lugs are fully cured when they are put in the autoclave with the non-cured skin. Up to now the lugs have been manufactured from prepreg, in a mix of tape and fabric (264 g/m^2 tapes and 370 g/m^2 fabrics). The thicker lugs have up to 134 layers. Curing takes place in metal moulds in the autoclave and under autoclave pressure. Owing to variations in prepreg physical properties, resin flow and fibre areal weight, thickness control was poor. Another big disadvantage was that pre-consolidation was necessary every four or five layers to get the quality required for parts such as this carrying such high loads. When RTM was being developed in 1992 we selected these parts for a demonstrator programme. First calculations on cost and performance showed some 40% cost advantage at equivalent performance. Early manufacturing trials have been extremely successful. Although a modified, metal tool designed originally for prepreg was used, the first parts were of high quality, even higher than prepreg. None of the first trials failed.

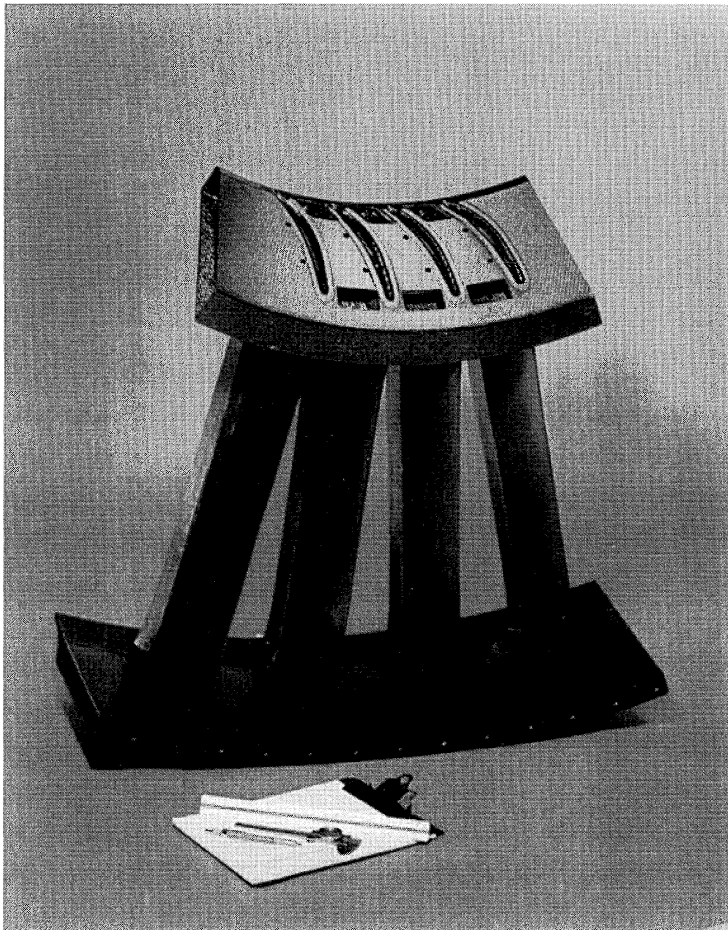


Figure 1.13 Fan exit case. Reproduced courtesy of Dow-UT.

A design-to-cost study was performed with the result that these parts can be introduced into service having a breakeven point of two years only. To reduce risk the tooling can be used for both prepreg and RTM. The first RTM parts started series production at the beginning of 1996. Certification was completed by the end of 1996.

A second important part to be replaced is the horizontal stabiliser cantilever beams (Figure 1.15). These parts are a complex metal design using both aluminium and titanium for fail-safe reasons. This rather complex design can be simplified by the application of composites. A single, monolithic beam of a certain thickness is sufficient because of the excellent fatigue performance of carbon fibre reinforced plastic (CFRP).

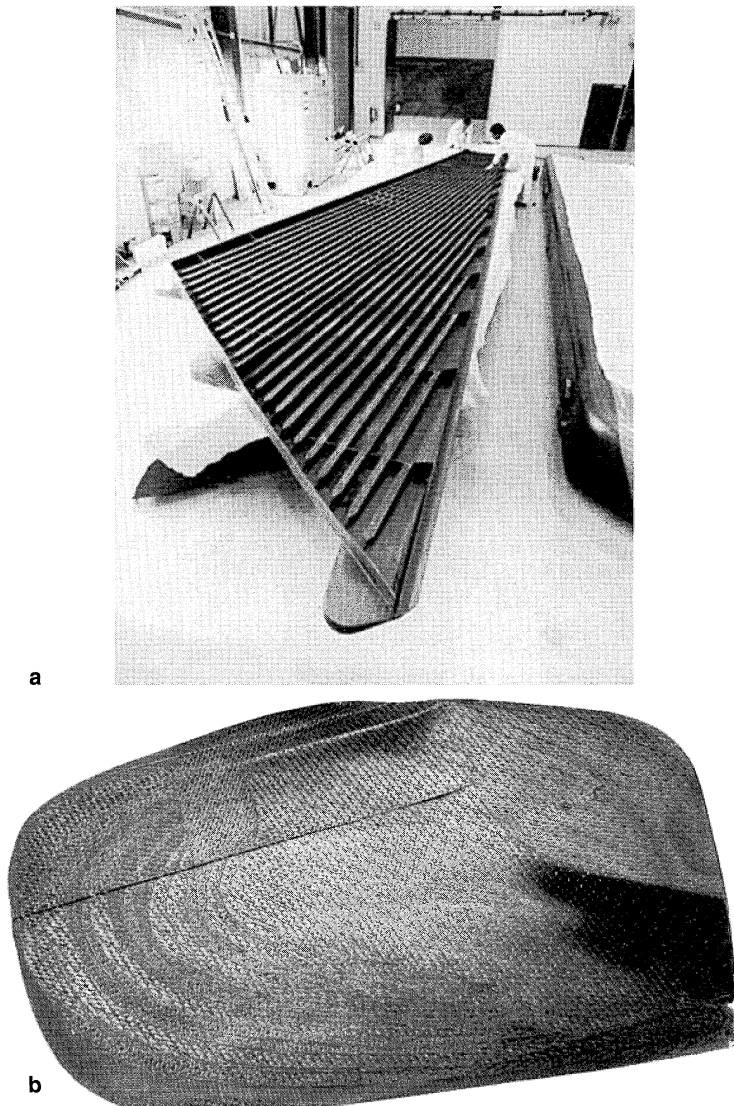


Figure 1.14 (a) Shell of an A310 fin box; (b) pre-cured fin-box attachment lugs.
Reproduced courtesy of Daimler-Benz Aerospace Airbus.

Early studies on the application of composites to this part came to the conclusion that composites have advantages, but use of prepreg would result in higher manufacturing costs. When RTM came up and resins and materials were qualified a new calculation showed both an approximate

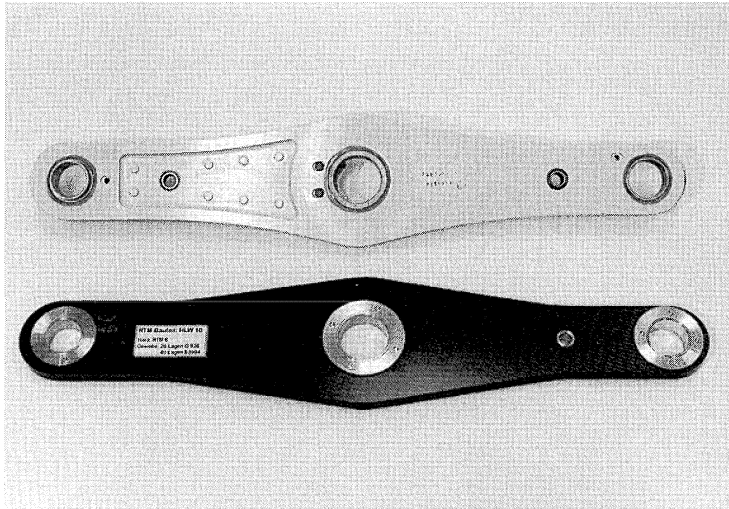


Figure 1.15 Horizontal stabiliser cantilever beam. Reproduced courtesy of Daimler-Benz Aerospace Airbus.

30% weight reduction and a dramatic cost reduction. Part costs are some 25% lower than those for the metal design.

These examples show very clearly that RTM can replace standard prepreg parts as well as metal parts. They also prove that most of the applications are of higher complexity than the parts realised in prepreg. With the success in the engine industry as an indication, RTM parts allow more freedom in design and can outperform metal design by weight and cost if the specific advantages are used. The better the understanding of preform technology in the future the more applications RTM will gain, even against low-cost aluminium parts.

1.2.2 OUTLOOK FOR RESIN TRANSFER MOULDING IN AEROSPACE APPLICATIONS

As discussed before, RTM technology has already proven its position in the composites world as a complementary technology to prepreg technique rather than as a replacement. RTM will not allow the manufacture of large, shell-type parts because of limited flow time and length. Even improvements in tool design and reinforcement permeability will not allow RTM to make these parts in a more cost-effective way than prepreg.

Therefore RTM will not be able to be a stand-alone technology in the composites world. A mix of different techniques and processes will be the future for composites. Each technique will have its specific application. Prepregs will be faced with strong competition from the RFI tech-

nology, which is aimed at basically the same group of applications. The first demonstrator programmes have successfully proven the capability of RFI.

Several reasons indicate an increase of applications produced in RTM. The most important opportunity for RTM (as well as for RFI) is the implementation of advanced textile reinforcements. Modern textile processes such as stitching, weaving, braiding, knitting and the multiaxial warp knitting (NCF) have been adopted for the processing of carbon fibre. These processes have become attractive in the use of advanced composites.

The combination of textile preforms and RTM will allow the manufacture of parts which were not possible in composites until now. Substitution of complex-shaped metallic parts will be a major opportunity for RTM. Such parts will not only be cost competitive but also will provide all the benefits of carbon-fibre-reinforced plastics. Corrosion and fatigue resistance will no longer be a problem for ageing aircraft. Frequent inspection of parts will not be required because composite parts have no loss in performance during the predicted life of an aircraft.

Many of the projected RTM parts are not in damage-critical areas or are simply too thick to be subject to damage-tolerance criteria. Nevertheless, sufficient damage tolerance can be achieved by 3D reinforcement if necessary.

Additional specific advantages of RTM parts are excellent tolerance control and net shape capability with high surface quality. This will depend on the quality of the tooling. Therefore, good tool design is a prerequisite for high-quality RTM parts.

All these advantages of RTM will contribute to competitive components, which will match the requirements from design, stress and manufacturing at lower costs. Compared with metal parts RTM will provide the same weight gain as conventional prepreg parts: 15%–30% for structural parts, depending on design and requirements. This weight gain will be achieved without having higher part costs, unlike many prepreg parts.

Of course, the success of RTM depends on more research, development and introduction work in order to understand fully the advantages and disadvantages. Serious development work will lead to more RTM applications, including some outside aerospace.

This book will give a much more detailed outlook on RTM and the benefits it will give to the aerospace composites family. It will help to provide an understanding of RTM and the development of RTM parts which will match today's and future requirements. Although the use of composites has not increased over the past number of years they should have a prosperous future – RTM technology will help to achieve this.

References

1. Wurtinger, H. (1970) Herstellung großflächiger Glasfaser/Kunststoff-Teile im Injektionsverfahren (Manufacture of glass fibre composite parts by an injection process). *Kunststoff-Rundschau*, 9, (September), 475–9.
2. Johnson, C. F. (1987) Resin transfer molding, in *Engineered Materials Handbook, Volume 1: Composites*, ASM International, Metals Park, OH, pp. 564–8.
3. AEG Isolier- und Kunststoffe GmbH, (undated) Product information, Kassel.
4. DOW-UT (1995) Presentation to Daimler-Benz Aerospace Airbus, November.
5. Karlheinz Hörsting (1994) *Rationalisierung der Fertigung langfaserverstärkter Verbundwerkstoffe durch Einsatz multiaxialer Gelege*, Shaker, Aachen.
6. Gliesche, K. and Rothe, H. (1994) Neue Gestaltungsmöglichkeiten für Composite-Bauteile durch kraftflußorientierte Textilkonstruktionen. *Techtextil-Symposium*, presentation number 328.
7. Sigle, C.H. (1996) Das DP-RTM Verfahren, eine Fertigungstechnologie zur wirtschaftlichen Herstellung hochwertiger Faserverbundbauteile. *AVK-Tagung*, A17-2–A17-7.
8. Mir, L., Leblond, E., Auduc, H. and Bazerque, G. (1994) RTM – a process for aircraft structural composite parts. *15th International European SAMPE Conference*, June 8–10, Society for the Advancement of Materials and Process Engineering, 1161 Parkview Drive, Covina, CA 91724–3748, pp. 171–9.
9. Morgan, D. (1989) Design of an aero engine thrust reverser blocker door. *34th International SAMPE Symposium*, May 8–11, Society for the Advancement of Materials and Process Engineering, 1161 Parkview Drive, Corvina, CA 91724–3748.
10. Kauffmann, C. (1994) Development of organic matrix composites in thrust reversers. *15th International European SAMPE Conference*, June 8–10, Society for the Advancement of Materials and Process Engineering, 1161 Parkview Drive, Covina, CA 91724–3748, pp. 201–11.
11. McCarthy, R.F.J. (1994) Polymer composite applications to aerospace equipment. *Composite Manufacturing*, 5(2), 83–93.
12. Warwick, G. (1996) Building the F-22. *Flight International* (17–23 January), 35–6.
13. Warwick, G. (1996) Moulded for success. *Flight International* (24–30 January), 65.

Injection equipment

2

Mitch Petervary

2.1 INTRODUCTION

Injection equipment represents one of the three primary components to a successful resin transfer moulding (RTM) set-up, the others being tooling and materials. The old axiom, 'the right tool for the right job' holds true even in the aerospace industry. The proper choice of injection equipment from the outset can eliminate many production heartaches and financial burdens resulting from slipped schedules, rework and high scrap rates. The selection requires a thorough review of the intended application, listing the requirements in as detailed a fashion as possible. This list should evaluate several considerations, including but not limited to: the types and variety of materials being processed, the size of the part (capacity of the apparatus), the size of the production run (total number of parts), the production rate, data acquisition features for quality control records, and, of course, price [1, 2, 3]. This chapter will discuss these various considerations, as well as the basic elements involved in an RTM injection system and the different types of equipment available, contrasting their advantages and disadvantages. It will also offer examples from some of the leading popular manufacturers: Ashby Cross, Graco, Liquid Control, Radius Engineering and Venus Gusmer. (A list of manufacturers and their contact details is given at the end of this chapter.)

2.2 SELECTION CONSIDERATIONS

Selection criteria can be broken down into manufacturer-specific and application-specific considerations.

2.2.1 SELECTION OF A MANUFACTURER

The selection of the appropriate apparatus requires forethought as to the current and potential future applications. The unit should afford room for growth and versatility, unless a single production programme is large enough to warrant a dedicated machine. Generally, the greater the versatility the greater the cost, particularly in upgrades. Most manufacturers offer an assortment of options and upgrades to custom configure their products to the customer's specific needs. The selection and availability of such additions therefore may become a consideration, as well as an indicator of product support. It should be noted, however, that all injection systems include at a minimum three basic components: the resin reservoir, a resin feed system and a resin delivery hose (these will be described in greater detail later in section 2.3.1).

Manufacturers offer a vast background of knowledge and experience with which to assist the customer. Such knowledge often extends past injection equipment to tooling designs as well [2]. This resource can prove invaluable when setting up for the first time and can continue throughout production as an asset to manufacturing and/or process engineering. This knowledge should not be overlooked but rather considered part of the purchase. The actual equipment represents only part of the product. Customer service and support is the other. The manufacturers mentioned in this text have set the standards for such support and as such are separated primarily by different design philosophies, specific features, assortment of add-on options and packaging of their equipment.

2.2.2 APPLICATION-SPECIFIC CONSIDERATIONS

The first and most crucial consideration is the determination of the materials to be processed, in particular the class of resin systems. The service requirements of the apparatus will ultimately be defined by the processing parameters of the resin system(s). In general, aerospace-grade resin systems tailored for high strength, temperature resistance and toughness require adherence to narrow processing parameters to maximise part quality. Many resin systems mandate a preheat in order to lower the viscosity of the resin to a processable state. Low viscosity is essential for good wet-out of the preform in a reasonable amount of time. It is also crucial to mixing the resin with curative systems, additives and

fillers as required as well as degassing and injection. (The interdependence of temperature, viscosity and gel time will be discussed in detail in Chapter 3, Section 3.1.2.) This processing requirement usually necessitates use of heated resin reservoirs, pumps, injection lines, valves and dispense heads. It therefore is important to match the temperature requirements of the resin system to the service limits of the selected injection equipment (while incorporating a reasonable margin of safety).

The size of the part will define the capacity and flow rate requirements of the apparatus. It is important that the injection system (or systems if multiple units are used in parallel) provide an ample supply of resin sufficient to fill and burp the mould cavity. Interruption of an injection to refill the resin reservoir should be the last option. Flow rate is determined through an interplay of material pot-life, the injection system's capacity and the production rate. The pot-life of the resin system and the number of the systems utilised will define the frequency of cleaning and maintenance. [1, 4–7]. Here, meter/mix injection machines such as the Liquid Control Corp. unit shown in Figure 2.1 offer an advantage. Multiple reservoirs provide a limited storage capability where resin components are stored separately. In this type of system the resin is mixed just prior to entry into the mould, thus reducing the amount of clean-up. Many injection systems offer solvent reservoirs and 'self-cleaning' options [1, 4, 5, 8]. If, however, the frequency of use is low or resin systems are switched often, a manual cleaning may prove more effective by providing a more thorough cleaning, eliminating resin build up, deposits and contamination. Modularity in many of the current units results in

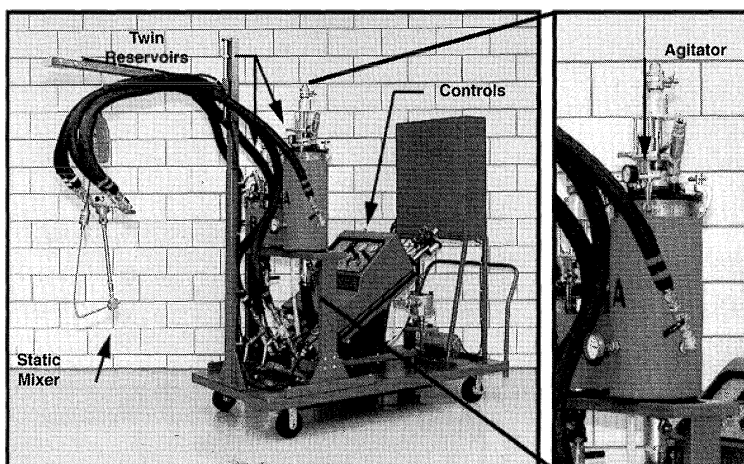


Figure 2.1 Liquid Control CMF™ mix/meter injection system. Reproduced courtesy of Liquid Control Corporation.

28 Injection equipment

easier tear-down and further facilitates cleaning and maintenance, thereby reducing subsequent costs.

Production rate will define the degree of automation involved in the injection system. Large production runs and high manufacture rates can better afford the costs associated with automation. Quality control requirements will define the specific data-acquisition features needed. These include temperature and pressure (of the reservoir, dispense line and tooling), flow rate, volume injected, viscosity, elapsed time and dielectric properties of the resin (used to determine position of the resin flow front and state of resin cure) [3,8,9]. Last, all these considerations will combine in the total cost of the unit.

2.3 BASIC PRINCIPLES OF RESIN DELIVERY FOR RESIN TRANSFER MOULDING

All injection equipment possesses three common components, as mentioned previously: the resin reservoir, a resin feed system (pump or valve in the case of a pressure-pot system) and a delivery hose, as seen in Figure 2.2. This section will discuss each component, offer basic construction (for the 'do-it-yourselfer') and some incorporated advanced features offered by the aforementioned manufacturers. Because most aerospace-grade resin systems require a preheating prior to injection, the schematics shown will incorporate heating elements.

2.3.1 BASIC ELEMENTS

Resin reservoir

The reservoir in general is simply a tank capable of holding a vacuum (for the degassing operation) and, in the case of a pressure-pot type resin

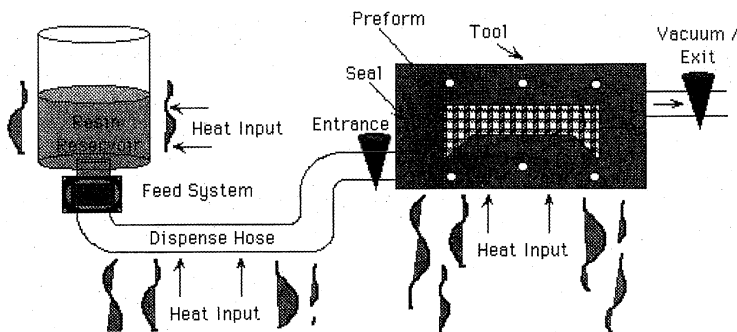


Figure 2.2 Schematic of a basic resin transfer moulding set-up.

feed system, holding pressure (Figure 2.3). The reservoir often incorporates some type of agitator which allows for mixing, assists in degassing and provides for uniform heating of the resin as required. The lid frequently supports air or vacuum line quick connects and as a recommendation should incorporate a sight glass or window when possible. This window should be large enough to accommodate illumination into the tank as well as a view of the interior.

Heat input is usually accomplished through the use of electric resistance heater blankets. The heater blanket is wrapped about the exterior wall of the tank and can be secured with high-temperature silicon RTV sealant or fibreglass tape. A series of thermocouples are sandwiched between the heater blanket and tank to allow for a temperature monitoring and control feedback loop and associated quality control data acquisition systems. Such blankets and controllers can be purchased through companies such as Briskheat and Omega Engineering. Their extensive customer support and available literature will assist the 'do-it-yourselfer' in determining requirements and equipment selection. Next, the blanket is overwrapped by several layers of thin insulation such as coarse-weave fibreglass such as 285–500 g (10–18 oz) boat cloth or a similar material. Finally, a cosmetic overwrap is applied which will seal the cloth or insulation and prevent it from fraying.

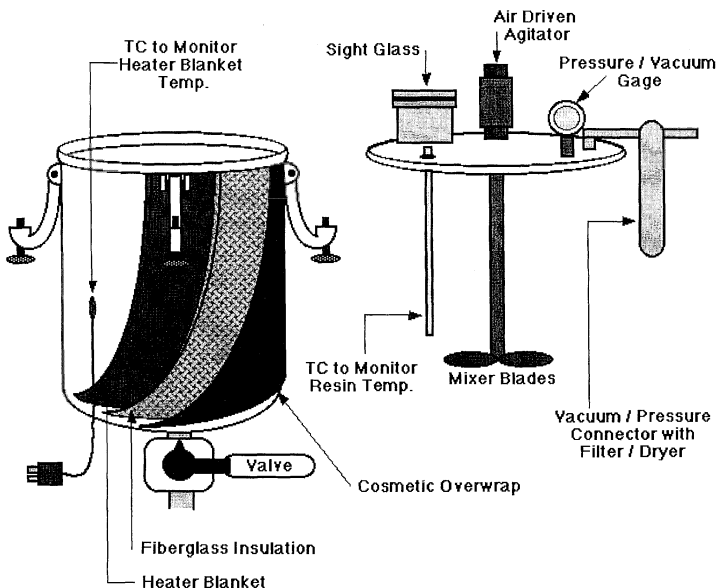


Figure 2.3 Schematic of a basic reservoir.

30 Injection equipment

Some units such as the Graco unit (shown in Figure 2.4) were designed without such a reservoir. Rather, the resin shipping container acts as the reservoir for the unit. The model shown unloads single-part (precatalysed, premixed and degassed) resin right from its one-gallon (3.8 l) shipping container. A heated plunger is inserted into the pail from the top and forms a seal with the walls. The plunger heats the resin only as it is used. Heated resin immediately beneath the plunger flows into a piston-action pump which pressurises the resin through the dispensing hose and ultimately in the tooling. Such a design affords efficiency in a very compact unit through the minimisation of resin waste and virtually no clean-up. Portable yet powerful, this elegant design provides injection pressures to 5.86 MPa (850 psi) on 0.689 MPa (100 psi) shop air. Other versions are available for larger resin shipping containers [10, 11]

Heated dispensing hose

The heated dispensing hose functions as a bridge between the resin reservoir and the tooling. It is typically a simple design. High-temperature, high-pressure PTFE teflon tubing [typically 6.4 mm (1/4") inner diameter] is used to carry the hot resin. This tubing can be reused or configured as a disposable liner (as shown in Figure 2.5) to reduce clean-up or possible contamination if multiple resin systems are used in the apparatus. The tubing lines a metallic flexible conduit similar to that

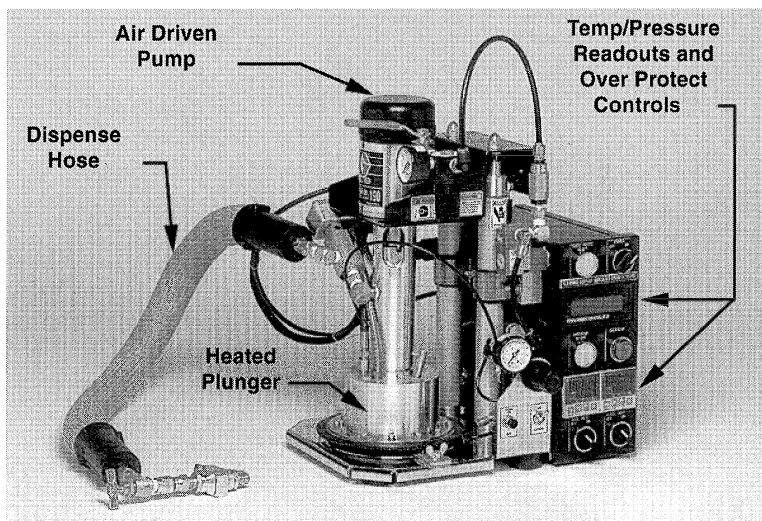


Figure 2.4 Graco one-gallon heated resin transfer moulding unit (HRTMU). Reproduced courtesy of Graco.

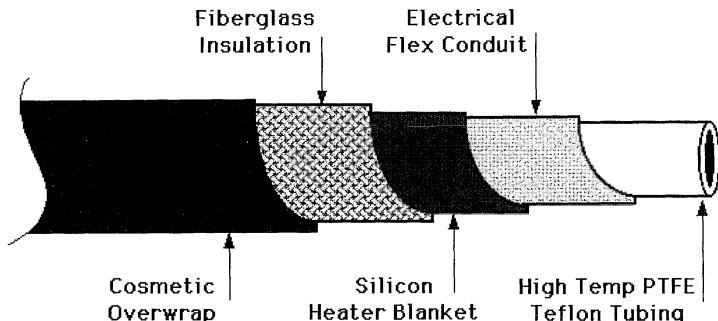


Figure 2.5 Schematic of heated dispensing hose.

used by electricians. Next, a long silicon strip heater blanket is helically wrapped about the flex conduit and secured with high-temperature silicon RTV sealant or fibreglass tape. Thermocouples are sandwiched between the strip heater and the conduit as part of the monitor/controller feedback loop and any quality control data acquisition systems. The hose is then wrapped with several layers of insulation, again coarse weave fibreglass boat cloth or similar thin flexible insulation. Finally, a cosmetic overwrap is applied such as a tight weave nylon braid or shrink tubing to prevent fraying and damage to the insulation and subsequent layers. For low-pressure injections and to facilitate the disposable liner approach to the dispense hose, barbed nipples and hose clamps may be used. It is always crucial to know the processing limits of the equipment used, especially the tubing. Engineered burst pressure and temperature limits must never be exceeded.

Manufactured injection equipment generally rely on hard plumbing connections where possible, offering the greatest degree of safety and reliability. These configurations involve the use of copper tubing instead of PTFE tubing. The copper tubing is quite inexpensive and offers excellent burst strength and a high thermal conductivity (making heating a simple matter with strip heaters or even a heat gun). However, because the tubing is rigid, it must be custom bent to the configuration of the RTM set-up and plumbed using fittings and valves. Such a system is best incorporated into fixed RTM set-ups where flexibility is not a necessity. This system requires careful cleaning and/or replacement of the tubing and subsequent fittings and valves.

Resin feed systems

Resin feed system refers to the method by which the heated resin flows through the dispense hose into the tooling. Such methods may utilise piston-driven pumps, reciprocating piston pumps, rotary pumps, or

32 Injection equipment

simply vacuum or pressure differentials generated by connections to shop lines. A heated pressure pot in a configuration similar to that shown in Figure 2.3 exemplifies the use of the pressure differential method where atmospheric pressure is increased in the reservoir. The vacuum infusion technique is identical in principle; however, the pressure is instead reduced below atmospheric pressure in the tooling. In either case, it is a pressure differential driving the resin flow [12–14]. The other systems rely on an integrated pumping system which provides the advantages of high pressure (greater than shop air) and/or constant flow rate but require heating and present the difficult issues of proper sealing, security from contamination and the need to clean. Resin feed systems can be broken down into two categories: constant pressure and constant flow rates. These will be discussed further in section 2.3.3.

2.3.2 ADDITIONAL FEATURES AND VARIATIONS

Mix/Meter

Manufacturers such as Ashby Cross, Liquid Control and Venus-Gusmer offer a wide variety of mix/meter apparatuses. Such units actually mix the resin components automatically to a ratio set by the user. These companies boast accurate mix ratios and broad mix ratio ranges to meet a variety of applications. These units, listed in Table 2.1, are differentiated by varying capabilities in resin capacity, resin flow rates, resin viscosity, filled resin and output pressure capabilities. Multiple reservoirs store the resin components separately. Although most units are configured in a twin reservoir arrangement, companies such as Liquid Control offer an optional third tank for pigments, additives or other components [1]. In the mix/meter system the resin is mixed just prior to entry into the

Table 2.1 Selected meter/mix machines from various manufacturers

Manufacturer and Model	Ratio Capability	Accuracy
Ashby Cross:		
2500 Series	1:1 to 25:1	±1.0
1125 Series	1:1 to 10:1	±1.0
Liquid Control:		
Posiratio	1:1 to 30:1	±0.1–0.5
MultiFlo-CVR	1:1 to 148:1	±0.7
MultiFlo-41:1 to 148:1		±0.7
MultiFlo-61:1 to 200:1		±0.5
TwinFlo CVR 1:1 to 500:1		±0.1–0.5
Venus Gusmer		
EPO-1, EPO-2, EPO-3	1:1 to 8:1	±0.1

mould, thus reducing the amount of clean-up. The actual metering occurs at the pump where the piston stroke for reservoir B is set at a fraction of the piston stroke on reservoir A (Figure 2.6). This is accomplished by a boom arm which connects and drives power to piston B. As a unit volume of resin is pumped through a full stroke, the catalyst at a fraction of the resin volume is simultaneously pumped [1,8].

Mixing of the resin is accomplished via a static mixer. There are no moving parts. Helical intertwined elements within a mix-tube force separate resin and catalyst streams to intersect and mix as seen in Figure 2.7. These mixers are offered both in reusable and in disposable forms [1,8,15].

Mix/meter systems are best suited when multipart resin systems are utilised in a production-line format, where there is a large resin throughput and a limited number of resins used. The reservoirs allow limited storage of the resin as no mixing takes place. Mixing occurs for only the required amount of resin, therefore waste is greatly reduced. If a variety of resin systems are used, or production quantities are low, a premix system may be a simpler and more cost-effective option. This has been the case particularly in the aerospace industry where production volumes are traditionally low (as compared with the automotive and sporting goods industries) and one-component resin systems are often preferred. The cleaning and purging of previous resins from the components becomes easier and may be virtually eliminated by using disposable liners. The costs saved on the premix unit and cleaning operations may easily offset reductions in waste. This is especially attractive and applicable in the areas of prototyping, characterisation and research and development [3].

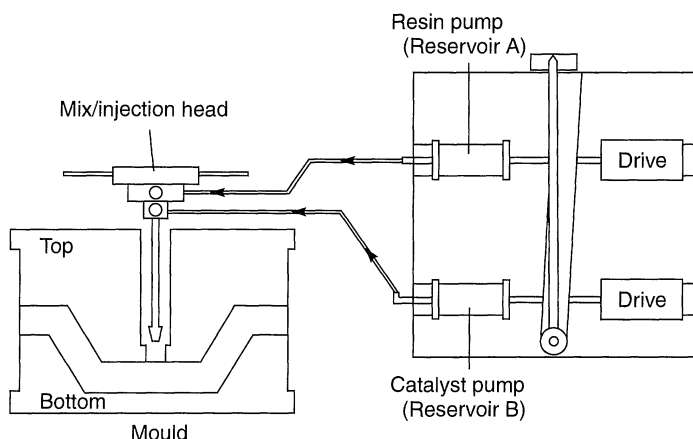


Figure 2.6 Schematic of Liquid Control metering system.

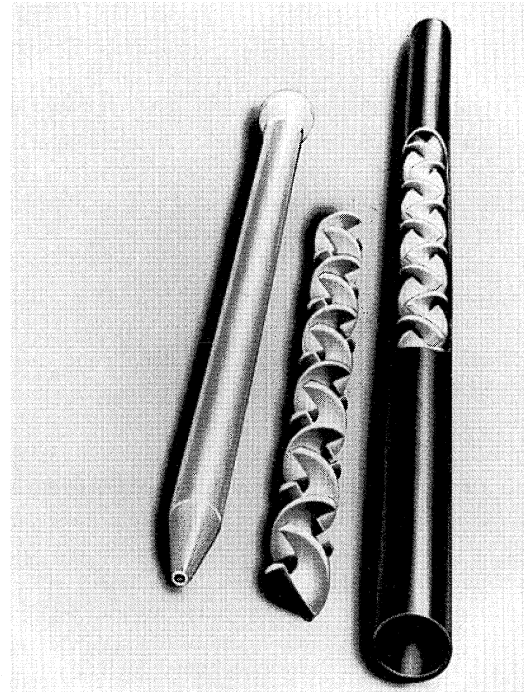


Figure 2.7 Typical static mixers. Reproduced courtesy of Liquid Control Corporation.

Data acquisition systems

All units are designed with on-board pressure and temperature read-outs which split from the feedback loops to the controllers as can be seen on one of the products from Radius Engineering (Figure 2.8). Pressure transducers at the pump exit usually measure output pressure. J-type thermocouples are generally used to monitor resin-reservoir and dispensing-hose temperatures, whereas pump and mix-head temperature measurement is optional. These systems also offer temperature and pressure 'overprotects' which automatically shut the unit down when the user-defined upper processing limit is exceeded. The read-outs usually provide an output to a chart recorder, computer or other data storage device, allowing for a permanent record of the part manufacture for quality control purposes. If the unit does not offer such outputs it is usually a simple matter to incorporate them.

Additional monitoring may be incorporated into the unit such as resin supply levels, resin flow rates, pump cycles and volume injected or piston displacement information. Further data can be accumulated through the integration of computer software and the injection system, as

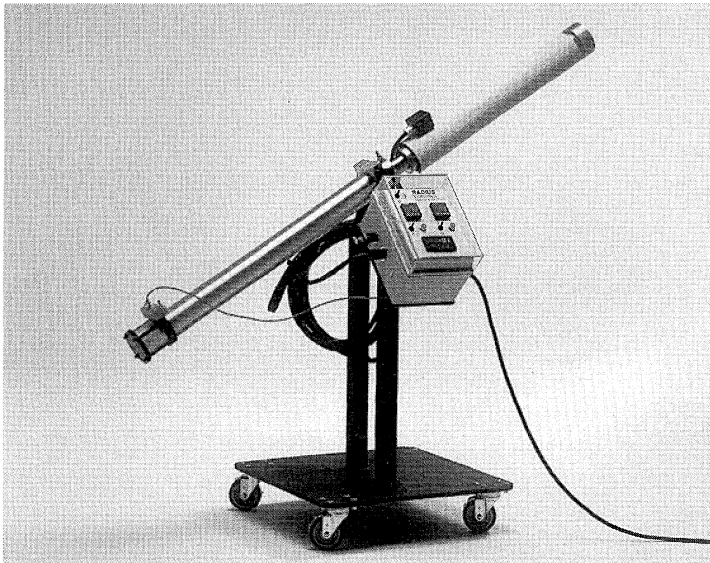


Figure 2.8 Radius Engineering RTM 2100 cc system. Reproduced courtesy of Radius Engineering.

shown in Figure 2.9. These software systems are offered by several manufacturers such as Radius Engineering's FloWare® and Venus-Gusmer's computer-controlled process monitor which can be tied into the entire RTM set-up offering control and measurement data to enhance process control [2, 8]. Currently, information such as viscosity (pot-life alarm), flow-front position in the mould, degree of resin advancement and peak exotherm can be determined through the use of dielectric sensors imbedded within the apparatus and tooling [2, 8, 9, 16, 17].

Ultimately, computer control of the injector, press and even robotic motion tables translating tooling and dispense heads can be incorporated into a totally automated system. Such robotic motion tables are offered by Liquid Control Corp. For one particular case study Radius designed an automated system utilising their FloWare® on a 486/33 MHz personal computer and a shuttle press for Boeing Commercial Airplane group. Data acquisition includes:

1. actual volumetric flow rate;
2. initial resin volume;
3. injected volume;
4. percentage completion;
5. elapsed time;
6. injection pressure;
7. cylinder temperature;



Figure 2.9 Radius Engineering RTM 5000 interfaced with FloWare®.

8. line temperature;
9. pressure data measured at one user-defined point;
10. temperature data measured at four user-defined points;
11. definition by user of parameters and limits;
12. data file archiving.

2.3.3 CONSTANT PRESSURE VERSUS CONSTANT FLOW RATE

Two primary philosophies prevail in the design of injection equipment: the use of constant pressure or constant flow rate. When constant fluid pressure is in effect, flow rates vary during impregnation owing to resistance generated by the preform. It will be shown that under constant pressure conditions the flow rate will decrease with increasing distance from the flow source. Conversely, when there is a constant flow rate, the fluid pressure varies as a function of the preform's permeability. The preform's permeability, the resin viscosity, the distance traversed by the resin and the flow speed determine the fluid back pressure seen at the pump. If the permeability is constant (assuming only minor regional fluctuations) the back pressure will increase with distance traversed by the resin. This relationship can be visualised mathematically and described by Darcy's law for flow through a semi-permeable membrane [for simplicity, the one-dimensional case is shown in equation (2.1)]:

$$v = -\frac{1}{\mu\epsilon} \kappa \Delta P \quad (2.1)$$

where

- v is the fluid velocity incorporating distance and time;
- κ is the preform permeability;
- ΔP is the fluid pressure change;
- μ is the resin viscosity;
- ϵ is the preform porosity.

Equation (2.1) more accurately models the RTM process when considering flow in two directions, requiring consideration of κ and ΔP in both the x and the y directions [16–20]. This will be discussed further in Chapter 8. It is this interdependence which motivates injection equipment manufacturers when designing their resin feed systems.

Constant flow rate

Constant flow rate machines allow the user consistent, repeatable injection times important for production-line manufacturing. These systems are usually driven by reciprocating piston pumps which provide a quasi-constant flow rate. The term ‘quasi’ is applied because the flow is briefly interrupted during the piston upstroke, or fill stroke. With each down-stroke the piston discharges a set volume of resin. Therefore flow rate is defined by the pump cycle rate. Many of the products by Liquid Control (Figure 2.10), Graco, and Venus-Gusmer fall into this category. Their advantages include constant flow-rate control, higher injection pressure capabilities and the ability to connect to larger resin reservoirs or even shipping containers as is the case with the Graco unit (Figure 2.4) and the Venus-Gusmer Hydrajector series [2,8]. The Hydrajector series allows the manufacture of very large parts without the need for injection interruptions to refill the reservoir.

The disadvantage of such a system results with increasing back pressure as the resin flow progresses through the preform. If the fluid pressure is too high the preform fibres may be ‘washed’ or displaced out of orientation. Further, the fibres must be given adequate time to be wetted by the resin. If the resin fills the preform but fails to wick into the bundles (capillary action) and wet the individual filaments intrabundle porosity will result. The flow front, moving too swiftly, will pass over the bundle, allowing insufficient time for bundle infiltration, and thus lead to the entrapment of voids [12–14]. Overpressurisation may also result in tooling deflection and even leakage and/or bursting of the equipment. Careful planning, control and supervision of the injection is required to prevent these occurrences.

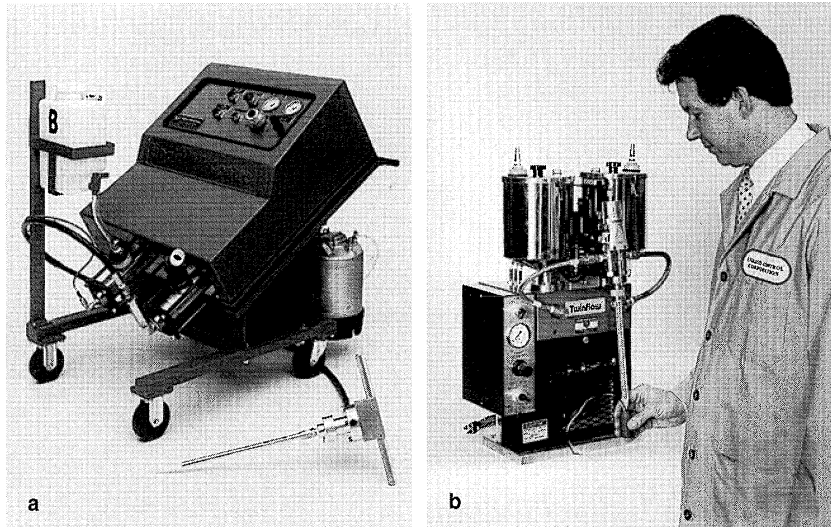


Figure 2.10 (a) Liquid Control MultiFlow-6; (b) Liquid Control TwinFlow mini. Reproduced courtesy of Liquid Control Corporation.

Constant pressure

A heated pressure pot is an example of a constant-pressure machine. The shop air will exert a constant pressure on the resin but the result will be variation in the flow rate. For example, if the pot is pressurised and the flow valve opened, the resin will flow through the hose at a high rate to the mould entrance. At the mould entrance the resin will encounter the preform and a significant resistance to the flow will result [16, 17]. There will be a subsequent drop in resin flow. The advantage of such a system is the complete control over system injection pressure. The disadvantages include limited control over the flow rate during injection. Also, in a pressure-pot system, pressurisation is limited by the available shop air pressure [generally about 700 kPa (100 psi)]. The resin must be held in a pressurisable reservoir making a large-volume capability bulky and expensive. In addition, this limitation may prevent the use of high-viscosity filled resin systems. Some of these problems have been alleviated through innovative design features such as quick refill access and higher pressure capability, found in the Radius Engineering products and the Ram by Venus-Gusmer.

Somewhere in-between

The fact is that a combination of both control types are needed to allow the manufacture of a high-quality part under a production-rate format.

All the manufacturers listed offer a combination of both by providing controls and feedback loops which allow for a compromise: adjustment of flow rate to within user-specified pressure limits or adjustment of pressure to within user-specified flow rate limits. This is accomplished through set-points, overprotects, cycle counters, etc., which add safety, security and reliability to the RTM set-up. Innovative designs in pumps such as the rotary valve system developed by Ashby Cross provide true constant flow rate or pressure by providing resin flow on both the up-stroke and the downstroke of the reciprocating piston pump. Again, the requirements must be identified for the application and be applied by the user. The versatility of all these machines make each option viable; however, one machine will probably work more efficiently than another for a given application.

2.4 CONCLUSIONS

Injection equipment represents one of the three primary components of a successful RTM set-up. As such it is an important investment and choice of such equipment demands a thoughtful decision process. The information provided is intended as a background for the selection process and to educate the consumer before speaking to a distributor or manufacturer. It is not meant to replace their assistance but rather to promote it. It is essential to utilise their knowledge when purchasing equipment. These manufacturers and others have developed a wide experience base. Their job is to understand the process, the intended application, and the budget and then ascertain which equipment (if any) they carry is suited to the task at hand. The selection process will require a thorough understanding of the application requirements, including: types and variety of materials being processed, the size of the part, the size of the production run, the production rate, data acquisition features for quality control records and, of course, price. With this list in mind and the fundamental principles and features of injection equipment presented in this chapter, the reader should be well-equipped to make an effective selection.

References

1. Jacobs, K.A. (1989) Primary processing equipment for resin transfer molding. *Fabrication News*, (September), 3–17.
2. Radius Engineering Inc. (1996) *Products and Services for Resin Transfer Molding*, Radius Engineering Inc., Salt Lake City, UT.
3. Milovich, D. and Nelson, R. (1990) Aerospace resin transfer molding: a multidisciplinary approach. SME technical paper presented at Resin Transfer Molding for the Aerospace Industry, Manhattan Beach, CA, March.
4. Liquid Control Corp. (1996) *Innovative Dispensing Solutions*, Liquid Control Corp., North Canton, OH, USA.
5. Larsen, M. (1996) *Resin Transfer Molding*, Liquid Control Corp., North Canton, OH, USA.
6. Smoluk, G.R. (1986) New appeal in resin transfer. *Modern Plastics* (July).
7. Galli, E. (1982) Resin-transfer molding: a cost effective alternative. *Plastics Design Forum* (March/April), 47–57.
8. Venus-Gusmer (1993) *Catalog, Volume 1: Sprayup, Resin Injection, Cast and Pour*, 7th edn, Venus-Gusmer, Kent, WA, USA.
9. Kranbuel, D., Kingsley, P. and Hart, S. (1992) Sensor-model prediction, monitoring and in-situ control of liquid RTM advanced fiber architecture composite processing. *37th International SAMPE Symposium*, March, Society for the Advancement of Materials and Process Engineering, 1161 Parkview Drive, Covina, CA 91724-3748, pp. 907–11.
10. Graco Inc. (1992) *1 Gallon Heated RTM Resin Supply System*, form 304-887 rev. 3/92 098, Graco Inc., Minneapolis, MN, USA.
11. Graco Inc. (1992) *5 Gallon Heated RTM Resin Supply System*, form 304-888 rev. 8/92 098, Graco Inc., Minneapolis, MN, USA.
12. Michaeli, W. and Dyckhoff, J. (1994) Production of fibre reinforced components with high surface quality using a modified RTM technique. *39th International SAMPE Symposium*, April, Society for the Advancement of Materials and Process Engineering, 1161 Parkview Drive, Covina, CA 91724-3748, pp. 144–53.
13. Hamada, H., Ikegawa, N., and Maekawa, Z. (1994) Void flow behavior in structural resin transfer molding with twin injection system. *39th International SAMPE Symposium*, April, Society for the Advancement of Materials and

- Process Engineering, 1161 Parkview Drive, Covina, CA 91724-3748, pp. 120-32.
14. Lundström, T.S. (1994) Void formation and transport in the RTM process. *39th International SAMPE Symposium*, April, Society for the Advancement of Materials and Process Engineering, 1161 Parkview Drive, Covina, CA 91724-3748, pp. 108-15.
 15. Ashby Cross Company Inc. (1996) *Meter Mix and Dispense Equipment*, Ashby Cross Company Inc., Topsfield, MA, USA.
 16. Aoyagi, H. (1992) *Filling Process Simulation in the Mold for RTM and SRIM*, CCM Report 92-26, University of Delaware, Newark, DE, USA.
 17. Chan, A.W. and Huang, S. (1991) Modeling of the impregnation process during resin transfer molding. *Journal of Polymer Engineering and Science*, **31** (15), 1149-56.
 18. Gutowski, T.G., Wineman, S.J. and Cai, Z. (1986) Applications of the resin flow/fiber deformation model. *31st International SAMPE Symposium*, April, Society for the Advancement of Materials and Process Engineering, 1161 Parkview Drive, Covina, CA 91724-3748, pp. 245-54.
 19. Gauvin, R., Chibani, M. and Lafontaine, P. (1986) The modeling of pressure distribution in resin transfer molding. *41st Annual Conference, Reinforced Plastics/Composites Institute, The Society of the Plastics Industry*, Society of the Plastic Industry, April, session 19-B, pp. 1-5.
 20. Coulter, J.P., Smith, B.F. and Selçuk, G.I., (1987) Experimental and numerical analysis of resin impregnation during the manufacturing of composite materials. *Proceedings of the American Society for Composites, Second Technical Conference*, American Society for Composites, September, pp. 209-17.
 21. Dave, R., Kardos, J.L., Choi, S.J. and Dudukovic, M.P. (1987) Autoclave vs. non-autoclave composite processing. *32nd International SAMPE Symposium*, April, Society for the Advancement of Materials and Process Engineering, 1161 Parkview Drive, Covina, CA 91724-3748, pp. 325-37.

MANUFACTURERS

- Ashby Cross Company, Inc., 418 Boston Street, Topsfield, MA 01983 USA. Tel.: (508) 887-2887. Fax: (508) 887-3929.
- Briskheat Corp., 1055 Gibbard Avenue, PO Box 628, Columbus, OH 43216-0628, USA. Tel.: 1-800-848-7673. Fax: (614) 294-2672.
- Graco Inc., PO Box 1441, Minneapolis, MN 55440-1441, USA. Tel.: 1-800-367-4023 (sales); 1-800-543-0339 (technical assistance).
- Liquid Control Corp., 7567 Freedom Avenue NW, PO Box 2747, North Canton, OH 44720-0747, USA. Tel.: (216) 494-1313. Fax: (216) 494-5383.
- Omega Engineering Inc., PO Box 2669, Stamford, CT 06906, USA. Tel.: 1-800-826-6342. Fax: (203) 359-7700.
- Radius Engineering Inc., 3474 South 2300 East, Salt Lake City, UT 84109, USA. Tel.: (801) 227-2624. Fax: (801) 277-7232.
- Venus-Gusmer, 1862 Ives Avenue, Kent, WA 98032, USA. Tel.: (206) 854-2660. Fax: (206) 854-1666.

3

Materials

Mac Puckett and Mitch Petervary

3.1 RESINS

The volume of structural composites used globally has grown slowly but surely through the decades of the 1970s, 1980s and into the 1990s. The growth of resin transfer moulding (RTM) as a preferred fabrication method for composites results from the versatility and economy of the process compared with the traditional materials of construction in the aerospace arena. RTM as a manufacturing method allows the use of fibre and resin in close to their most economical form. It also allows a flexibility in part geometry that is not available through prepreg fabrication.

The common feature shared by all structural composites is the manner in which reinforcing fibres are used in combination with a plastic material to carry structural loads more efficiently than can metal. The performance of composites in load-bearing applications is directly dependent on the ability of a well-designed part to provide an anisotropic pathway through the reinforcement to produce the strength and stiffness required from the part as it is loaded. The resin matrix is the essential 'glue' required to hold the fibre in place and transfer the load from fibre to fibre. Four commonly used reinforcements for structural composites are E-glass, S-glass, carbon, and aramid fibre. The ability of these strong yet lightweight fibres to carry and transfer loads is the basis of composite functionality compared with metals.

The role of the resin in the composite is also critical. The resin selection results in a set of characteristic processing parameters and performance properties (e.g. thermal, flammability, environmental resistance) for the

composite. The resin properties are also critical factors in understanding some of the mechanical performance of the composite. A well-designed composite carries the highest direct loads with the fibrous reinforcement. However, the imposition of shear or compression loads on the composite forces the resin to carry more of the stress applied to the part. A comparison of resin matrix properties with the most commonly used reinforcing fibres shows that the properties of the reinforcement are at least one order of magnitude greater than the resin (Table 3.1). Therefore, the greater the volume percentage reinforcement used in a composite the higher the load-carrying capability of the part.

As fibre volume increases, resin volume decreases. This puts an increasing performance demand on less and less resin to provide a path for load transfer from fibre to fibre. The modulus and the elongation (ductility) of the resin are critical to generating these optimum composite properties. Typically, Young's modulus values in excess of 2.76 GPa (400 ksi) and tensile strain to failure values in excess of 4% are required to provide a tough resilient composite system. An optimised RTM resin will be one that wets out the fibre surfaces and forms a strong interfacial bond that is not degraded with time and environmental exposure. This allows loads to be uniformly distributed across the composite reinforcement and forms a system that will act as a unit and not as a series of individual fibres. The role of the interface between the polymer matrix and the fibre in producing a quality composite should not be underestimated [1, 2].

3.1.1 BACKGROUND: THERMOPLASTIC AND THERMOSET MATERIALS

As a resin is chosen for use in aerospace RTM there are a series of trade-offs that must be made, not the least of which are resin cost and availability of a performance database (design allowables) for a given material. In the market from the mid-1980s to the mid-1990s there were

Table 3.1 Comparison of matrix and fibre properties

	Matrix Properties	Fibre Properties		
		Glass	Aramid	Carbon
Tensile Strength (GPa) ^a	0.04–0.08 (0.006–0.012)	3.1–4.1 (0.45–0.6)	3.4–4.1 (0.5–0.6)	3.4–4.5 (0.5–0.65)
Tensile Modulus (GPa) ^a	2.1–4.1 (0.3–0.6)	69–83 (10–12)	83–186 (12–27)	207–276 (30–40)
Tensile elongation (%)	1–8	4–5	2–4	1–2
Density (g/cm ³)	1.0–1.3	2.5	1.45	1.8

^a Values in parentheses below are in ksi.

44 Materials

many RTM materials introduced but only a relatively few remain. It is anticipated that the dynamics of the aerospace market and its suppliers has changed significantly enough that fewer materials will be introduced in the next 10 years. It is impossible to guess what these resin formulations will be. The resin choice automatically results in a set of windows that define the processability of the material and the properties obtainable. Therefore it is appropriate to explain the chemical and engineering basics that control the interrelationship of the resin and the process and then discuss a few specifics of materials available in today's market.

Thermoplastics

Resins which are used to make structural parts can be divided broadly into two classes: thermoplastics and thermosets. Thermoplastic polymers are made by reaction of small monomeric molecules to form very high molecular weight molecules. These solid resins have very little or no cross-linking of the polymeric chains. The thermal and mechanical performance of these materials is a result of the nature of the backbone molecules, the degree of branching and the entanglement of these long strands of molecules. The resin sold to someone fabricating with a thermoplastic is a solid, high molecular weight polymer, not a monomer. Therefore, the polymeric molecular weight, branching, processability, glass transition temperature (T_g) and melt flow properties are controlled by the plastic producer not the composite fabricator.

Thermoplastics are typically moulded by applying heat until the solid plastic material becomes liquid and it is then injected into a mould, drawn into a fibre and extruded as a bar or sheet or is formed in a similar fashion as it cools and resolidifies. No chemical reactions have occurred during the fabrication process of melting and moulding thermoplastics; therefore the molecules that go into the process are in theory identical to the molecules that come out. The change that has occurred is a phase (state) change, much like heating ice until it becomes water and then cooling to once again form ice. Some thermoplastics are shaped by dissolving them in a solvent and then removing the solvent. This solvent-forming process, like the thermal process, does not change the molecular structure. Therefore, the thermoplastic materials at least in theory can be moulded and remoulded time and again [3].

Many of the engineering thermoplastics are high-elongation, impact-resistant systems that show real potential for use as a matrix for aerospace composites. Even though in many ways these materials appear as ideal candidates to produce durable aerospace composites, the current state of technology makes it impractical or impossible to achieve a viscosity (because of the high polymeric molecular weight) that would allow this type of material to be used in RTM applications. Owing to the

excellent properties available this class of material finds continued use in aerospace composites, formed by processes other than RTM. Research is ongoing in several laboratories to develop high-performance engineering thermoplastic materials that can be generated *in situ* during a fabrication process [4, 5].

Thermosets

Thermoset resins are the materials used in RTM, and the primary reason for this is their processability. Thermoset resins are almost always liquid or semi-solid at room temperature and conceptually are more like the monomers from which thermoplastics are made than the finished thermoplastic resin. Thermosets can be formed or moulded into a variety of shapes before they are 'set'. However, once these materials are set by use of catalysts and/or heat they cannot change form again. This is because the thermosetting process involves the formation of chemical bonds that convert the relatively small molecules of the resin into a rigid high molecular weight three-dimensional cross-linked polymeric structure.

Composite fabricators must realise that selection of a reactive thermoset resin for use in their RTM process will force them to deal with a large number of chemical engineering choices. In the RTM process there is a strong interrelationship between the resin chemistry selected and the engineering of the process [6, 7]. Process parameters such as moulding time, temperature and pressure cannot be selected without considering the resin chemistry to be used. Alternatively, selection of a resin for use in RTM based on its properties, without considering how it will process, is impractical. The factors to consider when choosing a resin system for use in RTM can be broken down into two broad categories: processing and performance. Process parameters to consider in selecting a resin and curing agent formulation for RTM are:

1. initial viscosity;
2. moulding life (pot-life).

Both of these parameters are a direct function of temperature. Once the operational temperature for a process has been chosen, this will determine the initial viscosity of the selected resin system. The temperature selected also governs the time available for moulding (moulding life). The moulding time is dependent on the rate at which the reaction between the resin and curing agent occurs, and this rate is directly proportional to temperature.

The organic polymer of the matrix to a large extent will determine how the composite will perform following moisture absorption, either in cold or in hot conditions, under impact or fatigue loads, or with a high sustained load, or some combination of these. Before producing composites

46 Materials

and running a full battery of tests the best indicators of polymer performance properties when selecting a resin and curing agent combination include:

1. tensile (Young's) modulus;
2. glass transition temperature (T_g);
3. moisture absorbance;
4. toughness (tensile elongation).

Other performance properties are often used as the basis for selecting one resin rather than another (e.g. flammability and solvent resistance).

The composites fabricated from an RTM process, like any other composites, must operate in a real-world environment which typically involves use at elevated temperatures, exposure to high humidity, often under constant load or while being fatigued. Therefore, the thermal and mechanical performance characteristic of the selected resin must be evaluated. Load-bearing structural aerospace applications are compression critical and require a stiff polymer adequately to support the fibre reinforcement and prevent premature buckling during compression. A Young's modulus of 2.76 GPa (400 ksi) or greater is needed for these applications.

The maximum use temperature of a polymer is governed by its glass transition temperature and the amount of moisture absorbed. Absorbed moisture plasticises the polymeric matrix which then lowers the glass transition temperature and the modulus [8, 9]. The less moisture absorbed the less detrimental the observed effect. Depending upon the amount of moisture absorbed by a polymer, the dry T_g should be generally at least 28°C (50°F) higher than the use temperature, preferably 56°C (100°F).

The thermoset resin selection (phenolic compared with epoxy compared with bismaleimide, etc.) will determine the thermal, mechanical and environmental resistance of the cross-linked polymer that results. A typical thermoset resin used in RTM fabrication is formulated with a primary resin (e.g. epoxy), a curing agent and catalyst package. The selection of this resin formulation and the temperature of the reaction sets the kinetics (cure rate), the chemorheology (temperature-dependent change in viscosity with time), and the thermodynamics (heat release) of the ensuing chemical reactions. The selection of a reinforcement type and complexity, along with the size and shape of the part (mould), and the fabrication process parameters chosen (tool type, temperature, resin injection pressure, inlet-outlet distribution, etc.) determines the rates of heat and mass transfer experienced during the moulding process.

Partially because of the complexity experienced in processing RTM materials, there has been an increasing demand for one-part resin systems in RTM applications, particularly for fabrication of aerospace

composites [10]. The customer's requirement for a simple resin formulation is one reason for this trend, but the primary driver is an issue of quality. Purchase of a one-part liquid moulding resin by the fabricator reduces their quality concerns by removing the requirements for purchasing, for metering and mixing and for tracking multiple resin components through the entire part-production process. There is a great deal of perceived and real value provided to the fabricator that can purchase a one-part resin that comes with a specification sheet, a suggested process profile and thermal and mechanical performance characteristics that are well characterised.

3.1.2 ENGINEERING THE RESIN TRANSFER MOULDING PROCESS: THE INTERACTION OF CHEMISTRY AND PHYSICS IN A REACTIVE PROCESS

It is important to understand the fundamentals of chemistry and physics that affect the engineering decisions made in the RTM process. A discussion of material properties and their associated processing characteristics will be emphasised in this section.

For the thermoset resins used in RTM, the reactive process by which bonds are formed, molecular weight increases and the resin is finally gelled and cross-linked to form a final polymer is similar for all materials. To understand thermoset resin processing the concepts of gelation and curing and of how the increase in molecular weight leads up to and through these stages is important. Figure 3.1 shows the thermosetting process as a function of viscosity increase versus time. Curve T-1 shows the isothermal viscosity of a resin system at a temperature where it is non-reactive. This is usually accomplished by using a catalyst or curing agent that is either non-reactive and/or non-soluble at temperatures below some given heat activation temperature. This is the basis for many one-component (one-part) resin systems. Curve T-2 shows the viscosity profile of the same resin system at a slightly higher temperature. At this higher temperature the resin has a lower initial viscosity, the reaction rate is increased, and the time required for the resin and curative to build molecular weight (and viscosity) is reduced. Curve T-3 shows the lowest initial viscosity and the most rapid increase in resin viscosity because it is the highest temperature system of the three [11].

A rule of thumb from kinetics suggests that for each 10°C increase in temperature the rate of reaction doubles [12]. This approximation can be useful for estimation of the rise in viscosity to a specified point in a reactive resin system. (Example: If a given resin with a viscosity of 200 cps at 100°C requires 50 min to increase in viscosity to 1000 cps, then the same resin system at 110°C will have an initial viscosity less than 200 cps and will require about 25 min to reach a viscosity of 1000 cps.)

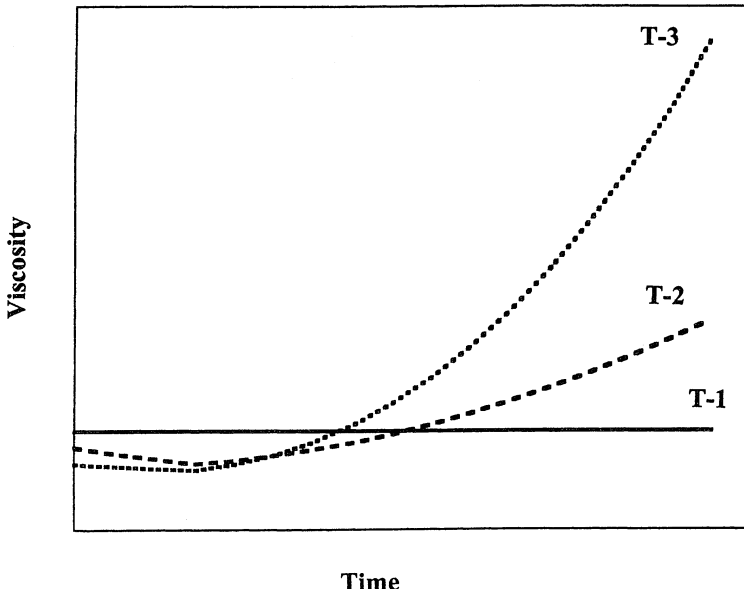


Figure 3.1 Resin viscosity change as a function of an isothermal hold. Temperature increases from T-1 to T-3; — = T-1; - - - = T-2; · · · = T-3.

As a material is processed by RTM the fabricator must choose a moulding temperature. The selection of this parameter not only sets the initial viscosity of the resin but also sets the rate at which it cures and therefore the rate at which it increases in viscosity.

The importance of viscosity to the time required for wetting a composite preform (which is equivalent to fluid flow through a fixed bed) can be described by Darcy's Law [13–18]:

$$\text{flow rate} = \frac{\text{permeability} \times \text{cross-sectional area}}{\text{resin viscosity}} \times \frac{\text{pressure drop}}{\text{unit length}} \quad (3.1)$$

The rate at which a resin will flow through a fibrous preform (typically 55%–60% by volume) in an RTM mould is inversely proportional to the viscosity of the resin. Empirical evidence suggests that viscosities above 500 cps are very difficult to handle; there are some reports of resins with viscosities approaching 1000 cps being moulded at 100 psi. Attempts to push resin systems with viscosities greater than 500 cps through high fibre volume fraction preforms leads to mould pressures which cannot be easily handled and produces dry and voidy composites caused by poor fibre wet-out. To obtain good impregnation of the reinforcement and reasonable production rates a resin viscosity of 100–200 cps is an ideal

range for moulding high fibre volume fraction complex preforms. Beyond the inherent viscosity of a resin formulation the only practical way to adjust viscosity of a material is to adjust the mould temperature. The choice of moulding temperature not only sets the initial resin viscosity (and therefore flow rate through the mould) but, as described previously, the rate at which the viscosity increases per unit time.

The moulding life of a resin is defined here as the time required at a given temperature for the resin system's viscosity to reach a viscosity too high to continue flowing through the preform (approximately 500 cps for most systems). Depending on the size and complexity of a preform, anywhere from 60 s to 60 min can be required to complete resin impregnation of the part. Analysis of resin suitability for RTM application must include viscosity profiles of a resin under isothermal conditions to insure that sufficient moulding life is available (total time below 500 cps) to wet out the preform. Selection and precise control of a moulding temperature can be crucial in fabricating a quality part, as the dynamics of balancing the chemistry of reaction rates and the physics of fluid flow must be simultaneously achieved. Figure 3.2 shows the boundary conditions for these parameters [2,7].

As reaction occurs in a thermosetting resin, the monomeric starting materials are reacting with one another to form larger and larger molecules which eventually cross-link to form very high molecular weight polymers that possess a three-dimensional network. The point in the

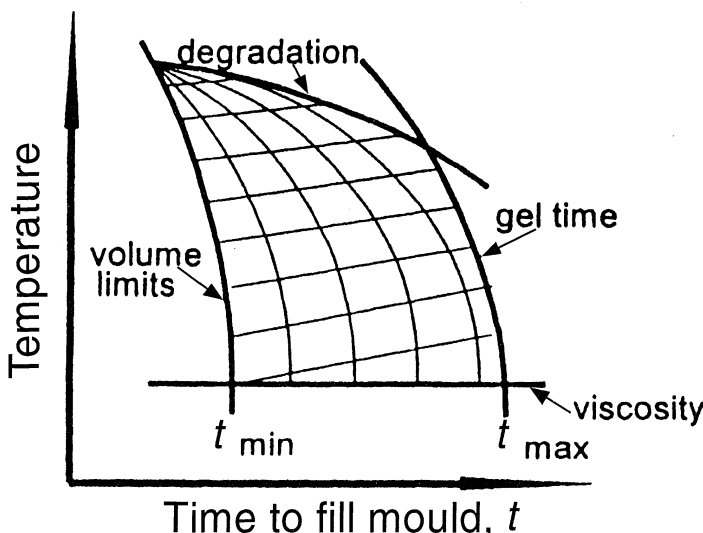


Figure 3.2 The effects of temperature and time on mould filling. Reproduced courtesy of Professor L. T. Drzał.

50 Materials

reaction process at which conversion from liquid to solid becomes irreversible is known as the gelation, or gel, point. For a given class of thermoset resins (epoxy, cyanate, bismaleimide, etc.) the gelation point occurs at approximately the same percentage conversion of monomer. For polyesters and vinyl esters a conversion of 5%–10% of the initial monomeric materials in the resin leads to gelation. In an epoxy, bismaleimide or phenolic, a conversion of approximately 50%–60% of the initial monomeric materials into high molecular weight species is required to gel. At higher temperatures, even though initial viscosity decreases, the reaction rate increases and the time required to convert a given percentage of low molecular weight species (monomers) to higher molecular weight polymers is shortened. The total percentage conversion to reach gelation is relatively unchanged for a class of thermoset materials, usually regardless of route or rate of conversion. The choice of resin type therefore sets the gelation point for a material and sets practical limits on the times and temperatures which must be used to convert the material in the moulding process.

Once a resin system has been injected into a preform the process continues with cure of the polymer to obtain the final part. The rate at which a polymer cross-links and builds a glass transition temperature (T_g) at a given temperature determines the curing time necessary to mould a part. When sufficient ‘green strength’ has developed, a part can be demoulded. As a thermoset material is cured, the glass transition temperature of the forming polymer increases. Measurement of T_g is not a direct measure of cross-link density but a correlation can be made. Figure 3.3 shows the increase in T_g versus time that occurs with a thermoset resin at three different isothermal cure temperatures ($T_3 > T_2 > T_1$). The glass transition temperature achieved for a thermoset resin is strongly correlated to the highest temperature used in the cure or postcure cycle [19, 20]. Any given polymer formed in a thermoset reaction has an ultimate glass transition temperature that can be achieved. Heat treatment at temperatures above this ultimate T_g will not increase the polymer T_g . Obviously, the higher the isothermal cure temperature used in moulding a part the faster the reaction occurs and the more rapidly the ultimate polymer T_g is approached and hence the faster a part can be demoulded. This faster cure cycle can lead to some unexpected consequences, as described below. A free-standing post-cure of the composite is a typical part of most fabrication cycles. The post-cure step serves the dual function of allowing a part to complete its cure of resin (if any residual cure remains) and relieving moulding stresses in the part.

When thermoset resins cure, heat is released. This heat is generated by bond formation (i.e. the increase in polymeric molecular weight and cross-linking). The more bonds that are formed per unit time and per unit volume the more energy is released. The energy content found in

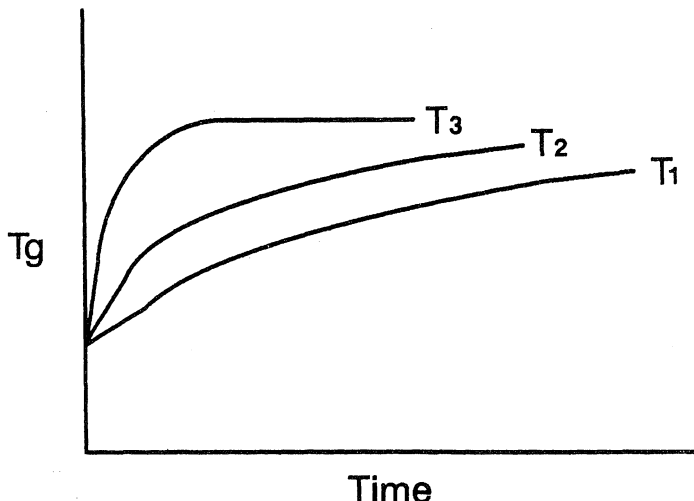


Figure 3.3 Polymeric T_g build as a function of an isothermal hold. T_g = glass transition temperature; T = temperature, where $T_3 > T_2 > T_1$.

most classes of thermosets is sufficient to produce large temperature increases during polymerisation. Reaction energies of greater than 300 J/g are common in most thermoset materials. The heat transfer coefficients for resins and the polymers that they produce are quite low. Therefore, the heat produced during polymerisation, especially in thick sections, cannot be transferred out of the part as fast as it is generated. This increasing heat leads to reactions (bond formation) occurring at faster rates, which generates more heat. This form of self-accelerating reaction will produce an adiabatic exotherm (runaway reaction) which usually leads to stress cracking or part degradation. (Quantities of resin as small as 200 g, when heated in a container, can produce surprisingly large exotherms. This type of uncontrolled reaction should be avoided and care should be taken in handling the leftover resin that was used for injection into the part or that was collected after exiting the mould.) Heat loss to the environment in thin sections moderates the temperature rise and in many cases can even lead to undercured parts which require application of additional heat to finish the cross-linking reactions.

Volumetric shrinkage in thermosets is dependent on the type of resin chemistry used and upon the degree of conversion (percentage of cross-linking sites available that are actually reacted). Shrinkage cannot be controlled by a change in resin composition without also affecting the reactivity and the thermal and mechanical properties of the resultant material. An idealised curve showing density variations for a thermoset resin as it reacts and converts from starting monomers to final cured

polymer is shown in Figure 3.4. Even though the exact profile will change from resin to resin, these types of transitions will occur for every thermoset resin as it cures. As the reaction begins (segment A–B), heat applied or generated internally causes a reduction in system density. As the system gels (segment B–C–D) it rapidly increases in density until it reaches a maximum at full cure. As the fully cross-linked polymer cools (segment D–E–F) its density continues to increase. When the cooling of the polymer passes through the glass transition temperature (point E), there is a large decrease in the rate of change in density per degree. Segments D through F

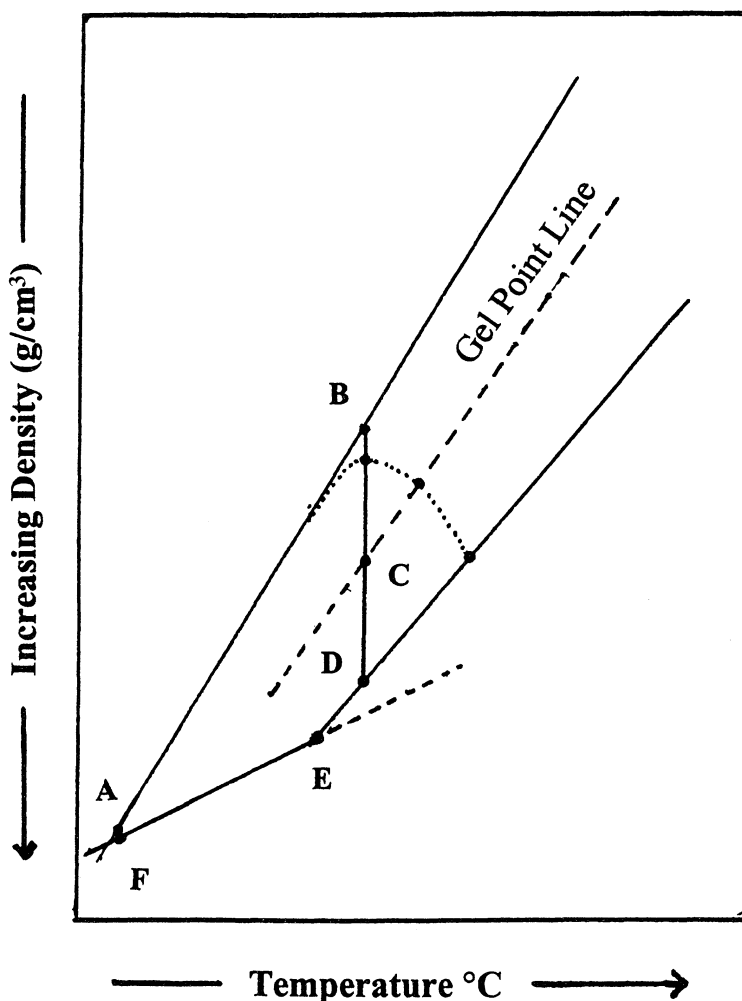


Figure 3.4 Density changes during the cure of a thermoset resin.

of this cycle are analogous to the volume changes plotted in a thermal mechanical analysis (TMA) of a polymer. One implication that can be drawn from Figure 3.4 is that for any given resin cure shrinkage can be minimised by reducing the temperature at which gelation occurs.

Each resin formulation (e.g. epoxy A, epoxy B, BMI C, phenolic D) has an inherent shrinkage on full cure. The gel line in Figure 3.4 is determined by the nature of the polymer; that is, the resin formulation chosen determines the conversion point at which gelation occurs and the temperature at which it becomes practical to mould the part. As seen in Figure 3.4, this shrinkage occurs primarily during the gelation phase of the reaction. Density change (shrinkage) that occurs in the liquid phase cannot produce internal stresses. Shrinkage that occurs when the resin is in the gelled (solid) state inevitably leads to production of internal stresses. Therefore, the process temperature and the nature of the resin (i.e. the percentage conversion and amount of shrinkage experienced at gelation, and the strength of the gel and the gel-fibre interface on formation) will determine the stress state of the composite on cure completion. The process temperature also sets the amount of expansion that the reinforcement has experienced as the resin gels and forms an interface with the fibre. The difference in coefficients of thermal expansion between polymer and fibre during the cool-down can lead to additional stresses being set in the part. Reduction of the moulding temperature to adjust cure shrinkage and other thermal stresses set in the composite will, of course, slow the rate of reaction and increase the initial viscosity of the system (i.e. slower mould-fill rates and slower cure rates).

3.1.3 TOUGH COMPOSITES: TOUGH RESINS AND COMPOSITE ARCHITECTURE

Polymeric and composite toughness is a topic that receives a great deal of investigation and debate. There are numerous methods by which toughness can be evaluated including, mode I and II opening energies, microcrack resistance, retention of compression strength after impact, fatigue crack propagation and others. Material toughness is an important issue because it can be critical to the performance of these systems. In this section a very simplistic approach to evaluating polymer toughness will be used. The tensile elongation is a common measure of polymeric toughness because it gives an indication of the ductility of the material. If some amount of damage tolerance is expected, the elongation should be at least 3%–5%. If the polymer strain does not at least match the theoretical strain of the fibre there is no way it will be able to transfer the load from fibre to fibre because it will crack and fail before the reinforcement.

One of the most challenging sets of requirements for an aerospace RTM resin formulation is the production of a tough, high T_g , polymer.

54 Materials

Toughening of thermoset resins is normally done with the addition of rubber or thermoplastic. The addition of toughening agents to a brittle (glassy) thermoset matrix immediately begins the cycle of trade-offs on processability, toughness, modulus and thermal performance. Even with these compromises, state of the art prepreg materials (e.g. TorayTM T800/3900-2, HerculesTM IM-7/8551-7, FiberiteTM IM-7/977-2) have been developed that can provide very tough damage-tolerant composite products [21–27]. These impact-resistant prepreg-based composites, a staple of the aerospace market, typically possess a resin-rich interlaminar region that has been toughened by the addition of relatively large elastomeric or thermoplastic particles.

This type of composite microarchitecture cannot be used in applications when the composite is formed by the RTM process. It is difficult to control the thickness of the interlaminar regions in a dry preform into which a liquid is injected. The use of large elastomeric or thermoplastic particles in an RTM formulation is unworkable, primarily because the preform acts as a filter, trapping particles as the resin flows through the fibre bundles. Furthermore, addition of particles to a resin formulation increases the viscosity to a level that can dramatically inhibit fibre impregnation.

An approach to generating impact-resistant composites without using toughened resin formulations is the use of a three-dimensional (3D) preform [28–31]. Impact of a typical composite causes development of interlaminar cracks, which lead to delamination and eventually to failure. The use of through-the-thickness stitching (z-axis) in a standard preform lay-up of woven or knitted fabric (or a 3D braid) drastically reduces the possibility that failure can occur via delamination, as the plane of failure is constrained by the z-axis reinforcement. It has been demonstrated that composites made from brittle thermoset resins, that would typically have compression-after-impact (CAI) values of 138–172 MPa (20–25 ksi), can exhibit CAI values of 207–241 MPa (30–35 ksi) by stitching the preform through the thickness [32, 33].

The use of these ‘tough’ 3D reinforced preform structures is compatible with resin impregnation via RTM. However, the 3D structure of the preform produces a triaxial stress on the polymer in the resin-rich interstitial pockets of the preform. The stress is generated during the cure by a combination of resin shrinkage and the dissimilar thermal expansion (contraction) coefficients between the polymer and fibre. As discussed in previous sections, these problems are magnified as the cure temperature of the process is increased and the cure shrinkage of the resin increases. Most of the relatively brittle thermoset polymers used in RTM relieve this stress by microcracking. Even though there has been no reduction observed in static mechanical properties that can be directly related to the presence of these microcracks, they can lead to increased

moisture absorption and an increased probability of interlaminar and intralaminar crack formation. These problems are exacerbated by thermal cycling in a moist environment. Therefore, selection of an RTM resin that has a minimum tendency to microcrack would be desirable in production of aerospace-quality composites when using a damage-tolerant 3D preform.

3.1.4 EPOXY SYSTEMS

Epoxy resins are well known materials for the production of aerospace composites. The wide range of available epoxies and curing agents makes these systems very versatile in terms of processing latitude and attainable physical properties [34, 35]. The most commonly used epoxies for production of structural composites are the glycidyl derivatives of bisphenol A (DGEBA), bisphenol F (DGEBF), phenol formaldehyde novolacs and methylene dianiline (Figure 3.5). Although there has been a large body of innovative work in developing new epoxy resin formulations for prepreg, RTM, filament winding and other aerospace applications in the past two decades, there has been limited commercialisation of new types of epoxy resins. Some of these new epoxy resins provide a whole new level of performance in their respective RTM formulations (e.g. diglycidyl ether of bishydroxyphenylfluorene from Shell, used in 3M® PR-500).

When liquid epoxy resins such as DGEBA and DGEBF are used in RTM systems they are typically part of a two-component system. There are many liquid epoxies available of this type which have slight variations in epoxy, hydroxyl and oligomeric content. These slight variations in molecular structure lead to some variability in the processing of these materials, particularly as the molecular structure has an effect on initial viscosity and the reaction rate for the system. However, there is a remarkable amount of similarity in the way these materials process and there is very little real difference in the polymeric properties formed when any of these materials is reacted with any given curing agent. Table 3.2 provides a list of the common liquid epoxy resins available in the market place. The three principal suppliers of epoxy resins are Ciba Resins, Dow Chemical and Shell. (A list of manufacturers and their contact details is given at the end of this chapter.)

Epoxy resins require a curing agent to form the finished polymer. In no other thermoset chemistry is the choice of curative so important. With polyester and vinyl ester resins the curing catalysts alter the time of cure but do not substantially affect the viscosity of the resin or the final polymeric properties. When phenolic resins, cyanates or bismaleimides are used there are a limited number of curing agents available or, more typically, a fully formulated system is used. There is a staggeringly large

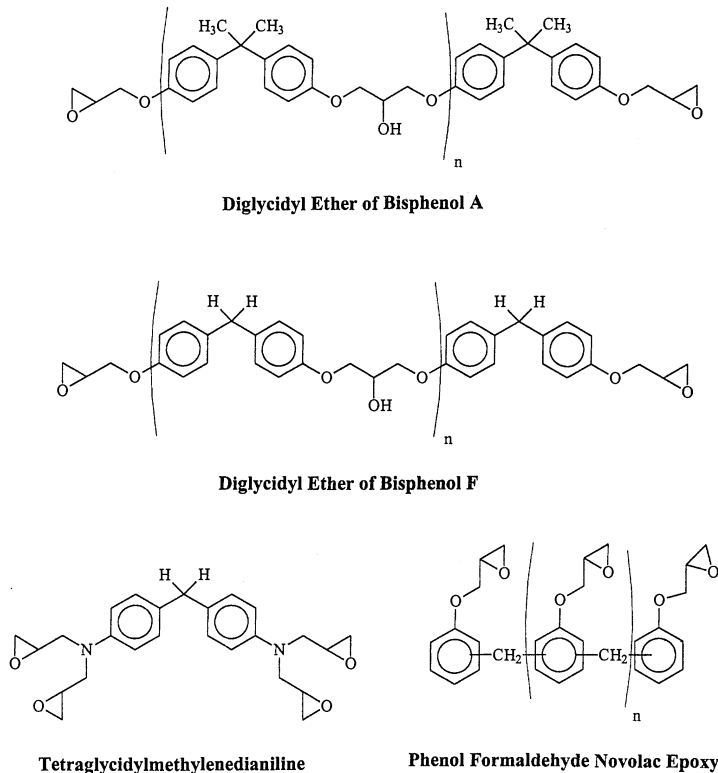


Figure 3.5 Chemical structures of some commonly used epoxies.

choice available in curing agents for epoxy resins. The choice in curing agent is crucial in the use of an epoxy because it determines the ultimate thermal and mechanical properties of the polymer formed as well as defining the temperature-dependent viscosity change which controls the processability of the system. Among the most useful curing agents for epoxy resins are the aromatic and (cyclo)aliphatic amines, anhydrides and phenolics. Epoxies can also be cured successfully with catalytic agents such as imidazoles or Lewis acids.

Diethyltoluenediamine (DETDA), a liquid aromatic amine, has found wide acceptance as a primary hardener component in many RTM formulations. (It is the principal curing agent found in Shell's Epon Curing Agent® W and Dow's TACTIX® H41 epoxy curing agent). DETDA is an alkylated aromatic diamine and is representative of the processing characteristics and polymer properties available from this class of curing agent. It is a liquid at room temperature and provides good RTM processability as part of either a one-part or a two-part system. The slow

Table 3.2 Some common liquid epoxy resins: (a) bisphenol A epoxy resins (DGEBA); (b) bisphenol F epoxy resins (DGEBF)

Manufacturer and Resin Tradename	Viscosity (mPa s)	Epoxy Equivalent Weight
(a)		
Ciba Resins:		
Araldite® LY 556	9000–12 000	179–187
Araldite® GY 6008	6500–9500	177–188
Araldite® GY 6005	7500–9500	182–196
The Dow Chemical Company:		
DER 330	7000–10 000	176–185
DER 331	11 000–14 000	182–192
DER 332	4000–6000	172–176
DER 383	9000–10 500	176–183
TACTIX® 123	4400–5600	172–176
TACTIX® 138	9200–9800	178–182
Shell Chemical Company:		
Epon 825	5000–6500	175–180
Epon 826	6500–9500	178–186
Epon 828	11 000–15 000	185–192
(b)		
Ciba Resins:		
Araldite® PY 306	1200–1800	159–170
Araldite® LY 9703	3000–4000	160–180
Araldite® GY 281	5000–7000	158–175
The Dow Chemical Company:		
DER 354	3000–5500	158–175
Shell Chemical Company:		
Epon DPL 862	3000–4000	166–177

even cure rate of an epoxy with DETDA allows these systems to be processed over a wide temperature range. The introduction of catalysts into a DETDA formulation can significantly speed the cure and/or lower the cure temperature with an epoxy resin [36–38]. DETDA produces a polymer with a high glass transition temperature [typically >177°C (350°F)] when fully cured. The Young's modulus of polymers made by curing an epoxy with DETDA is normally less than 3.1 GPa (450 ksi) and is often less than 2.76 GPa (400 ksi). Therefore, the use of liquid aromatic amines such as DETDA as a curative provides excellent processability as well as a polymer with a good high glass transition temperature but with a modulus value that is possibly too low for demanding aerospace applications.

Aliphatic and cycloaliphatic amines are useful curing agents for most epoxy resins. These materials are almost always low-viscosity liquids [e.g. diamocyclohexane (DACH), isophoronediamine (IPDA), *para*aminocyclohexylamine (PACM), etc.] that are readily soluble in epoxy resin formulations. The reactivity of these amines is relatively high and

58 Materials

therefore formulation as the B component of a two-part system is the only practical use of these curing agents. Thermal and mechanical properties achieved from this class of epoxy curing agent combination is usually somewhat less than that of an aromatic-amine-cured epoxy. With use of these curing agents, glass transition temperatures of 121°C–177°C (250°F–350°F) and polymeric modulus values of 2.4–3.1 GPa (350–450 ksi) are routinely obtained.

Anhydrides have been widely used as epoxy curing agents in filament winding applications for many years. This class of epoxy curing agent has not received much attention as a potential curing agent for RTM formulations. The liquid nature of most of the commonly used anhydrides [e.g. methyltetrahydrophthalic anhydride (MTHPA), nadic methyl anhydride (NMA), etc.] and their good solubility with epoxy resins means they could be used in either one-part or two-part RTM systems. The ready accessibility of a range of catalysts for the epoxy–anhydride reaction makes it possible to formulate a system that will meet specific process requirements [39–41]. Anhydride-cured liquid epoxy resins (i.e. DGEBA, DGEBF) typically form polymers with glass transition temperatures of approximately 140°C–150°C (283°F–301°F), modulus values of 3.45 GPa (500 ksi), tensile elongation of 3%–5% and moisture pick-up of 1.5%.

Cure of an epoxy resin with an amine is a simple reaction mechanically. Reaction of an epoxy with an anhydride curing agent is relatively complex and is subject to competitive side-reactions. The primary side-reaction is the homopolymerisation of epoxy groups to form ether linkages. This homopolymerisation reaction can be acid-catalysed or base-catalysed and competes with the desired epoxy anhydride reaction. Homopolymerisation reactions use up epoxy functionality and leave excess anhydride (acid) functionality in the polymer. Basic catalysts tend to be more effective than acidic ones in catalysing epoxy–anhydride chemistry. The course of the reaction and the resultant ratio of epoxy–epoxy reaction versus epoxy–anhydride reaction is driven predominantly by the choice of catalysts.

Reactions of epoxy with anhydride that depend on trace quantities of acid from anhydride hydrolysis or those in which catalytic amounts of acid (e.g. BF_3 , sulphuric acid, acetic acid, etc.) have been added lead to a polymer in which 20%–50% of the stoichiometric amount of anhydride is unreacted. Acid catalysis of epoxy–anhydride reactions therefore has proven ineffective. When tertiary amines and imidazoles are used as catalysts for epoxy–anhydride reactions the amount of anhydride used is typically about 85% of stoichiometry to account for the increased epoxy homopolymerisation. When reaction catalysts such as quaternary ammonium salts are used the epoxy–epoxy reaction is less competitive, and a stoichiometric amount of anhydride is used.

Mechanistically, the reaction of an epoxy with an anhydride can be shown to form two intermolecular linkages at the site of the oxirane group. This effectively increases the cross-link density of these systems as compared with an amine-cured resin. There are several important consequences of the cure mechanism. Since the epoxy has an effective functionality of four and the anhydride an effective functionality of two, a large amount of anhydride must be used in curing. Functionally, it is equivalent to the epoxy acting as a cross-linker for the anhydride. The highly cross-linked polymer formed from this reaction has a relatively high modulus and a low strain to failure. The use of flexibilisers such as modified anhydrides [polyazelaic anhydride (PAPA)] or epoxies (butyl glycidyl ether or DER 736 epoxy resin) to increase the strain to failure of anhydride-cured epoxies has not been completely effective.

Another result of this cure mechanism is the formation of two ester linkages from the oxirane and no pendant hydroxyls. This generates a polymer with low moisture absorption (typically 1%–1.5%). Even though anhydrides tend to form polymers with slightly lower glass transition temperatures than many amine-cured epoxies, the lower moisture absorption of the anhydride provides a polymer that has a higher final use temperature in many cases. The high fraction of anhydride in a formulation and the low viscosity of most anhydrides leads to a system viscosity that can be processed without the addition of diluents. The relatively low cost of anhydride systems means that these materials normally provide the lowest cost epoxy composites.

When anhydride curing agents are exposed to moisture, typically with long-term storage in a moist environment, they hydrolyse to form acids. These acidic components interact with the basic catalyst and inhibit the cure of the epoxy anhydride while catalysing the competing epoxy homopolymerisation (discussed above). The polymer formed with epoxy and anhydride that is contaminated with acid is inferior because of its lower cross-link density, which leads to lower modulus, lower glass transition temperature, and greater moisture absorption. The presence of acid (hydrolysed anhydride) is often observed in liquid systems as a white crystalline material. Care should be taken when using anhydride curing agents to minimise the absorption of water.

Some of the most successful RTM systems in the aerospace market place are one-part epoxy systems. There are numerous reasons for the success of these materials, as discussed previously, including ease of use, quality control of process and materials and excellent thermal and mechanical properties. Table 3.3 provides a listing of some one-part RTM systems which are available from Hexcel, Dow, and 3M.

Table 3.3 One-part epoxy systems for aerospace resin transfer moulding Applications.

Manufacturer and material	Glass transition temperature (°C)	Density (g/cm ³)	Moisture Uptake (%)	Tensile Strength (MPa) ^a	Tensile Modulus (MPa) ^a	Tensile Strain (%)
3M: PR-500	193	1.25	1.6	56.6 (8.2)	3640 (528)	1.9
PR-520	158	1.25	1.7	91 (13.2)	3544 (514)	6.0
The Dow Chemical Company: XUS 19022.00	165	1.30	1.0	82.7 (12)	3034 (440)	5.0
Hexcel: RTM 6	183	1.14	2.5	75 (10.9)	2890 (419)	3.4

^a Values in parentheses below are in ksi.

3.1.5 PHENOLIC THERMOSET MATERIALS

The condensation reaction of either a phenol or an amine (urea or melamine) with formaldehyde to generate a cross-linked polymer and liberate water is one of the oldest polymerisation reactions known. Phenolic polymers have been produced since before 1920 and the amino polymers since the mid-1920s.

Phenolic resins are made by the reaction of phenol or a phenolic material (e.g. cresol) with an aldehyde. The aldehyde used is almost always formaldehyde. This is because formaldehyde is the most economical aldehyde, it reacts faster and it cannot undergo most of the side-reactions possible for the higher aldehydes. However, the use of substituted phenols or aldehydes other than formaldehyde formulated into the resin can provide different properties and processing characteristics. By adjusting the temperature at which the resin is made, the catalyst or the ratio of phenol to formaldehyde a variety of polymeric material properties can be achieved. There are basically two types of phenolic resins: resoles and novolacs. Base resins and formulated systems are available from Borden and Georgia Pacific.

Resole resins are made in a single-stage process (using a basic catalyst and excess formaldehyde) by carefully controlling the reaction conditions to produce a non-cross-linked relatively low molecular weight system that is a phenolic methylol. The cure of a resole resin is finished in either a second heat-activated step, or by activation from an acidic catalyst that produces reaction at relatively low temperatures to cross-link the system and form the finished polymer with elimination of water.

Novolac resins are made in a two-stage process using an acidic catalyst and excess phenol to generate a low molecular weight non-cross-linked system that is a methylene-linked phenolic. The 'glassy' novolacs isolated from this first step will not cross-link with additional heating but require a curing agent (hardener) to form a polymer. The hardener used with novolacs is usually a formaldehyde derivative, such as hexamethylenetetramine (hexa). On heating, the hexa decomposes to formaldehyde and ammonia, which serves as a basic catalyst for the cross-linking reaction between the novolac and formaldehyde.

Approximately 91000 tonnes (200 million pounds) of phenolic moulding materials are produced each year. Only a relatively small percentage of this resin is used in structural composite applications. Most of the material is used in filled moulding compounds for electrical applications (e.g. switchgear and connectors), appliances (e.g. steam irons and handles), automotive applications (e.g. water pump housings and solenoids) or in decorative laminates. Phenolic polymers demonstrate excellent dimensional stability over a wide temperature range, good electrical insulation properties, creep resistance, hardness, resistance to

62 Materials

degradation from a variety of automotive fluids and flammability resistance and low smoke generation. The low viscosity and very high char yield of these materials is the reason they are used in forming many carbon/carbon composite structures.

Phenolic (novolac and resole) resins are classified as condensation polymers because they generate volatiles (water) during the curing process. These volatiles have an impact on the processability of all these materials in structural composite applications where the void content of the part can have a dramatic effect on the mechanical properties of the part. The tightly cross-linked nature of these polymers causes them to be generally quite brittle, resulting in systems that are characterised by low tensile strength and elongation and high flaw sensitivity. Even with the difficulties found in processing and the relatively poor mechanical behaviour of these materials the excellent low fire and smoke properties of these resins is leading to an increasing role for phenolic resins in structural applications. The only resin that comes close to providing composites with the same relatively high resistance to flammability and low smoke generation are bismaleimide formulations which are typically at least an order of magnitude more expensive.

In RTM the closed-mould nature of the process makes it more difficult to deal with the volatiles evolved during the cure of phenolics than in more open processes such as pultrusion. However, some fairly clever ways to work around these problems are being developed. A very interesting approach to solving the volatiles problem is use of a catalyst that will allow gelation of the resin at temperatures below 100°C (212°F). If water is formed during the RTM process but the reaction is held at temperatures below the boiling point of water then the water will remain in the liquid phase and act as a polymeric plasticiser. Obviously, if the reaction temperature rises above 100°C during the initial gelation phase of cure then water will vaporise and leave the part as steam, causing massive degradation. An elevated temperature post-cure, ramping up very slowly and carefully through 100°C, will drive water from the gelled structure and finish cross-linking the polymer without degrading the part. These volatile problems are compounded by the fact that most phenolic formulations are based on aqueous solutions of relatively low boiling materials such as phenol and formaldehyde. The acidic nature of the catalysts used in many phenolic formulations can cause corrosion in some tooling materials.

3.1.6 CYANATE RESINS

Cyanate (sometimes called cyanate ester) resins have a relatively small niche use in the fabrication of composites. The very high glass transition temperature and the excellent electrical properties of polymers based on

these resins is the primary driver for their use. The relatively high cost of formulated systems of cyanate (US\$44.00–US\$220.00 per kilogramme) are obviously preventing entry of these materials into any markets other than those for the most demanding applications. The cyanate resins are all made by reaction of a phenolic precursor and a cyanogen halide with base catalysis. The resultant cyanate is usually cured with the addition of heat and a transition metal catalyst [Co(III), Cu(II), etc.]. The reaction, as seen in Figure 3.6, is the formation of a triazine ring. The energy released (typically 300–400 J/g) in forming an aromatic network provides the driving force for this reaction, while the transition metal catalyst forms a template for the ring formation. Phenolic materials are often added as catalysts for the trimerisation reaction when a lower temperature cure is required.

The phenolic triazine (PT) resins are materials in which the capping of the phenolic precursor with cyanogen halide is controlled to leave some residual amount of phenolic functionality in the presence of a large excess of cyanate capping. The presence of this incipient phenolic functionality leads to an increased reaction rate for these resins compared with typical cyanates. Therefore, less catalyst is needed to cure a PT resin than for a similar cyanate resin. The greater reactivity of these resins tends to generate uncontrolled exotherms if moulding temperatures are not carefully controlled. The polymers formed by trimerisation of cyanate functionality (cyanate and PT resins) develop a modulus of 3.1–3.45 GPa (450–500 ksi) but a fairly low strain to failure (2%–4%) because of the tightly cross-linked network.

The gelation of a cyanate resin occurs at about 50%–60% conversion, similar to that in epoxy resin chemistry. However, cyanates are quite unusual in that they have very little to no densification on cure. The coefficient of thermal expansion is also relatively small, at about 50 ppm/°C. This lack of cure shrinkage and low coefficient of thermal expansion allows production of composite parts with very low internal stresses even when elevated temperature cures are used. The resins as a class of materials process very much like aerospace epoxies except that a

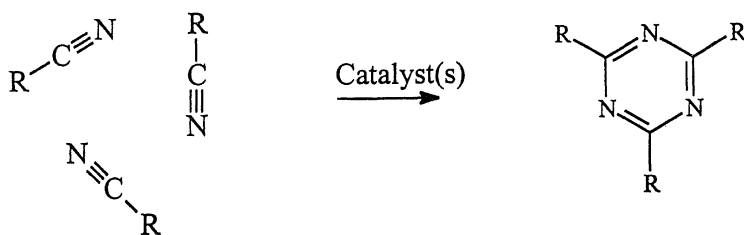


Figure 3.6 Thermosetting reaction of a cyanate resin.

64 Materials

very high-temperature post-cure (>240°C) is required if a polymer with very high glass transition temperature is desired. Cyanate resins are often formulated with epoxy resin or maleimides in order to modify the processability or properties of the resultant polymer. Typical formulations also include curing catalysts such as transition metal salts and phenolic species. There are very few formulations of cyanate resin that were specifically developed for RTM. Most systems were produced for prepreg or adhesive applications. There are a variety of cyanate resins and formulated systems which are available commercially from Ciba Resins, Dow, Fiberite, Lonza, Bryte and YLA.

Cyanate resins typically produce a polymer with high glass transition temperature, low moisture absorption, good mechanical properties and excellent electrical properties. The use of cyanates in radome structures is driven by the need for a high glass transition temperature coupled with a low dielectric constant and dissipation factor to prevent degradation from high-energy radiation transmitted and received through the structure. Some cyanate formulations have been developed that have a very flat response in both dielectric and dissipation across a very wide range of temperatures and electromagnetic radiation wavelength. The use of carbon fibre/cyanate composites in satellite structures is driven by the need for an extremely stiff structure, with high glass transition temperature and low moisture absorption that can endure repeated thermal cycling without failure generated by internal stresses [42].

3.1.7 BISMALEIMIDES

Bismaleimide (BMI) resins currently supply a niche market in the fabrication of structural composites, for those parts requiring a very high glass transition temperature and good thermal oxidative stability and low flammability. The relatively high cost of formulated BMI resin systems (US\$44.00–US\$220.00 per kilogramme) is slowing entry of these materials into any markets other than those for the most demanding applications.

BIMIs are made by reaction of an aromatic diamine precursor with maleic anhydride. The resultant BMI is usually cured with the addition of heat; additional catalysts are not usually required. Unmodified BMIs form a very brittle polymer, with strain-to-failure values typically of <2%. In order to toughen these systems a highly formulated mixture containing co-reactants of amines, vinyl monomers or epoxy resins are used. These formulated resins require process conditions that are very similar to aerospace epoxy systems. The polymers formed in this way are reasonably tough, but as elevated temperature post-cures are used to generate higher glass transition temperatures an increasingly brittle polymer is generated [43, 44].

A typical BMI resin is made by reaction of methylene dianiline (MDA) with maleic anhydride, using heat to remove the water generated and force the reaction to completion. Of course, a variety of diamines can be used in this process to make the BMI. By altering the backbone of the BMI structure and formulating with co-reactants one may obtain a variety of processing characteristics and thermal, mechanical and environmental resistance properties [45–47]. There are a variety of BMI resins and formulated systems available commercially from Ciba Resins, Shell, Cytec, and Hexcel.

The use of BMIs is driven by their exceptional high-temperature performance, particularly their ability to retain useful mechanical properties above 149°C (300°F) following moisture saturation. The other BMI characteristics that drive their use in particular applications are their good electrical properties, their long-term thermal oxidative stability at temperatures in excess of 177°C (350°F) and their exceptionally low flammability and smoke generation characteristics when exposed to high heat flux. These excellent high-temperature properties are key drivers in moving these formulated systems into aerospace applications, but currently their largest single application [more than 454 tonnes per year (1 million pounds per year)] is in the manufacture of high-temperature electrical circuit boards.

A disadvantage that seems to be present across the entire family of BMI resin systems is the very long cure schedule. The very desirable high-temperature properties of these resins is obtained only when a high-temperature post-cure is used. The high-temperature cure and post-cure cycle leads to relatively brittle polymer systems with a significant amount of built-in stress. The elevated temperature cures, with relatively high cure shrinkage, quite often leads to stress relief via microcracking. Most moulders use slow ramp rates, particularly for the cool-down schedule, to minimise the problems with the built-in stress.

The BMI resins are available as formulated systems for liquid moulding applications and as prepgres. Table 3.4 provides a listing of some typical one-part formulated bismaleimide RTM systems.

3.2 FIBRE REINFORCEMENTS

Fibre reinforcements represent the main load-bearing component in advanced composites. As such, careful attention is paid during the design of the part when selecting the specific fibre material and its form. The most basic categories of fibrous reinforcement are whiskers, continuous fibres and wire. Whiskers are short fibres with very small aspect ratios and they posess high degrees of crystalline perfection (i.e. few to no defects). As such, they are often very expensive and are rarely used in structural components because of difficulties in processing, such as little

Table 3.4 One-part bismaleimide systems for aerospace resin transfer moulding applications

Manufacturer and material	Glass transition temperature (°C)	Density (g/cm ³)	Moisture uptake (%)	Flexural strength (MPa) ^a	Flexural modulus (MPa) ^a	Moulding life (h)
Cytec: 5250-4-RTM	300	1.25	4.2	163 (23.6)	4480 (650)	~2 at 121°C
Hexcel: F650	310	1.27	4.3	86.9 (12.6)	4410 (640)	
HX-1601	265	1.25	3.7	141 (20.4)	4220 (612)	>3 at 115°C
Shell Chemical Company: Compimide® 65FWR	265	1.29	2.5	163 (23.6)	4509 (654)	~1 at 110°C

^a Values in parentheses below are in ksi.

control over orientation, low fibre volume fraction and poor interfacial bonding with the matrix material, which lead to poor load-bearing performance [48]. A continuous fibre is defined as a fibre whose length is past a critical value, somewhere between 20–100 times longer than its diameter [48, 49]. In aerospace applications, however, continuous fibres are meters long. It is this category which will be discussed in this chapter since these fibres provide the necessary structural load-bearing capacity which meet the demands of most aerospace components. The fibre diameters are typically in the order of 5–15 µm. This is a result of the fact that the material strength is a function of the number of flaws present. The fibres minimise volume with respect to surface area and thereby reduce the probability of failure from internal flaws (this property is the basis of Weibull statistics used to predict the strength of brittle materials). Continuous fibres are usually bundled into tows or spun into yarn containing 1000–12 000 filaments. [48, 50]. Finally, the term ‘wire’ generally refers to larger-diameter metallic fibres most commonly used in the reinforcement of rubbers as seen in tires and high-pressure hoses. This section will cover continuous fibres of various materials, their utility in specific applications, the general types and forms in which these fibres can be utilised and various surface treatments commonly applied to enhance the performance of these fibres.

3.2.1 MATERIALS FOR FIBRE REINFORCEMENTS

A wide selection of materials have been, and continue to be, developed as reinforcements for composite materials. They span the full spectrum of materials: metals, polymers and ceramics. Each offers specific advantages tailored individually to target application requirements. The primary characteristics considered include strength, modulus (stiffness), density, service temperature capability, fatigue resistance and price. The most common reinforcements for structural aerospace parts are polymeric or ceramic in nature.

Fibreglass

Fibreglass is the most popular reinforcement available. It offers the best value providing intermediate strengths [1.5–2.0 GPa (217–290 ksi)], fair stiffness, [76–86 GPa (10–12 msi)] and low cost [around US\$12 per kilogramme (US\$6 per pound)] [48, 51]. Fibreglass is, however, heavier than other popular reinforcements such as carbon fibre and aramid fibre. It has a density of 2.5 g/cm³. The structure of the fibre is an amorphous ceramic based on silica glass (SiO₂). Silica exists in a tetrahedral crystal structure in which oxygen atoms occupy the corners and the silicon atom resides inside [Figure 3.7(a)]. These tetrahedra link together to form a

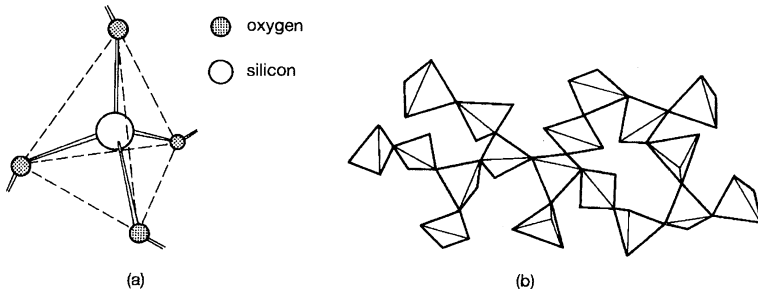


Figure 3.7 (a) Structure of silica; (b) silica in an amorphous configuration (non-crystalline network). Source: Callister, W.D. Jr, *Materials Science and Engineering*, 3rd edn; published by John Wiley & Sons, Inc, New York, 1994.

non-crystalline or vitreous network [Figure 3.7(b)] which is modified by other ions and oxides. They are drawn from a melt through a prescribed orifice, called a bushing, at a precisely determined velocity resulting in a consistent fibre diameter.

The fibres must be totally amorphous because the presence of crystals would act as stress concentrations in the fibres and greatly weaken them [49]. Several forms of fibreglass are commercially available and are differentiated by properties controlled by composition. Composition is varied by the type and relative amounts of secondary component oxides and impurities [48, 53]. The most common forms in aerospace are E-glass, S-glass and C-glass. E-glass, also called ‘electrical glass’, is the most popular for the reinforcement of polymers. It is a borosilicate glass with properties and cost representing the low end of the glass category. Applications of E-glass include aircraft radomes and antennas. S-glass, or ‘structural glass’, is a magnesia/alumina/silicate glass with higher tensile strength, necessary for applications experiencing primary structural loads, and is subsequently more expensive. Its applications include seals, access doors and even armour systems. C-glass is a calcium borosilicate glass and was developed for enhanced environmental durability and provides better chemical resistance to attack from water and acids. It is often used for applications involving containment or disposal of chemicals [48, 51–53].

Fibreglass offers the advantages of intermediate to high strengths, low cost, high temperature resistance (it softens at 850°C), transparency to visible light and isotropy of thermal expansion. Because its structure is amorphous, the coefficient of thermal expansion is the same in both the longitudinal direction and the transverse direction. Disadvantages include a higher density than other reinforcements, susceptibility to surface damage and high sensitivity to attack by moisture [48, 49].

Carbon (Graphite) Fibre

Carbon fibre is a higher-strength, stiffer and lighter-reinforcement option. The most common fibres offer strengths around 77 MPa (530 ksi) and a modulus of 234 GPa (34 msi) at a density of 1.8 g/cm³. Many grades, however, are available based on modulus, which can vary from low [227–241 GPa (33–35 msi)], intermediate [275–345 GPa (40–50 msi)] to high [345–965 GPa (50–140 msi)]. Costs range from US\$14–US\$5000 per kilogramme (US\$7–US\$2500 per pound), the average grade being around US\$60 per kilogramme (US\$30 per pound). These fibres are based on the specific properties and methods of manufacture [48, 50–52]. The structure is composed of carbon atoms arranged in the graphite configuration [Figure 3.8(a)]; hence it is often referred to as graphite fibre. Carbon atoms pack hexagonally in very ordered sheets or planes [Figure 3.8(b)] along which primary covalent bonds carry the load, resulting in their high strength. The strength properties are thus reliant upon the degree to which the planes lie parallel to the fibre axis and the extent to which defects (i.e. voids, impurities, misalignment) are present. Interplane bonding, however, is weaker and results in low transverse axis properties [48].

These fibres are manufactured via several different methods. Each method starts with a different precursor material. The predominant method synthesises fibre from polyacrylonitrile (PAN). PAN fibres provide the best compressive strength properties and are used in structural applications such as aircraft skins, wing elements, stiffeners, nacelle systems and access doors. Pitch fibres are synthesised from petroleum or coal tar pitch. Originally used for producing lower performance fibres this method has been developed and now produces fibres of extremely high modulus and near-zero values for the coefficient of thermal expansion (CTE). These exotic carbon fibres represent the high end of

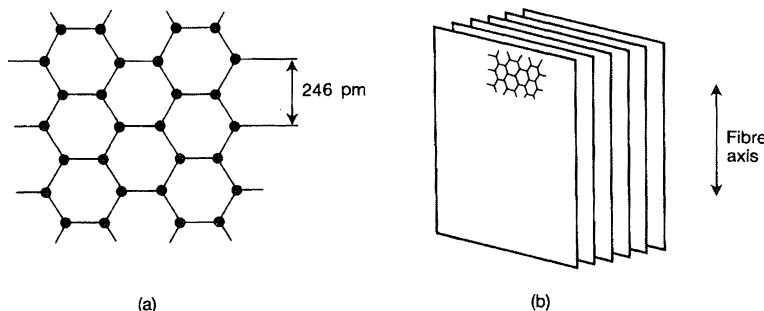


Figure 3.8 Structure of carbon fibre: (a) hexagonal packing arrangement of carbon atoms; (b) series of graphitic planes composing carbon fibre. Source: McCrum, N. G., Buckley, C. P. and Bucknall, C. B., *Principles of Polymer Engineering*; published by Oxford University Press, Oxford, 1989.

70 Materials

carbon fibre technology and are used in performance-driven applications such as launch vehicles and space systems. Carbon fibres are also manufactured through the carbonisation of rayon fibres. Though less structural in performance, these fibres have excellent wear and ablative properties for applications such as heat shields, rocket nozzles and brake systems [52].

The advantages of carbon fibre encompass high stiffness, high strength and reduced weight. Carbon fibres are chemically inert, provide high electrical and thermal conductivity and have low CTE values. Their disadvantages include high cost, high anisotropy (transverse properties are much lower than longitudinal properties) and greater brittleness than fibreglass and aramid. In the presence of aluminum a galvanic couple will form, resulting in corrosion of the aluminum. This effect is often prevented through the use of a barrier material, usually fibreglass/epoxy [48, 52].

Aramid Fibre

Aramid fibres are the primary structural polymeric reinforcement currently used in aerospace applications. Unlike other polymers the long-chain molecules of this aromatic polyimide (hence 'aramid') are rigid because of the presence of benzene rings in the backbone. This prevents the chains from folding back upon themselves, allowing for higher degrees of alignment parallel to the fibre axis. This in turn allows the fibre to make better use of the polymer's strong covalent bonds. KevlarTM 49 is one of the most popular aramid fibres in use today. It is based on the polymer poly(*paraphenylene terephthalamide*) (Figure 3.9).

The molecules pack together lengthwise and bond firmly to their neighbours via hydrogen bonds, furthering fibre rigidity. The fibre is drawn or extruded from a solution. As they are stretched the lengthy molecules are preferentially aligned in the draw direction. There are no discrete amorphous regions in the structure [48].

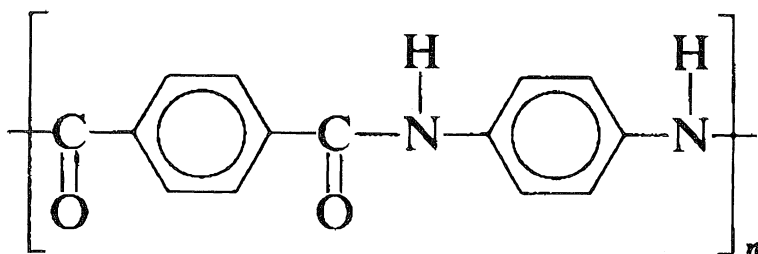


Figure 3.9 Poly(*paraphenylene terephthalamide*).

Kevlar® 49 by DuPont possesses a strength of 3.5 GPa (500 ksi) and a modulus of 130 GPa (19 msi). Its specific weight is 1.45 g/cm³ and costs on average about US\$24–US\$30 per kilogramme (US\$12–US\$15 per pound). The advantages are its light weight and strength over a wide range of temperatures (down to –196°C). Aramid fibres provide superior fatigue resistance, chemical resistance, toughness, weathering and wear resistance [48–50]. Applications include blade containment on aircraft engine nacelle systems, ballistic shielding, seals, solid rocket motors and helicopter rotor blades. Applications are limited, however, by a relatively weak axial shear strength and a tendency to absorb moisture. Aramid lies somewhere in-between carbon and glass with respect to both price and performance (Figure 3.10).

Ceramic and other exotic fibres

The list of available fibre reinforcements continues to grow as materials research progresses, driven by the increasing performance requirements of the aerospace industry. Fibreglass, carbon and aramid fibres are the most widely used, but special applications require the performance of more exotic reinforcements. These include high-grade ceramic fibres where strength, oxidation and creep resistance are required at service temperatures of over 1000°C (1800°F) and where increased cost is justified by performance. These systems are generally used to reinforce ceramic or metallic matrices but offer utility with high-temperature polymeric matrices in functions such as heat shielding and ablative applications. These fibres include boron, quartz, aluminum oxide, single-crystal alumina (sapphire), silicon carbide and boron nitride.

Boron fibre is manufactured through the chemical vapour deposition of elemental boron onto a thin tungsten filament. These fibres offer strengths five times greater than steel and are two times as stiff. Fibre reinforced plastic (FRP) applications include the empennage structure of the F-15, the box beams in the B-1 bomber and truss members on the space shuttle in conjunction with boron/aluminum. It is also widely used as a patching material over cracked structures in aircraft [48, 51, 52].

Quartz fibres are high-purity (99.95% pure) fused silica fibres. They offer a low CTE, high service temperature capabilities (to 1500°C), excellent torsional and flexural stiffness and chemical stability. They are particularly attractive when low dielectric loss properties are required. Quartz fibres are also well suited to high-energy applications, where they are transparent to ultraviolet radiation and resist neutron capture. Disadvantages include susceptibility to hydrofluoric acid and strong alkalis and a lower tensile strength (on par with fibreglass) compared with other high-temperature reinforcements [50].

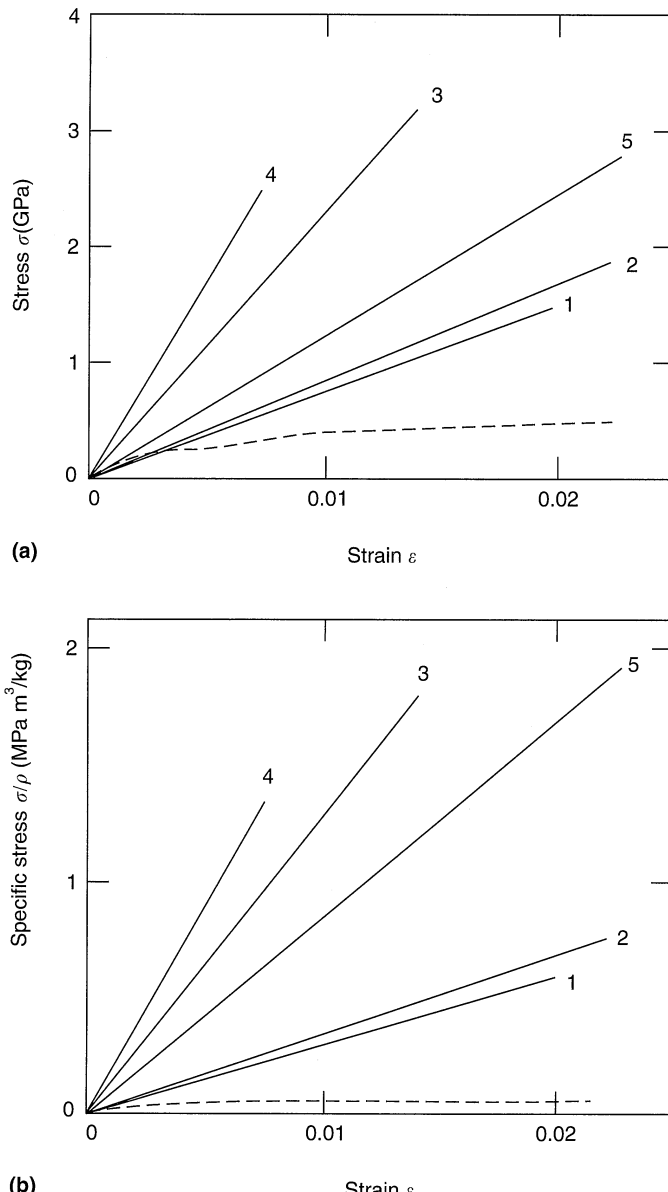


Figure 3.10 Comparison of the mechanical properties of six materials. (a) stress versus strain; (b) specific stress versus strain. 1 = E-glass; 2 = S-glass; 3 = high-strength carbon; 4 = high-modulus carbon; 5 = KevlarTM 49; - - - = 0.1% carbon steel.

Aluminum oxide fibres come in various grades defined by their composition and structure, thereby determining their mechanical properties and temperature limits. An example is the 3M line of Nextel® fibres [54] which predominately contain alumina (Al_2O_3) in various phases such as the α , γ , δ and mullite phases as shown in Table 3.5. They provide excellent temperature, abrasion and oxidation resistance. Their low thermal conductivity and high thermal shock resistance makes them attractive for gaskets, seals, heat shielding and firewall applications for aircraft and spacecraft. They are used in high-temperature shielding of cowlings, engine struts and auxiliary power units. For the ultimate in high-temperature performance, single-crystal alumina (sapphire) continuous fibres are used where creep resistance and strength at continuous service temperatures over 1500°C is a priority. Such fibres manufactured by Saphikon Inc. possess a room-temperature strength of 3.0 GPa (435 ksi) and a modulus of 450 GPa (65 msi) and retains approximately 40% of its strength and 90% of its stiffness at 1200°C [55]. Again, these fibres, like the others in this category, are driven by performance to justify costs.

Silicon carbide (SiC) and silicon nitride (Si_3N_4) offer excellent chemical resistance in addition to their high-temperature strength and stiffness capabilities. Manufactured by the pyrolysis of polycarbosilanes, continuous SiC fibres are used in a variety of matrix materials, from metals, such as aluminum, to ceramics, including carbon, alumina and silicon carbide. Nicalon™ fibres manufactured by Dow Corning have been used in high-temperature structural engine applications such as exhaust nozzles, ducts and hot gas filters. The ceramic grade Nicalon™ has a strength of 3.0 GPa (430 ksi) and a modulus of 193 MPa (28 msi) and is comparable to carbon fibre in density.

Table 3.5 Properties of Nextel® fibres. Source: Tompkins, T.L., Ceramic oxide fibers: building blocks for new applications, *Ceramic Industry* (April), 1; published by 3M, 1995

	Nextel® 312	Nextel® 440	Nextel® 610	Nextel® 720
Composition (wt%)	62 Al_2O_3 24 SiO_2 14 B_2O_3	70 Al_2O_3 28 SiO_2 2 B_2O_3	+99 Al_2O_3	85 Al_2O_3 15 SiO_2
Density (g/cm ³)	2.70	3.05	3.88	3.40
Tensile Strength (MPa) ^a	1700 (247)	2000 (290)	2930 (425)	2100 (305)
Tensile Modulus (GPa) ^b	150 (21.8)	190 (27.6)	373 (54.1)	260 (37.7)

^aValues in parentheses below are in ksi.

^bValues in parentheses below are in msi.

Hybrids

Hybridisation of fibre reinforcements is an effective means of achieving superior performance at reduced costs. Different fibres are bundled or woven together to obtain a blend of properties and ultimately costs. Popular mixtures such as glass and carbon provide high strength and stiffness with weights less than glass and costs less than carbon. Carbon/aramid provides the damage tolerance, vibrational damping and lighter weight of aramid and the carbon provides higher stiffness. In today's competitive markets where the cost-to-performance ratio is ever-shrinking, hybrid fabrics are increasingly becoming prevalent in designs. Properties for common reinforcements are shown in Table 3.6.

3.2.2 BUNDLING FIBRES: TOWS, YARNS AND WOVEN FABRICS

Single fibres or filaments are far too brittle and small to be handled and effectively incorporated into composites individually and thus they are bundled together in thousands. The first stage is to combine individual fibres into macroscopic strands. These strands may be in the form of a tow or roving where fibres are merely strung together and held in a coherent bundle by a sizing. Tows or bundles are usually designated by the number of filaments contained in each tow. For example a 6K bundle contains on average 6000 filaments. Fibres may also be grouped into twisted bundles then plied together with similar bundles by twisting them into yarns. Yarns are typically specified by the number of filaments and the number of twists per inch [50–52]. These tows or yarns may then be woven into a variety of fabric styles, each with its own characteristics: strength, toughness, stiffness and drapability. These will be covered in greater detail in Chapter 4.

3.2.3 FINISHES, SIZINGS AND COATINGS

Most fibres whether woven or spooled in tow form are delivered with some surface treatment applied. Though the terms 'coating', 'sizing', and 'finish' are often used interchangeably each describes a specific treatment and performs a particular task.

Finishes are surface treatments designed to promote interfacial bonding between the fibre and the matrix material. They provide a means of achieving compatibility in the composite. Fibreglass finishes fall into two basic categories: chrome finishes and organofunctional silanes. Chrome finishes (Volan type) are very versatile, providing bonding enhancement for polyester, epoxy or phenolic resin systems. Organofunctional silane finishes are specifically tailored to enhance interfacial bonding for three individual classes of resins: polyesters, epoxies and vinyl esters, and thermoplastics [50].

Table 3.6 Properties of common reinforcements. Source: Callister, W. D. Jr, *Materials Science and Engineering*, 3rd edn; published by John Wiley & Sons, Inc., New York, 1994. Copyright © 1994 W. D. Callister Jr. Data used by permission John Wiley & Sons, Inc.

Material	Specific Gravity	Tensile Strength (Mpa) ^{a,b}	Specific Strength (Mpa) ^{a,c}	Elastic Modulus (Mpa) ^{a,b}	Specific Modulus (Mpa) ^{a,c}
Whiskers:					
Graphite	2.2	20 (3)	9.38 (1.36)	1000 (142)	445 (64.5)
Silicon carbide	3.2	20 (3)	6.48 (0.94)	480 (70)	152 (22)
Silicon nitride	3.2	7 (1)	2.14 (0.31)	380 (55)	119 (17.2)
Aluminum oxide	3.9	14–28 (2–4)	3.4–7.0 (0.5–1.0)	700–2400 (100–350)	177–618 (25.6–89.7)
Fibres:					
Aramid (Kevlar®)	1.4	3.5 (0.5)	2.50 (0.36)	130 (19)	93.1 (13.5)
E-Glass	2.5	3.5 (0.5)	1.38 (0.20)	72 (10.5)	29 (4.2)
Graphite	1.4	1.7 (0.25)	1.24 (0.18)	255 (37)	182 (26.4)
Nylon 6,6	1.1	1.0 (0.14)	0.90 (0.13)	4.8 (0.7)	4 (0.6)
Asbestos	2.5	1.4 (0.2)	0.55 (0.08)	172 (25)	69.0 (10.0)
Metallic wires					
High-carbon steel	7.8	4.1 (0.6)	0.55 (0.08)	210 (30)	27 (3.9)
Molybdenum	10.2	1.4 (0.2)	0.14 (0.02)	360 (52)	35 (5.1)
Tungsten	19.3	4.3 (0.62)	0.21 (0.03)	400 (58)	21 (3.0)

^a Values in parentheses below are in ksi.

^b All values are as given in the original table.

^c The values in Mpa in this column are calculated from those given in the original table (in ksi) by dividing by 0.14504.

As mentioned previously these reinforcements (particularly the more brittle ones) are susceptible to surface damage which ultimately decreases strength. In an effort to protect the fibre through the bundling and/or weaving process, shipping and subsequent handling, sizings have been developed to limit the occurrence of incidental surface damage [50]. Sizings also serve the purpose of promoting tow integrity through the weaving and preforming operations [48]. In some instances sizings may be incorporated directly into the matrix material and may even serve as a finish. In most instances, however, the size is an organic

low molecular weight polymer which must be removed prior to incorporation into the matrix. This is particularly true for the more exotic ceramic fibres. Two such sizings are polyvinyl alcohol and hydroxypropyl methyl chloride.

Coatings refer to a third material applied to the fibre and are designed to tailor the interfacial characteristics of the matrix/fibre bond or to provide performance enhancements to alleviate certain shortcomings of a particular reinforcement. Such coatings are widely utilised in ceramic matrix composites to provide oxidation resistance and to toughen the overall composite. These coatings include carbon, boron nitride and silicon oxycarbide.

For RTM, coatings are currently being developed as an aid to pre-forming. Such coatings are referred to as binders or tackifiers. When the coating is of similar chemistry to that of the injected resin system the coating is referred to as a tackifier. These coatings are often applied to one or both sides of the fabric in amounts of 2%–7% of the total resin content. Binders and tackifiers provide the fabric with a degree of rigidity, allowing it to be manipulated, handled and draped without the misorientation of fibres and the fabric spring-back associated with tool loading. The binder or tackifier would then be incorporated into the matrix material provided they are compatible. Ciba Geigy offers a line of such fabrics in a selection of materials [57]. Other coatings are also being investigated as a means of promoting faster wet-out of the fabric and thus reducing injection times.

3.3 CONCLUSIONS

Resin transfer moulding has evolved into a process that is capable of producing high-quality, high-performance composites. As a fabrication process RTM has many advantages, including production of complex shapes in one shot, the production of low-cost composite parts with rapid cycle times, reproducible high fibre volume with excellent surface finish and tight dimensional tolerances and low-pressure closed-tool moulding that can incorporate a variety of resins, reinforcements and inserts. The quality of RTM parts can be equal to the quality of parts produced by the autoclave prepreg process. In order to obtain this quality there is much that must be done correctly because the process is deceptively simple looking.

To fabricate parts via RTM successfully the critical parameters that must be integrated are a combination of process engineering and proper tool and part engineering design. The relationship between chemistry and its effect on processability and performance must be well defined and understood in order to select the correct resin system. This process provides tremendous flexibility in choice of resins, curing agents, rein-

forcements and processing times and temperatures that will meet the application requirements of most users. The fabricator that can successfully integrate both the chemical and the engineering aspects of this process will be rewarded with high-quality composites that are produced rapidly, economically and to specification time after time.

References

1. Ishida, H. and Kumar, G. (eds) (1985) *Molecular Characterization of Composite Interfaces*, Plenum Press, New York.
2. Drzal, L.T. (1996) Fibre/resin interfaces in liquid molding: sizings and finishes. *OSU/NIST/MSU/UD Liquid Molding Workshop*, Columbus, OH, June 13.
3. Berins, M. L. (ed.) (1991) *Plastics Engineering Handbook of the Society of the Plastics Industry, Inc.*, Van Nostrand Reinhold, New York.
4. Salem, A. J. (1996) Liquid composite molding with cyclic thermoplastic oligomers. *Proceedings from the Second Workshop on Liquid Composite Molding (OSU/NIST/MSU/UD)*, Columbus, Ohio, June 14.
5. Laursen, L.J., Bertram, J.L., Bishop, M. T. *et al.* (1994) Novel matrix resins for composites for aircraft primary structures. NASA Contractor Report 194886 (NAS1-18841).
6. Martinez, E. C., Puckett, P. M., Millard, T. G. and White, D. W. (1992) A comparison of epoxy resin systems useful for resin transfer molding. *Resin Transfer Molding Clinic for the Aerospace Industry*, Society of Manufacturing Engineers, Los Angeles, CA, April 1-2.
7. Macosko, C. W. (1989) *RIM Fundamentals of Reaction Injection Molding*, Hanser Publishers/Oxford University Press, New York.
8. Clancy, H. M. and Lufti, D. E. (1986) Moisture in composites – a reminder. *18th International SAMPE Technical Conference*, October 7–9, Society for the Advancement of Materials and Process Engineering, 1161 Parkview Drive, Covina, CA 91724-3748, pp. 135–41.
9. Vieth, W. R. (1991) *Diffusion in and through Polymers*, Hanser Publishers/Oxford University Press, New York.
10. Puckett, P. M. (1994) Tough one-pot epoxy systems for liquid molding applications. *Proceedings from The Epoxy Formulators*, A Division of The Society of the Plastics Industry, Inc., St. Louis, MO, September 28.
11. Goodman, S. H. (ed.) (1986) *Handbook of Thermoset Plastics*, Noyes Publications, Park Ridge, NJ.
12. Carey, F. A. and Sundberg, R. J. (1977) *Advanced Organic Chemistry, Part A: Structure and Mechanisms*, Plenum Press, New York.

13. Friedman, H.L., Johnson, R.A., Miller, B. *et al.* (1996) In-plane movement of liquids through curved fabric structures. *Proceedings from The Second Workshop on Liquid Composite Molding (OSU/NIST/MSU/UD)*, Columbus, OH, June 14.
14. Shafi, M. A. (1996) Applications of flow modeling past, present, and future. *Proceedings from The Second Workshop on Liquid Composite Molding (OSU/NIST/MSU/UD)*, Columbus, OH, June 14.
15. Advani, S. G. (1996) Fundamentals of flow modeling in resin transfer modeling. *Proceedings from The Second Workshop on Liquid Composite Molding (OSU/NIST/MSU/UD)*, Columbus, OH, June 14.
16. Wisler, E. H. (1971) Viscoelastic effects on the flow of non-Newtonian fluids through a porous medium. *Ind. Eng. Chem. Fundamentals*, **10**(3), 411–17.
17. Coulter, J. P. and Guceri, S. I. (1988) Resin impregnation during the manufacturing of composite materials subject to prescribed injection rates. *Journal of Reinforced Plastics and Composites* (March).
18. Gauvin, R. and Chabani, M. (1988) Modelization of the clamping force and mold filling in resin transfer molding. *43rd Annual Conference, Composites Institute, The Society of Plastics Industry, Inc.*, Session 22-C/1-4, February 1–5.
19. Hale, A., Macosko, C. W. and Blair, H. E. (1991) Glass transition temperature as a function of conversion in thermosetting polymers. *Macromolecules*, **24**(9), 2610–21.
20. Gillham, J. K. (1989), In *Time-Temperature-Transformation (TTT) State Diagram and Cure*, in *The Role of the Polymeric Matrix in the Processing and Structural Properties of Composite Materials* (eds J. C. Seferis and L. Nicolais), Plenum Press, New York, pp. 127–45.
21. Bucknall, C. B. (1989) Approaches to toughness enhancement, in *Advanced Composites* (ed. I. K. Partridge), Elsevier Applied Science, New York, pp. 145–61.
22. Almen, G., Mackenzie, P., Malhotra, V. and Maskell, R. (1990) 977: Characterization of a family of new toughened epoxy resins. *35th International SAMPE Symposium*, April 2–5, Society for the Advancement of Materials and Process Engineering, 1161 Parkview Drive, Covina, CA 91724-3748, pp. 419–31.
23. Grande, D., Iliewicz, L. B., Avery, W. B. and Bascom, W. D. (1990) Effects of intra- and inter-laminar resin content on the mechanical properties of toughened composite materials. *First NASA Advanced Composite Technology Conference (NASA CP-3104)*, Seattle, WA, October 29, pp. 455–75.
24. Lee, F. W., Boyle, M. A. and Lefebvre, P. (1990) High service temperature, damage tolerant prepreg systems based on cyanate chemistry. *35th International SAMPE Symposium*, April 2–5, Society for the Advancement of Materials and Process Engineering, 1161 Parkview Drive, Covina, CA 91724-3748, pp. 162–74.
25. Recker, H. G., Alstadt, V., Eberle, W. *et al.* (1990) Toughened thermosets for damage tolerant carbon fiber reinforced composites. *SAMPE Journal*, **26**(2), 73–8.
26. Rice, B. P. and Kim, R. Y. (1990) Fracture characterization of toughened bismaleimide/graphite composites. *35th International SAMPE Symposium*, April 2–5, Society for the Advancement of Materials and Process Engineering, 1161 Parkview Drive, Covina, CA 91724-3748, pp. 455–67.

80 Materials

27. Recker, H. G., Alstadt, V. and Strangle, M. (1992) Rigidite 5276 – a highly damage tolerant epoxy system for primary aircraft structure applications. *37th International SAMPE Symposium*, March 9–12, pp. 493–505.
28. Dexter, H. B., Camponeschi, E. T., Peebles, L. (eds) (1985) *Conference Proceedings: 3-D Composite Materials (NASA CP-2420)*, Annapolis, MD, November 5–7, 1985.
29. Funk, J. G. and Deaton, J. (1989) The interlaminar fracture toughness of woven graphite/epoxy composites. NASA TP-2950.
30. Brookstein, D. S. (1990) Interlocked Fiber architecture: braided and woven. *35th International SAMPE Symposium*, April 2–5, Society for the Advancement of Materials and Process Engineering, 1161 Parkview Drive, Covina, CA 91724-3748, pp. 746–56.
31. Brosius, D. and Clarke, S. (1991) Textile preforming techniques for low cost structural composites. *Advanced Composite Materials: New Developments and Applications Conference Proceedings*, Detroit, MI, September 30–October 3, pp. 1–10.
32. Dow, M. B., Smith, D. L. and Lubowinski, S. J. (1988) An evaluation of stitching concepts for damage tolerant composites. *Fiber-Tex Conference (NASA CP-038.)*, Greenville, SC, September 13–15.
33. Palmer, R. J., Dow, M. B. and Smith, D. L. (1990) Development of stitching reinforcement for transport wing panels. *First NASA Advanced Composites Technology Conference (NASA CP-3104)*, Seattle, WA, October 29–November 1, pp. 621–46.
34. May, C. A. (ed.) (1988) *Epoxy Resins Chemistry and Technology*, 2nd edn, Marcel Dekker, New York.
35. Lee, H. and Neville, K. (1967) *Handbook of Epoxy Resins*, McGraw-Hill, New York.
36. Wiggins, P. L. (1986) Curing acceleration of a hindered aromatic diamine–epoxy system. *41st Annual Conference, Reinforced Plastics/Composites Institute, The Society of Plastics Industry, Inc.*, Session 5-A, January 27–31.
37. Urech, K., Habermeier, J. and Moser, R. (1982) US Patent 4,366,108.
38. Shimp, D. (1984) US Patent 4,447,586.
39. Lucas, P. A., Plohocki, B. A. and Tacca, J. M. (1986) Trends in controlling reactivity in epoxy formulations. *Proceedings from The Epoxy Formulators, A Division of The Society of the Plastics Industry, Inc.*, May 1986.
40. Lindau Chemicals (1988) *Anhydride Manual*, Lindau Chemicals, PO Box 13565, Columbia, SC 29201, USA.
41. Hancox, N. L. (1987) The influence of processing on an anhydride cured epoxide resin. *SAMPE Quarterly*, 18(2), 1–6.
42. Millard, T. G. and Puckett, P. M. (1994) XU-71787.02 and XU-71787.07 high performance polycyanate resins. *Proceedings of the American Chemical Society Division of Polymeric Materials: Science and Engineering*, Washington, DC, August, pp. 625–6.
43. Morgan, R. J., Shin, E. E., Lincoln, J. E. et al. (1996) The structure–property relations of bismaleimide composite matrices and durability of high temperature polymer matrix composites. *28th International SAMPE Technical Conference*, November 4–7, Society for the Advancement of Materials and Process Engineering, 1161 Parkview Drive, Covina, CA 91724-3748, pp. 213–24.

44. Shin, E. E., Morgan, R. J., Wilenski, M. *et al.* (1996) The effects of processing conditions and service environmental exposures on high temperature polymer matrix carbon fiber composites. *28th International SAMPE Technical Conference*, November 4–7, Society for the Advancement of Materials and Process Engineering, 1161 Parkview Drive, Covina, CA 91724-3748, pp. 225–35.
45. Stenzenberger, H. D., Herzog, M., Konig, P. *et al.* (1989) Bismaleimide resins: past, present, future. *34th International SAMPE Symposium*, May 11, Society for the Advancement of Materials and Process Engineering, 1161 Parkview Drive, Covina, CA 91724-3748, pp. 1877–88.
46. Boyd, J. D., Chang, G. E. C., Eisenbarth, P. and Webb, W. E. (1989) An improved damage tolerant bismaleimide system for aerospace applications. *34th International SAMPE Symposium*, May 8–11, Society for the Advancement of Materials and Process Engineering, 1161 Parkview Drive, Covina, CA 91724-3748, pp. 2365–76.
47. Boyd, J. D. and Chang, G. E. C. (1993) Bismaleimide composites for advanced high temperature applications. *38th International SAMPE Symposium*, May 10–13, Society for the Advancement of Materials and Process Engineering, 1161 Parkview Drive, Covina, CA 91724-3748, pp. 357–69.
48. McCrum, N.G., Buckley, C.P. and Bucknall, C.B. (1989) *Principles of Polymer Engineering*, Oxford University Press, New York.
49. Callister, W. D. Jr (1994) *Materials Science and Engineering*, 3rd edn, John Wiley, New York.
50. Hexcel Corp (1990) *Fabric Handbook*, Hexcel Trevarno Division, Pleasanton, CA.
51. McDermott, J. (1993) The structure of the advanced composites industry. *Journal of Advanced Composites*, 8(6), 4–15.
52. McConnell, V.P. and Stover, D. (1995) Advanced composites: performance materials of choice for innovative products. *High Performance Composites*, 2(6), 8–19.
53. Hartman, D.R., Greenwood, M.E. and Miller, D.M. (1994) High strength glass fibers. *39th International SAMPE Symposium*, April, Society for the Advancement of Materials and Process Engineering, 1161 Parkview Drive, Covina, CA 91724-3748, pp. 521–33.
54. 3M Corporation (1996) *Fiber Products for High Temperature Applications*, 3M Corporation, St. Paul, MN.
55. Tompkins, T.L. (1995) Ceramic oxide fibers: building blocks for new applications. *Ceramic Industry*, (April).
56. Goto, T. and Anderson, O.L. (1988) Apparatus for measuring the elastic constants of single crystals by a resonance technique up to 1825 K. *Rev. Sci. Instrum.*, 59(8), 1405–8.
57. Thirion, J., Girard, H. and Waldvogel, U. (1992) *New Developments for Producing High Performance Composite Components by the RTM Process*, Ciba Geigy/Brochier S.A., Neuilly.

MANUFACTURERS

Borden Industrial Products, 610 Meidinger Tower, Louisville, KY 40202, USA.
Tel.: (502)-587-7111.

82 Materials

Bryte Technologies Inc., 2025 O'Toole Avenue, San Jose, CA 95131, USA. Tel.: (408)-434-9808.

Ciba Specialty Chemicals, Three Skyline Drive, Hawthorne, NY 10532, USA. Tel.: (914)-347-4700.

Cytec Engineered Materials, 1440 North Kraemer Blvd., Anaheim, CA 92806, USA. Tel.: (714)-630-9400.

Dow Corning, Nicalon Product Information Sheet, Dow Corning Corp, Midland, MI, USA.

Du Pont, PO Box 80713, Wilmington, DC 19880-0713, USA. Tel.: (1800-441-7515).

Fiberite, 2055 East Technology Circle, Tempe, AZ 85284, USA. Tel.: (602)-730-2000.

Georgia-Pacific Resins, 2883 Miller Road, Decatur, GA 30035, USA. Tel.: (770)-593-6828.

Hexcel, 5794 Las Positas Boulevard, Pleasanton, CA 94588, USA. Tel.: (510)-847-9500. [Re: bismaleimide resins and formulated systems.]

Hexcel Composites, Z.I. Les Chartinières – BP 27, Dagneux 01121 Montluel, France. Tel.: (33) 72 25 26 27. [Re: one-part resin transfer moulding systems.]

Lindau Chemicals, PO Box 13565, Columbia, SC 29201, USA. Tel.: (803)-799-6863.

Lonza, 17-17 Route 208, Fair Lawn, NJ 07410, USA. Tel.: (201)-794-2400.

3M, 3M Center, Building 220-7E-01, St. Paul, MN 55144-1000, USA. Tel.: (800)-235-2376.

Saphikon, 33 Powers Street, Milford, NH 03055, USA. Tel.: (1800-899-5831).

Shell Chemical Company, 3200 Southwest Freeway, Suite 1230, Houston, TX 77027, USA. Tel.: (800)-872-7435.

The Dow Chemical Company, 2040 Building, Midland, MI 48674, USA. Tel.: (800)-441-4369.

YLA, 2970 Bay Vista Ct., Benicia, CA 94510, USA. Tel.: (707)-747-2750.

Advanced reinforcements

4

Michael Bannister and Israel Herszberg

4.1 INTRODUCTION

Improved structural performance from lightweight materials has been the goal of design engineers and materials scientists in the aerospace industry for decades. The bright future that was initially predicted for composite materials has not yet been realised owing to a number of problems inherent in the composite manufacturing process and the mechanical behaviour of the materials themselves.

The current manufacturing process utilises prepreg material which is relatively expensive to purchase, requires cold storage and has only a finite lifetime. Production of composite components can be very labour intensive and often leads to a significant amount of material wastage. The process also involves the use of autoclaves which can be very expensive to run. These issues result in the manufacturing process becoming very costly, which is not necessarily improved by a move to use more automated equipment, such as tape-laying machines, as they can be limited in their application.

The resultant composite material structure also has its problems. Although composite materials are capable of producing lightweight structures they are very sensitive to impact. Owing to the essentially two-dimensional arrangement of fibres in the composite structure the material has very little strength in the thickness direction. Impact upon the composite from a dropped tool or ballistic event, for example, can result in cracks forming between the fibre layers (delaminations) and across the fibres themselves. This damage results in a dramatic decrease in material strength. The aeronautical engineer must design structures after allowing

Resin Transfer Moulding for Aerospace Structures. Edited by T. Kruckenberg and R. Paton. Published in 1998 by Chapman & Hall, London. ISBN 0412731509.

for this decrease in material strength and thus may not realise the potential weight savings over more conventional metallic structures.

A novel area of manufacturing that has been at the centre of an intense research effort for a number of years has taken its inspiration from the traditional textile industry. Weaving has been used for some time to produce two-dimensional cloth for use in prepreg material, but a number of innovative textile manufacturing processes have been developed [1] in the search for a cost-effective methods of producing composite structures with improved performance. These can be generally grouped into the four textile areas of stitching, weaving, braiding and knitting (which includes non-crimp fabrics).

Using these textile processes it is possible to manufacture net-shape fibre preforms, that have a three-dimensional fibre architecture, in a highly automated method of production. As a result of the three-dimensional nature of the fibre architecture such structures are less prone to delamination and their impact resistance is increased significantly. These textile manufacturing processes, combined with resin transfer moulding (RTM), have the potential to produce high-quality composite structures with improved mechanical performance at a reduced cost. Table 4.1 provides a brief description and evaluation of the various techniques under development.

4.2 STITCHING

Of the textile manufacturing routes that will be described here, stitching is arguably the simplest process and one which can be performed with the smallest investment in specialised machinery. Stitching equipment currently used in the textile industry is capable of manufacturing preforms from aerospace-grade materials and there is an increasing supply of glass, aramid and carbon thread specifically sold for stitching. Aramid yarns are relatively easy to use in stitching machines as they are more resistant to rough handling than are glass and carbon. However, the use of aramid stitching threads can cause difficulties in the final composite component because of their propensity to absorb moisture and the difficulty in bonding the aramid yarn to standard aerospace resins. The manufacturer must therefore be aware that these problems may lead to a reduction in the mechanical performance of the component in certain situations. Glass and carbon yarn do not have the problems of moisture absorption and weak interfaces that aramid yarn does but they are significantly more difficult to use in stitching machines. This is because of their inherent brittleness which can lead to yarn breakage when stitch knots are being formed and fraying of the yarn in its passage through the stitching machine. Apart from trying to minimise the potential fraying on the stitch thread the main requirement for a suitable stitching machine is

Table 4.1 Description of advanced textile manufacturing techniques

Textile process	Preform style	Fibre orientation	Productivity and set-up
Stitching	Complex preforms are possible by combining several structures Additional fibres are incorporated onto basic fabric	Dependent upon basic preforms	High productivity; short set-up time
Embroidery		Complex fibre orientations are possible, e.g. in the maximum stress direction	Moderate productivity; short set-up time
Three-dimensional Weaving	Flat fabrics, integral stiffeners, integral sandwich structure and simple profiles Open and closed profiles (I, Z, O, U...) and flat fabrics	Wide range of through-thickness architectures possible, but in-plane fibres are generally limited to 0° or 90° directions 0° fibres; braiding fibres between 0°–80°, 90° fibres possible	High productivity; long set-up time
Three-dimensional Braiding		Highly looped fibres in mesh-like structure	Medium productivity; long set-up time
Knitting	Flat fabrics and very complex preforms	Multiaxial in-plane orientation 0°, 90°, +45°, -45°, up to eight layers possible	Medium productivity; short set-up time
Non-crimp	Flat fabrics and integral sandwich structures		High productivity; long set-up time

that the needle be capable of penetrating through the number of fabric layers to be stitched together.

Stitching has a number of advantages over other textile processes. First, it is possible to stitch both dry and prepreg fabric, although more damage is created within the prepreg material by the stitching process. Stitching also utilises the standard two-dimensional fabrics that are commonly in use within the aerospace industry and therefore there is a sense of familiarity concerning the material systems. The use of standard fabric also allows a greater degree of flexibility in the fabric lay-ups that can be stitched together. It is therefore relatively simple to incorporate a stitching step into the overall manufacturing process as it is not necessary to change the component design or tooling. Through the use of robotic mechanisms it is also possible to automate the stitching of the fabric and thus create a highly automated and economical production process.

Stitching is not restricted to a 'global' stitching of the complete component. If required, stitches can be placed only in areas which would benefit from through-thickness reinforcement, such as along the edge of the component or around holes. The density, stitch pattern and thread material can also be varied as required across the component, therefore this technique has a great deal of flexibility in the arrangement of the through-thickness reinforcement.

Stitching can also be used to construct complex three-dimensional shapes by stitching a number of separate components together (Figure 4.1). This not only increases the through-thickness strength of the final component but also produces a net shape preform which can be handled without fear of fabric distortion.

There are disadvantages with the stitching process, the main one of which is a reduction of the in-plane properties of the resultant composite component (i.e. tension, compression, shear, etc.). As the needle penetrates the fabric it can cause localised in-plane fibre damage and fabric distortion which has been found to reduce the mechanical performance of the composite. This reduction in performance, which is generally between 10%–15%, can be aggravated by the surface loop of the stitch which can also crimp the fabric in the thickness direction if the tension in the stitch thread is high. The presence of the stitch thread and the distortion in the fabric that it creates also causes a resin-rich pocket to be formed within the composite. This pocket can act as a potential crack initiator which could possibly affect the long-term environmental behaviour of the material.

A version of stitching which can be used to provide localised in-plane reinforcement together with through-thickness reinforcement is technical embroidery. In this process a reinforcement yarn is fed into the path of the stitching head and is thus stitched onto the surface of the preform (Figure 4.2). With current computer-controlled embroidery heads it is

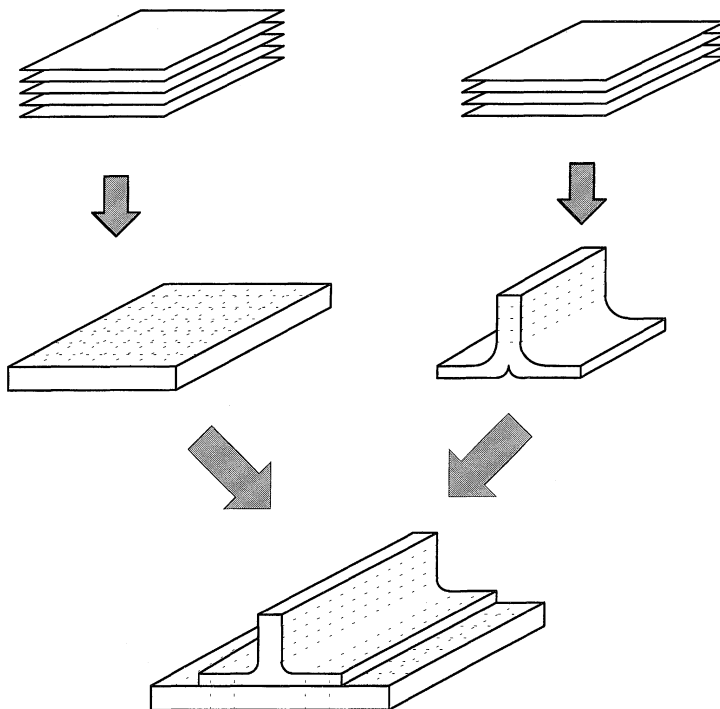


Figure 4.1 Preform manufacture via stitching.

possible to place this in-plane yarn accurately in quite complex paths, which allows high-stress regions of a component to be reinforced by fibres laid in the maximum stress direction. This process could therefore be considered a version of optimised fibre placement.

Two alternative methods to the standard stitching process were described by Evans and Boyce [2]. The first consists of embedding previously cured reinforcement fibres into a thermoplastic foam which is then placed on top of a prepreg, or dry fabric, lay-up and vacuum bagged. Through judicious choice of the material, the foam will collapse as the temperature and pressure are increased, allowing the fibres to be pushed slowly into the lay-up (Figure 4.3). This method can be used during the normal autoclave cure of prepreg and, for both prepreg and dry fabric, can be performed whilst the lay-up is on the tool surface itself, thus saving extra steps in the manufacturing process. The second method is used primarily for prepreg as it utilises an ultrasonic horn that heats up a local area of resin, thus allowing a plunger to push the pre-cured reinforcement yarn into the lay-up (Figure 4.4). Both methods have been successfully applied to carbon/epoxy composites with silicon carbide, boron and carbon reinforcement yarns.

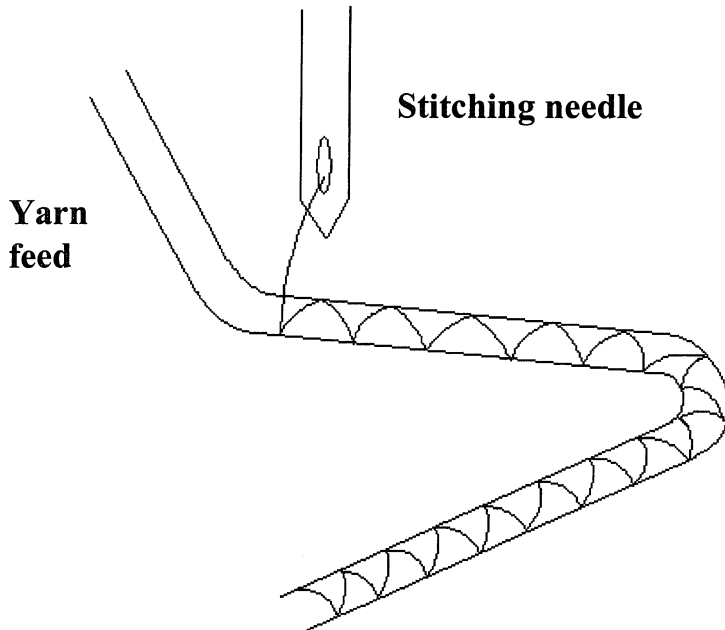


Figure 4.2 Illustration of technical embroidery.

The mechanical performance of stitched composites has been widely investigated for a number of years. Initially, work concentrated upon prepreg materials that had been stitched with a variety of thread materials, but as the technique of RTM was developed, dry stitched preforms that were later moulded became the specimen of choice because of the problems inherent in stitching prepreg. It is not possible in this chapter to cover in detail the results of all the research work. This is particularly true as the variables in the stitching process, such as thread type, thread diameter, fabric type, thread tension, stitch density, etc., have all been found to have a critical effect on the change in mechanical performance [3]. However, it is certainly true that the presence of stitches dramatically

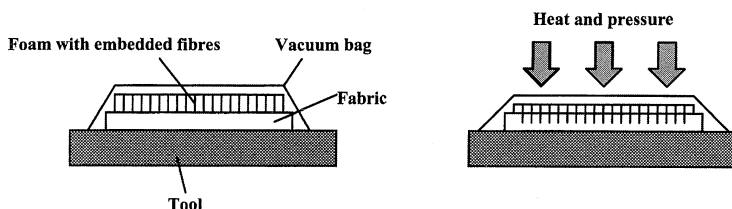


Figure 4.3 Thermoplastic foam used to insert through-thickness fibres.

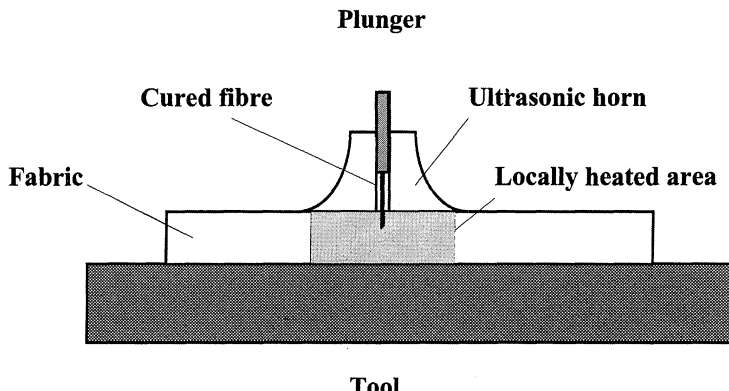


Figure 4.4 Ultrasonic horn used to insert through-thickness fibres.

increases the delamination resistance of the composite material in both mode I and mode II crack propagation. Increases of up to a factor of 30 have been reported for the steady-state value of the mode I fracture toughness G_{1C} [4]. Table 4.2 [5] illustrates the typical improvement observed for G_{1C} with various stitch densities and thread materials. This increase in fracture toughness directly improves the damage resistance of the composite, with many researchers observing a reduction in the damage area under impact [3,4,6,7]. As might be expected, this behaviour of the stitched composites was generally shown to lead to an improvement in their compression after impact performance. Figures 4.5(a) and 4.5(b) (data from references [8] and [9], respectively) illustrate these improvements for different stitch densities and thread material and demonstrate that significant improvements in impact performance can

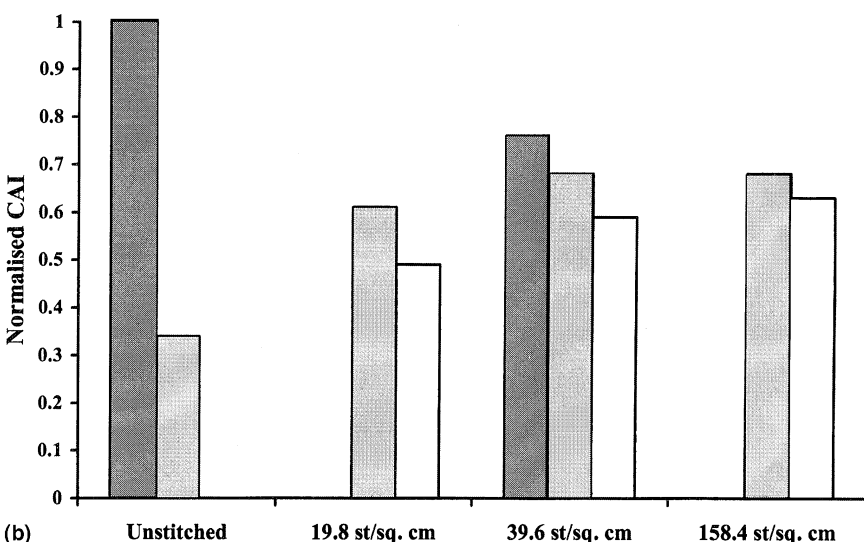
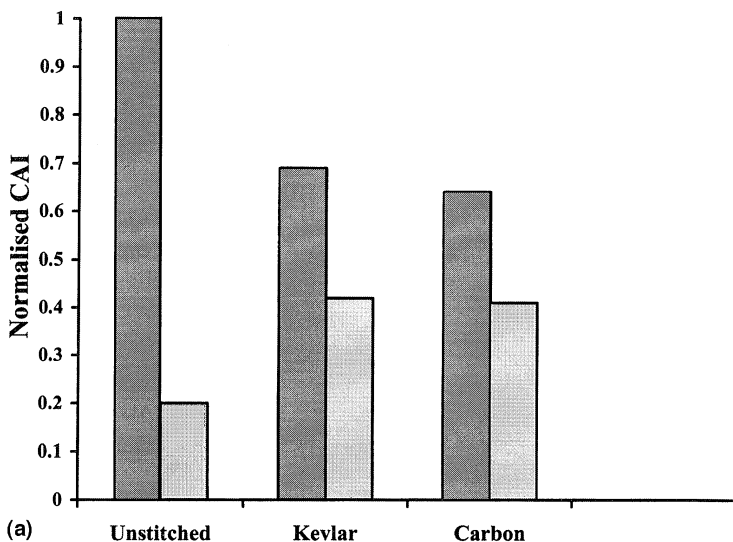
Table 4.2 Improvement in mode I fracture toughness, G_{1C} , with stitching [stitches per square inch (stitches/in²)]: T300-3K 5 harness satin weave, [0]₁₄, Dow Tactix 123 epoxy and H41 hardener, KevlarTM 1319 tex, Glass 1376 tex and carbon 1387 tex. Source: Morales, A., Structural stitching of textile preforms, *Proceedings of the 22nd International SAMPE Technical conference*, November 6–8, Society for the Advancement of Materials and Process Engineering, 1161 Parkview Drive, Covina, CA 91724-3748, pp. 1217–30

No stitch ^a	Carbon (stitches/in ²)			Glass (stitches/in ²)			Kevlar ^a (stitches/in ²)			
	5	10	45	5	10	45	5	10	45	
G_{1C} (kJ/m ²)	0.25	>0.98	1.62	3.68	0.62	1.13	2.05	1.05	2.0	6.9

^a Unstitched, resin transfer moulded T300 five-harness satin weave composite material.

be made through stitching the composite. It should be noted, however, that recent work [10, 11] performed upon relatively thin laminates (less than 6 mm) has shown less benefit from stitching with regard to impact performance. This work implies that there may be a cut-off value of component thickness below which stitching may be of limited benefit.

A comparison between stitched and unstitched composites of their in-plane mechanical properties is not so clear-cut and possibly reflects the



influence that stitch and specimen variables have upon the mechanical performance of the composite. Early work with tape [12] had shown limited benefit from stitching whereas the previously mentioned work on relatively thin composites [10, 11] had demonstrated a decrease of the in-plane mechanical properties. In spite of these sometimes conflicting results, with the current understanding of stitched composites it is generally accepted that the in-plane properties of the composite material will be reduced by approximately 10%–15%. It is therefore important if utilising the stitching process carefully to optimise the parameters so that any benefits gained from improvements to impact performance are not outweighed by degradation to the in-plane performance.

The use of stitching to join two or more components to form a structure has also been observed to have benefits not only in the increased handling capability of the structure but also in its mechanical performance. Stiffeners that have been stitched on to a panel are more resistant to the spread of delamination under the stiffener and thus prevent 'stiffener pop-off' occurring [13, 14], with improvements in the load-carrying capability of approximately 15% being observed [14].

4.3 WEAVING

The weaving process is already familiar to the aerospace industry as it is the manufacturing method used to produce the standard two-dimensional carbon and glass fabric that is used to form the composite components. However, the same weaving equipment can also be used to manufacture more intricate, net-shaped preforms that have a three-dimensional fibre architecture.

The basic weaving process is illustrated in Figure 4.6. Warp yarns are fed into the weaving loom from a source of yarn, which can consist of individual packages of yarn (a creel) or a number of beams onto which



Figure 4.5 Compression after impact (CAI) strength for stitched and unstitched laminates (normalised with respect to the undamaged compression strength of the unstitched laminate): (a) AS4/3501-6 [(0/90)₂/0/(90/0)₂], KevlarTM 1100 denier and carbon T900-1000A [4.9 stitches/cm² (st/sq. cm), 6.4 mm thick]. Impact: ■ = 0 J/mm, □ = 6.56 J/mm; (b) AS4/3501-6 (quasi-isotropic), Kevlar[®] 1500 denier, glass S2 3678 denier and carbon T900 1440 denier. Impact: ■ = 0 J/mm, □ = 4.45 J/mm, □ = 6.67 J/mm. Data in part (a) from Farley, G., Smith, B. and Maiden, J., Compression response of thick layer composite laminates with through-the-thickness reinforcement, *Journal of Reinforced Plastics and Composites*, **11** (July 1992), 787–810; data in part (b) from Dow; M. B. and Smith, D. L., Damage tolerant composite materials produced by stitching carbon fabrics, *Proceedings of the 21st International SAMPE Technical conference, September 25–28*, Society for the Advancement of Materials and Process Engineering, 1161 Parkview Drive, Covina, CA 91724-3748, pp. 595–605.

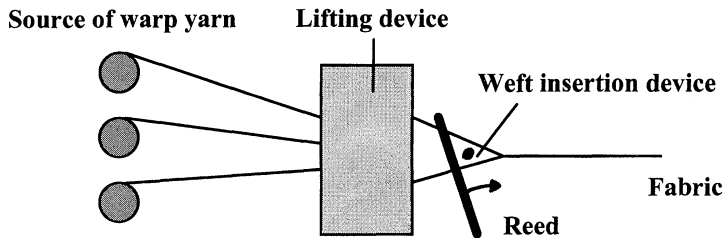


Figure 4.6 Schematic of the standard weaving process.

the necessary amount of yarn has been pre-wound (warp beams). The warp yarns are then fed through a lifting mechanism which selects and lifts the required yarns and creates a space (the shed) into which the weft yarns are inserted at right angles to the warp. The sequence in which the warp yarns are lifted controls the interlinking of the warp and weft yarns and thus the pattern that is created in the fabric. A comb-like device (reed) is used to space the warp yarns correctly across the width of the fabric and to compact the fabric after the weft yarns have been inserted. This same process can be used not only to produce standard single-layer fabric but also to create more complex, multilayer fabrics that have yarns in the thickness direction linking the layers together. Examples of such weave architectures that are currently capable of being manufactured are illustrated in Figure 4.7. The three-dimensional architectures that are shown in Figure 4.7 would play a dual role. First, the through-thickness yarns would provide the composite with an improved delamination resistance, much as the stitching fibres have been shown to do. Also, these yarns bind the layers together and produce a net-shape preform that can be easily handled, which will reduce the manufacturing time associated with the lay-up of individual fabric layers.

Flat, multilayer fabrics are not the only structures that can be woven on standard looms. By correctly programming the sequence in which the warp yarns are lifted it is possible to weave a fabric with slits that can be opened out to form a complex three-dimensional structure. This concept is illustrated in Figure 4.8, which demonstrates how I-beams and box structures can be formed from initially flat fabric. Being able to construct integrally woven, net-shaped preforms such as these should again lead to a reduction in the manufacturing time for such products compared with use of standard two-dimensional fabric. An example of such an integrally woven I-beam is shown in Figure 4.9, and these types of components are already in use in the civil engineering field [15].

More specialised looms have been developed that allow complex-shaped structures to be woven in the final shape without the need to have slits in the fabric that are then opened up. Techniques such as polar weaving [16], XYZ weaving [17] and proprietary techniques developed at

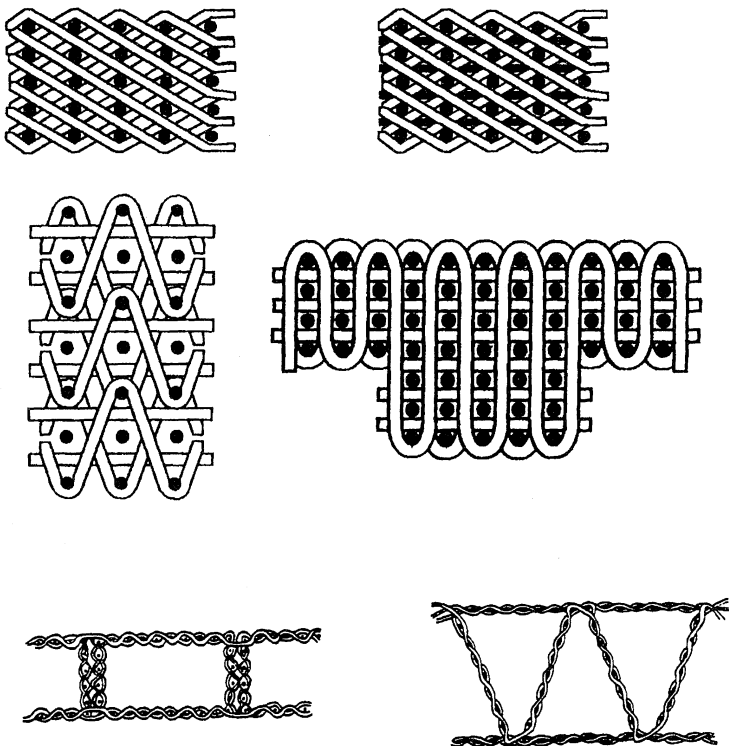


Figure 4.7 Examples of three-dimensional weave architectures.

companies such as Techniweave Inc. in the USA allow items to be woven such as those illustrated in Figure 4.10. Structures of such complexity are often difficult to manufacture using normal prepreg technology; therefore the use of weaving technology can result in substantial cost savings which open new potential markets for composite materials.

One of the main problems facing the use of multilayer woven fabrics is the difficulty in producing a fabric that contains fibres orientated at $\pm 45^\circ$. Standard industry looms which are capable of producing multilayer fabric cannot manufacture this fabric with fibres at angles other than 0° and 90° . This restricts the potential components that can be made using multilayer fabric as the necessity to add $\pm 45^\circ$ fabric will often negate the advantages that can be gained in using a single, integrally woven pre-form that contains fibres in the thickness direction. Owing to this limitation, a great deal of research is being carried out on developing the machinery and techniques that will allow the cost-efficient manufacture of multilayer fabric containing fibres in all four major directions. An example of such a fabric that is now beginning to become commercially

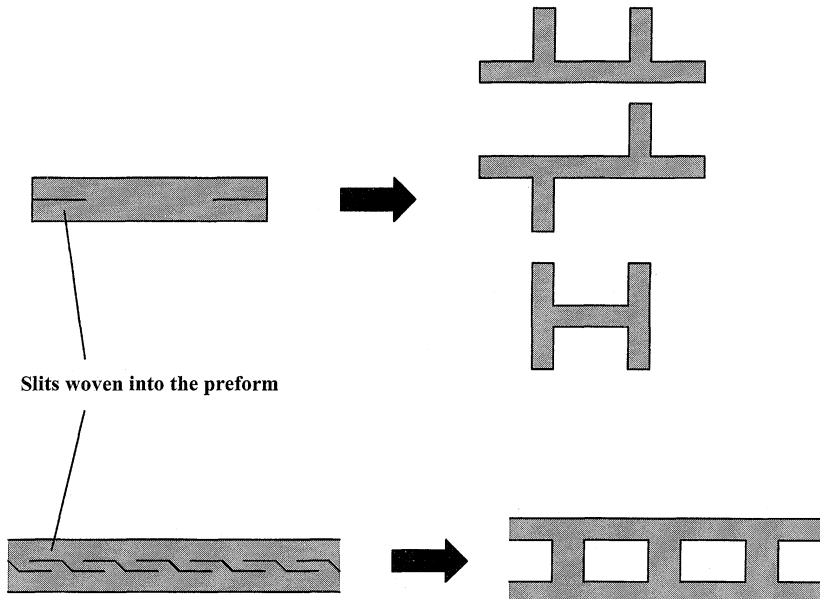


Figure 4.8 Three-dimensional structures formed from flat fabrics.

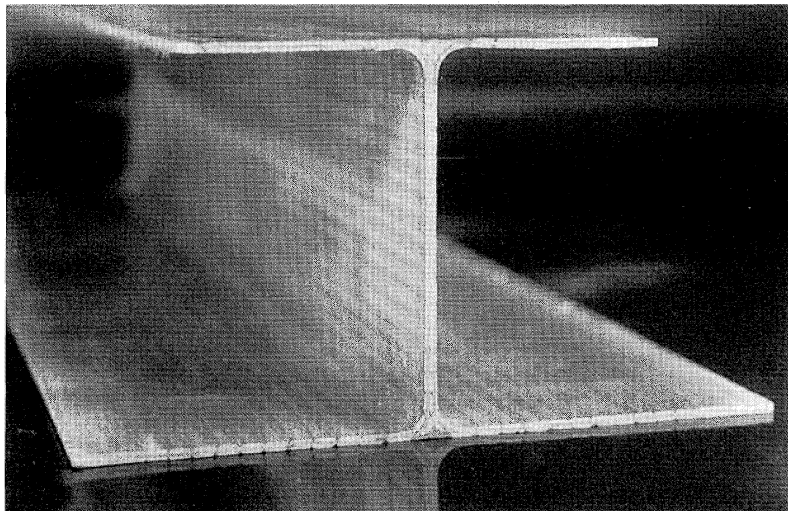


Figure 4.9 Composite I-beam manufactured from multilayer woven fabric. Reproduced courtesy of Cooperative Research Centre for Advanced Composite Structures Ltd, Fishermens Bend, Vic., Australia.

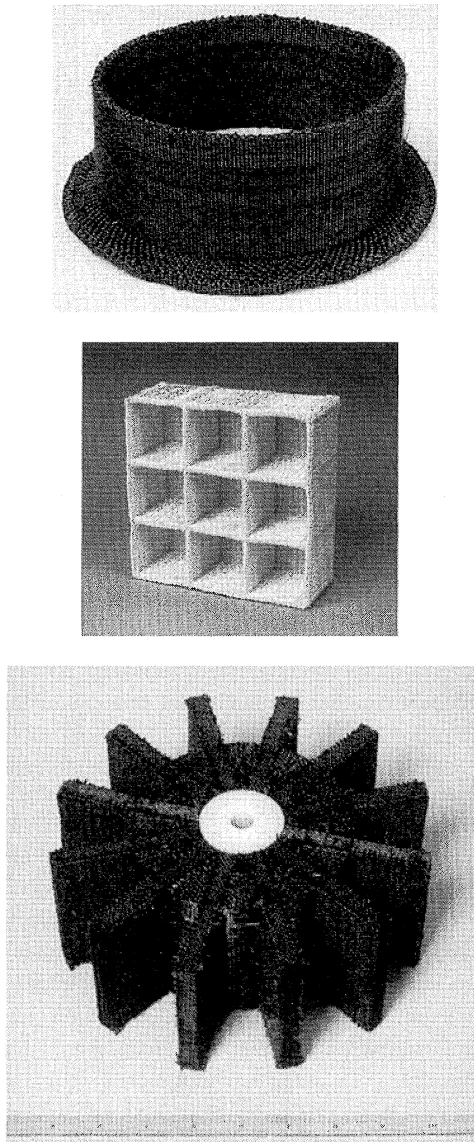


Figure 4.10 Examples of three-dimensional woven preforms. Reproduced courtesy of Techniweave Inc., Rochester, NH, USA.

available is shown in Figure 4.11 and was produced by the French company CTMI (Cotton Textiles pour Materiaux Innovants). At the moment there are restrictions in the relative proportions of fibres that can be placed in each of the four directions and in the positioning of the $\pm 45^\circ$

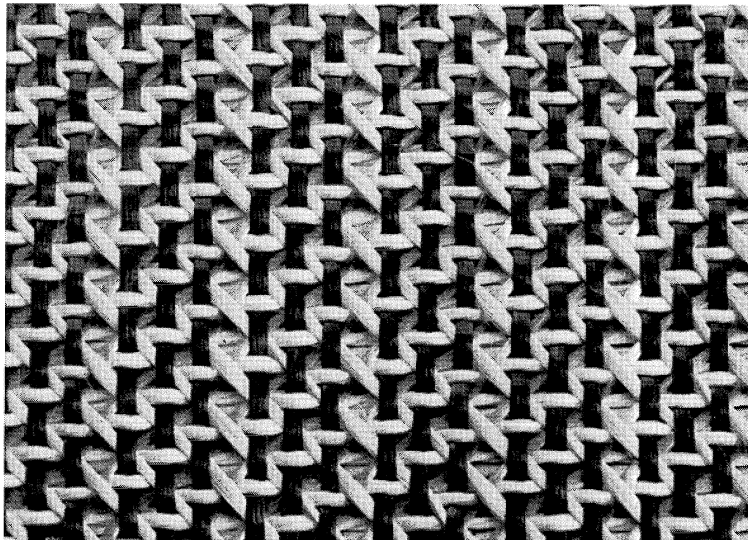


Figure 4.11 Example of multilayer woven fabric containing 0°, 90° and $\pm 45^\circ$ yarns. Reproduced courtesy of CTMI (Cotton Textiles pour Materiaux Innovants), La Sone, France.

layers but as new manufacturing methods are developed fabric of this form will become more readily available.

As can be imagined, the very large range of weave architectures that can be produced in a multilayer fabric will lead to a correspondingly large range in the mechanical performance of these structures. However, in general, tests performed upon composites reinforced with multilayer fabric [8, 17, 18] have shown that, although the undamaged in-plane properties of such composites are often degraded by the three-dimensional architecture, properties such as the compression after impact (CAI) are significantly improved (typically by at least 50%) compared with composite specimens reinforced with standard fabric. An example of this behaviour is shown in Table 4.3 (from reference [18]). This improvement in impact performance arising from the three-dimensional architecture is already being utilised in a variety of aerospace and non-aerospace applications, including ballistic resistant articles [19].

4.4 BRAIDING

The braiding process is familiar to many fields of engineering, as standard two-dimensionally braided carbon and glass fabric has been used for a number of years in a variety of high-technology items such as golf clubs, aircraft propellers, yacht masts and lightweight bridge structures [20].

Table 4.3 Mechanical performance of composites based upon various three-dimensional woven fibre preforms: woven carbon fabric (two-dimensional) orthogonal carbon preform (three-dimensional) GY30-500 Celion® fibres with Shell HPT 1071/1062 epoxy and 6 mm thick (advanced three-dimensional). Source: Brandt, J., Drechsler, K., Mohamed, M. and Gu, P., Manufacture and performance of carbon/epoxy 3D woven composites, *Proceedings of the 37th International SAMPE Symposium, March 9–12, 1992*, pp. 864–75

	Tensile strength (MPa)	Tensile Modulus (GPa)	Compression Strength (MPa)	Compression after impact of 6.7 J/mm (MPa)
Woven carbon fabric	615	65	506	168
Orthogonal carbon preform	410	48	285	219
GY 30-500 Celion™ fibres	674	72	535	301

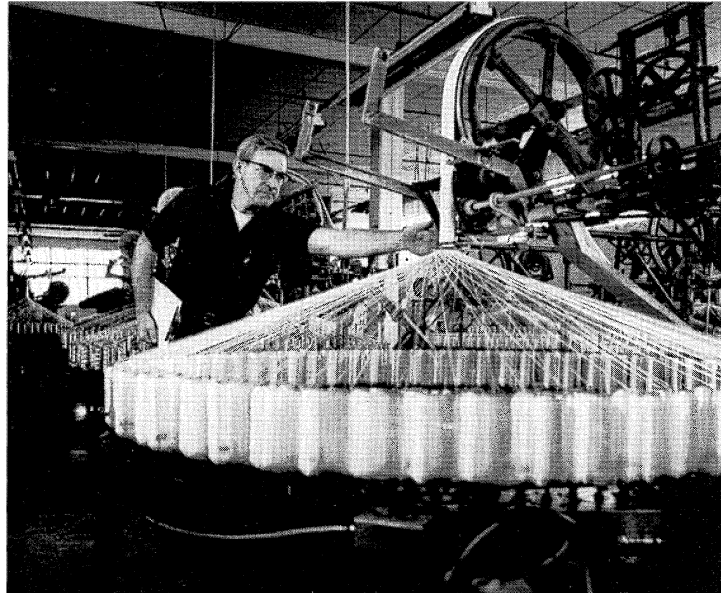


Figure 4.12 Standard two-dimensional braiding. Reproduced courtesy of A&P Technology Inc., Covington, KY, USA.

The braiding technique is illustrated in Figure 4.12 which demonstrates how the counter-rotation of two sets of yarn carriers around a circular frame forms the braided fabric. The style and size of the braided fabric and its production rate are dependent upon a number of variables [21], amongst which are the number of braiding yarns, their size and the required braid angle. The equations that relate these variables dictate the range of braided fabric that can be produced on any one machine. Typical large braiding machines tend to have 144 yarn carriers; however, larger braiding machines (up to 500 carriers) are now coming into commercial operation and this will allow braided fabric to be produced in larger diameters with a faster throughput.

The braiding process can also be used with mandrels, to make quite intricate preform shapes (Figure 4.13). By suitable design of the mandrel and selection of the braiding parameters braided fabric can be produced over the top of mandrels that vary in cross-sectional shape or dimension along their length. Attachment points or holes can also be braided into the preform thus saving extra manufacturing steps and improving the mechanical performance of the component by retaining an unbroken fibre reinforcement. Thus, within the limitations of fabric size and production rate, braiding is seen to be very flexible process in the range of

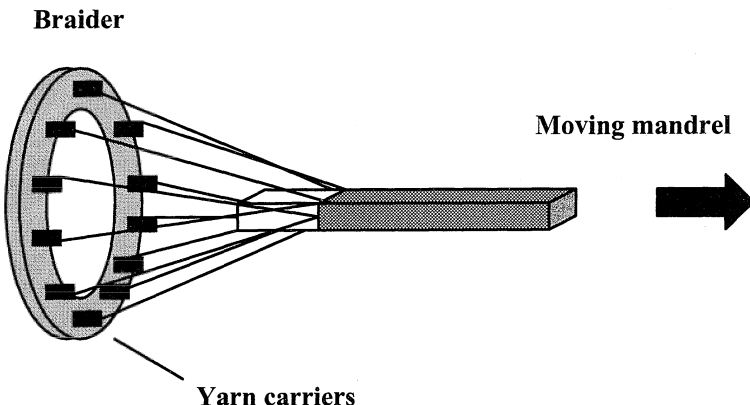


Figure 4.13 Braiding with mandrels.

products that are capable of being manufactured. In particular, unlike the standard weaving process, braiding can produce fabric that contains fibres at $\pm 45^\circ$ (or other angles) as well as at 0° . However, fibres placed in the 90° direction are not possible with the standard braiding process.

The primary difficulty with the traditional braiding technique is that it cannot make thick-walled structures unless the mandrel is repeatedly braided over. This can be done but it produces only a multilayer structure without through-thickness reinforcement. To manufacture true three-dimensional braided preforms it was necessary for new braiding techniques to be developed.

The late 1960s saw the development of three-dimensional braiding to construct carbon/carbon rocket motor components [22]. These first processes were examples of a style of three-dimensional braiding known as four-step (or row-and-column) braiding. This process utilises a flat bed containing rows and columns of yarn carriers that form the shape of the required preform (Figure 4.14). Additional carriers are added to the outside of the array, the precise location and quantity of which depends upon the exact preform shape and structure required. There are four separate sequences of row and column motion, shown in Figure 4.14, which act to interlock the yarns and produce the braided preform. In a similar process to the use of a reed in weaving, the yarns are mechanically forced into the structure between each step to consolidate the structure.

The second generic class of three-dimensional braiding is referred to as two-step braiding [23]. Unlike the four-step process, the two-step process includes a large number of yarns fixed in the axial direction and a smaller number of braiding yarns. The arrangement of axial carriers defines the shape of the preform to be braided (Figure 4.15) and the

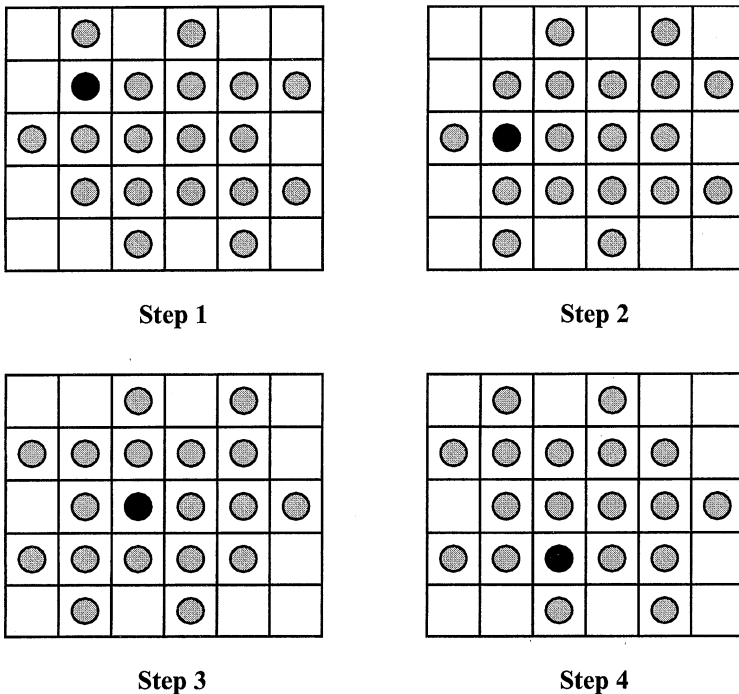


Figure 4.14 The four-step braiding process.

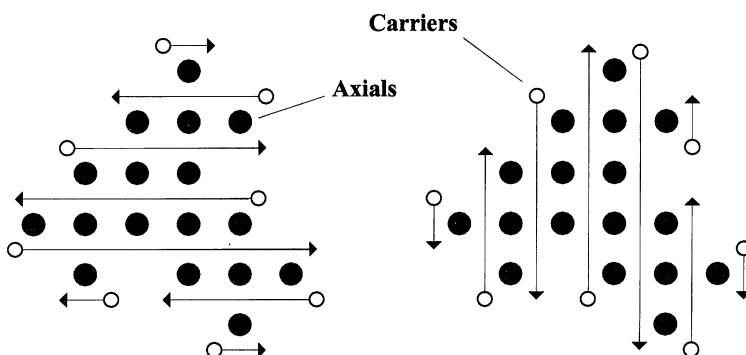


Figure 4.15 The two-step braiding process.

braiding carriers are distributed around the perimeter of the axial carrier array. The process consists of two steps in which the braiding carriers move completely through the structure between the axial carriers. This motion allows the braid to be pulled tight by yarn tension alone and thus the two-step process does not require mechanical compaction.

Both of these braiding processes are capable of forming quite intricate shapes and have been used successfully with a range of fibre materials: glass, carbon, aramid, ceramic and metal. It is possible to braid inserts or holes into the structure that have a greater degree of stability than holes that have been machined. The braid pattern can be varied during operation so that a change in cross-sectional shape is possible, including the introduction of a taper to the preform. A bend is also possible as well as a bifurcation, which will allow junctions to be produced, and these processes even allow 90° yarns to be laid into the preform during manufacture. These possibilities make three-dimensional braiding a very adaptable process, and modern versions of these braiding techniques are currently being developed into commercially available braiding machines (Figure 4.16).

The third generic class of three-dimensional braiding does not rely upon a 'flat-bed' process and is considered to be less versatile than the previous techniques in the range of preforms that can be made. This proprietary braiding process, called multilayer interlock braiding, was developed at Albany International Research Corporation [24] and the machinery is analogous to a number of standard circular braiders being joined together to form a cylindrical braiding frame. This frame has a number of parallel braiding tracks around the circumference of the

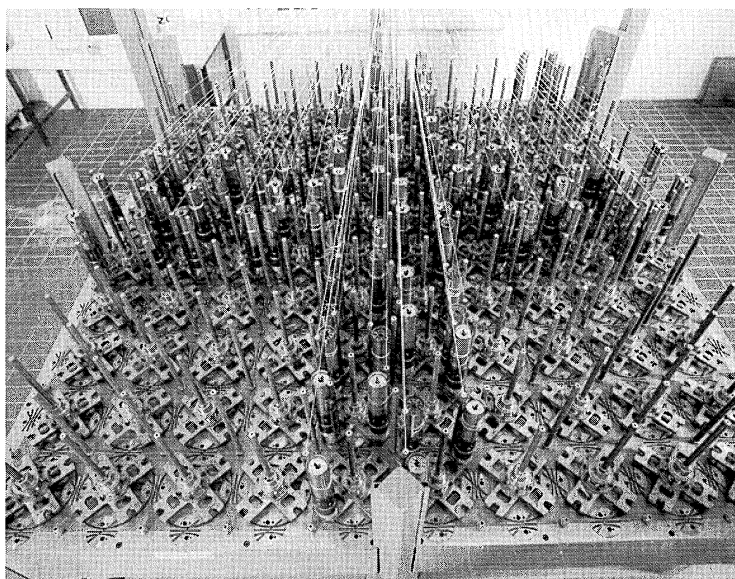


Figure 4.16 Herzog three-dimensional braiding machine. Reproduced courtesy of Daimler Benz AG , Munich, Germany.

cylinder but the mechanism allows the transfer of yarn carriers between adjacent tracks, thus forming a multilayer braided fabric with yarns interlocking adjacent layers. The benefit that this technique has over others is that it is capable of producing larger preform sizes with in-plane properties that should be superior to flat-bed preforms.

Information currently published in the open literature on the mechanical performance of three-dimensional braided fabric has, in general, shown that composites manufactured with three-dimensional fabric have improved damage tolerance and resistance when compared with composites made from two-dimensional woven and braided fabric. However, as with woven and stitched material, the variety of three-dimensional braided material is quite large and a comprehensive analysis of the mechanical performance of this type of material is not yet available.

There are a number of disadvantages both with the two-dimensional and with the three-dimensional braiding processes. First, braiding can make preforms of small scale only (relative to other textile processes) because of the restrictions of machinery size. Also, the length of preform that can be braided before resupply of the yarn is necessary is limited by the need for the yarn to be on the moving carriers, which ideally must be small and light for rapid braid production. The three-dimensional braiding process is also still very much at the machinery development stage; therefore there are limitations to the type of preform that can be made commercially and the range of companies that have the necessary experience and equipment to manufacture these preforms.

4.5 KNITTING

Knitting may not at first appear to be a manufacturing technique that would be suitable for use in the production of aerospace components. However, the knitted carbon and glass fabric which can be produced on standard industrial knitting machines has particular properties that potentially make it ideally suited for certain composite components.

Two basic knitting processes – weft knitting and warp knitting – are available to manufacture preforms for composite structures. In warp knitting multiple yarns are fed into the machine in the direction of fabric production, and each yarn forms a line of knit loops in the fabric direction. For weft knitting there is only a single feed of yarn coming into the machine at 90° to the direction of fabric production, and this yarn forms a row of knit loops across the width of the fabric. Figure 4.17 shows examples of weft and warp knitted fabric, and it is clear from this figure that the primary difference between knitted fabric and fabric made by the other textile processes described in this chapter is in the high degree of yarn curvature that results from the knitting process. This architecture results in a fabric that will provide relatively little structural

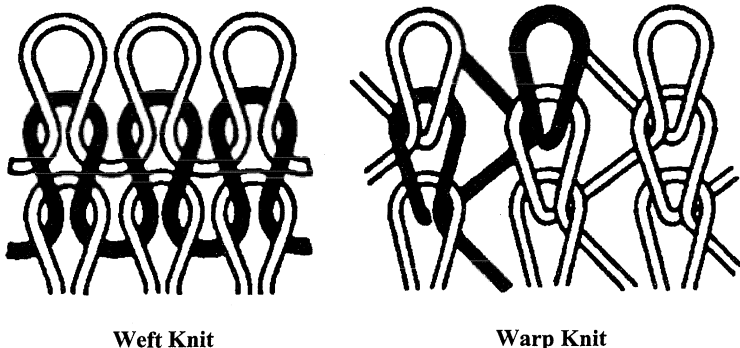


Figure 4.17 Typical warp and weft knitted fabrics.

strength to a composite but is highly conformable and thus ideally suited for manufacturing non-structural components of complex shape, such as fairings. This conformability means that layers of knitted fabric can be stretched to cover the complete tool surface without the need to cut and overlap sections. This will reduce the amount of material wastage and help to decrease the costs of manufacturing complex-shaped components. An example of such a component is shown in Figure 4.18.

The properties of knitted fabric itself can be varied quite significantly by changing the knit architecture. In this fashion, properties such as fabric extensibility, areal weight, thickness, surface texture, etc. can all be controlled quite closely. This allows knitted fabric to be tailor-made to suit the particular component being produced.

The mechanical performance of composites reinforced with knitted fabric is currently under investigation. In general, the undamaged tensile and compressive properties of knitted composites are inferior to standard woven composites [25]. The properties are anisotropic and these can be exaggerated by any stretching of the knit and may have taken place during manufacture; therefore it should be noted that any mechanical characterisation of a knitted composite should be performed under similar deformation states to the component to which it relates.

The area in which knitted composites appear to have improved performance over standard woven composites is in energy absorption and damage tolerance. Research conducted on flat panels [26] and tubes [27] has shown that composites manufactured from knitted preforms are capable of absorbing much larger amounts of energy than those utilising standard woven fabric. The knitted composites also retained a greater proportion of their undamaged strength. This behaviour would indicate that knitted composites should be considered for applications requiring high impact energy absorption capabilities, such as automotive bumpers, side rails and helmets.

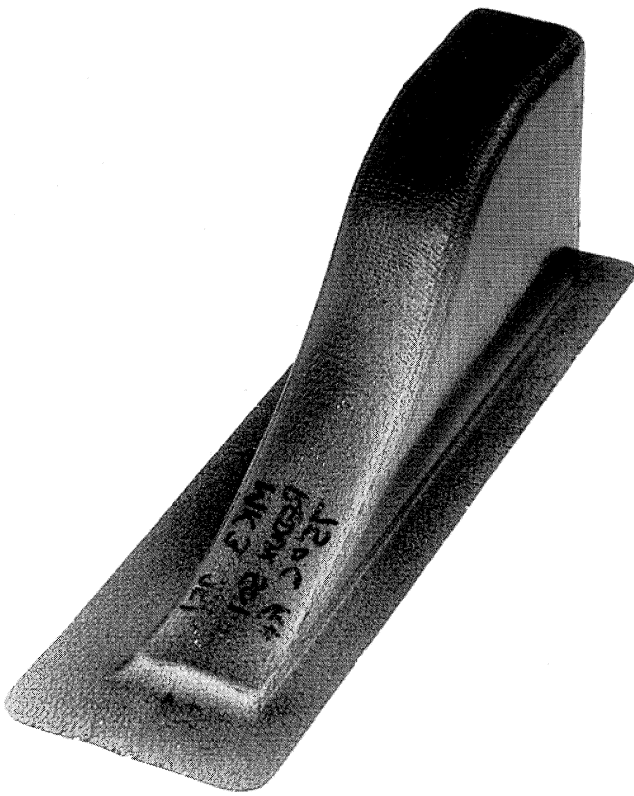


Figure 4.18 Helicopter door track pocket manufactured with use of knitted fabric. Reproduced courtesy of the Cooperative Research Centre for Advanced Composite Structures Ltd, Fishermens Bend, Vic., Australia.

As well as producing highly conformable flat fabric the knitting process can be used to manufacture more complex-shaped items. The sophisticated computer design and control mechanisms that are available with advanced knitting machines allow the knitting process to be designed such that as the fabric is manufactured it will form itself into the required three-dimensional preform shape with a minimum of material wastage. This can be accomplished without fabric overlap or seams and with the fabric properties capable of being designed to be uniform throughout the whole structure. This process is capable of cutting the manufacturing costs for complex-shaped components as the time required to form the component shape will be dramatically reduced compared with the use of prepreg techniques. Net-shaped components that have already been demonstrated in continuous filament glass and carbon yarn include T-pipe junctions, cones, flanged pipes and domes [28].

4.6 NON-CRIMP FABRIC

A manufacturing technique that combines aspects of weaving and knitting is known as either multiaxial warp knitting or stitch-bonding, but is perhaps, most commonly referred to by the style of fabric it produces – non-crimp fabric (NCF). This fabric can be produced with glass, carbon or aramid yarn (or with combinations of these) and is unique in that fabric can contain relatively uncrimped yarns orientated at 0° , 90° and at angles that can vary between $\pm 30^\circ$ to $\pm 60^\circ$. There are a number of generic manufacturing processes which can be employed to produce NCF. The most commonly used process is that developed by the LIBA Machine Company of Germany. A schematic of this process is shown in Figure 4.19(a) together with an example of the type of fabric that can be produced [Figure 4.19(b)].

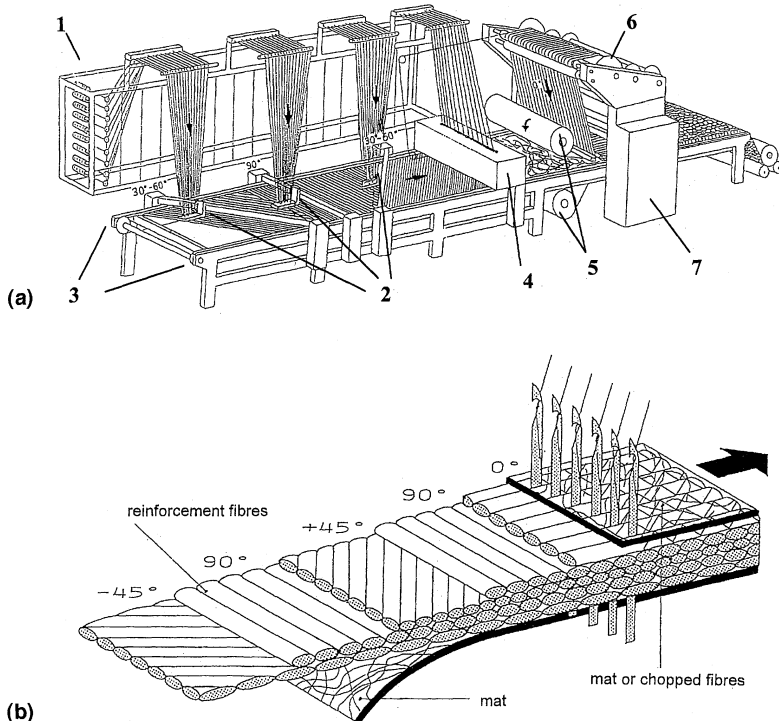


Figure 4.19 (a) Schematic of the LIBA process for manufacturing non-crimp fabric. 1 = creel system; 2 = placement heads; 3 = needles; 4 = chopper system; 5 = roll-carriers; 6 = beam to feed 0° fibres; 7 = warp knitting machine. (b) An example of the type of fabric which can be produced with use of this process. Reproduced courtesy of LIBA-Maschinenfabrik GmbH, Naila, Germany.

As illustrated in Figure 4.19(a), yarns are feed from a creel system (1) and are laid onto a long table at the orientations required via placement heads (2), an example of which is shown in detail in Figure 4.20. These placement heads travel across the table and secure the yarns at either side on a chain of needles (3) that travel along the table as the fabric is manufactured. The lay-up of the final fabric is dictated by the order in which the placement heads are angled. As well as angled fibres, a chopped strand mat can be incorporated into the fabric by the use of a chopper system (4), and further fleeces or mats can be inserted through the use of two roll-carriers (5). The 0° fibres are the last to be placed and can be feed from a beam (6) or a creel system and the multiple layers of the fabric are linked together by a warp knitting machine (7). This machine has specially designed sharp-head needles that are positioned such that the knitting process does not penetrate and damage any yarns but instead forms the knit loop in between the yarns (Figure 4.21). In current, commercially available, fabric the knit thread is usually polyester, but techniques are being developed to manufacture high-quality fabric with glass or carbon knitting thread. During the manufacturing process thermoplastic films can also be incorporated between each fabric layer, thus allowing the NCF to be used in thermoplastic forming operations. Honeycomb and foam materials can also be fed between the layers to enable on-line production of sandwich structures.

The process is flexible in that the variety of lay-ups is dictated only by the number and order of the 'stations' (i.e. 90° , 45° , chopped fibre, fleece

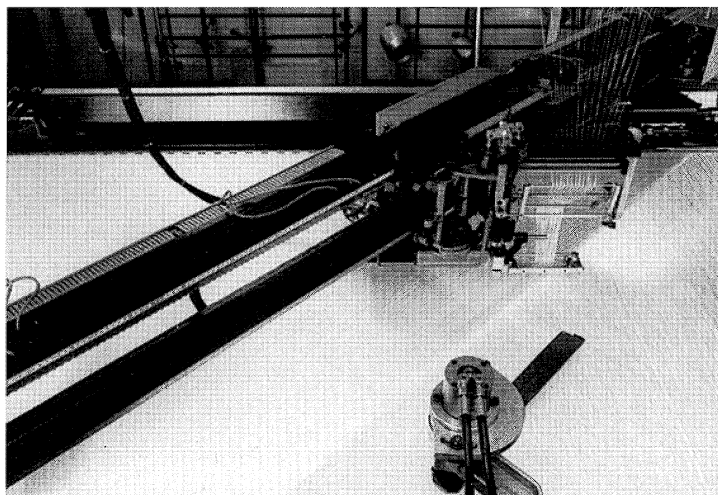


Figure 4.20 Detail of fibre placement head. Reproduced courtesy of LIBA-Maschinenfabrik GmbH, Naila, Germany.

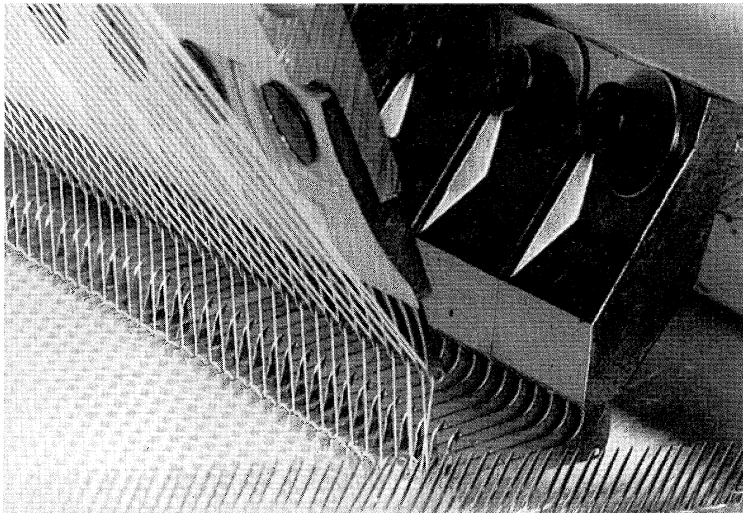


Figure 4.21 Knit loop formation. Reproduced courtesy of LIBA-Maschinenfabrik GmbH, Naila, Germany.

mats, etc) that are linked together along the length of the production table. However, owing to the need to locate the angled yarns on the needle chains precisely and to ensure the knitting needles do not damage the yarns, there are some restrictions on the size of yarns used and the areal weights that can be obtained for each layer of oriented yarn. Also, current production machines are capable only of producing fabric with a maximum of eight layers, and the 0° yarns must be placed on an outer layer.

In spite of these restrictions, NCF is extensively used in the marine industry for the manufacture of high-performance yachts and is currently under investigation for potential use within the aerospace industry. This fabric has the advantage that fewer numbers of layers need be used to build up the required structure, therefore reducing the cost of labour. Owing to the relatively uncrimped nature of the yarns, laminates produced using NCF have been found to exhibit superior in-plane properties for a given volume fraction of reinforcement than do laminates produced using woven fabric in which yarns can be more highly crimped [29]. However, unlike the true three-dimensional structures described in sections 4.2–4.4 the polyester knitting thread does not improve the impact performance of the composite. NCF has also shown a much greater ability to conform to relatively complex shapes without the wrinkling that is usually produced in standard woven fabric. This is a result of the ability of the fabric layers to shear a certain amount relative to each other without the knit loops restricting this movement.

4.7 CONCLUSIONS

It should be stated that the manufacturing processes described in this chapter will not be applicable for all aerospace components. Design or manufacturing criteria which favour the use of a particular textile process for one application may not necessarily be relevant for another. It is also possible that for some structures it may be necessary to combine a number of the textile processes in order to achieve a cost-effective product with the required performance. Of particular importance is the intimate connection between the textile manufacturing process, the required preform design, the cost and the performance of the resultant component. It has been mentioned in the descriptions of the various textile processes that there is a very large range of possible preform architectures that can be produced, each with its own mechanical performance and associated cost. It is therefore critical that in the design of any component early consideration is given to the method of manufacture, as only slight, relatively unimportant changes to component shape or required performance may result in significant changes to the cost of manufacturing the preform.

In spite of the relative youth of these manufacturing techniques, advanced textile preforms are beginning to be used in the manufacture of aerospace components. The potential savings in cost and improvements in performance that can be realised through the use of these processes are sufficiently attractive that extensive efforts are being put into further developing these processes. It is not yet clear how far these developments will go, but as designers and manufacturers become more familiar with the advanced textile techniques on offer the use of these techniques will become more commonplace.

References

1. Ko, F. K. (1989) Three-dimensional fabrics for composites, in *Textile Structural Composites* (eds. T-W. Chou and F. K. Ko), Elsevier, Amsterdam, pp. 129–71.
2. Evans, D. A. and Boyce, J. S. (1989) Transverse reinforcement methods for improved delamination resistance. *34th International SAMPE Symposium, May 8–11*, Society for the Advancement of Materials and Process Engineering, 1161 Parkview Drive, Covina, CA 91724-3748, pp. 271–82.
3. Pelstring, R. M. and Madan, R. C. (1989) Stitching to improve damage tolerance of composites. *34th International SAMPE Symposium, May 8–11*, Society for the Advancement of Materials and Process Engineering, 1161 Parkview Drive, Covina, CA 91724-3748, pp. 1519–28.
4. Dexter, H. B., and Funk, J. G. (1986) Impact resistance and interlaminar fracture toughness of through-the-thickness reinforce graphite. *27th Structures, Structural Dynamics & Materials Conference, May 19–21*, AIAA/ASCE/AHS, American Institute of Aeronautics and Astronautics, Suite 500, 1801 Alexander Bell Drive, Reston, VA 20191-4344, pp. 700–709.
5. Morales, A. (1990) Structural stitching of textile preforms. *Proceedings of the 22nd International SAMPE Technical Conference, November 6–8*, Society for the Advancement of Material and Process Engineering, 1161 Parkview Drive, Covina, CA 91724-3748, pp. 1217–30.
6. Liu, D. (1990) Delamination resistance in stitched and unstitched composite plates subjected to impact loading. *Journal of Reinforced Plastics and Composites*, **9**, 59–69.
7. Kang, T. J. and Lee, S. H. (1994) Effect of stitching on the mechanical and impact properties of woven laminate composites. *Journal of Composites Materials*, **28** (16), 1574–87.
8. Farley, G., Smith, B. and Maiden, J. (1992) Compression response of thick layer composite laminates with through-the thickness reinforcement. *Journal of Reinforcement Plastics and Composites*, **11** (July) 787–810.
9. Dow, M. B. and Smith, D. L. (1989) Damage tolerant composite materials produced by stitching carbon fabrics. *Proceedings of the 21st International SAMPE Technical Conference, September 25–28*, Society for the Advancement of Materials and Process Engineering, 1161 Parkview Drive, Covina, CA 91724-3748, pp. 595–605.

10. Herszberg, I. and Bannister, M. K. (1993) Tensile properties of thin stitched carbon/epoxy laminates. *5th Australian Aerospace Conference, September 13–15*, Institute of Engineers, Australia, 11 National Circuit, Barton, ACT, pp. 213–18.
11. Thuis, H. and Bron, B. (1996) The effect of stitching density and laminate lay-up on the mechanical properties of stitched carbon fabrics. National Aerospace Laboratory Contract Report NLR CR 96126 L, National Aerospace Laboratory, The Netherlands.
12. Mignery, L. A., Tan, T. M. and Sun C. T. (1985) The use of stitching to suppress delamination in laminated composites, in *Delamination and Debonding, ASTM STP 876* (ed. W. S. Johnson), American Society for Testing and Materials, Philadelphia, PA, pp. 371–85.
13. Yeh, H. Y. and Dufour, P. B. (1995) Structural instability and material failure of a J-stiffened stitched composite shear panel. *Proceedings of the 4th Japan International SAMPE Symposium, September 25–28*, Society for the Advancement of Materials and Process Engineering, 1161 Parkview Drive, Covina, CA 91724-3748, pp. 71–6.
14. Mitchell, L. and Herszberg, I. (1995) Analysis and testing of stitched stiffened carbon/epoxy shear panels. *6th Australian Aerospace Conference, March 20–23*, Institute of Engineers, Australia, 11 National Circuit, Barton, ACT, pp. 593–8.
15. Müller, J., Zulliger, A. and Dorn, M. (1994) Economic production of composite beams with 3D fabric tapes. *Textile Month* (September) 9–13.
16. Bruno, P., Keith, D. and Vicario A. (1986) Automatically woven three-directional composite structures, *SAMPE Quarterly*, 17 (4), 10–17.
17. Fukuta, K., Kinbara, M., Amano, M. et al. (1995) Research and development of 3D fabric reinforced composites, *Proceedings, of the 4th Japan International SAMPE Symposium September 25–28, Tokyo*, Society for the Advancement of Materials and Process Engineering, 1161 Parkview Drive, Covina, CA 91724-3748, pp. 736–41.
18. Brandt, J., Drechsler, K., Mohamed, M. and Gu, P. (1992) Manufacture and performance of carbon/epoxy 3D woven composites. *Proceedings of the 37th International SAMPE Symposium, March 9–12*, Society for the Advancement of Materials and Process Engineering, 1161 Parkview Drive, Covina, CA 91724-3748, pp. 864–75.
19. Lundblad, W., Dixon, C. and Ohler, H. (1995) Ballistic resistant article comprising a three dimensional interlocking woven fabric. *US Patent 5,456,974*, October 10.
20. Popper, P. (1991) Braiding, in *International Encyclopaedia of Composites Vol. 1* (ed. S. M. Lee), VCH Publishers, New York, pp. 130–47.
21. Soebroto, H. B., Pastore, C. M. and Ko, F. K. (1990) Engineering design of braided structural fibreglass composite. *Proceedings 6th Annual ASM/ESD Advanced Composites Conference, 8–11 October 1990*, ASM International, 9639 Kinsman Road, Materials Park, OH, pp. 435–40.
22. Ko, F. K. (1982) Three-dimensional fabrics for composites – an introduction to the Magnaweave structure. *Proceedings of the International Conference on Composite Materials IV, Tokyo, 1982*, pp. 1609–16.
23. Popper, P. and McConnell, R. (1987) A new 3D braid for integrated parts manufacture and improved delamination resistance – the 2-step process. *Proceedings of the 32nd International SAMPE Symposium, April 6–9, 1987*, Society

- for the Advancement of Materials and Process Engineering, 1161 Parkview Drive, Covina, CA 91724-3748, pp. 92–103.
- 24. Brookstein, D., Preller, T. and Brandt, J. (1993) On the mechanical properties of three-dimensional multilayer interlock braided composites. *Proceedings of the Techtextil Symposium 93, June 7–9, 1993, Frankfurt am Main*, Techtextil Symposium 93 secretariat, Messe Frankfurt GmbH, Postfach 150210, D-6000, Frankfurt am Main, paper 328.
 - 25. Ha, S.-W., Mayer, J., De Haan, J. et al. (1993) Knitted carbon fibers reinforced biocompatible thermoplastics, mechanical properties and structural modelling, in *6th European Conference on Composite Materials September 20–24, 1993, Bordeaux, France* (eds A. R. Bunsell, A. Kelly and A. Massiah), Woodhead Publishing, Cambridge, pp. 637–42.
 - 26. Bannister, M. and Herszberg, I. (1995) The manufacture and analysis of composite structures from knitted preforms. *4th International Conference on Automated Composites, September 6–7, Nottingham, UK*, Institute of Materials, London, pp. 397–404.
 - 27. Ramakrishna, S. (1995) Energy absorption characteristics of knitted fabric reinforced epoxy composite tubes. *Journal of Reinforced Plastics and Composites*, **14**, 1121–42.
 - 28. Epstein, M. and Nurmi, S. (1991) Near net shape knitting of fiber glass and carbon for composites. *Proceedings of the 36th International SAMPE Symposium, April 15–18, 1991*, Society for the Advancement of Materials and Process Engineering, 1161 Parkview Drive, Covina, CA 91724-3748, pp. 102–13.
 - 29. Hogg, P. J., Ahmadnia, A. and Guild, F. J. (1993) The mechanical properties of non-crimped fabric-based composites. *Composites*, **24** (5), 423–32.

Fabric drape modelling and preform design

5

Andrew C. Long and Chris D. Rudd

5.1 INTRODUCTION

As described in Chapter 6, on preforming, there are a variety of methods available for producing preforms for resin transfer moulding (RTM). Although there are a number of textile-based techniques which can be used to produce relatively complex preforms directly from yarns or rovings, these are usually limited to specific component geometries such as regular prismatic sections and it is often necessary to produce preforms by forming or stamping reinforcement fabrics. However, the formability of the fabrics, which are usually bidirectional and may be either woven or stitch-bonded ‘non-crimp’ materials, is limited by their construction. In particular, fabric wrinkling can occur in areas with complex curvature, which would lead to rejection of the preform on grounds of quality. This may be alleviated by selecting an alternative reinforcement, by reorientating the fabric or by constraining the reinforcement in a blank-holder or ‘pinching frame’ to ensure that the fibres are held in tension during forming. In practice this is usually achieved by trial and error, although ideally it would be desirable to have a computer-aid engineering (CAE) system based on a reinforcement deformation model to support preform design. Another important application for such a system is the prediction of the fabric net-shape, which would allow the reinforcement layers to be cut prior to deformation.

Another associated problem with reinforcement deformation is that the resulting variations in fibre volume fractions and orientations inevitably lead to variations in the processing and performance characteris-

tics of the preform. As well as leading to a non-uniform distribution of mechanical properties across the component there may also be a significant effect on the impregnation properties of the preform. Conventional methods for preform, component and process design usually rely on data measured from flat plaques, which are not necessarily representative of the fibre architecture within the preform. Once again a CAE approach is required if these problems are to be accounted for at the design stage. Ideally, this would follow the route outlined in Figure 5.1, pro-

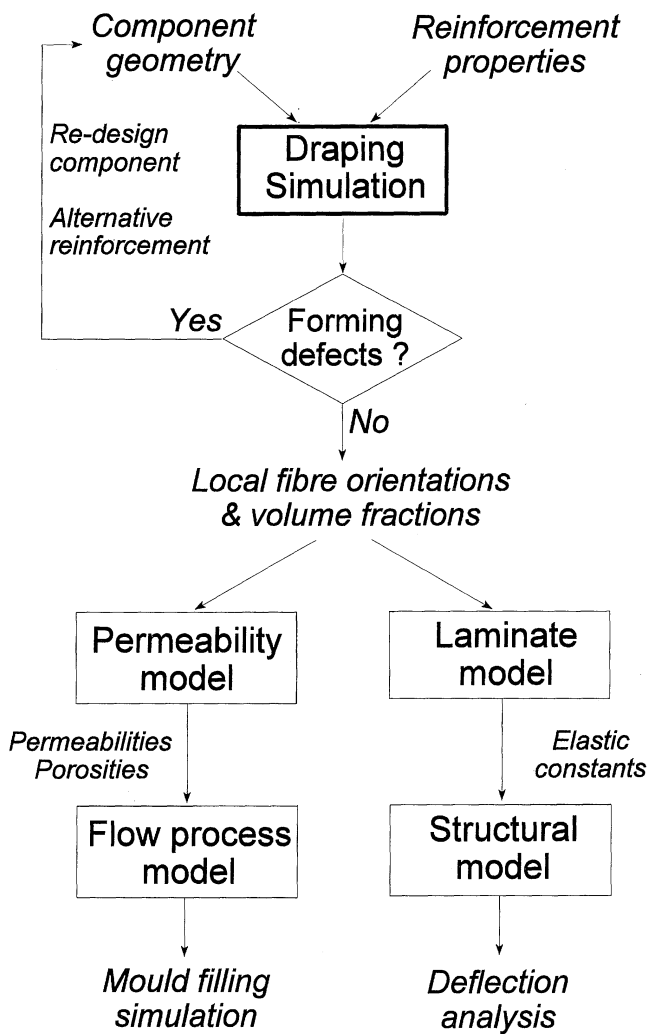


Figure 5.1 Computer-aided engineering approach to preform design.

viding an integrated design system encompassing fabric deformation, flow simulation and component structural analysis.

While manufacturing simulations are useful in their own right it is usually the case for aerospace structures that the ply orientations within the preform stack are dictated by performance considerations, with little scope for modification to suit the preforming process. It is also evident that many applications involve either single curvature or shallow deformations. In these cases the application of drape modelling may at first appear to be rather academic. However, as weight reduction becomes critical then even minor changes in laminate stiffness, such as those arising from fibre movements during fabric forming, can have significant effects on structural performance and these can be estimated conveniently by using a drape-modelling approach.

In recent years a number of researchers have developed fabric-deformation or ‘drape’ models. These are usually based on a kinematic mapping of the fibres onto the component surface, based on the assumption that fabric deformation is restricted to interfibre shear. This kinematic modelling approach is described in detail in the following sections, with a number of examples included to demonstrate the degree of deformation which may be expected for relatively complex component geometries. Methods for characterising reinforcement-deformation mechanisms are also described and demonstrated for a range of sample fabrics. The effects of deformation on the preform permeability and laminate mechanical properties are then discussed and demonstrated for a relatively complex component geometry.

5.2 FUNDAMENTALS OF FABRIC DEFORMATION

5.2.1 DEFORMATION MECHANISMS

Reinforcement fabrics are able to conform to non-developable surfaces via a number of deformation mechanisms. The behaviour of a particular material will depend on the fibre architecture, although a number of common mechanisms exist (as discussed in detail by Potter [1]). These are demonstrated in Figure 5.2 and can be summarised as follows:

- (a) Interfibre shear: fabrics are sheared as the fibres rotate about their crossover points (stitch or weave centres). The degree of shear is limited by the construction of the fabric, with each material exhibiting an effective “locking angle” which determines the limit of shear deformation. This is described in more detail in section 5.2.2.
- (b) Interfibre slip: some fabrics can deform by slippage at the fibre crossovers, so that the fabric is effectively stretched locally. This will usually only be significant when the fabric approaches the limit of

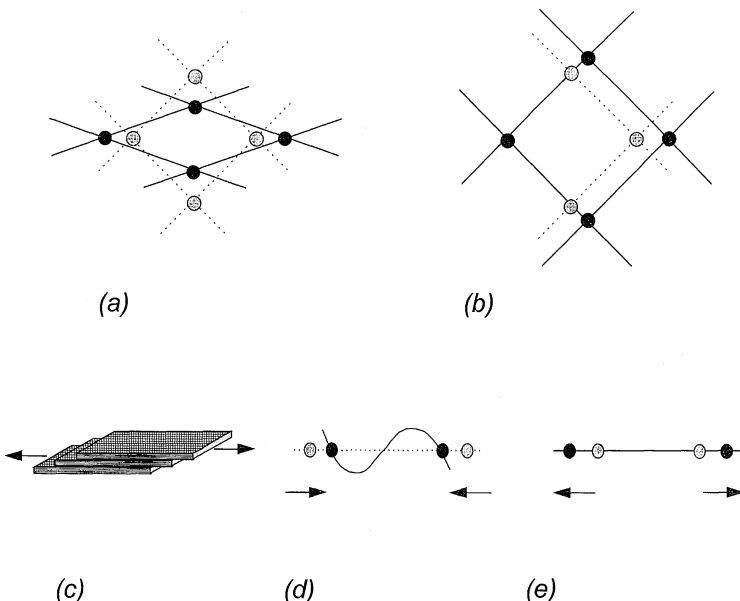


Figure 5.2 Fabric-deformation mechanisms: (a) interfibre shear; (b) relative slip; (c) interply slip; (d) fibre buckling; (e) fibre extension.

shear deformation, although it may be an essential mechanism in the production of complex component geometries.

- (c) Interply slip: when several layers of reinforcement are used the individual layers may slide relative to each other. This is most apparent when forming a region of single curvature.
- (d) Fibre buckling: this will occur when the fabric is subjected to local in-plane compression, resulting in the occurrence of wrinkles or folds in the preform. Fibre buckling is likely to occur when the limit of slip or shear deformation has been reached. Within a fabric drape simulation this may be anticipated by identifying regions where the interfibre angle has reached the measured fabric locking angle.
- (e) Fibre extension: this is likely to be negligible for most reinforcements, where the fabric shear stiffness is several orders of magnitude lower than the modulus of the individual fibres.

As will be described in section 5.3, in the development of fabric forming or ‘drapé’ simulations reinforcement deformation is usually assumed to be accommodated by fabric shear. This allows a relatively simple kinematic approach to be used. Other modes of deformation are not usually included, although as has been mentioned fabric wrinkling may at least be anticipated by specifying the fabric locking angle. In reality, the relative importance of each of the above mechanisms will be fabric-specific.

These may be characterised experimentally using the techniques described in the next section.

5.2.2 EXPERIMENTAL CHARACTERISATION

The useful deformation modes for fabric reinforcements differ according to the fibre architecture, although the two mechanisms of primary interest are in-plane shear and out-of-plane bending. The draping of fabrics over complex surfaces is a problem which occurs frequently in the garment industry and although reinforcement fabrics differ in that fibres are generally considered to be inextensible the two problems are closely related. Several international textile standards exist for the mechanical testing of fabrics, some of which have been adapted for application to composite materials and the more relevant tests are summarised here. For a useful review of the methods used for composite applications readers are referred to Yu *et al.* [2].

Simple shear testing

For materials which deform predominantly by the simple shear or scissoring mode of deformation, as described in section 5.2.1, this is an extremely informative test. The shear compliance and the deformation limit for a fabric can be measured by constraining the fabric sample in a simple shear test fixture. Two possible experimental approaches are illustrated in Figure 5.3. The parallelogram fixture [Figure 5.3(a)] can be used to constrain the fabric on either two or four sides, whereas the Treloar apparatus [Figure 5.3(b)] provides two-sided clamping only, with lateral tension applied via either a suspended mass or a light spring. In either case, a shearing force is applied in the bias direction while measuring the axial displacement. The stiffness or compliance is derived from the load versus displacement data (usually at modest shear angles) and a locking angle can be inferred by defining some arbitrary point beyond which no useful deformation can be induced. This is usually taken to occur when the slope of the force versus displacement curve approaches infinity or when visual indication of wrinkling occurs. Typical locking angles in the range 28° to 37° have been measured by Wang *et al.* [3].

Test results for glass and carbon fibre fabrics have been reported by several workers [2–4]. Figure 5.4 includes a number of characteristic loading curves obtained using the approach shown in Figure 5.3(b). This demonstrates the non-linearity of the shear compliance quite clearly. The maximum shearing angle (and by implication the potential for conformability) is associated with the transverse compaction of the fibre bundles and therefore increases with the tow spacing. The shear com-

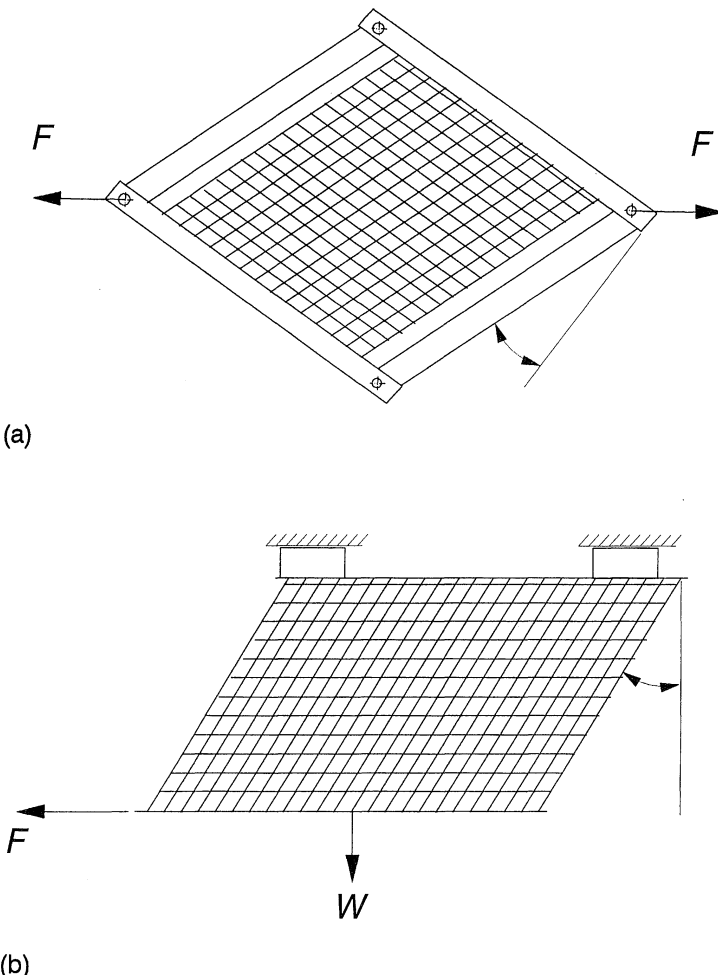


Figure 5.3 Experimental arrangements for measuring fabric in-plane shear properties: (a) parallelogram fixture; (b) Treloar shear apparatus.

pliance appears to be governed by friction at the tow crossovers and generally increases as the crossovers per unit area decrease. This causes a difficulty when attempting to apply relationships which are used for conventional sheet materials since the crossovers lie in the plane of the fabric and no relevant thickness effect can be calculated as in the case of solids. Consequently the data in Figure 5.4 are presented in terms of force per unit width (length of specimen clamped parallel to the shear direction). High superficial density fabrics made from heavy tows tend to have fewer crossovers per unit area and therefore less resistance to shear

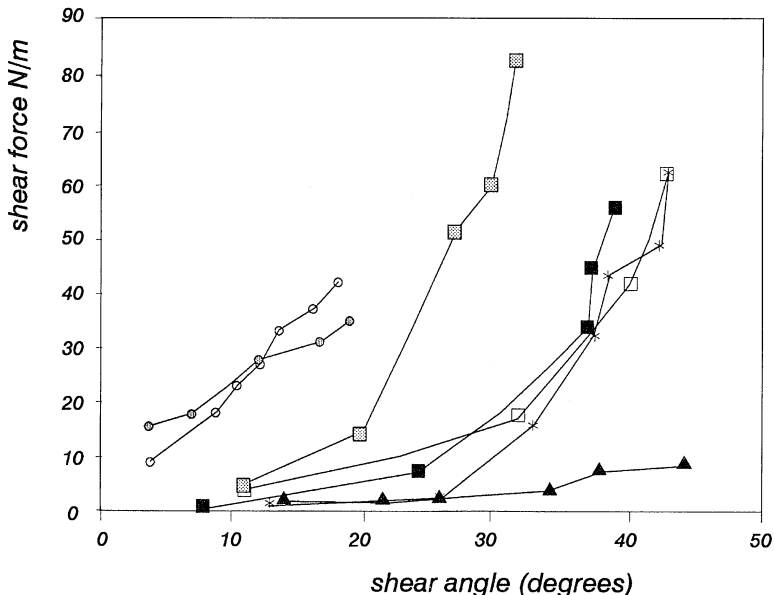


Figure 5.4 Typical shear data for fabric reinforcements. ▲ = plain weave, 85 g/m²; ○ = plain weave, 196 g/m²; ★ = plain weave, 160 g/m²; ■ = twill weave, 175 g/m²; × = twill weave, 300 g/m²; □ = satin weave, 300 g/m². Data from Robroek, L.M.J., *The Development of Rubber Forming as a Rapid Thermoforming Technique for Continuous Fibre reinforced Thermoplastic Composites*, PhD thesis, Delft University of Technology, 1994.

than have lighter fabrics. For woven materials this effect is complicated by the weave pattern used, and plain weaves (with the maximum degree of crimp) generally provide higher resistance than equivalent twill or satin weaves. The normalised fabric shear stiffness or shear rigidity (1/radians) can be defined by the following equation and provides a useful basis for comparing the relative formability of different fabrics [2]:

$$E_s^* = \frac{\Delta F_s}{\Delta \phi} \frac{1}{W h V_f E_f} \quad (5.1)$$

where

E_s^* is the normalised fabric shear rigidity;

ΔF_s is the change in applied force during testing;

$\Delta \phi$ is the change in the fabric shear angle;

W is the fabric width parallel to the direction of shear testing;

h is the height (thickness) of the reinforcement or laminate;

V_f is the volume fraction of the fibre reinforcement;

E_f is the tensile modulus of the fibre reinforcement.

Comparison of the shear stiffness of typical woven fabrics shows that these are typically several orders of magnitude lower than those for equivalent solid sheet materials such as metal foils and thermoplastic sheet. The ratio of shear compliance to tensile compliance for woven fabrics can be of the order of 10^5 . Although the precise values will obviously be a function of the fibre architecture it is apparent during forming that if any shear components exist then the fabric will probably shear to the maximum extent possible.

Bias ($\pm 45^\circ$) tensile testing

Although the test described in the previous section provides fabric shear stiffness and locking angles a dedicated system needs to be built for that purpose. An alternative approach is to use conventional in-plane tensile testing for $\pm 45^\circ$ fabric samples. The load versus displacement data can be interpreted to assess the tensile rigidity of the fabric, and it is also possible to determine the locking angle if the degree of shear is monitored during the test. If the transverse contraction is also measured an estimate of yarn slippage can be made using the method described by Potter [1]. This involves comparing the measured dimensional change with that of an ideal, pin-jointed net:

$$\text{Percentage slip} = \left(\frac{e_{\text{act}}}{e_{\text{th}}} - 1 \right) \times 100\% \quad (5.2)$$

where the actual extension ratio, e_{act} , can be measured in either the longitudinal or the transverse direction, and the theoretical value, e_{th} , is calculated from the measured shear angle and is based on pin-jointed behaviour.

Specimens usually exhibit a distinct 'hourglass' shape during testing, with a central region undergoing uniform deformation based predominantly on shear. The specimen size is typically much larger than that used in conventional laminate testing in order to overcome edge effects. Some care also needs to be taken with the test arrangement as the use of rigid clamps at the ends of the specimen introduces a region which cannot deform fully. Specimens thus need to be sufficiently long to provide a suitable gauge length in the fully deformed region. Care is also needed with the clamping arrangements, and the use of taped or rubberised jaws is common, although the latter method needs care in order to avoid introducing errors in the measurement arising from compliance of the rubber. Like the simple shear test, the load versus deflection curve is highly non-linear owing to the effects of crimp and yarn locking. This is demonstrated in Figure 5.5, which shows the variation in force per unit fabric width with axial strain for a zero-crimp (stitch-bonded) glass fabric. In this case the specimen width was 100 mm and the gauge length

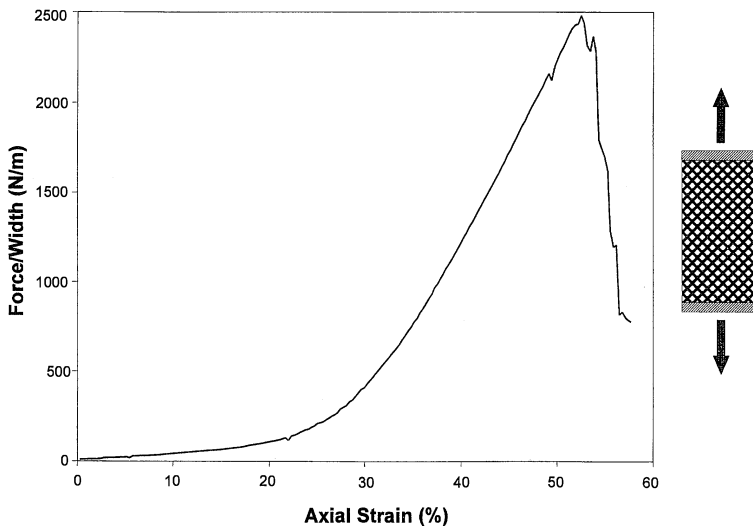


Figure 5.5 Typical uniaxial tensile data for a $\pm 45^\circ$ zero-crimp glass fabric (Tech Textiles E-BXhd 936).

was 250 mm. The peak force was observed to coincide with stitch failure in the fabric, which occurs when the material has reached the effective locking angle.

Fabric bending stiffness

Standard textile test methods (BS 3356, ASTM D1388-64, ISO 4604) provide the basis for measurements of fabric bending stiffness. The simplest of these involves the bending of the fabric under its own weight. This provides an approximate indication of the fabric conformability under low pressures. The method involves sliding a standard strip of fabric off the edge of a platform until the self-weight causes the fabric to bend to a specified reference angle for comparative purposes. The length of the strip which is necessary to reach this threshold value is recorded and normalised using its superficial density, which gives a relative bending stiffness.

An alternative method, which also characterises the response to single curvature bending, involves the use of a flexometer. A square sample is held rigidly on one edge while the other edge is constrained to move through an orbit such that a uniform curvature is induced in the sample. The bending curvature calculated from the position of the moving jaw and the bending moment (and thereby the flexural rigidity) is measured through a torque meter which is mounted on the fixed jaw. The test yields the bending rigidity and the shear hysteresis. The test is continued up to the point of critical curvature which is defined as the point at which

the fabric starts to buckle and therefore at which the bending load reduces. As with most fabric properties the bending rigidity is generally much higher in the warp and weft directions than in the bias direction, although unlike the in-plane shear tests the stiffness of the individual yarns has an important effect, thus carbon fabrics are generally more rigid than those produced from glass fibres (as demonstrated by Wang *et al.* [3]).

5.3 KINEMATIC DRAPE MODELLING

5.3.1 ASSUMPTIONS

A relatively simple approach has been developed by a number of researchers to simulate the deformation of both bidirectional fabric reinforcements and prepregs [5–11]. This is based on a simple kinematic algorithm, relying on the following assumptions which were first suggested by Mack and Taylor [12]:

- (1) the fibres are inextensible;
- (2) fibre crossovers (or nodes) act as pin-joints with no relative slip;
- (3) fibre segments are straight between joints;
- (4) uniform surface contact is achieved;
- (5) fabric layers are infinitely thin.

This approach allows the fabric to be approximated as an orthogonal network of threads which are connected by pin-joints and is thus usually referred to as the ‘pin-jointed net’ or ‘fishnet’ model. This is clearly an oversimplification of the real situation where a number of other deformation mechanisms exist, although as has been demonstrated in the previous section fabric shear would appear to be dominant for the majority of bidirectional reinforcements. The pin-jointed net model also provides a useful design limit, as it represents the ‘worst case’ scenario in which the effects of deformation on fibre orientations and volume fractions are maximised. However, the main advantage is the simplicity of the resulting algorithm, which effectively involves a geometric mapping of the fibres onto the component geometry.

5.3.2 FUNDAMENTAL EQUATIONS

To determine a unique deformed fibre pattern it is first necessary to specify two intersecting fibre paths on the component (or preform tool) surface. These paths determine the initial orientation of the reinforcement and are usually represented by means of geodesic paths which intersect at the initial contact point between the fabric and the pre-forming tool. Each node is described by the indices (m, n) , which rep-

resent the position relative to the intersection of the initially constrained paths (0,0). The position of each node can be determined by solving the equations of intersection between the fabric and the component surface. Given the assumptions described earlier this is equivalent to finding the point of intersection between the surface and two spheres representing the possible end points of each warp and weft fibre segment (as shown in Figure 5.6). Thus the necessary equations to locate each draped node are as follows:

$$(x_{m,n} - x_{m-1,n})^2 + (y_{m,n} - y_{m-1,n})^2 + (z_{m,n} - z_{m-1,n})^2 = S_m^2 \quad (5.3)$$

$$(x_{m,n} - x_{m,n-1})^2 + (y_{m,n} - y_{m,n-1})^2 + (z_{m,n} - z_{m,n-1})^2 = S_n^2 \quad (5.4)$$

$$f(x, y, z) = 0 \quad (5.5)$$

where

x, y and z are the draped coordinates of the node;

S is the interfibre spacing (in direction m or n).

Equation (5.5) describes the required component surface, which may be represented using a number of approaches. For a relatively simple geometry this may be described by a single expression. For example Robertson *et al.* [5] presented a simulation of fabric draping for a hemispherical surface, which was represented by means of a single implicit equation which allowed the equations of intersection to be solved explicitly. However, in most practical situations the component surface is unlikely to be described by a single expression and it is necessary to employ geometric modelling techniques (e.g. as described by Faux and

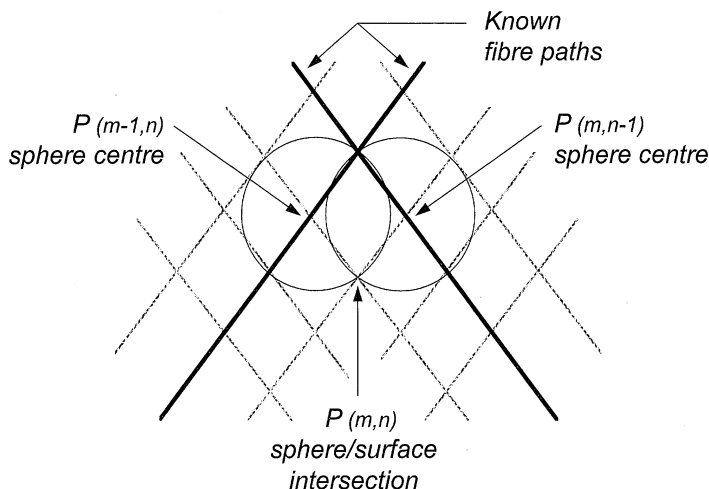


Figure 5.6 Intersection of surface with idealised reinforcement fabric.

Pratt [13]). The most convenient approach is to describe the surface by using a collection of adjoining patches or elements. Note that allowing for assumption (5) above it is most appropriate to represent the geometry by using the component mid-plane, ensuring that the resulting draped fibre pattern represents the ‘average’ properties of the reinforcement stack. There are several possible representations for each patch, which may be described by the general parametric form, $\mathbf{p}[u, v]$:

$$\mathbf{p}[u, v] = \mathbf{u} \mathbf{M} \mathbf{B} \mathbf{M}^T \mathbf{v}^T \quad u, v \in [0, 1] \quad (5.6)$$

where \mathbf{u} and \mathbf{v} are vector polynomial expressions in the surface patch parameters u and v , respectively; \mathbf{B} is a matrix defining the coordinates and continuity at the patch boundaries; and \mathbf{M} is a transformation matrix associated with the patch representation.

The order of the vector polynomials defines the level of continuity at the boundaries which can be achieved, although high-order polynomials require a larger number of constants for each patch definition. Van West *et al.* [7] used bicubic surface patches in a simulation of fabric draping for an arbitrary surface geometry. A combination of equations (5.3) and (5.4) with the appropriate parametric equation for a particular patch was used to determine the parameters u and v corresponding to the nodal position. Owing to the non-linear nature of this representation, an iterative solution was required based on the Newton–Raphson method.

In practice it may be difficult to determine the coefficients required to describe a surface using bicubic patches. A simpler approach involves the use of flat patches, allowing a conventional finite element mesh to be used to represent the component. An arbitrary bilinear (quadrilateral) plane surface patch with corners at \mathbf{p}_{00} , \mathbf{p}_{01} , \mathbf{p}_{10} and \mathbf{p}_{11} is defined by the parametric form

$$\mathbf{p}[u, v] = (1 - \mathbf{u} \quad \mathbf{u}) \begin{pmatrix} \mathbf{p}_{00} & \mathbf{p}_{01} \\ \mathbf{p}_{10} & \mathbf{p}_{11} \end{pmatrix} \begin{pmatrix} 1 - v \\ v \end{pmatrix} \quad (5.7)$$

Once again it is not possible to find an explicit solution to equations (5.3), (5.4) and (5.7), and a numerical solution is required. Alternatively the implicit form of the equation defining the plane containing the patch may be used:

$$ax_{m,n} + by_{m,n} + cz_{m,n} - d = 0 \quad (5.8)$$

where the coefficients a , b and c represent the element normal vector and can be calculated from

$$\begin{pmatrix} a \\ b \\ c \end{pmatrix} = (\mathbf{p}_{10} - \mathbf{p}_{00}) \times (\mathbf{p}_{01} - \mathbf{p}_{00}) \quad (5.9)$$

and d can be found by substituting the coordinates of any of the corner points into equation (5.8). This approach allows the location of each node to be determined explicitly [14]. The major disadvantage is the large number of elements required for an accurate surface representation. In practice this may be outweighed by the reduction in processing time enabled by the explicit solution of the intersection equations, and hence this is likely to be the most efficient approach.

5.3.3 DRAPING ALGORITHM

The draped fibre pattern can be determined by solving the equations of intersection between the surface and the possible positions of each node as described above. This is initiated by positioning nodes at equal spacings along the constrained fibre paths. As has already been mentioned in the previous section, these are usually defined as geodesics which intersect at the initial tool contact point during forming (the validity of this approach is discussed in section 5.4). In the majority of cases the constrained paths will divide the surface into four quadrants which may be simulated independently. The draping algorithm within each quadrant involves determining the position of each node along parallel fibre paths until the region is completely covered. As the surface is usually composed of a number of elements it is first necessary to determine the appropriate patch for each node. This can be achieved by testing for a solution to the intersection equations for each patch within the surface model. In the examples included below the surface is composed of flat patches so that the intersection equations may be solved explicitly. In this case a valid solution will produce a point which is both in the plane and within the boundaries of the patch (with the latter condition assessed by means of a containment algorithm). If a valid solution is not found, then it is assumed that the edge of the surface has been reached and the next parallel fibre is placed on the surface. If no solutions are found for subsequent fibres the quadrant must be completely covered and the process is repeated for the next quadrant.

5.3.4 EXAMPLES

The examples included in this section were generated using a personal-computer-based drape simulation developed at the University of Nottingham [9,14]. In each case the surface geometry is described by a collection of triangular or quadrilateral flat patches, with the initially constrained fibre paths represented by means of geodesics. An explicit solution was applied to the equations of intersection between the reinforcement and the surface geometry, as described in the previous section.

Bead stiffened panel

The first example is based on an analysis performed for the Cooperative Research Centre for Advanced Composite Structures (CRC-ACS), and is reproduced with their kind permission. The surface model represents a bead stiffened panel, which was to be produced by RTM using a woven carbon fabric reinforcement. One of the major objectives of the study was to determine the feasibility of a number of preform lay-ups based on combinations of $0/90^\circ$ and $\pm 45^\circ$ fabric orientations (as illustrated in Figure 5.7). During the drape analyses it was necessary to consider only one quarter of the component geometry, because of symmetry. The predicted fibre pattern for $0/90^\circ$ layers is shown in Figure 5.8. Maximum shear is anticipated towards the top right of Figure 5.8, in the region adjacent to one of the stiffening channels. The minimum interfibre angle in this region is predicted to be 40° , which may well lead to wrinkling during preform manufacture. Figure 5.9 demonstrates that a less severe problem is expected for $\pm 45^\circ$ layers. In this case, maximum deformation occurs at the top of the central stiffening channel, where the interfibre angle is reduced to 55° .

Local reinforcement shearing has the effect of drawing more material into a particular region, which will result in an increase in fibre volume fraction if the component thickness is to remain constant (as is usually the case for RTM). This will have a significant effect both on the impregnation characteristics of the fabric and on the mechanical properties of the moulded component, as will be discussed in section 5.5. The

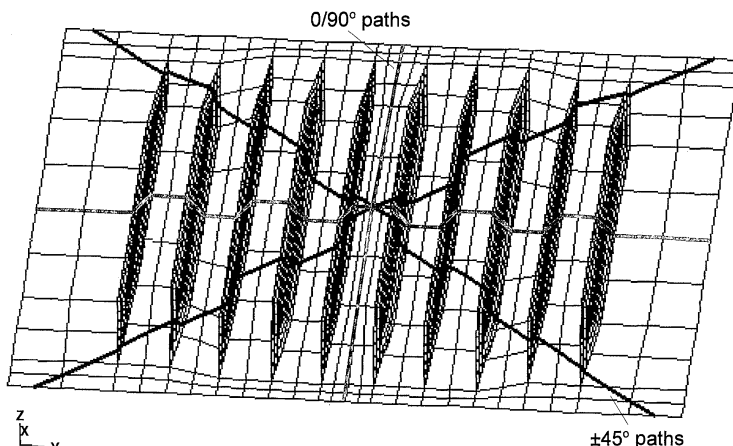


Figure 5.7 Surface model for bead stiffened panel, showing constrained fibre paths for alternative fabric orientations. Reproduced courtesy of the Cooperative Research Centre for Advanced Composite Structures Ltd, Fishermens Bend, Vic., Australia.

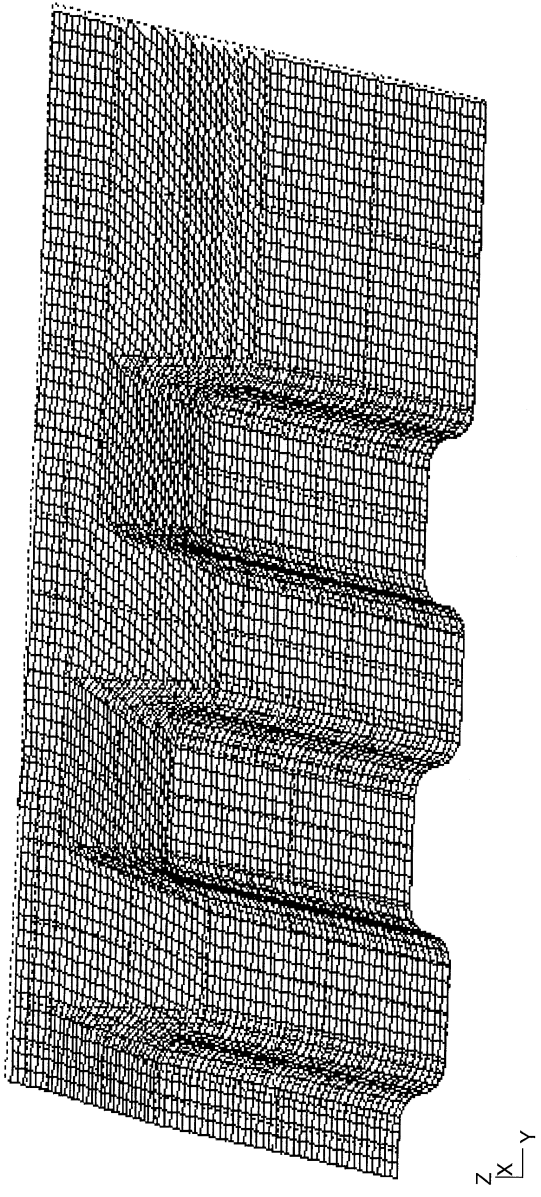


Figure 5.8 Predicted fibre pattern for bead stiffened panel draped with a 0°/90° fabric orientation. Reproduced courtesy of the Cooperative Research Centre for Advanced Composite Structures Ltd, Fishermens Bend, Vic., Australia.

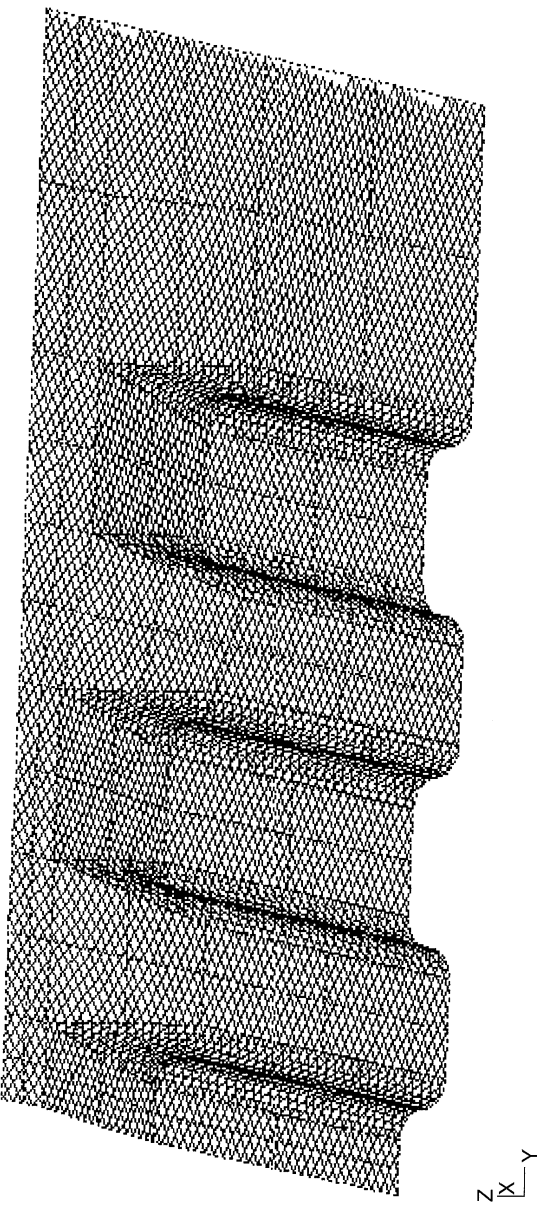


Figure 5.9 Predicted fibre pattern for bead stiffened panel draped with a $\pm 45^\circ$ fabric orientation. Reproduced courtesy of the Cooperative Research Centre for Advanced Composite Structures Ltd, Fishermens Bend, Vic., Australia.

relationship between volume fraction, V_f , and the interfibre angle, β , is given by:

$$V_f = \frac{V_{f_0}}{\sin \beta} = \frac{D_0^s}{\rho_f h \sin \beta} \quad (5.10)$$

where

V_{f_0} is the initial volume fraction of the undeformed material;

D_0^s is the reinforcement superficial density (mass per unit area) for the undeformed material;

ρ_f is the density of the fibre reinforcement;

h is the thickness of the reinforcement.

This expression can be used to calculate the average fibre volume fraction for each element within the surface model. The proposed stack for the stiffened panel consisted of eight layers of satin weave carbon fabric, each with an initial (undeformed) superficial density of 290 g/m². For a constant component thickness of 2.24 mm and a given fibre density of 1800 g/m³, this equation gives a fibre volume fraction of 57% for un-sheared reinforcement. Figure 5.10 shows the predicted variation in volume fraction for a 0°/90° reinforcement orientation. In this case the volume fraction is expected to increase to 74% in the most highly sheared

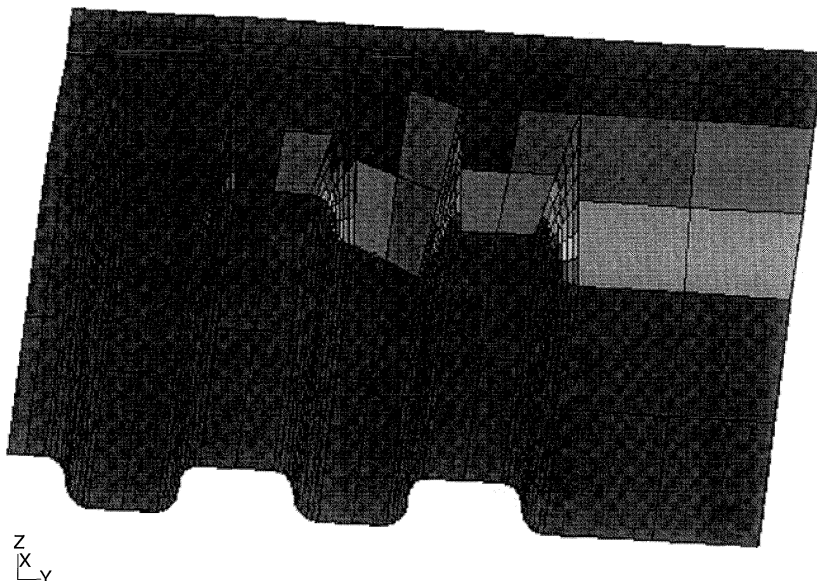


Figure 5.10 Predicted fibre volume fraction variation for bead stiffened panel based on a 0°/90° fabric orientation. Reproduced courtesy of the Cooperative Research Centre for Advanced Composite Structures Ltd, Fishermens Bend, Vic., Australia.

region. This is likely to exceed the maximum fibre fraction which can be achieved with the woven fabric. The equivalent maximum value for a $\pm 45^\circ$ orientation was 62%, which is less likely to be problematic.

Prototype wheel-hub

This component is based on the geometry of an automotive wheel-hub and represents a component with a significant amount of draw. The component is essentially dish-shaped, with a diameter of 396 mm, a depth of 118 mm and a thickness of 8 mm in the base and 6 mm elsewhere. Owing to symmetry it was only necessary to use a one quarter surface model for drape analysis. The constrained fibre paths were located along the edges of the surface model, intersecting at the axis of symmetry. Figure 5.11 shows the predicted draped fibre pattern, indicating that deformation is most pronounced in the central region of the rim, where the interfibre angle is reduced to 28° . The corresponding variation in fibre volume fraction is shown in Figure 5.12, which is based on five layers of zero-crimp glass fabric with a superficial density of 1134 g/m^2 . The volume fraction is significantly lower in the base of the component (at the top of the figure), where the component thickness is greatest. Within the thinner (6 mm) region, the initial (undeformed) volume fraction of 36% is expected to increase to 63% in the region of maximum deformation. This variation has been confirmed experimentally, as discussed in the next section.

The output from the draping simulation can be used to generate the fabric net-shape required to form the component to the exact perimeter

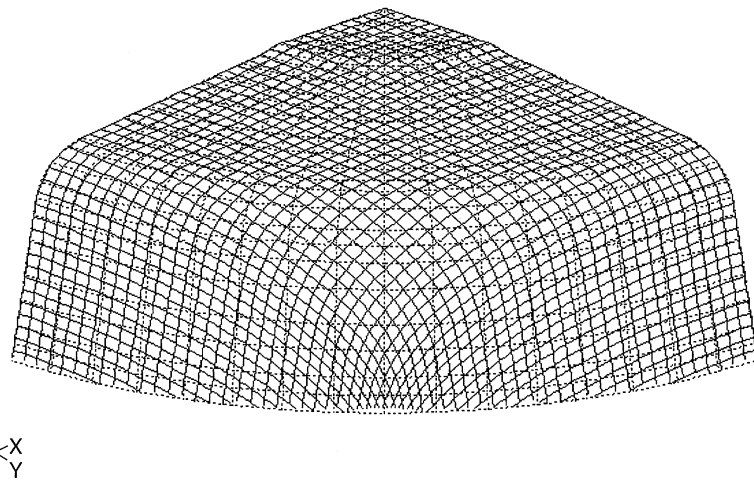


Figure 5.11 Predicted fibre pattern for prototype wheel-hub.

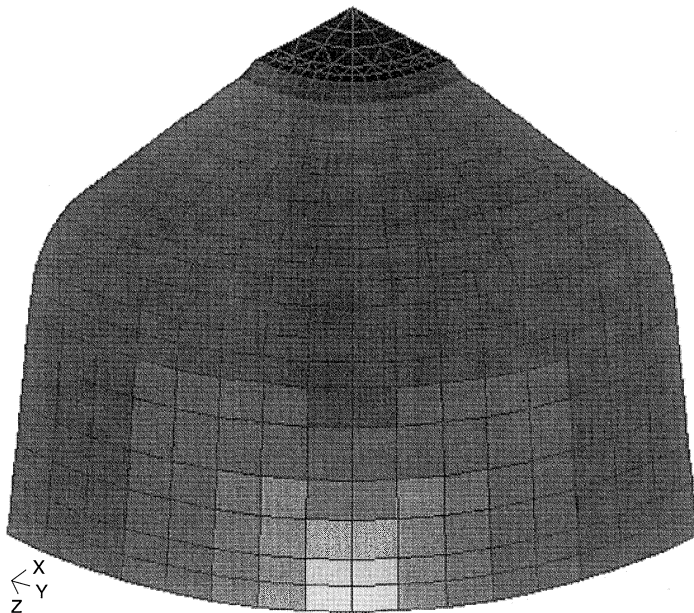


Figure 5.12 Predicted variation in fibre volume fraction for prototype wheel-hub.

of the mould. This is achieved by mapping each node back to its original position in the undeformed sheet. Figure 5.13 shows the predicted fabric net-shape for the wheel-hub. This was subsequently used as a template for reinforcement layers within the actual preform stack, proving to be extremely accurate, as no further trimming was required after forming.

5.4 DRAPE MODEL VALIDATION

Although a number of kinematic draping simulations have been developed, relatively little evidence has been published to verify the accuracy of this approach. To validate the model a technique is required to measure the positions and orientations of fibres within the deformed fabric. Such a technique would also be of use in determining the relative importance of the fabric deformation mechanisms described in section 5.2. In this section, methods which can be used to obtain a quantitative measure of fabric deformation are described. These are used to establish the validity of the kinematic drape model.

5.4.1 FIBRE VOLUME FRACTION VARIATION

As discussed in section 5.3, one measurable effect of fabric shear is a local increase in fibre volume fraction [given by equation (5.10)]. The pre-

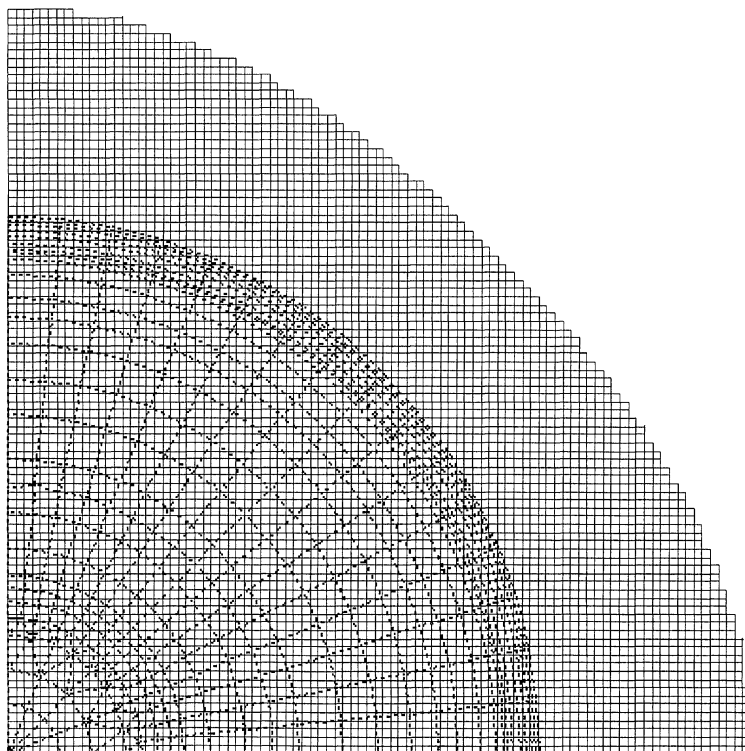


Figure 5.13 Predicted net-shape for wheel-hub reinforcement layers.

dicted variation in volume fraction for a particular component can be compared with measured values at specific locations using burn-off (loss on ignition) or acid digestion tests. This is demonstrated in Figure 5.14, which compares the predicted and measured volume fractions around the rim of the prototype wheel-hub described in section 5.3.4. Two experimental values are included at each location representing different quadrants of the component. The predicted and measured values are in close agreement, apart from one value in the most highly sheared region which may indicate the onset of interfibre slip or fabric wrinkling. However, it should be noted that this correlation applies only to the behaviour of a specific fabric and for a single geometry. It is likely that an alternative fabric or geometry may provide a less satisfactory correlation.

5.4.2 AUTOMATED STRAIN ANALYSIS

This method involves measuring the deformation of a square grid which has been printed onto the reinforcement fabric, and it is based on a

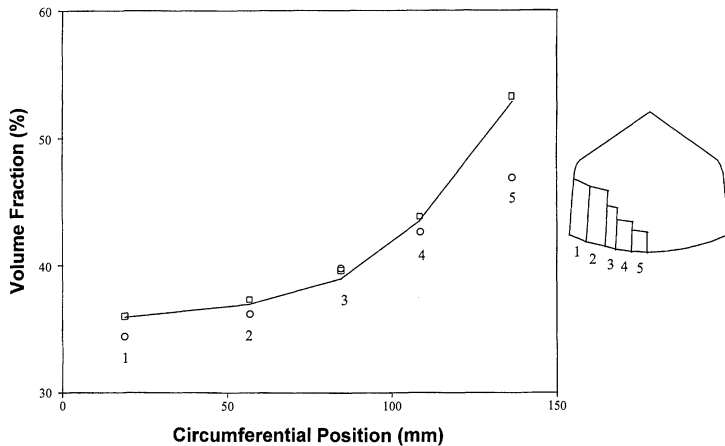


Figure 5.14 Comparison of predicted and measured fibre volume fractions around the wheel-hub rim (with burn-off specimen locations shown on the inset figure). — predicted value; □ ○ = experimental values.

technique developed by Ford Motor Company to characterise sheet metal formability. Figure 5.15 shows a schematic representation of the system, known as the CAMSYS Automated Strain Analysis and Measurement Environment (ASAME). This consists of a turntable on which the deformed specimen is placed and a digital camera positioned using

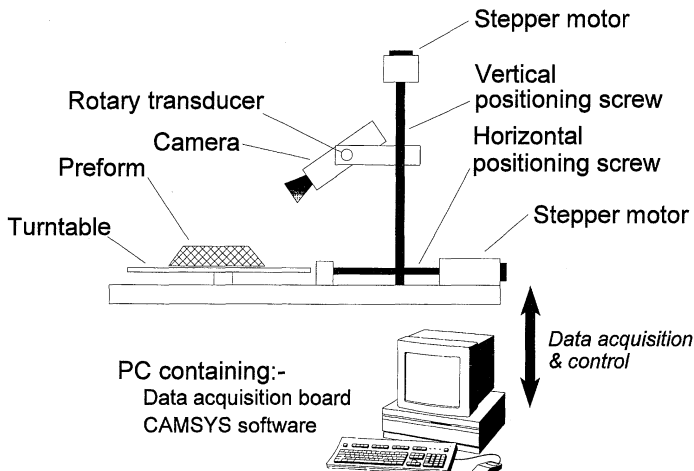
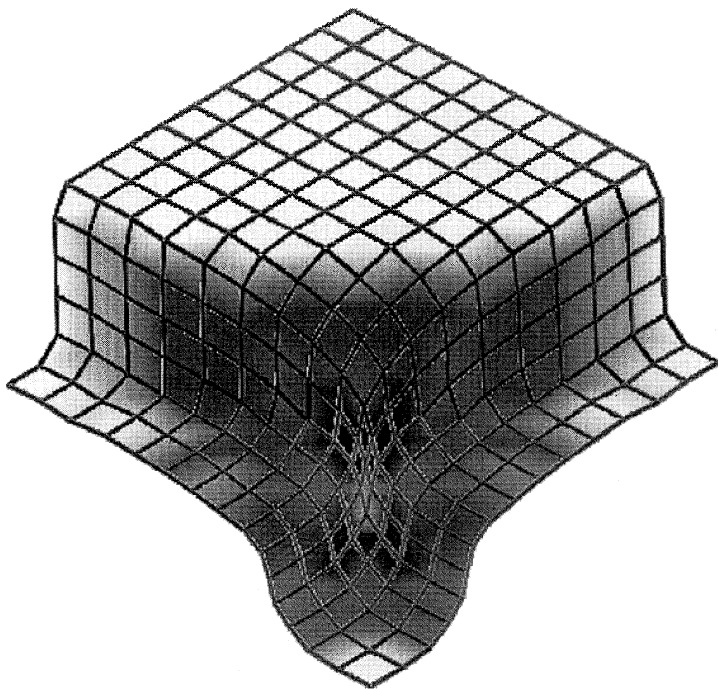


Figure 5.15 Schematic of the CAMSYS Automated Strain Analysis and Measurement Environment, developed by the Ford Motor Company.

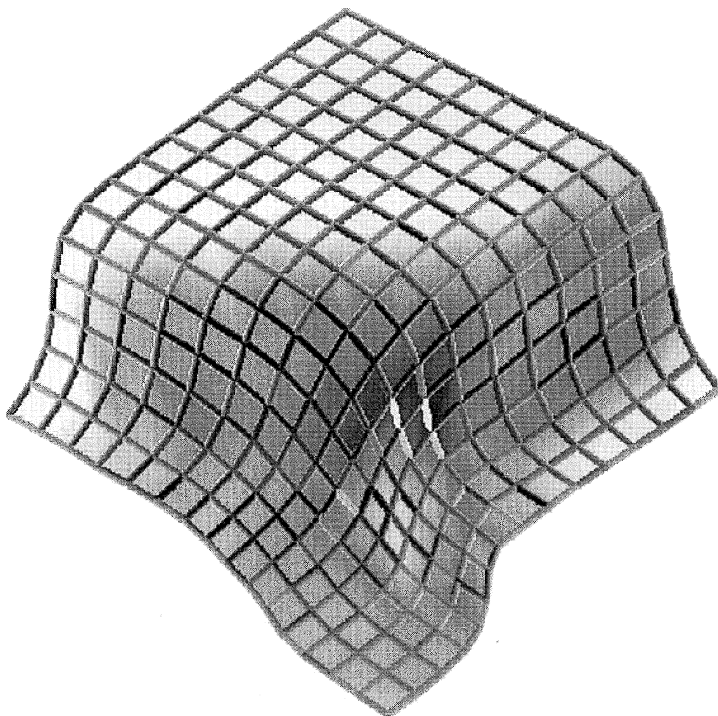
stepper-motor-driven lead screws. Deformation is measured by capturing two digital images of the grid from different orientations. A more detailed description of the system and data analysis methodology is given by Vogel and Lee [15].

To establish the applicability of this process to reinforcement deformation, experiments were carried out [16] using a zero-crimp $\pm 45^\circ$ glass reinforcement. This material is of particular interest as it is designed to be a 'high drape' reinforcement in which interfibre slip may be an important deformation mechanism because of the relatively 'loose' stitching. A 6.4 mm square grid was screen printed onto one surface of each fabric specimen. The material was deformed over a number of male forms by means of a vacuum bag and was subsequently rigidised using an aerosol varnish. The deformed grids were then scanned to provide the positions of each grid intersection, which were post-processed to provide information relating to the fibre architecture. Although this information is generally used to provide the material surface strains, which are of relevance when forming sheet metals, in this case the local interfibre angles and grid spacings were of more interest.

Five 120 mm diameter discs with heights of between 7 mm and 38 mm were used to establish the effect of depth of draw on fabric deformation. Drape analyses were carried out for each of the discs to enable comparison between the predicted and measured fibre architectures. This is demonstrated in Figures 5.16(a) and 5.16(b), which show, respectively, the predicted and measured fibre patterns for the 26 mm disc. A comparison of the fibre patterns would suggest that the drape model is reasonably accurate except in the most highly deformed regions, where interfibre slippage becomes significant. The minimum measured fibre angles (corresponding to maximum deformation) for each quadrant and at each disc height are compared with the predicted values in Figure 5.17. Whereas the predicted minimum interfibre angle continues to reduce with increasing disc height, the measured values level off at approximately 32° owing to fibre locking. After this point any further deformation was accommodated either by interfibre slip or by fabric wrinkling. It should, however, be noted that although there is a significant discrepancy between the predicted and measured orientations in the region of maximum shear, the agreement is significantly better for the majority of measurements. More generally, this study would suggest that, for this particular reinforcement fabric, the pin-jointed deformation model is reasonably accurate for relatively simple geometries where the fabric does not approach its deformation limit. However, as the geometric complexity is increased, other deformation mechanisms, including interfibre slip or fabric wrinkling, which are likely to be fabric-specific phenomena, may become increasingly important.



a



b

Figure 5.16 Deformed fibre distributions for a 26 mm high disc (where surface shading indicates the local degree of fabric shear): (a) predicted pattern; (b) measured pattern.

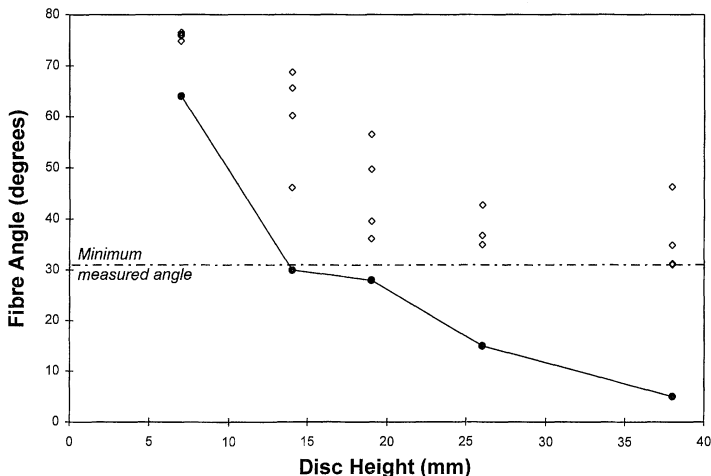


Figure 5.17 Comparison of predicted (●) and measured (◊) minimum interfibre angles for discs of increasing height.

5.5 EFFECTS ON PROCESSING AND PERFORMANCE CHARACTERISTICS

The variations in fibre orientation and volume fraction associated with fabric deformation are likely to have a significant effect both on the impregnation characteristics of the preform and on the mechanical properties of the resulting component. The accuracy both of structural analyses and of flow simulations is dependent on the quality of the input data, which is in turn a function of the fibre architecture. As the fibre architecture is a function of the preform manufacturing process, an effective design solution should be based on a combination of the predicted fibre distribution with structural analysis and flow simulation packages (as outlined in Figure 5.1). This section describes experimental and analytical methods for obtaining the necessary material property data to achieve such a combination. Although the intended application is for preforms produced by forming of aligned fabrics, it is likely that the results are applicable to other preforming processes such as braiding.

To assess the effect of fabric shear on reinforcement permeability and laminate mechanical properties, reinforcement layers were sheared by means of a four-bar linkage, as shown in Figure 5.18. The reinforcement was clamped along two edges, with one edge attached to the laboratory bench and the other edge free to move to achieve the desired level of shear. Sheared fabric samples were subsequently used in flow experiments to determine their in-plane permeabilities and as preforms for moulding by RTM, with the resulting laminates tested for mechanical

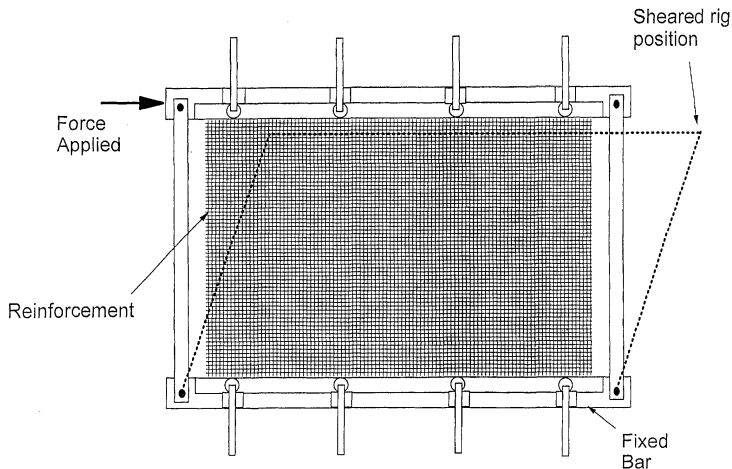


Figure 5.18 Schematic of the four-bar linkage used to produce sheared reinforcement samples.

properties. A more detailed description of the techniques involved is given elsewhere [16, 17].

5.5.1 IMPREGNATION PROPERTIES

Simulations of the injection phase during liquid composite moulding (LCM) rely on an accurate knowledge of the reinforcement permeability. This is defined by Darcy's Law (which is described in Chapter 7, on preform permeability) as the ratio between the fluid velocity and the pressure gradient and is considered to be a property of the reinforcement which expresses the ease of impregnation. Permeability is usually determined by means of a simple flow experiment within a two-dimensional cavity. This is conventionally applied to undeformed (roll-stock) reinforcements and thus neglects the effects of reinforcement deformation. In particular, local reinforcement shear causes changes in both fibre orientation and volume fraction. From equation (5.10) it is clear that shear deformation will lead to an increase in fibre content, which is likely to result in a significant reduction in permeability.

The permeability of a deformed bidirectional reinforcement can be estimated by assuming the fabric to be composed of two unidirectional (UD) layers. Several models exist for predicting the permeability of a UD reinforcement from the fibre architecture. Probably the most commonly used expression is the Kozeny–Carman equation, which relates permeability to the fibre radius and volume fraction. The axial permeability, (k_1), can be calculated as follows:

$$k_1 = \frac{r_f^2}{4c} \frac{(1 - V_f)^3}{V_f^2} \quad (5.11)$$

where r_f is the fibre radius and c is the Kozeny constant and is dependent on the geometric form of the reinforcement. In general the value of this constant must be determined experimentally, although this can be problematic for UD reinforcements as the fibre architecture is susceptible to washing during flow experiments.

The principal permeabilities of the combined bidirectional reinforcement can be approximated by applying a transformation to the axial values and employing a simple addition rule. For a reinforcement with ply angle $\pm\theta$, the fibre volume fraction can be calculated by means of equation (5.10) (setting $\beta = 2\theta$). The axial permeability is then determined by using the Kozeny–Carman equation, with appropriately selected values for the fibre radius and Kozeny constant. As the transverse permeability (k_2) of a UD reinforcement is negligible in comparison with the axial value, it is assumed to be zero to simplify the analysis presented here. This gives the following expression for flow parallel to the major axis of the fabric (which corresponds to the bisector of the two fibre axes):

$$k_x = k_1 \cos^2 \theta \quad (5.12)$$

Note that this is a simplified version of the expression derived by Advani *et al.* [18], which is based on a more rigorous treatment of the permeability tensor transformation:

$$k_x = k_1 \cos^2 \theta + k_2 \sin^2 \theta - \frac{(k_2 - k_1)^2 \sin^2 \theta \cos^2 \theta}{k_1 \sin^2 \theta + k_2 \cos^2 \theta} \quad (5.13)$$

Equation (5.13) is appropriate if experimentally determined values are used both for the axial and for the transverse permeabilities. However, equation (5.12) is preferred in this analysis as it results in reduced complexity when determining the appropriate constants for the semi-empirical axial permeability equation.

To determine the validity of this approach, permeability tests were carried out for a range of sheared reinforcements using a constant flow-rate radial flow arrangement (as described elsewhere [19]). An example of the resulting variation in permeability is shown in Figure 5.19, which represents the behaviour of a 0%90° zero-crimp fabric (Tech Textiles E-LT 850). Four layers of reinforcement fabric were used, with a cavity thickness of 4 mm, resulting in an unsheared fibre volume fraction of 32.6%. The appropriate value for the Kozeny constant (0.0404) was obtained by means of a least squares method based on the experimental data, and the fibre radius (7.5 μm) was obtained from manufacturers' data. Reference to Figure 5.19 suggests that there is generally excellent agreement between predicted and measured permeabilities over the

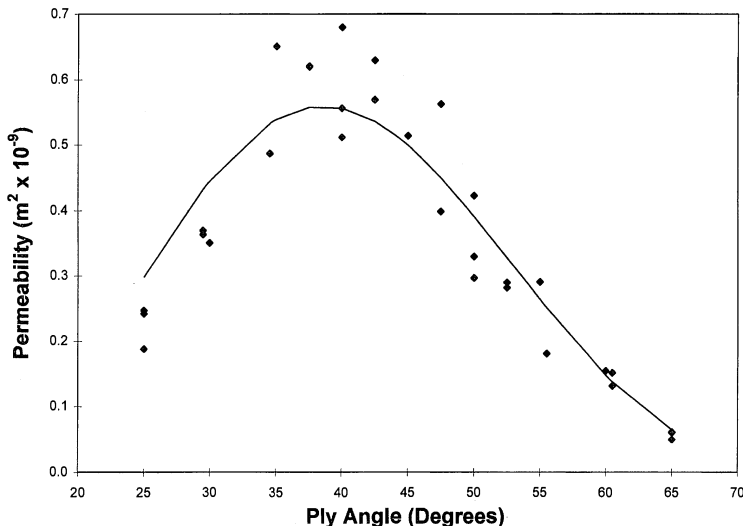


Figure 5.19 Variation in permeability with shear angle for a 0°/90° zero-crimp glass fabric. — = Theoretical value curve; ◆ = experimental value.

range of ply angles. The permeability decreases for ply angles above $\pm 45^\circ$ owing to the combined effects of fibre reorientation and increased volume fraction. For ply angles below $\pm 45^\circ$, a slight increase occurs for low levels of shear as fibres become aligned towards the direction of flow. However, as the ply angle is decreased (below 40°), the associated increase in fibre volume fraction becomes dominant and the permeability begins to fall. A similar trend has been observed in a number of other studies, as demonstrated in Figure 5.20, which compares the permeability–shear relationship for a plain weave fabric obtained by the present authors with data from Smit [20] and Ueda and Gutowski [21]. In each case the data have been normalised by using the undeformed ($\pm 45^\circ$ ply angle) permeability to account for the differing fibre volume fractions used in each study. The results show a reasonably good correlation, despite the fact that each study was based on different materials (Ueda and Gutowski used a seven harness satin weave, whereas Smit used Ten Cate RP0280 plain weave).

To establish the effect of fabric deformation on the filling phase during liquid moulding it is necessary to combine the draping simulation with a flow modelling package. This has been demonstrated for the prototype wheel-hub described earlier [14]. The predicted fibre orientations and volume fractions were used to establish the principal permeabilities for each element within the surface model. This information, along with the fabric porosity distribution, was used as input data for a control volume/

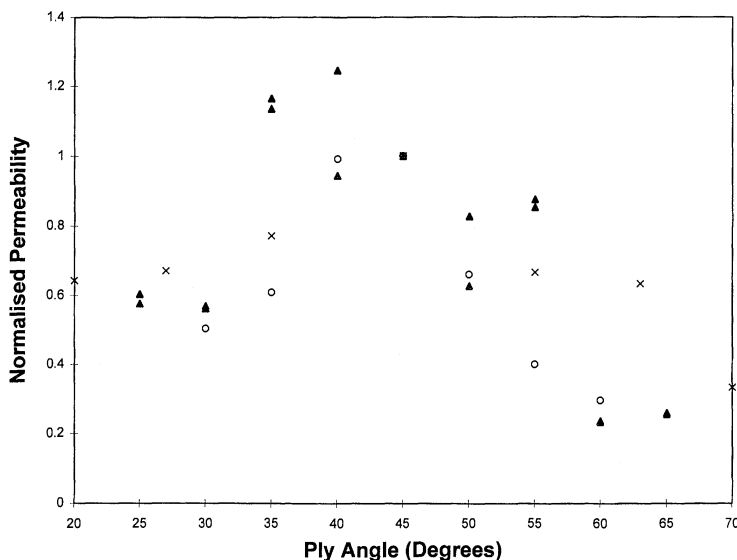


Figure 5.20 Comparison of published permeability data for sheared woven glass fabrics. ▲ = plain weave (data from Smith *et al.*); ○ = plain weave (data from Smit); x = satin weave (data from Ueda and Gutowski). Sources: Smit, A., The effect of shear deformation on the permeability of reinforcement fabrics for resin transfer moulding, MSc thesis, Delft University of Technology, 1995; Smith, P., Rudd, C. D. and Long, A. C., The effect of shear deformation on the processing and mechanical properties of aligned reinforcements, *Composites Science and Technology*, 1996; Ueda, S. and Gutowski, T. G., Anisotropic permeability of deformed woven fabrics, submitted to *Composites*, 1996.

finite element flow modelling package (known as CFILL, developed by Crescent Consultants Ltd [22]). It was assumed that the resin was injected through a central pin-gate at a constant flow rate sufficient to fill the mould in approximately 3 s [corresponding to the structural resin injection moulding (SRIM) moulding cycle used in practice]. Two analyses were carried out to study the effects of various factors associated with reinforcement deformation. The first was intended to isolate the effect of fibre orientation and used permeabilities based on the predicted fibre orientations with the fibre content held constant. Figure 5.21(a) shows the predicted flow front locations throughout filling, indicating that flow is promoted in the most highly sheared region, where the fibres are orientated in the radial direction. The results of the second analysis, which included both fibre orientation and volume fraction changes, are shown in Figure 5.21(b). Although the effects are less significant than in the previous analysis, a clear flow leader still exists in the most highly sheared region. This is despite the local reduction in permeability caused by the increased fibre content in this region, as the corresponding

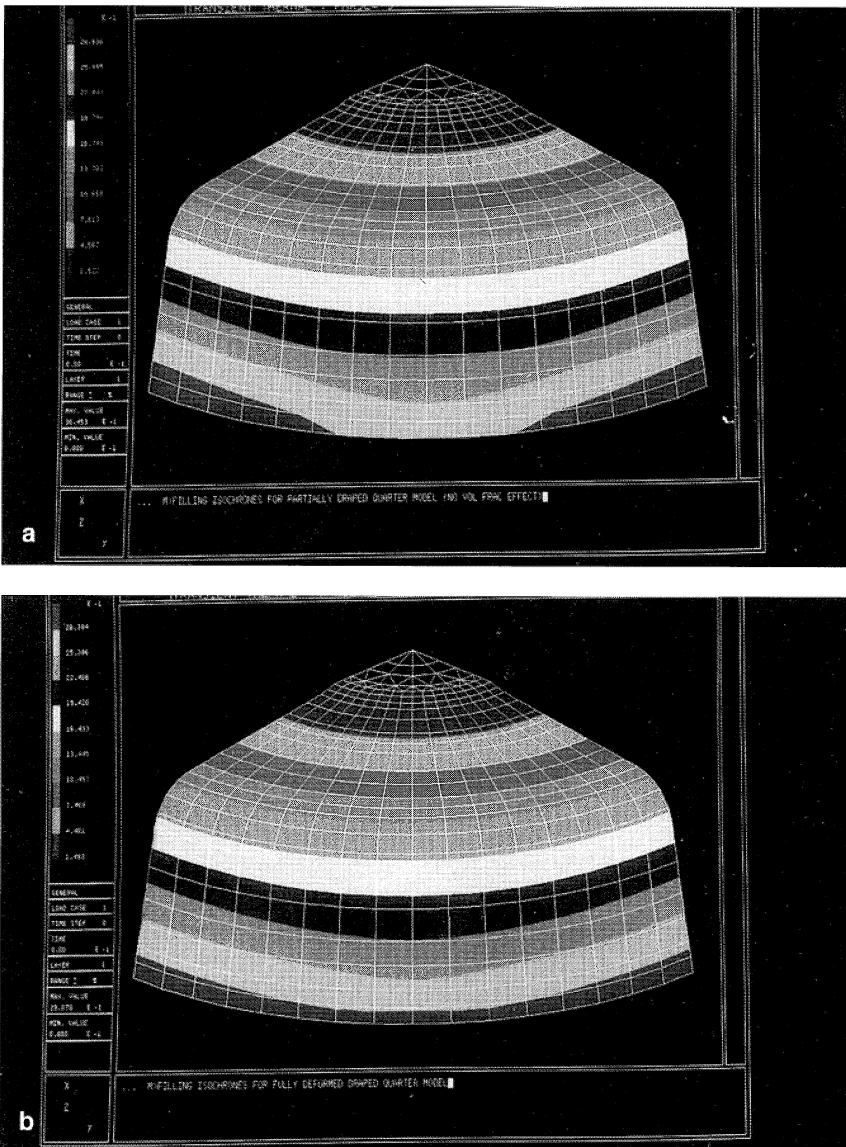


Figure 5.21 Predicted flow front locations for a prototype wheel-hub based on 'draped' fibre architectures: (a) fibre reorientation only; (b) combination of fibre re-orientation and volume fraction variation.

decrease in porosity implies a reduced volume of resin required for impregnation. To validate this analysis, a number of short shots were carried out at intervals corresponding to the isochrones in Figure 5.21.



Figure 5.22 Short shot for the wheel-hub, demonstrating preferential flow.

An example is shown in Figure 5.22, which shows the flow front position after injection for 2.8 s. The flow is most advanced in the most highly sheared region, as anticipated by the flow analysis.

5.5.2 MECHANICAL PROPERTIES

The effect of fabric shear on the subsequent laminate mechanical properties can be estimated by means of classical laminate theory. This can be achieved by assuming the laminate to be comprised of two unidirectional (UD) plies corresponding to the warp and weft fibres within the fabric reinforcement. The properties of each UD ply may be estimated by using the Halpin-Tsai equations. The longitudinal modulus, E_1 , and Poisson's ratio, ν_{12} , of a UD composite can be estimated from the properties of the constituent materials from the following expressions:

$$E_1 = E_r(1 - V_f) + E_f V_f \quad (5.14)$$

$$\nu_{12} = \nu_r(1 - V_f) + \nu_f V_f \quad (5.15)$$

in which subscripts r and f refer to the resin matrix and the fibre reinforcement, respectively. The transverse and shear moduli are calculated by the expression

$$M = M_r \frac{(1 + \xi \lambda V_f)}{(1 - \lambda V_f)} \quad (5.16)$$

where

$$\lambda = \frac{(M_f - M_r)}{(M_f + \xi M_r)} \quad (5.17)$$

M is the appropriate modulus and ξ is dependent on factors such as the aspect ratio and the packing arrangement of the fibres. Generally, the appropriate values of ξ are determined empirically from experimental results, although Halpin [23] suggests that for fibre volume fractions of up to 65% values of 2.0 and 1.0 are appropriate for the transverse modulus and the shear modulus, respectively.

By employing a transformation based on the required ply angle and then applying a unit stress to the off-axis compliance matrix it is possible to predict the corresponding laminate tensile modulus and Poisson's ratio (as described in more detail elsewhere [17]). To assess the validity of this approach, flat plaque mouldings were manufactured by RTM with use of aluminium tooling with a cavity thickness of 3.5 mm. Preforms were produced with use of a range of reinforcements which were pre-sheared by the method described above. One example is included here, based on three layers of 0°/90° zero-crimp reinforcement (Tech Textiles E-LT 850) with a vinylester resin (Dow Drekane 8084 with 1% by mass Interox TBPEH catalyst). This resulted in a fibre volume fraction of 28% for laminates with unsheared reinforcement. After post-cure at 130°C for 24 h the elastic properties were measured with an Instron 1195 Universal Testing Machine to a method encompassing BS 2782. The fibre and matrix properties used in this analysis are included in Table 5.1.

Figure 5.23(a) compares the experimental moduli at a range of ply angles with those predicted using the classical laminate model. The predicted and measured values agree reasonably well, with both showing a reduction in modulus as the ply angle is increased up to ±55°. Above this value the associated increase in fibre volume fraction causes a slight increase in modulus. The variation in Poisson's ratio with shear is demonstrated by Figure 5.23(b), which compares the measured values with those predicted using the classical laminate approach. Poisson's ratio appears to reach a peak at a ply angle of approximately ±30°, and then reduces gradually as the ply angle is increased. Similar trends have been observed for a range of reinforcements including zero-crimp and woven fabrics. The next stage in this work is to apply this procedure to predict the distribution of elastic constants for a complex component, based on the fibre architecture predicted by the draping simulation.

Table 5.1 Fibre and matrix properties. Source: Manufacturers' data, except where stated

Material	Tensile modulus (GPa)	Shear modulus (GPa)	Poisson's ratio	Density (kg/m ³)
Glass fibre	73.0	29.9	0.22	2605
Vinylester resin	3.3	1.2	0.38	1120 ^a

^a Measured value from cured resin sample.

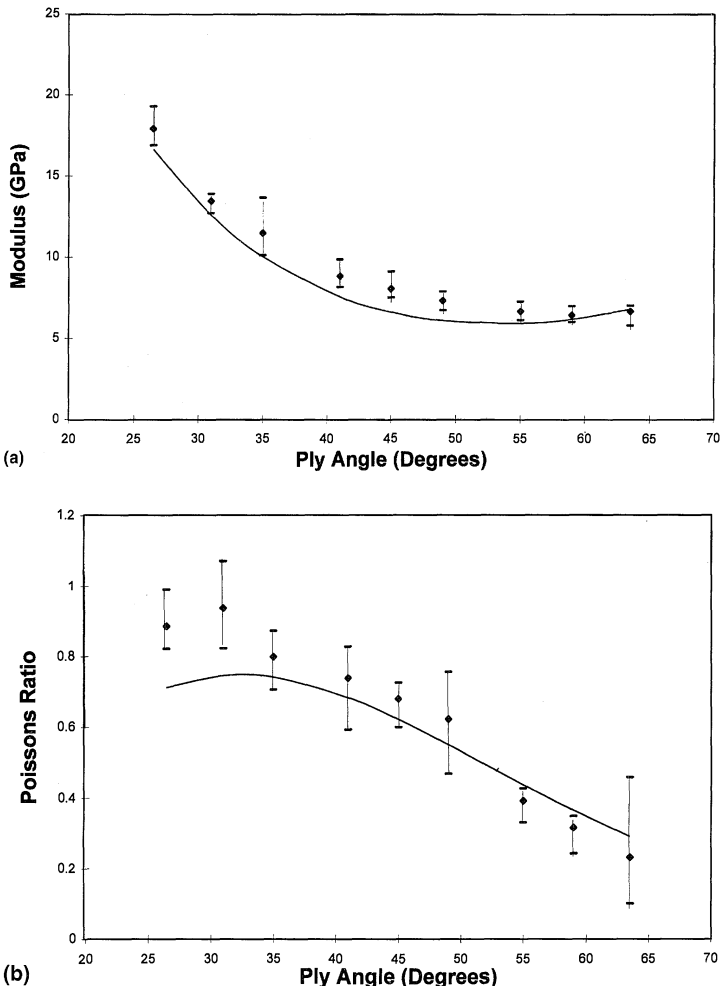


Figure 5.23 Variation in (a) tensile modulus; (b) Poisson's ratio with shear angle for 0°/90° zero-crimp glass fabric/vinylester resin laminates. — = Laminate theory curve; ♦ = experimental value.

These data could then be used within a structural analysis to establish the effects of fabric deformation on the deflections under specific load cases. Preliminary experimental work in this area has shown that the effects can be significant [24]. However, although the results above would suggest that tensile modulus and Poisson's ratio can be predicted with reasonable accuracy, less success has been obtained in estimating the shear modulus using classical laminate theory. It is hoped that an alternative approach may be used to produce more accurate data, which

would allow the link between drape modelling and structural analysis to be completed.

5.6 DISCUSSION

The kinematic or ‘pin-jointed net’ approach to drape modelling has been shown to be reasonably accurate for relatively simple geometries, where the fabric does not approach its locking angle. However, there are a number of deficiencies which must be addressed to develop a more useful and robust design tool. Perhaps the most important of these is that the kinematic model has no way of distinguishing between different reinforcements, other than in the specification of a locking angle representing the onset of wrinkling. In reality, fabric deformation must be dependent on the fibre architecture. This is particularly evident for so-called ‘high drape’ fabrics, which may allow a significant degree of inter-fibre slippage to enable the forming of complex geometries. Another difficulty is in the specification of the initially constrained fibre paths. At present, these are specified by use of geodesic paths, although the validity of this approach for components which do not exhibit any symmetry has yet to be established. Van West *et al.* [7] have demonstrated that the initial constraints can have a significant effect on the draped fibre pattern. An alternative approach is to simulate the forming process sequentially, with the position of each node determined iteratively at each stage to minimise the energy required for the fabric to conform to the surface. Such an approach has been developed by Bergsma [8], although a number of difficulties were reported and it was generally felt that this resulted in a far more complex and less robust draping algorithm.

An alternative approach to fabric deformation modelling may arise from the extensive research carried out into more conventional forming operations. In particular, a number of commercial packages are now available for simulating sheet-metal forming. These generally employ the finite element method to solve large strain problems within an incremental deformation scheme (an overview of the analytical methods usually employed is provided by Kobayashi *et al.* [25]). It may be possible to apply a similar approach to reinforcement fabrics by using the appropriate fabric mechanical properties, in particular the fibre moduli and the shear stress–strain relationship (which may be non-linear, as demonstrated in section 5.2.2). At each stage it would be necessary to redefine the fibre directions within each element, representing a single fabric unit cell, based on the local shear strain. Boisse *et al.* [26] applied this type of analysis to model the deformation of woven fabrics, using the finite element method with membrane elements used to represent the fabric. In this simulation, the shear forces were neglected as they were shown to be several orders of magnitude lower than the tensile forces within warp and

weft fibres. However, although this approach removes the need for specifying constrained fibre paths, it is not clear how it could be extended to include alternative deformation mechanisms such as interfibre slip.

Despite the deficiencies discussed above, it is clear that fabric drape modelling should play an important role in preform design. The use of drape simulations to establish the feasibility of producing a particular geometry, and to determine the optimum fabric orientation, is becoming increasingly popular, with a number of commercial packages now available. The ability to predict the fabric net-shape is also of benefit, not only to assist in lay-planning and fabric-cutting but also as a design tool for fibre placement systems [27]. This chapter has demonstrated the use of drape modelling for a number of components and has shown the associated property changes which may be significant for complex geometries. It seems likely that the CAE approach outlined in Figure 5.1, based on a combination of a draping simulation with flow modelling and structural analysis software, may provide the only sensible preform design solution.

References

1. Potter, K.D. (1979) The influence of accurate stretch data for reinforcements on the production of complex structural mouldings. Part 1. Deformation of aligned sheets and fabrics. *Composites*, **10**, 161–7.
2. Yu, J.Z., Cai, Z. and Ko, F.K. (1994) Formability of textile preforms for composites applications. Part One: Characterisation experiments. *Composites Manufacturing*, 113–21.
3. Wang, J., Page, J.R. and Paton, R. (1996) Experimental investigation into the draping properties of reinforcement fabrics. *Proceedings of the 2nd International Symposium on Aeronautical Science and Technology in Indonesia* (Vol. 2), Jakarta, June 1996.
4. Robroek, L.M.J. (1994) The Development of Rubber Forming as a Rapid Thermoforming Technique for Continuous Fibre Reinforced Thermoplastic Composites. PhD Thesis, Delft University of Technology.
5. Robertson, R.E., Hsiue, E.S., Sickafus, E.N. and Yeh, G.S.Y. (1981) Fiber rearrangements during the moulding of continuous fiber composites. 1. Flat cloth to a hemisphere. *Polymer Composites*, **2**, 126–31.
6. Smiley, A.J. and Pipes, R.B. (1988) Analysis of the diaphragm forming of continuous fiber reinforced thermoplastics. *Journal of Thermoplastic Composite Materials*, **1**, 298–321.
7. Van West, B.P., Pipes, R.B. and Keefe, M. (1990) A simulation of the draping of bidirectional fabrics over arbitrary surfaces. *Journal of the Textile Institute*, **81**, 448–60.
8. Bergsma, O.K. (1993) Computer simulation of 3D forming processes of fabric reinforced plastics. *Proceedings of the 9th International Conference on Composite Materials* (Vol. IV), Madrid, July 1993, pp. 560–7.
9. Long, A.C. and Rudd, C.D. (1994) A simulation of reinforcement deformation during the production of preforms for liquid moulding processes. *Proceedings of the Institution of Mechanical Engineers, Part B: Journal of Engineering Manufacture*, **208**, 269–78.
10. Laroche, D. and Vu-Khanh, T. (1994) Forming of woven fabric composites. *Journal of Composite Materials*, **28**, 1825–39.
11. Trochu, F., Hammami, A. and Benoit, Y. (1996) Prediction of fibre orientation and net shape definition of complex composite parts. *Composites Part A* **27**, 319–28.

12. Mack, C. and Taylor, H.M. (1956) The fitting of woven cloth to surfaces. *Journal of the Textile Institute (Transactions)*, **57**, 477–88.
13. Faux, I.D. and Pratt, M.J. (1979) *Computational Geometry for Design and Manufacture*, Ellis Horwood, Chichester, Sussex
14. Long, A.C. (1994) *Preform Design for Liquid Moulding Processes*. PhD thesis, University of Nottingham.
15. Vogel, J.H. and Lee, D. (1990) Analysis method for deep drawing process design. *International Journal of Mechanical Science*, **32**, 891–907.
16. Long, A.C., Rudd, C.D., Blagdon, M. and Smith, P. (1996) Characterizing the processing and performance of aligned reinforcements during preform manufacture. *Composites Part A*, **27**, 247–53.
17. Smith, P., Rudd, C.D. and Long, A.C. (1997) The effect of shear deformation on the processing and mechanical properties of aligned reinforcements. *Composites Science and Technology*, **57**, 327–44.
18. Advani, S.G., Bruschke, M.V. and Parnas, R.S. (1994) Resin transfer molding flow phenomena in polymeric composites, in *Flow and Rheology in Polymer Composites Manufacturing* (ed. S.G. Advani), Elsevier Science, Amsterdam.
19. Chick, J.P., Rudd, C.D., Van Leeuwen, P.A. and Frenay, T.I. (1996) Material characterization for flow modelling in structural reaction injection moulding. *Polymer Composites*, **17**, 124–36.
20. Smit, A. (1995) The effect of shear deformation on the permeability of reinforcement fabrics for resin transfer moulding. MSc thesis, Delft University of Technology.
21. Ueda, S. and Gutowski, T.G. (1996) Anisotropic permeability of deformed woven fabrics. Submitted to *Composites Part A*.
22. Rice, E.V. (1993) *Computer-aided-engineering Techniques for Resin Transfer Moulding*. PhD thesis, University of Nottingham.
23. Halpin, J.C. (1984) *Primer on Composite Materials: Analysis*, Technomic Publishing, Lancaster, PA.
24. Cucinella, F., Long, A.C., Rudd, C.D. and Pappalettere, C. (1996) Analysis of an anisotropic prototype composite wheel-hub. *Proceedings of the International Conference on Material Engineering* (Vol. 1), Gallipoli–Lecce, September 1996, pp. 519–28.
25. Kobayashi, S., Oh, S. and Altan, A. (1989) *Metal Forming and the Finite-element Method*, Oxford University Press, Oxford.
26. Boisse, P., Cherouat, A., Gelin, J.C. and Sabhi, H. (1995) Experimental study and finite element simulation of a glass fibre fabric shaping process. *Polymer Composites*, **16**, 83–95.
27. Turner, M., Rudd, C.D., Long, A.C., Middleton, V. and McGeehin, P. (1995) Net-shape preform manufacture using automated fibre placement. *Advanced Composites Letters*, **4**, 121–4.

Overview of fibre preforming

6

Vivek Rohatgi, L. James Lee and Adrian Melton

6.1 FIBRE PREFORMING – WHY IS IT NEEDED?

Unlike the traditional process of autoclave curing of prepregs, in which the fibres and the resin are pre-mixed before lay-up and moulding, the fibre reinforcement in the resin transfer moulding (RTM) process is initially dry and is often assembled outside the mould in the shape of the finished part (Figure 6.1). The fibre assembly, called a preform, is then placed in the mould and impregnated with the liquid resin which polymerises to yield a rigid composite. The preforming process thus converts the fibre reinforcement into the part geometry.

The manner in which the fibre reinforcements are held together to form a fibre mat determines its architecture and is dictated by the size and performance requirements of the end application. During fibre assembly many single-fibre filaments are first brought together in the form of a bundle, also called a roving or a tow. The fibre tows are then held together and assembled by different preforming methods. Predominant fibre materials are glass, graphite and Kevlar®. Typical fibre reinforcements for aerospace applications include bidirectional wovens, unidirectional or bidirectional stitched mats and various other combinations of stitching, weaving, knitting, braiding and filament winding. Apart from the mechanical strength, a fibre reinforcement is also characterised by additional attributes such as the bulk factor, which is the ratio of the volume of the given mass of 'loose' reinforcement to the volume of the same mass after forming, and by drapeability, the ability of a fabric to conform to the contours of the mould cavity. Currently, one of the

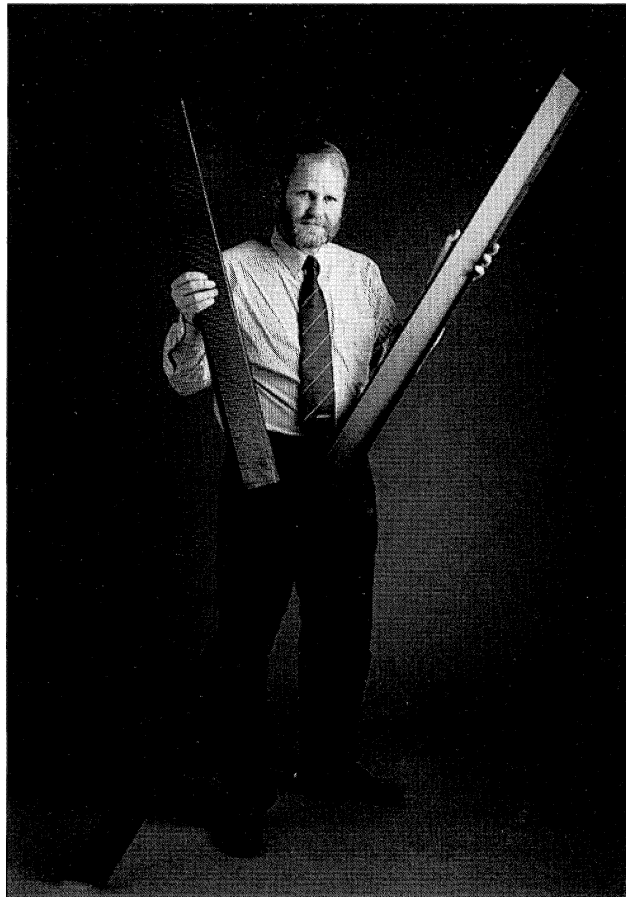


Figure 6.1 Carbon fabric stiffener preforms. Reproduced courtesy of the Co-operative Research Centre for Advanced Composite Structures Ltd, Fishermens Bend, Vic., Australia.

bottlenecks in RTM process is the preforming stage. Usually, individual layers of the reinforcement must be cut and shaped to conform to the various curvatures of the tool surfaces, a process which can be very time consuming and therefore very cost-ineffective. In a way, the mould represents a 'prison cell' and the fibre reinforcement may not go quietly into it (Figure 6.2). Fasteners such as tape and staples are often needed to hold the fibre reinforcement in shape until the mould is closed, greatly slowing the turnaround time. Another challenge is to hold the fibres in place within the closed mould, as the pressure of the injected resin can shift the preform into unpredictable contours [1]. Moreover, parts with complicated geometries make accurate placement of the fibre reinforcement

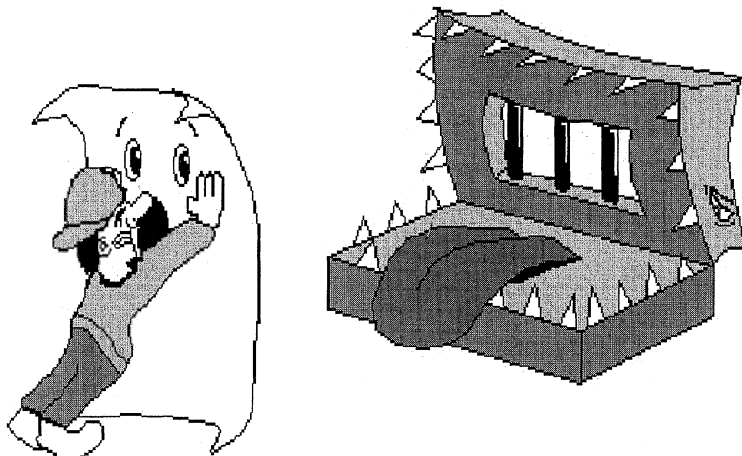


Figure 6.2 Schematic of preform placement in the mould.

quite cumbersome and may induce a number of defects. Stretching causes fibre thinning and reorientation. Bending results in thickness reduction and springback. In-plane compression causes wrinkles through buckling. Wrinkle formation and fibre thinning are undesirable from the point of view of the mechanical strength of the preform, and thickness reduction may lead to gaps between the preform and the mould surface. This together with fibre reorientation can cause channeling or 'race-tracking' of the resin in regions of high permeability, resulting in the formation of voids and/or 'dry spots'. Incomplete fibre wet-out is detrimental to both the surface quality and the mechanical strength of moulded composite. Dimensional changes due to preform springback are also undesirable as they lead to additional machining costs to achieve the required tolerances. Obtaining net-shape preforms is therefore perceived as a prerequisite for cost-effective production of parts from the RTM process.

Although there are several commercial preform fabrication methods, the technology is not as well developed as other well-established net-shape manufacturing techniques such as sheet metal stamping. The major hurdle is the lack of a sufficient knowledge base and reliable technology to produce preforms consistently with accurate dimensions and the desired fibre orientations. Nonetheless, owing to the sustained interest in recent years among researchers both in industry and in academia, preforming methods are gradually changing from art-based to engineering-based techniques. An understanding of the preform fabrication techniques and mechanisms governing the formability is important for optimal preform design of the wide range of reinforcements used

in the RTM process. This chapter covers the various aspects of forming the fibre reinforcement into net-shape assemblies that can be moulded into the final product. Extensive details of each preforming process are beyond the scope of this chapter, but can be found in the references cited.

6.2 USE OF BINDERS AND TACKIFIERS FOR FIBRE PREFORMING

Binder and tackifier materials form an important part of the preforming process. Their use not only facilitates stabilisation of the fibre mats but also allows for part consolidation (attachment of ribs, inserts and foam cores, etc.) to yield more integrated structural components.

Binders and tackifiers are thermoplastic or thermoset resins that are usually solid at room temperature but melt easily upon heating. On cooling, the resin resolidifies, bonding the fibre tows or plies together. The glass transition temperature (T_g) of the binder or tackifier should be low enough so that the preform can be shaped without overheating or overcuring the binder or tackifier. At the same time the T_g should be high enough so that the preform can be handled and stored at room temperature [2, 3]. In high-performance aerospace composites a partially reacted matrix resin, commonly termed a reactive tackifier, is often used to achieve effective consolidation of fibre preforms. Another reason for using the tackifier is to obtain sufficient tack to reduce slippage between the layers and to minimise springback. The latter occurs when the elastic stresses stored in the fibres during deformation is greater than the adhesion forces due to tack [4].

The choice of a binder or tackifier is governed by several factors, such as compatibility with the matrix resin to be injected during the mould-filling stage, operational effectiveness, process environment control, final product performance and the preforming technique. Typical thermoset binders are based on unsaturated polyester, polyurethane and epoxy resins. However, thermoplastics are the preferred binder materials as it is easier to control their rheological properties. The trade-off is that the mechanical properties of the moulded composite may be reduced because of incompatibility with the thermoset matrix. A commonly used thermoplastic for glass fibres is nylon; for carbon fibres, polyether-etherketone (PEEK) and polyphenylene sulphide (PPS) are often used. Binder concentration is typically limited to the range of c.4–8 wt% of the preform to provide sufficient rigidity to the preform without adversely affecting the mechanical properties of the finished part [5].

Tackifiers are mostly thermoset resins. The reactive tackifier can be either an uncatalysed or a catalysed thermoset resin, which is generally a partially reacted matrix resin. Typical examples are epoxy, polyester/vinyl ester (with suitable initiators and promoters), phenolic, polyimide

and bismaleimide resins [6]. Particularly suitable epoxy resins include polyglycidyl ethers of polyhydric phenols (compounds having an average of more than one phenolic group per molecule) such as diglycidyl ethers of bisphenol A having an epoxide equivalent weight from c.650–750. Vinyl ester resins include acrylates or methacrylates of polyglycidyl ethers of compounds having an average of more than one phenolic hydroxyl group per molecule. Reaction products (with an average molecular weight of 800–1400) of diglycidyl ether of bisphenol A and acrylic or methacrylic acid have been found to perform quite satisfactorily [6]. Consideration of the molecular weight of the tackifier is important for controlling the rheological properties of the resin during the heating and cooling stages of the preforming process. The effectiveness of the tackifier in minimising fibre springback strongly depends on the rheological properties of the polymer melt [7]. It is also desired that the tackifier dissolves in and reacts with the resin injected into the mould cavity during mould filling. The concentration of the tackifier ranges from 4–7 wt% of the preform [8]. As the density of the fibres is typically nearly twice that of the resin, the tackifier constitutes about 8%–14% of the total resin in the moulded part. Therefore, to obtain a homogeneous matrix and to avoid any deterioration in the mechanical properties, it becomes important that the chemistry of the tackifier chosen is compatible with the matrix resin [6, 9]. It is, however, not necessary that the tackifier chemistry be identical to the matrix resin as long as the tackifier can react with the matrix. As an example, an epoxy resin tackifier can be used with a cyanate ester matrix, and *vice versa* [2, 3].

6.3 FIBRE PREFORMING TECHNIQUES

Fibre preforming techniques can generally be classified into two broad categories, depending on whether the formation and the assembly of the fibre tows (mat forming) and conversion (shaping) into the final geometry of the part is carried out simultaneously or sequentially. Both the mat forming stage and the shaping stage, however, may involve several substages or processing steps. Another difference in the preforming techniques arises from whether or not the shaping process utilises a thermoplastic or a thermoset binder or tackifier.

6.3.1 SIMULTANEOUS PREFORMING PROCESSES

As shown in Figure 6.3, filament winding and overbraiding can be classified as simultaneous processes. To make preforms by filament winding, continuous fibre tows are wound tightly over a collapsible mandrel having the desired shape of the part. This approach is good for achieving high fibre content but is usually limited to axisymmetric

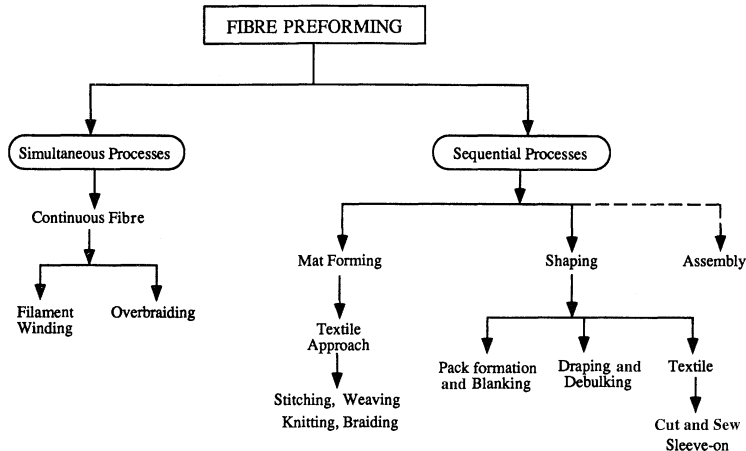


Figure 6.3 Classification of fibre preforming techniques for aerospace applications.

shapes. It is also difficult to 'lock' the fibre tows in place, which results in comparatively low interlaminar shear strength [10]. Overbraiding circumvents this limitation, and like filament winding produces preforms via helical wrapping of fibres onto a mandrel which duplicates the shape of the final part [11]. The overbraiding process produces an interlaced system of yarns which conforms to the shape of the mandrel, eliminating the need for subsequent cutting and shaping. The lay-up parameters for the fibre tows or yarns can be automated for precise placement and orientation. Three-dimensional braiding offers more flexibility in fibre placement [12] and improved through-the-thickness properties over two-dimensional braided preforms.

6.3.2 SEQUENTIAL PREFORMING PROCESSES

Mat Forming Techniques

Most of the continuous fibre preforms are made by sequential processes. In these processes, the final fibre assembly or the preform is obtained by first forming the fibre mats, which are then shaped and assembled by one of the following methods.

Preform fabrication techniques for aerospace applications include methods based on traditional textile operations such as stitching, weaving, knitting and braiding (hence the name textile preforms). Textile processes, however, need to be carefully controlled to avoid any detrimental effect on the fibres (Figure 6.4). A convenient and economical way for holding the fibre tows together and maintaining their orientation is

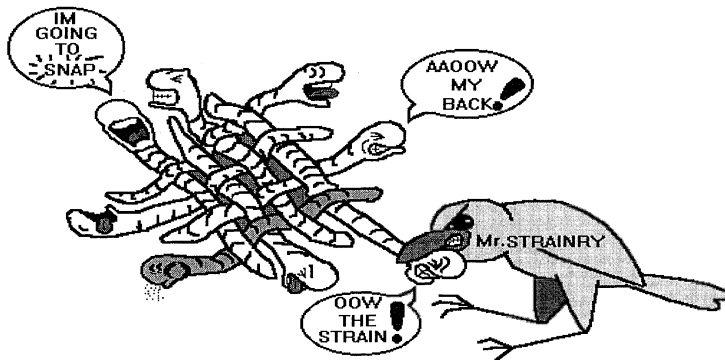


Figure 6.4 Schematic of forces inflicted on the fibres during the weaving process.

by using a continuous stitch. The crossover or tricot, and the standard or chain stitch, are two types of stitches used [13]. Benefits of stitching include better interlaminar shear properties, damage tolerance and fibre alignment [14]. However, the use of stitches is not without disadvantages. Stitches can create high-density areas that may interfere with the flow and result in the formation of voids [15, 16]. Also, as a result of the presence of stitches anisotropic microcracking in composite parts has been observed [15]. To avoid these drawbacks other ways have been devised to hold the fibre tows. These include weaving, knitting and braiding the fibre tows in different patterns to obtain a self-supporting structure.

In weaving, yarns in one set, which runs along the length of the fabric, interlace by passing under and over the yarns in another set, which cross the fabric. Woven materials have good drapeability depending on the weave pattern and the tow size. Three basic weave patterns are plain, twill and satin. Depending upon the weave pattern, satin weaves can be further subdivided into different harness types (e.g. 3HS, 4HS, 8HS, etc.). Harness weaves are more common in aerospace preforms. Mock Leno weaves or other tight styles, though very tough, are not good in compressive modes. The main characteristic of woven fibres is the formation of crimp caused by the under-and-over weave pattern at the intersection of the warp (0°) and weft (90°) tows or yarns. Triaxially woven fabrics are made of three yarns interlaced at 60° angles. Woven fabrics can also be produced with through-the-thickness reinforcement. These include layer-to-layer interlock, through-the-thickness angular interlock and orthogonal and net-shape weave patterns [17, 18].

The knitting process produces little crimp and results in a less bulky reinforcement. In knitting, the interlacing is done by loops formed between neighbouring tows in one set (introduced sequentially in weft knitting, and in parallel in warp knitting). Knitted fabrics are ideal re-

inforcements for highly curved shapes because of their extremely high deformability [19]. Multiaxial warp-knit (MWK) fabrics also provide good conformability to complex shapes. The MWK fabric consists of warp, weft and bias ($\pm\theta^\circ$) yarns held together by a chain or tricot stitch through the thickness of the fabric [20].

Like filament winding, braiding is used primarily when the desired fibre orientation is symmetrical about an axis [21]. The braiding process can be divided into three major categories: flat braiding [22], tubular braiding [23] and through-the-thickness, three-dimensional, braiding [12, 24]. Moreover, depending on the orientation of yarns in the braids, tubular or flat braids can be further classified into biaxial and triaxial braids. In biaxial braiding, two groups of yarns within the same plane intersect each other at a certain angle, $\pm\theta^\circ$, to the longitudinal axis of the braid. Triaxial braid is formed by inserting unidirectional yarns parallel to the longitudinal braid axis in the same plane as the biaxial yarns [25]. Other preforming techniques involve forming a hybrid structure consisting of different combinations of textile and chopped or continuous strand random fibre mats.

Binder and tackifier application techniques

The methodology of binder or tackifier application for stabilising layers of fibre mats into net-shape or near-net-shape preforms is quite similar to the use of thermoplastic powders in prepgs. Some of the common methods of binder and tackifier application utilise veils, liquid/solvent spray and powder. Veils can be placed between adjacent layers of fibre mat and then the ply stacks fused with heat and pressure to form the preform [9]. Alternatively, spraying of liquid with dissolved binder or tackifier onto each layer can be used, but this is not a very practical approach as it tends to increase the scrap factor and slows the production because of the need for the liquid/solvent to evaporate during bonding. Also, conventional liquid binders include stabilisers that present an environmental concern [1]. Application of the binder or tackifier in the form of small granules or thin fibres ($c.100\text{--}400\ \mu\text{m}$ in diameter) is a better approach. This method offers the additional benefit of being environmentally friendly. The conventional method is to disperse the binder or tackifier between the layers of the fibre mat. Shields and Colton [26] have proposed a different method which involves application of the powdered resin to the fibre tows instead, with subsequent assembly of the tows to form the fibre mat. However, this approach limits the use of such tows to a specific application and thus is not very practical for large-scale commercial production of fibre preforms.

The most effective method of applying the powder binder or tackifier to the fabric is to use a coating machine. The two most commonly used

coating machines are of the overhead hopper type in which the amount of powder is metered onto the fabric by a fine bristle-covered roller [Figure 6.5(a)] and of the dip tank type [Figure 6.5(b)]. In the latter the fabric is passed through powder in a tank. Heat is applied to partially melt the particles thereby causing them to adhere to the fabric. The main components of both designs are an 'off-let reel', a 'wind-on reel', a 'heater bank' with 'shield plate', and an applicator hopper or tank. The fabric is wound from the off-let reel, under or through the hopper, between the heater bank and shield plate and then rewound on the wind-up reel. The optimum energy setting is gauged when the powder particles are well attached to the fibres but not dissipated into the fabric (Figure 6.6). If the heat relative to the feed speed is too high the particles will dissipate into the fibre tows. Conversely, insufficient heat will fail to bond the particles and the powder will fall off the fabric. The best results are obtained when the tackifier particle is bound to the fabric as shown in Figure 6.6. The overall

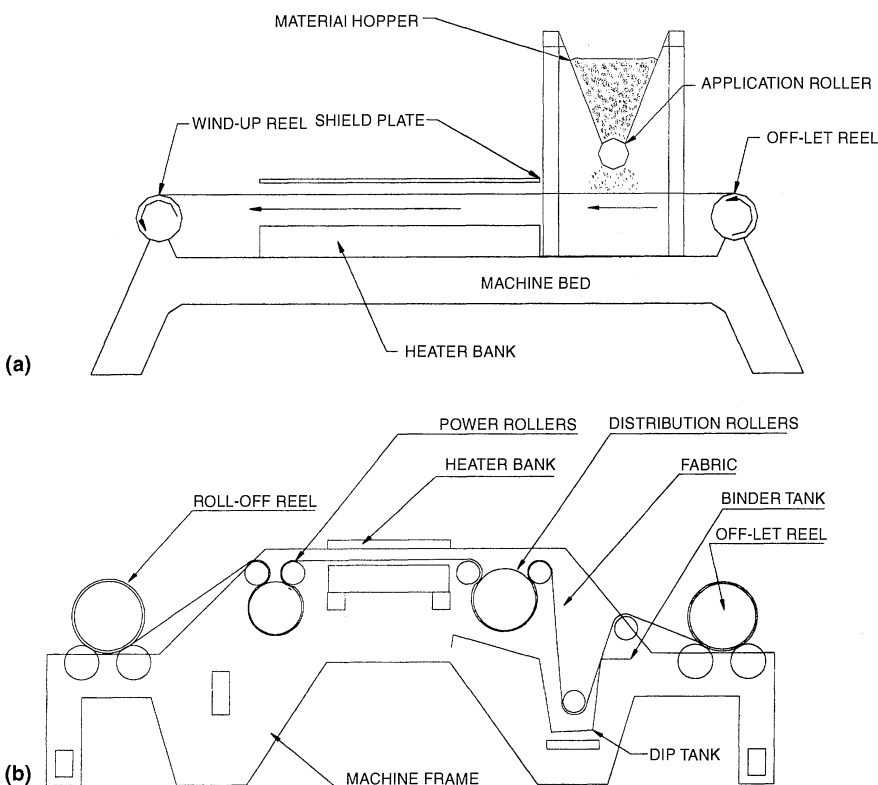


Figure 6.5 Powder coating machines: (a) overhead type; (b) dip tank type.

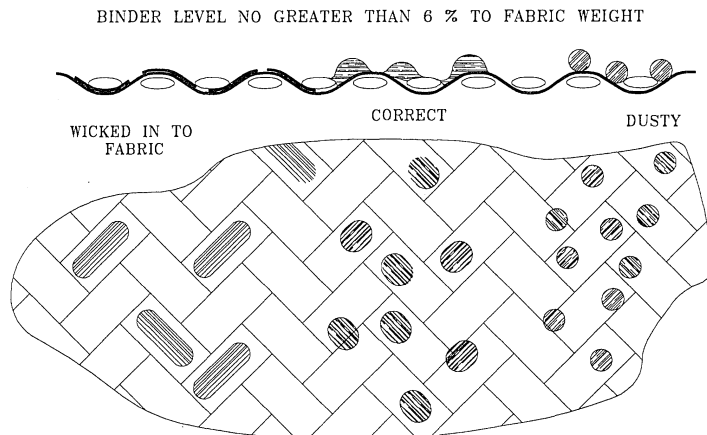


Figure 6.6 Schematic of the ideal distribution of binder or tackifier on the fibre preform.

appearance should be dull or dusty on the surface of the fabric. If after application of the tackifier the appearance has returned to the original shiny lustre (especially so with carbon fabric), the binder or tackifier will be ineffective.

Assembly and shaping techniques

For applications in which the final preform consists of several components with complex geometry it becomes very difficult to obtain a consolidated net-shape preform by means of a single method to replicate the shape of the entire part. It then becomes advantageous to break down the preform in several modules, fabricate the preforms separately for each module and then assemble the different preform structures as a single unit (Figure 6.7). In some cases, the subassemblies can be stitched, stapled or pinned together to improve the through-the-thickness properties. Shaping techniques which use binders and tackifiers are blanking and draping or debulking. Other methods are cut-and-sew and sleeve-on.

Blanking

Older methods of stabilising textile preforms with binder or tackifier involved selective application and removal of a hot iron. Since most reinforcing fabrics are poor heat conductors, hot iron tacking was done one ply at a time, which made the process both time and labour intensive. An improvement of this method involves laying up the individual plies over a diaphragm press, as shown in Figure 6.8, and directing a

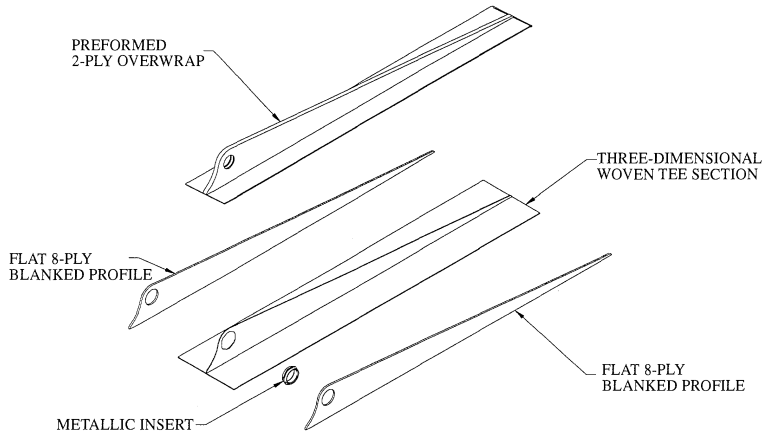


Figure 6.7 Assembly of various preforms and a metallic bush (all preassembled before being placed into the mould).

stream of heated air through all the layers to melt the resin. This results in faster heating as a result of convective heat transfer. Application of vacuum pressure behind the perforations serves three important functions. First, in the fabric lay-up process the vacuum can facilitate holding the individual plies in place until hot air is applied. Second, the vacuum can be used to promote hot air penetration through the laminate. Last, subsequent to the melting stage, the vacuum can be used to draw colder

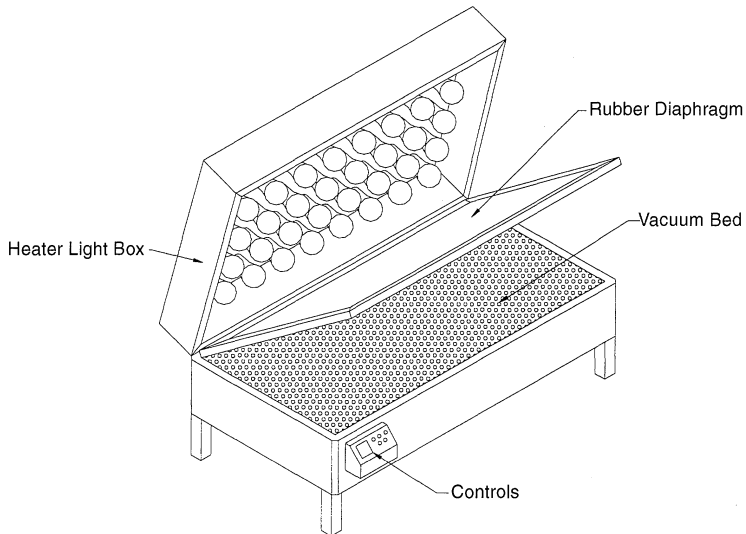


Figure 6.8 Heated diaphragm mat consolidation press.

ambient air through the plies to cause the melt to solidify rapidly [27]. This not only enhances the production rate but also causes the resin modulus to increase quickly. Increase in resin modulus results in increased resistance to the relaxation of deformed elastic fibres, thereby minimising preform springback. Low-inertia infra-red heaters offer even faster heating rates as a result of heat transfer by radiation. For most epoxy-based tackifiers the typical heat setting temperature is 100°C for 1–5 min followed by cooling under pressure for the same amount of time. This process produces a dry workable sheet or board-like material which can be cut into blanks with multiple blade cutting tools or a roller press (Figure 6.9). It is usually much more economical to cut the dry fabric to net-shape than to machine a cured laminate with diamond cutters.

Draping and debulking

The term draping refers to the forced conformance of the fibre reinforcement over the tool surface. In contrast to blanking, in which the edges of the fibre reinforcement are clamped, draping involves deformation of a free boundary. Thus the dominant deformation mode is interfibre shear rather than stretching or compression as in blanking. Owing to the interfibre shear during draping, the initial angle between the weft and warp fibres may decrease [Figure 6.10] until the 'locking angle' is reached [28].

Draped preforms are often debulked to the desired fibre volume fraction and thickness with the aid of vacuum or a hydraulic press. Vacuum debulking is similar to vacuum bagging of prepgs. It involves placing the draped preform in a vacuum bag assembly. A typical as-

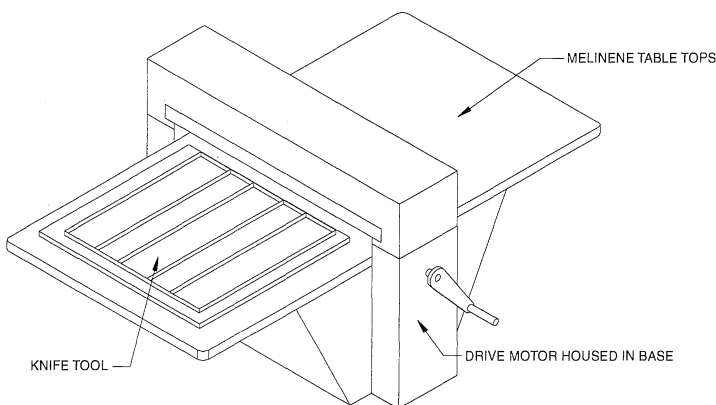


Figure 6.9 Blank form cutting roller press.

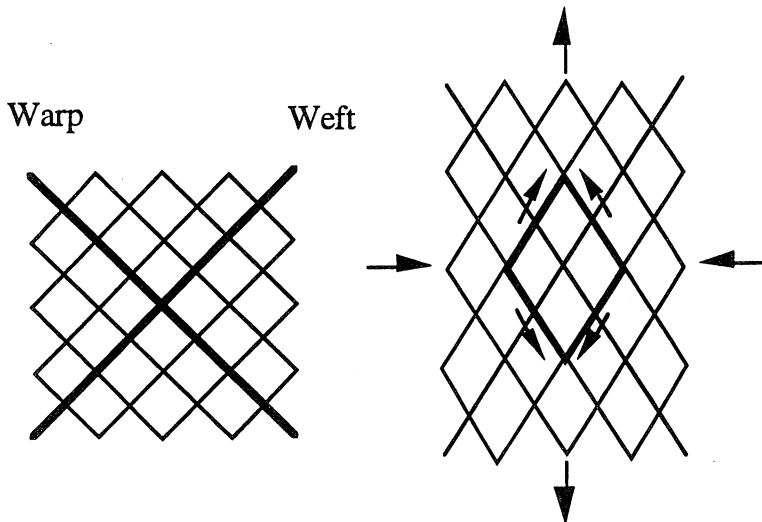


Figure 6.10 Schematic depicting the change in fibre orientation during draping of woven fibre mat.

sembly consists of an envelope (made of high-temperature plastic film sealed to the perimeter of the mandrel). A runner (connected to a vacuum source) serves to pull the vacuum from the bag. Often, debulking is carried out in a heated oven to melt the tackifier resin dispersed between the adjacent fibre layers. After applying the vacuum for a specified time period the assembly is allowed to cool to room temperature. The solidified or cured tackifier bonds the fibre layers together, thereby imparting dimensional rigidity to the stacked laminate.

Cut-and-sew

Some low-volume applications utilise the cut-and-sew preforming technique. In this method laminates are precut and assembled into the shape of the part being produced, including the positioning of inserts or cores. The plies are held together by sewing in the thickness (z) direction. Common sewing threads are polyester, glass and KevlarTM, although carbon has also been used [29]. Although the process is slow, the structural efficiency is high because of the exact reinforcement placement and orientation [30].

Sleeve-on

This method is employed for shaping biaxial and triaxial braided fibre mats which are in the form of a 'sock'. The sock is then 'sleeved-on' to the

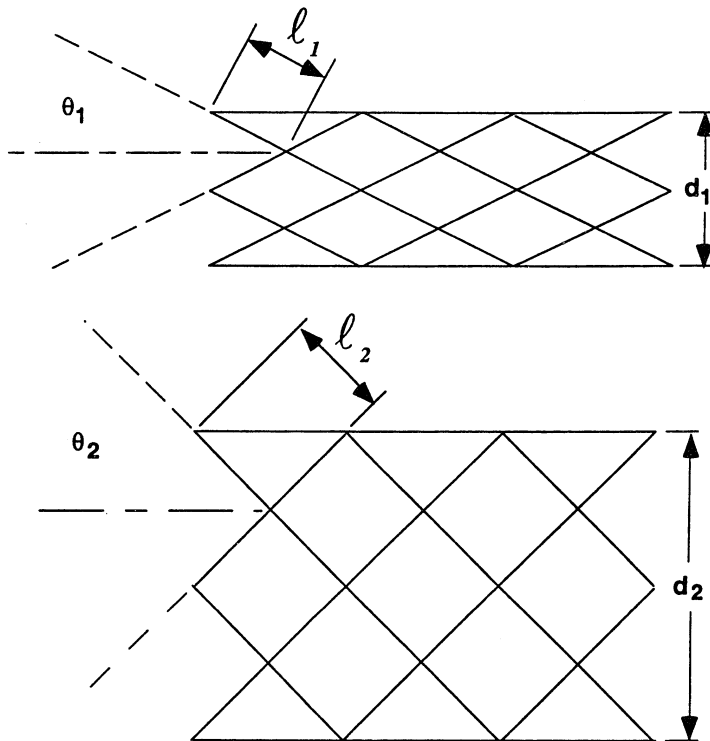


Figure 6.11 Schematic depicting the change in fibre orientation during sleeve-on of a braided sock. θ = intertow angle; l = interfibre distance; d = tool diameter.

mandrel having the shape and geometry of the part to be moulded. As in draping, the sleeve-on method also results in a change in fibre orientation from the initial configuration. The extent to which the intertow angle, θ , changes is a function of the radius of curvature and diameter, d , of the tool (Figure 6.11).

6.4 NET-SHAPE PREFORMING OF WOVEN FIBRE MATS BY MEANS OF TACKIFIERS

Although some patents describing the methodology for obtaining stabilised preforms for liquid composite moulding (LCM) processes exist [2, 3, 5, 6, 27], few studies have investigated in depth the relevant mechanisms for better design of preforming conditions to obtain near-net and net-shape preforms. Kittelson and Hackett [9] studied the influence of chemical compatibility of epoxy tackifier (PT 500) with an epoxy matrix resin (PR 500) on mechanical properties of moulded composites. They also did experiments to observe the effect of tackifier concentration and

debulking conditions on fibre springback in C-Spar preforms [Figure 6.12(a)] made of plain weave graphite fabric. However, the mechanisms causing the springback phenomenon were not addressed. A systematic investigation of the issues involved in preforming of tackified fibre mats has been conducted [7]. A reactive bismaleimide (BMI) and a non-reactive polymethylmethacrylate (PMMA) tackifier (*c.* 100 mm, powder) were used with woven (6k, 4HS) graphite fibre mats. Preforming experiments were carried out with the use of two different modes of fibre deformation, namely, U-shape bending and lateral compression [Figures 6.12(b) and (c)]. The basic approach used and a summary of the findings obtained from that study is presented here. The specifics of the experimental set-up and other details are reported elsewhere [31].

The U-shape bending and lateral compression experiments both showed that at a specified concentration level increasing the degree of

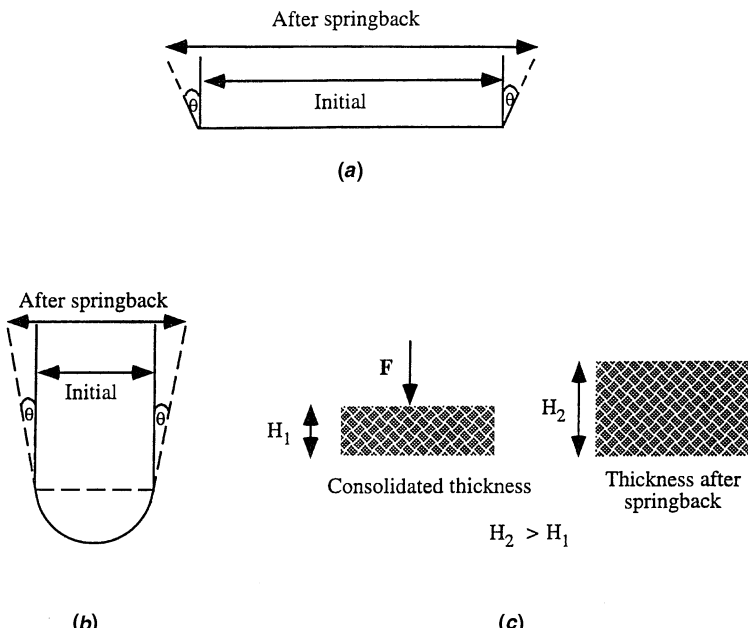


Figure 6.12 Schematic of springback (sb) phenomena for three types of preform geometry deformation: (a) C-spar ($sb = \theta^0$); (b) U-shape ($sb = \theta^0$); (c) lateral compression ($sb = \Delta H = H_2 - H_1$). Source, part (a): Kittelson, J. L. and Hachett, S. C., Tackifier/resin compatibility is essential for aerospace grade resin transfer moulding, *Proceedings of the 39th International SAMPE symposium*, Society for the Advancement of Materials and Process Engineering, 1161 Parkview Drive, Covina, CA 91724-3748, pp. 83–96, 1994. Source, parts (b), (c): Rohatgi, V. and Lee, L. J., Moldability of tackified fibre preforms in liquid composite moulding, *Journal of Composite Materials*, **31**, 720–44, 1997.

cure of BMI tackifier reduced the amount of springback. Also, for the same tackifier conversion, an increase in the concentration resulted in lower springback. These results concur with the general observations of Kittelson and Hackett [9] for the C-spar type geometry. An interesting phenomenon, observed from U-shape bending experiments, was that when the same amount of tackifier was applied dissolved in acetone solvent, instead of in the powder form, fibre springback reduced from 5.3° to 2.2° (for eight layers, the fibre volume fraction, V_f is 0.55). The tack or interply adhesion, however, was greater in the case of the powder technique compared with when the tackifier was applied by the solvent method. The reason for this behaviour can be explained from the scanning electron micrographs [Figures 6.13(a) and (b)] which show the distribution of the tackifier in the two cases. When applied as a powder most of the tackifier remained on the fibre mat surface as coagulated chunks. In contrast, when applied from a solvent, very little remained on the surface and most of it formed a thin coating on the filaments.

In order to elucidate the mechanism for the observed preform springback, fibre layers were consolidated in a mould to different extents. The resulting microstructure was 'locked' by impregnating the fibres with an unsaturated polyester and subsequently curing the resin. Cross-sections of the moulded samples were then examined by means of scanning electron microscopy. Figure 6.14(a) is a micrograph of the cross-section of the sample with a fibre volume fraction, V_f of 0.32. The figure shows a gap between the adjacent layers. However, with an increase in the fibre volume fraction [Figure 6.14(b), $V_f = 0.45$], the interlayer gap disappears, and fibre tows of adjacent layers start touching each other. Compaction beyond $V_f = 0.45$ causes further consolidation of the fibre tows as the smaller gaps between the filaments of the fibre tows start to get compressed [Figure 6.14(c), $V_f = 0.67$]. These photomicrographs indicate two levels of consolidation and consequently suggest that there should also be two levels of springback – one arising from the deconsolidation of the small gaps within the fibre tows and the other arising from deconsolidation between the fibre layers.

Based on the experimental results, it was hypothesised that springback occurs when the force exerted by the elastic fibre preform is greater than the 'holding force' provided by the tackifier. The ratio of forces driving and opposing fibre springback can be expressed as in equation (6.1). The rationale is that the driving force exerted by the fibres depends on the relaxation characteristics of the preform, F_f , whereas the holding force is the product of the modulus, E_r , which is a function of degree of cure for the reactive tackifier, and the wetted surface area coverage, A_w :

$$\frac{\text{driving force}}{\text{holding force}} = f \left(\frac{F_f}{E_r A_w} \right) \quad (6.1)$$

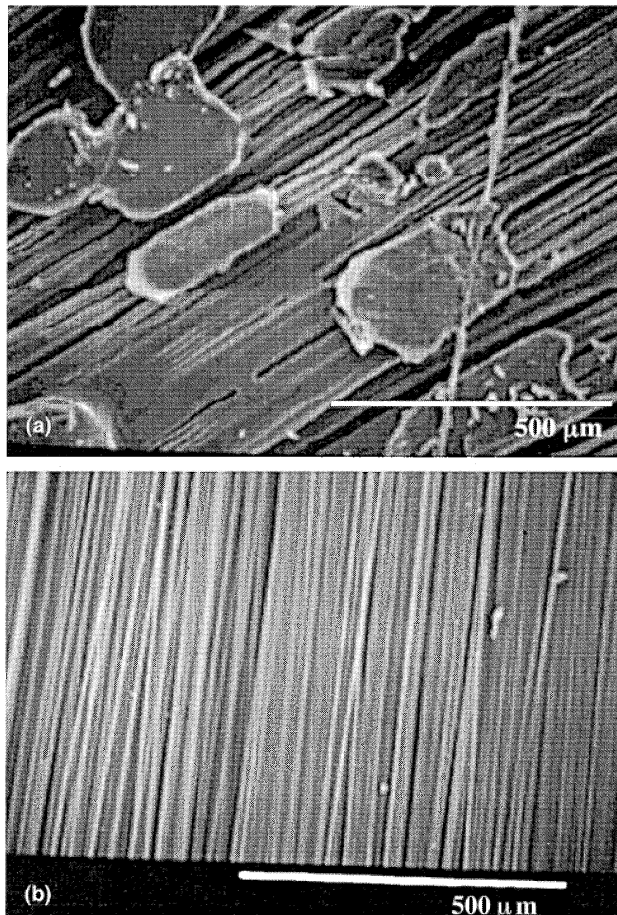


Figure 6.13 Photomicrographs of debulked fibre preforms with bismaleimide tackifier applied (a) as a powder; (b) dissolved in acetone. Source: Rohatgi, V. and Lee, L. J., Moldability of tackified fibre preforms in liquid composite moulding, *Journal of Composite Materials*, **31**, 720–44, 1997.

It was proposed in the study that the magnitude of the force exerted during springback for any number of fibre layers could be estimated from a model describing the compaction behavior of fibres, such as the finitely extendable non-linear elastic (FENE) spring model [equation 6.2] [32]:

$$P_a = k \left\{ \frac{V_{fi} - V_{f0}}{V_{fi}} \left[1 - \left(\frac{V_{fi} - V_{f0}}{V_{fi}} \right) \left(\frac{V_f^{\max} - V_{f0}}{V_f^{\max}} \right)^{-1} \right]^{-n} \right\} \quad (6.2)$$

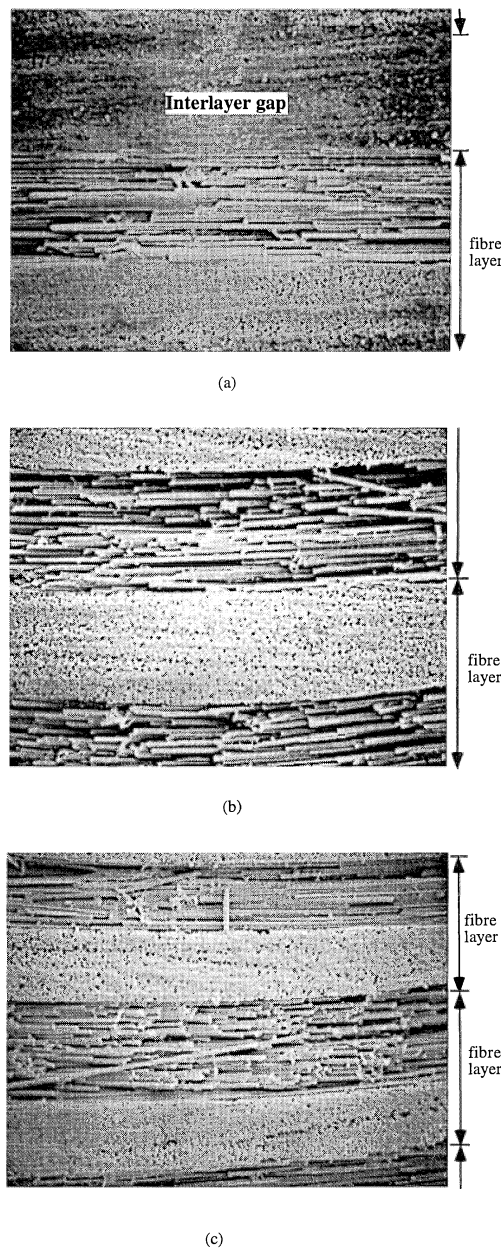


Figure 6.14 Photomicrographs (magnification $\times 200$) showing the consolidation of interlayer and intralayer gaps with increasing fibre volume fraction, V_f : (a) $V_f = 0.32$; (b) $V_f = 0.45$; (c) $V_f = 0.67$. Source: Rohatgi, V. and Lee, L. J., Moldability of tackified fibre preforms in liquid composite moulding, *Journal of Composite Materials*, **31**, 720–44, 1997.

where

P_a is the applied pressure;

k is the spring constant of the fibres;

V_{f0} is the initial fibre volume fraction;

V_{fi} is the fibre volume fraction at any instant i ;

V_f^{\max} is the maximum fibre volume fraction achievable;

n is a constant.

The underlying assumption of the proposed approach is that the force required to compress the fibres to a certain volume fraction should be similar (for minimal hysteresis) to that exerted by the fibres at the same volume fraction during the relaxation process. Thus information from compressibility curves, as shown in Figures 6.15(a) and 6.15(b) can be used to calculate the pressure required for achieving compaction to a desired fibre volume fraction and also to estimate the amount of fibre springback, which can be used for effective mould design. Figure 6.15(b) illustrates the applicability of the FENE model to describe the consolidation behaviour of eight layers of 6k, 4HS graphite fabrics (assuming $V_f^{\max} = 0.901$).

Analysis of the holding force for a reactive tackifier is complicated because of the combined effects of the increase in the modulus from chemical reaction and the increase in the area coverage by the melted tackifier. Thus, in order to decouple the effects of increase in modulus and surface area coverage, lateral compression experiments were conducted with PMMA tackifier. Different temperatures beyond the melting point of the tackifier were chosen to cover a broad range of melt viscosity. The premise was that for a thermoplastic tackifier the modulus would be the same for all cases upon cooling to room temperature, unlike the case for BMI tackifier. Any observed differences in the spring-back values should therefore come from differences in the surface area coverage by the tackifier rather than from differences in modulus. Since quantification of the actual surface area coverage is difficult because of the complex nature of spreading of a viscoelastic melt over a porous substrate, changes in the wetted area coverage were studied qualitatively. Figures 6.16(a)–(c) show the photomicrographs of the preforms after debulking for three of the runs, at 220°C, 250°C and 287°C, respectively. Although there is more spreading for debulking at 250°C as compared with the 220°C run, the melt remains on the surface and there is little intralayer coverage. At 287°C, however, the polymer melt migrates from the surface to within the fibre tows [Figure 6.16(c)] and forms a coating on the filaments. The reason for this can be explained by analysis of the forces favouring and resisting impregnation of the tackifier into the fibre tows. The capillary pressure, P_c , provides the main driving force favouring bundle impregnation, whereas resistance to deformation comes from the viscoelastic modulus of the polymer melt.

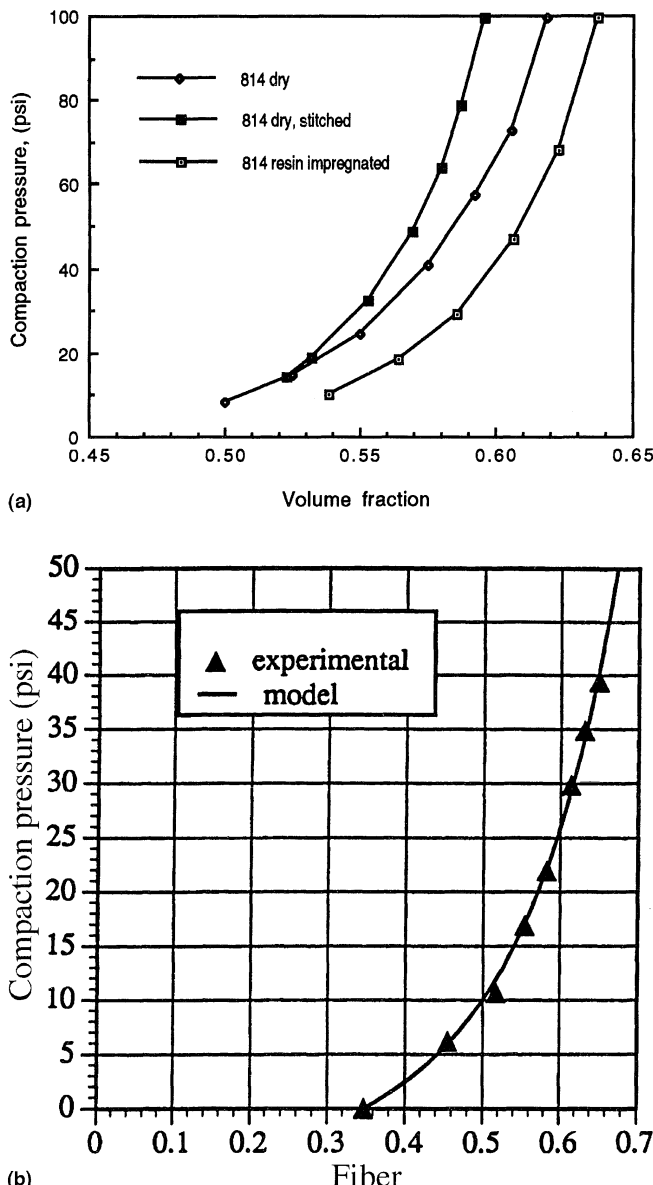


Figure 6.15 Compaction pressure versus fibre volume fraction: (a) 3k plain weave graphite fabrics (Brochier 814); (b) 6k, 4HS woven graphite fabrics. Source, part (b): Rohatgi, V. and Lee, L. J., Moldability of tackified fibre preforms in liquid composite moulding, *Journal of composite Materials*, **31**, 720–44, 1997; part (a) reproduced courtesy of the Cooperative Research Centre for Advanced Composite Structures Ltd, Fishermens Bend, Vic., Australia.

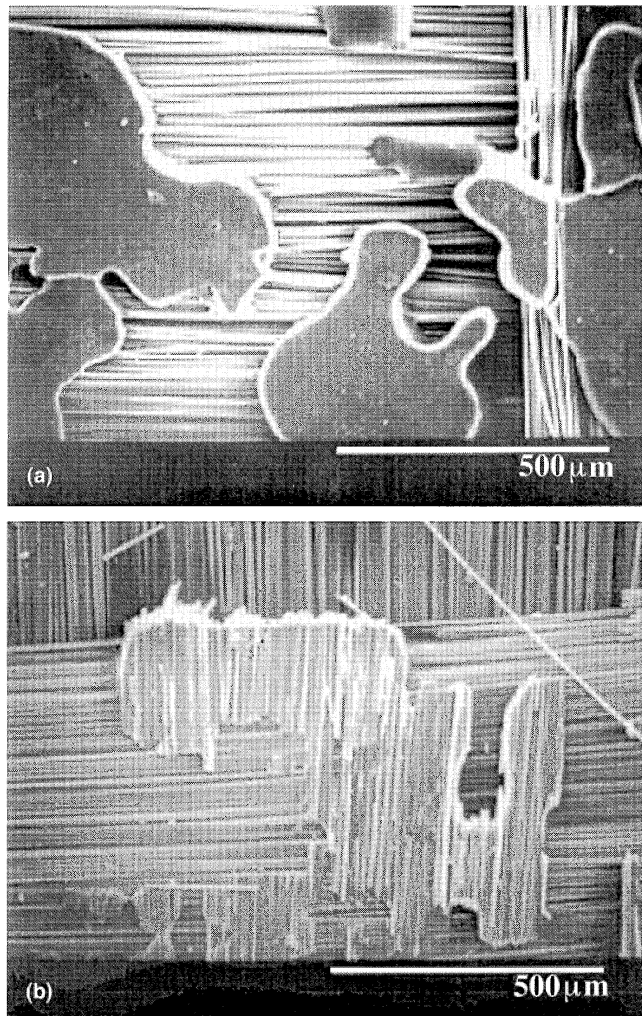


Figure 6.16 Photomicrographs of surface of polymethylmethacrylate tackified preforms debulked at: (a) 220°C; (b) 250°C; (c) 287°C; at (i) low magnification, (ii) high magnification. Source: Rohatgi, V. and Lee, L. J., Moldability of tackified fibre preforms in liquid composite moulding, *Journal of Composite Materials*, **31**, 720–44, 1997.

Consequently, when the driving force equals or exceeds the resisting force it results in ‘wicking’ of the tackifier resin inside the fibre tows.

Figure 6.17 depicts the springback values as a function of debulking temperature for 3 wt% and 8 wt% of PMMA tackifier. Springback remains the same up to 235°C, then decreases gradually with increasing temperature, and levels off after 287°C. As the modulus should be the

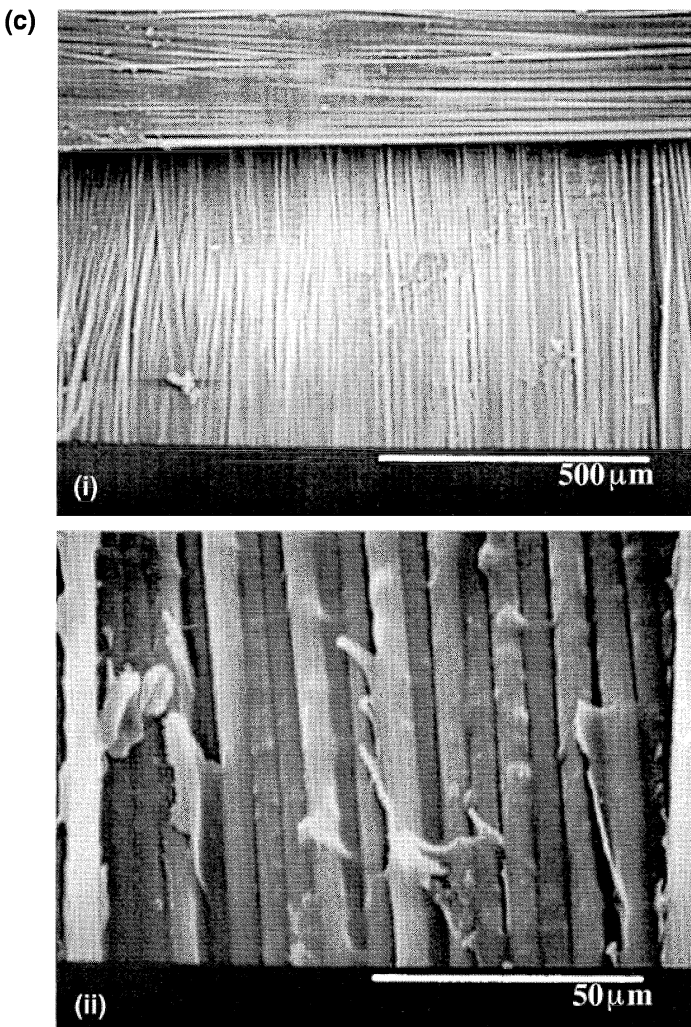


Figure 6.16 c(i) & (ii)

same in all cases, initial decrease in springback can be attributed to the increase in the interlayer wetted area coverage arising from a decrease in the melt viscosity. Further decrease in springback is a result of the transition of the tackifier area coverage from interlayer to intralayer. Since for a given tackifier concentration tow impregnation implies complete intralayer spreading, the springback levels off beyond the transition region.

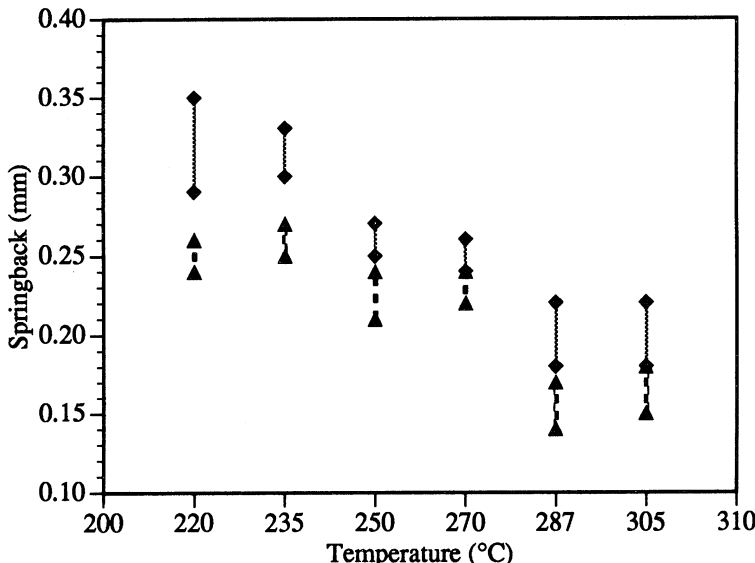


Figure 6.17 Springback as a function of debulking temperature in fibre preforms with polymethylmethacrylate tackifier. $\sim\sim$ = 3 wt%, $-\cdot-$ = 8 wt%. Source: Rohatgi, V. and Lee, L. J., Moldability of tackified fibre preforms in liquid composite molding, *Journal of Composite Materials*, **31**, 720–44, 1997.

The general conclusions drawn from this study are that the processing variables affecting fibre springback include tackifier concentration, preform debulking temperature and the location of tackifier (i.e. between the layers compared with within the fibre tows). The study revealed two levels of fibre consolidation: interlayer consolidation or compression of gaps between the layers, followed by intralayer consolidation or compression of gaps within the fibre tows. It was therefore reasoned that there should also be two levels of springback, one arising from the deconsolidation of the small gaps within the fibre tows and the other arising from between the fibre layers. Thus, for optimal interply adhesion and reduced springback, the preforming conditions should be controlled such that the tackifier is present at both the interlayer and intralayer levels.

6.5 DESIGN OF PREFORM TOOLS

The principal section of a preform tool is the plug form. The heated fabric blank is forced over and around the plug by a ring or matching cavity. Typically, tools are made from hard wood, plastics or of light metal. When the shape is simple the fabric can be formed over a plug-type tool with an elastomeric diaphragm. Where sharp corners exist in the plug

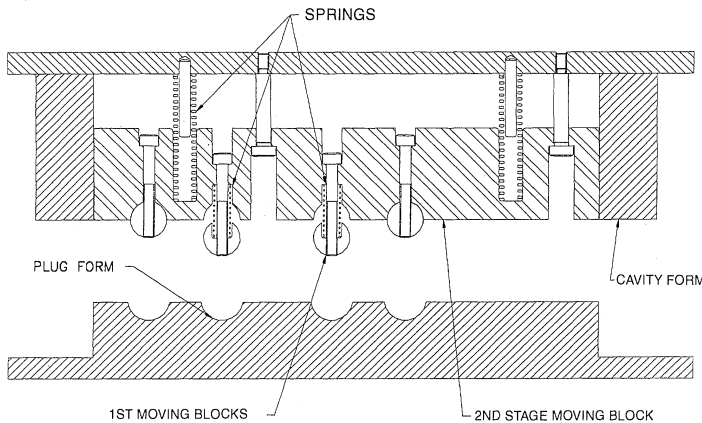


Figure 6.18 Section through spring staged preform tooling.

form an intensifier should be used under the diaphragm to assist in forming such detail. Since the fibres are inextensible, special forming techniques are required for complex shapes, in which the fibre must be fed progressively into the shape, pulling material in from the sides. Spring-loaded tool sections can achieve this, as shown in Figure 6.18.

6.6 DESIGN OF PREFORMING EQUIPMENT

There are three simple stages in the preforming process:

1. locating the fabric;
2. heating the fabric to soften the binder or tackifier;
3. pressing the fabric to form.

The order of these steps can be changed to locating, pressing, heating and then cooling. A light metal frame can be used to locate the fabric and hold it in a controlled fashion. This must be carefully designed as the fabric will have the tendency to sag as the tackifier softens. The other concern with regard to location is that the frame should be indexed over the press tool in a consistent fashion to make the process repeatable.

The principal types of preforming equipment are linear [Figure 6.19(a)] and rotary [Figure 6.19(b)]. The first fixes the process stages in a consecutive line; the second arranges them around a column. The linear system (also known as the shuttle system) is often the first choice as it takes progressive steps to a goal and is then repeated. It is, however, the less efficient of the two in that the return of the fabric holding tray for the

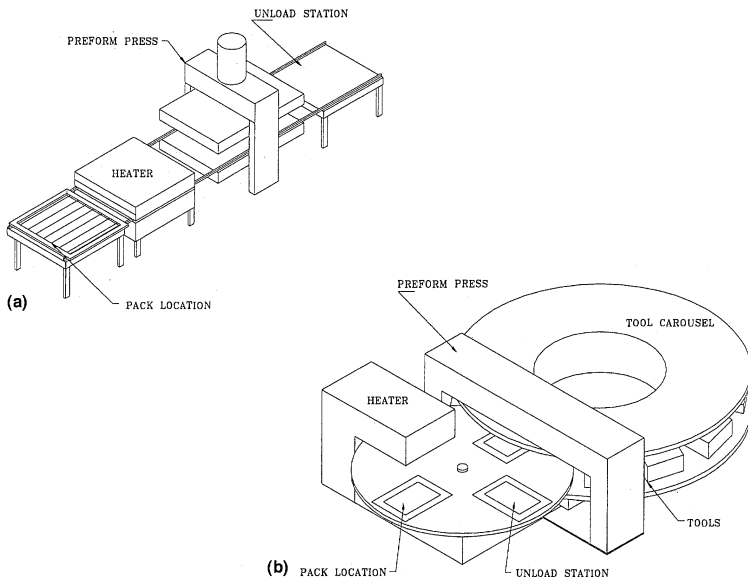


Figure 6.19 Typical preforming machines: (a) shuttle type; (b) carousel type.

next part constitutes lost time. Rotary or carousel-type rigs are more efficient in that the process is a continuous cycle, lending itself more easily to automation. The fibre blank is placed on to the table, rotated into the heater and is finally rotated into the press and formed. As each preform is retrieved from the press the vacant stage is filled with another fibre blank. This system can produce preforms at a rate of one every 45 s (based on a rib channel section 12" (308 mm) long, 3" (77 mm) wide and 1.5" (38 mm) deep). Refinements to the rig such as an automatic tool changer and simple pick-and-place, load and unload devices can automate the whole process.

6.7 PREFORM STORAGE

As a general rule, storage of preforms for prolonged periods of time should be avoided whenever possible. However, when storage becomes a necessity it is important to support the shape to prevent gradual relaxation. The shape of the preform does not need to be perfect as the mould will realign it to shape. However, the developed trim length must be maintained. A support block or a formed kit tray provides the best storage medium. The temperature and humidity of the storage space should be carefully controlled to avoid any post-forming problems with stored preforms.

6.8 CONCLUSIONS

This chapter has provided an overview of the different methods available for manufacturing fibre preforms for the RTM process. Characteristics of different preforming methods were discussed. The choice of one preforming method over the other is determined by several factors, such as the processability (drapeability, bulk factor, wetting and permeability characteristics of the preform), the feasibility of obtaining net-shapes, the desired mechanical properties of the moulded part and, of course, the cost of production. Although all these factors are important, net-shape preforming is a prerequisite for RTM to reach the desired commercial potential. This necessitates a broader experimental database and simple though realistic models to characterise the mechanisms governing the changes in the fibre orientation during preforming. Moreover, in order to optimise the existing liquid moulding technology, it becomes imperative to integrate preforming analysis with mould-filling characteristics and mechanical properties of the moulded composite parts.

References

1. Fisher, K. and McDermott, J. (1995) Preform molding hits the fast lane. *Composites Technology*, (July/August), 19.
2. White, W. D., Cook, P. H., Wai M. and Davis, W. (1995) Process for resin transfer molding and preform used in the process. *US Patent*, 5,427,725.
3. White, W. D., Cook, P. H., Wai M. and Davis, W. (1995) Process for resin transfer molding using a partially cured tackifier. *US Patent*, 5,427,726.
4. Gutowski, T. G. and Bonhomme, L. (1988) The mechanics of prepreg conformance. *Journal of Composite Materials*, **22**, 204–23.
5. Reavely, R. T. and Kim, W. (1991) Method of fabricating fibre reinforced composite articles by RTM. *US Patent*, 4,988,469.
6. Heck, H. G. and White, W. D. (1991) Preforms for molding processes. *US Patent*, 5,071,711.
7. Rohatgi V. and Lee, L. J. (1997) Moldability of tackified fibre preforms in liquid composite molding. *Journal of Composite Materials*, **31**, 720–44.
8. Hansen, R. S. (1990) RTM processing and applications. SME Technical Papers, EM 90-214, Society of Manufacturing Engineers, 1 SME Drive, PO Box 930, Dearborn, Michigan 48121.
9. Kittelson, J. L. and Hackett, S. C. (1994) Tackifier/resin compatibility is essential for aerospace grade resin transfer molding. *Proceedings of the 39th International SAMPE Symposium*, Society for the Advancement of Materials and Process Engineering, 1161 Parkview Drive, Covina, CA 91724-3748, pp. 83–96.
10. Martin, J. (1996) Braided reinforcements enhance properties in structural composites – a case study. *Proceedings of the 41st International SAMPE Symposium*, Society for the Advancement of Materials and Process Engineering, 1161 Parkview Drive, Covina, CA 91724-3748, pp. 1245–52.
11. Sharpless, G. C. (1991) Advancement of braiding/resin transfer molding from commercial to aerospace applications. *Proceedings of the 7th Annual ASM/ESD Advanced Composites Conference*, ESD, The Engineering Society, Ann Arbor, Michigan 48105, pp. 11–21.
12. Florentine, R. A. (1991) The designer of 3-D braided preforms and the automotive design engineer; communications for innovation and profit. *Proceed-*

- ings of the 7th Annual ASM/ESD Advanced Composites Conference, ESD, The Engineering Society, Ann Arbor, Michigan 48105, pp. 23–8.
- 13. Harris, H., Schinske, N., Krueger, R. and Swanson, B. (1991) Multiaxial stitched preform reinforcements for RTM fabrication. *Proceedings of the 36th International SAMPE Symposium*, Society for the Advancement of Materials and Process Engineering, 1161 Parkview Drive, Covina, CA 91724-3748, pp. 521–33.
 - 14. Stark, E. B. and Beitingam, W. V. (1987) Resin transfer molding materials, in *Engineered Materials Handbook 1*, ASM International, Metals Park, OH, pp. 168–71.
 - 15. Shim, S. B. and Seferis, J. C. (1994) Characterization of binder interactions with lightly crosslinked thermosets. *Science and Engineering of Composite Materials*, 3, 191–207.
 - 16. Rohatgi, V., Patel, N. and Lee, L. J. (1996) Experimental investigation of flow induced microvoids during impregnation of unidirectional stitched fibreglass mat. *Polymer Composites*, 17, 161–70.
 - 17. Brookstein, D. S. (1990) Interlocked fibre architecture: braided and woven. *Proceedings of the 35th International SAMPE Symposium*, Society for the Advancement of Materials and Process Engineering, 1161 Parkview Drive, Covina, CA 91724-3748, pp. 746–56.
 - 18. Shafer, M. P. (1995) Three dimensional preforms for structural applications. *Proceedings of the 40th International SAMPE Symposium*, Society for the Advancement of Materials and Process Engineering, 1161 Parkview Drive, Covina, CA 91724-3748, pp. 945–51.
 - 19. Gommers, B., Wang, T. K. and Verpoest, I. (1995) Mechanical properties of warp knitted fabric reinforced composites. *Proceedings of the 40th International SAMPE Symposium*, Society for the Advancement of Materials and Process Engineering, 1161 Parkview Drive, Covina, CA 91724-3748, pp. 966–70.
 - 20. Du, G. W. and Ko, F. K. (1996) Analysis of multiaxial warp-knit preforms for composite reinforcement. *Composites Science and Technology*, 56, pp. 253–60.
 - 21. Schwartz, M. (1992) *Composite Materials Handbook*, McGraw-Hill, New York.
 - 22. Soebroto, H. B. and Ko, F. K. (1989) Composite preform fabrication by 2-D braiding. *Proceedings of the 5th Annual ASM/ESD Advanced Composites Conference*, ESD, The Engineering Society, Ann Arbor, Michigan 48105, pp. 307–16.
 - 23. Du, G. W. and Popper, P. (1994) Analysis of a circular braiding process for complex shapes. *Journal of the Textile Institute*, 85, 316–37.
 - 24. Li, W., Hammad, M. and El-Shiekh, A. (1990) Structural analysis of 3-D braided preforms for composites, part I: the four step process. *Journal of the Textile Institute*, 81, 491–514.
 - 25. Ramasamy, A., Wang, Y. and Muzzy, J. (1994) Braiding and molding of powder coated towpregs. *Proceedings of the 39th International SAMPE Symposium*, Society for the Advancement of Materials and Process Engineering, 1161 Parkview Drive, Covina, CA 91724-3748, pp. 844–56.
 - 26. Shields, K. and Colton, J. (1993) Resin transfer molding with powder coated preforms. *Polymer Composites*, 14, 341–8.
 - 27. Flonc, N. P. and Brace, M. W. (1993) Stabilized complex composite preforms. *US Patent*, 5,217,766.
 - 28. Tsai, J. S., Li, S. J. and Lee, L. J. (1996) Preforming analysis and mechanical properties of composite parts made from textile preform RTM. *Proceedings of the 41st International SAMPE Symposium*, Society for the Advancement of

- Materials and Process Engineering, 1161 Parkview Drive, Covina, CA 91724-3748, pp. 1230–44.
- 29. Brosius, D. and Clarke, S. (1991) Textile preforming techniques for low cost structural composites. *Proceedings of the 7th Annual ASM/ESD Advanced Composites Conference*, ESD, The Engineering Society, Ann Arbor, Michigan 48105, pp. 1–10.
 - 30. Johnson, C. F. (1990) Resin transfer molding, in *Composite Materials Technology – Processes and Properties*, (eds P. K. Mallick and S. Newman), Hanser, New York, Ch. 5.
 - 31. Rohatgi, V. (1995) *Liquid Molding of Textile Reinforcements: Analysis of Flow Induced Voids and Effect of Powder Coating on Preforming and Moldability*. PhD dissertation, The Ohio State University, OH.
 - 32. Hou, T. H. (1986) A resin flow model for composite prepreg lamination process. *Proceedings of the Society of Plastics Engineers, Annual Technical Conference*, pp. 1300–5.

Preform permeability

Richard S. Parnas

7.1 INTRODUCTION

The need for the resin to flow over long distances through a preform of complex structure is unique to liquid composite moulding (LCM) in comparison with other composite manufacturing methods. However, an extensive literature on the general topic of flow through porous media exists and is helpful for understanding the effects of geometrical complexity on flow behaviour [1–3]. A brief summary of the salient points of the general literature will serve as an introduction to the historical problem of measuring the critical parameters required to characterise the flow of resins into a mould containing a preplaced reinforcement preform.

7.1.1 FLOW THROUGH POROUS MEDIA

A porous medium may be characterised by several length scales, as illustrated in Figure 7.1. In general, a porous medium consists of a small scale ℓ , characteristic of the particles or interstitial spaces from which the medium is constructed, and a large-scale \mathcal{L} , which determines the overall extent of the medium. A number of intermediate length scales may also be envisioned, especially if the porous medium contains particles of several sizes. Additionally, other types of length scales may exist that depend upon other properties of the porous medium such as the fluid flow behaviour.

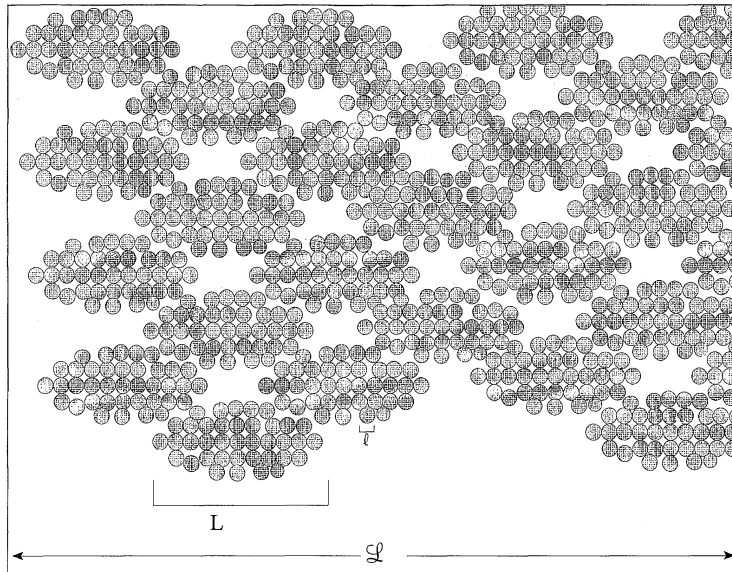


Figure 7.1 Schematic diagram of a fibrous porous medium with multiple length scales. The macroscopic length scale, \mathcal{L} , indicates the overall size of the medium, and the microscopic scale, ℓ , represents the smallest elements such as the individual filaments or the pores between the filaments. One of the mesoscopic scales is shown as L and indicates the size of the tows forming the medium.

The detailed flow behaviour of typical liquid resins within the porous medium can be described with the Navier–Stokes fluid mechanics equations for incompressible flow [4]:

$$\rho \frac{D\mathbf{v}}{Dt} = -\nabla P + \mu \nabla^2 \mathbf{v} \quad (7.1)$$

where the notation on the left-hand side represents the ‘material’ derivative of the fluid velocity vector. An immediate simplification can be made since the flows of concern in composites processing are typically slow enough, even for structural resin injection moulding (SRIM), to neglect the non-linear momentum terms contained in the material derivative, leading to the Stokes flow equation:

$$0 = -\nabla P + \mu \nabla^2 \mathbf{v} \quad (7.2)$$

Equation (7.2) still presents a formidable problem since the solution is subject to the no-slip boundary condition on the very complex shape of the porous medium surface.

The classical solution to the problem of solving the flow behaviour within the complex geometry of porous media has relied on the procedure of volume averaging to further simplify equation (7.2) [1]. Volume

averaging makes use of an intermediate length scale, L (Figure 7.1), which is small enough to preserve enough information for most practical purposes, such as process design, but is large enough to eliminate most of the geometrical complexity. If the volume average of a scalar quantity B is defined as

$$\langle B \rangle = \frac{1}{V} \int_V B \, dV \quad (7.3)$$

where V is the averaging volume, and $V \propto L^3$, then similar relations can be defined for vector and tensor properties, and the momentum equation, equation (7.2), can be volume averaged. When that operation is performed, and the porous media is also assumed infinite in extent, then the Darcy relationship is obtained:

$$\langle v \rangle = \frac{\mathbf{K}}{\mu} \langle \nabla P \rangle \quad (7.4)$$

where \mathbf{K} is the permeability tensor and depends only on the geometry of the porous medium through the volume averaging operations. Thus the difficulty of computing the detailed flow behaviour in a geometrically complex porous medium has been replaced by the difficulty of computing averaged flow behaviour with an equation containing an unknown quantity, \mathbf{K} . \mathbf{K} is indeed unknown in realistic porous media since the geometries of such media are not precisely known. For model porous media or reconstructed porous media \mathbf{K} can be computed analytically for simple cases or numerically for more complex cases [3]. For example, in a medium containing only straight parallel tubes, each of radius R , the scalar permeability is $\epsilon R^2 / 8$, where ϵ is the porosity of the medium and $R^2 / 8$ is the equivalent permeability of a single tube.

7.1.2 THE IMPORTANCE OF PERMEABILITY IN LIQUID COMPOSITE MOULDING

The importance of the permeability is that one can compute flow behaviour in large complex moulds with use of equation (7.4), if one knows \mathbf{K} , whereas the required computational resources are prohibitive for computing flow behaviour on the scale of the mould with equation (7.2), even if the detailed porous medium geometry were known. Thus an important problem in the process design of LCM is obtaining permeability values for reinforcements of industrial interest. Note, however, that the permeability, as defined above, pertains to the steady flow of fluid in a fully saturated porous medium where the no-slip boundary condition is satisfied on the porous medium surface in contact with the fluid. In contrast, the resin injection process in LCM involves unsteady flow of resin into an unsaturated preform. Therefore, the permeability

alone is not expected to characterise fully the LCM flows. Nevertheless, mould-filling simulations in current usage rely exclusively on solving Darcy's law [equation (7.4)] in conjunction with a flow front boundary condition to account for the front movement.

In large parts of complex geometries, LCM simulations can help in designing the mould by locating optimal positions for fill ports and vents [5]. Since the permeability tensor of many reinforcements is highly anisotropic, the pathways of resin flow are often counterintuitive, requiring simulation and visualisation. In such simulations, knowledge of the heat transfer behaviour and thermal gradients is just as important as knowledge of the permeability, since the temperature strongly influences the resin viscosity, and the viscosity appears in Darcy's law along with the permeability [6]. Once the fill port and vent locations are designed, the mould-filling simulations continue to play a useful role by predicting the pressure distributions throughout the mould. The pressure distributions are found in the simulations by substituting Darcy's law into the equation of continuity, $\nabla \cdot v = 0$, and solving the resultant partial differential equation for the pressure distribution. Note that the governing parameters in the partial differential equation are the components of the permeability tensor [equation (7.30), section 7.3.2]. The pressure distributions that accumulate in the mould help define the required pumping power, the required clamping pressure to hold the mould closed and the required stiffness of the mould to retain its shape during the moulding operation.

The permeability is determined by the structural features of the reinforcement, including the fibre volume fraction, the reinforcement architecture and the tow construction. The classical model for the dependence of permeability on porosity, the Carmen–Kozeny model [7], was developed for isotropic particulate porous media and does not work well for the anisotropic fibrous media used in composites [8]. More recent models have enjoyed limited success in describing particular types of reinforcements (e.g. unidirectional, random mat, etc.), and the limits of such models may be a result of the wide variety of microgeometries that can be created by combining the fibres in various architectures. The difficulties such models confront may be summed up by noting that the permeability of different fabrics may vary by as much as an order of magnitude at the same fibre volume fraction [9]. Thus, a model that purports to predict the permeability of fibrous media must account for the fabric architecture in addition to the fibre volume fraction. Finally, recent experimental and modelling work also indicates that the structure of the tows themselves can play a significant role in determining the permeability [10]. Thus the permeability is related to structural features of the reinforcements at several length scales [11], and predicting the permeability directly from the structure is a subject of intense current research.

Currently, the most reliable way of assessing preform permeability is with fluid flow experiments. Consequently, the remainder of this chapter will focus on experimental measurements of permeability and their interpretation. After describing the measurement methods for assessing the permeability of reinforcement preforms, additional discussion will assess methods for determining the contributions to the flow behaviour that arise from the unsaturated flow near the flow front during moulding operations.

7.2 EXPERIMENTAL METHODS

The two most widely used methods of characterizing the flow of viscous fluids through the reinforcements typically used in LCM are the unidirectional flow method and the radial flow method. The unidirectional experiment allows the unsaturated flow data to be directly compared with the saturated flow data, providing insight into differences that may be expected during mouldings as compared with pure permeability-based flow behaviour. The radial experiment permits the rapid determination of both components of the in-plane permeability tensor but only for unsaturated flow. Each method will be described, typical data presented and mistakes to be avoided discussed.

7.2.1 UNIDIRECTIONAL FLOW METHOD

Saturated flows

Unidirectional flow experiments are typically conducted in flat moulds with a transparent top of glass or acrylic (see Figure 7.2). A variety of mould sizes and thicknesses have been reported in the literature, and an example design is given typical of that used in the National Institute of Standards and Technology (NIST) laboratories [12]. The mould contains a $15.24 \text{ cm} \times 15.24 \text{ cm}$ ($6'' \times 6''$) sample section, and the thickness of the test sample can be adjusted between 0.3175 cm ($\frac{1}{8}''$) and 1.27 cm ($\frac{1}{2}''$). It is important that the sample size be large compared with the size of the tows, the thickness of the layers and the dimension of the repeat pattern in the fabric construction to ensure that volume-averaged flow behaviour is observed. Additionally, the sample is constrained by inlet and outlet gates, as shown in Figure 7.2, to prevent sample movement during the experiment and to allow for uniform fluid distribution at the inlet and outlet. The top of the mould was 2.54 cm thick acrylic to permit observation of the flow front as the fluid initially filled the mould. Such observation is important, even in saturated flow experiments, since non-uniform filling indicates an improperly constructed experiment.

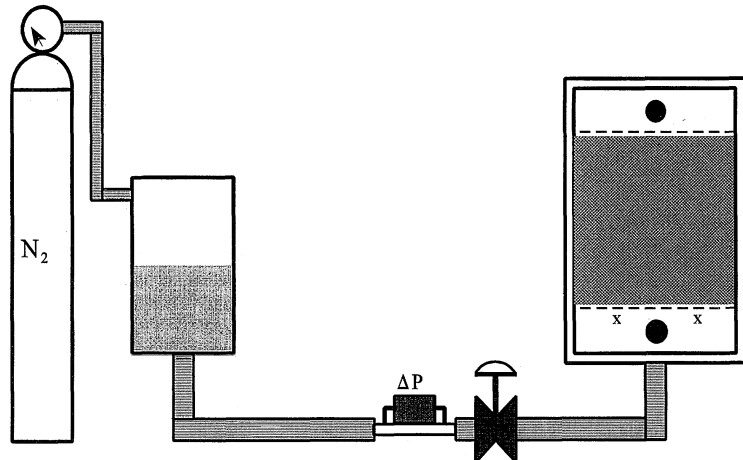


Figure 7.2 Apparatus for conducting unidirectional flow experiments with non-reactive fluids. A nitrogen cylinder provides pressure to force the fluid from the tank. Fluid flow into the mould is measured by a differential pressure cell and controlled by a valve. Mould inlet pressure is measured by transducers located at the positions marked 'X'.

Saturated flow experiments are conducted by forcing a test fluid through the mould and measuring the steady-state relationship between the flow and the pressure drop across the length of the mould. The pressure-pot system shown in Figure 7.2 is a convenient and inexpensive method of pumping the test fluid. The fluid flow is measured as it enters the mould with a differential pressure cell and may also be monitored at the mould exit with volumetric measurements. Pressures at the mould inlet are measured by calibrated transducers that are mounted at two positions on the back face of the mould, located at the lower boundary of the reinforcement sample. The pressure at the outlet of the mould is assumed equal to the atmosphere. Once a steady flow and pressure are established, data are recorded. If the test fluid has a Newtonian rheology then a linear relationship is obtained between the steady-state flows and pressure-drops, as indicated in Figure 7.3 [13]. Although the flow of non-Newtonian fluids in porous media is of interest in a number of applications [3], the determination of permeability is most accurately accomplished by utilising a Newtonian test fluid.

The data shown in Figure 7.3 indicate that the flow/pressure drop relationship may depend upon the direction of fluid flow through the sample, as is expected if the permeability tensor is anisotropic. The upper line is the best fit to the data (\blacksquare) collected for flow through the fabric parallel to the warp fibres, and the lower line fits the data (\bullet) for flow through the fabric parallel to the fill fibres. An effective permeability, K_e^θ ,

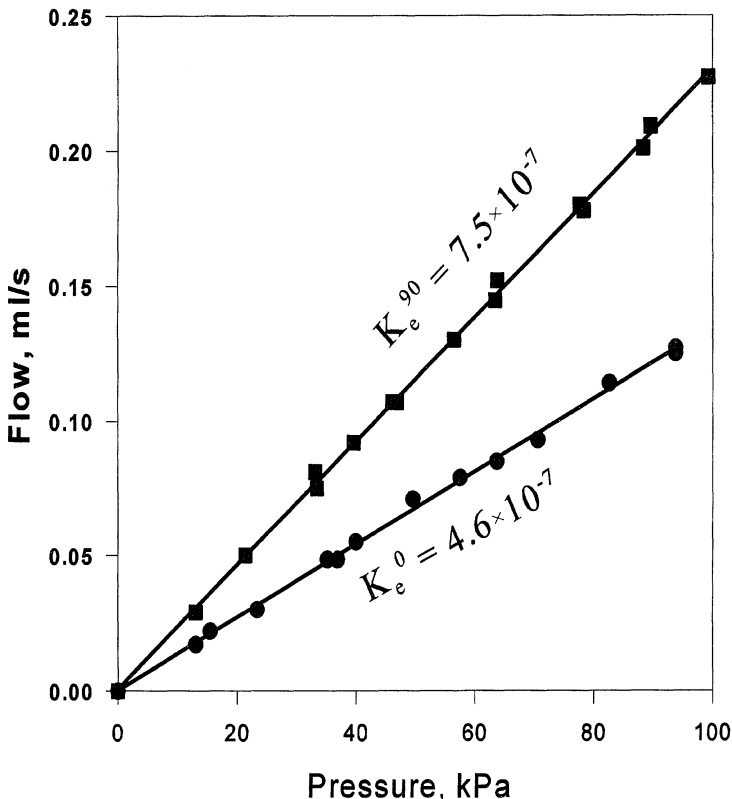


Figure 7.3 An example of saturated unidirectional flow data collected for a corn syrup/water solution in a crowfoot weave glass fabric at approximately 49.1% fibre volume fraction. Owing to anisotropy in the permeability tensor, the flow/pressure relationship for flow in the direction of the warp fibres (■) is different from that in the direction of the fill fibres (●).

can be obtained from each set of data, the superscript θ indicating the angle of fluid flow relative to a predefined fabric coordinate system (Figure 7.4). A scalar form of Darcy's law is used to relate the flow and pressure gradient in the unidirectional flow experiments, and the relationship between the scalar form of Darcy's law [equation (7.5) below] and the tensorial form, [equation (7.4)], is as follows [equations (7.26)–(7.35)]:

$$\langle v \rangle = \frac{Q}{A} = \frac{K_e^\theta}{\mu} \frac{\langle \Delta P \rangle}{\mathcal{L}} \quad (7.5)$$

where \mathcal{L} is the length of the porous medium and where the ratio of the pressure drop $\langle \Delta P \rangle$ to the mould length is used to approximate the

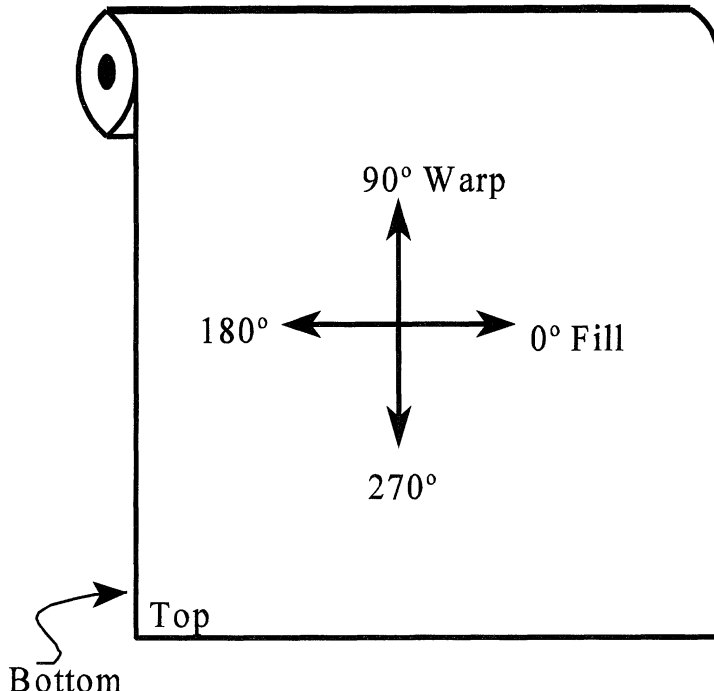


Figure 7.4 The coordinate system used to describe orientation for the permeability experiments reported here and in several of the references.

pressure gradient. The averaged velocity, $\langle v \rangle$, is simply the total fluid flow, Q , divided by the cross-sectional area of the mould, A . Thus, a plot of Q against ΔP , as in Figure 7.3, has a slope of $K_e^\theta A / \mu \mathcal{L}$, from which K_e^θ is obtained. For example, the effective permeabilities for the data shown in Figure 7.3 and for several other glass fabrics are given in Table 7.1 and Figure 7.5 [12, 13]. Further analysis is required to derive the permeability tensor, K , since the principal orientation angles of the permeability are not known *a priori*; such analysis will be described after the discussion of the experimental techniques is completed [equations (7.22)–(7.26)]. Unidirectional experiments with several materials were not conducted at all four listed orientations in Table 7.1 because of handling or other considerations [12], but a method of combining radial flow and unidirectional flow data will be discussed below which allows the determination of the missing information. The data in Figure 7.5 illustrate several important general points:

1. chopped mats (◻) behave differently from continuous strand random mats (⊕);

Table 7.1 Effective permeability values of glass fabrics at several flow angles, θ

Fabric	Effective Permeability (cm^2) ^a			
	$\theta = 0^\circ$	$\theta = 90^\circ$	$\theta = 45^\circ$	$\theta = 135^\circ$
JPS 8-harness satin	3.91×10^{-8} (55.5)	4.49×10^{-8} (55.5)	2.04×10^{-8} (55.7)	2.40×10^{-8} (55.7)
CNF crowfoot	4.57×10^{-7} (49.1)	7.50×10^{-7} (49.1)	1.02×10^{-6} (45.3)	9.52×10^{-7} (45.3)
Three-dimensional woven			1.03×10^{-6} (52.3)	8.70×10^{-7} (52.2)
Cotech™ $\pm 45^\circ$ stitched	8.92×10^{-8} (55.13)	9.09×10^{-8} (55.04)		
Vetrotex™ continuous strand random mat	6.34×10^{-5} (15.45)	6.23×10^{-5} (15.41)		

^a Percentages are given in parentheses below.

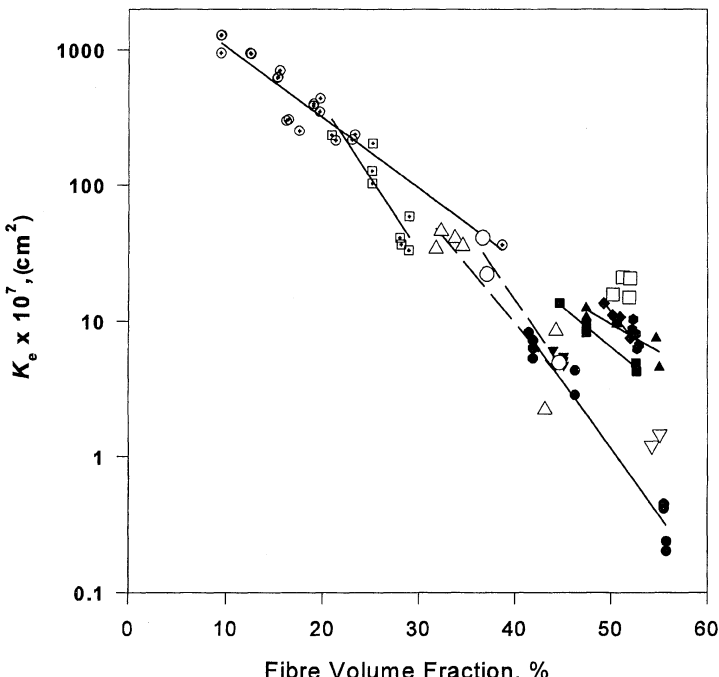


Figure 7.5 Example permeability (K_e) data obtained from saturated, unidirectional flow experiments with several types of glass fabrics. The permeabilities illustrated for highly anisotropic materials (unidirectionals) are the larger component of the in-plane permeability tensors, K_{xx} . ○ = woven warp unidirectional; □ = weft unidirectional; -△- = Knytex™ $\pm 45^\circ$; ▽ = Cotech™ $\pm 45^\circ$; -●- = JPS 8-harness woven; -■- = CNF 5-harness woven; -▲- = CNF crowfoot woven; -▼- = CNF 8-harness woven; -◆- = TTI three-dimensional woven; ◉ = SRM three-dimensional woven; ⊕ = continuous strand random; ▨ = chopped random.

2. woven fabrics may have very different permeabilities at the same fibre volume fractions (\bullet , \blacksquare , \blacktriangle , \blacktriangledown);
3. unidirectional fabrics may also have very different permeabilities at the same fibre volume fraction (\circ , \square).

A number of errors may reduce the accuracy of the unidirectional flow method, and the three major errors are illustrated schematically in Figure 7.6. The error most commonly associated with the unidirectional flow experiment is the ‘edge effect’ error in which small gaps between the edges of the preform and the mould wall contribute inordinately to the total flow through the mould. In such cases, erroneously high measurements of the effective permeability are obtained since at each pressure drop a flow is obtained that is larger than would have been obtained without the edge effects. An important point to note is that even with edge effects a linear relationship between the flow and the pressure drop is often obtained, so the linearity, or lack thereof, of the plotted data is not an indicator of edge effects. An analysis of edge effects during

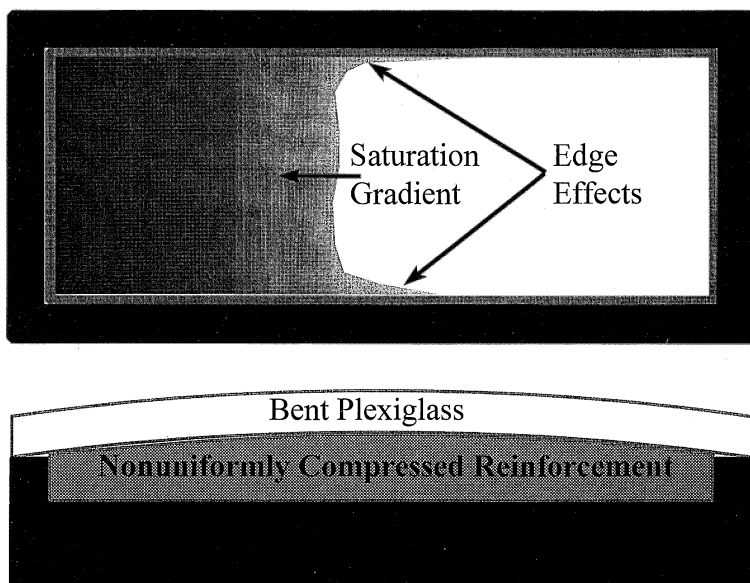


Figure 7.6 Three experimental artifacts that can reduce the accuracy of the measured permeability in unidirectional flow experiments. Edge effects occur when the fluid flows preferentially along the edges of the sample, and will result in an overestimation of the permeability. Saturation gradients occur during the filling of multi-scale media, and if saturation is not completed then the permeability may be either overestimated or underestimated. Non-uniformly compressed samples occur as a result of the use of pliable transparent mould tops and if not corrected will cause an overestimate of the permeability.

saturated flow, based upon the Brinkman equation, is illustrated in Figure 7.7 to demonstrate the sensitivity of the unidirectional flow experiment to edge effects [14, 15]. An important point to note is that the sensitivity is a function of the width of the mould, and that wider moulds are less sensitive to edge effects. For example, if the permeability of the preform is 10^{-6} cm^2 , then a gap δ of 0.2 mm along the mould edge would produce an error in the permeability measurement of approximately 10% in a mould of half-width $Y = 30 \text{ cm}$, and an error of about 50% in a mould of half-width $Y = 3 \text{ cm}$. Most importantly, however, is the large increase in the fluid velocity in the edge region, compared with the Darcy velocity, required to produce a significant error in the measured flow. For the example stated above, the velocity in the edge region is expected to exceed the Darcy velocity by more than a factor of five during sat-

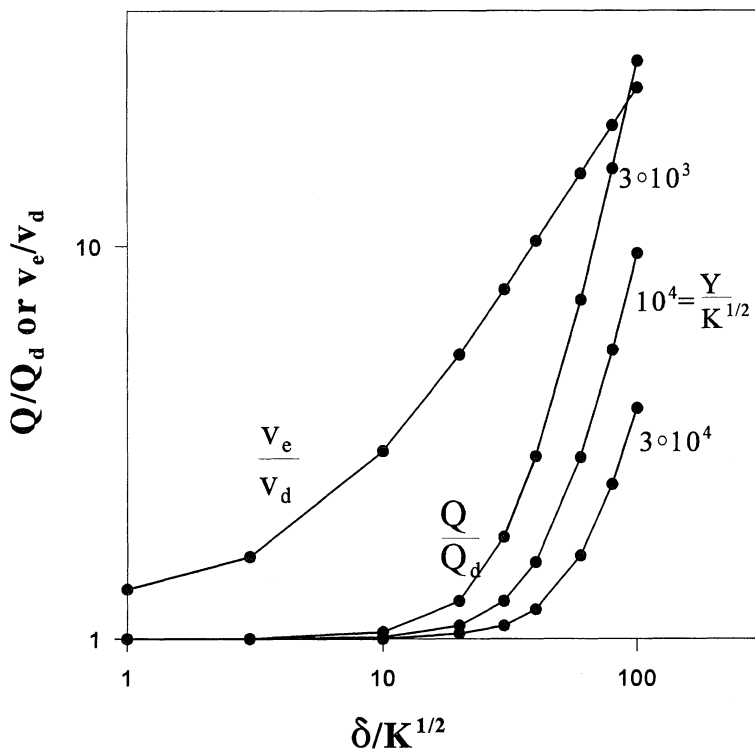


Figure 7.7 An analysis of edge effects in saturated flow based on the Brinkman equation. For edge gaps, δ , in excess of $10K^{1/2}$ the measured flow, Q , becomes significantly larger than the expected Darcy flow, Q_d , if there were no edge gap. By the time such an increase in flow occurs, the velocity in the edge gap, v_e , is several times larger than the Darcy velocity, v_d , providing a sensitive visual check on the significance of edge effects. Note: Y = mould half-width; K = permeability.

rated flow. Simulations of unsaturated flows indicate that easily detectable non-uniform flow fronts may be expected to occur for such cases. The large velocity in the edge region means that edge effects are easily observable through a transparent mould and that badly constructed experiments can therefore be detected and eliminated. The elimination of edge effects requires either sealing the edges of the preform to the mould sides or designing the mould tooling to seal the edges during the closure procedure.

A second error that can effect unidirectional flow experiments is mould deflection, especially when transparent plastic mould lids are used to detect edge effects. Deflection of a mould lid can arise from two sources: the initial clamping pressure required to compress the sample and the additional hydrodynamic pressure developed during the experiment owing to fluid flow. Both sources of deflection are easily treated by use of a bolt-on metal top that is attached to the mould after the initial mould filling is completed, and it is verified that edge effects are minimal. If such a precaution is not taken, erroneous results can be obtained such as apparently non-Darcian behaviour where the effective permeability appears to increase as the flow and pressure-drop increase. In that case, a non-linear relationship between the flow and pressure-drop is obtained as a result of increasing mould deflection as the pressure-drop and flow are increased. In the coordinates of Figure 7.3, a concave upwards curve would be obtained as the flow would increase disproportionately with the pressure-drop. A more subtle error occurs if the clamping pressure is much larger than the hydrodynamic pressures, and mould wall deflection occurs solely as a result of clamping pressure. In that case, a linear flow/pressure-drop relation is obtained but the measured permeability is too large.

The third common error in the unidirectional flow experiment is caused by not completely saturating the reinforcement sample before taking measurements; incomplete saturation manifests itself in a variety of ways in the measured data. After taking each steady-state data point, and changing the flow or pressure, a long period of time will be required for the system to settle to a new steady state. After acquiring several data points at increasing flows, a trend in the data may become apparent in which the permeability appears to increase. Upon acquiring several additional points at decreasing flows a second curve manifests itself, and if enough data are acquired over a broad enough flow range a hysteresis cycle may become apparent. Such behaviour may be due to the re-equilibration of the trapped air within the sample that occurs at each different flow.

The problems caused by incomplete saturation are usually obvious enough that the experiment is halted. However, the first two errors of mould deflection and edge effects can be subtle enough to go unnoticed.

Unsaturated flows

During the initial mould filling of a unidirectional experiment it is possible to log the mould inlet pressure, flow and flow front position as functions of time and to analyse those data to determine the unsaturated permeability, K_u^θ . Such data will include the effects of incomplete sample saturation and a moving flow front, even if mould deflection and edge effects are minimised. Thus, if a Darcy analysis, based on equation (7.5), is used to determine K_u^θ , misleading conclusions may be obtained unless care is taken in interpreting the results. It is important to note that K_u^θ obtained directly from equation (7.5) is not a permeability in the Darcy sense but is a measure of the overall flow behaviour. Nevertheless, values of K_u^θ may be valuable for simulation purposes as the currently available simulations rely only on Darcy's law.

An example of unsaturated flow data is shown in Figure 7.8 for the case where the flow was controlled to a constant value during injection

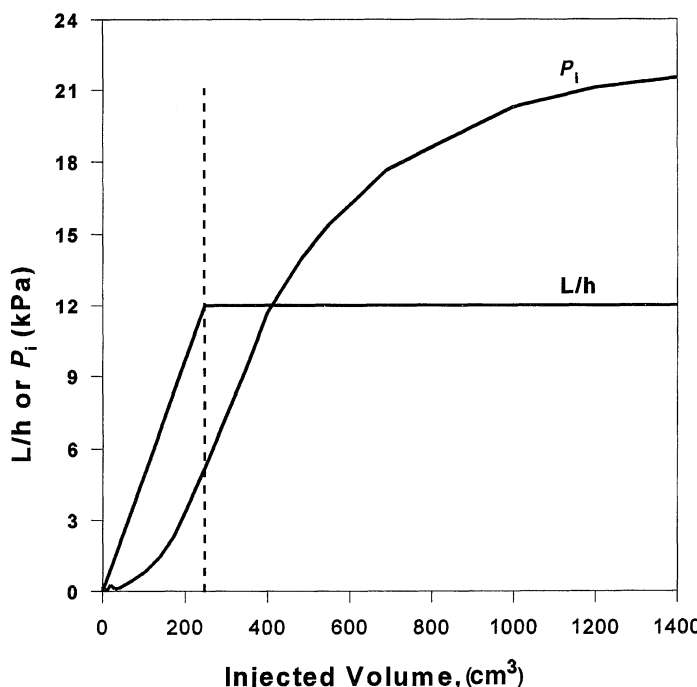


Figure 7.8 The flow front progression (L/h) and mould inlet pressure (P_i) evolution during unidirectional unsaturated flow into a continuous strand random mat. At constant injection rate, the average flow front location advances as a linear function of time, but the mould inlet pressure does not increase significantly until the flow front has nearly reached half the length of the mould.

into a random continuous mat [12]. The progression of the flow front is illustrated in Figure 7.8 and, as expected, the position of the flow front increases linearly with time for this case of constant injection rate. However, the build-up of mould inlet pressure, also shown in Figure 7.8, did not proceed in a simple manner, indicating a more complex relationship between the flow and pressure-drop than seen previously in the saturated flow experiments described above (Figure 7.3). Additionally, the mould inlet pressure continued to rise long after the flow front reached the end of the reinforcement, indicated in Figure 7.8 by the vertical dotted line, and fluid began exiting the mould.

The straightforward Darcy analysis of the unsaturated unidirectional flow experiments requires the manipulation of the transient pressure data collected as the mould filled. At any given time t during the mould filling, the value of K_u^θ may be obtained with the one-dimensional expression of Darcy's law [equation (7.5) suitably rearranged] if the mould inlet pressure, P_i , and flow front location, \mathcal{L} , are known:

$$K_u^\theta(t) = \frac{\mu v}{P_i(t)/\mathcal{L}(t)} \quad (7.6)$$

where ΔP in equation (7.5) has been replaced by P_i since the pressure at the flow front is zero, and the angle brackets, $\langle \rangle$, denoting volume averaging, have been dropped for brevity. The symbol \mathcal{L} is used to denote the flow front location as it is the macroscopic length scale of interest (Figure 7.1). The flow front location is well known in an experiment conducted at constant flow because the average flow front location may be obtained by a simple mass balance on the mould:

$$\mathcal{L}(t) = \int_0^t \frac{v}{1 - V_f} d\tau = \frac{Qt}{A(1 - V_f)} \quad (7.7)$$

where V_f is the fibre volume fraction. In addition to using the condition of constant flow to integrate the expression in equation (7.7) the fibre volume fraction has also been assumed to be constant throughout the flow domain.

The analysis of the constant flow experiment illustrated in Figure 7.8, according to equations (7.6) and (7.7) yields values of the unsaturated permeability, K_u^θ , that are not constant during the experiment, as shown in Figure 7.9. The value of K_u^θ , obtained by the procedure outlined above [equation (7.5)] first increased, passed through a maximum and then decreased to a value very close to the saturated permeability. Such behaviour is due to the advancement of the flow front without a proportional increase in the mould inlet pressure (Figure 7.8). The mould inlet pressure did not initially rise as the fluid entered the sample owing to wicking effects that sucked the fluid into the sample faster than it was being injected. Such wicking behaviour has been observed in a number of

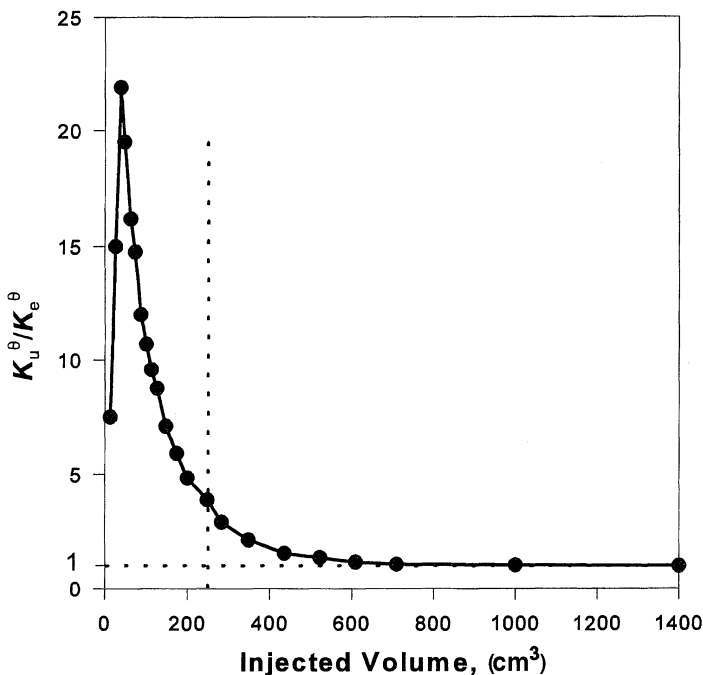


Figure 7.9 The unsaturated permeability, K_u^θ , derived from the data in Figure 7.8 and neglecting the effects of incomplete saturation. In this case incomplete saturation was caused by wicking. K_e^θ is the effective permeability at angle of fluid flow θ .

materials. Note that since P_i did not rise initially, the computed values of K_u^θ early in the experiment may not be accurate because of high levels of noise in the pressure measurement which always occurs when instruments are read at the extremes of their ranges. However, the computed values of K_u^θ at injected volumes larger than about 50 cm^3 are expected to be accurate since the value of P_i had increased above the noise level of the instrumentation.

As the fluid penetrated further into the sample a saturated region developed behind the flow front where wicking effects diminished and pressure was required to drive the flow, leading to a rise in mould inlet pressure, P_i . The effects of incomplete saturation persist for a period of time after the flow front reaches the end of the mould, as indicated by the rise in P_i and the decrease in K_u^θ after the flow front reached the end of the mould. Thus, an experiment based purely on unsaturated flows, and interpreted with use of equations (7.6) and (7.7), may be subject to very large errors if an accurate determination of permeability is the goal.

If the unsaturated flow experiment were conducted with a constant value of mould inlet pressure instead of constant fluid flow, the flow

front would not advance at a constant rate. Rather, it advances according to

$$\frac{d\mathcal{L}}{dt} = \frac{v}{1 - V_f} = \frac{K_u^\theta P_i}{\mu \mathcal{L}(1 - V_f)} \quad (7.8)$$

where Darcy's law [equation (7.5)] has been used to substitute for the fluid velocity, v . If K_u^θ remains constant then equation (7.8) can be integrated as a first-order differential equation to give

$$\frac{\mathcal{L}^2}{2} = \frac{K_u^\theta P_i}{\mu(1 - V_f)} t \quad (7.9)$$

Thus, for constant pressure injection, the position of the flow front is expected to increase as $t^{1/2}$, and a plot of \mathcal{L}^2 against t could be used to determine K_u^θ . Such work has been carried out [16]; a linear relationship was observed between \mathcal{L}^2 and the time t , but a more complete analysis of unsaturated flows will show why analyses based on equations (7.6) and (7.7) or on equations (7.8) and (7.9) are incomplete.

The following analysis is also the beginning of a discussion that reconciles the differing behaviours observed in constant pressure and constant flow unsaturated experiments, and that discussion will be concluded in the section on radial flows. Wicking effects were primarily responsible for the large fluctuations in the value of K_u^θ observed in Figure 7.9, and an analysis method has been developed to account for simultaneous pressure driven and wicking flows [17, 18]. In this method, Darcy's law is written for unsaturated flow [equation (7.5)] as above, but a term for the capillary pressure at the flow front is included:

$$v = \frac{K_u^\theta}{\mu} \nabla P = \frac{K_u^\theta}{\mu} \left(\frac{\Delta P_h + \Delta P_c}{\mathcal{L}} \right) = (1 - V_f) \frac{d\mathcal{L}}{dt} \quad (7.10)$$

where ΔP_c is the capillary pressure and ΔP_h is the hydrodynamic pressure included in the previous equations. Note that equation (7.10) implies that measurements of the mould inlet pressure, P_i , may be less than ambient at early times in experiments with strongly wicking reinforcements. Thus, vacuum pressure transducers may be required for such experiments, which was not the case for the results illustrated in Figures 7.8 and 7.9. Nevertheless, the portion of the results during which the pressure was clearly greater than zero (injected volume greater than 50 cm³ in Figure 7.8) remain valid, illustrating that K_u^θ can vary during such experiments if wicking is not taken into account.

In the work of Miller and Friedman [18] experiments were conducted at constant hydrodynamic pressure, which produced flow fronts expected to advance according to

$$\mathcal{L}^2 = \frac{2K_u^\theta}{\mu(1 - V_f)} (\Delta P_h + \Delta P_c) t \quad (7.11)$$

since the capillary pressure was also assumed to be constant. In such unsaturated flow experiments run at constant pressure the slope $d(\mathcal{L}^2)/dt$, s , where

$$s = \frac{d\mathcal{L}^2}{dt} = \frac{2K_u^\theta}{\mu(1 - V_f)} (\Delta P_h + \Delta P_c) \quad (7.12)$$

taken at a single value of ΔP_h has been used to determine the permeability K_u^θ by other workers. However, that is only possible if the effects of wicking are neglected or ΔP_c is known beforehand. More generally, one can obtain both the permeability and the capillary pressure if several values of ΔP_h are used during a single experiment [18].

A different value of the slope s is obtained at each level of ΔP_h , and if the values of s are subsequently plotted against ΔP_h then a straight line should be obtained with slope

$$S = \frac{ds}{d\Delta P_h} = \frac{2K_u^\theta}{\mu(1 - V_f)} \quad (7.13)$$

from which the permeability can be obtained, and with a y -intercept, y_0 , given by

$$y_0 = \frac{2K_u^\theta}{\mu(1 - V_f)} \Delta P_c \quad (7.14)$$

from which the capillary pressure can be obtained. This type of analysis was originally applied to experimental data taken by measuring the mass uptake of fluid in the porous medium, and the quantities discussed above are easily related to the mass uptake quantities by suitable use of the fluid density [18].

Modelling the effects of wicking by including a single value of ΔP_c in Darcy's law, as in equation (7.10), is an oversimplification of the true nature of unsaturated flow. In unsaturated flows a saturation gradient exists behind the flow front (Figure 7.5) and the capillary pressure is a strong function of the saturation level in the porous medium [19]. Nevertheless, a single value of ΔP_c , as used in equation (7.10), may be sufficient to describe capillary effects well enough for the purpose of extracting the permeability from unsaturated flow data. For the purpose of qualitative judgement, dimensionless numbers such as the capillary number [equal to $(\gamma \cos \theta)/(\mu v)$] can provide useful relationships for judging the importance of wicking effects during unsaturated flow, where γ is the fluid surface tension and θ is the contact angle between the fluid and the fibre.

The inclusion of capillary pressure has improved the analysis of unsaturated flows in some materials, and would improve the interpretation of the data illustrated in Figures 7.8 and 7.9. However, such an analysis would not explain the additional pressure rise observed after the flow

front reached the end of the mould, and shown by the pressure data to the right of the vertical dotted line in Figures 7.8 and 7.9 [12, 19]. That behaviour arises from the continuing saturation of the reinforcement after the flow front reaches the end of the mould. Thus, if the long-term flow behaviour is ignored in an unsaturated flow experiment, the measured value of K_u^θ may be in error even if wicking is accounted for with equations (7.10)–(7.14). When the time scale of saturation differs considerably from the time scale of mould filling, the flow has occurred very unevenly throughout the material, and such uneven flow behaviour is a symptom of a multiscale porous medium [11]. Most composite reinforcements have multiple length scales, as can be seen by examining Figure 7.1. Although the single intermediate scale L may have been sufficient for the volume averaging operation and to explain the saturated flow behaviour, a single intermediate scale is not sufficient to explain the unsaturated flow behaviour. For example, the interstitial spaces between the tows in Figure 7.1 are clearly much larger than the interstices within the tows themselves. Furthermore, typical reinforcements have a much more complex structure than illustrated in Figure 7.1 owing to weaving, braiding, stitching or other construction techniques that lead to the creation of several additional length scales [20]. Thus, depending upon the fluid surface interaction and the rate of fluid movement (i.e. the capillary number), the smaller spaces may fill first or the larger spaces may fill first. In either case, the reinforcement will fill unevenly. Figures 7.8 and 7.9 provide an example where the smaller spaces filled first as wicking dominated the filling process.

An example where the larger spaces have filled first is shown in Figure 7.10, in which unsaturated flow data are given for a three-dimensionally woven fabric. The mould was filled at a constant injection rate so the flow front position \mathcal{L} advanced at a constant rate just as for the random mat discussed above. However, the curve of mould inlet pressure displayed a very different shape for the three-dimensionally woven fabric than for the random mat, and the apparent unsaturated permeability also followed a very different trend [12]. In this case, the value of K_u^θ , computed with equations (7.6) and (7.7), appeared to decrease at first, then to increase to a value larger than the saturated permeability and finally to decrease to the saturated permeability after the flow front reached the end of the mould. The initial decrease in K_u^θ occurred because of the sharp initial rise in mould inlet pressure which was brought about by the confinement of the flow to the exterior regions around the tows [10, 21]. The rise of K_u^θ to values larger than the saturated permeability follows because of the subsequent tow infiltration process that occurs behind the flow front as the pressure in the porous medium rises. Finally, after the flow front reaches the end of the mould, and the saturation process becomes complete, or nearly so, the pressure completes its rise to

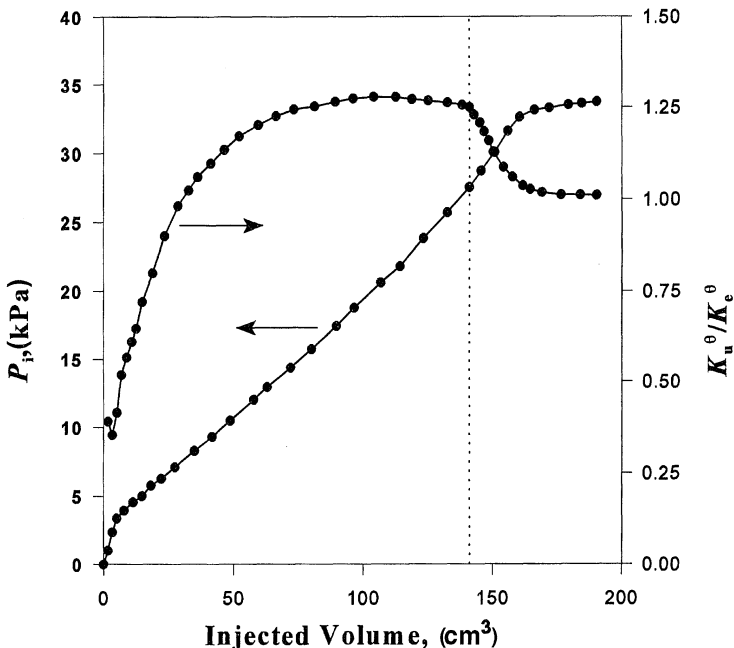


Figure 7.10 The mould inlet pressure, P_i , and the unsaturated permeability, K_u^θ , for a constant injection rate experiment with a three-dimensional woven material. The mould inlet pressure increased rapidly at first owing to incomplete saturation caused by resistance to tow filling (the opposite of wicking). K_e^θ is the effective permeability at angle of fluid flow θ .

the saturated value and the permeability appears equal to the saturated value.

The examples discussed above and illustrated in Figures 7.8–7.10 show that unsaturated flow behaviour can be quite complicated, and that permeabilities obtained from such experiments are not true permeabilities in the classical sense. Further, although it has been reported that injection at constant pressure rather than at constant flow can mitigate the effects of unsaturation, such reports were made for only one or two particular fabrics that wicked strongly, and the relationship of constant pressure injection to constant injection rate measurements will be brought out below in the discussion on the radial flow method. Before proceeding to discuss radial flow experiments, however, one more important issue remains to be mentioned in the context of unidirectional flow experiments.

A major effect not accounted for in the permeability measurements discussed above is reinforcement deformation arising from the pre-forming process. The measurements discussed above are performed on

flat stacks of material, but often the reinforcement is curved around corners in the mould to produce parts of complex shape. Some deformations can be approximated by in-plane shear of the reinforcement, and experiments have been conducted for such geometries [22]. In those cases, a sheared fabric can be placed into a flat mould for standard permeability measurements, and the shear strain significantly affects K . However, a more accurate representation of the types of fabric deformation commonly encountered during preforming is illustrated in Figure 7.11. The L-shaped mould shown in Figure 7.11 can be adjusted to provide curvatures of varying radii to measure the change in fabric permeability caused by bends. As shown, the experiment would measure the effects of fabric curvature on the behaviour of fluid flowing around the bend, and similar moulds can be developed to measure the effects of curvature on fluid flowing along the line of the bent fabric.

The analysis of the data obtained from such an experiment is quite complex and so will not be reproduced entirely (unpublished data and ref. 23). However, the major points of the analysis and example results

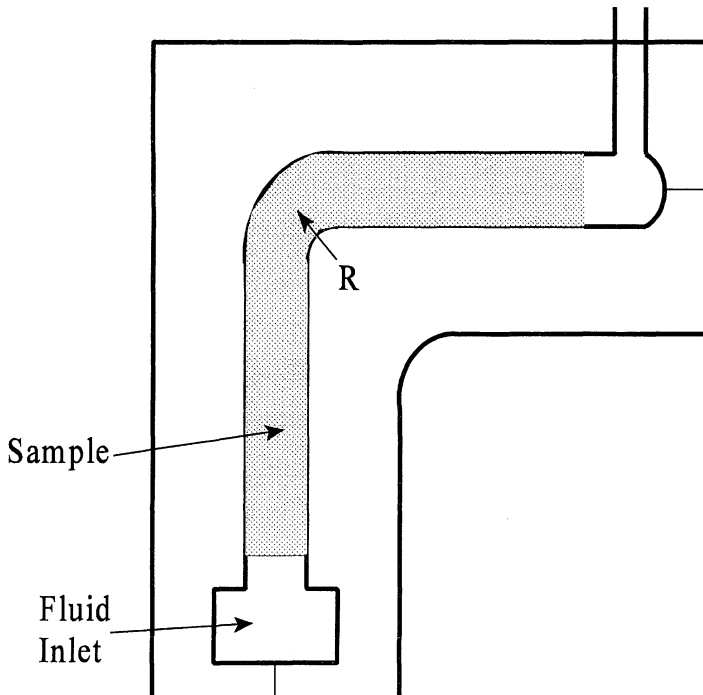


Figure 7.11 The L-cell developed to measure the permeability changes arising from fabric deformation around curves.

are discussed. The starting point of the analysis is Darcy's law, written as

$$v = \frac{K_u^\theta}{\mu \mathcal{L}} (\Delta P_c + \Delta P_h - \rho g h) \quad (7.15)$$

where the hydrostatic head, ρgh (ρ = is the density; g = is the acceleration due to gravity; h = height), is included since a portion of the experiment includes vertical flow. If we assume that the first part of the flow is vertical, so that $h = \mathcal{L}$, and that the hydrostatic pressure ΔP_h is held constant, as discussed above, then the following differential equation is developed:

$$\mathcal{L} \frac{d\mathcal{L}}{dt} = \frac{K_u^\theta}{\mu(1 - V_f)} (\Delta P_c + \Delta P_h - \rho g \mathcal{L}) \quad (7.16)$$

It is solved by integration to give

$$\frac{\mathcal{L}_u^\theta t}{\mu(1 - V_f)} = \frac{1}{(\rho g)^2} (\Delta P_c + \Delta P_h) \ln \left(\frac{\Delta P_c + \Delta P_h}{\Delta P_c + \Delta P_h - \rho g \mathcal{L}} \right) - \rho g \mathcal{L} \quad (7.17)$$

which relates the location of the flow front to the time t after the beginning of the flow. After the fluid traverses the curve in the fabric and begins travelling horizontally, the height h becomes constant and a solution to equation (7.15), similar to that developed for the unsaturated flow experiment described above, is obtained:

$$\mathcal{L}^2 - \mathcal{L}_i^2 = \frac{2K_u^\theta}{\mu(1 - V_f)} (\Delta P_c + \Delta P_h - \rho g h)(t - t_i) \quad (7.18)$$

except that the hydrostatic head term appears as a constant, t_i is the time the flow front reaches the horizontal section and \mathcal{L}_i is the flow front location at the beginning of the horizontal section.

The equations describing unsaturated flow in deformed fabric have been used to analyse data obtained for a non-woven polyester and three-dimensionally woven glass fabrics. Table 7.2 summarizes the results obtained to date and they should be regarded as somewhat preliminary.

Table 7.2 The effect of fabric deformation on the permeability, $K_u^\theta \cdot \Delta P_c$ = capillary pressure; V_f = volume fraction

Material	K_u^θ (cm ²)		ΔP_c (Pa)
	vertical	horizontal	
Non-woven Polyester ($V_f = 5\%$)	14.0×10^{-6}	7.6×10^{-6}	393.2
Non-woven Polyester ($V_f = 23\%$)	3.2×10^{-6}	2.4×10^{-6}	810.0
Three-dimensional Woven	8.9×10^{-6}	5.7×10^{-6}	621.0
Glass ($V_f = 48\%$)			

The radius of curvature for all the experiments was 12.7 mm measured on the outer curved surface. The permeability measured in the vertical stage is representative of the permeability of the undeformed material since the flow occurred in the vertical stage first. The permeability measured in the horizontal stage includes the resistance to flow in the vertical region, curved region and horizontal region and is lower in all cases than the permeability measured in the vertical region. Thus, the deformation caused by the curvature lowered the permeability of each material. An exact expression for the permeability in the curved region has not yet been derived, but methods for extracting it from the data obtained for flow in the L-cell are being developed.

7.2.2 RADIAL FLOW METHOD

One of the drawbacks of the unidirectional flow method for determining permeability is that it is time consuming. Several experiments are necessary to determine the permeability tensor, K , and each saturated flow experiment may take several hours. In an effort to reduce the time required to determine the permeability tensor, the radial flow method was developed to determine both principal components of K in the plane of the sample with a single fast experiment [24]. However, in addition to the problems with unsaturated flow experiments outlined above, the analysis of the typical radial flow experiment assumes that two of the principal components of K are in the plane of the fabric. Recently, efforts have begun to conduct three-dimensional radial flow experiments [25–27]. In either two or three dimensions it is extremely difficult to gather radial flow data in saturated flow for direct comparison with the unsaturated flow because for anisotropic flows the shape of the flow front is not circular. The material used in the flow experiments would have to be carefully cut to a special shape to ensure uniform flow boundary conditions during the saturated flow. Nevertheless, the radial flow experiment has gained in popularity because of its ease of use.

A typical planar flow cell used to gather radial flow data as viscous fluids radially penetrate fibre reinforcements at room temperature is illustrated in a simplified schematic in Figure 7.12. A radial in-plane flow is achieved by injecting the fluid through a central 1.27 cm (0.5") diameter gate into a 30.48 cm × 30.48 cm (12" × 12") region between two parallel plates containing the reinforcement. A spacer between the parallel plates set a cavity thickness of 6.35 mm (0.25"). Each layer of reinforcement has a 1.27 cm (0.5") diameter hole, created by a steel punch, centred over the injection gate to permit the fluid to penetrate evenly through the thickness of the sample. A 2.54 cm (1") thick acrylic upper plate permits visual recording of the flow front progression. The thickness of the upper plate was chosen to permit no more than a 6.35×10^{-2} mm deflection (1% of

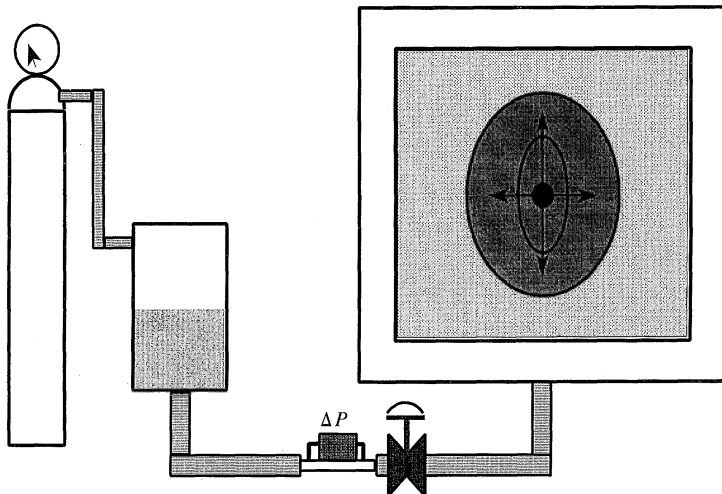


Figure 7.12 Apparatus for conducting radial flow experiments with non-reactive fluids. Pressure-driven flow is used as for the unidirectional flow hardware, but the mould is centre-gated rather than end-gated. ΔP = pressure.

the cavity thickness) at the centre of the plate for a total pressure of $3.45 \times 10^5 \text{ N/m}^2$ (50 psi). Nevertheless, mould top deflection is a major problem in most radial flow experiments, and two remedies are discussed later in this section.

The data required from a radial flow experiment depend upon the type of radial flow experiment conducted. In the typical radial flow experiment, a transparent mould lid is used to permit recording of the shape of the expanding flow front as fluid is injected, and the shape is used in the data analysis. The expanding flow fronts create elliptical shapes that are related closely to the geometry of the permeability tensor if the permeability tensor lies in the plane of the fabric [24]. The orientation of the major axis of the flow front coincides with the orientation of the permeability tensor in the plane of the fabric, and the ratio of the major and minor axes, squared, equals the ratio of the principal components of the in-plane permeability tensor:

$$\frac{K_{xx}}{K_{yy}} = \left(\frac{a}{b}\right)^2 \quad (7.19)$$

where a is the length of the major axis of the elliptical flow front and b is the length of the minor axis. Typical flow front data from a radial experiment are depicted in Figure 7.13 for the same woven glass fabric as shown in Figure 7.3, and data for other woven fabrics are shown elsewhere [12, 13, 28]. Best-fit ellipses are also shown in Figure 7.13 for each flow front. The orientation and anisotropy of the permeability tensor

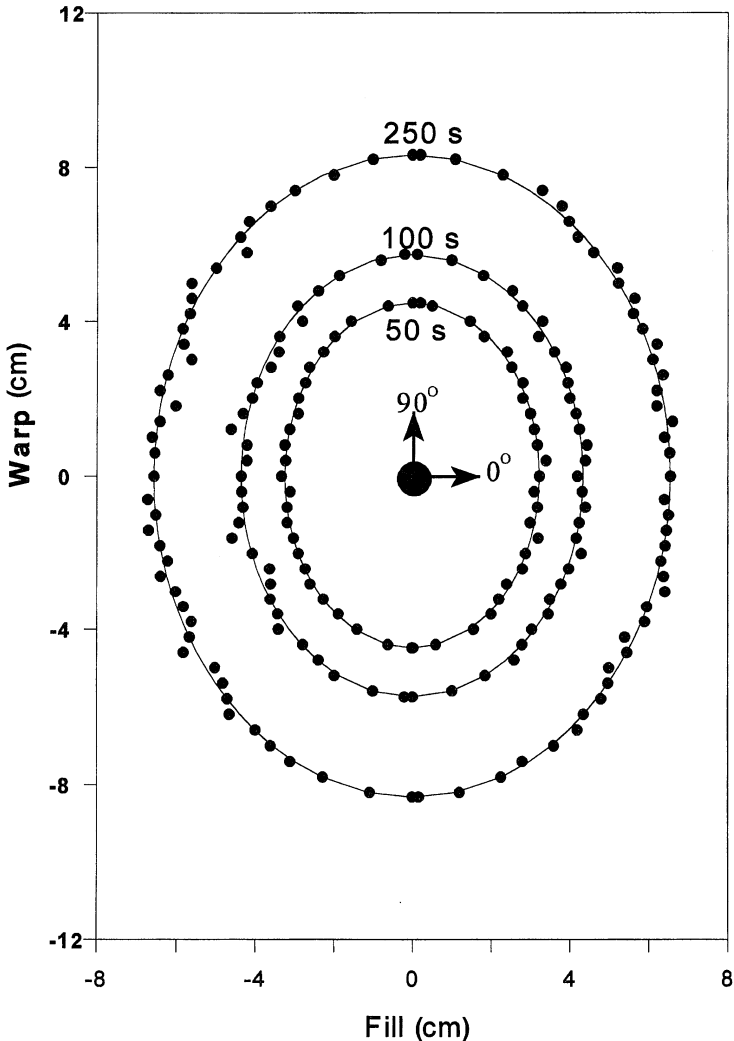


Figure 7.13 An example of radial flow data collected for a corn syrup/water solution in a crowfoot weave glass fabric. Owing to anisotropy in the permeability tensor, the shape of the flow fronts is elliptical, and the major axes of the flow fronts are oriented at 90°.

derived from the elliptical functions fit to the raw data have been shown in several cases to be equal to the equivalent information derived from saturated unidirectional flow experiments. Table 7.3 summarises such data, including a special case in which the geometrical information was not similar for the two experimental techniques. The differences in anisotropy and orientation for the five-harness satin weave fabric arose from

Table 7.3 A comparison of the geometrical properties of the permeability tensor, \mathbf{K} (components K_{xx} and K_{yy}) obtained from radial and unidirectional flow experiments

Fabric	Radial Flow		Unidirectional flow	
	K_{xx}/K_{yy}	Angle°	K_{xx}/K_{yy}	Angle°
JPS eight-harness satin	0.85	107	0.81	115
CNF eight-harness satin	0.83	79	0.73	75
CNF five-harness satin	0.68	94	0.85	121
CNF crowfoot	0.60	90	0.61	94

packing and nesting considerations unique to five-harness satin weave architecture because the angles formed by the fabric crimps were identical on the two sides of the fabric [13]. Note that the orientation of the permeability tensor does not necessarily correspond to the fibre directions but may follow the angle formed by the fabric crimp, as was the case for the two eight-harness satin weave fabrics. Several architectural features of the woven fabric can play a role in determining the orientation and magnitude of the permeability, including the weave pattern, yarn construction and interlayer packing arrangements. Analogous features in braided or knitted reinforcements also influence the permeability. Analytical models explicitly relating fabric architecture to flow behaviour are currently restricted to relatively simple, idealised architectures and saturated flows. Numerical models are being applied to more complex geometries and flows [29, 30].

To obtain the values of each component of the in-plane permeability tensor, K_{xx} and K_{yy} , the mould inlet pressure is required if the injection rate is fixed, and the injection rate is required if the mould inlet pressure is fixed. For the case of fixed mould inlet pressure, an asymptotic relationship between the radius of the flow front and the time may be derived that is valid for all except very short times [24]:

$$\frac{1}{2} \left(\frac{R_{gm}}{r_0} \right)^2 \left[\ln \left(\frac{R_{gm}}{r_0} \right) - \frac{1}{2} \right] = P_i \frac{K_{gm} t}{(1 - V_f) \mu r_0^2} - \frac{1}{4} \quad (7.20)$$

where

R_{gm} is the geometric mean of the major and minor radii of the elliptical flow front, $(ab)^{1/2}$;

K_{gm} is the geometric mean of the major and minor components of the in-plane permeability tensor;

r_0 is the radius of the hole punched in the fabric.

Thus, if R_{gm} is known from measurements and the left-side of equation (7.20) is plotted against time, K_{gm} may be obtained from the slope of the

resulting line. Since $K_{gm} = (K_{xx}K_{yy})^{1/2}$, and as the ratio K_{xx}/K_{yy} is known from the ellipticity of the flow front [equation (7.19)], the individual components K_{xx} and K_{yy} are easily obtained. It has been reported that permeabilities obtained from constant injection pressure radial flow experiments are identical to those obtained from saturated unidirectional flow experiments [31]; however, it has also been found that large fabric deformations can occur in such experiments as a result of the very large initial flows [32].

In the case of constant injection rate, a relationship has been derived relating the mould inlet pressure P_i to time t :

$$P_i = \frac{\mu Q}{4\pi h K_{gm}} \ln \left[1 + \frac{Qt}{(1 - V_f)\pi h r_0^2} \right] \quad (7.21)$$

where h is the thickness of the mould and Q is the fixed injection rate. The geometric mean permeability K_{gm} can be obtained from the slope of the data when plotted as $4\pi h P_i / \mu Q$ against the logarithmic term on the right-hand side of equation (7.21). Knowledge of the shape of the flow fronts obtained from the same experiments provides the other required information, as discussed above, to give each component of the in-plane permeability tensor. Results for constant injection rate radial flow experiments are illustrated in Figure 7.14, and these results were obtained with use of the same random mat fabric used to illustrate the effects of wicking in unidirectional flow experiments (Figures 7.7 and 7.8). Note that a monotonic decrease in the unsaturated permeability is obtained in the radial flow experiment, in contrast to the initial increase, peak and then decreasing trend observed in the unidirectional flow experiments. However, data at very early times in the radial flow experiment were not available owing to poor shape development of the flow front. Thus, the radial flow experiment is thought to depict the equivalent information as the latter stages of the unidirectional flow experiment, in which wicking effects become less and less evident as more of the reinforcement becomes saturated with fluid. A similar relationship was also observed between the radial and unidirectional flow results for a three-dimensional woven fabric (Figure 7.10). In that case, the radial flow experiment showed an increasing trend in unsaturated permeability, as did the unidirectional flow experiment during the latter part of the unsaturated flow process [12].

The results shown in Figure 7.14 also indicate that larger flows appear to suppress the effects of wicking on the computed permeability, and this is consistent with the analyses above [equations (7.10)–(7.14)] for unidirectional flows where the effects of capillary pressure were included. The larger injection rate caused a more rapid increase in hydrostatic pressure leading to dominance of the hydrostatic pressure term over the

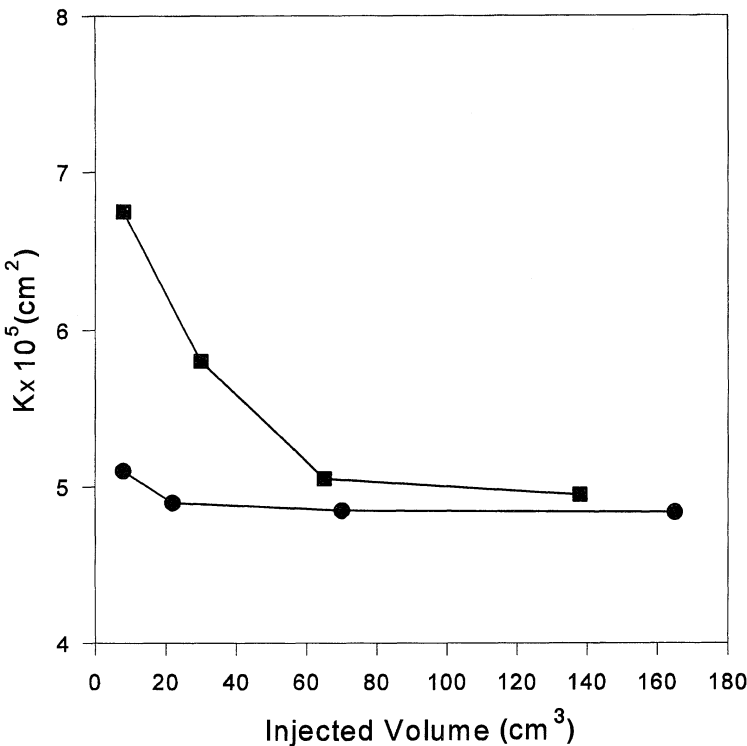


Figure 7.14 The unsaturated permeability, K , derived from radial flows in a continuous strand random mat. The permeability appears to decrease during the experiments because of wicking and is also a function of the injection rate, Q , used for the experiment. -●-, $Q = 1.5 \text{ cm}^3/\text{s}$; -■-, $Q = 1 \text{ cm}^3/\text{s}$.

capillary pressure term in Darcy's law. This result also explains why constant injection pressure experiments can give similar results to saturated flow results if the preform is not deformed in the constant pressure experiment [28, 31]. In that case, the initial flow is very high, leading to the case where the hydrostatic pressure term dominates the capillary pressure term. The first-order analysis of the radial flow experiment with a capillary pressure term, in which the capillary pressure is assumed to be independent of direction, is straightforward and left as an exercise for the reader. Nevertheless, there are cases where very large flows do not lead to equality between the unsaturated and saturated measurements. Rudd *et al.* [32] showed that the permeability of a quasi-unidirectional non-crimp fabric decreased by over 50% as the flow was increased in a series of radial flow experiments.

The values of unsaturated permeability change during the radial flow experiment for the same reason they vary during the unidirectional flow

measurements; the analysis of the measurements is based only on Darcy's law and is therefore incomplete. For example, analyses according to Darcy's law predict that the orientation and anisotropy of the radially expanding flow front should be constant after a very short time required for an adjustment from the shape of the injection hole to a shape determined by K , and that is often the case in monofilament fabrics [24]. However, because previous analyses did not account for unsaturated flow effects, the prediction of constant shape and orientation is not expected to hold universally, as indicated by the results shown in Figure 7.15. Significant changes in flow front shape occurred over long time scales for several woven fabrics, including the flow fronts illustrated for the crowfoot weave in Figure 7.13. Thus, a number of cases exist in which interpretation of the results of a radial flow experiment can be quite difficult by means of existing data analysis tools. The anisotropy and orientation results from radial flow experiments presented in Table 7.3 were those at the end of the radial flow experiment after most of the change had occurred. In general, the results of an unsaturated flow ex-

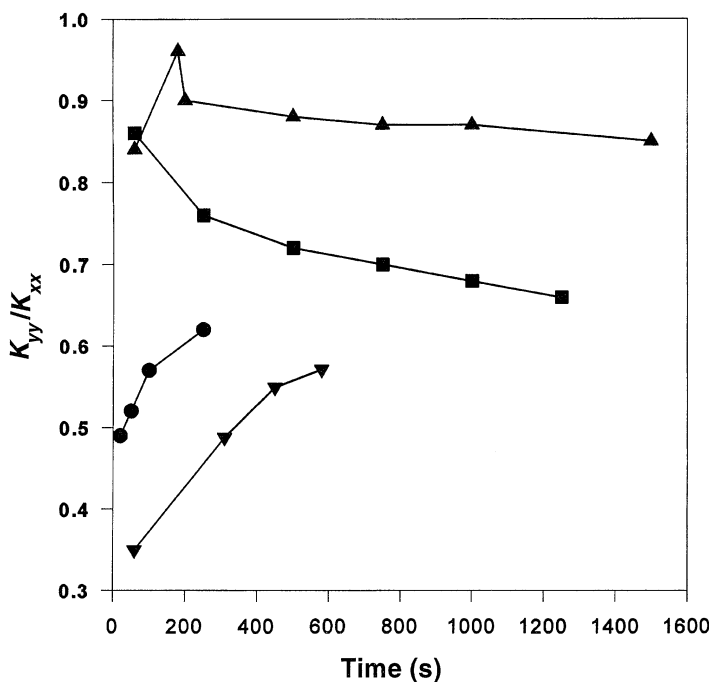


Figure 7.15 The apparent anisotropy of the unsaturated permeability for several woven fabrics changed appreciably during each radial flow experiment. Fabric: Δ = eight harness; \blacksquare = five-harness; \bullet = crowfoot; \blacktriangledown = three-dimensional woven. K_{yy} and K_{xx} are components of the permeability tensor, K .

periment may be expected to approach asymptotically the results of the equivalent saturated flow experiment if the medium becomes fully saturated at some point behind the moving flow front.

The results of radial flow experiments conducted with several glass fabrics are summarised in Figure 7.16 and compared with saturated flow results. In all cases, except for the random continuous mat, the permeabilities observed at the end of the radial flow experiments were significantly larger than the permeabilities obtained from the saturated flow experiments. In counterpoint, the results illustrated in Figure 7.16 probably overstate the differences between radial and saturated flow results since all the radial flow data presented were obtained by means of

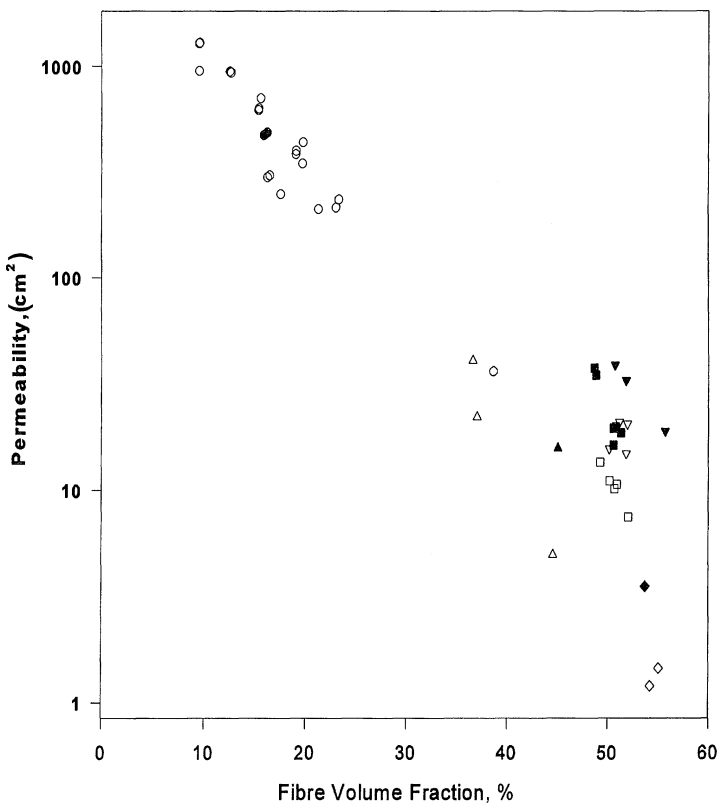


Figure 7.16 Example permeability data obtained from radial flow experiments with several types of glass fabrics (filled symbols). The corresponding permeabilities from Figure 7.5, obtained by saturated flow experiments, are also shown for comparison (unfilled symbols). The permeabilities illustrated for anisotropic materials are the larger principle component values of the in-plane permeability tensor, K_{xx} . Fabric: ○, ● = U-750; □, ■ = three-dimensional; △, ▲ = A130 unidirectional; ▽, ▼ = D155 unidirectional; ◇, ◆ = Cotech ± 45°.

constant injection rates. Nevertheless, these results and others available in the literature document a systematic difference in which reported values of unsaturated permeabilities are larger than the corresponding saturated permeability values.

In addition to the analytical problems that may be encountered with the radial flow experiment, mould top deflection can contribute significant measurement error, as was the case for the unidirectional flow experiment (Figure 7.5). Often, mould deflection is worse in the radial flow experiment than in the unidirectional experiment because the radial flow moulds are usually larger than the unidirectional flow moulds [28]. Two remedies are available to alleviate mould deflection problems in radial flow experiments: reinforce the mould top in a way that does not interfere with flow front visualisation, or eliminate the need for flow front visualisation and use a metal mould top. A rib-stiffened metal structure is usually sufficient to minimise mould top deflection while preserving the ability to do flow front visualisation.

Eliminating the transparent mould top entirely requires a mould that provides an alternative means of detecting the shape of the flow front. One reported solution to this problem has been given in which several pressure transducers mounted in two orthogonal rows are used [32]. One complication arises in cases where the principal orientation of the permeability tensor does not correspond to the orientation of the pressure transducers. In such cases, a preliminary visualisation experiment is needed to determine the orientation of the permeability tensor. The reinforcement sample is subsequently placed into the mould with the principal permeability axes aligned with the orthogonal rows of pressure transducers. Then, a radial flow experiment is conducted and the mould inlet pressure data analysed according to equation (7.20) or (7.21) to provide the geometric mean permeability. The additional data from the pressure transducers may be used in several ways, but the simplest is to construct a graph of the initial response of each transducer against time. Then, by noting the location of each transducer, one obtains the location of the flow front along the principal directions as a function of time, thereby providing the ellipticity of the flow front and hence the anisotropy of the permeability tensor via equation (7.19). As noted above, once both the geometric mean permeability and the anisotropy of the permeability are known, one can easily find each component of the permeability tensor.

7.3 THE GENERAL THREE-DIMENSIONAL CASE

The experimental methods described above provide either the effective permeability for flow in a particular direction (unidirectional) or the unsaturated approximation to the in-plane permeability tensor (radial). However, numerical simulations used for design and optimisation of

liquid moulding processes may require the complete three-dimensional permeability tensor, especially if thick multilayer preforms are to be used. A more general treatment of the data analysis to extract the three-dimensional permeability tensor is therefore warranted.

7.3.1 ANALYSIS OF UNIDIRECTIONAL FLOW DATA

The following analysis was recently presented to analyse saturated, unidirectional flows within a fully three-dimensional framework [33]. No prior assumptions have been made concerning the orientation of the permeability tensor except that it is orthotropic. One may begin by expressing Darcy's law in three dimensions:

$$\mu v_{x'} = -K_{xx'} \frac{\partial P}{\partial x} - K_{xy'} \frac{\partial P}{\partial y} - K_{xz'} \frac{\partial P}{\partial z} \quad (7.22)$$

$$\mu v_{y'} = -K_{yx'} \frac{\partial P}{\partial x} - K_{yy'} \frac{\partial P}{\partial y} - K_{yz'} \frac{\partial P}{\partial z} \approx 0 \quad (7.23)$$

$$\mu v_{z'} = -K_{zx'} \frac{\partial P}{\partial x} - K_{zy'} \frac{\partial P}{\partial y} - K_{zz'} \frac{\partial P}{\partial z} \approx 0 \quad (7.24)$$

where x' is the flow direction, y' is perpendicular to the flow direction in the plane of the material and z' is perpendicular to the flow direction through the thickness of the material. Additionally, we assume that $v_y = 0$ and $v_z = 0$ in a one-dimensional flow experiment [equations (7.23) and (7.24)], and this assumption will be tested below.

If the permeability tensor is orthotropic, then $K_{xy'} = K_{yx'}$, $K_{xz'} = K_{zx'}$, $K_{yz'} = K_{zy'}$, and there exists a principal coordinate system (x, y, z) with a principal permeability tensor, \mathbf{K} :

$$\mathbf{K} = \begin{pmatrix} K_{xx} & 0 & 0 \\ 0 & K_{yy} & 0 \\ 0 & 0 & K_{zz} \end{pmatrix} \quad (7.25)$$

The relationship between the laboratory and principal coordinate systems may be envisioned with the help of Figure 7.17, which also shows a schematic illustration of a permeability tensor. Before proceeding to the general three-dimensional analysis, however, a simplified case exists that is worth considering first since many materials may be adequately treated with this approach. If the z principal direction of the permeability tensor is perpendicular to the plane of the material (i.e. the z and z' axes are coincident), then the in-plane and through-the-thickness measurements may be decoupled and analysed separately. In that case, a through-the-thickness permeability measurement would provide K_{zz} directly with no further analysis. This simplification holds in many cases and can be validated with a simple flow visualisation experiment that

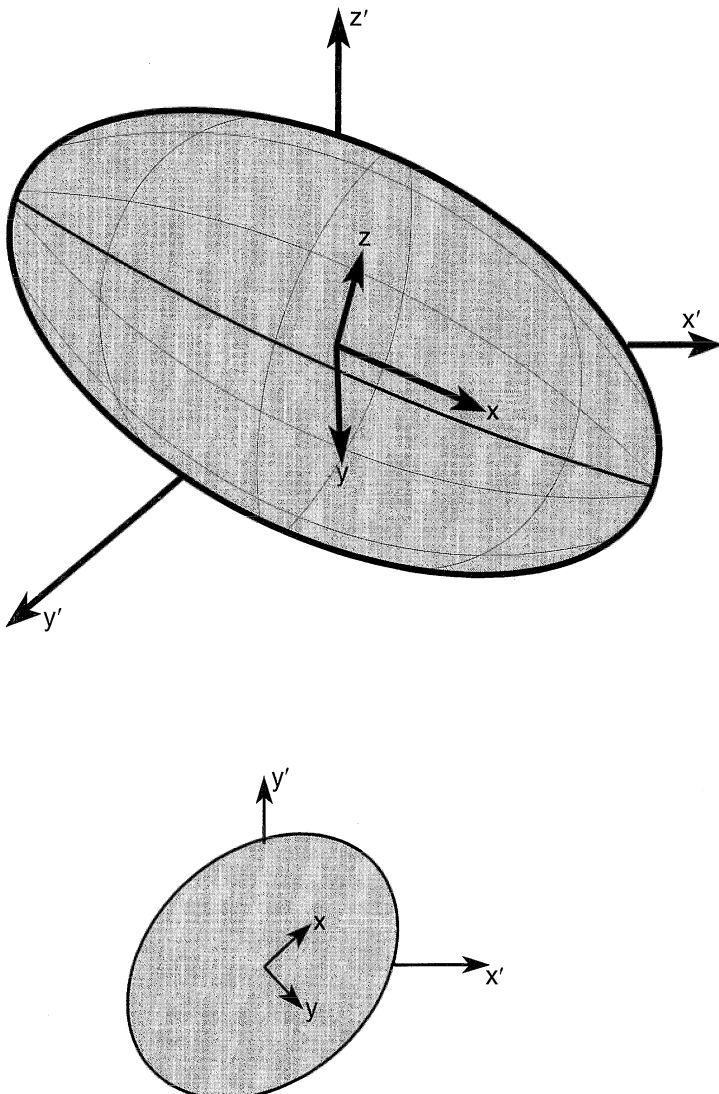


Figure 7.17 (a) Three-dimensional and (b) two-dimensional permeability tensors with respect to their laboratory coordinate systems. The three-dimensional permeability tensor is represented by an ellipsoid; the two-dimensional permeability tensor is depicted by an ellipse. x , y , z = principal coordinates; x' , y' , z' = laboratory coordinates.

allows one to observe the progress of the advancing front from the side of the mould. If the mould is orientated horizontally, and the flow front remains vertical, on average, then the z and z' axes are coincident.

However, if the flow front assumes an angle then the more general analysis discussed below is warranted.

If the z and z' axes are coincident, the in-plane unidirectional flow measurements may be analysed to provide the in-plane components of the permeability tensor according to [13, 31]

$$K_e^\theta = K_{yy} \left(\sin^2 \theta + \frac{K_{yy}}{K_{xx}} \cos^2 \theta \right)^{-1} \quad (7.26)$$

where θ is the angle between the principal orientation of the permeability (x axis) and the flow direction of the unidirectional flow experiment (x' axis). Since there are three unknowns (K_{xx} , K_{yy} and θ) at least three unidirectional flow experiments are required to determine the three unknowns, and details concerning the use of equation (7.26) are given elsewhere [13]. Equation (7.26) was used to treat the unidirectional flow data provided in Table 7.1 to generate the comparisons of the geometric properties of permeability tensors determined by the radial and unidirectional flow experiments given in Table 7.3. Given the good comparison between the geometric properties generated by radial and unidirectional flow experiments, equation (7.26) also suggests an efficient method of combining the radial flow and unidirectional flow methods to obtain accurate estimates of the in-plane permeability tensor. A single radial flow experiment can provide both θ and the ratio K_{yy}/K_{xx} , a single unidirectional experiment can provide one value of K_e^θ , leaving only K_{yy} as an unknown in equation (7.26). Thus, by performing one unidirectional flow experiment and one radial flow experiment, the saturated and unsaturated values of the in-plane permeability may be obtained at a particular fibre volume fraction, V_f .

The through-the-thickness permeability has been measured for a limited number of cases by saturated unidirectional flow methods utilising specialised flow cells [12, 34]. Specialised flow cells are required because the flow path is typically much shorter in a through-the-thickness flow geometry than in an in-plane flow geometry, leading to a higher susceptibility to edge effects in the through-the-thickness case. To prevent edge effects, a through-the-thickness flow cell was designed to permit the sides of the mould to squeeze together after the mould was closed, compressing the preform sample on its sides and thereby sealing the edges. Such a design permits the flow to be observed as the mould fills, whereas layers of sealant may obscure the flow preventing visual observation.

The through-the-thickness permeability was found to be substantially lower than the in-plane permeability. Examples of such measurements are shown in Table 7.4 and Figure 7.18 for the random mat, three-dimensional woven fabric, and other materials, and the corresponding in-plane permeability values are included for comparison. The data indicate that the through-the-thickness permeability lies in the range 10%–20% of

Table 7.4 Examples of through-the-thickness permeability measurements (K_{zz}). In-plane geometric mean permeability measurements (K_{gm}) are given for comparison. V_f = fibre volume thickness

Material	V_f (%)	$K_{zz} \times 10^{-7}$ (cm 2)	$K_{gm} \times 10^{-7}$ (cm 2)
Random Mat	17.7	38.6	251.0
Random Mat	27.3	8.99	57.2
Three-dimensional Woven	52.0	1.65	11.44
Knytex D155 unidirectional	49.9	0.412	3.23

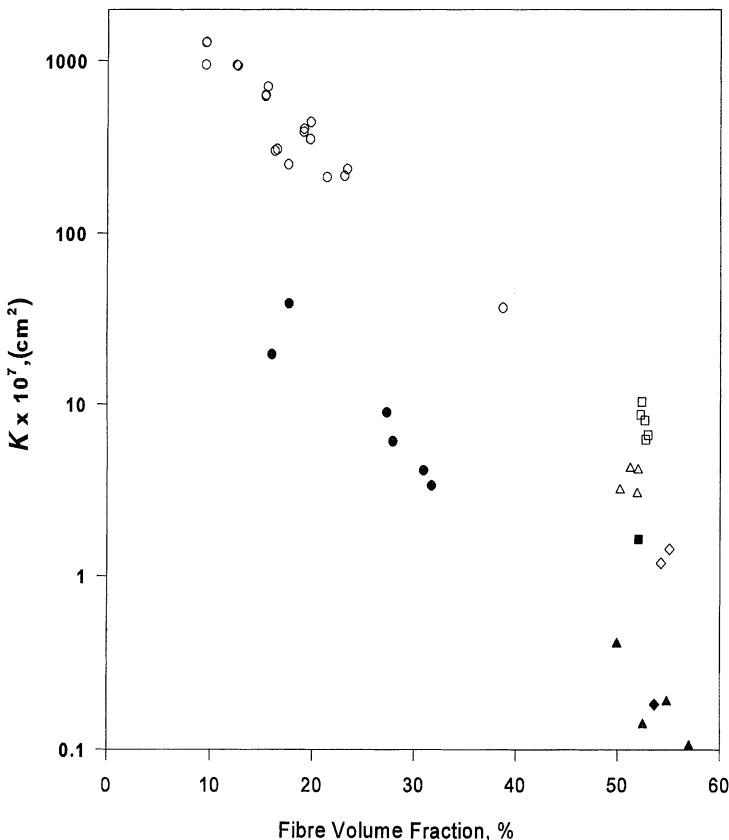


Figure 7.18 Example permeability (K) data obtained from through-the-thickness (z) flow experiments (filled symbols) with several types of glass fabrics. The corresponding in-plane permeabilities, obtained by saturated flow experiments, are also shown for comparison (unfilled symbols). The in-plane permeabilities of anisotropic materials are the geometric mean values $(K_{xx}K_{yy})^{1/2}$. Fabric: ○, ● = random; □, ■ = three-dimensional weave; △, ▲ = D155 unidirectional; ◇, ♦ = Cotech ± 45°.

the in-plane permeability. The in-plane permeability value shown for each anisotropic material is the geometric mean $(K_{xx}K_{yy})^{1/2}$ of its in-plane principal permeabilities. If a principal axis of \mathbf{K} is perpendicular to the plane of the fabric, one in-plane unidirectional, one radial flow and one through-the-thickness flow experiment can characterise the complete three-dimensional \mathbf{K} tensor.

In the more general case, where the z and z' axes are not coincident, the flow front is expected to assume an angle through the thickness of the material, and that has been observed for $\pm 45^\circ$ stitched bidirectional fabrics. If a unidirectional flow experiment is performed with the flow along one of the laboratory axes, say the x' axis, then the experimental orientation, or the (x', y', z') coordinate system is related to the principal (x, y, z) system by rotating the (x, y, z) coordinate system by θ_x degrees about the x -axis, by θ_y degrees about the second generation y -axis and by θ_z degrees about the third-generation z -axis. It should be noted that in this case θ_z is the angle between the z -axis and the z' -axis; however, θ_y does not represent the angle between the y -axis and the y' -axis, nor does θ_x represent the angle between the x -axis and the x' -axis [35]. The components of the permeability tensor for a particular experimental orientation are defined as follows:

$$\mathbf{K}^\theta = \begin{pmatrix} K_{xx'} & K_{xy'} & K_{xz'} \\ K_{xy'} & K_{yy'} & K_{yz'} \\ K_{xz'} & K_{yz'} & K_{zz'} \end{pmatrix} \quad (7.27)$$

where

$$\begin{aligned} K_{xx'} = & K_{xx} \cos^2 \theta_y \cos^2 \theta_z \\ & + K_{yy} (-\cos \theta_z \sin \theta_x \sin \theta_y + \cos \theta_x \sin \theta_z)^2 \\ & + K_{zz} (\cos \theta_x \cos \theta_z \sin \theta_y + \sin \theta_x \sin \theta_z)^2 \end{aligned} \quad (7.28)$$

$$\begin{aligned} K_{xy'} = & -K_{xx} \cos^2 \theta_y \cos \theta_z \sin \theta_z \\ & + K_{zz} (\cos \theta_x \cos \theta_z \sin \theta_y + \sin \theta_x \sin \theta_z) \\ & \times (\cos \theta_z \sin \theta_x - \cos \theta_x \sin \theta_y \sin \theta_z) \\ & + K_{yy} (-\cos \theta_z \sin \theta_x \sin \theta_y + \cos \theta_x \sin \theta_z) \\ & \times (\cos \theta_x \cos \theta_z + \sin \theta_x \sin \theta_y \sin \theta_z) \end{aligned} \quad (7.29)$$

$$\begin{aligned} K_{xz'} = & -(K_{xx} \cos \theta_y \cos \theta_z \sin \theta_y) \\ & - K_{yy} \cos \theta_y \sin \theta_x (-\cos \theta_z \sin \theta_x \sin \theta_y + \cos \theta_x \sin \theta_z) \\ & + K_{zz} \cos \theta_x \cos \theta_y (\cos \theta_x \cos \theta_z \sin \theta_y + \sin \theta_x \sin \theta_z) \end{aligned} \quad (7.30)$$

$$\begin{aligned} K_{yy'} = & K_{xx} \cos^2 \theta_y \sin^2 \theta_z \\ & + K_{zz} (\cos \theta_z \sin \theta_x - \cos \theta_x \sin \theta_y \sin \theta_z)^2 \\ & + K_{yy} (\cos \theta_x \cos \theta_z + \sin \theta_x \sin \theta_y \sin \theta_z)^2 \end{aligned} \quad (7.31)$$

$$\begin{aligned} K_{zy'} &= K_{xx} \cos \theta_y \sin \theta_y \sin \theta_z \\ &\quad + K_{zz} \cos \theta_x \cos \theta_y (\cos \theta_z \sin \theta_x - \cos \theta_x \sin \theta_y \sin \theta_z) \\ &\quad - K_{yy} \cos \theta_y \sin \theta_x (\cos \theta_x \cos \theta_z + \sin \theta_x \sin \theta_y \sin \theta_z) \end{aligned} \quad (7.32)$$

$$K_{zz'} = K_{zz} \cos^2 \theta_x \cos^2 \theta_y + K_{yy} \cos^2 \theta_y \sin^2 \theta_x + K_{xx} \sin^2 \theta_y \quad (7.33)$$

These components of \mathbf{K}^θ may be used to define the effective permeability, K_e^θ , measured in the x' direction:

$$\begin{aligned} K_e^\theta &= -\mu v_{x'} \left(\frac{\partial P}{\partial x'} \right)^{-1} \\ &= K_{xx'} + K_{xy'} \left(\frac{\partial P}{\partial y'} \right) \left(\frac{\partial P}{\partial x'} \right)^{-1} + K_{xz'} \left(\frac{\partial P}{\partial z'} \right) \left(\frac{\partial P}{\partial x'} \right)^{-1} \end{aligned} \quad (7.34)$$

where the superscript θ is now given in vector notation (bold) to express the three orientation angles θ_x , θ_y and θ_z . The pressure gradient ratios, $(\partial P / \partial y')(\partial P / \partial x')^{-1}$ and $(\partial P / \partial z')(\partial P / \partial x')^{-1}$ may also be expressed in terms of \mathbf{K}^θ components by using the approximations $v_y = v_z = 0$ [equations (7.23) and (7.24)]. A highly complex expression for the effective permeability resulted from making all of the proper substitutions. In an effort to simplify the equation, a matrix tool known as the Schur complement was employed (H. J. Woerdeman, 1992, private communication; ref. 36) which yielded

$$\begin{aligned} K_e^\theta &= K_{xx} K_{yy} K_{zz} \left\{ -[K_{xx} \cos \theta_y \sin \theta_y \sin \theta_z \right. \\ &\quad + K_{zz} \cos \theta_x \cos \theta_y (\cos \theta_z \sin \theta_x - \cos \theta_x \sin \theta_y \sin \theta_z) \\ &\quad - K_{yy} \cos \theta_y \sin \theta_x (\cos \theta_x \cos \theta_z + \sin \theta_x \sin \theta_y \sin \theta_z)] \\ &\quad + (K_{zz} \cos^2 \theta_x \cos^2 \theta_y + K_{yy} \cos^2 \theta_y \sin^2 \theta_x + K_{xx} \sin^2 \theta_y) \\ &\quad \times [K_{xx} \cos^2 \theta_y \sin^2 \theta_z + K_{zz} (\cos \theta_z \sin \theta_x \\ &\quad - \cos \theta_x \sin \theta_y \sin \theta_z)^2 + K_{yy} (\cos \theta_x \cos \theta_z \\ &\quad + \sin \theta_x \sin \theta_y \sin \theta_z)^2] \left. \right\}^{-1} \end{aligned} \quad (7.35)$$

Although strict algebraic equivalence between the three-dimensional expressions obtained with and without the Schur complement can be very difficult to show, it can easily be shown algebraically that the expression for the effective permeability in two dimensions [equation (7.26)] derived with the Schur complement is equivalent to the one derived without the Schur complement [13]. A number of numerical tests with the three-dimensional expressions have been conducted and in each case the expressions derived with and without the Schur complement have yielded exactly the same results.

The equation for the in-plane case [equation (7.26)] contains three variables, which means at least three unidirectional flow experiments

must be conducted in order to extract the in-plane permeability tensor and its orientation angle. The three-dimensional expression for the effective permeability [equation (7.35)] contains six unknowns: K_{xx} , K_{yy} , K_{zz} , θ_x , θ_y and θ_z . At least six different flow experiments would have to be conducted in order to solve for a sample's three-dimensional permeability tensor. To conduct the six experiments, a laboratory coordinate system should first be established with respect to a geometrically favourable flow direction. After measuring the effective permeability for flow in that particular orientation, five different directions should be chosen and effective permeability data measured at each.

Figure 7.19 summarises six experimental flow orientations that could be used in conjunction with this analysis. Under tensor rotation algebra, six different equations of the form of equation (7.35) were derived for the effective permeability, corresponding to the six experiments illustrated in Figure 7.19. The six equations relating K_e^θ to the permeability tensor constitute an approximate analytical solution to Darcy's law, in three dimensions, for the simple one-dimensional flow geometry and are given elsewhere [33].

7.3.2 NUMERICAL TESTS

The six equations relating the measured K_e^θ values from six experiments to the six unknowns are highly non-linear and require a robust root-finding algorithm to obtain solutions. The solver [37] consists of a binary search algorithm that operates in six-dimensional space and which converges to a small region in the neighbourhood of a sign inversion of the system of equations. One can use the equation solver to find the three-dimensional permeability tensor and its orientation angles upon entering six values for the effective permeability measured for six different flow directions.

To provide an example of the derivation of a three-dimensional K tensor with the binary search equation solver, a three-dimensional K tensor will be constructed based on the measured data for the crowfoot weave fabric. The in-plane components of the permeability tensor were previously reported for the fabric, and it was assumed that K for that fabric lies in the fabric plane [13]. Additionally, the through-the-thickness permeability was measured and was assumed to be the third principal component of K , K_{zz} . In order to show the ability to extract a three-dimensional permeability tensor that is tilted out of the fabric plane, a hypothetical out-of-plane orientation angle was chosen for the numerical work presented below. Presented in the first numerical column of Table 7.5 are the constructed permeability tensor and orientation angles which were used to test the equation solver. Note that $\theta_x = 0.3$ rad means the tensor is rotated out of the plane of the material by 0.3 rad (*c.* 17.2°). The

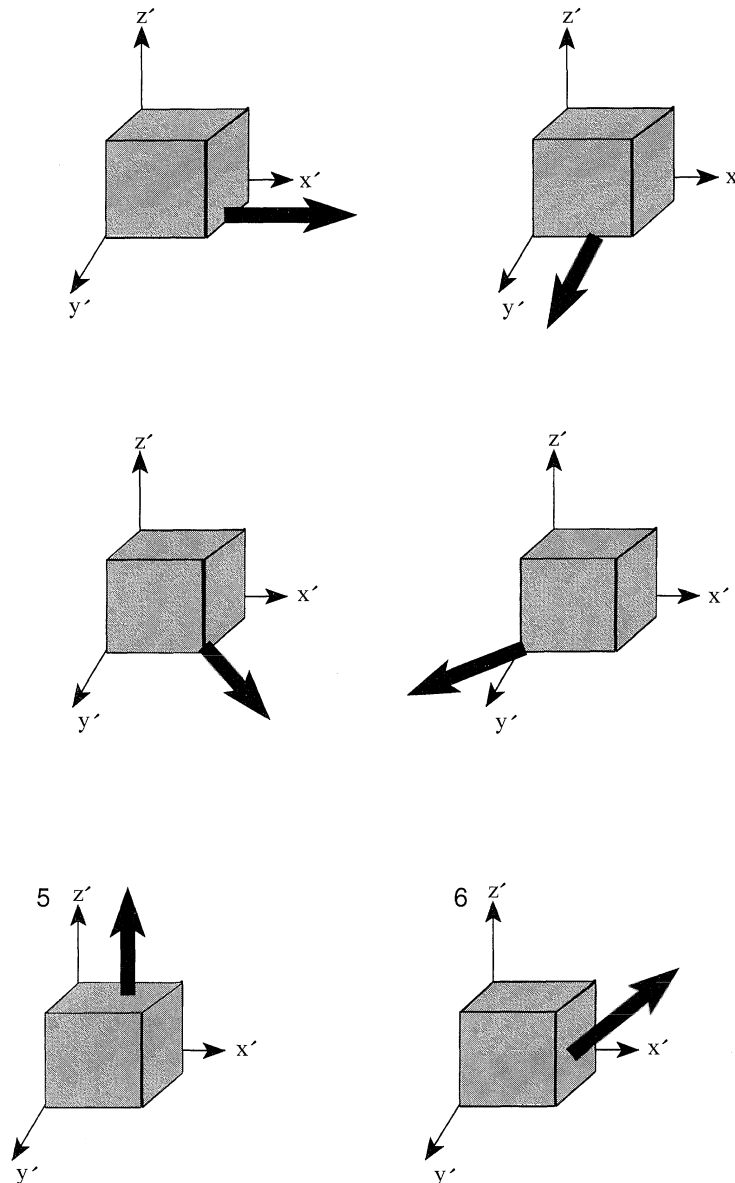


Figure 7.19 Six experimental flow orientations relative to the reference coordinate system (x', y', z') .

data in this column of Table 7.5 were used in equations of the form of equation (7.35) to compute the K_e^θ values shown in the second numerical column. These values were entered into the binary search root finder to

Table 7.5 The permeability tensor \mathbf{K} constructed for numerical tests; computer values relate to K_e^θ , the effective permeability; the inverted tensor was generated from K_e^θ by means of a binary root finder

	Constructed	Computed	Inverted
$K_{xx} (\text{cm}^2)$	7.51×10^{-7}	3.76×10^{-7}	7.49×10^{-7}
$K_{yy} (\text{cm}^2)$	4.58×10^{-7}	6.52×10^{-7}	4.58×10^{-7}
$K_{zz} (\text{cm}^2)$	1.0×10^{-7}	3.82×10^{-7}	0.99×10^{-7}
$\theta_x (\text{rad})$	0.3	6.33	0.3
$\theta_y (\text{rad})$	1.0×10^{-3}	1.07	6.0×10^{-3}
$\theta_z (\text{rad})$	1.2	2.54	1.2

invert those equations for the permeability tensor \mathbf{K} , which returned the values shown in the third numerical column. Although the solver is not accurate to a large number of decimal places, the accuracy is sufficient for estimating permeability tensors from experimental data. A comparison of the first and third numerical columns indicates that all six components of the permeability tensor were accurately found by the root finder except for θ_y . However, the correct value of θ_y , 1.0×10^{-3} rad, is quite small relative to the other angles, and the root finder computed a solution that maintains that relationship among the orientation angles. Note that the first four K_e^θ values in the second numerical column of Table 7.5 do not correspond to the values in Table 7.1 for the crowfoot weave fabric because of the out-of-plane orientation presumed for the permeability tensor in the calculations presented in Table 7.5.

After verifying that the non-linear equations, of the form of equation (7.35), relating experimental measurements of K_e^θ to the components of the permeability tensor and its orientation angles could be solved, the accuracy of the approximate solution to Darcy's law was checked by comparing it with numerical solutions for different flow cases [33]. An initial calculation was performed in two dimensions to check the accuracy of equation (7.26). The simulation predicts the flow front position and the pressure field as a function of time for unsteady RTM mould fillings [38]. The simulation algorithm was constructed by substituting Darcy's law into the equation of continuity, $\nabla \cdot \mathbf{v} = 0$, which gives a single partial differential equation for the pressure field of the fluid. The pressure equation is parameterised by the components of the permeability tensor. For two-dimensional flow, this is expressed as:

$$K_{xx'} \frac{\partial^2 P}{\partial x^2} + 2K_{xy'} \frac{\partial^2 P}{\partial x \partial y} + K_{yy'} \frac{\partial^2 P}{\partial y^2} = 0 \quad (7.36)$$

assuming the permeability tensor to be spatially invariant.

A comparison of the approximate solution for K_e^θ , [equation (7.26)] to the numerical solution of Darcy's law in two dimensions is illustrated in

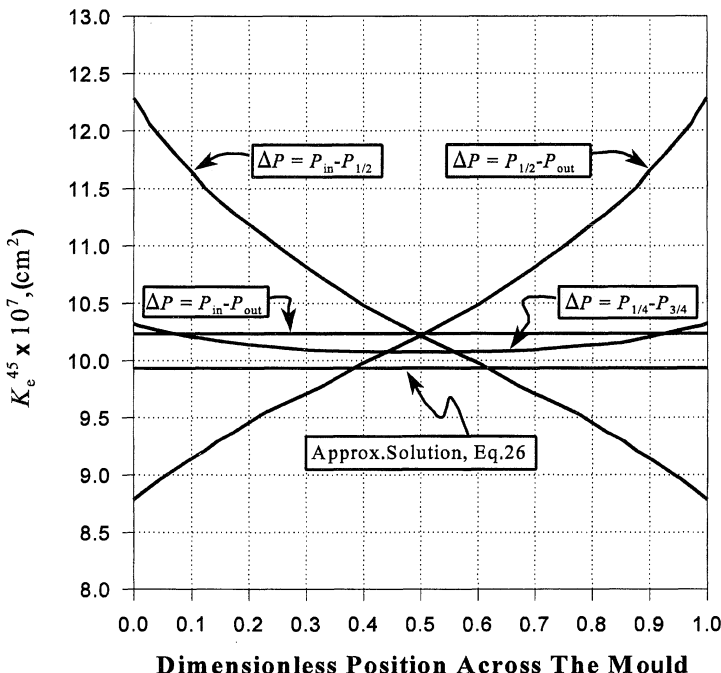


Figure 7.20 A comparison of the approximate solution for K_e^θ [equation (7.26) in text] to the numerical solution of Darcy's law in two dimensions, [equation (7.36) in text], for various pressure transducer positions. The particular flow orientation chosen is at a 45° angle to the principle orientation of the \mathbf{K} tensor. The components of the \mathbf{K} tensor used in the calculation are the K_{xx} , K_{yy} and θ_z components of \mathbf{K} for the crowfoot weave fabric so the value of $K_e^{45^\circ}$ calculated for the line labeled ' $\Delta P = P_{in} - P_{out}$ ' equals the value reported for $K_e^{45^\circ}$ in Table 7.1 for the crowfoot material. $P_{1/4}$, $P_{1/2}$ and $P_{3/4}$ = pressure at a quarter, half and three-quarters along the mould length, respectively; P_{in} and P_{out} = pressure at the entry and exit of the mould, respectively.

Figure 7.20, and the two-dimensional permeability tensor used for the comparison consists of the K_{xx} , K_{yy} , and θ_z components of \mathbf{K} listed in Table 7.5. The flow geometry was chosen for which the largest error in the approximate solution was expected. More specifically, the flow axis was chosen to bisect the principal directions of the permeability tensor. The most notable point of the two-dimensional analysis is the predicted dependence of the measured value of K_e^θ on the location of the pressure measurements. For example, the line in Figure 7.20 labelled ' $\Delta P = P_{in} - P_{1/2}$ ' compiles the results for the cases where the pressure drop was computed from the inlet boundary to a point half of the way along the length of the mould and at various locations across the width of the mould. Clearly, if one chooses to measure the pressure drop over the

first half (or over the second half) of the mould length the measured value of K_e^θ may vary significantly depending upon the placement of the pressure measurement ports across the width of the mould. However, if one measures the pressure drop over the entire mould length (the line labelled ' $\Delta P = P_{in} - P_{out}$ '), the dependence of the measured value of K_e^θ on the choice of widthwise placement of the measurement ports is eliminated.

The accuracy of the approximate solution is subject to the mould design as the difference between the approximate solution and the numerically accurate solution depends on the choice of pressure measurement port locations. For the purposes of judging the error introduced into the previous in-plane measurements reported by Salem and me [13], a comparison between the lines labeled 'Approx.Solution, Eq. 26' and ' $\Delta P = P_{in} - P_{out}$ ' is most appropriate since the mould used for the saturated one-dimensional flow measurements in that work was designed to measure the pressure drop over the entire length of the porous sample. Thus, the error caused by the use of the approximate analysis was probably no larger than 5%, which is smaller than the expected experimental errors. An even smaller analysis error could be achieved by placing the pressure transducers at locations a quarter and three-quarters along the length, and at the midline of the mould.

A comparison of the full three-dimensional approximate solution [equation (7.35)] with a three-dimensional finite element solution was also conducted, using the out of plane permeability tensor given in Table 7.5. A detailed illustration of the effect of pressure port location would be very difficult in the three-dimensional case as each line of Figure 7.20 from the two-dimensional case becomes a curved surface in the three-dimensional case. Results are provided only for the specific mould geometry used in the author's laboratory. For this case, the approximate solution to Darcy's law was found to be within 2% of the numerical solution for all six flow orientations, as Figure 7.21 indicates. The 'approximate' K_e^θ values in Figure 7.21 were computed directly from K (Table 7.5) with equation (7.35), and were given above. The 'course mesh' K_e^θ values in Figure 7.21 were computed numerically with a finite element mesh of $8 \times 8 \times 4$ elements within the simulated mould cavity. The 'refined mesh' K_e^θ values in Figure 7.21 were computed numerically with a finite element mesh of $24 \times 24 \times 8$ elements within the simulated mould cavity, and demonstrate that the finite element calculation is converged to an accurate solution.

The accuracy of the three-dimensional approximate solution, for reasonable choices of mould design, demonstrates that permeability tensors can be obtained for general anisotropic materials from a limited set of experimental measurements. Additional calculations are expected to show the limitations of the approximate solution. A probable limitation in the approximate solution is a loss of accuracy for very high levels of

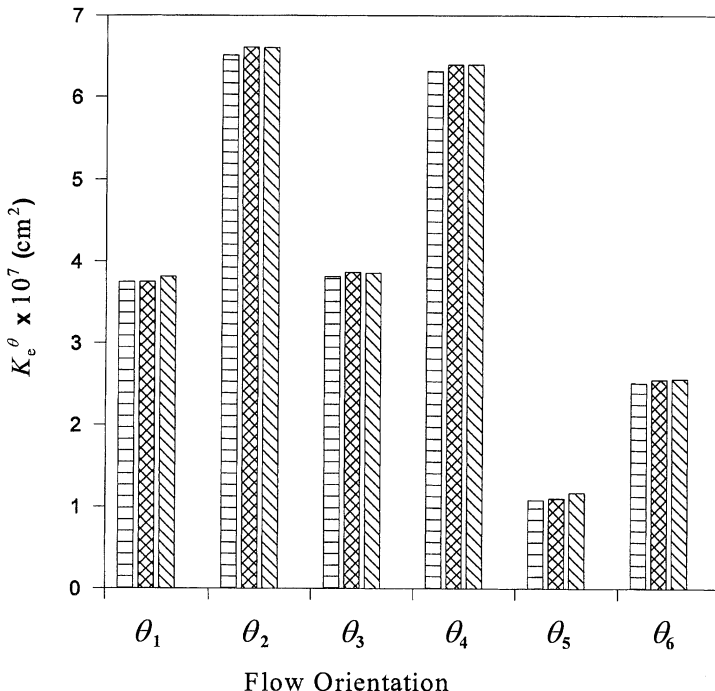


Figure 7.21 A comparison of the approximate solution for K_e^θ , to the numerical solution of Darcy's law in three dimensions for a specific set of pressure transducer positions. \square = 'approximate' values [equation (7.35) in text]; \boxtimes = 'course mesh' ($8 \times 8 \times 4$ elements in the simulated mould cavity); \square = fine mesh ($24 \times 24 \times 8$ elements in the simulated mould cavity).

anisotropy. In the case of composite reinforcements such a limitation may not present a problem as most materials with large degrees of anisotropy are unidirectional fabrics, and the principal orientation of the permeability tensor is known to lie along the tow direction in the plane of the fabric. Another likely limitation of the measurement and analysis methods presented above does not involve the approximate solution but is directly related to the required experimental measurements (Figure 7.19). Although five of the suggested measurements use standard in-plane or through-the-thickness flow geometries, the final measurement illustrated requires a flow orientation 45° out of the fabric plane, and it may be quite difficult to construct the mould and cut the reinforcement to fit such a flow orientation.

7.3.3 THREE-DIMENSIONAL FLOW EXPERIMENTS

To shorten the time required to obtain three-dimensional permeability tensors, efforts are being made to conduct three-dimensional flow ex-

periments. The experiments are similar in concept to the two-dimensional radial flow experiments, except that elaborate methods are required to detect the movement of the flow front in the nearly opaque porous medium. A fluid is injected into a mould containing a thick stack of reinforcement, and the progress of the flow front is observed in all three dimensions by means such as X-ray imaging or by placing an array of small detectors throughout the reinforcement stack [25–27]. One important difference in the injection strategy for two-dimensional compared with three-dimensional radial flow experiments is that a hole is not punched in the stack of material when conducting a three-dimensional experiment, thereby forcing the fluid to penetrate through the thickness of the preform in addition to travelling in the plane of the preform. These efforts are quite recent and the results are therefore only preliminary. If such measurements are refined and can be made relatively routine, they could become valuable for assessing the complex three-dimensional flows that occur in fibrous reinforcements. However, it should be noted that such experimental measurements may not provide accurate estimates of the permeability because of the unsaturated nature of the flow and the difficulties associated with such complex experiments. For example, high flows are required in unsaturated flow experiments to obtain reasonably accurate permeability data, but fabric deformation can become a problem at high flows. Further, the fabric deformation problem is expected to be worse in the three-dimensional than in the two-dimensional radial flow geometry because the punched hole used in the latter to permit through-the-thickness penetration is specifically omitted in the former in order to force a three-dimensional flow. Experimental and analytical results confirm that even small fabric deformations near the mould wall can dramatically alter the flow behaviour [39, 40]. Rather, the value of such measurement technology may be greater for assessing flows in complex stacks of reinforcements or in reinforcements deformed inside of moulds.

7.4 SUMMARY

Permeability tensors are key parameters for models of LCM. For this reason it is crucial that they be measured and interpreted properly. However, the permeability does not entirely govern the flow behaviour in LCM because the flow is unsaturated during resin injection. Thus other physical phenomena such as capillary forces and structural heterogeneity introduce dynamic behaviour not accounted for by Darcy's law. Despite these complex fluid mechanical issues, current LCM simulations rely exclusively on Darcy's law and therefore interest has developed in measuring the so-called unsaturated permeability and in developing improved models.

In this chapter the standard measurement techniques for measuring both the saturated effective permeability, K_e^θ , and the unsaturated permeability were discussed. Measurement of K_e^θ is conceptually very simple, requiring only steady-state measurements of flow and pressure as a fluid moves unidirectionally through a preform packed into a mould. A number of practical problems such as edge effects, incomplete saturation and mould wall deformation combine to complicate considerably the measurement of K_e^θ . For those reasons, as well as the large amount of time needed to complete all the measurements of K_e^θ required to generate a complete permeability tensor, \mathbf{K} , a faster method based on unsaturated radial flow was developed.

Measurement of the radial flow of fluid into a preform requires the collection of transient flow, pressure and flow front shape information. Analyses based on Darcy's law may sometimes yield values of unsaturated permeability that compare well with the saturated flow measurements but often yield a collection of permeability values that are difficult to interpret. Such cases arise because of the unsaturated nature of the flow and are manifested by transient values of anisotropy, orientation and permeability. As a result, researchers often report the results from radial flow experiments obtained very late in the experiment when the rate of change in the values appeared to have slowed. Nevertheless, such 'terminal' results often display a dependence on the flow or pressure used to inject the fluid into the mould. More complete analyses of the radial flow experiment would be helpful to improve the interpretation of radial flow data. More recent efforts to shorten the time required to measure \mathbf{K} involve three-dimensional radial flow experiments, and those experiments are expected to suffer additional difficulties beyond those already complicating the standard radial flow experiment.

The unidirectional flow experiment permits a direct comparison of unsaturated and saturated flow behaviours within the limited range of injection rates that can be used if one intends to saturate fully the preform. Within this range, the unsaturated permeability, K_u^θ , has been found to be larger than K_e^θ in some cases, smaller than K_e^θ in other cases or both smaller and larger than K_e^θ during the course of an experiment. Much of the interesting behaviour of K_u^θ can be explained by accounting for capillary pressure, even with simplified treatments where the capillary pressure is added to the hydrodynamic pressure within a Darcy's law formalism. Additional types of behaviour observed for K_u^θ , such as the decrease in K_u^θ after the flow front reaches the end of the mould, can be explained only by more complex models that explicitly account for the structural heterogeneity of the preform. Models that include unsaturated flow phenomena are relatively primitive at this time and so cannot account quantitatively for many flow behaviours in realistic preform architectures.

Preform architectures used in liquid moulding have become quite intricate recently as preform technology has improved. It is quite possible that preforms with intricate three-dimensional fibre architectures possess a permeability tensor tilted out of the plane of the material. Therefore, it may be inadequate to treat the in-plane and through-the-thickness permeability data independently when estimating the permeability tensor of these braided, woven or stitched reinforcement materials. A general methodology was presented in this chapter for interpreting unidirectional measurements of K_e^θ in a three-dimensional reference frame. The components of an out-of-plane permeability tensor can be obtained from a set of one-dimensional saturated flow results by using an approximate solution to Darcy's law. Six highly non-linear, algebraic equations relating K_e^θ to K were presented, along with a robust root-finding algorithm for obtaining solutions. The accuracy of the approximate solution to Darcy's law was checked by comparison with a nearly exact numerical solution to Darcy's law. The approximate solution to Darcy's law was found to be within 5% of the numerical solution for all of the flow directions.

References

1. Slattery, J.C. (1981) *Momentum, Energy and Mass Transfer in Continua*, Robert E. Kreiger Publishing, Huntington, NY.
2. Greenkorn, R.A. (1983) *Flow Phenomena in Porous Media*, Marcel Dekker, New York.
3. Adler, P.M. (1992) *Porous Media*, Butterworth-Heinemann, Boston, MA.
4. Bird, R.B., Stewart, W.E. and Lightfoot, E.N. (1960) *Transport Phenomena*, John Wiley, New York.
5. Rudd, C.D., Middleton, V., Owen, M.J. et al. (1994) Modelling the processing and performance of preforms for liquid moulding processes. *Composites Manufacturing*, **5**(3), 177–86.
6. Dessenberger, R.B. and Tucker, C.L. (1995) Thermal dispersion in resin transfer molding. *Polymer Composites*, **16**(6), 495–506.
7. Carman, P.C. (1937) Fluid flow through granular beds. *Transactions of the Institute of Chemical Engineers (London)*, **15**, 150–66.
8. Lam, R.C. and Kardos, J.L. (1989) The permeability and compressibility of aligned and cross-plied carbon fiber beds during processing of composites. Annual Technical Conference of the Society of Plastics Engineers, May 1–4.
9. Phelan, F.R., Leung, Y. and Parnas, R.S. (1994) Modeling of microscale flow in unidirectional fibrous porous media. *Journal of Thermoplastic Composite Materials*, **7**, 208–18.
10. Sadiq, T.A.K., Advani, S.G. and Parnas, R.S. (1995) Experimental investigation of transverse flow through aligned cylinders. *International Journal of Multiphase Flow*, **21**(5), 755–74.
11. Parnas, R.S., Salem, A.J., Sadiq, T.A.K. et al. (1994) The interaction between micro- and macroscopic flow in RTM preforms. *Composite Structures*, **27**, 93–107.
12. Parnas, R.S., Howard, J.G., Luce, T.L. and Advani, S.G. (1995) Permeability characterization: part 1. A proposed standard reference material for permeability. *Polymer Composites*, **16**(6), 429–45.
13. Parnas, R.S. and Salem, A.J. (1993) A comparison of the unidirectional and radial in-plane flow of fluids through woven composite reinforcements. *Polymer Composites*, **14**(5), 383–94.

14. Neale, G. and Nader, W. (1974) Practical significance of Brinkman's extension of Darcy's law: coupled parallel flows within a channel and a bounding porous medium. *Canadian Journal of Chemical Engineering*, **52**, 475–78.
15. Parnas, R.S. and Cohen, Y. (1987) Coupled parallel flows of power-law fluids in a channel and a bounding porous medium. *Chemical Engineering Communications*, **53**, 3–22.
16. Gebart, B.R. (1992) Permeability of unidirectional reinforcements for RTM. *Journal of Composite Materials*, **26**(8), 1100–33.
17. Williams, J.G., Morris, C.E.M. and Ennis, B.C. (1974) Liquid flow through aligned fiber beds. *Polymer Engineering Science*, **14**(6), 413–19.
18. Miller, B. and Friedman, H.L. (1993) Evaluating in-plane absorption capabilities. *The New Nonwovens World*, **2**(3), 83–88.
19. Patel, N. and Lee, L.J. (1996) Modeling of void formation and removal in liquid composite molding. Part I: wettability analysis. *Polymer Composites*, **17**(1), 96–103.
20. Ko, F.K. (1989) Three dimensional fabrics for composites, in *Textile Structural Composites*, Eds. T.W. Chou and F.K. Ko, Elsevier, Amsterdam, pp. 129–71.
21. Parnas, R.S. and Phelan, F.R. Jr (1991) The effect of heterogeneous porous media on mold filling in resin transfer molding. *SAMPE Q*, **22**, 53–60.
22. Rudd, C.D., Long, A.C., McGeehin, P. and Smith, P. (1996) In-plane permeability determination for simulation of liquid composite moulding of complex shapes. *Polymer Composites*, **17**(1), 52–9.
23. Friedman, H.L., Johnson, R.A., Miller, B. et al. (1995) In-plane movement of liquids through curved fabric structures. (I) Experimental approach. *Proceedings of the ASME Materials Division, MD-Volume 69-1*, pp. 817–40.
24. Adams, K.L., Russel, W.B. and Rebenfeld, L. (1988) Radial penetration of a viscous liquid into a planar anisotropic porous medium. *International Journal of Multiphase Flow*, **14**(2), 203–15.
25. Ahn, S.H., Lee, W.I. and Springer, G.S. (1995) Measurement of the three-dimensional permeability of fiber preforms using embedded fiber optic sensors. *Journal of Composite Materials*, **29**(6), 714–33.
26. Bréard, J., Saouab, A., Bouquet, G. et al. (1995) Experimental study of a three-dimensional resin flow through a fiber reinforcement material, in *Proceedings of the International Conference on Composite Materials and Energy*, Technomic Publishing Lancaster, PA, pp. 327–33.
27. Weitzenböck, J.R., Sheno, R.A. and Wilson, P.A. (1995) Flow front measurement in RTM, in *4th International Conference on Automated Composites*, The Institute of Materials, Nottingham, UK, pp. 307–14.
28. Gebart, B.R. and Lidström, P. (1996) Measurement of in-plane permeability of anisotropic fiber reinforcements. *Polymer Composites*, **17**(1), 43–51.
29. Ranganathan, S., Phelan, F.R. and Advani, S.G. (1996) A generalized model for the transverse permeability of unidirectional fibrous media. *Polymer Composites*, **17**(2), 222–30.
30. Marty, N.S., Torquato, S. and Bentz, D.P. (1994) Universal scaling of fluid permeability for sphere packings. *Physics Reviews E*, **50**(1), 403–8.
31. Lidström, P. (1992) Measurement of in-plane permeability of anisotropic media. Swedish Institute of Composites SICOMP technical report 92-013, SICOMP, Piteå, Sweden.

32. Rudd, C.D., Morris, D.J., Chick J.P. and Warrior, N.A. (1995) Material characterization for SRIM, in *4th International Conference on Automated Composites ICAC '95, Volume 1*, The Institute of Materials, Nottingham, UK, pp. 211–18.
33. Woerdeman, D.L., Phelan, F.R. and Parnas, R.S. (1995) Interpretation of 3-D permeability measurements for RTM Modeling. *Polymer Composites*, **16**(6), 470–80.
34. Luce, T.L., Advani, S.G., Howard, J.G. and Parnas, R.S. (1995) Permeability characterization, part 2. Flow behavior in multiple-layer preforms. *Polymer Composites*, **16**(6), 446–58.
35. Nye, J.F. (1957) *Physical Properties of Crystals: Their Representation by Tensors and Matrices*, Oxford University Press, Oxford.
36. Cottle, R. W. (1974) *Manifestation of the Schur complement, Linear Algebra and Applications*, **8**, 189.
37. Press, W.H., Flannery, B. P., Teukolsky, S. A. and Vetterling, W. T. (1986) *Numerical Recipes, The Art of Scientific Computing*, Cambridge University Press, Cambridge, MA.
38. Phelan, F.R. (1992) Flow simulation of the resin transfer molding process, in *Proceedings of the American Society for Composites 7th Technical Conference*, p. 90.
39. Han, K., Trevino, L., Lee L.J. and Liou, M. (1993) Fiber mat deformation in liquid composite molding. I: experimental analysis. *Polymer Composites*, **14**(2), 144–50.
40. Parnas, R.S., Schultheisz, C.R. and Ranganathan, S. (1996) Hydrodynamically induced preform deformation. *Polymer Composites*, **17**(1), 4–10.

Modelling and simulation of flow, heat transfer and cure

8

Suresh G. Advani and Pavel Simácek

8.1 INTRODUCTION

8.1.1 THE RESIN TRANSFER MOULD FILLING PROCESS

The resin transfer moulding (RTM) process consists of five consecutive stages, as shown in Figure 8.1. These are:

- draping of the mould with a preform;
- closing the mould;
- resin injection;
- curing;
- demoulding.

The complexity of each stage will depend on the mould shape, preform architecture and, obviously, the design of the mould. The mould shape and preform architecture will be dictated primarily by the part design. The design details of the mould, such as gate and vent locations, runners for resin and similar factors, can be adjusted for ease of manufacturing only as long as the design criteria are satisfied. The ability to take advantage of this fact and design a fast, reliable and cheap process depends on our understanding of the RTM process and the ability to model it by analytical or numerical means.

This chapter is primarily interested in the third and fourth stages, filling the mould with resin and, consequently or simultaneously, curing

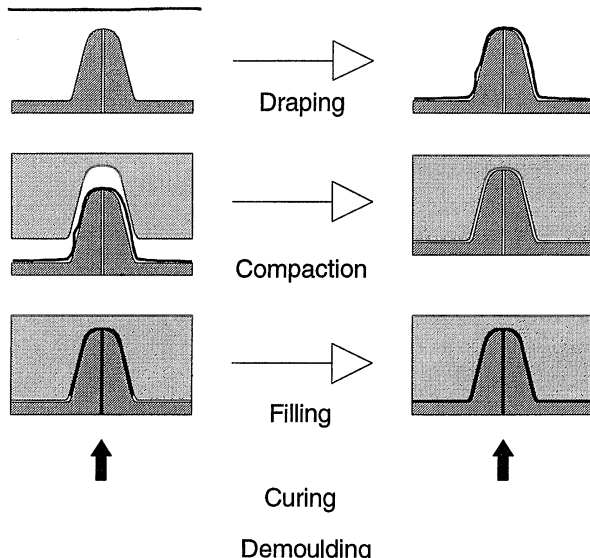


Figure 8.1 Resin transfer moulding process stages.

it to a sufficient degree, so that demoulding is possible. The traditional approach to RTM modelling assumes that this is the only part of the process that needs to be modelled. However, the preceding stages of draping and closing influence the filling process significantly, and more recent approaches include them, at least partially, in the model. We will therefore discuss these preforming stages in connection with the subsequent filling and cure.

8.1.2 THE NEED FOR A PROCESS MODEL OF RESIN IMPREGNATION

Successful mould design is fully dependent on our ability to simulate the complete process. The principal reasons are apparent: the need to keep down cost and time. Figure 8.2 shows a fairly complex part (an Apache helicopter keel beam). The mould for such a part involves enormous cost and, if improperly designed, can easily end up as a total failure. The flow progression in the mould can entrap air pockets which will lead to undesirable dry spots. Also, the injection pressure can be higher than expected. This can introduce unacceptable deformation of the mould or, in extreme cases, mechanical failure of one of the components.

The simulation of filling such a part can predict the qualitative flow progression fairly well. Also, if the estimates of input data are reasonable, the filling pressure or flow rate can be predicted fairly reliably.

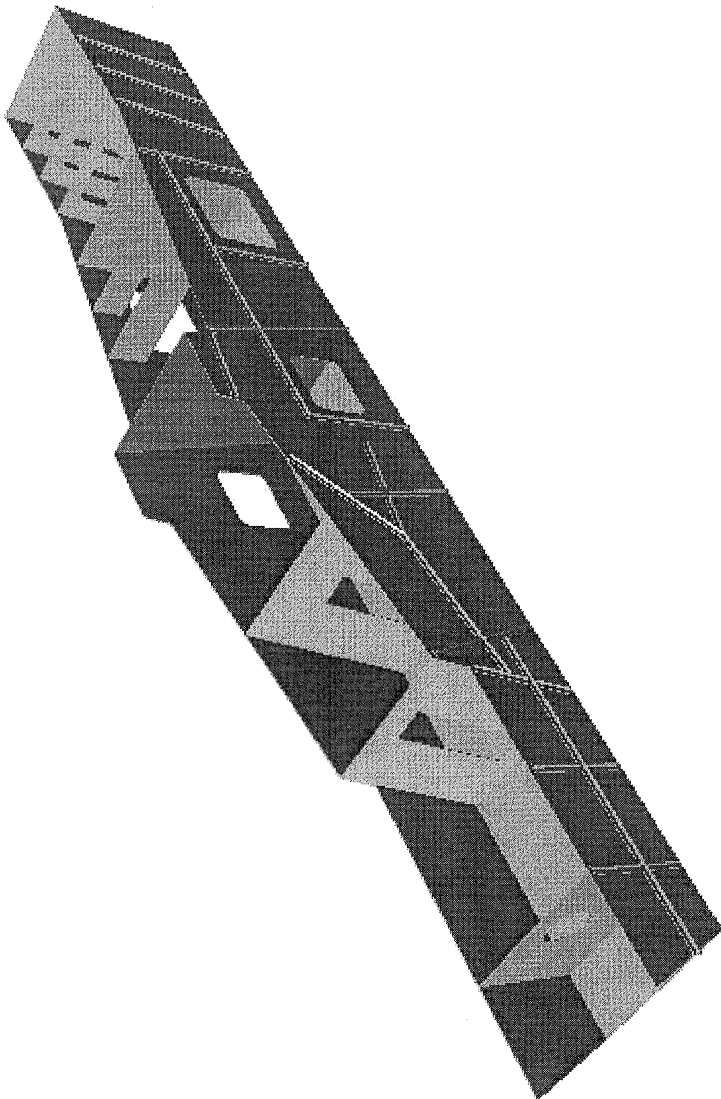


Figure 8.2 Apache helicopter keel beam.

This leads us to the key question at the heart of simulation and numerical modelling: the acquisition of the necessary input data for the simulation. Some parameters, such as permeability, cannot be estimated without substantial numerical modelling and/or analytic work. Other phenomena, such as heat dispersion, are not well understood and in

addition suffer from lack of experimental data. We will discuss the individual input parameters as they are introduced.

8.1.3 MICROSCOPIC AND MACROSCOPIC FLOW

The flow through the preform is modelled as a flow of viscous fluid (resin) through a porous continuum (preform). However, in real situations most preform materials do not qualify as a continuum if one uses the rigorous definition. The dimensions of the microstructure (typically the fibre tow diameter) are not much smaller than the smallest overall dimension, usually the thickness. Actually, the difference between fibre tow diameter and thickness is usually about an order of magnitude but sometimes they can even be of the same order.

Fortunately, we know from countless experiments performed in various laboratories over a decade that the continuum model works. The usual way to justify its use is to compare a single fibre diameter with the total thickness. Then we have a proper continuum! This is hardly a proper justification, but it emphasises the dual character of the flow.

The visible preform structure usually consists of fibre tows woven, braided or stitched together and a network of empty spaces – channels and pores. This can be defined as the **macrostructure** and it is obviously a porous medium. However, the fibre tows are not solid reinforcement but are rather bundles of well-aligned fibres, containing a significant volume percentage of voids. The arrangement within fibre bundles can be labeled as the **microstructure**.

Resin will flow preferentially through the channels and pores in the macrostructure. However, in addition to this **macroflow** the resin will fill in and flow through the individual fibre tows. The significance of this effect (**microflow**) has yet to be estimated. Nonetheless, it is certain that it contributes considerably to void formation and complicates permeability measurements [1]. It is also possible to conceive a simple analytic problem where the influence of the microflow will govern the macroflow characteristics [2].

8.2 FLOW AND PREFORM ARCHITECTURE

The preform within the mould presents a two-phase system. Prior to filling there is a structure of solid reinforcing particles (fibres) and free space. If it is assumed no preform deformation occurs during the flow, the fibres remain stationary and resin fills in and flows through the space between fibres. There might actually be a significant period of a three-phase flow when fibres, resin and air coexist within the volume. The difficulties in using the ‘exact’ description to model the flow are formi-

dable. The models we are going to introduce later will invariably treat the flow through the preform as a flow through a porous Darcian medium. In such a material, the flow Darcian velocity v and the pressure in fluid p are coupled via the generalised Darcy's law:

$$\mathbf{v} = -\left(\frac{\mathbf{K}}{\eta}\right) \cdot (\nabla p) \quad (8.1)$$

Here η the resin viscosity and \mathbf{K} is the preform permeability. This quantity is a second-order symmetric tensor and consequently has three independent components for two-dimensional problems and six components in fully three-dimensional equations. Thus, for a two-dimensional problem (i.e. solution in the plane of the preform only) the equation can be written as:

$$\begin{pmatrix} v_x \\ v_y \end{pmatrix} = -\frac{1}{\eta} \begin{pmatrix} K_{xx} & K_{xy} \\ K_{yx} & K_{yy} \end{pmatrix} \begin{pmatrix} \frac{\partial p}{\partial x} \\ \frac{\partial p}{\partial y} \end{pmatrix} \quad (8.2)$$

and for a fully three-dimensional problem as:

$$\begin{pmatrix} v_x \\ v_y \\ v_z \end{pmatrix} = -\frac{1}{\eta} \begin{pmatrix} K_{xx} & K_{xy} & K_{xz} \\ K_{yx} & K_{yy} & K_{yz} \\ K_{zx} & K_{zy} & K_{zz} \end{pmatrix} \begin{pmatrix} \frac{\partial p}{\partial x} \\ \frac{\partial p}{\partial y} \\ \frac{\partial p}{\partial z} \end{pmatrix} \quad (8.3)$$

Most of the research concerning the simulation of flow through a preform hinges upon the determination of the components of \mathbf{K} in these equations [3, 4].

We will examine the flow through the preform and its dependence on the preform architecture and point out certain potential complications with this approach, as well as issues that require further research. The reasons are that occasionally certain assumptions of Darcy's law are violated. Most notably, the law was derived for Newtonian fluids but is used indiscriminately with whatever fluid model suits the resin. Although experience shows that reasonable results might be obtained even in these cases a certain caution is advisable.

Moreover, the preform geometry displays a distinct dual length-scale character, as mentioned above [5–7]. The effect is demonstrated in Figure 8.3. The equivalent permeability tensor \mathbf{K} has to take into account both the macroflow and the microflow through the actual structure.

In most cases the flow depends mainly on the macrostructure, and whatever happens at the fibre tow level does not really influence it very much. This statement does not extend to some other areas, such as void formation. Depending on the type of preform it is even possible that there is just a single length scale (unidirectional fibres, random mats).

Since both the macrostructure and microstructure change with preform deformation, we will need to accommodate preform deformation

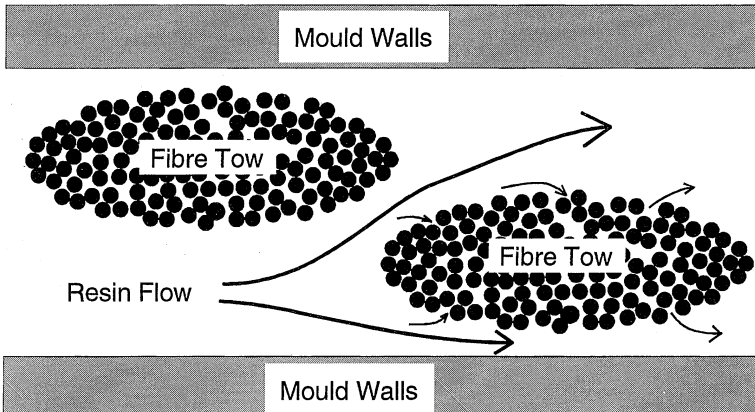


Figure 8.3 Dual length scale within the woven fibrous preform: schematic.

when we evaluate the permeability tensor \mathbf{K} . This means that the in-plane deformation during the draping as well as the compaction of the preform have to be accounted for if we want to obtain reasonable values of \mathbf{K} [8, 9].

8.2.1 FLOW IN RANDOM FABRICS

The simplest possible preform is the random fibre mat. Its structure is depicted in Figure 8.4. The structure is homogeneous, the typical dimension being the fibre diameter. The length of the fibres relative to their diameter (aspect ratio) is usually large.

In most cases, the thickness of the preform is indeed much larger than the fibre diameter and the material does behave as a continuum on the length scale of its thickness. There seems to be no objection to this type of material being treated as a Darcian medium.

Additionally, the properties of the fibre bed are unlikely to change in the plane of the preform. This means that the material should show isotropy relative to flow in the plane of preform. The only complication might be that of a different value of the permeability tensor through the thickness because of preferential fibre orientation.

Most random mats do not shear well, so in-plane deformation and its effect on permeability is non-existent. However, fibre volume fraction is low and the structure can be compacted considerably in the transverse direction so we cannot neglect preform deformation altogether. The measured permeability will depend on compaction and the original preform volume fraction only. Thus the permeability measurement can be obtained with relatively few experiments. Consequently, we will not discuss flow through or permeability of random mats any further.

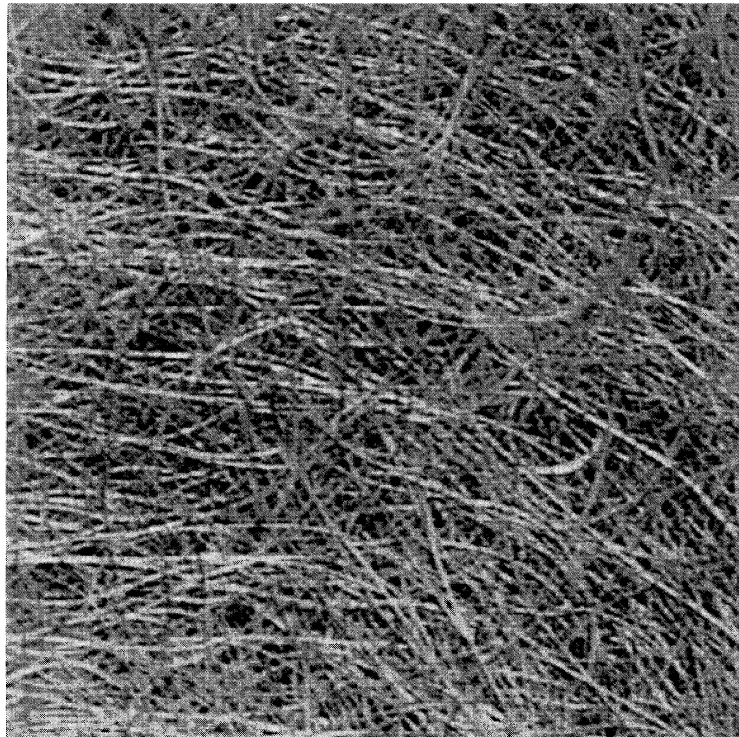


Figure 8.4 Random mat structure.

8.2.2 FLOW IN WOVEN OR STITCHED FABRICS

Typical woven or stitched fabric looks fairly different from a random mat (Figure 8.5). The preform is prepared in two steps: first the individual fibres are assembled into fibre tows, then the tows are woven, braided or stitched together to make the preform.

Sizes of the individual tows vary greatly with the preform. Usually 1K to 100K fibre tows (1000–100 000 fibres per tow) are used. This creates the above-mentioned dual length-scale structure; the individual tows are themselves a porous medium. The assumption of these being a continuum seems fairly reasonable.

However, the macrostructure created from tows by weaving, braiding or stitching creates one additional level of complexity. With the exception of some stitched preforms, fibre tows show a considerable degree of undulation and a description of this structure might be extremely difficult. The empty space between fibre tows is usually a continuous network of open pores or channels and will attract most of the flow; consequently a description of this network is necessary for any analytic

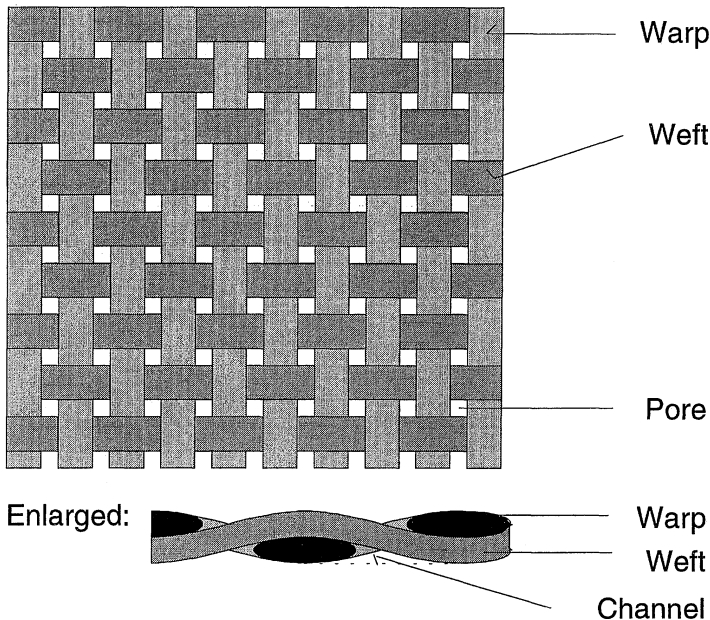


Figure 8.5 Simple woven fabric.

permeability predictions. The dimensions of this network are rarely more than one order of magnitude smaller than the overall thickness and this fact puts a continuum assumption into jeopardy.

The resin flow has to fill both the empty space within the macro-structure (called channels or pores) and the interfibre space within the fibre tows. To use equation (8.1) we need to find an equivalent permeability that will include both mechanisms.

The intuitive way is to skip the problems and use a measured permeability, K . There is a strong reason not to rely exclusively on this approach. Woven preforms can deform both in-plane and in the transverse direction. To accommodate these deformations, one would have to measure permeability for various degrees of shearing deformation and compaction for each type of preform being used [1, 7]. The necessary data and charts for each case would make a thick volume.

There are some analytic algorithms available to predict permeability. A simple analytic model such as the one we presented elsewhere [2] does not eliminate the necessity for measurements. These remain necessary in order to verify the model and adjust any geometric parameters within the geometry description. However, the number of experiments necessary for a full description is reduced considerably if a reasonable analytic model is used for guidelines.

Microflow within tows

Fibre tows are a nearly ideal porous medium. Flow through an aligned fibre bed has been studied thoroughly [10–12] and can be easily modelled. What has to be realised is that the permeability of this medium is anisotropic. The permeability tensor might be transversely isotropic if the deformation of fibre tow is negligible, but the principal value in the fibre direction will be larger than its value in the transverse direction. Obviously, the model might be more complex than Darcian flow, but there is no need for such a complication in usual cases.

Flow in open channels

If one assumes a low fluid velocity (more precisely low Reynolds number Re), flow within the spatial structure of channels can be basically treated as Stokes flow through a very complex domain. Simplifications to the Stokes equations can be made by using appropriate dimensional analysis.

There are two crucial problems in analysing the flow. First, it is rather difficult to obtain some sort of 'representative' geometry for an arbitrary preform. Second, the boundary conditions on the surface of fibre tows are fairly uncertain. Although one can apply a no-slip condition similar to the condition applied at the surface of the mould this condition is really not compatible with Darcian flow within the fibre tows.

8.2.3 UNSATURATED FLOW

So far we have described the flow of fluid through the solid preform. However, in a real filling process in a dual length-scale medium the flow will progress with different speeds in the channel network and within the fibre tows. The result is that [1, 7] the permeability seems to have a transient character until the saturated state is reached. The magnitude and orientation of this effect depends on the rate of injection. Obviously, this might be of some importance, especially if the part being filled is small and filling time is short. There are some analytical models to address this problem [13] but the analysis of this effect is in its infancy.

8.2.4 TRANSVERSE FLOW IN MULTILAYER PREFORMS

The preform within the mould is generally three-dimensional. To classify the flow within a preform, tensor K has nine components, of which six are independent because of symmetry, and the velocity and pressure varies both in the plane of the preform and through the thickness.

In the real world, the RTM manufactured part is usually a flat shell, possibly with large curvature, and the thickness is negligible. Under certain conditions, which are discussed later and are usually satisfied, we

can then assume that the pressure varies within the plane of preform only and that the velocity vector lies in the plane of preform and does not vary through the thickness. This is rather an attractive simplification since it reduces the dimension of the problem and considerably simplifies the measurement of permeability.

The difficulty is that the preform is not necessarily homogenous in the transverse direction. There might be several layers of quite different structure and consequently of different permeability. We would like to be able to use the in-plane permeability predicted for individual layers to obtain the in-plane permeability of the layered preform. Because of the importance of this topic, both experimental [14] and analytic [15] work on this topic are available. The simplest scheme, that works well if the difference in permeabilities is not very large, is to average the permeability through the thickness, that is:

$$\bar{K}_{ij} = \frac{1}{h} \sum_{k=1}^n h_k K_{ij,k} \quad (8.4)$$

where

i and j are the in-plane directions;

K_{ij} is the average permeability through the thickness;

h is the thickness of the preform;

h_k is the thickness of layer k of the preform;

$K_{ij,k}$ is the permeability of layer k of the preform;

n is the total number of layers in the preform.

If the permeability of individual layers differs by an order of magnitude, some corrections might be necessary [16, 17].

8.3 DEFORMATION OF FABRICS AND ITS IMPACT ON FLOW

Quite recently it was casually assumed that the permeability of a preform material could be measured once and applied to any flow through the same preform. Unfortunately, recent work has clearly demonstrated that this is not the case [8, 9, 18].

The flow through the preform depends on its macrostructure and on its microstructure. During the preforming stage the preform structure undergoes considerable changes:

- the angles between yarns are changed as the preform is draped over the tool surface;
- the thickness is reduced as the mould is closed (or vacuum drawn), usually by a significant percentage;
- empty spaces may remain along sharp edges in the mould, where the preform does not follow the surface exactly.

Since these changes can drastically change both the magnitude and the principal directions of the permeability tensor it is necessary to include preforming into the simulation.

8.3.1 IN-PLANE DEFORMATION

A typical woven preform will consist of two families of fibre tows, labelled as warp and weft. These are initially perpendicular to each other and equally spaced in the fabric, as shown in Figure 8.5. If the fabric is draped on the surface of the mould, then given that the surface is not developable, this geometry will change.

Obviously, the fibre tows allow only very little extension, but, depending on the preform structure, two modes of deformation are possible. These are depicted in Figure 8.6. The first one, shearing, changes the angle between warp and weft. The second is the tow–tow slip which changes locally the spacing between the neighboring tows.

The possible amount of deformation will depend on the structure of the preform. Very tight preforms may not allow much deformation; looser ones can shear by over 40°. Tow–tow slip is traditionally considered to be a less important deformation mode, but it seems from our

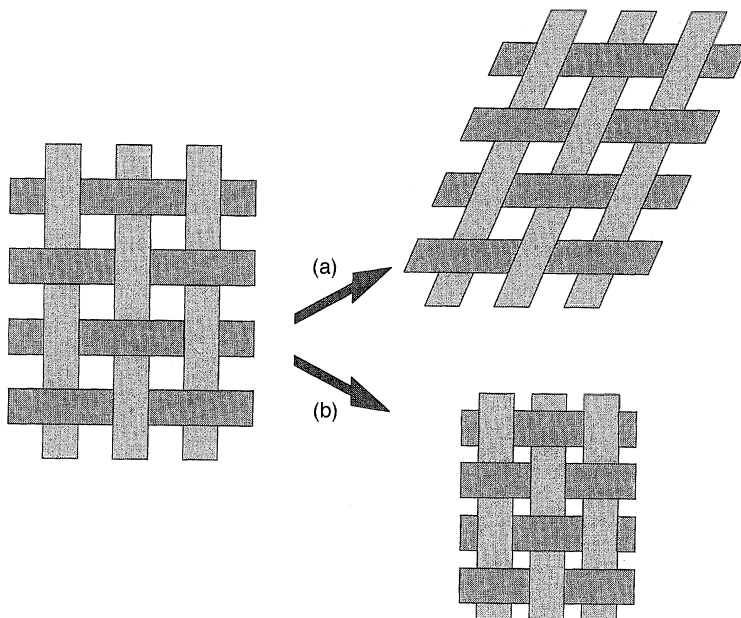


Figure 8.6 In-plane deformation of woven fabric: (a) fibre-fibre shearing; (b) fibre-fibre (or tow-tow) slip.

experimental experience [8] that once the potential for shearing deformation is exhausted tow–tow slip deformation occurs and is no longer negligible.

The impact of this deformation on the flow is twofold. First, deformation reduces the size of the channel and pore network, as well as the spacing within the fibre tows. Thus it reduces the magnitude of permeability. It also rotates the principal axes of permeability. Second, the fibre volume fraction is also increased.

8.3.2 TRANSVERSE COMPACTION

After the preform is placed in the mould, the mould has to be closed, either by another rigid piece or by some type of bagging maintained by vacuum. In either case, transverse pressure is applied to the preform. The pressure is necessary to hold preforms in place during the filling stage. In the case of a rigid form being used, the compaction force that the rigid mould exerts on the preform is unpredictable by current means of analysis. If one assumes the mould to be rigid one can, however, make an estimate from the final thickness of the preform. Often it is much less than its thickness prior to compaction.

In the case of a vacuum being used, corresponding to resin infusion or similar processes, we do not know the final thickness of the preform as only a flexible surface is used, but we know exactly the pressure that was applied. Again, the pressure reduces the thickness of the preform. For some types of preform this reduction can be considerable.

There are two deformation mechanisms at work during the compaction stage, as depicted in the Figure 8.7. The individual layers are compacted. Also, the individual layers can interpenetrate, thus reducing the thickness of the preform, possibly without any deformation. The presence of both mechanisms complicates experimental evaluation; predic-

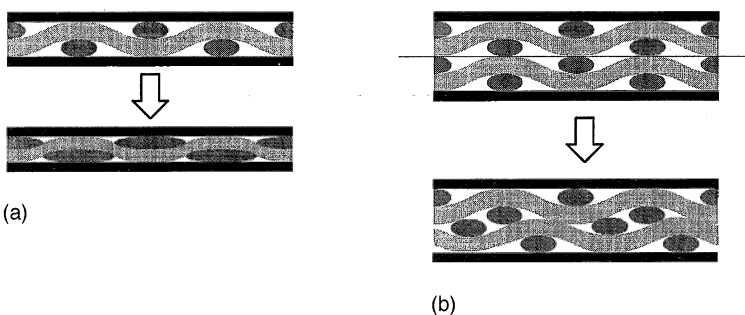


Figure 8.7 Deformation mechanisms in transverse compaction: (a) intralayer (single-layer) compaction; (b) interlayer compaction (layer ‘nesting’).

tive models for the compaction of preforms exist only for the case of aligned fibre beds [19, 20] and, in great variety, for random mats [21–25]. Attempts to deal with woven preforms are few [25–27]. There is no predictive model and experimental data are scarce for the second deformation mechanism.

Since both mechanisms reduce the spacing in both microstructure and macrostructure, compaction reduces the permeability of the preform to an unknown degree.

8.3.3 RACETRACKING

The third problem is associated with the finite bending stiffness of a preform and the precision of its preparation. In the corners and along the edges of the mould there might be some free space left, as shown in Figure 8.8. The same effect might be intentionally created to speed up the filling process. This will result in flow through the gap, usually faster than that in the other parts of the mould, as has been demonstrated [18, 28].

Since we presume the mould is filled with continuous preform we have to handle the channels as a part of the preform and assume that the presence of a channel increases the permeability of the preform in this range [18, 28]. A detailed analysis of the phenomenon is beyond the scope of this chapter, but, obviously, a way to estimate this ‘permeability’ would be extremely useful for the prediction of flow front patterns and other quantities [28].

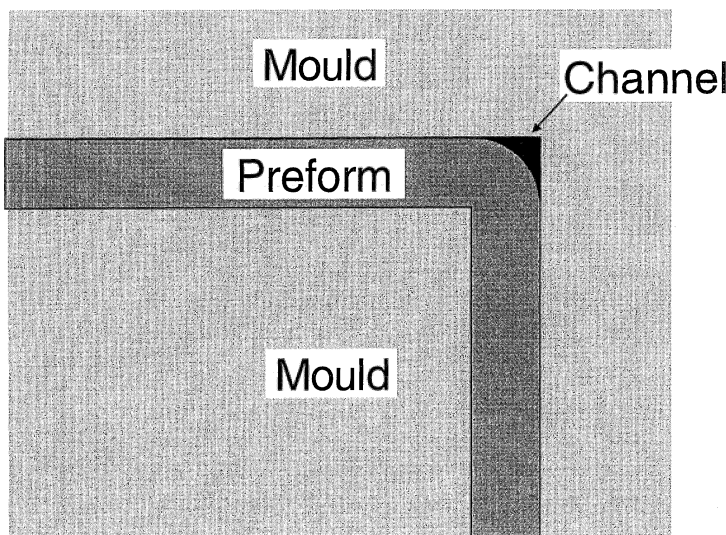


Figure 8.8 Channels in the corner of the mould that result in racetracking.

8.4 ANALYTIC AND NUMERICAL MODELS FOR THE PREFORMING STAGE

Measurement of the above-mentioned factors would be a complex task. Moreover, it would not help the design process very much, since the mould would have to be constructed prior to any data being collected. Consequently, we would like to model all the factors – draping, compaction and, finally, the permeability prediction – by analytic tools.

Current models introduce a number of simplifications that will be stated. The consequences of these assumptions limit the range of validity and reduce the accuracy. Nonetheless, the application of these models prior to the actual filling simulation presents a considerable improvement when compared with the case where preforming deformation is ignored.

8.4.1 PREFORM DEFORMATION

Preform deformation consists of two steps: draping and compaction. If the surface is developable, draping will not result in shearing deformation but it might still be important if the permeability of the undeformed preform is anisotropic because it maps the principal axes of the permeability to the surface. Note that this task is trivial only if the surface consists of a limited number of planar surfaces, as is the case with plates or boxes.

Currently there are models available for compaction of aligned fibres and random mats [19, 21–24]. There is no analytical model available for a typical dual length-scale medium such as a woven, braided or even stitched preform. The model suggested by Hearle and Shanahan [26, 27] does not specifically treat microscale deformation.

Draping

Models of draping start with the shape of the mould and possibly the preform and give us the following information:

- the direction of warp and weft tows on the surface;
- the shearing deformation of the preform;
- the change in the fibre volume fraction as a function of position.

We will examine the behaviour of woven preforms. The conclusions are usually directly applicable to bidirectional stitched preforms as well and can also be applied to bidirectional braided preforms. As far as other fibrous media are concerned (random mats, multidirectional stitched or braided preforms) these do not allow any in-plane deformation.

The numerical or analytic simulation of the draping process raises several issues. From the numerical point of view, non-uniqueness of the

solution is a very critical problem. Hence in order to obtain a solution we have to introduce additional criteria (boundary conditions) to warrant a unique solution. Unlike in most engineering problems, these conditions tend to be purely geometric and completely arbitrary.

Behaviour of the media is the second issue. The woven material has two directions of inextensibility and a wide range of low-resistance shearing deformations. This deformation is not unlimited and at a certain angle a fabric will lock, which means it will not deform any more and any attempt to increase the shearing deformation leads to either tow–tow slip (Figure 8.6) or wrinkling.

This creates difficulty in establishing the proper locking angle from an experimental point of view. From the simulation point of view, the possibility of a wrinkled surface will require changes to certain geometrical aspects (boundary conditions) of draping according to the shearing deformation attained and may even require additional cutting of the preform and removal of a section of the fabric to allow draping without wrinkling or slippage.

The geometric solution

The geometric solution of the draping process is based upon kinematic constraints. The fibre tows are considered inextensible and there is no slip of tow–tow intersection allowed. Only shearing deformation is allowed. The validity of these assumptions seems to depend on the severity of shearing deformation of the preform relative to its limit [8].

The fabric is replaced by a net representing the warp and weft tows. Usually, the net is considerably more coarse than the actual fabric structure. The net is then mapped onto the surface by using the inextensibility of the sides of individual cells. The algorithm starts with the known position of certain nodes and finds the position of additional nodes based on a fixed length of warp and weft between the nodes already placed and the node being placed, as shown in Figure 8.9. The scheme has the distinct advantage of being incremental; one node at a time is being placed on the surface, which resembles the actual draping process.

If it is assumed there are no interactions, the tow (warp or weft) connecting two points follows the geodesic curve, that is, the shortest possible line. On a flat surface this reduces to a straight line. On non-planar developable surfaces, this curve maps onto a straight line after developing the surface. For a general surface, a differential equation has to be solved to obtain the geodesic curve. Most researchers [29–32] are utilising these facts. The actual solver depends on an approximation of the surface, which allows two distinct possibilities.

First, the surface can be modelled as an assembly of flat elements (i.e. linear triangles). Then the geodesics reduce to straight lines and can be

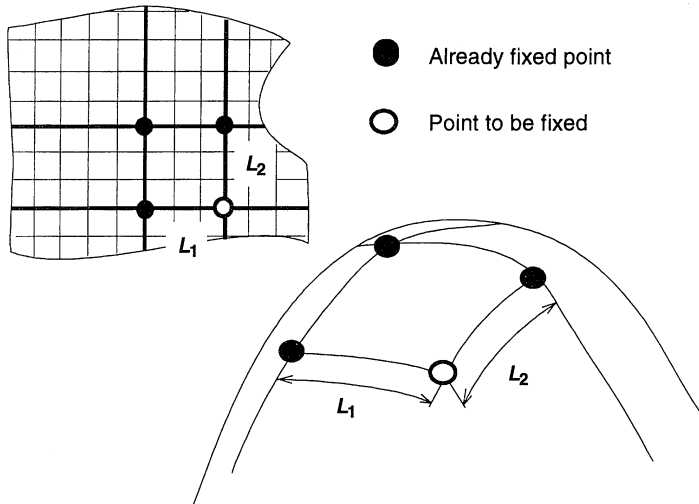


Figure 8.9 Draping: placing an additional intersection on the surface. ● = points already fixed; ○ = point to be fixed.

solved easily. In fact, since the surface is developable, a closed-form solution is available regardless of how many triangles the line crosses. However, unless carefully optimised the closed-form solution will require development of about 2^N panels to a plane, where N is the number of triangles the yarn segment crosses. This renders the solution unsuitable for large N , that is for small panels and long distances between nodes on the fabric. As a result, existing implementations restrict the number of triangular boundaries crossed [30].

Second, the surface can be modelled as a smooth (C^1) assembly of curved elements. The geodesics then have to be followed numerically. For a geodesic given by an initial point and a tangent this is a straightforward approach. Unfortunately, if we want two geodesics of given starting points to intersect at given distances, some iterative scheme is necessary to solve for the initial tangents. This involves a non-linear system of equations with two unknowns. Obviously, the problem can be cast into a non-linear minimisation problem of two variables.

There is a third possibility, that is, the surface can be modelled as curved panels on a C^0 surface, but it does not offer much of an advantage other than possibly an easier description of the surface. It is, at least in theory, possible to obtain an elastic solution for the fabric treated as a membrane with two directions of inextensibility, with a progressively stiffening-shearing response and with large deformations [33–35]. Nonetheless, a number of problems persist, rendering this solution impractical:

- The solution is non-unique. Since all points are being placed at once, this requires the specification of boundary conditions and optimisation criteria to obtain a properly posed system. Any change to these conditions requires the whole problem to be recomputed.
- The inextensibility is problematic as it requires a mixed formulation and usually yields spurious modes in the stress (tension) part. This is a difficulty with use of one direction of inextensibility. To our knowledge, the use of two directions of inextensibility in a finite element method (FEM) formulation has not been treated yet. Use of extensible tows with large stiffness may help but may run into problems[36].
- The reactions between the mould and the fabric are necessary for this approach truly to work. These would need to be specified, but it is extremely difficult to obtain even an estimate of realistic values. The repeatability of these values in a real process is also questionable.
- Wrinkling would not be easily predicted, since the sheared elements would become absolutely rigid instead of yielding to load owing to instability (buckling). However, if large deformations are allowed, buckling on length scales larger than the element size could be modelled.
- The constitutive equation of the fabric should be at least elastoplastic. No such constitutive equation is available.

Because of these difficulties the geometric model is currently the only way to obtain a solution in real time with the data currently available to us. The available 'elastic' solutions [29, 33, 35] actually assume a large elastic extensional stiffness of the fibres in the fabric and zero shearing stiffness. This solution is actually very close to the geometric one and has nothing to do with a true elastic (or rather elastoplastic) problem. The only difference is that the geometric approach uses pointwise collocation, whereas the 'elastic' solution uses the Galerkin method to enforce the condition of no extension in the fibre direction. Comparison of this 'elastic' solution with the geometric approach considered above is presented by Van Der Wee  n [29]. However, this work should not be considered the final word, since only a hemispherical surface is compared. Since the proposed algorithm depends on the smoothness of the surface it might be more problematic to apply the method to a general geometry described by a typical FEM mesh.

Compaction

Compaction models should take the preform geometry, possibly already subjected to shearing deformation and compaction pressure to predict the resulting thickness, or alternatively they should use the resulting thickness to predict the compaction pressure and the micro structure and the macrostructure of the preforms.

There are a number of models describing the compaction of random mats or aligned fibres [19, 21–23]. The problem is a bit more complex with a dual-scale medium. To describe deformation of a macrostructure by any means one has to model fibre tows as a continuum with sufficiently accurate behaviour (i.e. an elastoplastic medium). Although there are some suggestions as to how the medium should behave [37–39] there is little or no experimental evidence for these models.

Once the constitutive equations are known the structure of the preform can be analysed as a large-deformation non-linear elastic (or elastoplastic) problem, for example viFEM. Also, use of the mosaic model (or some other Raileigh–Ritz approximation) provides a valid upper bound on the stiffness of the preform.

However, at this time, there is no publication offering a comprehensive attempt to characterise compaction as a whole. Some of the above-mentioned approaches have not been properly tested; none of them includes prediction of the nesting behaviour, although experimental work shows that this phenomenon does occur [3, 25].

8.4.2 PERMEABILITY

Permeability models

If we want to predict permeability we have to select the method suitable for the data we need and the reinforcement type. Depending on the model we use for filling we might need either a two-dimensional permeability tensor (in-plane components only) or a three-dimensional tensor. Since there is very little data on measurements of three-dimensional permeability components, we will concentrate mostly on prediction of the in-plane permeability tensor.

The other question that arises concerns the type of preform we are dealing with. For random mats or unidirectional fibres we can utilise a number of existing equations [11, 12, 17, 40, 41] that usually correlate well with experimental data. For woven (or stitched or braided) preforms the situation is more involved [6].

Although there are many attempts to model flow past an array of variously arranged cylinders [17, 40], there is fairly little accomplished in this area, although some models do exist [2, 42, 43].

In-plane permeability of a woven preform

In this subsection we present basic ideas to model in-plane permeability for a woven preform. Utilising a unit cell, we can compute permeability by comparing the total flow in two directions for a specified applied pressure drop [44]. Under typical conditions for a woven preform one

can considerably simplify the problem while maintaining accuracy [2]. These conditions imply that the preform is flat; that is the tow cross-sections are flat ellipses rather than circular sections.

The simplified problem reduces to flow through a layered system, as depicted in Figure 8.10. There are alternating layers of reinforcement (fabric, stitched fibre tows) saturated with resin, and channels filled with only resin. The number of preform layers can vary. In the example in Figure 8.10 there are two layers. The flow through the channels can be described as a two-dimensional (x - y plane) lubrication flow. The only significant flow within the preforms is the transverse (z -direction) Darcian flow. The problem can be reduced to a set of coupled two-dimensional elliptic partial differential equations [2]. There will be one equation for each channel, coupled with the neighbouring equations. For the example in Figure 8.10, the equations will be as follows:

$$\frac{K_{zz}}{\eta h_1} (p_B - p_A) - \frac{1}{6\eta} \nabla(h_A^3 \nabla p_A) = 0 \quad (8.5)$$

$$\frac{K_{zz}}{\eta h_2} (p_C - p_B) - \frac{K_{zz}}{\eta h_1} (p_B - p_A) - \frac{1}{6\eta} \nabla(h_B^3 \nabla p_B) = 0 \quad (8.6)$$

$$\frac{K_{zz}}{\eta h_2} (p_C - p_B) - \frac{1}{6\eta} \nabla(h_C^3 \nabla p_C) = 0 \quad (8.7)$$

where the gradient operator, ∇ , is in the x - y plane only (the direction of y goes out of the plane of the Figure 8.10) and where,

K_{zz} is the transverse permeability of the reinforcement;

η is the resin viscosity;

p_A , p_B and p_C are the pressures in channels A, B and C, respectively;

h_1 and h_2 are the thicknesses of fabric layers 1 and 2;

h_A , h_B and h_C are the thicknesses of channels A, B and C, respectively.

Since the unit cell is of a simple (rectangular) shape, the finite difference method might be sufficient to solve the problem. The geometry of the reinforcement is described in terms of dimensions (thicknesses), as given

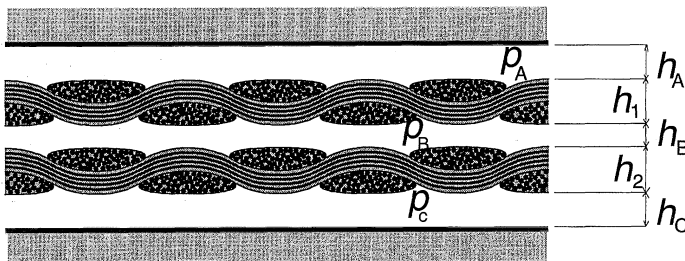


Figure 8.10 Permeability model: flow geometry. p_A , p_B and p_C are the pressures in channels A, B and C, respectively.

in Figure 8.10. The fibre reinforcement thickness data may be given at discrete points rather than by an analytic expression. The boundary conditions are specified by periodicity and the pressure drop in the x and y directions.

The unknown in equations (8.5–8.7) is the pressure inside individual channels. Once the pressure fields are evaluated the velocities are known from pressure gradients and lubrication assumptions, and can be integrated to obtain the flow. Then the appropriate permeability components can be evaluated. To obtain all in-plane components, two computations are necessary (one with pressure drop in the x direction and one with pressure drop in the y direction, respectively).

The ‘unit’ cell concept

The above-mentioned ‘periodic’ boundary conditions are a consequence of the more general approach to the unit cell we have described elsewhere [2]. The unit cell is a representative repetitive unit of the entire domain. In most cases, when this concept is invoked, the boundaries of such a cell are lines of symmetry. This fact allows ‘special’ boundary conditions to be specified. Usually these are very advantageous for solving the problem. An example of these conditions for our case of an undeformed cell are given in Figure 8.11 (a).

Generally, the boundaries of the unit cell do not have to be lines of symmetry. The repetitive character of the unit cell enforces only the idea of ‘periodic’ boundary conditions. In our case, the primary unknown is the pressure, p . The periodicity will thus require that the pressure field on one end has the functional dependence that might smoothly connect to the pressure field on the opposite end, possibly shifted by a prescribed

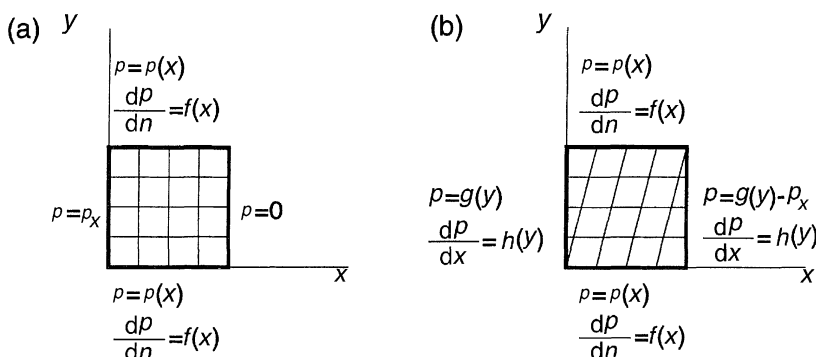


Figure 8.11 Permeability model: in-plane boundary conditions for (a) an undeformed cell; (b) a deformed cell. p = pressure variable; p_x = specific value of p ; $p(x)$ and $f(x)$ = functions of x ; $g(y)$ and $h(y)$ = functions of y ; n = normal direction.

pressure drop. For a rectangular cell, this leads to conditions as shown in Figure 8.11(b). These conditions complicate the solution and, more significantly, they slow the solution process. Nonetheless, they are necessary if the unit cell describes a deformed fabric, as in this case there is no symmetry to justify the formulation of a cell as shown in Figure 8.11(a).

The above-mentioned model provides surprisingly good correlation with the experimental data [8]. Obviously, this approach is of little help if the geometric restrictions do not apply or when three-dimensional permeability is required.

The permeability evaluation as described above really allows solving for the permeability of a lay-up of different preforms at once. The Darcian flow through the preforms will account for the transverse flow.

Nonetheless, it is simpler to solve for a permeability of a simple preform and combine the permeability tensor either by a weighted average [equation (8.4)] or one of the other available recommended methods [16, 17].

Generally, to obtain the three-dimensional permeability one will use similar methods to the previous case. A typical repetitive volume of reinforcement has to be selected, a pressure gradient imposed and flow solved in both the channels and within the fibre tows, with use of some matching boundary condition on channel-tow boundaries [2]. The flow through the cell can then be compared with the applied pressure gradient to obtain permeability components. But despite its conceptual simplicity, this undertaking is a very demanding one as all directions will be of importance. Scaling analysis will not produce any simplifications [such as those in lubrication theory and equation (8.4)] and full three-dimensional Stokes flow through a complex domain has to be modelled [44].

8.5 GOVERNING EQUATIONS

8.5.1 ISOTHERMAL FLOW MODELLING

We will assume the domain in which there is resin to be a fully saturated domain in order to model the mould filling process. This implies that we have to split the mould into two domains: the already-filled part, where we use the equations presented below to solve for pressure and velocities, and the part that is as yet empty, where we either assume zero pressure or the presence of some inviscid compressible gas. There is an alternative formulation available, which uses the fill factor as another unknown and does not dissect the domain [45–47], but we will not present it here.

Darcy's law [equation (8.1)] describes the relations between velocity and the pressure gradient. Note that there are more general relations between velocity and pressure [48], such as Forchheimer's equation or

Brinkmann's equation [49, 50]. Applicability of any of them has limits; for example Darcy's equation is valid only for the saturated flow of a Newtonian fluid with a Reynold's number relative to pore size being of the order of 1 or less. However, Darcy's law seems to be acceptable for all practical cases of RTM analysis. For a steady-state flow we can use the conservation of mass:

$$\nabla \cdot \mathbf{v} = 0 \quad (8.8)$$

and combine it with equation (8.1) to obtain the governing equation in terms of resin pressure as:

$$\nabla \cdot \left(\frac{\mathbf{K}}{\eta} \cdot \nabla p \right) = 0 \quad (8.9)$$

This equation is going to be either two-dimensional or three-dimensional, depending whether we solve for flow through a thin shell or for a fully three-dimensional geometry. It is necessary to realise that the velocity, \mathbf{v} , is the volume-averaged fluid velocity [48] and that this equation is valid only for saturated flow. Despite these limitations, it can be used to handle most analysis of the RTM process.

The boundary conditions for equation (8.9) are zero pressure at the free flow front end and, if there is no leakage through the mould walls, a velocity component of zero normal to the mould wall. For an anisotropic medium this condition translates to:

$$\mathbf{n} \cdot \left(\frac{\mathbf{K}}{\eta} \right) \cdot \nabla p = 0 \quad (8.10)$$

where \mathbf{n} is the vector normal to the mould wall. Additionally, at inlets either the pressure or the flow rate can be prescribed. The latter condition translates into prescribing some measure of velocity, or, by virtue of equation (8.1), pressure gradient.

8.5.2 THE TWO-DIMENSIONAL PROBLEM

A typical RTM part is shown in Figure 8.12. The structure is obviously a thin shell. If we assume that the pressure and velocities do not depend on the transverse coordinate (z), we can solve equation (8.8) or (8.9) in the two-dimensional domain. True, the local coordinates will depend on position, and the coordinate system might actually be curvilinear, but it is no problem to generate local orthonormal systems if the surface is discretised by finite elements. Then, equation (8.9) becomes:

$$\frac{\partial}{\partial x} \left(\frac{K_{xx}}{\eta} \frac{\partial p}{\partial x} \right) + \frac{\partial}{\partial x} \left(\frac{K_{xy}}{\eta} \frac{\partial p}{\partial y} \right) + \frac{\partial}{\partial y} \left(\frac{K_{yx}}{\eta} \frac{\partial p}{\partial x} \right) + \frac{\partial}{\partial y} \left(\frac{K_{yy}}{\eta} \frac{\partial p}{\partial y} \right) = 0 \quad (8.11)$$

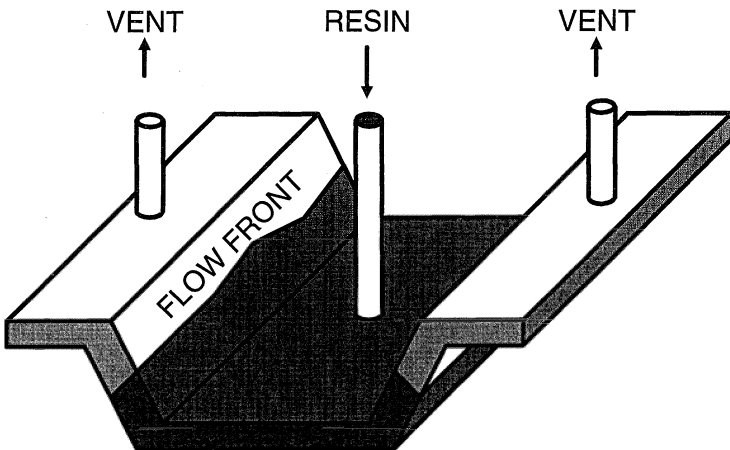


Figure 8.12 A typical resin transfer moulding part.

and the boundary condition [equation (8.10)] can be rewritten [16, 51] as:

$$\frac{1}{\eta} \left(K_{nn} \frac{\partial p}{\partial n} + K_{nt} \frac{\partial p}{\partial t} \right) = 0 \quad (8.12)$$

The permeability tensor, \mathbf{K} , is reduced from being three-dimensional to two-dimensional by omitting the z row and column in the matrix of its x , y and z components. If the permeability is not homogeneous through the thickness it is necessary to introduce some assumptions and an 'equivalent' permeability model, such as that described by equation (8.4). Additional methods for equivalent permeability are available [14, 15, 17, 51, 52].

8.5.3 FORMULATION USING A FILL FACTOR

The previous equations are used to solve for fully saturated flow in the domain containing the resin. The velocities at the flow front are then used to update the boundaries of the filled domain in an explicit fashion. This has some disadvantages, as it introduces a limit on time step, usually depending on discretisation. For each time step, the problem has to be solved for pressure. Although it is possible to build an extremely fast solver [53] for such a system, it might be possible to use a hybrid formulation that solves the flow problem on a complete domain, using two unknowns – pressure and a fill factor, ϕ [45–47]. Then the combined mass and momentum conservation equation will be:

$$\frac{\partial \phi}{\partial t} = \nabla \cdot \left(-\frac{\mathbf{K} \cdot \nabla p}{\eta} \right) \quad (8.13)$$

An additional equation is then needed to describe the transport of the fill factor:

$$\frac{D\phi}{Dt} + \mathbf{v} \cdot \nabla \phi = 0 \quad (8.14)$$

where $D\phi/Dt$ denotes the total derivative. This formulation has some advantages – few steps are required to solve the whole filling process and co-injection can be handled gracefully. If the system [equations (8.13) and (8.14)] is directly discretised it will result in a larger, non-symmetric system and an implicit (non-linear) solver will be required even for a Newtonian fluid. However, equation (8.13) can be used as a basis for an implicit FEM by itself.

8.5.4 THE ENERGY EQUATION

Mould filling is not necessarily an isothermal process. The temperatures of mould and injected resin may differ. If cure is initiated, the reaction-generated heat may influence the temperature as well. Since resin viscosity depends strongly on temperature and on degree of conversion the temperature and degree-of-conversion distribution can influence the mould filling pattern significantly.

By using the local equilibrium model (i.e. the local temperature of the resin is the same as the temperature of the preform) we may arrive at the energy equation [48]:

$$\begin{aligned} & \left[\phi(\rho \cdot c_p)_f + (1 - \phi)(\rho \cdot c_p)_s \right] \frac{\partial T}{\partial t} + (\rho \cdot c_p)_f \mathbf{v} \cdot \nabla T \\ &= \nabla \cdot \left[(\mathbf{k}_e + \mathbf{K}_D) \cdot \nabla T \right] + \phi \dot{s} + \eta \mathbf{v} \cdot \mathbf{K}^{-1} \cdot \mathbf{v} \end{aligned} \quad (8.15)$$

where

\mathbf{k}_e is the effective conductivity;

\mathbf{K}_D is a heat dispersion coefficient;

\dot{s} represents heat generation arising from the curing reaction;

c_p is the specific heat capacity at constant pressure;

ρ is the density.

subscripts f and s refer to the properties of the fluid (resin) and solid (preform), respectively.

Temperatures and velocities are volume-averaged values.

In most cases, this equation can be simplified considerably by means of dimensional analysis. For small Brinkman numbers the last term (viscous dissipation) can be neglected. For thin parts we can also neglect heat conduction in the plane of the preform ($x-y$) and convection in the

transverse direction [16, 54, 55]. The resulting equation, applicable to two-dimensional mould filling, is:

$$[\phi(\rho c_p)_f + (1 - \phi)(\rho c_p)_s] \frac{\partial T}{\partial t} + (\rho c_p)_f \left(v_x \frac{\partial T}{\partial x} + v_y \frac{\partial T}{\partial y} \right) = k \frac{\partial^2 T}{\partial z^2} + \phi \dot{s} \quad (8.16)$$

where k now describes both conductivity and the heat dissipation coefficient. Factor \dot{s} will couple the energy equation with the resin cure. The coefficient k is related to equation (8.15) by:

$$k = (0 \quad 0 \quad 1) \cdot (\mathbf{k}_e + \mathbf{K}_D) \cdot \begin{pmatrix} 0 \\ 0 \\ 1 \end{pmatrix} \quad (8.17)$$

Moreover, evaluation of \mathbf{K}_D is rather difficult [48, 56]. If we neglect \mathbf{K}_D , the effective conductivity, k , can be evaluated from the properties of the resin and preform by [16]:

$$k = k_s \frac{k_s + k_f + (1 - \phi)(k_s - k_f)}{k_s + k_f - (1 - \phi)(k_s - k_f)} \quad (8.18)$$

where k_s is the heat conductivity of the preform, k_f the conductivity of the resin and ϕ the volume fraction of the resin [54, 55].

Note that the 'two-dimensional' model described by equation (8.16) still has a three-dimensional temperature field, whereas both pressure and velocity are assumed to be constant through the thickness. This introduces some complications for the numerical model, as will be demonstrated later.

Note that the validity of the equation (8.16) will depend on local equilibrium and the magnitude of certain non-dimensional parameters (Peclet, Graetz and Brinkman numbers [48]).

8.5.5 BOUNDARY CONDITIONS FOR ENERGY TRANSFER

To solve equation (8.15) or (8.16), certain boundary conditions have to be prescribed. Equation (8.15) is a second-order, elliptic, partial differential equation in all spatial coordinates and is first-order in time. Consequently, it is necessary to prescribe the temperature boundary condition all along the spatial boundary in addition to initial temperature.

There is no difficulty with boundary conditions on the mould walls. The simplest approach is to prescribe the mould wall temperature. A little more complex and realistic approach is to couple heat flux and temperature at the boundary in the form:

$$\frac{\partial T}{\partial n} + C_{bc}T = C_{bc}T_\infty \quad (8.19)$$

where T_∞ is the temperature of the heating medium in the mould and C_{bc} is a boundary condition constant dependent on the dimensions and heat transfer coefficients both within the mould and between the mould and the cavity. For the situation depicted in Figure 8.13 this coefficient can be evaluated by the following equation:

$$C_{bc} = \frac{1}{k} \left(\frac{1}{h_h} + \frac{1}{h_m} + \frac{a}{k_m} \right)^{-1} \quad 8.20$$

where

k_m is the conductivity of the mould material;

a is the distance of the mould wall from the heating pipe;

h_h and h_m are the heat transfer coefficients between the mould and the heating medium and between the mould and the resin, respectively [55].

At the inlet gate, the temperature boundary condition is likely to be a prescribed temperature of resin. The only boundary condition that is difficult to model is the transient boundary at the flow front. Here it is necessary to account for the internal energy of the preform being impregnated and to perform a local heat balance which takes into account convection into the unsaturated medium.

For a two-dimensional model, the situation is quite different, as the order of the partial differential equation in the plane of the mould is only one because of the simplifications justified by the non-dimensional analysis. Thus there will be no conditions in the in-plane mould edges, only at the inlet gate. The condition of equation (8.19) will hold on the top and bottom mould plate. The energy balance at the flow front will influence the initial condition only.

8.5.6 CURE KINETICS COUPLING

There is still one term that needs to be described in equations (8.15) and (8.16), the heat source term arising from the reaction. The following model, presented by Kamal *et al.* [57–59], is widely used for thermoset-

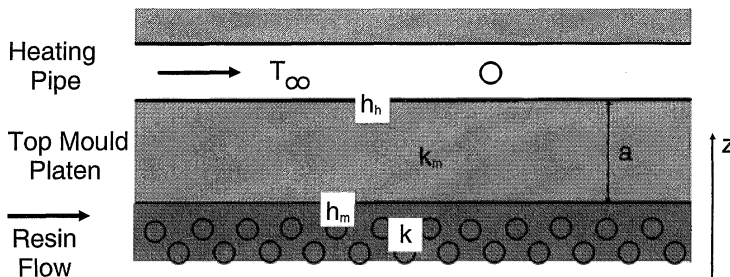


Figure 8.13 Configuration to obtain the temperature boundary condition at the mould surface.

ting polymers, both polyester and epoxy resins. It assumes the specific energy generated during curing to be proportional to the rate of the reaction:

$$\dot{s} = R_\alpha E_\alpha \quad (8.21)$$

where R_α is the rate of reaction and E_α is the heat of reaction. The reaction rate itself is a function of the temperature and the extent of reaction, α :

$$R_\alpha = (k_1 + k_2 \alpha^m)(1 - \alpha)^n \quad (8.22)$$

The values k_1 and k_2 are dependent on temperature:

$$k_1 = A_1 \exp\left(\frac{E_1}{RT}\right) \quad (8.23)$$

$$k_2 = A_2 \exp\left(\frac{E_2}{RT}\right) \quad (8.24)$$

where R is the universal gas constant and the parameters m , n , A_1 , A_2 , E_1 and E_2 are dependent on the resin system and have to be determined experimentally.

There are many other models describing resin kinetics. The range of applicability varies greatly; many will describe the behaviour of a certain system extremely well but fail to approximate the behaviour of different systems. Also, it seems to be uncertain how well the models created for pure resins can model reaction kinetics in the presence of a considerable fibre volume fraction [60].

Obviously, the degree of conversion depends on time and the location within the mould, and it is subject to the conservation of species. Thus it has to obey the continuity equation:

$$\phi \frac{\partial \alpha}{\partial t} + \mathbf{v} \cdot \nabla \alpha = \phi R_\alpha \quad (8.25)$$

or, in the two-dimensional problem:

$$\phi \frac{\partial \alpha}{\partial t} + v_x \frac{\partial \alpha}{\partial x} + v_y \frac{\partial \alpha}{\partial y} = \phi R_\alpha \quad (8.26)$$

The left-hand side of this equation represents the total time-derivative of the degree of cure; the reaction rate on the right-hand side represents a source term. Equation (8.25) or (8.26) has to be solved simultaneously with the energy equation [(equation (8.15) or (8.16)]. They are coupled through the right-hand side of equation (8.15) or (8.16).

8.5.7 TEMPERATURE-DEPENDENT VISCOSITY

The resin viscosity is dependent on the resin temperature and can change significantly with a small change in temperature. Consequently, if the

filling process is not isothermal, the viscosity should be described as a function of temperature. This relation is traditionally described by the Arrhenius equation as exponential:

$$\eta = \eta_0 \exp[-a(T - T_0)] \quad (8.27)$$

where T_0 is the reference temperature at which $\eta=\eta_0$.

Additionally, the viscosity of the resin changes as cure proceeds. The chemorheological model that describes this dependence reasonably [61] gives:

$$\eta = A \exp\left(\frac{E}{RT}\right) \quad (8.28)$$

where the activation energy E and the coefficient A are given by:

$$E = a + b\alpha \quad (8.29)$$

$$A = a_0 \exp(-b_0\alpha) \quad (8.30)$$

where a, b, a_0 and b_0 are material parameters.

There is no universal agreement which chemorheological models to use, similar to the case of cure kinetics models. Most models are empirical and tailored to suit well a certain category of resins. The model above works well with polyester and epoxy resins, but can obviously be replaced by others.

For the two-dimensional flow model, one more note concerning the temperature dependence of viscosity can be made. Since the temperature field varies through the thickness, so does the viscosity [equation (8.27)]. This would undermine the assumptions of constant velocity through the thickness. Consequently, the viscosity has to be averaged through the thickness as well to be used in the two-dimensional case of Darcy's law [equation (8.2)] or in derived equations. The average viscosity $\bar{\eta}$ can be evaluated as

$$\frac{1}{\bar{\eta}} = \frac{1}{h} \int_0^h \frac{1}{\eta} dz \quad (8.31)$$

where h is the thickness of the mould cavity.

8.5.8 THE HEAT DISPERSION EFFECT

The heat dispersion coefficient K_D in equations (8.15) and (8.17) is caused by the fact of local velocity in the porous media being misaligned from the volume-averaged velocity v both in direction and magnitude. Consequently, this term essentially represents convective heat transfer due to the velocity oscillations.

An analytic method to obtain K_D , based on a knowledge of unit cell geometry, is described by Tucker and Dessenberger [48, 56]. Generally, it is not possible to evaluate this coefficient for all preforms. To make

matters worse, the scaling analysis really does not exclude this term from equations (8.15) or (8.17) for all RTM processes.

Methods of finding K_D experimentally are not readily available either. Moreover, releasing the assumption of local thermal equilibrium introduces some additional terms in equation (8.15). This problem limits the usefulness of the heat transfer analysis in RTM simulations at the current time. This may not be an issue as the goal in RTM seems to be moving towards room temperature cure in which isothermal filling is all that is needed.

8.5.9 NON-NEWTONIAN FLUIDS

Strictly speaking, Darcy's law is not valid for non-Newtonian fluids. As such it cannot accommodate viscoelastic behaviour, which certain polymers exhibit. Fortunately, it has been shown [62] that, for Deborah numbers up to about five, the viscoelastic effects do not cause a significant deviation from Darcian behaviour.

Shear-thinning behaviour can be modelled – albeit it is again in violation of Darcy's law assumptions – by utilising an effective viscosity dependent on local strain rates. This means one replaces the ratio K/η by a tensor of flow mobility, which includes the effects of both the preform architecture and the fluid viscosity [16].

8.6 NUMERICAL FORMULATIONS AND SIMULATIONS

In this section we will provide pertinent details concerning the numerical solution of governing equations for the filling stage presented in the previous chapters; the flow equation [equations (8.9) or (8.11) or (8.13) and (8.14)], the heat transfer equation [equation (8.15) or (8.16)] and the species conservation equation [equation (8.25) or (8.26)].

We will concentrate on methods for solving the flow part of the problem [equation (8.9)] and then briefly discuss the incorporation of temperature and cure into this model.

Any applicable numerical method can be and has been applied to the problem. The basic differences in approach will be dependent on the method used (finite element, finite difference, boundary element) and the discretisation or meshing of the domain. Since the flow front position is transient, the solution domain changes with each time step. This offers two approaches for the discretisation of the domain.

- A boundary-fitted discretisation fits the mesh or grid to the current flow front. This method provides fine approximation of the flow boundary but creates a number of problems. First, it is necessary to remesh with each time step. This might be a complex problem if mul-

tiple flows are running together etc. Second, if multiple injection ports are used, multiple problems are to be discretised, solved and merged when the flow fronts merge. These problems limit the use of this discretisation [63].

- A stationary finite-element or finite-volume mesh is virtually free of the problems mentioned above. It uses one discretisation and approximates the flow front to the closest node of the fixed mesh. This is its drawback; the approximation is accurate to about an element size. Obviously, this reduces the accuracy of the method. This method seems to be the preferred one for most implementations [51, 64, 65] and we will describe it in more detail. Note that if the hybrid formulation [equations (8.25) and (8.26)] is used [45, 46] the fill factor takes care of problems with the flow front approximation.

8.6.1 COMPLEXITY OF GEOMETRY

The typical RTM part is sketched in Figure 8.12. This leads to the previously discussed possibility of using a two-dimensional, shell approximation of the geometry. The one and only variable within the system is pressure, which is a scalar. The geometry of the part does not deform during the filling process in any way. This means that there will be no trouble with triangulation or continuity of the pressure approximation as long as it is C^0 . Note, however, that thick-walled parts are gaining popularity and a three-dimensional approximation of the geometry or an approach to handle them effectively is needed for these parts.

The governing equation for the problem is equation (8.9) or (8.11), depending on whether the model is two-dimensional or three-dimensional. Boundary conditions are described in section 8.5.1: there is assumed to be zero pressure at the flow front and a prescribed pressure at the constant pressure inlet; there is assumed to be no velocity normal to the walls [equation (8.10)] and inflow at the constant flow-rate gates.

8.6.2 THE FINITE ELEMENT/CONTROL VOLUME APPROACH IN TWO DIMENSIONS

This method utilises a finite element approach to solve for pressure at a given step. It then uses the control volume formulation to compute flow among the nodes and to advance the free surface (flow front). This method is pragmatic and fairly efficient [51, 52].

First, the surface of the shell is discretised into finite elements. This discretisation will also serve as the discretisation for the finite volumes. The finite volumes may either be associated with individual elements [16] or with individual nodes. The former case provides better approximation of the free boundary; the latter case is slightly more efficient. We

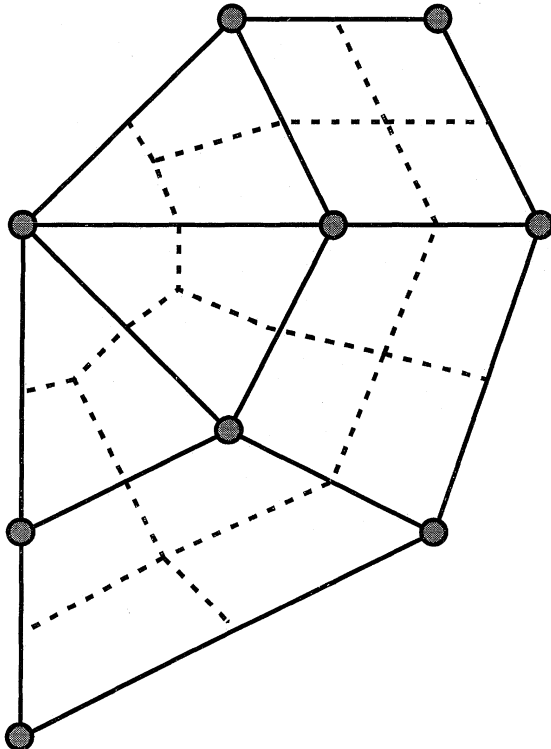


Figure 8.14 Finite element/finite volume discretisation. ● = finite element mesh node/finite volume centroid; - - - = finite volume boundary; — = finite element mesh boundary.

will use the latter one. The control volumes are created around nodes, with borders passing through the midpoints of individual elements and their borders as shown in Figure 8.14.

Then the nodes are assigned a fill factor – 1 for being filled, 0 for being empty. Then equation (8.11) is solved on the finite element mesh (actually, just for the nodes with the fill factor equal to 1) with proper boundary conditions. The flow front position is approximated by using the fill factor. Nodes for which the fill factor is 1 are inside the filled domain, nodes where it is 0 are outside. The value between 0 and 1 indicates that the free boundary passes through the control volume associated with the node (Figure 8.15).

Once the pressure field is known, we may continue with computation of flow in the part. Obviously, one might use Darcy's equation [equation (8.1)] to evaluate the velocities, but it is more natural to work with flows between individual control volumes. Actually, in the two-

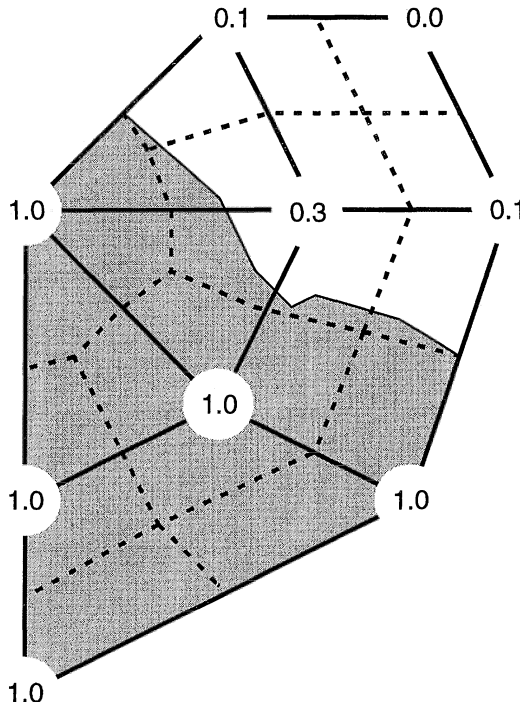


Figure 8.15 Nodal fill factors. Shaded area = resin.

dimensional case we might have some problem in defining velocities at some locations (Figure 8.16), but flow from one control volume to another is still well defined. Obviously, flow between two control volumes is simply an integral measure of velocity, and Darcy's law is used to compute it.

Thus, to compute the flow from one control volume (i) to another control volume (j) we can use the following:

$$q_{ij} = - \int_{s_{ij}} \left(\frac{h}{\eta_{eff}} \mathbf{n} \cdot \mathbf{K} \cdot \nabla p \right) ds_{ij} \quad (8.32)$$

where s_{ij} is the boundary between two control volumes, h is the thickness of the gap at the point of the boundary and η_{eff} is the effective (since we are in two-dimensional space) viscosity. The gradient is only in the plane of the preform, and \mathbf{n} is the unit vector normal to the boundary between two control volumes in the plane of the preform (Figure 8.17). Note that actual integration will have to be carried out in several steps, as the pressure gradient is not continuous from one element to another. Actually, for the case shown in Figure 8.16, s_{ij} is not a single line.

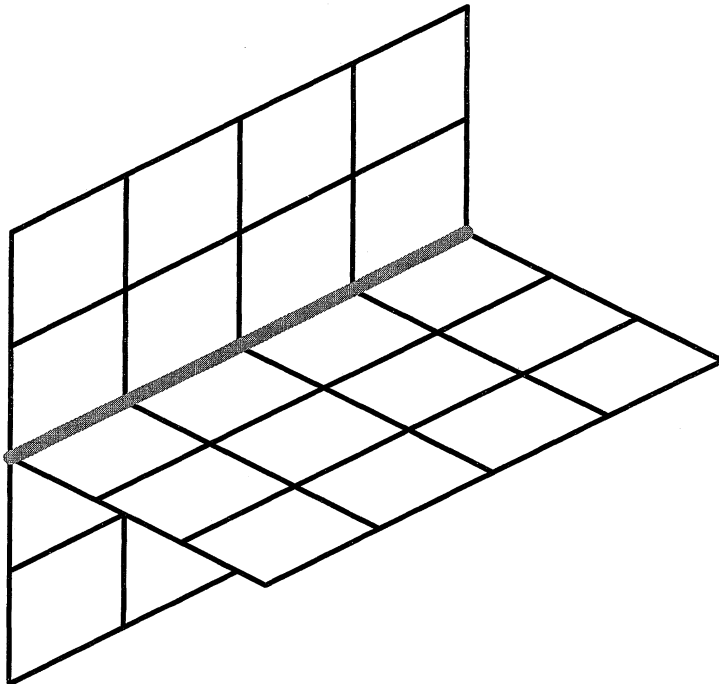


Figure 8.16 T-connection on the part – a location where a two-dimensional velocity is not properly defined.

Note also that the formula given [ref. 16] is a special case and is not applicable generally.

Once the flows q_{ij} have been computed, the net flow, Q_i , into control volume i may be calculated by a simple summation:

$$Q_i = \sum_{j=1}^n q_{ij} \Delta t \quad (8.33)$$

where n is the number of control volumes connected to the control volume i and Δt is the size of the time step.

These flows are used to update the nodal fill fractions. The size of the time step is calculated so that only one control volume fills up in each time step. The fill factors in all volumes are updated and the boundary conditions around the filled node are adjusted.

This technique allows one to fill thin cavities of complex shapes in three-dimensional space. Moreover, under certain conditions (the problem being isothermal) only a very small part of the finite element system used to evaluate the pressures has to be changed. This allows extremely

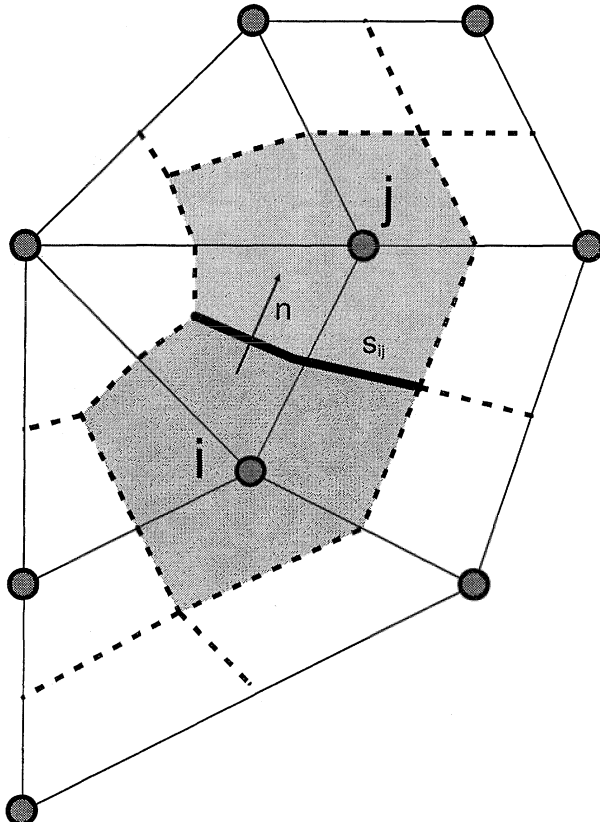


Figure 8.17 Typical geometry for evaluation of flow between control volumes. s_{ij} = the boundary between control volumes i and j ; \mathbf{n} is the unit vector normal to the boundary between the two control volumes in the plane of the preform.

efficient incremental factorisation of the system matrix [53] to be utilised. Consequently, the method is very efficient.

Extension to three-dimensional problems

The previously described algorithm can easily be used for a three-dimensional system as well. The governing equation for pressure evaluation will be equation (8.9). The discretisation will be analogous to the one described above. Only minor changes are needed to evaluate flows between control volumes. Instead of equation (8.32) we have:

$$q_{ij} = - \int_{S_{ij}} \left(\frac{1}{\eta} \mathbf{n} \cdot \mathbf{K} \cdot \nabla p \right) dS_{ij} \quad (8.34)$$

where S_{ij} is now the area between control volumes, not the arc length, η is the true viscosity (possibly dependent on location) and the thickness h is no longer needed as it has been incorporated into the area S_{ij} . All the other features of the two-dimensional problem, including the evaluation scheme described in ref. 53 remain applicable even in the three-dimensional domain. Obviously, the finite elements will be tetrahedrons or bricks instead of triangles and quadrilaterals.

8.6.3 COUPLING WITH HEAT TRANSFER AND CURE – THE TWO-DIMENSIONAL MODEL

As stated beforehand, despite the fact that the pressure/velocity solution is a two-dimensional one, the conduction term in the energy equation [equation (8.16)] requires that the temperature (and cure) be solved in three dimensions. Consequently, each control volume used for flow analysis has to be re-discretised in the transverse direction, as shown in Figure 8.18.

The solution to equations (8.16) and (8.26) can be evaluated by a partially implicit (explicit in time and the x - y plane, implicit in the z direction) method [55], which does not require excessive memory. Unfortunately, the method is only conditionally stable, so in some cases it might require very small time steps.

Convective terms in the energy equation [equation (8.16)] and the conversion equation [equation (8.26)] are handled consistently with the

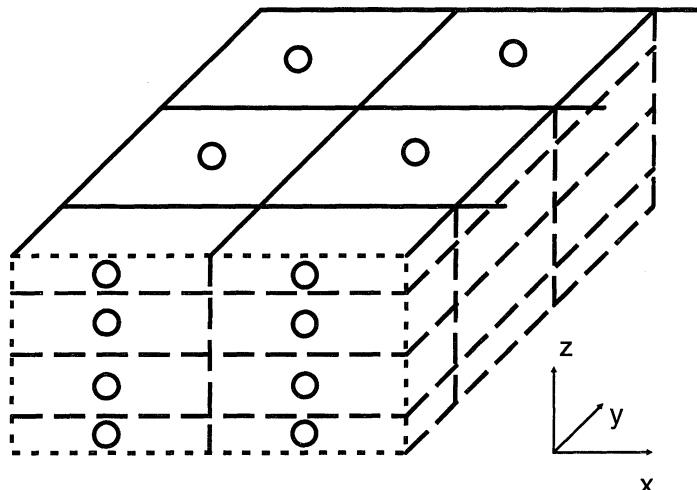


Figure 8.18 The control volumes used in the temperature and cure analysis for the two-dimensional model; — = finite element mesh; - - - = through-the-thickness control volumes; ○ = temperature nodes.

control volume approach used for the computation of flows. The pseudo-three-dimensional discretisation is used only to handle the conduction terms in equation (8.16).

As the source term in equation (8.16) is non-linearly dependent on temperature, an iterative solver has to be used for temperature evaluation [54]. Once the temperature is known, the rate of conversion can be computed by means of equation (8.22) and updated in all control volumes by equation (8.26). Then, the viscosity throughout each control volume can be computed from equation (8.28) and the effective viscosity evaluated by means of equation (8.31).

Extension to three-dimensional model

Since the problem is already fully three-dimensional, the existing discretisation might be used to solve equations (8.15) and (8.25). However, it seems that replicating the previous approach would not work too well. It might be better to solve a non-linear mixed system (pressure, temperature, conversion) within each step.

Note that among the codes that solve for three-dimensional flow in a permeable medium most assume isothermal flow, although the temperature and cure variations are much more important in the cases that require three-dimensional modelling. The reason is mainly the computational efficiency. So far there is no possibility to compute a full three-dimensional problem on a personal computer or ‘common’ workstation in real time.

8.6.4 THE PURE FINITE ELEMENT APPROACH TO MOULD FILLING

The pure finite element approach to mould filling simulation is a mixed finite element method. Instead of solving the problem for pressure only, the governing equation is defined in terms of the fill factor ϕ and the pressure p [equation (8.13)]. Obviously, one other equation has to be added, the equation for preservation of the fill factor [equation (8.14)].

The resulting equations would produce a non-linear and non-symmetric system, consequently requiring seemingly more computational power. However, there are possibilities to eliminate equation (8.14) and, since it is possible to fill the whole mould in one step, the method can actually be very efficient [45–47].

8.6.5 OTHER NUMERICAL APPROACHES

Some numerical approaches not based on finite elements or volumes, such as the finite difference [63] or boundary element method, have been applied to the above-described problem. These, however, seem to be of

limited importance, as most researchers favour methods based on finite elements.

There is a number of implementations of the finite element/volume method available [16, 66–71]. Some follow a similar approach to that described herein [53], trying mainly to improve the efficiency of the scheme. Others introduce more profound changes to allow, for example, for a one-step solution for filling time or flow fronts. The description of these works is beyond the scope of this chapter. The hybrid formulation [45–47] seems to be gaining popularity.

8.7 CRITICAL ISSUES

The flowchart for process modelling of RTM is shown in Figure 8.19. There are two distinct areas to the model, the preforming stage and the filling/curing stage. The output from the model of the preforming stage (draping and compaction) has to provide a considerable part of the input data for the filling simulation, which has been traditionally considered to be the only part of the process modelling.

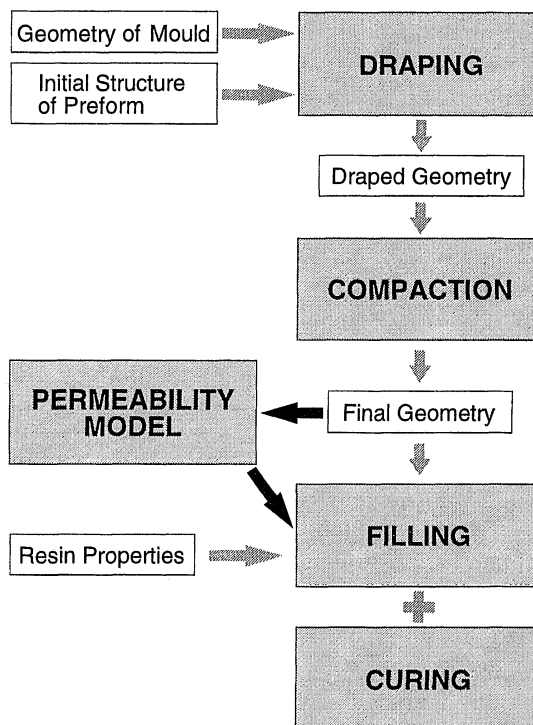


Figure 8.19 Flowchart for the process model.

The models for filling have been around for about a decade now and are reasonably well understood. Flow is modelled as a Darcian flow through a porous continuum, and utilising a mass-conservation principle one obtains a governing equation for the pressure. There are several approaches for the handling of moving flow fronts, such as a control volume approach [16] or by using a fill factor as an additional unknown [46], which differentiate individual models currently in use. Another major difference is whether the filled preform is handled as a fully three-dimensional domain [47], or whether it is declared flat and then handled as a shell-like two-dimensional structure [16].

With general agreement about the governing system, the most important issue concerning the filling simulation is that of computational efficiency. Since most of the codes around are a result of the endeavours of engineers and designers rather than of computational wizards and applied mathematicians, there is a lot of improvement possible [53] and such improvement is likely to take place in the near future.

The heat transfer part and the curing process are, however, still shrouded in mystery. The heat transfer part poses most importantly the question concerning the validity of the local equilibrium model, on which the usual governing equations [16, 48] are based. Second, there remains the question of the heat dissipation coefficient and its estimation. Finally, although the developers of equations clearly state the assumptions and limits of their applicability [48], the code developers and, above all, users, seem to be quite good at ignoring them.

There are some empirical and semi-empirical formulas available for curing [57–59] but the reliability of these is rather questionable. This doubt is magnified by the fact that the usual subject for kinetics studies is a pure resin and the presence of reinforcement has been shown to change these kinetics considerably. Consequently, quite a few models assume isothermal filling with no reaction during filling. In most cases, this is not a real drawback, considering that the majority of real processes comply with this assumption very well. If this is not the case, further fundamental studies in this area are necessary. A general model can be implemented and successfully used only if there is a reasonable description of resin kinetics within the fibre–resin system [60].

In addition to the filling (and curing) there is another aspect to modelling, as shown in Figure 8.19. This model is independent of the filling simulation and deals with the deformation of the preform during the preforming stage, that is, the insertion of the preform into the mould and its compaction during closing of the mould. The filling model is dependent on the replacement of the complex structure of woven, braided or stitched preform by a simple continuum characterised by its resistance to flow (permeability), fibre volume fraction and possibly some thermal characteristics, and these quantities depend on the preform deformation [8, 9].

Not so long ago it was assumed that the properties collected for an undeformed preform were applicable as input characteristics. Unfortunately, this will provide appropriate data only for the modelling of the very same experiment used to collect the data! Any difference in the part shape or compaction pressure will deform the preform in a different way and thus change its permeability.

Draping (preform placement into the mould) can change the angle between the fibre tows by a significant amount and this change will cause a change in the fibre volume fraction [8]. Compaction (due to mould closure or drawn vacuum) will considerably reduce the thickness and increase the fibre volume fraction [15] and other properties as well [72]. Both will change the geometrical shape of the preform, the fibre tow cross-sections, etc. Also, another issue may arise with the creation of empty channels along sharp bends in mould corners (race-tracking [18]).

The deformation mentioned above will considerably change the filling behaviour, flow fronts and pressure/flow rate magnitudes. It is necessary to be able to predict these changes and incorporate them into the filling model. Although some work has been done [8, 9], further progress in this area is the key to progress in modelling the RTM process as a whole.

8.7.1 LEVELS OF SOPHISTICATION TO BUILD THESE MODELS

There are a number of complications that may or may not be included in a model of the RTM filling process. The parts manufactured by the RTM process are, obviously, three-dimensional heterogeneous structures. During the manufacturing process there is a two-phase (air, resin) flow through the spatial structure of the preform. Temperatures vary throughout the part, and the resin can react and cross-link if conditions are favourable. To make modelling nearly intractable, resin can behave as a viscoelastic continuum or show shear-thinning or other non-Newtonian properties.

The simulation of the manufacturing process cannot handle many of these problems realistically. Consequently, the following assumptions might be introduced.

- The part is actually shell-like. Consequently, pressure and velocity fields do not vary through the thickness and the flow part of the problem can be solved as a two-dimensional problem. This might involve computing 'equivalent' permeability, viscosity etc., as outlined above.
- Viscous dissipation in the energy equation can be neglected.

- The resin is actually not supposed to cure during the filling stage, since if this happens, the part has to be discarded. Thus we do not need to model the cure and can simplify the energy equation. Note that if the temperature is predicted during the filling it can be used to test whether the assumption of no conversion is sufficiently accurate.
- In many cases, both the resin and the tool will be at room temperature for filling. Consequently, there is no energy equation to solve and the only outputs are velocity components, flow fronts and pressure.
- The preforming stage may be neglected for some part shapes, such as a single curvature geometry.

Even a model using all the assumptions above can be a powerful and useful tool if properly applied, especially during the design stage. We will classify such a model as a **minimal** model. Obviously, we might want to verify its results with more complete models once the design is finalised.

Generally speaking, there are going to be three ways to separate the models used in simulation packages. First, depending on the flow assumptions, the model can be either two-dimensional or three-dimensional. Most RTM parts can be treated as two-dimensional shells. Some parts, however, defy this simplification. Also, some filling methods (resin infusion etc.) are intrinsically three-dimensional, even if the part is thin.

Second, the model can either neglect thermal and cure effects (isothermal) or include them (with varying degrees of simplification). Again, many times the simpler approach works but in some cases it is necessary to handle the temperature, mainly because of its influence on viscosity.

Last, the preforming stage can be modelled or ignored depending on the geometry of the surface and the type of preform. As the methods for modelling the preform deformation are in the early stage of development, the preforming models are essentially independent and are used to prepare data for filling simulations. Obviously, a well-integrated package would be desirable [73, 74].

The computational power at hand can decide what simplifications are to be made. The tool that runs on a personal computer using the minimal model has to sacrifice some features to provide an acceptable response time, whereas simulations running on high-end systems can afford more complexity. Nonetheless, there is an additional factor that comes into play: the required input data for the simulations to be useful tools.

8.7.2 INPUTS

There is another, more subtle limit to the complexity of flow models. If the media is described as a continuum following certain laws, its behaviour is characterised by a set of material properties that are necessary

for the solution of the governing equations. The values necessary for the minimal model – isothermal flow of a Newtonian fluid through a generalised Darcian porous medium – are as follows:

- fibre volume fraction – a scalar that describes the amount of space between the reinforcement;
- permeability – a symmetric second-degree tensor that describes the resistance of the preform to flow; if a two-dimensional flow is assumed, permeability is represented by three components; for three-dimensional flow the number is six;
- resin viscosity – a scalar that represents resistance of fluid to shearing deformation and replaces more complex general constitutive laws.

These values will allow us to determine pressure and flow front location within the mould. If we want to simulate additional effects, additional parameters will be required. For example, if we allow for temperature changes, and the heat transfer solution is desired, we will have to provide the heat conductivity tensor, density and the specific heat for the preform and resin, and, ideally, the heat dispersion tensor K_D . Allowing the resin to react will force us to provide a relation between temperature, degree of conversion and reaction rate as well as specific heats. For the models described in this chapter this will require about a dozen parameters to be extracted from experimental data.

Obviously, all the above-mentioned parameters are part of the solution. As a rigorous study of the sensitivity of the solution to the variation of these parameters is beyond our scope now, we will just state that some of these parameters influence profoundly the quantities we are searching for, at least under certain circumstances. Consequently, it is crucial to provide proper values or constitutive equations to obtain reasonable simulation results.

In the situation where some of the parameters have to be guessed, this might lead to an interesting paradox: a simpler model provides better estimates than a more complex one. The reason is obvious: simpler models usually require less input and replace some of the unknowns with a set of assumptions. If the more complex model forces the engineer to guess some parameters, the error caused by a wild estimate might just exceed the error caused by the assumptions in the first case.

A simple example of the above-mentioned question is that of two-dimensional compared with three-dimensional models. As stated above, we need some extra components of permeability for a three-dimensional model. However, for a flat part these might be difficult to obtain [how do you measure transverse flow through a 6.5 mm (1/4") plate?], whereas the assumption of two-dimensional flow actually works rather well. If a guess of missing components is incorrect, we might end up with a worse solution than the simpler, and more efficient, model provides.

There are two problems associated with obtaining the proper material parameters we need. One is that we do not know how to obtain some of these values and the second one is that we cannot afford to perform enough measurements. Both problems are obstacles to proper development and, above all, to use of the simulation tools.

The need for fundamental understanding

This chapter is about what we can model, but these paragraphs will outline what we really cannot do presently. There are several problems for which we miss essential relations.

The number one difficulty lies in the field of heat transfer and cure. Although a certain heat transfer (energy) equation has been set and is generally used [48], its acceptance is not absolute. The heat convection effects within the random porous media may go beyond the diffusivity coefficient.

Even in cases where the accepted model is applicable we are short of the value of the thermal diffusivity, K_D . The method for its evaluation [48] is extremely difficult in the case of dual length-scale and general geometries, and techniques of measurement are non-existent.

The dependence of conversion rate on temperature and degree of conversion is well established in the domain of pure resin. The data for pure resin are then used for solution of the cure/temperature problem in RTM. Unfortunately, the presence of fibres in typical volume fractions may change the reaction kinetics so much that it renders this scheme useless.

Obviously, these difficulties arise only if the filling is not isothermal. But there are also poorly understood issues in the area of isothermal flow. The apparent inability to handle preform deformation in a satisfying manner is very pronounced. Although the models for preform draping seem to provide reasonable estimates, there is no universal model for compaction of preforms as an elastoplastic deformation, barring some first-order attempts [37, 38]. Also, since the boundary conditions between the flow in the porous medium (say the fibre tows) and flow within the neighbouring channel are unclear, we are unable to describe exactly the flow through the preform in order to evaluate permeability [75].

Fortunately, in many cases, we can rely on experimental techniques to provide at least some data to allow for interpolation and reasonable simulation output.

Limitations of experimental characterisation

There are also two problems associated with obtaining the experimental data. First, in some cases, the experimental methods have not yet been established. This is true of three-dimensional permeability measure-

ments. As preform materials are flat, the length scale at which the measurement is to be done is very short and consequently the measurement will be very inaccurate [3, 14]. It seems to be more feasible to backtrack the missing components from some more complex flow predictions [15].

The second limit is less esoteric but more pressing. Too many experiments are necessary to gather the amount of required data. For example, the two-dimensional permeability is represented by three values. To provide each of them for several shearing angles and several compaction pressures is a demanding task. To do so for every preform material on the market is impossible. Also, if we want to obtain both the chemorheological constants and the temperature dependence of viscosity for the resin, it means, for models described herein, about 12 parameters. To do a proper ‘best’ fit, one needs to conduct hundreds of experiments, even if one does not introduce any additional complications.

The solution to the first problem is to develop reliable methods. The second problem can be solved by creating predictive models, based on elementary physical facts, and by using experimental data only to verify or fine tune these models.

8.8 CASE STUDY

We will present the simulation process for the case of a simple, yet intriguing, part, namely a conical part with a spherical tip (‘radome’ shape, Figure 8.20). Occasionally, reference will be made to other results, for the sake of comparison. The part was manufactured and various data were collected. On the other hand, the whole manufacturing process was simulated using only the very minimum of measured input parameters:

- resin viscosity;
- geometry of preform architecture;
- part geometry;
- injection pressure or flow rate.

Unless otherwise noted, there was no ‘fitting’ of the individual models to the experimental result, that is, the error was allowed to accumulate as the simulation progressed.

The simulation included permeability prediction, draping of the preform and isothermal flow simulation under both constant inlet pressure and constant injection rate. The preform compaction was not considered since there is no general model available yet. Also, the process was essentially isothermal and consequently there was no need to worry about temperature or cure.

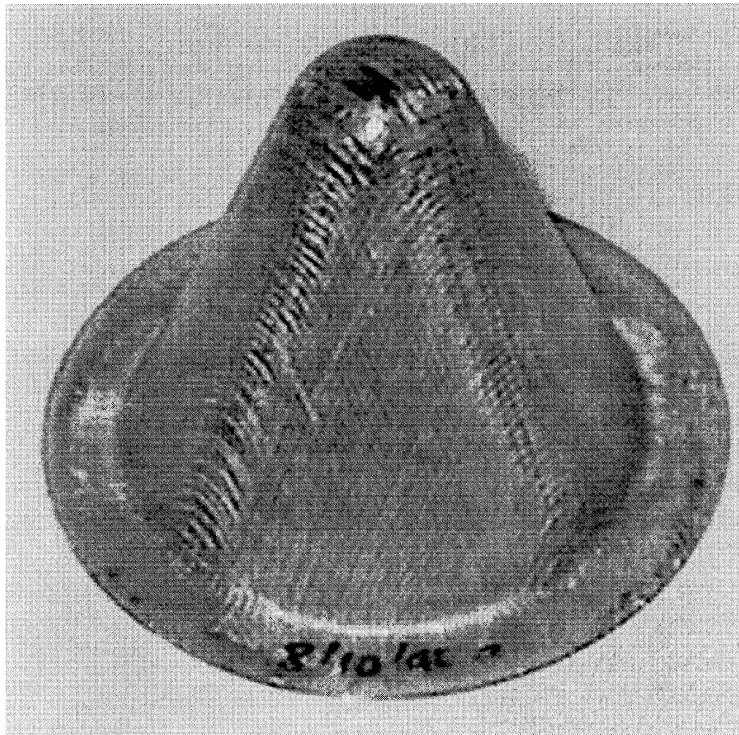


Figure 8.20 Conical part.

8.8.1 THE PERMEABILITY MODEL

The curvature of the part is quite large; consequently, the preform has to be able to deform considerably in-plane. For this reason, stitched preforms were chosen for the part. A schematic of the preform structure is shown in Figure 8.21(a). The structure was simplified by omitting part of the stitches parallel with the fibre tows, as depicted in Figure 8.21(b). In-plane dimensions were obtained by measuring the real preform. Thickness was estimated from the gap width and number of layers in the

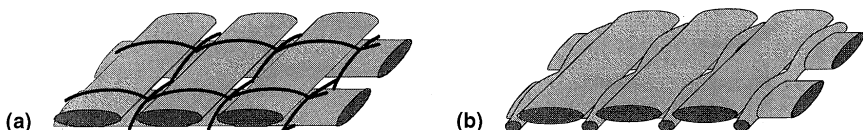


Figure 8.21 (a) Schematic of the preform illustrated in Figure 8.20; (b) preform geometry as modelled.

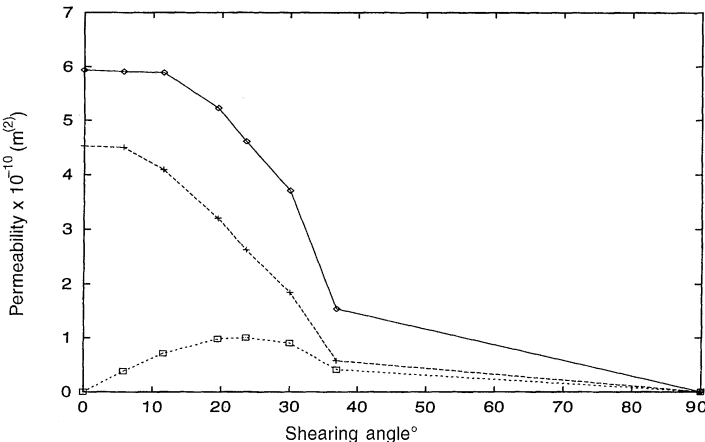


Figure 8.22 Permeability components K_{xx} (-◊-), K_{yy} (---) and K_{xy} (-□-) depending on the shearing angle.

actual part (thus, in a primitive fashion, adjusting for compaction). The cross-section of the binder was unknown beyond an order of magnitude and it was adjusted to provide a similar degree of anisotropy to that obtained by measurements.

The model we described in ref. 2 [equations (8.5)–(8.7)] was applied to the structure. Only one layer of preform was modelled. The structure itself was subjected to several shearing angles, providing full dependence of the permeability on shearing angle (Figure 8.22).

The results, when compared with the ‘quick ‘n’ dirty’ measurements, were promising. Note, however, that the range of prediction is between 0° and 37° of shearing deformation; the range of allowable deformation for the model [Figure 8.21(b)] material is between 0° and 42°. Actual shearing deformation measured on the material corresponds well with this range. For permeability predictions outside of this range (as a shear beyond this range can be predicted) extrapolation is needed, as shown in Figure 8.22.

8.8.2 DRAPING OF THE MOULD

Fabric draping over the mould was then simulated by means of the fishnet (geometric) model described previously. The numerically draped surface is shown in Figure 8.23(a). Figure 8.23(b) shows the shearing deformation.

As can be seen, the predicted deformation exceeds the allowable one by quite a significant margin. Shearing of such a magnitude is impossible for the given kind of preform. Comparison of the experimental data with



(b)

(a)

Figure 8.23 Draped cone surface: (a) fishnet geometry; (b) shearing angle (radians) contour plot.

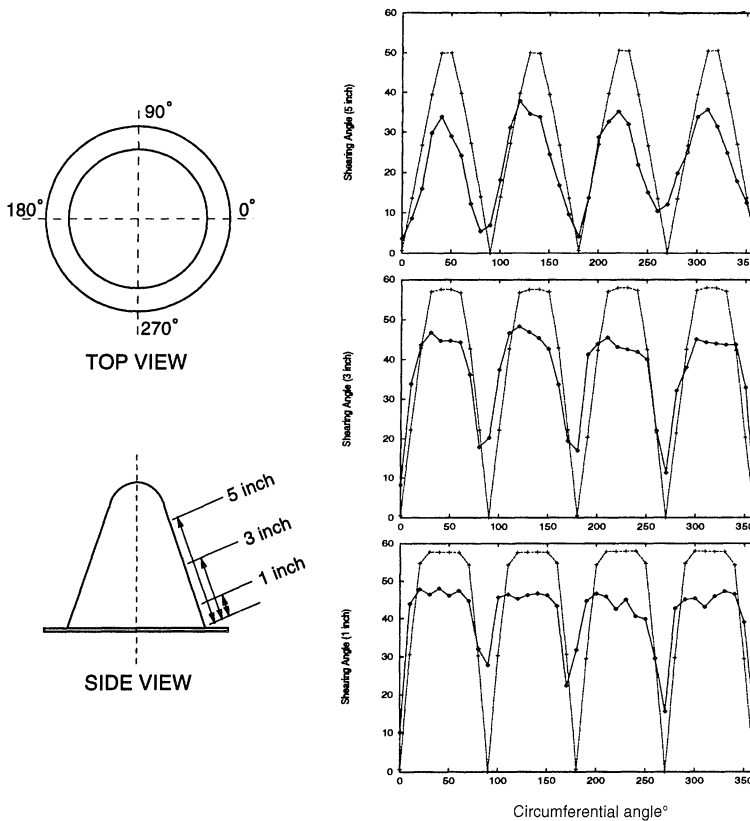


Figure 8.24 Draped cone surface: comparison of measured (-◇-) and predicted (-+-) shearing deformation.

the predicted values (Figure 8.24) confirms the doubt. The qualitative prediction is fine, but the experiment shows considerable smoothing of the shearing angle in the radial direction.

An explanation lies within the fabric deformation mode neglected by geometrical methods; tow-tow slip. Once the potential shearing deformation supply is exhausted, the fibre tows start to accommodate further deformation by mutual slipping. This was confirmed by analysis of the fibre volume fraction.

The problem has fairly serious consequences for our approach. Since the permeability model does not provide any data for shearing of this predicted magnitude, a significant part of the surface will have its permeability data created by extrapolation from the last known permeability value.

This problem is not commonplace but will appear wherever large shearing deformation is necessary. Note that if the area is sufficiently

Shearing Angle

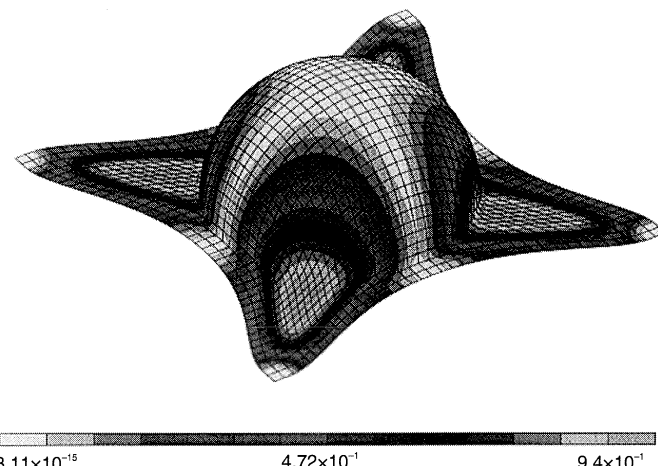


Figure 8.25 Draped hemispherical surface: shearing angle (degrees) contour plot.

small where the shear is high, such as in the case of a hemisphere (Figure 8.25), the mismatch is localised, and predicted values correlate well with experimental values.

8.8.3 FILLING SIMULATION

The data obtained from the permeability model and draping were, without correction, used as input into the filling simulation. Several experiments were simulated, both with constant inlet pressure and constant inlet flow rate. Two factors were compared with the experimental values: pressure (for constant inlet flow rate) or flow rate (for constant inlet pressure), and flow fronts.

The comparison is shown in Figures 8.26(a) (constant flow rate) and 8.26(b) (constant pressure). The correlation is very good and this result emphasises that a reasonable prediction of permeability magnitude is the crucial factor for realistic estimates of filling pressure and time.

The predicted flow fronts are illustrated in Figures 8.27(a) and 8.27(b), and Figure 8.28 presents the captured flow front from the experiment. Notably there is a considerable difference between these results; the anisotropy is more pronounced in the numerical results and the flow front shape does not correspond to the experimental value too well. This means that the difficulties with excessive predicted shear and associated problems with local permeability have reduced the accuracy.

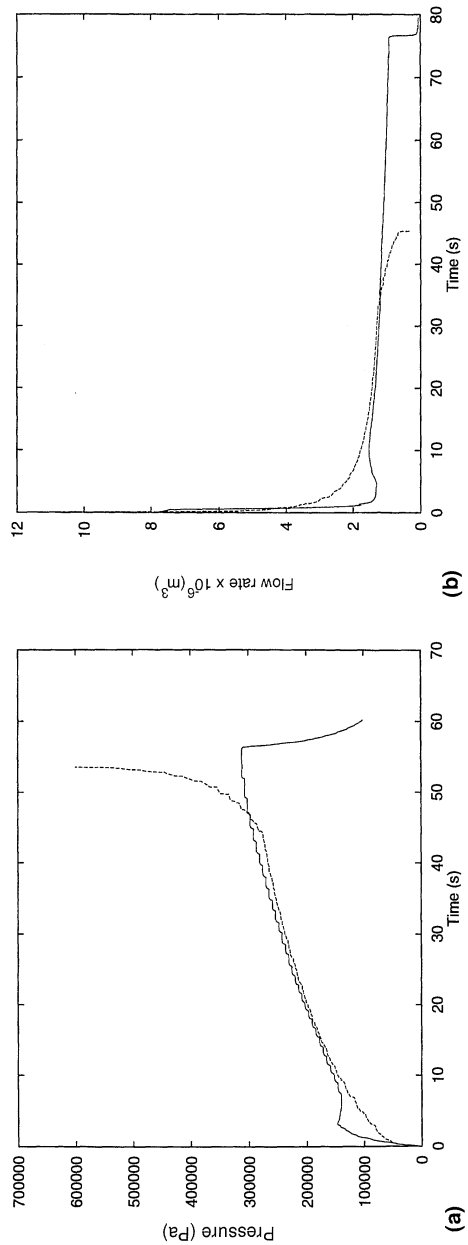


Figure 8.26 Predicted (---) and experimental (—) pressure: (a) constant flow rate experiment; (b) constant pressure experiment.

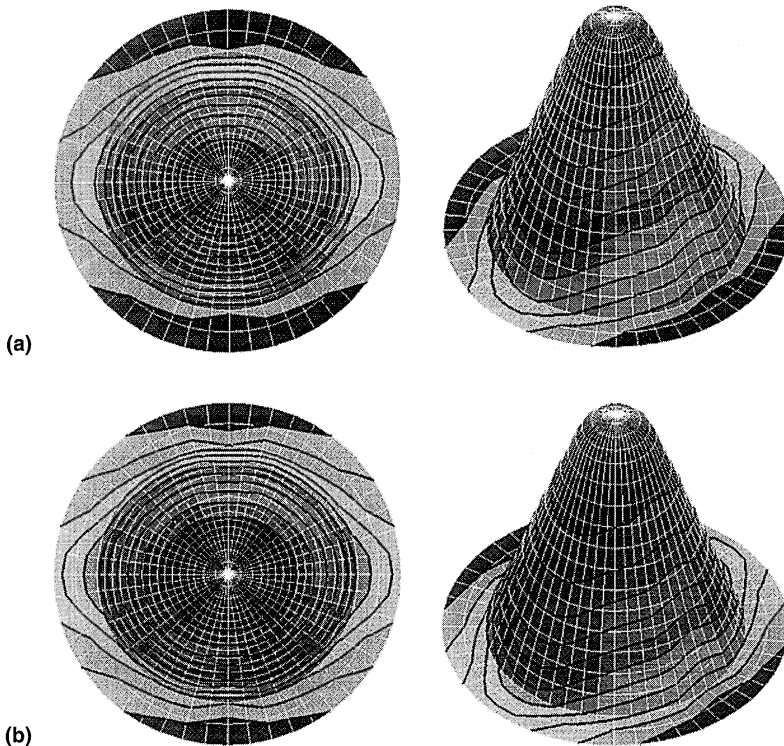


Figure 8.27 Predicted flow fronts: (a) constant flow rate experiment; (b) constant pressure experiment.

8.8.4 CONCLUSIONS

Despite the above-mentioned problems, the simulation predictions are vast improvements over the previous predictions that did not incorporate the predicted preform deformation at all. Using only basic data about the system we were able to make reasonable predictions of filling pressure and time. The obvious discrepancies in predicted preform deformation led to discrepancies in flow front prediction. Still, the flow front prediction fares better than the prediction that does not account for preform deformation.

Although there were some problems with the experimental data [8], these problems may be attributed to the extreme deformation of the preform necessary to fit it into the mould. At this point, the prediction of the fabric deformation fails as it does not allow for tow-tow slip, and the resulting error reduces the accuracy of subsequent steps. However, the existence of this problem suggests that in some cases the existing draping

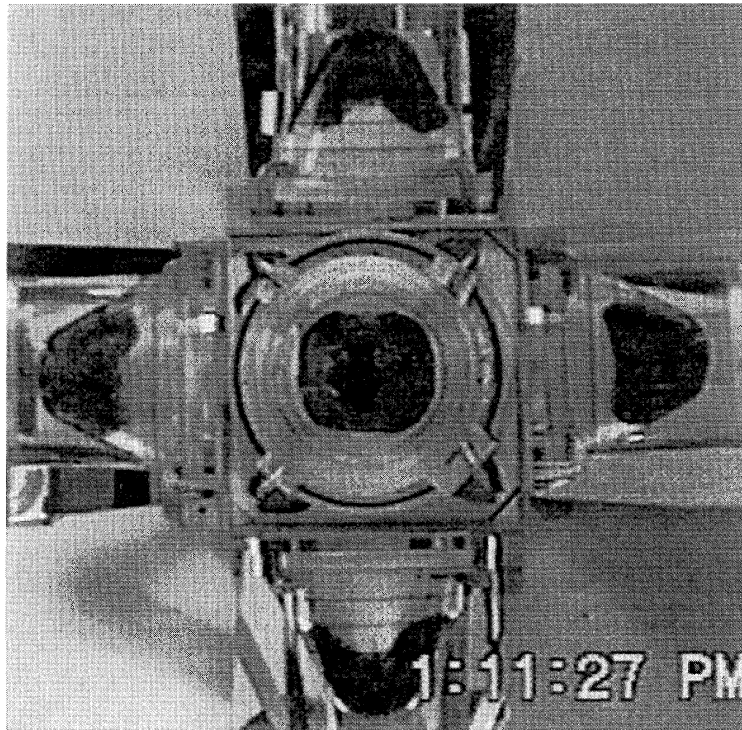


Figure 8.28 Video shot displaying the real shape of the predicted flow fronts illustrated in Figure 8.27.

model is inadequate and may require the inclusion of a slippage mechanism into the model.

8.9 THE USE OF SIMULATIONS AS A DESIGN TOOL

In a relatively short time the simulation of manufacturing processes has developed into an important tool used to verify many aspects of both product and manufacturing process design. However, the increase in computational power of low-end personal computer systems and workstations allows for a more comprehensive use of these tools during the design stage.

The process simulation is not necessarily only the domain of those who worry about how to manufacture the part. The part designer can greatly benefit from utilising the simulation.

As far as the RTM simulation is concerned, there are two clear steps to be modelled; the preforming stage, that includes the deformation of the preform necessary to comply with the final product geometry, and the mould filling and curing stage.

The former is of great interest both to the designer of the part (as fibre orientation and volume fraction will determine the functional properties of the part [72]) and to the designer of the processing equipment (as the permeability and fibre volume fraction of the preform is going to determine fill times and the forces necessary to manufacture the part). The latter is crucial for the proper design of moulds, inlets and vents, and also of the curing cycle, but should interest designers as well, since it can influence the cost of whatever they are designing.

Although the previous sections might read like a wish list of what we want to model compared with what we can model, there is a certain aspect of the simulation process that is absent here but will certainly prove very important in the future. It is the relation of the simulation to the part and/or to process equipment design.

The way current simulation codes operate, including the ones described herein, is that they provide the user with the expected orientation and deformation of a preform if it is placed in a mould as designed, with the parameters of process assuming the mould is built in a particular way.

The designer can use this type of simulation to conduct 'what if' type studies; he or she can compare several designs as far as the part performance or price is concerned. Although these are very useful, future simulation packages should allow a reverse approach to be taken. The questions to be answered during the design stage are more likely to be:

- How should the preform be cut and placed in the mould, in order to satisfy certain criteria on deformation or fibre orientation?
- How should the vents and gates be located to provide minimal filling time and pressure?
- How should the part be cured to minimise thermal stresses?

In other words, the designer is actually interested in solving the inverse problems. The 'what if' approach taken with the current packages does not really utilise the full potential of the simulation.

Besides developing the necessary models and their verification, simulations need to provide a way to solve these problems. This actually involves two subproblems: how to solve the inverse problem with a limited number of simulated processes; and the criteria for 'optimal' or just plainly 'better' fibre orientation, mould design etc. Only the solution to these problems will provide a design tool that can tap into the ultimate usefulness of process simulations.

References

1. De Parseval, Y. (1995) Experimental and analytical methods for the characterization of the permeability of fiber preforms. Masters thesis. Center for Composite Materials, Department of Mechanical Engineering, University of Delaware, Newark, DE.
2. Simacek, P. and Advani, S.G. (1996) Permeability model for a woven fabric. *Polymer Composites*, **12**, 887–99.
3. Luce, T., Advani, S.G., Howard, G. and Parnas, R. (1995) Permeability characterization: part 2: flow behavior in multiple-layer preforms. *Polymer Composites*, **16**, 447–58.
4. Parnas, R., Luce, T., Advani, S.G. and Howard, G. (1995) Permeability characterization: part 1: a proposed standard reference material. *Polymer Composites*, **16**, 430–46.
5. Pillai, K. and Advani, S.G. (1995) Numerical and analytical study to estimate the effect of two length scales upon the permeability of a fibrous porous medium. *Transport in Porous Media*, **21**(1), 1–17.
6. Pillai, K. and Advani, S.G. (1996) Wicking across a fiber bank. *Journal of Colloid and Interface Science*, **183**, 100–10.
7. De Parseval, Y., Pillai, K.M. and Advani, S.G. (1997) A simple model for the variation of permeability due to partial saturation in dual scale porous media. *Transport in Porous Media*, **27**, 243–64.
8. Bickerton, S., Simacek, P., Guglielmi, S. and Advani, S.G. (1996) Investigation of draping and its effects on the mold filling process during manufacturing of a compound curved composite part. *Composites – Part A: Applied Science and Manufacturing*, **28A**, 801–16.
9. Rudd, C.D., Long, A.C., McGeehin, P., et al. (1995) Processing and mechanical properties of bi-directional preforms for liquid composite molding. *Composites Manufacturing*, **3–4**, 211–19.
10. Bruschke M.V. and Advani, S.G. (1993) Flow of generalized Newtonian fluids across a periodic array of cylinders. *Journal of Rheology*, **37**, 479–98.
11. Gebart, B.R. (1992) Permeability of unidirectional reinforcements for RTM. *Journal of Composite Materials*, **8**, 1100–33.
12. Lam, R.C. and Kardos, J.L. (1988) The permeability of aligned and cross-plyed fibre beds during processing of continuous fiber composites. *Proceedings Of*

- The American Society For Composites, Third Technical Conference, 1988*, pp. 3–11.
- 13. Pillai, K. and Advani, S.G. (1995) Numerical and analytical study to estimate the effect of two length scales upon the permeability of fibrous porous medium. *Transport in Porous Media*, **21**, 1–17.
 - 14. Bruschke, M.V., Luce T.L. and Advani, S.G. (1992) Effective in-plane permeability of multi-layered RTM preforms. *Proceedings American Society Composites 7th Technical Conference*, 1992, 103–12.
 - 15. Calado, V.M.A. and Advani, S. G. (1996) Effective permeability of multi-layer preforms in resin transfer molding. *Composites Science and Technology*, **56**, 519–31.
 - 16. Advani, S.G., Bruschke, M.V. and Parnas, R.S. (1994) Resin transfer molding flow phenomena in polymeric composites, in *Flow and Rheology in Polymer Composites Manufacturing*, ed. S.G. Advani, Elsevier, Amsterdam.
 - 17. Bruschke, M.V. (1992) A predictive model for permeability and non-isothermal flow of viscous and shear thinning fluids in anisotropic fibrous media. Report 92-56, Center for Composite Materials, University of Delaware, Newark, DE.
 - 18. Bickerton, S.S. and Advani, S.G. (1997) Experimental investigation and flow visualization of resin transfer molding process in a non-planar geometry. *Composites Science and Technology*, **57**, 23–33.
 - 19. Gutowski, T.G. and Dillon, G. (1992) The elastic deformation of lubricated carbon fibre bundles: comparison of theory and experiments. *Journal of Composite Materials*, **16**, 2330–47.
 - 20. Djaja, R.G., Moss, P.J., Carr, A.J. and Carnaby, G.A. (1992) Finite element modeling of an oriented assembly of continuous fibers. *Textile Research Journal*, **8**, 445–57.
 - 21. Van Wyk, C.M. (1946) 20 – Note on the compressibility of wool. *The Journal of Textile Institute Transactions*, pp. 285–92.
 - 22. Carnaby, G.A. and Pan, N. (1989) Theory of compression hysteresis of fibrous assemblies. *Textile Research Journal*, **5**, 275–84.
 - 23. Batch, G.L. and Macosko, C.W. (1988) A model for two-stage fibre deformation in composite processing. *20th Internationa SAMPE Technical Conference*, Society for the Advancement of Material and Process Engineering, 1161 Parkview Drive, Covina, CA 91724-3748.
 - 24. Komori, T., Itoh, M. and Takaku, A. (1992) A model analysis of the compressibility of fibre assemblies. *Textile Research Journal*, **10**, 567–74.
 - 25. Mogavero, J. and Advani, S.G. (1997) Experimental investigation of flow through multi-layered preforms. *Polymer Composites*, **18**(5), 649–55.
 - 26. Hearle, I.W. and Shanahan, W.J. (1978) 11–An energy method for calculations in fabric mechanics; part I: principles of the method. *Journal of Textile Institute*, **4**, 81–91.
 - 27. Shanahan, W.J. and Hearle, I.W. (1978) 12–An energy method for calculations in fabric mechanics; Part II: examples of application of the method to woven fabrics. *Journal of Textile Institute*, 93–100.
 - 28. Bickerton, S. and Advani, S.G. (1995) Characterization of corner and edge permeabilities during mold filling in resin transfer molding. *Recent Advances in Composite Materials, MD*, **56**, 143–51.
 - 29. Van Der Weeën, F. (1991) Algorithms for draping fabrics on doubly curved surfaces. *International Journal for Numerical Methods in Engineering*, **31**, 1415–26.

30. Bickerton, S., Fong, L., Fickie, K.D. and Advani, S.G. (1995) Effect of draping of fiber preforms on process parameters during manufacturing with resin transfer molding. *Proceedings of 11th Annual ESD Advanced Composites Conference and Exposition*, 1995, 213–20
31. Long, A.C. (1995) Drape analysis for beaded stiffened panel. Report from the Department of Mechanical Engineering, University of Nottingham, Nottingham.
32. Van West, B.P., Pipes, R.B. and Keefe, M. (1990) Simulation of draping of directional fabrics over arbitrary surfaces. Report 90–14, Center for Composite Materials, University of Delaware, Newark, DE.
33. Postle, R. and Norton, A.H. (1991) Mechanics of complex fabric deformation and drape. *Journal of Applied Polymer Science: Applied Polymer Symposium*, **47**, 323–40.
34. Collier, J.R., Collier, B.J., O'Toole, G. and Sargand, S.M. (1991) Drape prediction by means of finite-element analysis. *Journal of Textile Institute*, **1**, 96–107.
35. Boisse, P., Gelin, J.C. and Sabhi, H. (1993) Experimental study and finite element simulation of glass fiber fabric shaping process. *Use of Plastics And Plastic Composites: Material and Mechanics Issues*, **46**, 587–608.
36. Simacek, P., Kaliakin, V.N. and Pipes, R.B. (1993) Pathologies associated with the numerical analysis of hyper-anisotropic materials. *International Journal on Numerical Methods in Engineering*, **10**, 3487–508.
37. Simacek, P. and Karbhari, V.M. (1996) Notes on the modeling of preform compaction: I – micromechanics at the fiber bundle level. *Journal of Reinforced Plastics and Composites*, **1**, 86–122.
38. Karbhari, V.M. and Simacek, P. (1996) Notes on the modeling of preform compaction: II – effect of sizing on fiber bundle micromechanics. *Journal of Reinforced Plastics and Composites*, **8**, 837–61.
39. Cai, Z. and Gutowski, T. (1992) The 3-D deformation behavior of a lubricated fiber bundle. *Journal of Composite Materials*, **8**, 1207–37.
40. Bruschke, M. (1992) *A Predictive Model for Permeability and non-isothermal Flow of Viscous and Shear Thinning Fluids in Anisotropic Fibrous Media*. PhD. thesis, Center for Composite Materials, Department of Mechanical Engineering, University of Delaware, Newark, DE.
41. Van Den Brekel, L.M. and De Jong, E.J. (1989) Hydrodynamics in packed textile beds. *Textile Research Journal*, **8**, 434–40.
42. Berny, C.A. (1993) Permeability of woven reinforcements for resin transfer molding. Master thesis, Department of Mechanical and Industrial Engineering, University of Illinois at Urbana-Champaign, IL.
43. Heitzmann, K.F. (1994) Determination of in-plane permeability of woven and non-woven fabrics. Masters thesis, Department of Mechanical and Industrial Engineering, University of Illinois at Urbana-Champaign, IL.
44. Ranganattan, S., Phelan, F. and Advani, S. G. (1996) A generalized model for the transverse permeability of unidirectional fibrous media. *Polymer Composites*, **17**, 222–30.
45. Lewis, R.W., Usmani, A.S. and Cross, J.T. (1991) Finite element modeling of mold filling, in *Finite Elements in the 90's*, eds E. Onate, J. Periaux and A. Samuelsson, Springer/CIMNE, Barcelona.
46. Voller, V.R. and Chen, Y.F. (1995) Prediction of filling times of porous cavities. *International Journal Numerical Methods*, **10**.

47. Gallez, X.E. and Advani, S.G. (1997) Resin infusion process simulation (RIPS): Proceedings of the 55th Annual Technical Conference, Antec, part 2 (of 3) 2454–8, Society of Plastics Engineers.
48. Tucker, C.L. III and Dessenberger, R.B. (1994) Governing equations for flow and heat transfer in stationary fiber beds, in *Flow and Rheology in Polymer Composites Manufacturing*, ed. S.G. Advani, Elsevier, Amsterdam.
49. Gupte, S. and Advani, S.G. (1997) Flow near the permeable boundary of aligned fibre preform, *Polymer Composites*, **18**, 114–24.
50. Gupte, S. and Advani, S.G. (1997) Non-Darcy flow near the permeable boundary of a porous medium: an experimental investigation using LDA. *Experiments in Fluids*, **22**, 408–22.
51. Bruschke, M. and Advani, S. G. (1990) A finite element/control volume approach to mold filling in anisotropic porous media. *Polymer. Composites*, **11**, 398–405.
52. Liu, B., Bickerton, S., and Advani, S.G. (1996) Modeling and simulation of RTM: gate control, venting and dry spot prediction. *Composites Part A*, **27**, 135–41.
53. Maier, R.S., Rohaly, T.F., Advani, S.G. and Fickie, K.D. (1996) A fast numerical method for isothermal resin transfer mold filling. *International Journal of Numerical Methods in Engineering*, **39**, 1405–22.
54. Liu, B. and Advani, S.G. (1995) Operator splitting scheme for 3-D temperature solution based on 2-D flow approximation, *Computational Mechanics*, **38**, 74–82.
55. Bruschke, M.V. and Advani, S.G. (1994) A numerical approach to model non-isothermal, viscous flow with free surfaces through fibrous media. *International Journal of Numerical Methods in Fluids*, **19**, 575–603.
56. Dessenberger, R.B. and Tucker, C.L. III (1994) Thermal dispersion in resin transfer molding, in *Advances in Computer-Aided Engineering (CAE) of Polymer Processing*, eds K. Himasekhar, V. Prasad, T.A. Osswald and G. Batch, ASME, 21–40.
57. Sourour, S. and Kamal, M.R.(1972) *SPE Technical Papers*, **18**
58. Kamal, M.R., Sourour, S. and Ryan, M. (1973) Integrated thermo-rheological analysis of the cure of thermosets. *SPE Technical Papers*, **18**, 187–91.
59. Kamal, M.R. and Sourour, S. (1973) Kinetics and thermal characterization of thermoset cure. *Polymer Engineering and Science*, **13**, 59–64.
60. Calado, V. and Advani, S.G. (1998) A review of cure kinetics and chemo-rheology for thermoset resins, in *Transport Processes in Composites*, eds A. Loos and R. Dave, (forthcoming).
61. Lee, D.S. and Han, C.D. (1987) A chemorheological model for the cure of unsaturated polyester resin. *Polymer Engineering and Science*, **27**, 955–63
62. Park, H.C, Hawley, M.C. and Blanks, R.F. (1975) The flow of non-Newtonian solutions through packed beds. *Polymer Engineering and Science*, **15**, 761–73.
63. Trochu, F. and Gauvin, R. (1992) Limitations of boundary fitted finite difference method for the simulation of resin transfer molding process. *Journal of Reinforced Plastics and Composites*, **11**, 772–86.
64. Hieber, C.A. and Shen, S.F. (1980) A finite element/finite difference simulation of the injection mold filling process. *Journal of Non-Newtonian Fluid Mechanics*, **7**, 1–31.
65. Osswald, T.A. and Tucker, C.L. (1988) *Polymer Engineering and Science*, **28**, 413–20.

66. Calhoun, D.R., Yalvac, S., Wetters, D.G., et al. (1994) Mold filling analysis in resin transfer molding. *Polymer Composites*, 251–64.
67. Kang-Moon-Koo, Lee-Woo-II, Yoo-Jung-Yul and Cho-Sung-Min (1995) Simulation of mold filling process during resin transfer molding. *Journal of Materials Processing and Manufacturing Science*, 3(3), 297–313.
68. Trochu, F., Boudreault, J.F., Gao, D.M. and Gauvin, R. (1995) Three-dimensional flow simulations for the resin transfer molding process. *Materials and Manufacturing Processes*, 1(10), 21–6.
69. Lee, L.J., Young, W.B. and Lin, R.J. (1994) Mold filling and cure modeling of RTM and SRIM processes. *Composite Structures*, 1–2 (27), 109–20.
70. Phelan, F.R. (1992) Flow simulation of the resin transfer molding process, in *Proceedings of the 7th Technical Conference of the American Society for Composites*, Technomic Publishing, Lancaster, PA, pp. 90–102.
71. Chang, W. and Kikuchi, N. (1995) Analysis of non-isothermal mold filling process in resin transfer molding (RTM) and structural reaction injection molding (SRIM). *Computational Mechanics*, 1 (16), 22–35.
72. Gupte, S. and Advani, S.G. (1997) Flow near the permeable boundary of aligned fiber preform. *Polymer Composites*, 18, 114–24.
73. Simacek, P. and Advani, S.G. (1996) DRAPE 1.00 – user manual. Report 96–21, Center for Composite Materials, University of Delaware, Newark, DE.
74. Fong, L.L., Liu, B., Varma, R.R. and Advani, S.G. (1995) Liquid injection molding simulation LIMS user's manual version 3.3. Report 95–06, Center for Composite Materials, University of Delaware, Newark, DE.
75. Falzon, P.J., Karbhari, V.M. and Herszberg, I. (1996) Effects of compaction on the stiffness and strength of plain weave fabric RTM composites, *Journal of Composite Materials*, 30(11), 1210–47

Tooling fundamentals for resin transfer moulding

9

Mark Wadsworth

9.1 INTRODUCTION TO RESIN TRANSFER MOULDING TOOLING

As with all processes where tooling is used, concurrent engineering of part and tooling will improve manufacturing and product performance. This is particularly true with resin transfer moulding (RTM), where more occurs inside the mould than with almost all other moulding processes. The mould may be used to form the fibre assembly, distribute and determine the quantity of the resin charge, cure the resin, restrain pressure differentials and allow part removal. Each of these factors can effect manufacturing and part performance. Tooling for RTM is similar to other closed moulds in many respects. The mould determines the geometry on the outside [outside mould line (OML)] of the part, and the inside when the part is hollow. For most composite manufacturing processes, the inside mould line (IML) may be less critical (except for items such as ducts). However, with RTM, thickness variations will not only alter the weight of the part but also cause processing variations. For this reason all surfaces of aerospace RTM applications must be accurately located.

Tooling can either be fabricated directly from stock or replicated from a pattern representing the geometry. The size of the mould may be scaled for thermal or chemical shrinkage and the shape may be distorted to compensate for anticipated part distortions. The tool must react to the physical loads of preform debulking, resin injection, mould sealing and any other pressurised bladder or mandrel inside the tooling. It must also accommodate process requirements such as injection ports (sprue), vents

and part demoulding features. The mould must also provide a means of distributing heat uniformly for cure and in some cases preheat the resin during injection.

With a rigid mould it is necessary to have at least two mould sections to define all sides of the part, allow placement of the preform and provide for removal of the part. The space between the two closed mould halves is the part cavity. The curve on the perimeter of the part where the mould halves meet is known as the parting line of the part. The mould parting plane is a reference plane normal to a mould opening axis. The surface beginning at the mould parting line and extending out is the tool flange, which contains an air-tight seal. Often the vents are also located in the tool flange, penetrating the seal to intersect the part cavity. Separate tooling sections that define the IML surfaces may be called mandrels, inserts or cores, details of which are discussed in the next chapter. When a primary tool section forms the inside part surface of a deep draw (commonly called a plug) it is usually considered an IML surface even though the part is not completely hollow. Other types of mandrels used for undercuts or as debulking aids are either supported by the preform, guided or locked into position while the OML tooling is closing (Figure 9.1).

When negative draft or undercuts preclude the use of simple two-piece OML tooling, mandrels can be used to define these surfaces without requiring that the primary mould be divided into more than two pieces. Generally, when more than two primary tool segments are required, more than one parting plane will exist and a simple single-axis press action cannot be used to open the mould, and sealing is more difficult.

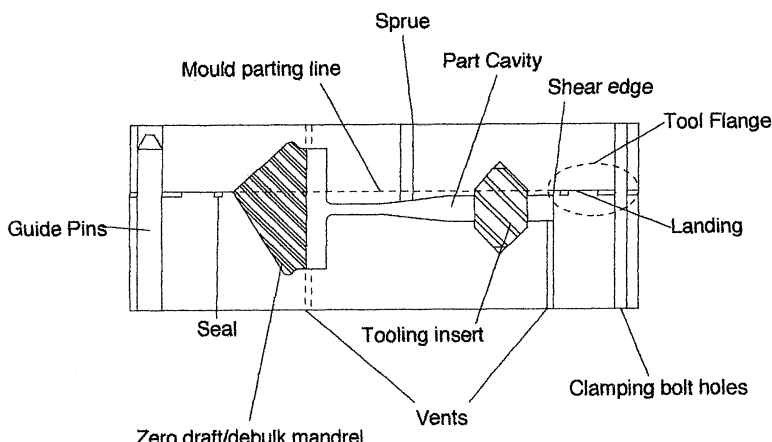


Figure 9.1 Resin transfer moulding: mould features.

Most of the time it is possible to accommodate undercut surfaces with mandrels contained within a two-piece primary tool set, simplifying mould clamping and sealing. Moulds with many OML sections can be used for complex geometry when necessary, but at the expense of cycle time. When tooling budgets are limited and production rate is low, one-sided tooling with a flexible bag can be considered.

Aerospace parts typically must endure temperatures which require that the resin be cured at elevated temperatures. The cure temperature required depends on the resin type and application but is commonly between 120°C and 175 °C. This temperature is a primary mould material selection criterion since it can have many effects on the mould material, geometry and physical properties.

The RTM mould must be clamped closed by a press or clamps which must be accommodated by or included in the mould. The debulking, injection and curing processes usually involve positive gauge pressures, so the mould must have enough stiffness to carry these loads to the clamps or press platens without excess deflection. Furthermore, the mould must have the surface properties to withstand the abrasion of dry fibre against the mould for the required number of cycles, without excessive maintenance. The mould surface must also be compatible with the chemicals in the uncured resin, release agents and mould cleaners.

9.2 RESIN TRANSFER MOULDING TOOLING MATERIALS AND PROCESSES

9.2.1 SELECTING MOULD MATERIALS

Mould material selection is often determined by production volume or rate. Low rate production can usually be most economically achieved with a composite laminate or with some other form of reinforced plastic tooling. When hard materials (such as steel) are used to make the mould, the initial tooling will be more expensive, but for high-volume applications the maintenance and shutdown costs of inferior materials can justify the initial investment. A hybrid approach is to employ a hard coating to provide surface durability with an easily fabricated or replicated base material to provide the structure. When using materials in combination, one must always consider the coefficient of thermal expansion (CTE) and other properties which might effect their compatibility in the mould environment. The mould-making process can also influence the mould material selection. For example, if a pattern of the part is available, the cost of replicated tooling may be much less. When the part is designed in three dimensions on a computer-aided design (CAD) system, the file can be converted to cutter paths for a computer

Table 9.1 Properties of various tooling materials

Material	CTE ^a × 10 ⁶ (°C)	Thermal conductivity (W/m °C)	Specific heat (kJ/kg °C)	Maximum Service Temperature (°C)	Specific gravity (g/m)	Yield strength (tensile) (MPa)	Modulus (tensile) (GPa)	Hardness (Rockwell scale)
Ductile Iron (spherical graphite)	12.1	80	0.5	>500	7.7	220	190	30 Rc
Cast Iron (gray)	12.1	80	0.53	>500	7.25	170	140	30 Rc
Steel:								
Mild (A-36)	11.7	76	0.42	>500	7.83	250	200	100 Rb
P-20	11.5	42.7	0.5	>500	8.19	300	200	38 Rc
4130	11.3	17.2	0.4	>500	7.8	300	200	32 Rc
Stainless (ANSI 420)	17.2	17.5	0.5	>500	8.0	206	192	40 Rc
Invar 42	2.3	10.5	0.5	>500	8.0	200	140	74 Rb
Invar 36	1.0	10.5	0.5	>500	8.0	215	141	73 Rb
Aluminum								
6061-T6	24.0	355	1.0	300	2.7	255	69	58 Rb
Cast	19-24	209	0.90	300	2.6	186	69	85 Rb
Aluminum Bronze	17	128	0.43	>500	7.7	241	120	100 Rb
High-Silicon Bronze	10.0	36	0.4	>500	8.5	375	117	100 Rb
Brass, Cast	18.7	113	0.41	>500	8.4	137	103	80 Rb
Electroformed Nickel	13.5	75	0.46	>500	8.9	205	205	95 Rb
E-glass Prepreg	10-14	0.86	0.1	220	2.1	310	22	
E-glass (Wet lay-up)	14-18	0.86	0.1	210	2.0	300	20	
Carbon Prepreg (fabric)	1.5-5	1.7	0.3	210	1.6	430	72	80-115 Rh
Mass cast epoxy	40	1.0	0.7	180	2.5	34		
Monolithic graphite	5	168	0.83	>500	1.9	13		
Glass (98% silica)	80	0.77	0.46	300	2.2	68	7	
Wood (ash)	9.5	0.16	1.6	200	0.75	50		
Teflon (neat)	17	0.24	1.0	300	2.2	9		
Ceramic (refractory)	1-5	1.8	1.0	>500	2.4	40	100	
Plaster	9	0.5	1.0	100	1.3	5	30	
Concrete	10	1	0.88	100	2.8	3.4	30	

Note: the above properties are for comparison; actual properties vary with specific composition, heat treat and service conditions.

^a Coefficient of thermal expansivity.

numerically controlled (CNC) mill, and machined metal tooling may be less expensive. Table 9.1 compares the important properties of various mould materials.

9.2.2 THE EFFECTS OF TOLERANCES ON TOOLING PROCESS SELECTION

The required part accuracy is an important consideration when selecting both the material and the manufacturing process used to make tooling. The tool tolerances should be considerably less than those applied to the part, often half. But since accuracy is expensive it should be no higher than absolutely necessary. Many times, the degree of accuracy required is not clear, even to the designer. CAD and geometric tolerances have improved the ability of engineers to predict interference and alignment problems, enabling them to allow more error by distributing it more effectively. When tolerances are not specific and explicit, the tool designer or contractor must allow enough budget to cover all possible contingencies, resulting in higher costs. A high-accuracy requirement will substantially increase the cost of a handmade pattern. In general high-precision moulds are most economical when machined from billet or castings, whereas replication processes are more commonly used for larger or less accurate moulds.

With most replication processes, final tool or intermediary distortions can result in inaccuracies if not modelled properly. Constant shrinkage in the laminate is compensated for by making the tool and/or pattern larger than the part. Shrink factors for aerospace tooling materials are usually very small and are often ignored, but where a high degree of accuracy is required the material manufacturer should be consulted to provide this information. Inconsistent shrinkage is often experienced in radii, where the fibre volume is not constant from the inside to the outside of the radius. This can lead to distortions, especially on an unsupported flange. When necessary, this spring-in effect can be compensated for in the pattern, or the cause (resin richness and temperature variations) eliminated by exact control of process parameters. For these reasons, the design of laminate tooling for very-high-precision applications is challenging, and experience with the material is important. Mass cast tooling can distort as a result of resin shrinkage and heat generated during cure. Substructure and internal reinforcement rods should be incorporated into the casting as early as possible to reduce out-of-plane warping (Figure 9.2). Improvements in tooling precision have been attempted by combining laminate tooling with a machinable face that can be CNC machined, after cure and substructure are complete. Since patterns can be stored in a relatively safe location and are not at risk, a replicated tool can often be replaced more readily than can a fabricated tool in the event the tool sustains massive damage.

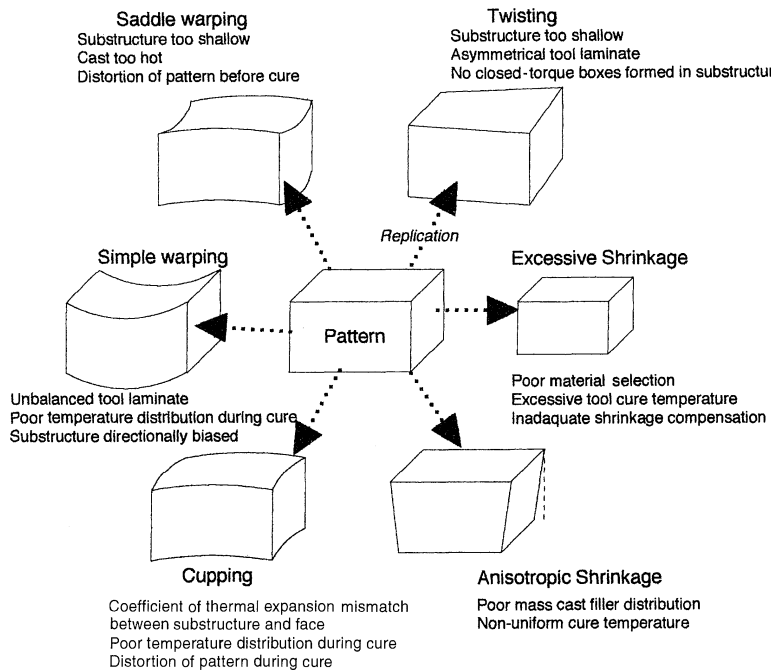


Figure 9.2 Types of replication distortion and common causes.

9.2.3 METHODS OF CREATING THE MOULD SHAPE

Tooling can either be fabricated directly from the tooling material or replicated from a pattern. A flow chart that can be used to compare fabricated with replicated tooling processes is shown in Figure 9.3. The mould manufacturing method can affect tooling costs dramatically. For example, the mould geometry is important when comparing the costs of cast-to-size with CNC machining metal moulds, even though similar metals can be used. Machining a deep cavity or a difficult-to-machine material can require a large billet and a lot of costly mill or electric discharge machining (EDM) machine time, but for castings, the depth is of less consequence. The following factors should be considered while selecting the method used to form the mould set:

- estimates of the number of parts and rate at which they are to be produced;
- number of moulds required;
- tooling budget;
- tolerances for moulded features;
- lead time available;
- tooling weight and associated handling systems;

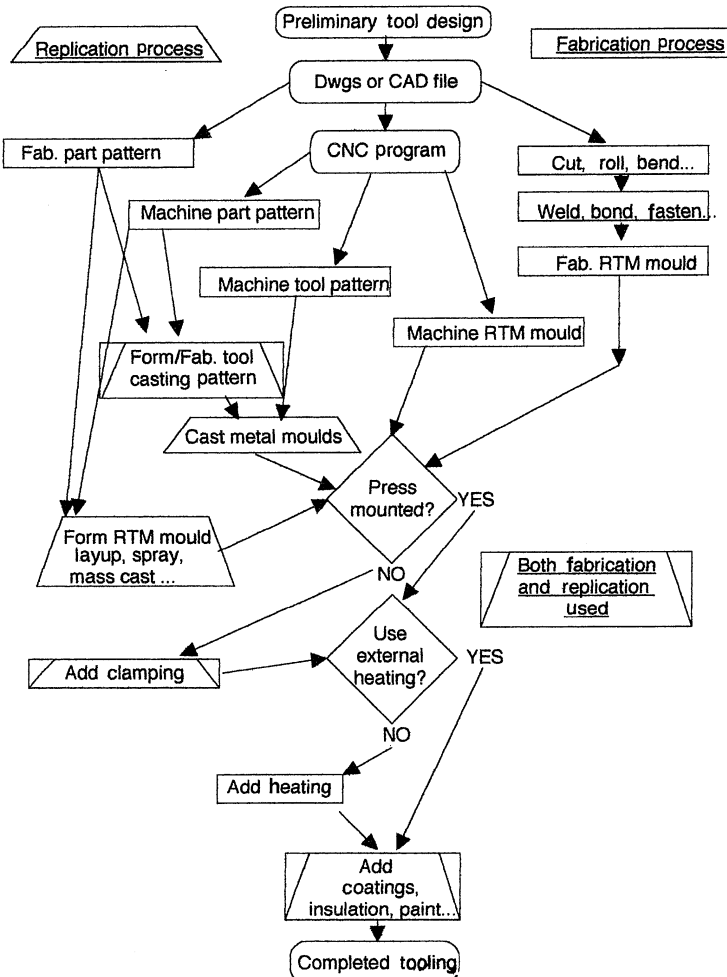


Figure 9.3 Comparison of fabrication and replication processes. CAD = computer-aided design; CNC = computer numerically controlled; Dwgs = drawings; Fab. = fabricate; RTM = resin transfer moulding.

- mould heat-up rate required;
- preform bulk factor and other tooling accommodations required.

9.2.4 FABRICATED TOOLING

With direct fabrication many steps in the tool building process can be eliminated, accelerating tool delivery and improving accuracy. After the tool is designed, drawings or a CAD file are used to machine or fabricate the tool directly from the desired material stock. Metals are most

conducive to this type of tooling since they can be machined, bent, formed, welded and fastened in many ways. Often large complex tools are fabricated in a manner similar to that used to make metal structures. A support network of frames and ribs are covered with partially or fully shaped skin sections, which are fastened to the frame and welded together. The entire assembly can then be machined and/or polished as necessary.

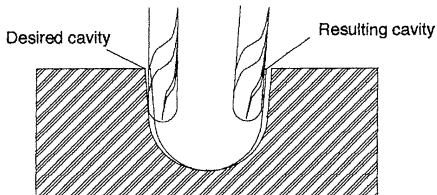
The second tool section is often more difficult to make by fabrication means, since the dimensional errors of the first and second section can combine to exceed tolerance. This can lead to excessive variance in cavity thickness. Moulds can be made adjustable to allow fine tuning of certain dimensions by means of threaded rod connecting the skin to the sub-structure.

A fabricated tool can be offset with sheet wax for the part thickness and the second half replicated. This combination of fabrication and replication eliminates the need for a dedicated pattern and provides some of the benefits of replicated tooling.

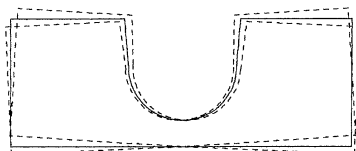
Machined tooling eliminates some of the manual tasks required with most other tooling methods. However, owing to the additional engineering and programming time required to 'fabricate' the tool design on the computer and expensive machine tool time, some moulds are more cost-effectively made manually. High machining costs are usually associated with deep cavity depth, narrow channel cavities, hard mould material and large tool size.

Most materials can be machined to shape with varying rates of material removal. Many tool steels made for cavity moulds, such as P-20, are usually pre-hardened to about 34 Rc but are still machinable. Such tool steels are durable but may take more than three times as long to machine as mild steel. Aluminium is about three times as easily machined as mild steel but is similarly less durable. Cast iron is between aluminium and mild steel in machinability and is comparable to steel in hardness.

Machined tooling is usually made from a billet large enough to leave sufficient material for the mould to retain its shape (Figure 9.4). The amount of remaining material required depends on the residual stress in the metal, the shape of the mould and the material stiffness. The residual stress depends on many factors, from the time the metal is poured into an ingot, reduced to a billet and heat treated. In some cases the billet size is determined by its stability during machining rather than by the RTM process loads. For this reason machined billet tooling is often massive and slower to heat up and cool. To reduce this problem, many moulds are made from even thicker billets that are machined on both sides to hollow-out material weight while maintaining stiffness. This is particularly useful when the tool is used in an oven or other situation where heat transfer is limited.

Cutter and Spindle Flexure**(a) Possible causes:**

- Inadequate cutter speed (increase speed)
- Feed rate too fast (use slower feed on final passes)
- Cutter dull (replace, use coolant)
- Cutter too small or long (for long reach use EDM)

Out-of-Plane Distortion
Cupping, warping or twisting**(b) Possible causes:**

- Inadequate billet thickness (add substructure, use thicker billet)
- High billet stress state (stress relieve)
- Mould overheated (remachine or replace)

Figure 9.4 Types of fabrication distortion and common causes: (a) cutter and spindle flexure; (b) out-of-plane distortion (cupping, warping or twisting). EDM = electric discharge machining.

9.2.5 REPLICATED TOOLING

The term 'replicate' is intended to describe any process whereby the inverse or 'replica' of a model is taken, whether by casting, spraying or any other deposition process. In the case where an existing pattern is available that can be used directly or with slight modification, the replication tooling option is most attractive. This tool type has been traditionally referred to as soft tooling, but since spray metal and cast metal tooling require a pattern but are 'harder' than some machined tooling, this term is not descriptive. Replicated tooling processes include: cast metal, cast plastic (mass casting), composite laminate, electroformed nickel, spray metal and others. All of these forming methods require a pattern of some type.

Tool patterns

Other than the part geometry, the pattern needs to include the parting line features such as seal grooves, guide pins and mandrel guides. The flange of the pattern should have excess area to allow casting forms to be attached or to allow the laminate to be trimmed after the substructure is attached. As many features as possible should be moulded in, because the machining of some materials is difficult and can result in mould damage, loss of vacuum integrity and/or distortion. The pattern should

have the same finish quality desired on the tool, porosity must be sealed and all surfaces treated with an appropriate release agent. In many cases the pattern represents the OML; the first tool half is replicated then offset for the part thickness with sheet wax before making the second half. In other cases, the pattern is free-floating and represents all sides of the part. For floating patterns, parting line features are usually located in a separate pattern base which nests the part pattern and defines the mould flange. The first section is replicated, cured and demoulded with the pattern intact. The second half can then be made from the first. Figure 9.5 depicts both of these replication processes.

The cost of making a pattern, which is usually a one-of-a-kind item, can be difficult to quote and is usually estimated by an experienced pattern maker on a similarity basis. Traditionally, this process is a series of steps where skilled craftspeople break the geometry into sections, profiles and other smaller or more easily fabricated components. These segments are then assembled into a pattern representing one or more surfaces of the part. The pattern may need to be scaled for a distributed dimensional change of a following process or offset for the part cavity thickness. A recent trend is to CNC machine a pattern from a highly machinable billet stock from which the tool can be replicated. This process combines the automation and precision of CNC with the benefits of a replicated tool.

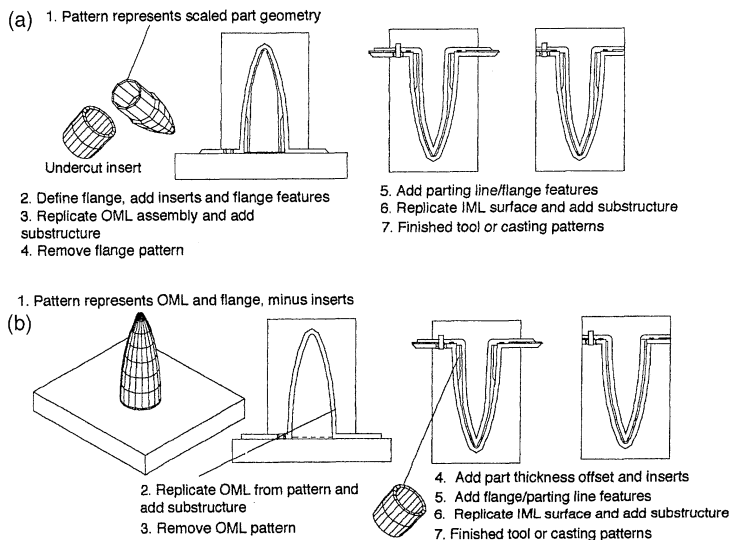


Figure 9.5 Replication techniques used for resin transfer moulding: (a) floating pattern technique; (b) surface offset technique. IML and OML = inside and outside mould line, respectively.

Reinforced plastic laminate tooling

Graphite composite tooling is particularly suitable for aerospace graphite parts because of the similar coefficients of thermal expansion (CTEs) and rapid heat-up with oven cures. The pattern used for composite tooling depends on the cure cycle used but almost all can be cured against plaster patterns. The primary reason for using laminate tooling is that it can be made in-house from the same material as the RTM part, with little lead time from a low-cost pattern. Epoxies are available which can be cured at room temperature and provide service to 200°C after a free-standing post-cure. For this reason, and because of low chemical shrinkage, epoxies are the most commonly used resin for aerospace tooling.

The laminates can be made by wet lay-up with liquid epoxy resins or with pre-impregnated reinforcement. An epoxy surface coat can crack and disbond after thermal cycles but is usually necessary with wet lay-up and vacuum bag preps to achieve a fine finish. Other surface coatings such as metal spray or electroformed surfaces can be used with laminate tooling. Tooling preps which are used without a surface coat may need to be autoclave cured in order to achieve a good surface and vacuum integrity. Systems used with a surface coat to provide vacuum integrity can usually be cured under a vacuum bag.

Consistent laminate shrinkage and thermal expansion is dependent upon the resin distribution; therefore the quality of wet lay-up tools is more skill dependent. With all laminate lay-up processes, the critical issues are bridging and wrinkling of the reinforcement on female and male radii during cure. Careful tailoring of the fabric to the surface and frequent vacuum bag debulk cycles are used to reduce these defects. Autoclave pressure greatly improves the tool durability by reducing void content and more evenly distributing the resin. For RTM the laminate should be thicker than for bag mould tooling; 12–19 mm is recommended, depending on the geometry and material. Substructure must be rigidly attached to the mould reinforced with wet lay-up or prepreg tape attachment. The substructure should be against the mould at least every 15 cm. The high laminate thickness partially compensates for the thermal and physical disruption that occurs where the substructure touches the face. A post cure is usually required after the substructure has cured. The moulds are usually clamped, holding the tool sections together tightly throughout post-cure.

Mass-cast resin tooling

The replication method that requires the least labour and frequently has the lowest cost is mass cast tooling. Mass-casting resin is a particle-reinforced plastic material containing fillers which reduce CTE and

shrinkage, increase stiffness and strength, improve heat conductivity and absorb heat from the cure exotherm. With as much filler as possible, the mixture must remain fluid enough to be poured into a form containing the pattern. The pattern can be less expensive than for laminate tools since vacuum integrity and heat resistance are usually not necessary. In the simplest case, the face coating is applied to the pattern which is then surrounded by a form to contain the liquid casting material.

Some cast materials involve pouring the solid fillers first, followed by the catalysed resin, whereas others have the filler mixed into the resin. With all methods, elimination of air entrapment by prior degassing, smooth pouring and vibration is advised. The casting material may generate heat which can distort the mould or the pattern, as can the resin shrinkage. The thermal capacity and conductivity of the pattern is important when one determines the maximum thickness that can be cast at once. It may be necessary to cast thick sections in layers when the pattern and form insulate the casting. The mould should include a thick base structure, a pre-welded steel frame or some other reinforcement that can be cast in place to stabilise the mould. Cores to displace mass cast (whether removed or left in place) save casting material, lighten the mould and reduce thermal mass. Heat-transfer tubing or electric heaters and thermocouple wells should also be cast in, since machining after cure is risky and often impossible. Plastic mass-casting resins are not the only materials that can be used in this manner. Ceramics, concrete, plaster and many other curing materials that can be poured and will maintain their shape can be used with this technique.

A variation on this process which increases accuracy is called the 'cast-face technique'. The bulk of the tool is cast into a pattern that is offset for the thickness of the face coating. Once the bulk of the tool has cured it is suspended over the finishing pattern and the face coat is poured or injected into the gap via a sprue hole moulded into the centre of the back-up casting, until it reaches vents or the edge. Owing to the small thickness of the surface, very little heat is generated and shrinkage is minimised (Figure 9.6).

Metal-faced tooling

Electroformed nickel tooling can be considered when longer lead times are permissible, high-production volumes are expected and when a high surface finish is critical. This process can use low-cost patterns usually made of plastic laminate. The plastic is made conductive by depositing a thin layer of silver on the surface. The pattern is immersed in a solution and current is applied to the silver layer. The thickness of the nickel is determined by the current and build-up time allowed. The mating mould can be made on a separate pattern at the same time or after a part offset is

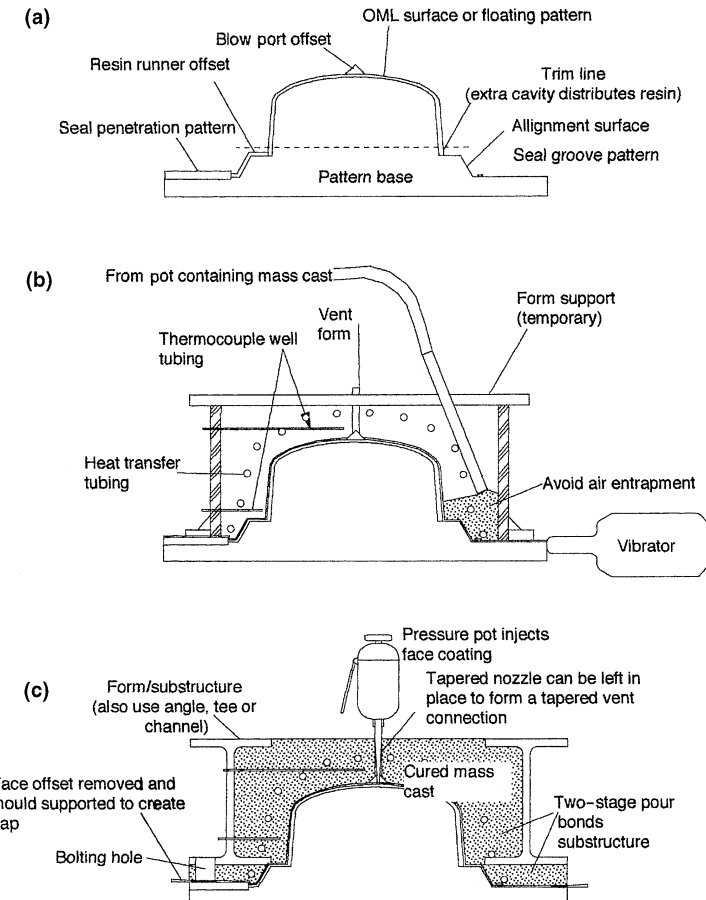


Figure 9.6 Mass-cast tooling processes: (a) preparing the pattern for face coating (or the sheet wax if face casting); (b) pouring the mass cast after the face coating has been applied; (c) the face casting technique. OML= outside mould line.

applied to the first half and the process is repeated. Then the mould face will need to be reinforced with epoxy laminate, welded substructure or mass casting. Welded substructure can be attached via threaded nuts or other inserts that are grown into the nickel. For RTM tooling with discontinuous substructure, extra thickness is advisable (7 mm minimum) and substructure should be very well distributed on no more than 15 cm centres. A metal mould can also be plated with nickel to improve its wear resistance, but existing surface imperfections will be amplified in this process.

An alternative to electroforming is the electroless nickel plating process. Since electrical conductivity is not necessary, a plastic mould or

pattern can be coated with a nickel layer after the surface is made catalytic. There is no theoretical limit on the thickness of the coating and it has a hardness of 49 Rc as plated. A heat treatment at 400°C for 1 h can increase the hardness to 70 Rc. Like electroformed tooling, the porosity should be almost zero and a very high surface polish can be obtained. Adhesion to the forming surface is not as good as with electroplating onto metal, so it is usually not used as a secondary mould treatment to increase the hardness of an existing metal mould. Electroless nickel is usually plated onto a pattern and backed up with substructure. The coating thickness is likely to be more consistent with the electroless process than with electroplating, especially on sharp radii and in narrow crevices.

Spray metallising involves melting a metal in a gun which uses a gas jet to propel the molten droplet onto a substrate (pattern). The droplets cool during flight and upon impact with the previous layer, forming a purely mechanical bond. The process results in a porous surface, with 1% void being a practical minimum. The temperature experienced by the pattern depends on the material and deposition rate, but metallising can be done on plastic and plaster patterns when tin, zinc and aluminium alloys are used. Kirksite is a common alloy used for heat-sensitive substrates, since temperatures less than 35°C are experienced. With a temperature-resistant pattern, use of extremely hard carbides and ceramics is possible. A back-up structure is necessary and is cast or laid on the mould back before demoulding from the parting line base. Often the tool surface must be sealed with a mould sealer or by electroplating, unless the back-up material penetrates into the face porosity.

Vapour deposition can be used to build up the desired tool or face thickness of almost any material onto a pattern. Many types of vapour deposition have evolved and vary in applicability. The cost may be higher than other replication systems but almost universal pattern compatibility, relatively high deposition rates and thickness uniformity with complex shapes are possible.

Cast metal tooling

A variety of metals can be cast and are suitable for tooling. Low melting point alloys can be poured into preheated moulds made from a tool pattern (often made from a part pattern). Each tool section is cast separately in a similar manner, preferably from the same ladle and with the moulds at the same temperature. The low-melt alloy can be selected to provide practically zero shrinkage against almost any mould material with good, as-cast accuracy and surface finish. But in service the mould temperatures are limited by the low melting point, as is the durability of these generally soft metals.

Higher melt temperature alloys are usually cast into green sand, investment or no-bake casting moulds. When investment casting is used the pattern is destroyed in the process of making the mould but no draft is required. When a removable (reusable) pattern is used the pattern must represent all mould surfaces and draft is necessary on the back as well as the front of the mould. The pattern usually must be larger than the required mould because of shrinkage upon casting, which is about 1% for iron. A parting plate, representing the parting surface of the mould, must be provided to create the mating surface between the sections of the foundry mould. This plate is removed after the first section is finished so that the next side can then be made with the pattern nested by the first. Finally, the pattern is removed from the mould and is replaced by molten metal. The mould is destroyed, exposing the rough mould segment. The casting risers and runners are removed and the surface must be ground or machined to final contour. The properties of the several castable alloys are shown in Table 9.1 (section 9.2).

Many ferrous alloys can be used for cast tooling and all can be heat treated to change their properties. Gray iron is the least expensive and is often subject to less distortion during casting than other castable ferrous alloys. Cast steel is preferred for its repairability, strength and hardness advantage, but is susceptible to slightly more distortion from casting. Ductile iron (also called spheroidal graphite or nodular iron) is in the middle and has higher strength and ductility than gray iron. Gray iron

Table 9.2 Comparison of heating systems

	Heat source	Advantages	Limitations
Integral Circulation	water	low cost, control ease	distribution tubing (channels)
	air oil	versatile, light cost efficient, control ease	bulky distribution ducting use low-wattage-density heating
Direct	electric blanket cartridge	integral, efficient	durability, distribution control
	strip	integral, efficient	quantity required, heat distribution irregular geometry
External Oven	air convection	versatile	slow heating, portable moulds
	radiant	fast	distribution depends on surface conditions
Press	heated platen	provides clamping and heating	mould must have a flat back

can be cast with an accuracy of approximately 3 mm/m. Most of the distortion will tend to be out-of-plane twisting, cupping or warping and is due to stresses created during phase change and cool down. Distortions are minimised by uniformity of casting thickness (no more than 20% variance in adjacent sections), adequate substructure depth and good foundry practice. Experience shows that out-of-plane distortions vary with geometry and degree of substructure. A circular tool 1.9 m in diameter with 25 cm deep substructure every 30° radially and around the perimeter distorts in a saddle shape with approximately 0.5 cm in total run-out when average foundry practices are used. Most ferrous alloys will polish to a high lustre but casting quality will vary. A class-A finish will be unlikely unless substantial machining is done to remove the surface voids (usually approximately 5 mm), otherwise casting pits must be welded. Invar is a ferrous alloy with about 36% nickel which exhibits a very low CTE and is popular for this reason. Since it is difficult to machine, invar is often cast to rough shape and then machined to final dimension. Alloys containing nickel generally have a higher melt temperature and are more difficult to cast but often have excellent corrosion resistance.

Aluminium alloys are excellent heat conductors and many are readily castable. Unless casting conditions are ideal, aluminium alloys tend to entrap more air under the surface than do higher density metals. Moulds are often pressure cast to reduce porosity. Aluminium has the highest heat conductivity of the common tooling materials and has enough durability for most aerospace applications, but the CTE of aluminium is nearly double that of iron. The higher material cost, lower durability and more expensive casting method are a disadvantage when compared with ferrous metals.

Aluminium bronze and beryllium copper alloys are often used to make plastics moulds, so their use for RTM should be considered. They have excellent corrosion resistance and high strength. Although pure copper cannot be cast, fair thermal conductivity combined with good hardness are the primary reasons for selecting cupric alloys. Silicon bronze is highly weldable using most conventional welding techniques and has good, well rounded, properties.

Almost unlimited possibilities exist for alloy selection, casting method and heat treatment. Investment casting can be used, where the budget will allow, for more precise or complex castings. Another advantage of cast tooling is that the substructure can be of the same material and can be cast directly onto the mould. The substructure provides support during casting cool-down, heat treating and machining and carries clamping loads in service. When designing a casting, the thickness should be as uniform as possible to minimise cold tearing, shrinkage cavities and other casting problems. The interface of the tool face with stiffening blades and other locations where the thickness necessarily

varies should be given a generous (1 cm minimum) fillet radius. Substructure members such as blade stiffeners, bosses, bathtub flanges and other features need draft on both sides of the parting plane if the use of expensive cores or investment casting is to be avoided.

A smooth finish is necessary on all surfaces of the casting pattern to reduce the force required to demould the pattern from the foundry moulds. Mould casting patterns can be made directly from the part pattern, using laminate with or without a sandwiched core of tooling dough (syntactic foam) to build up the required casting thickness. This is done while the part pattern is nested in a fixture that defines the parting plane and other flange features. The drafted substructure members are added to stabilise the laminate prior to demoulding. Once demoulded from the parting plane features the second tool section can be made from the first, with the part pattern still in place. Substructure and other features are then added to the second half as before. It is important that the substructure be well attached to the face in order to prevent disbond from the face while being demoulded at the foundry. Adhesive attachment alone is not recommended to connect the substructure but should be aided by screws or other mechanical fasteners. Also, it is advisable to lay reinforcement over the fillet and up the side of the substructure, overlapping both sides by 2–3 cm (Figure 9.7).

Most castings should be heat treated to relieve residual stresses before significant machining is done, and all heat treatment must be done before polishing. The amount of distortion which occurs upon hardening is of utmost concern, since machining a hardened material is difficult.

Ceramic tooling

Ceramic properties and processing methods vary widely, but some generalisations can be made. Ceramic's strong suits are hardness and a low CTE, often exceeding metals substantially in hardness and closely

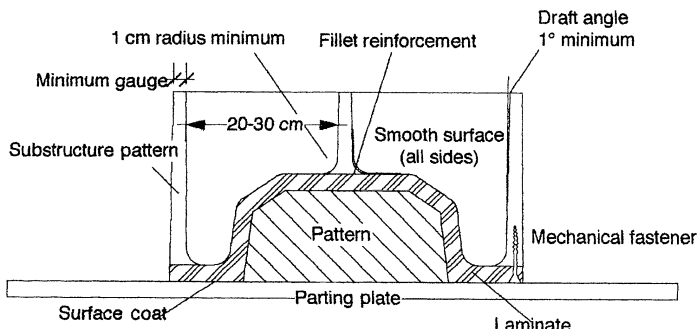


Figure 9.7 Features for cast tooling patterns.

matching graphite in CTE. Ceramic materials are usually made by replication processes and can have shrinkage, but some are machinable. Ceramics are usually at least slightly porous and are almost always brittle. Ceramic tooling is rarely used for RTM, but recent advances in properties and processing are likely to change that soon.

9.3 TOOLING COST CONSIDERATIONS

9.3.1 MANUFACTURING RATE AND VOLUME CAPACITY

The anticipated production volume and rate are the most important factors for selecting the best material and mould manufacturing process. When high volume and rate of production is expected the tooling efficiency becomes even more crucial and breakdowns are more expensive. The production capacity is proportional to the number of moulds and inversely proportional to the process cycle time. Reduction of cycle time is preferable to an increase in number of mould sets, and mould design can certainly affect the cycle time. It is difficult to obtain an accurate estimate of minimum cycle times before tooling has been designed. The designer should consider that while the mould is open it is not serving its function (making money). It is crucial that the mould designer minimises open mould time by proper selection and design of mould features. Open mould processes include mould preparation, preform placement, mould closure, clamping, mould opening and part demoulding. A simple feature to ease demoulding or preform placement can save many hours of open mould time over a production run. Closed-mould processes such as injection and cure represent the balance of the total cycle time and their duration should also be minimised. Tooling may also have an influence on these cycle times, but usually to a lesser degree. For example, heating rate or injection pressure can be limited by tooling and thereby influence closed-mould process times.

9.3.2 PROTOTYPE MOULDS

Even for an experienced RTM mould designer, cycle times and possible tooling difficulties are difficult to predict because of inevitable part variations. A prototype mould made from a less expensive material or on a smaller scale is very useful for debugging tooling and manufacturing details. Prototype moulds are also useful in marketing and testing prior to investing in production tooling. Various preform placement, injection and demould systems can be tested and the tooling modified for production as necessary. A useful advantage of cast metal tooling is that the foundry patterns can be used to make oversized RTM prototypes before casting metal.

9.3.3 RIGID VERSUS SEMI-RIGID TOOLING

Early on in the process of designing the RTM part, the use of semi-rigid tooling should be considered. Since only one mould half is rigid and the other is a flexible bag material the initial tooling costs are usually about half that of comparable rigid tooling. However, the recurring costs are higher, since the process has a higher labour content. The process is limited to atmospheric (or autoclave) pressure so there are no clamping requirements, but the process is usually slow, limiting production rate and resin selection. Semi-rigid tooling is most useful for prototypes or where the rate of production is limited. When bags are used to make hollow areas inside the part where it is surrounded by rigid OML tooling the pressures are not inherently limited and the bag serves as a mandrel rather than as a main tool segment. Internal bladders are discussed in Chapter 10 (Section 10.5).

9.3.4 THE EFFECT OF PRECISION ON TOOLING COSTS

The effects of precision on tooling costs depends upon the type of tooling to be made and the method used for its manufacture. Obviously, high precision influences the pattern making cost when traditional methods such as plaster sweeping are used. CNC machined patterns have good accuracy, which can be improved by using a higher density pattern stock, but this also increases the pattern costs. Lamine and mass-cast tooling must be carefully made and the pattern properly scaled when the tolerances are low. For high-precision applications additional sub-structure is required, also contributing to the tool cost. Precision is expensive and should be demanded only to the extent absolutely necessary.

9.3.5 ESTIMATING THE DURABILITY OF MOULDS

Mould durability directly affects tooling cost, and production costs as well if tool costs are amortised over the tool life. When estimating the durability of a mould one must first determine a failure mode. The useful life of a mould is ended for one of two reasons: normal wear or catastrophic failure. The mould surface is subject to chemical and physical deterioration by fibre abrasion, operator error or abuse, resin corrosion and frequent heat cycles, all of which can damage the mould. Moulds made of metal are generally harder and the contents are more easily released from them than is the case for plastic moulds, providing superior durability. Combinations of materials with drastically different properties (metal faced plastic tooling) can perform synergistically, being both cost efficient and durable. A well designed, hardened tool steel mould can last for 500 000–1000 000 cycles. Aluminium tools can last for 15 000–20 000 cycles and epoxy faced tools around 1000–5000 cycles if no

abuse occurs. As can be expected, the durability is also determined by the precision, surface finish requirements and the amount of maintenance provided. In most situations, the greatest threat to tool durability is the operator. Moulds can be damaged by a hurried operator while he or she demoulds a part or removes the resin from the ports. Handling precautions and restricted use of hard hand tools can extend the life of a mould.

Mould failure by wear

Wear from abrasion and scratching occurs when dry fibre rubs against the mould or when scissors, knives or other tools are allowed to contact the mould. A higher bulk factor in the preform will result in more wear during mould closure. The hardness of the mould surface is a primary determining factor in resisting abrasion for metal moulds. The abrasion resistance of a plastic face coating depends on the fillers used and the resin toughness. Surface hardness is important for abrasion resistance, but the overall material hardness is also important where severe forces are encountered. If the underlying material deforms, a hard surface cannot restrain the applied force and the surface will chip, crack or disbond. This condition can be worse than if no coating were applied at all since repair may require stripping, rebuilding the damage and replacing the coating. Steel tools that are not coated can be flame hardened on shear edges, and repairs on worn or dented areas can be made with a hard welding rod. Impact most often occurs during the demoulding process when demould difficulties are encountered. Reliable and redundant demoulding and mould release processes are advisable to extend tool life and avoid production delays. Guide pins, bushings and threads should be replaceable, or have replaceable inserts, since they are high-wear items.

Chemical compatibility of mould and process

Some resins, such as phenolics, polyesters and vinyl esters, can deteriorate vulnerable mould materials by acid or styrene attack. Therefore the chemical resistance of the surface may be important to mould durability. For this reason stainless steel is becoming popular for tooling, and in humid conditions moisture corrosion can also be avoided (not uncommon with ferrous tools, even overnight). It is advisable to store moulds sealed, with plugs in the ports and desiccant in the cavity. The porosity of the surface or coating also effects its resistance to chemical attack. A low-porosity, high-gloss finish minimises the surface area in contact with the resin and reduces the number of locations where chemical deposits can start to build up. Surface release agents can also be a factor in

chemical protection; in the extreme case a release film can be used to protect the mould surface but will require replacement for each cycle and must be removed from the part after demould. Usually this is done only with temporary prototype tooling which may be too porous otherwise.

Catastrophic mould failure

In some cases the failure is more catastrophic (if not more tragic), and can occur during clamping, heating, pressurising, demoulding or while moving the mould. These failure modes are not as predictable and should be avoided with conservative load estimates and high safety margins on all critical factors. Moulds with perimeter clamping are likely to be stiffness critical, so it is likely that more than adequate strength exists for unexpected loads. Very brittle materials, sensitive to stress concentrations, are not recommended for carrying clamping loads. Instead, brittle moulds should be used with a very rigid substructure or press platen to carry all but compressive loads. Runaway heaters or ovens have destroyed many moulds, usually when redundant high-limit safety controls are not properly installed or maintained.

9.4 GEOMETRIC CONSIDERATIONS FOR MOULDS FOR USE IN RESIN TRANSFER MOULDING

9.4.1 NET VERSUS EXCESS MOULDING

It is possible with RTM to produce parts that do not require trim after moulding. However, in most cases the most efficient way to produce the part is to mould it in excess, then trim it to size. Partially, this is because moulding a part net requires a higher degree of preforming precision. Furthermore, careful preform placement in a net situation usually consumes valuable mould time, whereas trim is usually a quick operation that may not require a mould. Many times both net and excess moulding are used in the same part. For example, long slender parts are often net in cross-section, but the length must be trimmed. This has benefits in both preform placement and flow control. The resin-rich end can be used to distribute the resin, promoting a smooth flow front. In cases where parts are moulded excess, a mould feature known as a pinch strip can be used to restrict flow around the resin-rich edge of a part. A pinch strip is a raised ridge in the mould that compresses the preform to a higher volume fraction locally, usually from 70% to 80%. The ridge ramp should be smooth enough so as not to be bridged by the preform and thus causing a new resin-rich area and associated flow problems. The ends of the pinch strip may need special consideration to prevent resin entrance and thereby bypassing of the preform.

9.4.2 MOULD GAP DESIGN

The majority of aerospace composite parts are made with bag moulding of prepreg where no precise way of controlling the thickness is available. With RTM the mould gap (thickness) determines the fibre loading of the part. The mould gap for a given area of a preform can be calculated by using equation (9.1):

$$\text{mould gap} = \frac{(\text{areal weight}) (\text{number of plies})}{(\text{volume fraction}) (\text{fibre density})} \quad (9.1)$$

9.4.3 PARTING LINE CONSIDERATIONS

One of the first concerns of the tooling designer is establishing the parting line geometry. The parting location on an existing pattern can be found for a particular parting axis by fixing this axis normal to a flat surface. A straight edge kept normal to the surface and moved around the perimeter of pattern will trace the parting line where it contacts the pattern. The angles between the straight edge and the pattern, on both sides of the point of contact, are the draft angles. The parting plane is a reference plane normal to the parting axis and would be parallel to the press platens if so mounted. Parallels to the parting axis (direction of draw) are the references by which draft is measured. When the draft is small the possibility of demould and preform placement difficulties are increased. The minimum draft angle varies depending upon the situation but is considered to be about 1° for an isothermal cycle. When the mould temperature is cycled the draft can be reduced to zero if the part has a substantially higher CTE than the OML tooling, or a lower CTE than the IML tooling. Figure 9.8 shows a process that can be used to select and optimise parting line location.

It is usually necessary to consider the preform placement method and estimated bulk factor when designing the mould parting line. The parting line need not stay in a single plane, but tooling costs are usually reduced when it does. There is usually more than one parting plane option to consider. However, one parting line option should provide the best combination of the following benefits:

- more draft;
- reduced cavity depth;
- inherent or easier mould guidance;
- more obtuse angle at shear edge;
- reduced displacement of material to machine part cavity and flange;
- more structural integrity to tool (or part prior to trim);
- simplified provisions for debulk of preform;
- the possibility of parting line injection and/or venting;

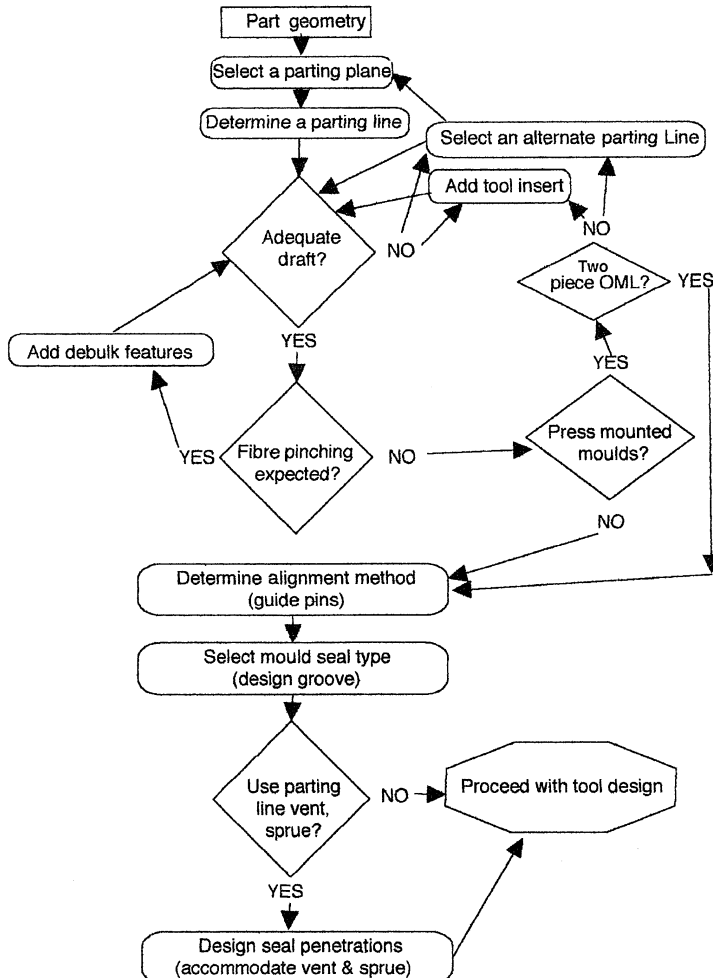


Figure 9.8 Parting line design process.

- more efficient tool loading procedure or verification thereof.

Figure 9.9 illustrates an example of a mould with a variety of parting line features.

9.4.4 DESIGNING THE TOOL FLANGE GEOMETRY

Once the parting line location has been determined the tool flange should be designed. The flange of the tool should be wide enough to accommodate any features and react landing loads over a safe area but should be no wider than necessary. Patterns, however, should have excess flange

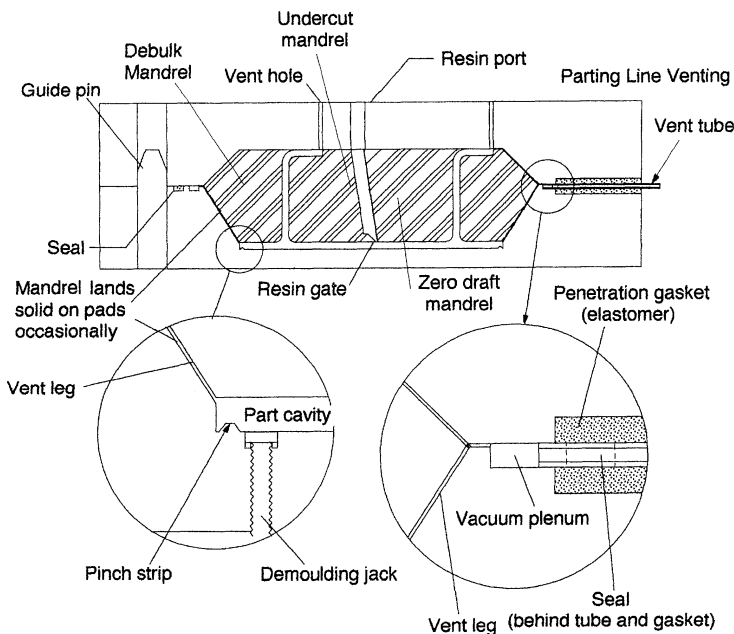


Figure 9.9 Parting line features.

with plenty of trim space or room for casting forms. The tool flange may contribute to or contain the following features:

- mould seal;
- cavities for seal penetration gaskets;
- resin distribution runners;
- injection ports;
- vacuum ports (vents);
- resin heating channels;
- resin entrance gates;
- purge resin traps;
- preform pinch-off strips;
- mould guide pins or guidance geometry;
- mould opening jacks;
- mould clamping bolt holes;
- necessary mould structure;
- demoulding access locations or stripping bypass;
- mould landing.

All cavities inside the seal groove, as well as all plumbing lines, will be filled with solid resin. When access to a port or vent is limited to the ends, the hole must be lined with an expendable tube, tapered and accessible to the knock-out resin plug, or be drilled out after each cure.

Where the hole contacts the part, the resin must be drilled out or broken off, making part demoulding more difficult. It is easy to realise the benefit of parting line plumbing, since the resin-filled cavities can be removed with the part and flashing. Features such as resin heating, distribution channels, resin entrance gates, purge resin traps and all other plumbing are more easily maintained when in the mould flange. Draft is usually not necessary on the sides of these channels since resin shrinkage will create some clearance, but drafted or half-round geometry will ease clean-up and tool replication processes.

Mould guidance features

The mould halves must be properly aligned before shear edges or the preform are encountered. When tapered pins or bosses are used the taper should end at the point where critical mould alignment is required. Parts with high draft may not require guidance until completely closed, requiring the mould to have only short cones to achieve alignment. With weaker mould materials it may be preferable to use a more distributed converging geometry in the flange. Situations with deep mandrels may require long guide pins with rounded or bevelled tips. These pins should be large enough to resist accidental bending.

Mould seal design

An important function of the mould flange is to contain and compress the seal in an appropriate groove. The mould must be sealed vacuum-tight for most aerospace applications since a vacuum is applied to the mould. The groove should be placed as close as possible to the part to minimise flashing, reduce resin flow around the edges, reduce the clamping force and allow the clamps to be placed closer. However, the seal groove must be outside any parting line feature that is to distribute resin and far enough away from the cavity so as not to be easily contaminated by stray fibres (usually about 4 mm away). The preferred seal design varies widely among the various RTM manufacturers and tooling vendors. Among the most common are O-ring and rectangular elastomer sections that are accommodated by a groove in either one or both adjacent surfaces. O-rings are used with a groove shallow enough to expose some of the elastomer for contact with the mating half and also in matched semicircular grooves in both halves. The amount of compression required depends upon many factors, but primarily on the amount of variance in the closure gap. More complicated seal cross-sections are finding use, as is redundancy, in an effort to improve seal integrity and reliability. It is necessary to compress the rubber until the required pressure sealing capacity is attained. The amount of compression depends on the width of the seal, the hardness of rubber and the amount of

deviation in the mould flange gap. Soft materials are easier to compress but must be compressed more to achieve the same pressure capacity. Thus soft rubbers and foams are generally only used where the seal must accommodate varying gaps and where pressures are low. Hard rubbers are more durable and achieve the desired pressure with less compression, but little mould flex or distortion is permissible. The seal groove must accommodate the expansion of the seal stock during compression and heat-up. Typically, this is accomplished by using a seal that is narrower than the groove, but some designs utilise an extrusion with a compressible foam rubber core. The best seal designs are durable, easy to clean of resin debris and are reliable (Figure 9.10).

Silicone and Viton® are the most common elastomers from which seal stock is made and are used in solid, foamed or combined form. High durometer (Shore A80) solid rubbers are used where clamping force and injection pressures are high. Some of the reasons why seals fail are: fibre or resin chips across the seal face, worn or cracked seal stock, the seal being covered with a thin layer of resin deposits, tool distortion allowing excessive gap, inadequate clamping force and improper seal stock. Seals are often held in place and repaired with a silicone RTV caulk. Complex seals can also be cast from liquid silicone into the groove before or after closing the mould. The interference can be provided by the very high

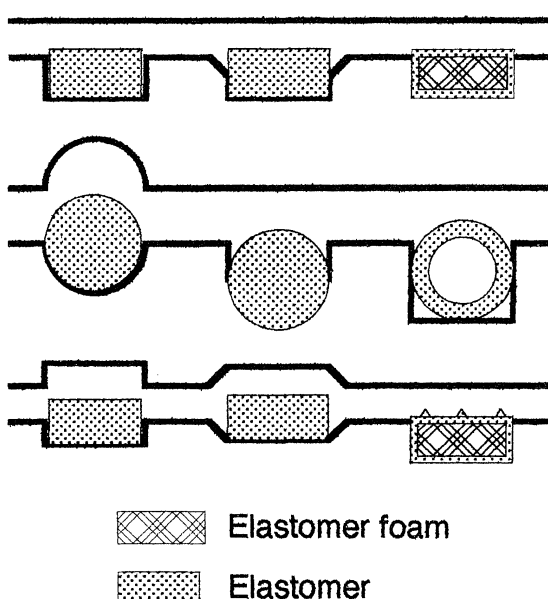


Figure 9.10 Various seal types and groove configurations.

CTE of the silicone when the mould is heated or by use of spacer tape to hold the mould sections apart during casting.

When more than two OML moulds sections are required, the seal must interface with an out-of-plane counterpart. The two seals can be butted to form a tee. It is crucial that both seals touch elastomer-to-elastomer with smooth surfaces. The seal-to-seal interface is a location where leaks often occur and should be avoided by using mandrels where possible. This problem and other trouble areas may benefit from the addition of vacuum grease or bagging tape to assist the seal, where preform contamination potential can be eliminated. The other location where seals frequently leak is where the ports cross over. Usually, this interface is sealed with an elastomer bushing that fits over the port tubing and is clamped in a cavity that compresses it against the mould seal.

Mould landing geometry

In order to close consistently, part of the mould flange needs to mate solidly. If the parting line is not used as a resin distribution channel it is usually landed everywhere inside the seal. This minimises resin channels around the part that might affect injection. It is not necessary to land the entire mould flange; clearance outside the seal may be useful for wedging the mould open and to reduce the possibility of a resin chip holding the mould open. A consistent space should be used around the perimeter to allow a thickness gauge to verify the mould gap, particularly when bolt clamping. When the parting line contains a resin distribution groove the landing may be outside the seal. The substructure carrying the clamping force should be as close as possible to the landing, minimising the moment arm on landing loads. The entire press capacity minus the preform debulk force must be carried on the landings until injection. The size of these pads varies widely depending on mould composition but should be sized according to the compressive strength of the material in contact, with a substantial safety margin. Even when the mould is not vented or injected through the parting line, the resin channelling potential of a gap in the parting line should be anticipated. It is preferable not to have a parting line gap parallel to the injection path, which can provide an alternate path of least resistance. Adjustment of the mould landing gap as well as a mould opening can be combined in a single jack screw system. This is especially useful for foam core moulds, which may not have the anticipated dimensions designed for in the RTM mould cavity.

9.4.5 ACCOMMODATING UNDERCUTS AND ZERO DRAFT SITUATIONS

When it is not possible to have a simple two-piece mould because of draft or anticipated preform placement restrictions, more tool segments,

or inserts, are necessary. Each undercut in the geometry is then considered with another parting plane, and a parting line for the insert is determined. More than one undercut can be defined by the same insert when the same direction of draw is suitable for all. The same criteria used for the OML parting line can be applied to that of the insert with more emphasis given to the preform placement, alignment and tool loading procedure. Each tool section must be cleaned, handled and treated with release agents, so inserts are used only when necessary.

9.4.6 GUIDANCE OF TOOL INSERTS

Guidance of inserts is usually provided by the closing action of the OML tool segments in combination with a tapered guidance boss or other self-aligning geometry. Truncated cones, pyramids and semi-ellipsoids are common since they provide a progressive alignment action and can be easily disassembled even when full of resin. One degree of draft (2° included angle) is a minimum for easy release, but will not provide for much misalignment. An included angle of 100° (50° of draft) can be used for maximum alignment motion but not with materials that tend to gall or that might deform or fracture under the high load that gentle inclines may require. Neither can these shallow angles be used for debulking force, since most of the force is lost to friction. Most guidance pins have between 60° and 90° included angle, since this combines moderate alignment motion with lower loads. For mandrels that contact more than one primary mould section, these angles do not need to be symmetric across the parting line. In fact for many applications where the part is twisted the guide angle varies on edge mandrels to allow the mould flange to be a plane.

9.4.7 DESIGNING PREFORM CONTROL AND DEBULK FEATURES

The preform may have a substantial bulk factor which must be accommodated by the mould. Difficulty arises when the fibre is pinched between two closing sections, damaging the reinforcement and the mould. Compaction normal to the parting plane is usually handled by offsetting the mould parting line from the part parting line by the expected uncompacted preform height. The part cavity is thereby recessed into one half so that the other half bypasses it before encountering the preform. When too high a bulk factor exists, the outermost plies are likely to exhibit wrinkling if the preform cannot distribute the compression along the fabric bias. Elimination of the preform bulk factor prior to placement is the best way to solve this problem, but where this is difficult or cost-prohibitive other tooling arrangements can be made.

Unlike simple undercuts, preform debulking inserts are expected to do work (exert force through a distance) and therefore must be more carefully designed. The closing action of the OML moulds is used to compress the preform by using a wedge-like geometry to transform the direction of motion. The smaller included angle will provide more precise control of the translation distance and greater mechanical advantage for debulking, whereas the larger angle will provide for more bulk. The insert should be constrained in all directions by appropriately drafted surfaces. When the mandrel has a much higher CTE than the OML tooling, longitudinal clearance should be provided for mandrel expansion. Once the debulking action is accomplished it is possible to lock the mandrel in position by using three surfaces to trap the mandrel, as shown in section 9.8 (Figure 9.15).

In cases such as a stiffener in the middle of a skin, the force used to debulk the stiffener preform must be generated by a perpendicular preform surface (the skin). When this is the case, it is necessary to design the mandrel such that the pressure from the skin preform gains a mechanical advantage over the stiffener preform. The area against the skin can be increased by placing a step in the wedge geometry, as shown in Figure 9.11. Without the step, any area increase on the skin is countered by a loss in mechanical advantage from the wedge angle. The wedge is usually truncated on the bottom to form a landing. This reduces the

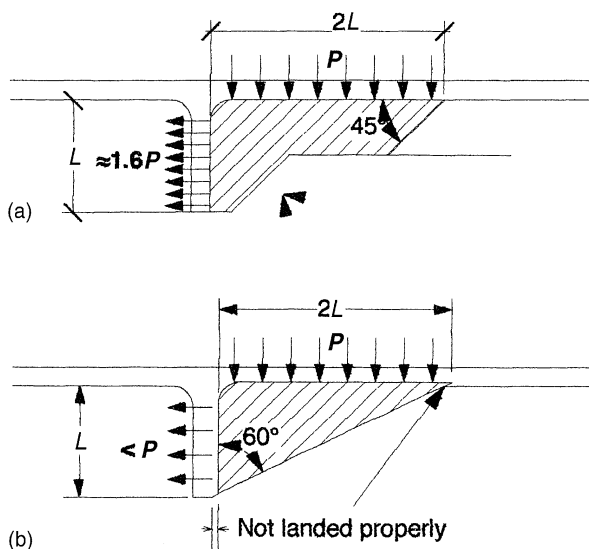


Figure 9.11 Debulking one preform with another: (a) good design (greater area with a steeper angle properly debulks the preform); (b) poor design.

likelihood of mandrel damage and provides a more solid stop. If these precautions are not observed, the mandrel may excessively compress the skin without debulking the stiffener, causing both quality and processing problems. If the mandrel can extend lengthwise beyond the part or can land on intermittent holes in the skin preform, the skin thickness distribution would be improved. When the stiffener preform can be pre-debulked to net size it may still be necessary to use a mandrel for pre-form placement and demoulding reasons.

To reduce the clean-up effort required to remove resin flashing from insert guide faces, clearance can be provided on the majority of the guide surfaces. This can be achieved if the alignment force is applied to raised bearing pads. These replaceable bearing pads are ideally composed of a low-friction, gall-resistant and self-releasing material, otherwise the rubbing action of closure can remove release agent from these areas, complicate clean-up and limit the tooling durability. When the majority of the non-part area is relieved, the resin is thick enough to be easily removed, but channels for resin bypass during injection are also opened. However, these channels may exist anyway, and should be given consideration when selecting the port locations. The pads can be used to restrict resin flow more easily when made from a more compressible material such as PTFE (polytetrafluoroethylene), but at the expense of a decrease in guidance precision. Steel mould surfaces with brass bearing pads can provide very precise and durable alignment.

When many mandrels in a row are used, the accumulated preform bulk between the mandrels can be substantial. Even when debulking mandrels are used on both edges, it can be difficult to position the last mandrel. In this situation it is useful to incorporate a feature in the ends of the first and penultimate mandrel. This allows a clamp to get a hold, providing some of the force required to compress the mandrels together. This system must be used on both ends simultaneously and possibly in the middle of long mandrels that might flex.

Long slender mandrels such as are used for control surface cavities are best supported at both ends, but should be clamped at least at one end to control the tendency for the mandrels to rotate slightly during final debulk. This can be accomplished by extending the mandrel out beyond the part, where a flat will become clamped in a similarly shaped cavity in the OML tools. Tooling example 4 demonstrates this configuration (section 9.8, Figure 9.18).

9.4.8 FREE-FLOATING INSERTS

Free-floating inserts depend on the preform to provide alignment, which can frequently allow variation in adjacent laminate thickness. The amount of variance depends on the mandrel weight, the weight distri-

bution, preform volume fraction and injection pressure distribution. With attention to these factors the volume fraction can be kept within 5% of the target. Fully floating mandrels and cores should be as light as possible and orientated to distribute the weight over a maximum amount of preform surface or directly into the OML sections. Where allowable the mandrel can be supported by tapered supports that penetrate the preform, creating moulded-in holes. Metal inserts in the preform can provide both support for the mandrel and a service function later.

9.4.9 PART DEMOULDING CONSIDERATIONS

The part may be flush with the parting line or recessed into one mould section, with no place to wedge under the part or apply demoulding force. Usually all that is required for part removal is access to the interface between the part and the offending mould section. By staggering the parting line from one side of the part to the other in a strategic location one can use a plastic or wood wedge and compressed air under the part. When the injection port is on the offending tool section, compressed air can be applied to the cleaned port to force the part from the mould. Otherwise, a blow port can be located in the mould half that the part will cling to. Sometimes this can be a difficult prediction to make, but most of the time the part will stay with the side having one or more of the following: the greatest wetted surface, the least draft, a male plug, mandrel guide pins or the roughest surface. To insure that the part will always cling to the same side, an intentional undercut or moveable pin can be used to restrain the part until the mould is open, then the parts sides are flexed or the pin removed to clear the undercuts. Blow port design should be kept simple but must provide a reliable seal and cover enough surface for the compressed air to crack the valve and part loose. A 2 cm diameter, 90° cone-shaped plug fitted into a countersunk hole through the mould usually has enough force to crack a thin part away from the mould. Unless composed of an elastomer, the plug may also require a seal to maintain vacuum integrity. Release of thick or sandwich panels is more difficult to initiate and may require the addition of a jack screw or provisions for a light hammer blow to the plug (Figure 9.12). Once the crack is started the air pressure may need to be regulated to prevent overpressuring and excessive flexing of the laminate.

Often thicker parts are best demoulded by a jacking action rather than by pneumatic pressure. A head, fitting flush with the mould, can be screwed into the mould cavity in a slow and controlled manner until the part is free. The head can contact with a gasket in a counter-bore while being retracted, maintaining a tight seal during injection and creating a smooth finish. The jack can create substantial force, so the location of the jack should be located where it will not bind the part and where the part

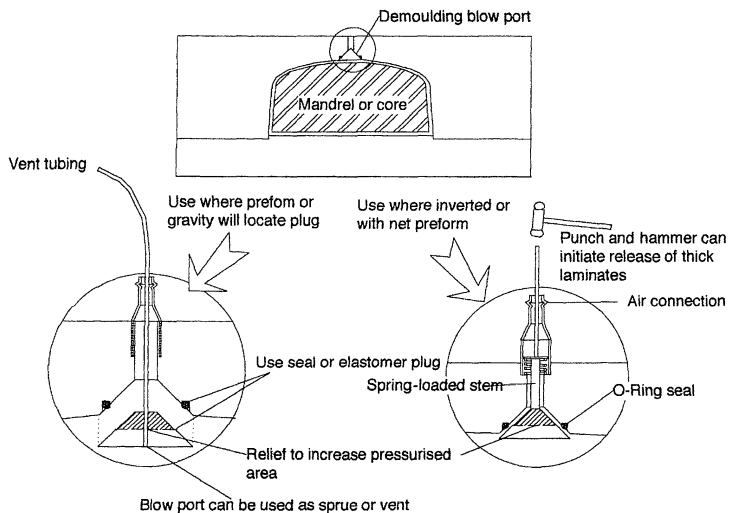


Figure 9.12 Examples of blow port designs.

is strong enough at demould temperature. Often a demoulding jack is applied or even attached to a mandrel where damage to the part is unlikely.

When the part can be much more easily extracted from one mould section than the others it is possible to bypass and undercut the part with a feature that can pull the part from the stubborn half. The undercut should be placed at necessary mould contours where possible, but can also be used explicitly for demoulding in an inconspicuous area. If semi-permanently mounted to one primary mould section this bypass should incorporate an undercut or ridge that can be cleared by flexing either the part or the bypass, or by pulling sideways on the part, as shown in Figure 9.13. In some cases the preform cannot be placed because of the bypass or undercut mandrel; in this case it must be temporarily removed and placed in the female cavity until the mould is closed. Then it is locked to the other section ready for service. A reliable demoulding process greatly aids in process automation.

For isothermal mould conditions the part will tend to remain on a male plug because of resin shrinkage. When the mould is allowed to cool before demould the CTE differential must be considered. A sizeable graphite part in an aluminium mould will become trapped in a female cavity if allowed to cool. In this situation part or mould damage can occur if precautions are not taken to provide relief around the edges. When parts are moulded in excess, the resin richness around the edge will shrink away from the edges and provide some clearance, as will the shrinkage in the rest of the part, to a lesser degree. CTE mismatch can aid

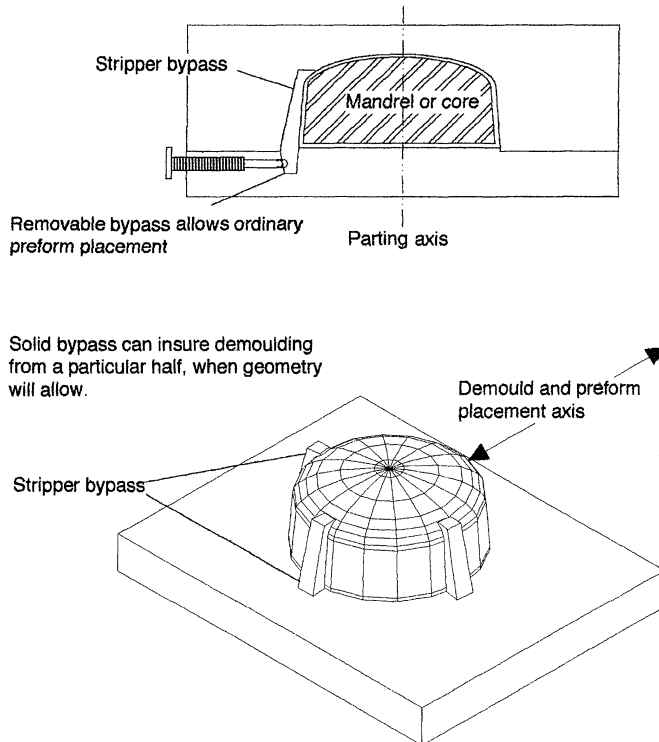


Figure 9.13 Demoulding aids for tooling in resin transfer moulding.

in demoulding when the appropriate differences exist for both OML and IML tools. Zero mould draft is possible under these conditions when a good surface finish exists on the mould. OML tool sections should have a CTE less than the part, whereas IML inserts should have a higher CTE when demoulding assistance is expected. A minimum CTE difference of $10 \times 10^{-6} \text{ }^{\circ}\text{C}$ is required to obtain reasonable demoulding ease for small internal cross-sections with gentle radii. Sharp edges should be avoided on all surfaces with little draft. Temperatures higher than 55°C are difficult and very uncomfortable for manual demoulding, so aids are more important in these situations.

9.5 THERMAL CONSIDERATIONS IN MOULD DESIGN IN RESIN TRANSFER MOULDING

9.5.1 MOULD HEATING

For aerospace applications it is necessary that the resin be cured at above ambient temperatures. Usually it is also necessary to inject at elevated

temperatures, since the viscosity of the resin at room temperature is likely to be too high. Ideally, the resin is injected and cured at the same temperature, but many situations do not allow isothermal processing. If the part can be partially cured in an isothermal mould hard enough to allow demoulding it may be possible to post-cure the part separately, either free-standing or in a support fixture. When an isothermal mould is possible, it can usually be cycled faster, it is easier to obtain a uniform temperature distribution and it requires less heater power with less frequent spacing. Mandrels may need separate heating when heat transfer is limited, because of insulating preforms, low mandrel thermal conductivity or time constraints. Integral electric heaters or fluid convection can be used to heat the mandrels or distribute the heat through the mandrel. Seals for fluid or power attachment should be on one end when mandrel thermal expansion may otherwise load the connection.

Selecting a heating system

There are many factors to consider when selecting a heating system. The mould heating and mould clamping systems must be compatible. For example, an oven and press are not likely to be compatible unless combined. In general, portable clamps lend themselves to a greater variety of heating systems. Consider the effects of heat on the clamps or how they can be insulated if necessary. Table 9.2 compares many heating systems. The following factors affect the selection of a heating system for RTM moulds:

- equipment availability (compatibility with other moulds);
- low production rate (use external heating such as an oven);
- clamping system (portable or stationary);
- temperature requirements (some systems are limited);
- mould material (thermal conductivity and specific heat);
- energy cost (electricity, gas, oil etc.);
- size of tool (plumbing logistics, weight of fluid, control)

Heat distribution

The thermal conductivity of the mould material is an important consideration when one is designing a mould heating system. A thick aluminium mould can be heated evenly with sparse heat input whereas a thin fibre glass tool requires thoroughly distributed heat input. Table 9.1, section 9.2, gives the thermal conductivity of some tooling materials. Metal moulds that operate at less than 125°C can be heated by sparsely spaced heat sources (3–6 times the distance from the face). Higher temperature metal moulds, or where heat-up rate is important, require more distributed heat input (less than 3 times the distance from the face). The

power requirements are usually determined by minimum heat-up times when ramping cure cycles are used. Isothermal moulds can be heated with much less heater power when heated continuously, and heat-up rate is not a problem. One must consider heat losses from conduction, convection and radiation and include 10% excess power as a safety margin.

Resin exotherm can require mould cooling when high production rates of thick laminates are sustained. Cooling can be provided easily with circulation heating but not with direct electric heaters. Another advantage of circulation heating systems is they are less likely to require as many control zones. The fluid flow paths should be designed to be short enough to carry enough fluid to minimise the temperature drop from inlet to exhaust. Multiple parallel fluid paths that interleave with each other and have opposing flow direction can further reduce temperature variations. The maximum length of tubing allowable depends on many factors, including the specific heat of the heat transfer fluid, the viscosity of the fluid and the size of the channel. For a low viscosity fluid (such as water) the fluid velocity should be approximately 60 cm/s to achieve good heat transfer with little back pressure. One must be sure that the plenum line feeding the various parallel legs is large enough to feed all with a similar pressure. For short distances it should have at least the sectional area as all the legs combined. For long plenums, at least twice this area should be used. It is possible to use 6 mm copper tubing, 8 m long, with water at 90°C through a cast iron mould with less than 2°C variation, but more, shorter, runs would improve uniformity for higher temperatures. The diameter of the tubing should be as large as possible while maintaining the bending radius required to conform to the tool surface. Other heat-transfer fluids can be used with similar results for higher temperatures.

Mould temperature control

In order to obtain a reliable and repeatable process, the mould temperature must be uniformly distributed and accurately controlled. The amount of control required depends upon the heating system, the heat-up rate and the temperature range. In all heated moulds a method of measuring the mould temperature is necessary. Even when the measurement is not used for control, such as when the mould is oven cured, the mould temperature may lag substantially behind the oven, so it should be verified. For integrally heated moulds the temperature sensor should be between the heater and the mould face. The sensor should be closer to the heater if slow heat-up rates are required; when faster heat-up rates are required the sensor should be closer to the mould face. Depending upon the geometry and control accuracy required, one or more heaters can be controlled in zones. The sensor should be located

near the centre of each zone. Zones can be large if power distribution is uniform, but where losses are high, such as around mounting bolts and a poorly insulated perimeter, temperature variations can occur. The heating controls and distribution systems should be designed to be expandable, in case cool or hot spots exist. Secondary limit controls should be used to assure over-temperature protection.

9.5.2 THERMAL EXPANSION OF THE MOULD

In order to mould a part with the correct final dimensions it is necessary that difference between the thermal expansion of the tooling and part is compensated for at the gel temperature of the resin. For an isothermal process, the mould temperature should be used. When the tooling is heated after injection, the temperature at which the resin gels can be estimated or measured experimentally. A more accurate method of determining the mould offset is to manufacture a test plaque under the expected mould conditions. This compensates for both CTE and resin shrinkage. The same tooling material is used and equipped with reference points scribed or other detail moulded into the plaque to allow measurement. The same ply lay-up configuration to be used for the part should be used in the plaque. Anisotropic CTE and shrinkage properties are typical for composites, therefore the scale factor may also need to be varied slightly in different directions. A good case can be made for invar or carbon tooling when large, high precision graphite parts are moulded. With carbon laminate tooling, the amount of thermal mismatch is reduced and even similar directional coefficients can be attained. The resin gel temperature is the point at which the part becomes a solid, and the mould temperature at this point determines its size. The part will then contract if cooled for service, and the resin may shrink. The resin shrinkage varies, depending upon the resin system, fibre orientation, cure schedule and part volume fraction. When epoxy resin is used with quasi-isotropic reinforcement at a 60% volume fraction it will shrink by approximately 0.03%. When part tolerance allows for some dimensional error, the mould scale factor can be disregarded as it is usually much less than 1%. For a desired part dimension, X_p , the tool dimension, X_M , can be determined by equation (9.2):

$$X_M = X_p [1 + (\alpha_M - \alpha_p)(T_{gel} - T_{use}) - S_r] \quad (9.2)$$

where

α_M and α_p are the coefficients of thermal expansion of the mould and part, respectively;

T_{gel} and T_{use} are the temperatures of the gel and the temperature used, respectively;

S_r is the resin shrinkage.

In-mould resin heating systems

Frequently, it is necessary when using one component resins to minimise the thermal history of the resin to extend the working life. One way of accomplishing this is by using a low resin temperature in the pot and heating only at the last minute. This is accomplished either by feeding the resin through a tortuous path or by fanning the flow into a thin cavity with sufficient surface area for uniform heat transfer. Resin heating may require additional heaters or heat transfer tubing to prevent localised cooling of the mould. The power required for resin heating can be estimated as follows:

$$P = Q_R C_P \Delta T_R \quad (9.3)$$

where

Q_R is the resin mass flow rate;

C_P is the specific heat of the resin;

ΔT_R is the change in temperature of the resin;

P is the power required.

Adequate power does not assure timely resin heat-up where flow rates are high or flow paths are short. For substantial resin heating, the heat transfer section should be controlled on a separate heat zone. It is possible to use the resin temperature as the control feedback signal in order to achieve more accurate control of resin temperature, but the surface of the heater must still have enough area so that it does not get too hot, causing premature resin cure against the heater. Heat transfer surfaces are usually sized for less than 1 W/cm^2 . For high demand, heat can be added by using a heated injection hose.

9.6 PHYSICAL REQUIREMENTS OF TOOLING IN RESIN TRANSFER MOULDING

9.6.1 SURFACE CHARACTERISTICS

It is necessary that the tool have the same surface finish or texture required on the part. Most composite parts made for aircraft do not need to have a high-gloss finish, and those that do will usually be painted. However, the mould finish will also effect the ease with which the part can be removed; the smoother the better. A high-gloss surface will also be more resistant to resin attack and delay deposit build-up. In all cases release agent and resin deposits will build up on the face, degrading the part finish. Eventually it will be necessary that deposits be stripped, possibly every 50 to 100 cycles for epoxy resins, depending on the release agent.

Hardness

The hardness necessary on the tool surface is dependent upon the durability expected, part geometry, operator care, reinforcement fibre type and part finish desired. For metal tools a gloss finish can be obtained and economically maintained on a tool surface with a Rockwell C30, but where a high lustre is required a Rockwell C50 or hard coating is recommended. Plastic faced and composite tools are typically softer than metal, but toughness and non-linear elastic properties can provide performance better than simple hardness numbers may imply. Some soft plastics resist abrasion an order of magnitude better than mild steel but may not be suitable mould materials for other reasons. The effect that surface properties such as hardness and finish have on durability often depends on the specifics of the preform placement process and geometry. Areas where fibre can be pinched are especially susceptible to abrasion and erosion from the dry reinforcement, particularly glass and carbon fibres (as aramid and polyethylene fibres are much less abrasive). Replaceable inserts of hard or tough material in these areas can extend mould life substantially. Tool erosion increases with bulk factor and fibre volume fraction. Wear is reduced when preform lay-up and debulking are done outside the RTM mould.

Methods for improving surface properties

Electroless plating, electroplating, vapour deposition, thermal spray, anodising and ion implantation are all means of hardening both physically and chemically. At least one of these methods can be used with almost every tooling surface. If selected and applied properly, hard coatings can increase the wear resistance of the mould by an order of magnitude. Keep in mind that some tool failures are not associated with wear, and a coating can reduce the repairability of the mould. The cost of applying these materials varies from an inexpensive hard anodised coating to a hard chrome electroplate which can cost as much as a mould set. With all materials, mould damage can occur, and a second backup set may be more useful than one that has been hard-coated.

Mould release and surface sealing

Dry fibre abrasion is the primary difference between RTM and other composites processes in release agent selection. The objectives are ease of release and minimum release agent transfer. Mould release agents are generally designed for a particular mould material and for specific temperature ranges. Most release agents are topical in nature, and act as a bonding barrier in a self-sacrificial manner. Semi-permanent release

agents bond to the mould and cure upon contact with air, moisture or heat. As their name would imply, semi-permanent mould releases can last for more than one cycle (as many as 20) and usually result in less release transfer to the part. Permanent mould releases are relatively thick coatings of materials which provide inherent release properties. PTFE and silicone can both provide inherent release properties (as do other plastics). They can be cured to the mould or applied with adhesive in sheet form. PTFE and silicone are available in film form with a self-adhesive backing to be used for this purpose. PTFE can be powder coated onto any mould that can withstand the 370°C temperatures required to consolidate the powder coating.

Repair characteristics and methods for various tool materials

All moulds will eventually become damaged and either can be repaired or must be replaced. Frequently the damage is on the face of the tool where it offends the appearance of the part or the demoulding process. Plastic faced tools are generally the easiest to repair by replacing the damaged area with similar material and curing. A surface coating (plating, anodise, PTFE etc.) may require that the entire mould surface be stripped, repaired and the coating replaced. For uncoated moulds, scratches and pits can usually be ground out using only abrasives. Metal tools can be welded and ground smooth to repair deep dents, cracks or blunted edges. The weldability of the alloy is an important factor in the selection of a metal tool material, especially for castings. Gray iron is slightly more challenging to weld than ductile (spheroidal graphite) iron, but most steels and other ferrous alloys are more easily welded. Cupric alloys are generally the most weldable, and many aluminium alloys weld well, with the right equipment.

9.6.2 PRESSURE FORCES ON THE MOULD

RTM tooling is subject to many forces but the primary design loads are generated by pressure in the mould cavity. These pressures are a result of the preform bulk factor, resin injection, resin cure and seal compression. These pressures must be countered by the clamping force without the mould deflecting more than allowed for by the dimensional or weight tolerances of the part.

Preform debulk pressure

A substantial amount of force can be required to compact the preform while clamping the mould. The main parameters influencing this force are fibre volume fraction, part geometry, fabric type and preforming

method. For abrupt contours, bulky fabric weaves with thick stacked ply preforms can easily require more than 4 bars of pressure to achieve a 60% fibre volume fraction, whereas flat sheets of satin weave fabric can be debulked to 55% volume fraction with only 1 bar of pressure. Thermoformed or stitched preforms may require very little pressure to be closed in the mould. As might be expected, the preform debulking pressure is reduced if it is debulked several times during lay-up, even if no binder is applied. The debulk pressure decreases slightly over time and also subsides somewhat during injection, as the resin lubricates the fibres and relieves interply friction. Despite this tendency, a conservative designer assumes that fibre debulk pressures will continue throughout injection. This also provides a higher margin of safety since bulk pressures may not be uniform across the part and may not be consistent from one part to the next as a result of variations in the lay-up technique. Even with flat panel compaction testing, is not easy to predict the magnitude of the pressure achieved in a particular mould. This is another situation where prototype tooling can provide valuable design insight. Debulk forces should not be ignored; it is not uncommon for clamping force and substructure size to be determined as much by debulk as by injection pressure.

When inserts utilise wedge action to debulk preforms, substantial force may be required. The force can be estimated in the same manner as for ordinary in-plane debulking except that the mechanical advantage the preform has on the clamps and friction must be considered.

Resin pressure

There are two different resin pressures that occur during the RTM process. Injection pressure typically varies from the injection port to the vents. However, in a worst-case scenario, the vents may get clogged, and the injection pressure will act over the entire mould area inside the seal. The other important resin pressure is static cure pressure, which is uniform across the part on all of the area inside of the seal groove. Only the higher of the two pressures need be considered when designing the mould, since they apply over the same area at different times. However, they may occur at a different temperature, which can be an important structural issue.

Seal compression pressure

It is necessary that the elastomer seal stock be compressed to a contact pressure greater than or equal to the highest injection pressure used. A higher seal pressure provides greater reliability. The contact area of the

seal stock multiplied by the pressure required for seal deflection will approximate the total seal compression force. O-ring-style seal stock has less area of contact than have square sections and therefore contributes more to the clamping force requirements. Owing to the thermal expansion of the seal after heating, a mould can be opened or deflected between sparsely spaced bolts if seal expansion space is not provided.

Total clamping loads

The total load on the substructure and clamping system should be estimated to size substructure and clamping systems. Studies suggest that preform debulk pressures subside over time and as wet with liquid resin. When long heat-up times or other some delay is expected to occur between clamping and injection processes, equation (9.4) may represent an overestimate of the total clamping force, F_{tot} :

$$F_{\text{tot}} = F_D + F_I + F_S + F_G \quad (9.4)$$

where

F_D is the average debulk pressure multiplied by the projected part area in the parting plane;

F_I is the maximum injection pressure or static cure pressure multiplied by the area inside the seal;

F_S is the seal compression pressure multiplied by the seal contact area;

F_G is the sum of all forces required for each debulk mandrel.

Substructure layout and sizing

The amount of substructure required to withstand the total clamping force depends on the geometry of the part and the location of the clamps. The clamps should be located as close to the seal as possible to reduce substructure span, and the structural members should be orientated to provide the most direct load path. A platen press mounted mould may not need any substructure for process loads since the platen can distribute the pressure evenly. The mould will most probably be stiffness critical, so the strength of the substructure is unlikely to be a large factor. Instead, the mould design process should focus on providing maximum stiffness by using a material with as high a modulus as can be applied. Steel is the most common substructure material, for many reasons. It can be easily fabricated, has a moderate CTE similar to fibreglass, it resists heat well and is stiffer than any material of comparable cost. A space frame or series of trusses on the back side of the mould is an efficient way to reinforce a perimeter clamped mould. Trusses should end near a clamping location and be interconnected with X-bracing. Isogrid arrangements are even more efficient but may be more complex to design

and build for some mould shapes. Egg-crating the back with sandwich panels or plate stock is also a common method of reinforcement. When flat surfaces are reinforced, there will be little stiffness contribution from the tool face. Compound curves generally stiffen a mould and allow the mould face to contribute substantially to the reacting pressure loads. Spherical surfaces can carry most of the pressure load in the face, but the flange still requires heavy reinforcement when perimeter clamps are used.

Unlike bag moulding tools, where the substructure does not directly contact the mould face, with RTM the substructure must be rigidly connected to the tool face. For laminate tooling this is usually accomplished by using liquid shim (filled epoxy) between the members prior to assembly, followed by a lay-up of reinforcement over the junctures. The substructure should contact the mould frequently and also be tied in with fabric reinforcement. Metal substructure should be pre-welded and connected to laminate moulds with fabric. Discontinuous welds can be used to attach the substructure to thick metal moulds. Threaded fasteners can connect the tool face and provide for adjustment.

9.6.3 SELECTING A MOULD CLAMPING SYSTEM

The mould clamping and handling system are factors that can influence many tooling decisions. For integrally clamped or shuttled tooling the moulds may need to be lightweight, whereas if a press is to be dedicated to a mould, weight is of little consequence. The following clamping systems have been used: perimeter bolts, toggle clamps, hydraulic clamps, air bladder presses, booking and plain platen presses, mould weight, C-clamps, pipe clamps and autoclave pressure. All types can be classified as either stationary or portable in nature. Portable clamping systems provide for oven and conveyer applications whereas stationary systems tend to be integrally heated or platen heated. A comparison of various clamping systems is shown in Table 9.3.

Portable clamping systems

When bolts or other concentrated clamps are to be used, the load can become concentrated if care is not taken to tighten the clamps evenly. Otherwise all sections must have a sufficiently stiff substructure to carry all the clamping load that can be created between two clamps without excessively flexing and damaging the mould. The bolt spacing should be less than 30 cm, even when heavy cast or steel tooling with deep substructure is used, and should be placed as close to the seal as possible. As a rule of thumb, for solid machined tools the bolts should be spaced less than three billet thicknesses for solid machined steel and less than

Table 9.3 Comparison of various clamping systems

	Portable Clamping Systems			Stationary Clamping Systems		
	Bolts	Toggle clamps	Hydraulic Perimeter	Platen press	Booking press	Latching press
Closing pressure	5–7	4–6	8	10	8–10	5
Clamping pressure	7	6	8	10	8–10	8
Speed	1	2	5	9	10	8
Stiffness contribution	0	0	2	10	5–9	9
Low initial cost	10	9	4	3	2	4
Automation	1	2	5	8	10	8
Durability	1	5	5	10	9	8
Mould alignment	1	1	1	10	10	10
Labour savings	0	2	5	7	9	7

Note: rankings are relative; 0 represents the least ideal and 10 the optimum.

two thicknesses for aluminium. The required number of bolts is usually determined by this spacing requirement rather than by the load carrying or clamping capacity of the bolts. However, the bolt size may be determined by clamping load, and should be sized conservatively. Large bolts with square threads are much more durable than small bolts at high torque. Oversized bolts are usually used since the cost difference is minimal. Nuts should be lubricated with high-temperature lubricant or graphite powder. Cast tooling should be bolted through thick areas where holes are drilled or cast. Often it is better to incorporate heavy bolting lugs around the perimeter to receive the clamping bolts. A forked design allows the bolts, washers and nuts to be placed and removed without unthreading the nut completely. Substructure should be designed to distribute the concentrated bolt loads as directly as possible to the rest of the mould. Clamping components are often loaded to less than 20% of yield strength in order to allow for unexpected loads, to reduce strain and to increase durability. Bolt holes must not come in contact with resin during the process so are usually outside the seal. When it is necessary to bolt in the middle of the tool the bolt hole should be surrounded by an O-ring groove to prevent vacuum or resin leaks. It is generally bad practice to thread one mould section for receiving the bolts, since galling is likely to occur and a seized bolt can cause much difficulty. Thread inserts are only a slight improvement for softer metals. A nut or nut plate on one side, that can be split or cut if a bolt is frozen, is preferable. It is advisable to locate the nuts on top or in some other position where gravity or a shield will prevent resin from getting on the threads.

Some situations may benefit from the use of a combination of bolts and platen press. The bolts can be used for rough debulk and restraint of the tooling assembly, then the system can be transferred to a press platen for final clamping. In these situations the bolts must be seated in recessed areas and bolt torque must be limited to avoid damaging the preferably lightweight moulds.

Hydraulic perimeter clamps can be applied more uniformly and therefore can be used with lighter mould substructures. Most were designed as hold-down clamps for fixturing, so a special cylinder and receiver may need to be made or cast into the mould. Although the force will be more evenly applied than with bolts, hydraulic clamps should also be mounted to distribute the load directly and provide for ease of mounting and replacement. This system may need to be isolated from the heat so it is not likely to be compatible with some heating methods.

Stationary clamping systems

When a rigid platen press is used, the loads are distributed by the platen, so the mould can transfer them in compression. This is advisable where low-tensile or brittle materials are used. There are several types of presses used for RTM, each with advantages. An ordinary platen press has rigid platens that provide excellent mould support with plenty of clamping force through the entire stroke with accurate mould guidance. A booking press rotates one platen to allow easier access to the mould for maintenance and demoulding. A booking press also has all the advantages of a platen press, with the possible exception of less accurate mould guidance. Often less expensive and lighter presses are used with RTM. These utilise a smaller hydraulic cylinder and clamping latches to hold the mould closed or use a scissor action to amplify the force just as the mould closes. These presses are made with rigid platens for flexible moulds or with lighter platens for moulds that have substantial integral substructure. With large moulds, the press may be assisted by perimeter clamping. Air bladders are also used as the source of clamping force in some presses but are usually less powerful when opening the mould and can accumulate force until release, moving the mould dangerously fast unless dampers are added.

9.7 PROCESS CONSIDERATIONS FOR RESIN TRANSFER MOULDING TOOLING

Because the mould not only forms the shape of the part but also is the location where the materials are combined and cured the preform must be partially shaped, debulked, evacuated, impregnated with resin and cured in the cavity before being demoulded. Each of these processes may require tooling accommodation.

9.7.1 RESIN INJECTION PORT

The orifice that allows the resin supply into the mould is often referred to as a resin port or sprue. The resin port must make a tight seal with the pumping equipment, be easily cleaned of cured resin and be reliable. Also, the port must not interfere with the demoulding process or ruin the part finish. The connection seal can be provided by an interference fit, a slightly tapered nozzle and seat or by an O-ring. For some applications it is possible to locate the sprue in the parting line where it can be easily cleaned and inspected; this is called parting line injection. In other cases the port must be away from any parting line and is referred to as face injection. The disadvantage of parting line penetrations is that the seal must be interrupted without leaking vacuum or resin. Often, disposable

resin hose is fitted into a silicone bushing that is constrained by a similarly shaped cavity in one or both halves of the mould where it crosses the mould seal. Face injection and venting locations are often merely holes sized for interference fit with tubing. Other moulds use compression, flare, threaded, barbed and quick connect fittings. Vacuum grease can be used on connections to aid sealing.

9.7.2 LOCATING INJECTION PORTS AND VENTS

The most common location for an injection port is at the lowest point in the mould, near the centroid of the part. Vents are placed at the extreme end of every flow path. The key is predicting the resin flow path, which can differ from simulations where perfect fibre distribution and tooling geometry are used. Anticipation of volume fraction variations, especially on parallel paths, allows the mould designer to optimise the venting and injection locations with fewer scrap parts. Corrugations or stiffeners may extend the flow path but flatten the wavefront when orthogonal to the flow direction. When parallel to the flow direction, stiffeners or other sudden transitions can cause the local flow to accelerate in the stiffener direction, bulging the wavefront and causing process variations.

Separate parallel flow paths that converge are a common cause of void entrapment problems. This problem may be avoided with correct sprue and vent placement. All sandwich structures have parallel flow paths, on each side of the core, and precautions should be taken to ensure that the sprue is in a location where the injection pressure is distributed evenly between the two opposing sides. When the flow front approaches the core or mandrel through solid laminate the distribution will take care of itself, but when the port is one side, the mandrel must be drilled or some other resin source provided for the second side with little pressure differential. Sheet metal laminates and other impermeable materials between preforms should have similar pressures on all sides with a substantial area.

Often when a part has spars or stiffeners primarily in one direction it is beneficial to inject with the flow path parallel to the spars. This eliminates many divergent flow paths at the stiffeners that would occur if the part were injected normal to the spars, with each one probably requiring venting. However, this flow and venting simplification can come at the expense of obtaining easily a smooth stable flow front; areas with stiffeners and free edges are likely to carry resin faster. This can result in dry spots, voids or a larger purge requirement because the resin may arrive at the vent before all of the space between the stiffeners has filled. With precision preforms, gentle corner radii, shallow pad-up ramp angles and vertical bottom-to-top injection the problem can be minimised and only one sprue and vent required with good distribution at both ends.

Another strategy is to inject the part through the centre, where the distance to the ends would be halved and where a combination of oblique and parallel flow would exist at different times. This injection method is a compromise, providing better flow stability, thanks to the lack of free edges initially and with less distance to go, but the top of each stiffener may require at least one vent at the top of each end. Free edges that are directly connected to the sprue are typically more problematic than when the resin must first flow through most of the preform before reaching the edges.

In many situations it is desirable to inject the part through the perimeter, via a resin distribution groove or through the space outside the trim line where the preform stops before the cavity. This system also offers the benefit of fewer vents; only one in the centre may be required. The resin distribution system should be large enough to distribute the resin evenly to all sides, even though the resin supply is located on one side. This injection method requires less pressure to achieve the same flow rate since the area of injection is greater.

9.7.3 PLUMBING REQUIREMENTS FOR SEQUENTIAL INJECTION

Since most aerospace RTM applications will use vacuum venting, a substantial amount of plumbing may be required for sequential injection. Often the static resin pressure behind the flow front are subatmospheric; this can introduce air into the resin if the port is vented to atmosphere during connection. Each port should be connected to both resin supply and vacuum sources from the start. Otherwise connections must be evacuated or purged of air prior to opening the flow control valve. During sequential injection, the location of the resin with respect to the port must be known; early injection can cause two flow fronts to converge which can result in voids, whereas late injection can nullify the injection time and pressure savings. A witness sight and resin trap provide for this and can be used to apply static pressure to the mould during cure as well.

Sequential injection plumbing is usually expendable, but for high volume this can be expensive. The process is used generally because of a combination of weak tooling, core compression failure or inadequate processing time with resin. It may be possible to solve these problems in some other manner that would be more cost-effective in the long term. By placing the plumbing in a parting line one can partially eliminate the expendable plumbing costs. It may be economical to incorporate a separate bolted or press-clamped parting line which contains the plumbing grooves against the back side of the mould and which can be cleaned after each cycle. Sight glasses, plug valves or other features may provide even greater control and cost savings. The pressure of the manifold

system does not contribute to the clamping loads if they are on the back side of the mould but can add area inside the seal if placed in the main parting line.

9.7.4 DESIGNING RESIN DISTRIBUTION MANIFOLDS

It is often necessary to route resin to various locations around the periphery or to various other locations on the part. This is accomplished by either internal or external plumbing. Internal plumbing usually consists of a groove in one or both mating tool surfaces, where it can be removed with minimum additional effort. External plumbing usually utilises disposable metal or plastic tubing which is sealed to the mould through a penetration in the mould. When more than one gate exists on a single path it is referred to as a distribution manifold or plenum and must be sized to accommodate the flow rate of the combined gates. When manifolds are used for extended distances, the cross-sectional area should be at least twice as great as the sum of the gate sections where possible, to minimise undesirable pressure variations. When only one gate exists or when only one gate will be open at once it is known as a runner or leg and is usually sized to carry the required flow volume over the required distance without an excessive pressure drop. For most fluids, flowing through smooth closed channels, frictional loss of pressure can be calculated using the Darcy–Weisbach expression given in equation (9.5). [1]:

$$\text{friction head} = \frac{flv^2}{2dg} \quad (9.5)$$

where

$$f \simeq 0.316 \left(\frac{vd\rho}{\mu} \right)^{-1/4}$$

and

- v is the average velocity;
- l is the length;
- d is the diameter;
- g is the acceleration due to gravity;
- μ is the viscosity;
- ρ is the fluid density.

When using semi-flexible tooling ease of resin distribution is more critical since injection pressure is limited. The resin is usually injected through the bag side into a port connected to the preform or a network of distribution channels. These channels may be separated from the preform by perforated separator film to allow them to be removed from the part after cure. The channels can be composed of coiled wire or other

highly permeable flexible stock that can withstand the vacuum without rupturing the bag. The channels can form an orthogonal or radial grid to feed the laminate in sections sized as large as possible but small enough to allow timely wet-out. Vacuum connections are usually made at the end of flow paths as with rigid tooling. Transparent bagging film allows the resin position to be monitored and alterations to plumbing to be made as necessary.

9.7.5 AIR VENT FEATURES

It is necessary that the air in the mould after closure be removed either before injection by using vacuum or be displaced during injection without vacuum. It is theoretically possible to use the same port for vacuum venting and resin injection, but this system is rarely used since any air in the mould at the time of injection or that leaks into the mould during injection cannot escape. Usually the vents are located at the end of the anticipated flow path where any air displaced by the advancing flow front can be evacuated from the mould before the vent is closed. The vents usually consist of a disposable tube originating in a hole through the mould intersecting the part cavity and ending at the resin trap. The interface with the mould cavity may cause demoulding difficulty or local delamination with partially cured laminates since the resin must be broken off to demould the part. Such difficulties can be alleviated by incorporating a gate restriction at the parting surface, which reduces the sectional area to be broken. With metal tubing this is easily accomplished, since a rotary tubing cutter naturally displaces metal into a restriction at the cut. Parting line vents can be removed with the part flashing without additional effort. When the injection cycle is complete the vents must be closed to prevent resin escape due to thermal expansion, static cure pressure or gravity. If the vents are not closed the resin will cure at ambient pressure. After cure the vents must be cleared for the next cycle.

9.7.6 DESIGNING PREFORM TOOLING

Preform tooling is often similar to the RTM tooling in part geometry, with the following exceptions:

- the preform may be formed with reinforcement fibre extending beyond the part edges;
- highly contoured surfaces may be preformed in stages by incremental dies;
- gently contoured part surfaces may not require any preform moulds;

- the mould composition may be of elastomer or other abrasion-resistant material;
- tooling components in contact with broad-goods should have rounded edges where snagging or other fabric damage can occur;
- spare mandrels and shaped cores can be used as preforming tools, conserving valuable RTM mould time.

9.8 EXAMPLES OF RESIN TRANSFER MOULDING TOOLING

Four examples of RTM tooling are outlined below. The first and second examples allow a comparison of cast and machined tooling with machined billet tooling, for similar generic wing rib designs.

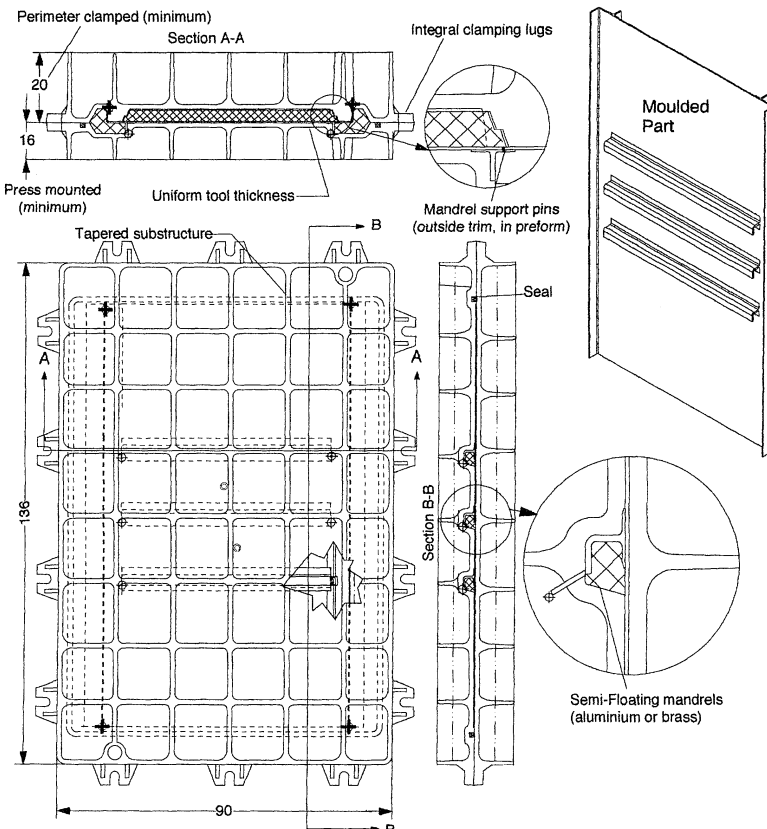


Figure 9.14 Tooling example 1. \oplus = vent location; \ominus = vent may be required; \odot = sprue location. Note: all dimensions are in centimetres.

9.8.1 EXAMPLE 1

The first tooling concept depicted in Figure 9.14 would be constructed with low-cost casting methods from a suitable metal alloy to rough dimension. The tooling is designed for central injection with vents at all corners of the part and at the ends of stiffeners. Divergent flow paths that reconverge are not necessarily encountered if the flow down the 'J' stiffener does not lead or lag the face flow. Alternative vent locations are shown where they may be required if voids occur in these areas. As shown, the mould is designed for perimeter clamping. It would be least expensive to machine this mould from a mild steel billet, since the cavity is shallow. However, machined invar castings would be less expensive than the same tooling machined from an invar billet, since it is difficult to machine. As indicated in Figure 9.14, a press mounted mould needs less substructure in service. However, the weight (cost) savings of the shallow design would increase the casting distortions, requiring more machining be done. Cast tooling works well with oven heating, since uniform thickness and high surface area promote even heat transfer. The substructure can be used to divide a circulated fluid into zones connected with a manifold on the back. The substructure and irregular contours make direct electric heating difficult with strip or rod heaters. The use of flexible blanket, infra-red or cable heaters would be possible but would be expensive to control. The sprue and vent would be drilled as a secondary operation, without cast-in features. Cast-in clamping lugs are superior to bolt holes since the nuts do not need to be removed to open the mould, and seized bolts can be slid off.

9.8.2 EXAMPLE 2

The mild steel OML mould design shown in Figure 9.15 utilises trapped and floating mandrels to confine the angle and hat-stiffened rib with no draft on most sides. The resin distribution plate on the back of one tool half heats the resin and distributes heat to two sprues positioned to avoid creating a pressure differential across the semi-floating hat-stiffener mandrels. The two wavefronts converge unless sequential injection techniques are used; one gate is delayed via a sliding valve that is accommodated in the resin distribution plate. More details on the plumbing are shown in Figure 9.16. Air is vented to the corners but may need vent assistance at the ends of both angle stiffeners. These vents may not be necessary; experience suggests that orthogonal members and edges tend to flow faster and might displace the air from the angles before the corners are reached. The mould can be press mounted or bolted shut. Heating could be of any type since a flat back and good heat conductivity exist, but oven heating would be slow. Note that if alu-

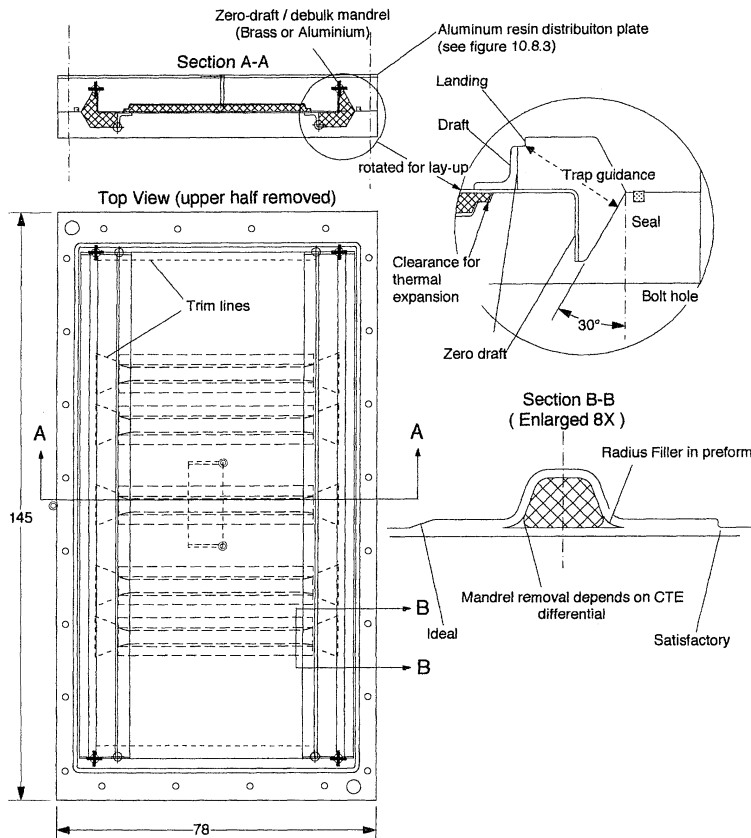


Figure 9.15 Tooling example 2. \blacksquare = vent location; \oplus = vent may be required; \odot = sprue location; all dimensions are in centimetres.

minimum hat-stiffener mandrels are used they cannot be removed because they will hit the rib flange. The part flange must be trimmed off in this area which would allow mandrel removal.

9.8.3 EXAMPLE 3

The mild steel generic fitting mould shown in Figure 9.17 is designed for central injection with venting at four corners and one end location. A resin distribution plate on both platens would facilitate press mounted operation. This mould design is intended for use with near-net preforms; a high bulk factor would otherwise make preform placement difficult. The part will likely remain in the female tool half when opened so the mould is equipped with two vents that also serve as mould jacks. This allows the resin in the vent to be sheared off in torsion rather than

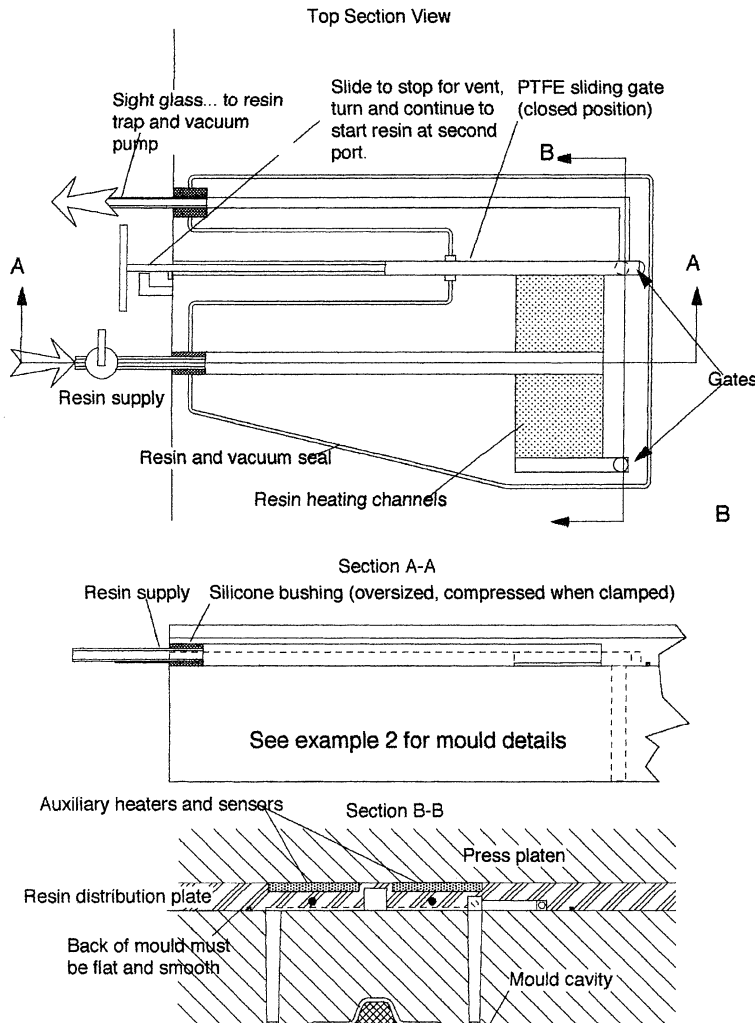


Figure 9.16 Sequential injection resin distribution plate. Example 2 is illustrated in Figure 9.15.

tension, and the vents are easily removed for cleaning or replacement. The guidance pads shown are to prolong mandrel life and ease mandrel clean-up. This mould can be clamped with bolts and oven heated and is also equipped with press mounting slots.

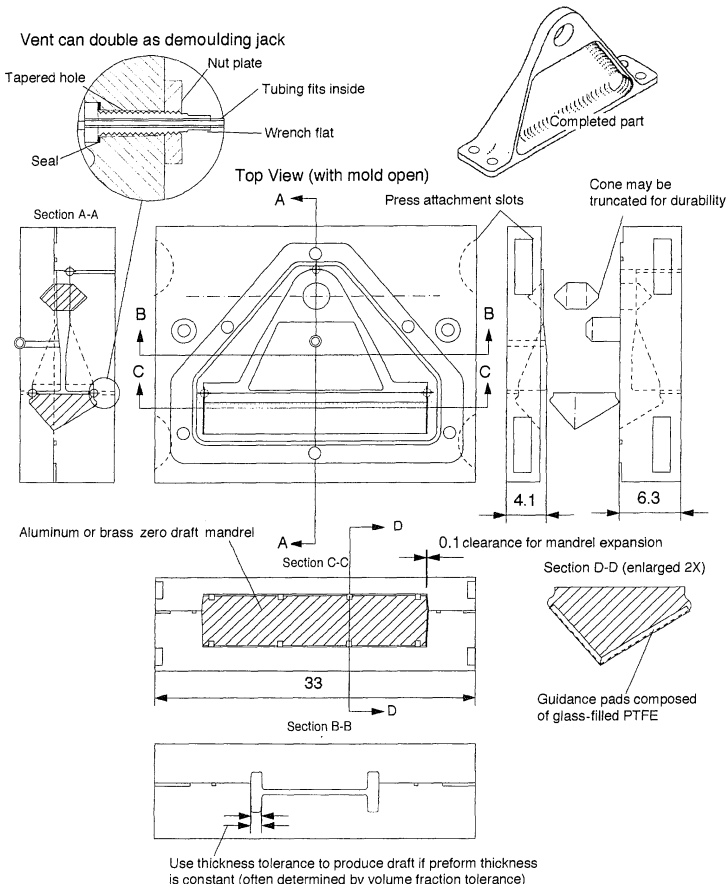


Figure 9.17 Tooling example 3. \blacksquare = vent location; \oplus = vent may be required; \circlearrowleft = sprue location; all dimensions are in centimetres.

9.8.4 TOOLING EXAMPLE 4

The generic flight control surface tooling depicted in Figure 9.18 is designed for mild steel OML and aluminium IML. The resin flow path is intended to be from end to end, using the excess mandrel length to distribute the resin. Central injection could also be done from both sides of the mandrels. In this situation it is beneficial to stand the mould on end during injection. This helps stabilise the flow front, since resin is more dense than vacuum. Furthermore, when this position is maintained throughout cure the mandrel weight is carried directly into the mould, reducing the need for the guidance shown on both ends. The part is designed to use braid which is slipped over the mandrels mounted to the

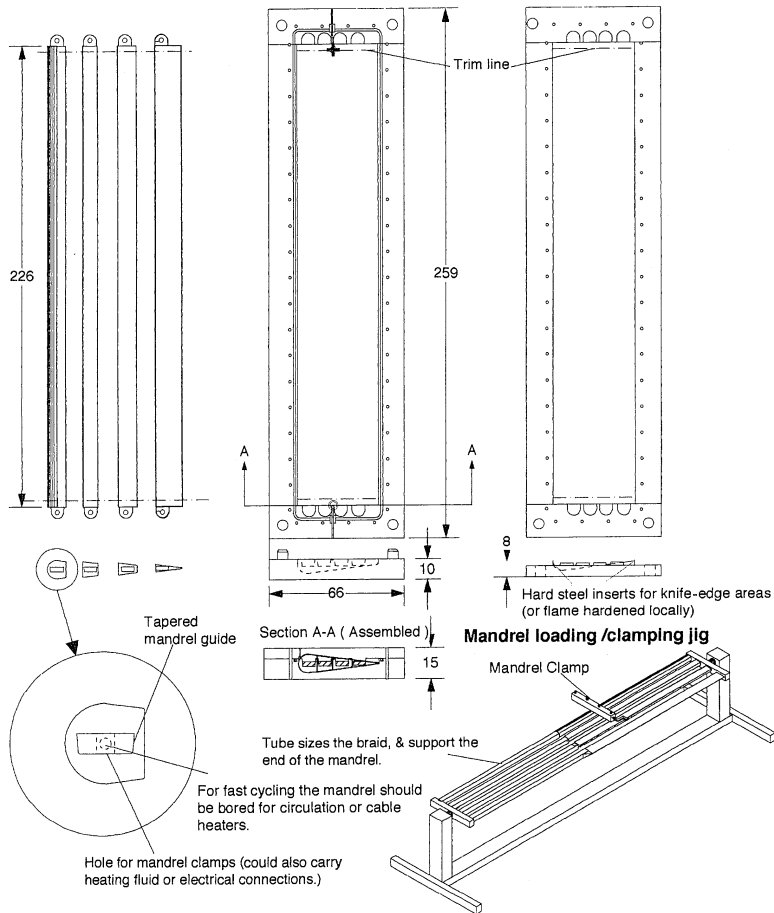


Figure 9.18 Tooling example 4. \oplus = vent location; \ominus = vent may be required; \odot = sprue location; all dimensions are in centimetres.

jig shown. The mandrels are clamped together after the braids are located over them and the assembly is then wrapped with fabric. The mandrels are held clamped until they are placed in the mould where the guidance is provided by the tapered tang. The part cavity is recessed into one mould half; the resulting bypass prevents fibre from being pinched between the halves.

Reference

1. Streeter, V. L. (1958) *Fluid Mechanics*, 4th edn, McGraw-Hill, New York, pp. 256–9.

FURTHER READING

- Beer, F.P. and Johnston, E.R. Jr (1981) *Mechanics of Materials*, McGraw-Hill, New York.
- Benjamin, W. P. (1972) *Plastic Tooling: Techniques and Applications*, McGraw-Hill, New York.
- DuBois, J.H. and Pribble, W.I. (eds) (1987) *Plastics Mould Engineering Handbook*, 4th edn, Chapman & Hall, London.
- Gentile, D.K. (1988) Size, shape and design detail factors in process selection, in *Engineering Plastics, Engineered Materials Handbook, Volume 2*, ASM International, Metals Park, OH.
- Harmon, B. D. (1988) Graphite epoxy tooling, in *Engineered Materials Handbook, Composites, Volume 1*, ASM International, Metals Park, OH.
- Hindle, R. and Harder, W. (1995) Abrasion-resistant steels meet more exacting mould needs, in *Modern Plastics Encyclopedia*, McGraw-Hill, New York.
- Marks, L. S. (ed) (1951) *Mechanical Engineers' Handbook*, McGraw-Hill, New York.
- Sheldon, D. L. (1988) Electroformed nickel tooling, in *Engineered Materials Handbook, Composites, Volume 1*, ASM International, Metals Park, OH.
- Van Vlack, L. H. (1985) *Elements of Material Science and Engineering*, Addison-Wesley, New York.

Tooling inserts for resin transfer moulding

10

Mark Thiede-Smet and Mark Wadsworth

10.1 INTRODUCTION

Tooling inserts are used together with the resin transfer moulding (RTM) mould to define the shape of the composite component during the RTM operation. Usually the tooling inserts define internal cavities as with a foam core or a melt-out metal alloy mandrel. External surfaces can also be defined by means of extractable steel tooling inserts or a pressurised bladder. Figure 10.1 shows the many choices for tooling inserts that are discussed in this chapter. They are categorised as 'fly-away cores' which remain in the moulded part, or as 'removable tooling inserts'. The section number for each type of insert is also listed to aid in locating each within the chapter.

Materials chosen for fly-away cores will have to meet the stringent requirements of aircraft testing, qualification and certification. This can be such an expensive undertaking that it is difficult to introduce a new material into an aircraft programme, regardless of how it simplifies the component or reduces the recurring cost.

The removable tooling inserts have the advantage of simply being tooling, therefore the designer has more freedom to incorporate them without extensive test programmes. Once these inserts are removed from the RTM component they usually expose hollow cavities. Designs incorporating these hollow cavities or unsupported laminate may not be the lightest weight designs, but they can be more damage tolerant than versions with internal cores.

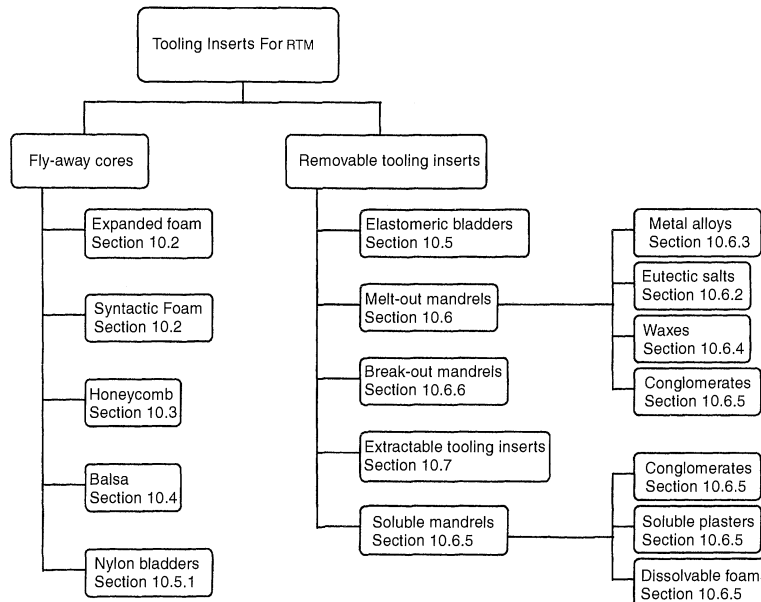


Figure 10.1 Options for tooling inserts for resin transfer moulding (RTM). Each option is discussed in text in the specified section.

10.2 FOAM CORES

Closed-cell foam has been the obvious and easy choice for core materials for the RTM process. Structural efficiency similar to a honeycomb sandwich panel can be designed into a foam core version, resulting in a light, stiff panel with a few added benefits. The strength properties of foam are nearly isotropic, allowing it to resist the resin injection pressure from all directions. This homogeneous foam structure allows sandwich panels to be moulded with steep ramp angles, such as the 45° and 60° ramps on the panel in Figure 10.2(a), or with internal walls, such as the panel with an internal box beam in Figure 10.2(b).

This section focuses on low-to-moderate-density expanded foams which are of interest for structural cores. Syntactic foams are another version of foam; they are combinations of resin and lightweight filler, usually hollow glass balloons. The densities for syntactic foams are usually above 480 kg/m³, making them too heavy for most cores. Their preferred applications are small inserts and hard points potted into honeycomb cores. Syntactic foam is available in many resin systems and can be cast into custom shapes for small, highly loaded RTM cores.

Another advantage of foam is that a panel with damaged skin and foam core is easier to repair than one with a honeycomb core, for two

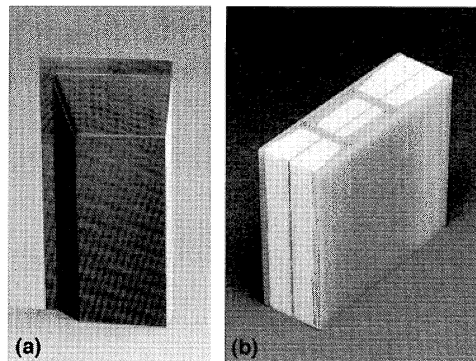


Figure 10.2 (a) Corner piece of foam core prototype access door panel; (b) foam core panel with integral box beam. Reproduced courtesy of Hexcel Structures, Kent, WA, USA. Photography by Tim Doty.

reasons. The damaged foam can be cut away revealing a uniform core capable of supporting the pressures of bonding in a replacement piece. Also the small closed cells of many foams do not fill with a large amount of water or hydraulic fluid which is typical in honeycomb panels and is very difficult to remove before the repair can take place. However, a disadvantage of foam cores is that some fluids, including jet fuel, can dissolve some foams.

One should use caution when designing a foam core structure for impact, and not choose thin composite skins and low-density foam. The localised compression and bending of the foam under impact can fracture it severely. As with matrix resins, the emphasis on high strength, modulus and temperature resistance in foams has lowered their toughness and resiliency. A Hexcel internally funded study demonstrated the fragility of light gauge RTM sandwich panels by impacting them to simulate damage from hail stones. The thin glass/epoxy skin was not damaged; however, the foam was fractured and the skins remained dented inwards. A Northrop study showed the advantage of thick composite skins with foam core. In impact tests with panels with 4.5 mm thick skins and a polymethacrylimide (PMI) foam core, the compression after impact strength decreased only 47% from panels impacted with 7 J of energy compared to those impacted with 135 J, a nineteenfold increase in impact energy [1].

Foam that will experience fatigue loading will require large design knock-down factors to adjust from ultimate strengths to design stresses. Fatigue testing has shown that PMI foam, a high specific strength foam, survived 20 000 bending cycles at 50% of ultimate static strength, and a million cycles at 30% [1]. This suggests that a conservative design approach should be used with thorough testing. This is even more im-

portant for parts which will be exposed to thermal cycling and moisture, as most exterior aerospace parts will be. There are sufficient opportunities for failures with foam cores, and any core for that matter, to implement a test programme that takes into account all the potential performance-degrading factors.

One design option for small cores that could eliminate much of the testing is to use the foam to create the interior shape of the composite but to assume that it does not contribute to the structural function of the part. This approach has been used for RTM components in areas that were uninspectable. Release film can be wrapped around the core in test parts to simulate a worst-case skin-to-core delamination.

10.2.1 FOAM SELECTION

This section describes the many different foam types that are produced and might be considered for an aerospace RTM component. Mechanical properties were available for some of these foams; they are compared graphically for compression strength [Figure 10.3(a)], for shear strength [Figure 10.3(b)] and for shear modulus [Figure 10.3(c)], all as a function of density. End-grain balsa and Nomex® honeycomb are included for comparison. These graphs are based on suppliers' data sheets. When designing thick cores one should note that shear strengths of some foams and honeycombs have been shown to decrease as core depth increases from 12 mm to 150 mm [1].

Since the properties at elevated temperature are critical for the RTM process, the relationship between compression strength and temperature is shown in Figure 10.4 for a few foams and for Nomex® honeycomb.

Polyurethane (PUR)

This foam is commonly used in the RTM of industrial parts and sporting goods and is produced in both rigid and flexible forms. Flexible PUR has been used in aircraft cockpit padding. The rigid foam is used in aircraft interiors as close-out strips for honeycomb panels in stowage bins. Rigid PUR is supplied by many companies in sheets and in two-component liquid kits for foaming into specific shapes. Densities from 32 kg/m³–480 kg/m³ are produced.

PUR is a closed-cell foam, with good solvent resistance. The impact and fatigue properties are low. The maximum recommended service temperature is 135°C, and the maximum processing temperature varies from 140°C to 160°C, depending on the manufacturer. PUR has the disadvantage of being somewhat friable, meaning that the surface dusts away when rubbed. It is moderately fire retardant and low in cost.

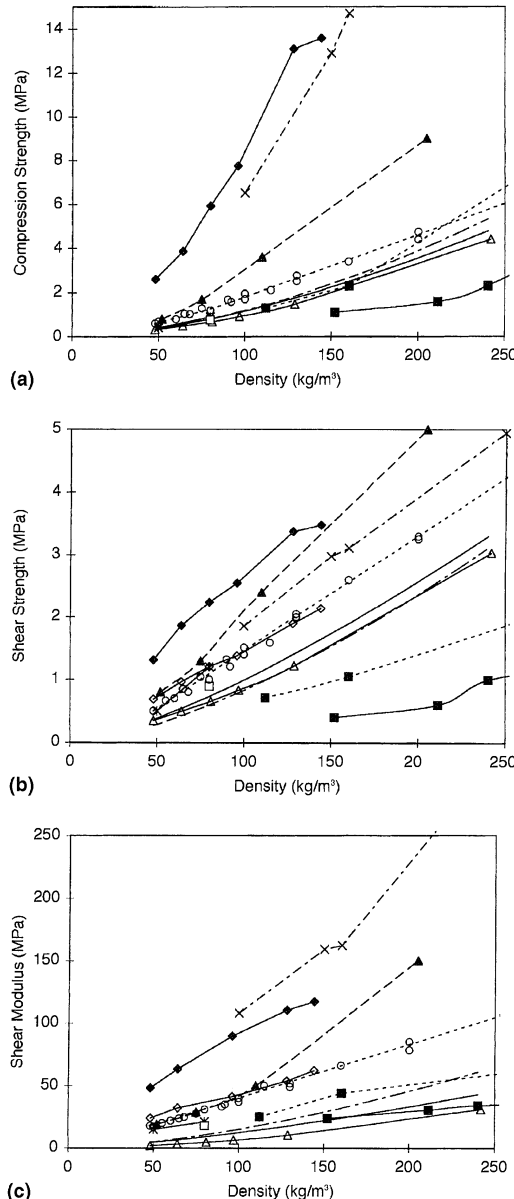


Figure 10.3 (a) Compression strength; (b) shear strength; (c) shear modulus as a function of density for core materials at 25°C. — = polyurethane foam; -Δ- = polyester foam; -★- = linear polyvinylchloride foam; -○- = cross-lined polyvinylchloride foam; -— = isocyanurate foam; -▲- = polymethacrylimide foam; --- = phenolic foam; ■ = phenolic syntactic; □ = polyetherimide foam; -×- = end-grain balsa; (a) -◆- Nomex™ honeycomb; (b, c) -◇- Nomex™ honeycomb, -◆- Nomex™ ribbon direction honeycomb. Note: PUR = polyurethane; PVC = polyvinylchloride; X-Linked = cross-linked; PMI = polymethacrylimide; PEI = polyetherimide; Nomex is a registered trademark.

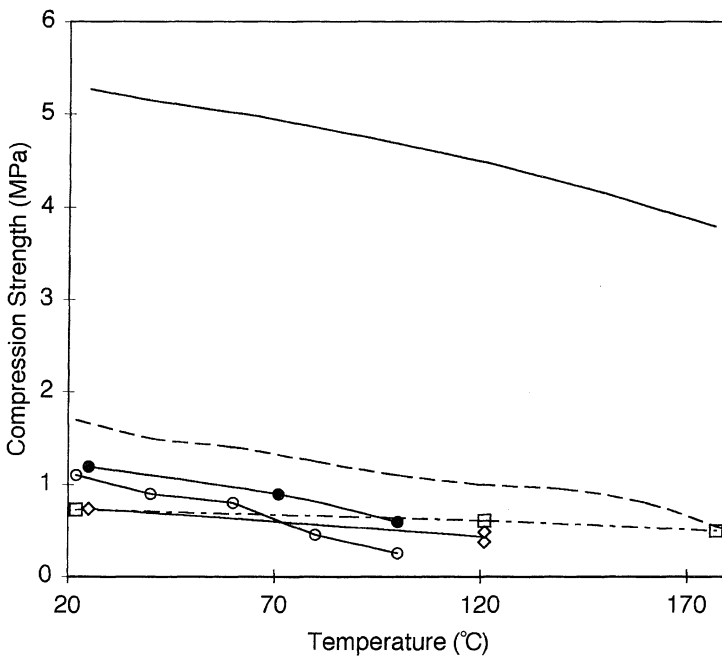


Figure 10.4 Compression strength versus temperature for core materials at 75 kg/m³. \diamond = polyurethane foam; ● = polyvinyl chloride foam (DivinycellTM HT); --- = polymethacrylimide foam; ○ = polyvinylchloride foam (DivinycellTM H); -□- = isocyanurate foam; — = NomexTM honeycomb.

Linear polyvinylchloride (Linear PVC)

This foam is used extensively in high-performance boat hulls because of its ability to sustain impact from waves. This comes from its unique rigid-elastic behaviour that allows greater than 40% elongation [2]. The maximum service temperature is 55°C to 60°C. It has a closed-cell structure, is self-extinguishing, thermoformable and vibration dampening. Linear PVC is available in densities of 50 kg/m³ and 80 kg/m³ from AIREX AG, referred to as the AIREXTMR62 and AIREXTMR63 series.

Cross-linked polyvinylchloride (PVC)

This more common version of PVC develops slightly improved mechanical properties compared with PUR; however, the properties degrade more severely with increasing temperature. In addition, PVC is less brittle (10%–15% elongation for low densities) and more fire resistant than PUR (considered self-extinguishing, yet the smoke evolution and heat release are high). This is a closed-cell foam. The maximum service

temperature varies between 65°C and 120°C, depending on the formulation and processing of the foam. It is slightly thermoformable at temperatures between 120°C and 140°C. PVC is used in aircraft interiors as close-out strips for honeycomb panels in stowage bins. PVC is produced in sheet form only, by several companies, in densities from 30 kg/m³ to 400 kg/m³.

Polymethacrylimide (PMI)

This is probably the foam most often chosen for structural aerospace RTM components. It has also been used with prepreg processes, from autoclave curing to thermal expansion moulding, for manufacturing propeller blades (for the CL-227 by Canadair), landing gear doors (for the Saab SF 340) and wing flap vanes and centre engine inlet duct (both for the MD-11 by Westland Aerospace) [3].

PMI foam is closed-cell and resists solvents but absorbs more water than does PVC foam. PMI is manufactured only by Röhm GmbH under the tradename Rohacell®, and is sold in several grades with densities from 31 kg/m³ to 300 kg/m³. As can be seen in Figures 10.3 and 10.4, the compression strength of PMI (Rohacell® WF series) is higher than the other foams, especially as density increases. The shear strength is higher than balsa and in the neighbourhood of Nomex® honeycomb. Rohacell® WF retains significant strength above 140°C and can be processed to 180°C.

Polyester

This closed-cell foam has mechanical properties similar to PUR, with lower temperature capability. The maximum service temperature is 90°C, and the maximum processing temperature is 120°C. Compared with PVC, it is more brittle, with 5%–8% elongation, and exhibits lower drum peel strength. The Diab Group supplies this foam under the tradename Estercore®. Densities from 65 kg/m³ to 600 kg/m³ are available in sheet form.

Polyisocyanurate

This closed-cell foam has mechanical properties similar to PUR, with improved dimensional stability and only a slight degradation in properties at higher temperatures. The maximum service temperature is 150°C, and the maximum processing temperature is 180°C. Polyisocyanurate generates little smoke when burned but is friable and brittle. It is available in sheets from General Plastics as Lastafoam® FR10100 in densities of 95 kg/m³ to 320 kg/m³, and from Dow Plastics as Trymer®

in densities from 26 kg/m³ to 96 kg/m³. The lower densities are used for insulation.

Phenolic

Two options are available for phenolic foam: blown foam and low-density syntactic. The blown foam from M.C. Gill Corporation, Gill-foam® 2019, has microscopic pores that are slightly open. It has been successfully used in the RTM of automotive parts, without a surface pore sealer. The maximum use temperature is 200°C, with intermittent exposure to 260°C possible. The compression strength is similar to PUR and isocyanurate; however, the shear strength is low. The phenolic resin is responsible for low smoke evolution and low heat release. This is one of the few blown foams that can be moulded into a specific shape, but only by the manufacturer. One source claims that this type of foam requires neutralisation of the acidic surface of the foam before use in RTM. Densities from 70 kg/m³ to 320 kg/m³ are produced.

Syntactic foams usually have very high densities (above 480 kg/m³), making them unsuitable for large structural cores. A low-density syntactic phenolic foam is made by Isorca Inc. under the tradename Alba-Core®. It has low moisture pick-up, but very low compression and shear strengths. This phenolic syntactic foam can be moulded into specific shapes. It has been used in automotive RTM at 250°C under 6 bars of pressure (0.6 MPa). Densities from 95 kg/m³ to 290 kg/m³ are produced.

Thermoplastic polyimide

This foam is a recent development of High Technology Systems Inc. (HTS). It is an open cell foam that can be sealed with liquid polyimide resin. The maximum temperature is 370°C; it exhibits thermoplasticity well above its 273°C glass transition temperature. No mechanical properties are available as of this writing. It can be supplied in sheets with densities from 48 kg/m³ to 130 kg/m³. Polyimide foam is made by other suppliers in very low densities only. It is used for thermal and acoustic insulation in high-temperature applications.

Polyetherimide (PEI)

This closed-cell foam is an expanded high-performance thermoplastic. It is a tough, resilient foam with isotropic mechanical properties. The compressive strength is low, the shear strength and modulus are moderate and peel strength can be higher than honeycomb. Compared with other high-performance thermoplastics, this foam has low evolution of

smoke and toxic gasses and low heat release. The maximum operating temperature under load is 180°C, yet load-free it remains dimensionally stable up to 190°C. PEI foam is thermoformable at 215°C. This foam has been proposed for nose cones because it is nearly radar transparent. AIREX AG produces this foam referenced as AIREX™R82. It is currently available in densities of 60 kg/m³, 80 kg/m³, and 110 kg/m³.

Unfortunately, epoxy resin can act as a solvent for PEI if the viscosity of the resin is low and the temperature of the PEI is high. Up to 120°C, RTM processing with epoxy resins is possible. If temperatures as high as 180°C are used, protection by the sealing technique described in section 10.3.1 (second subsection, on wrapping the honeycomb core with an impermeable film) can be used. RTM processing with phenolic resins presents no problems.

Relative cost for foams

Although this is too often ignored for aerospace design, it is necessary to understand the relative costs of the core options successfully to meet a cost target. Table 10.1 compares the approximate cost, for comparable density and thickness, of the foams listed above, and for end-grain balsa and Nomex® honeycomb. The foam types are listed in ascending order of approximate cost per unit area, for 75 kg/m³ density and 25 mm thickness, except for balsa, which has a density here of 150 kg/m³.

10.2.2 METHOD FOR FOAMING CORE SHAPES

The ability to cast a foam directly to the desired core shape is a definite advantage for many designs, and practically a necessity for high-volume production. Of the foam choices discussed above, only polyurethane, Gillfoam® (blown phenolic) and Alba-Core® (syntactic phenolic) can be directly produced into custom shapes.

Table 10.1 Relative cost of core materials

Core	Relative Cost
Polyester Foam	Low
Polyurethane Foam	Low
End-Grain Balsa	Low
Cross-Linked polyvinylchloride Foam	Low
Polyisocyanurate Foam	Low
Linear polyvinylchloride Foam	Moderate
Phenolic Foam	Moderate
Polyetherimide Foam	High
Polymethacrylimide Foam	High
Nomex™ Honeycomb	High

The most common method for moulding a core shape with two-component liquid polyurethane is to pour it into a mould, allow it to expand and cure. Key factors determining the suitability of the cores resulting from the open pour process are:

- the uniformity of the foam expansion;
- air pockets below the skin of the foam;
- consistency of the skin;
- adequate post-cure of the foam before RTM;
- distortion due to post-cure;
- the strength of the RTM resin-to-core bond.

A core mould is used which can react the substantial pressure of the expanding foam and define all core surfaces. The best moulds are polytetrafluoroethylene-coated steel (PTFE-coated steel). The core mould must be offset from the RTM mould by the required laminate thickness. However, the resulting cavity during RTM depends on many variables; it is often necessary to adjust the core size in order to obtain the targetted volume fraction in the laminate. For this reason it is useful to be able to mould cores for test runs before building the foam core mould. This can be done in the RTM mould with thickness offsets temporarily affixed. The stiffness of the mould and clamps is critical because the deflected mould geometry will be incorporated into the core. Test or limited-production cores can be offset from the outside mould line (OML) surface with adhesive-backed, high-temperature sheet wax. The wax is laminated to the mould with a thickness distribution corresponding to the preform. The wax is treated with a release agent that provides both ease of release and lubricity to make the cavity more durable. The pressure from the foam and demoulding can distort the sheet wax after only a handful of cycles. For a more durable offset, prepreg can be laid-up similarly and cured appropriately. After trimming off the excess material, the laminate offset should be smoothed on the inside and treated with release on all sides (including the RTM mould). A smooth interior surface can be achieved in some situations by using flexible or rigid caulk under the bag during cure or by coating with Teflon™ tape. In some cases this tape has been used for the entire offset. When attempting to position the offsets one may need to use a tack adhesive to hold them in position. The parting line seal should be removed for the foam casting process, as it is not necessary and may restrain escaping air.

Vents are required when the foam expands in such a way that air is trapped between the foam front and a sealed (dead end) cavity. The foam mixture will flow only downhill from the pour origin until expansion occurs and the mixture thickens. In general the mould will fill from bottom to top, but when the pour originates on top of a thin gentle incline, downhill expansion can be induced. In many cases the pour pattern is

critical to produce consistent void-free cores. Another key variable is the amount of foam dispensed into the cavity. Although the vents can act as a relief for foam and thereby affect the density, the density is more accurately controlled by varying the amount of foam poured. When vents are used to adjust the foam density, the distribution of density and foam cell uniformity are adversely affected. The volume of the core may be determined by water displacement. The weight of the foam resin mix can then be adjusted to provide the desired density. Small holes (1 mm) can be used as air vents where little or no foam venting is required. Air flow is not significantly restricted by the holes but the viscous foam is halted. If air is trapped in the core near the vent, more foam purge (a larger hole) can be incorporated and an appropriate amount of additional foam mixed. It is likely that where vents are required to mould a core they will not correspond with the vent locations of the RTM process; it is possible to drill or machine the laminate offset to provide a path on the back side for air to get to the closest vent. When sheet wax is used this cannot be done as easily, nor can high temperatures be used. If the core dimensions are not satisfactory, adjustments in the offset thickness can be made by adding plies or by making a new laminate. Even moderate production rates can justify a dedicated mould once the exact size is known.

The need to mix the two-component liquid foam sufficiently, but not excessively, is a key factor in obtaining uniform cell structure and a consistent skin quality. An air drill with a mixing paddle (Jiffy™ mixer) works well at about 1500 rotations per minute (rpm). The liquid foam should be mixed for a specific amount of time and in a constant pattern found to provide the best mix. Double cupping the mix will help if the foam mix time allows for it. It may be necessary to saw a core into sections to evaluate the cell structure, but the surface can reveal a great deal about the core quality. Swirls of colour variation indicate inadequate mixing whereas large cells on the surface or directly under the skin indicate overmixing, improper pour procedure or that insufficient expansion occurred. All foams have unique processing characteristics. When stubborn processing difficulties are encountered it is possible that the easiest remedy is to change brands. The mixer must be flushed with solvent before the foam cures if it is to be reused without burning off the build-up. Some water-based solvents might be effective but it is likely that MEK or acetone will be required. The solvent can usually be reused several times until it becomes saturated; gels and must be disposed of or recycled.

In most cases the mixed liquid foam is poured into the offset mould and the mould is closed as quickly as possible. Many foams expand quickly but can be slowed down by refrigeration. Many foam resins also have suspended particles that must be uniformly dispersed before the components are dispensed from the storage containers. The moulding temperatures vary widely for different foams, but some have a consid-

erable range for discretion. This can be beneficial since the size of a core, its density and its processing characteristics can be altered slightly by changing the mould temperature.

Demoulding of thin foam cores can be difficult because of the excellent adhesion properties of polyurethane, especially where draft is minimal. The removable mould offset discussed earlier may aid in core removal as it will provide rigidity and minimise contact with the mould. Then the offset or liner can be flexed to break the adhesion on the slightly drafted sides before pulling on or blowing compressed air under the core to free it.

All cores should be thoroughly cured and dried before proceeding with RTM. Subjecting the core at least to injection temperatures if not to full cure temperature can insure all outgassing and shrinkage has ceased. Often these conditions are obtained only on the surface while preheating the preform in the RTM mould.

Some urethane skins do not adhere to the inner core well, resulting in disbond after the cored structure is cured and subjected to heat. When necessary the skin can be removed by abrasion, but not easily, because of its high abrasion resistance. Removal of the skin of a urethane core is expensive, possibly approaching the cost of machining the core from a billet. For this reason thermal testing of sandwich coupons up front using the proposed materials is advisable to insure good core adhesion.

10.2.3 METHODS FOR MACHINING CORE SHAPES

Many of the high-performance foams require specific conditions for foaming which can be accomplished only at the foam factory. These foams are supplied in block or sheet form for subsequent machining to final size and shape. For low-volume aerospace parts this can be economical; after all, this is the approach currently used with honeycomb. Options for machining core shapes include band sawing, hand sawing, circular sawing, die cutting, planing, numerically controlled (NC) routing, shaping, hot-wire cutting, knife-blade cutting, drum sanding and almost any high-speed wood-working operation. Foams that absorb moisture may need to be dried and even post-cured to maximum RTM processing temperature before machining. Use caution; the dust from some foams may be hazardous.

Some of the foams supplied in sheet form can be thermoformed or densified from a rough cut piece to a more accurately moulded core. This process is recommended by the manufacturer of Rohacell™, for example.

10.2.4 PROCESSING CONSIDERATIONS WHEN USING FOAM CORES

When choosing the foam to use as a core material the maximum part service temperature and applied loads would naturally be important

considerations. In many cases, though, it will actually be the RTM processing temperatures and pressures inside the mould that will be worst-case. The compressive strength of the foam at the injection temperatures must be higher than the maximum resin injection pressure, and the compressive strength at cure temperature must be higher than the post-injection resin pressure. This requires a resin injection machine that controls the maximum pressure during and after injection.

Many foams absorb a small amount of moisture from the air, and because of the low density of the foam this moisture causes a significant percentage weight increase. The pressure caused by boiling off this absorbed water can blow the composite skin off the core. For most foams and RTM processing conditions it is recommended to dry the foam prior to loading it in the mould. The drying cycle will vary depending on foam type and thickness, but 120°C for 4 h is a good start.

Foam expands with increasing temperature. With some foams this is so dramatic that they are used in a process called thermal expansion RTM [4], where expansion occurs after resin injection, compacting the preform and squeezing out excess resin. In aerospace RTM, if there is a temperature increase after resin injection, both the foam and the resin will expand; the result will depend on the type of resin injection equipment used. If flow-controlled equipment is used, the resin pressure will increase. If pressure-controlled equipment is used, the expansion will cause resin to feed back into the resin pump.

One of the advantages of foam cores is the support they can provide during the preforming operation. Since the core provides rigidity, the preforming operation can be accomplished without a preform mould. The dry reinforcement can be adhered, stitched or stapled to the core during hand lay-up. The core provides the durability and handling properties required to transfer the preform to the mould, allowing less binder or fewer stitches to be used, which can affect physical properties. The foam can also be machined, providing a cavity for reinforcement to be placed, such as in a through-the-thickness spar or rib, without tooling changes. Cores can also be drilled, and reinforcement threaded through, to provide a column-like member. When thick laminates are to be used, the core can provide a 'mould' to debulk the plies around, allowing easy mould loading. Where foam cores are used for preforming, a number of preforms can be made at once, without the expense of multiple preforming moulds.

The resulting thickness of the composite skin moulded next to a foam core is influenced by many variables, including the size of the foam core, the stiffness of the foam at the processing temperatures and the bulk and compressibility of the reinforcement. It is necessary to adjust the core size after measuring the actual fibre volume in the composite skin.

After the cores have been covered with the preform they can be placed in the RTM mould, injected with resin and cured. An evaluation can then be done on the part to determine if the correct volume fraction has been obtained. If the first part is rejected on a visible quality basis it can be cut into sections and the laminates measured directly. When this is not the case it may be difficult to access the quality by means of traditional techniques. If the weight of the core and preform are measured prior to injection, the weight of resin added to the core and preform can be compared with the theoretical value. Determination of the part's centre of gravity and comparison of this with the ideal location can be used to reject parts with resin-rich pockets or resin-starved laminates that are not visible.

Non-destructive inspection (NDI) of foam cored panels can be more difficult than with honeycomb panels. The through-transmission ultrasonic (TTU) method, which is commonly used with honeycomb panels, functions with some foams up to 75 mm thick [1]. However, subtle changes in cell structure within the foam can attenuate the ultrasonic energy to the point that it does not transmit sufficient energy through the panel to detect any flaws. Shearography is effective on foam panels; it works on the principle of detecting very small deflections of the panel surface caused by an applied load, such as vacuum on the surface. Thermography has not been effective for foam panels; its operation is similar to shearography except that the applied load is replaced by a temperature change. Radiography (X-ray) detects variations in densities of the panels; it can detect locations of excess or insufficient resin but cannot detect cracks in the foam or disbonds that occur after moulding.

10.2.5 LESSONS LEARNED FROM USING FOAM CORES

The user should be wary when moulding parts with deep sections of foam at high temperatures because the high coefficient of thermal expansion (CTE) will cause dimensional changes upon cool-down. When a graphite composite web or an attachment passes through a foam core, as shown in the panel with integral lugs in Figure 10.5, the difference in CTE will result in surface waviness because the foam core shrinks more than the composite web.

A thin composite skin on low-density foam is not a durable combination. As previously mentioned (section 10.2), impact from hail can cause severe foam fracturing.

When closed-cell foams are sliced or machined, the cells on the surface are cut open. These act like small cups to hold resin. In addition, damage to these surface cells can admit resin into the layer of next deeper cells. The amount of resin admitted depends on the cell size and density of the foam (influencing the strength of the cell walls). Our experience with

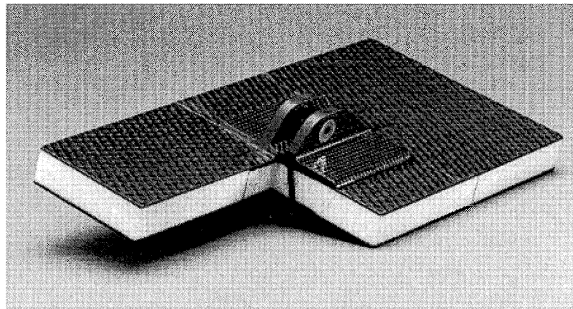


Figure 10.5 Foam Core Panel With Integral Lug Connected to Opposite Skin. Reproduced courtesy of Hexcel Structures, Kent, WA, USA. Photograph by Tim Doty.

Rohacell™ 51WF suggests about 600 g of resin will fill partial or broken cells per square meter of core surface.

As discussed above in section 10.2.4, it may be necessary to increase the size of the core to produce the desired composite thickness. This oversized core can lead to loading difficulties since it will not nest properly in the preform during loading. Some variability in final parts is likely.

Foam cores designed with a complex perimeter, such as varying ramp angles, curves and sharp corners, will likely cause more variation in composite thickness around this perimeter.

If the compressive strength of the foam at the RTM processing temperature is exceeded the foam will crush and the volume will be made up by resin. This may not be visible on the exterior of the part. Low-density foams are fragile. A slight tap with a hard object will make a dent which will be filled by pure resin during the injection.

When fabricating a preform with a tight male radius that will be placed over a foam core, one must remember to form the preform to the correct radius in the first place. Otherwise, one is relying on the foam to force a sloppy preform into a tight corner, and it is the foam that will give way. The outer radius of the part will be pure resin and prone to cracking. The fragile corners of the foam core will be strengthened by curing a surface coat of resin on to those corners.

10.3 HONEYCOMB AND OTHER OPEN-CELL CORES

In the conservative environment of aerospace design and certification the use of foam to replace honeycomb in sandwich panels can meet with scepticism. Some of this attitude comes from negative first impressions of foam cores, and some comes from more recent failures of foam cored components in testing. There are several advantages of honeycomb over foam:

- honeycomb is qualified for many existing specifications;
- Nomex™ honeycomb has a higher specific compression and shear strength (in the ribbon direction) than any other core material described in this chapter (Figures 10.3 and 10.4);
- the chemical resistance and the fire, smoke and toxicity properties of Nomex™/phenolic honeycomb are better than most foams;
- fatigue, durability and hot/wet performance of honeycomb is better understood than for foam;
- commonly used inspection techniques, such as TTU, perform well on honeycomb structures but not on many foams.

The obvious difficulty with the use of honeycomb in RTM is that the cells must be sealed to prevent the liquid resin from filling them. This can be solved by two approaches: by filling the honeycomb cells with closed cell foam, or by wrapping the honeycomb core with a film which is impermeable to the liquid resin. Both these methods will be discussed in section 10.3.1. below. Other core materials which normally are not compatible with the RTM process could be used when treated in the same way as honeycomb. Open cell foams could also be wrapped by an impermeable film to prevent resin entering the foam cells.

10.3.1 METHODS OF PREVENTING RESIN FROM FILLING THE HONEYCOMB CELLS

The two techniques for preventing resin from filling the honeycomb cells (filling the honeycomb cells with closed-cell foam and wrapping the honeycomb core with a film which is impermeable to the liquid resin) can each be achieved in either a one-step or a two-step process. The sequences for these processes are shown in Table 10.2. The one-step and two-step manufacturing processes are compared with a three-step approach which moulds two skins separately and secondarily bonds them to the honeycomb.

Filling the honeycomb cells with closed-cell foam

This method involves filling the cells of the honeycomb with one of three types of foam: a liquid foam-in-place closed-cell foam, a premixed expandable product such as Synspand™ from Dexter Hysol or a non-expanding syntactic filler. The non-expanding syntactic filler would have the highest density of the three and would be more suitable for small inserts, through fasteners and areas requiring accurate machining or drilling after filling.

Two blown foams listed in section 10.2.1 of this chapter may be useful for filling honeycomb: polyurethane and Gillfoam® phenolic. The latter

Table 10.2 Alternative processes for sealing honeycomb (H/C) before resin transfer moulding

Number of steps	Manufacturing Process		
Three	Fill H/C Core With Closed Cell Foam	Wrap H/C Core with Film	Bond
Two	Machine core shape; Fill H/C core with foam; Mould skin 1 and 2 around H/C core	Machine core shape; Wrap H/C core with film and cure; Mould skin 1 and 2 around H/C core	Mould skin 1; Mould skin 2; Machine core shape; Bond H/C core to skins
One	Machine core shape; Fill H/C core with foam; Expand foam in mould; Inject resin into skins 1 and 2 around H/C core;	Cure	Machine core shape; Wrap H/C core with Film; Cure in mould; Inject resin into skins 1 and 2 around H/C core; Cure

foam has been blown directly into honeycomb by the manufacturer, M.C. Gill. When choosing a foam to fill the honeycomb cells, look for a foam which bonds to the walls of the honeycomb, thus preventing the liquid RTM resin from squeezing between the two, adding weight. These foams should form a skin on the surfaces which will later contact the preform to reduce the amount of liquid RTM resin which would otherwise be deposited into the open surface cells of the foam. It is essential for proper load transfer that some of the honeycomb wall be exposed on both sides of the core for the resin to form a fillet during the RTM process.

Filling the honeycomb with foam will rigidise the core. In the two-step manufacturing process described (Table 10.2) the core is filled with foam prior to being combined with the preforms. This necessitates either post-machining of the core or accurate sizing during the foaming step to ensure accurate fit-up in the moulding step. The one-step process has the advantage of foaming while loaded in the mould with the preforms, which is a more robust approach to core sizing.

Unfortunately, this approach to sealing the honeycomb cells combines many of the disadvantages of foam with those of the honeycomb. The most notable disadvantages are the increase in weight of the core, the inability to use TTU inspection equipment on some foams, and low fatigue, impact and hot/wet properties. In applications where the honeycomb is the structural core and the foam is considered non-structural, foam failure may be tolerated.

Wrapping the honeycomb core with an impermeable film

This technique begins with machining the honeycomb core to size. The core is then wrapped, first with a film adhesive and then with a film which is impermeable to the RTM resin and is bondable on both sides. This wrapping operation must be complete with overlap splices throughout and no punctures. This 'gift wrapped' core is either cured as is (in the two-step manufacturing process) or placed in the RTM mould with the preforms (in the one-step manufacturing process) where the film adhesive cures prior to injection of the RTM resin. The film adhesive bonds the honeycomb to the impermeable film, and the RTM resin bonds the film to the composite skin. Core shapes should be kept simple to reduce the complexity of the film wrapping process. Commonly used film adhesives have performed well with this technique. The key to success is the choice of the impermeable film, which is often kept proprietary by the companies who have developed this method. The Boeing Company has patented a version of this method where the impermeability was achieved by a combination of a film adhesive and a carbon fibre prepreg [5].

A hybrid approach might be the best solution to honeycomb core sealing. Foam is expanded only in the honeycomb cells requiring extra

support against lateral forces (steep ramps) or where preforms penetrate the impermeable film and pass through the honeycomb. The prototype under-wing fixed panel for the Airbus A330/340 shown in Figure 10.6 was resin transfer moulded with honeycomb wrapped by an impermeable film. It incorporated moulded in-place metal bushings in the integral lugs that passed through the core to the opposite skin.

Little has been published on the mechanical performance of RTM honeycomb structures. Rohr Inc. has claimed that mechanical properties of the RTM components fall within acceptable ranges – not quite as strong as would be achieved with hand laid-up, pre-cured skins and secondary bonding technology, but stronger than would be achieved in a co-curing process [6].

10.3.2 HONEYCOMB SELECTION FOR RESIN TRANSFER MOULDING

The mechanical properties used to select honeycomb for a prepreg sandwich structure would also be used for an RTM application (e.g. shear strength, temperature limitations, compressive properties). When the honeycomb sealing technique of filling the cells with foam is to be used a larger cell size would be preferred and less resistance to lateral forces would be necessary since the foam in the honeycomb cells would significantly improve this property. When the honeycomb sealing technique of wrapping the honeycomb with an impermeable film is to be used a smaller cell size would be preferred since the film will act like a trampoline stretched across each cell opening. The honeycomb's resistance to lateral forces would depend on the steepness of the ramps and on the resin injection pressures used.



Figure 10.6 Fixed under-wing panel resin transfer moulding prototype for Airbus A330/340 with honeycomb core and integral lugs. Reproduced courtesy of Hexcel Structures, Kent, WA, USA.

10.3.3 SPECIAL CONSIDERATIONS

Core movement

As with autoclave processing of honeycomb panels the lateral forces created in the process must be resisted by the honeycomb, with or without the aid of auxiliary supporting techniques. For the RTM process the lateral forces come from the resin injection pressure and can cause the honeycomb to move laterally away from the preform. This is not obvious, unlike core movement seen in an autoclave cure. In the case of the RTM panel the movement may not be visible from an inspection of the exterior of the panel.

The hybrid approach mentioned in section 10.3.1 can reduce core movement. Foam is expanded only in the honeycomb cells of the steep ramps. Synspand® is useful for this purpose and can be incorporated in a one-step process where the foam expands as the film adhesive cures the impermeable film to the honeycomb walls prior to injecting the RTM resin. Additionally, the resin injection pressure can be reduced to further minimise core movement.

Design details

There is a fundamental difference between autoclave and RTM processing with honeycomb that opens up new design opportunities. In autoclave processing of prepreg it is essential that all areas of the lay-up experience consolidating pressure and thickness reduction in order to eliminate voids. Features shown in Figure 10.7 are not made in co-cured autoclave processing but can be moulded in RTM. These are examples of where honeycomb can provide weight reduction, part count reduction and increase in stiffness.

The designer also has latitude in selecting an angle for a ramp where the honeycomb tapers at an edge band. With autoclave processing, 30° is a common maximum without the need to resort to high-density honeycomb. It is possible to mould RTM parts with ramp angles of 90°. The ramp angles in the fixed panel shown in Figure 10.6 were 30°, 65° and 90°; however, compromises in the injection pressure were necessary along with proprietary techniques to support the honeycomb against the pressure of the resin at the steep ramp angles.

Honeycomb core machining

Honeycomb is commonly machined with equipment ranging from five-axis NC mills to hand-held pneumatic disk sanders. This discussion will not attempt to educate the reader on the details of honeycomb machin-

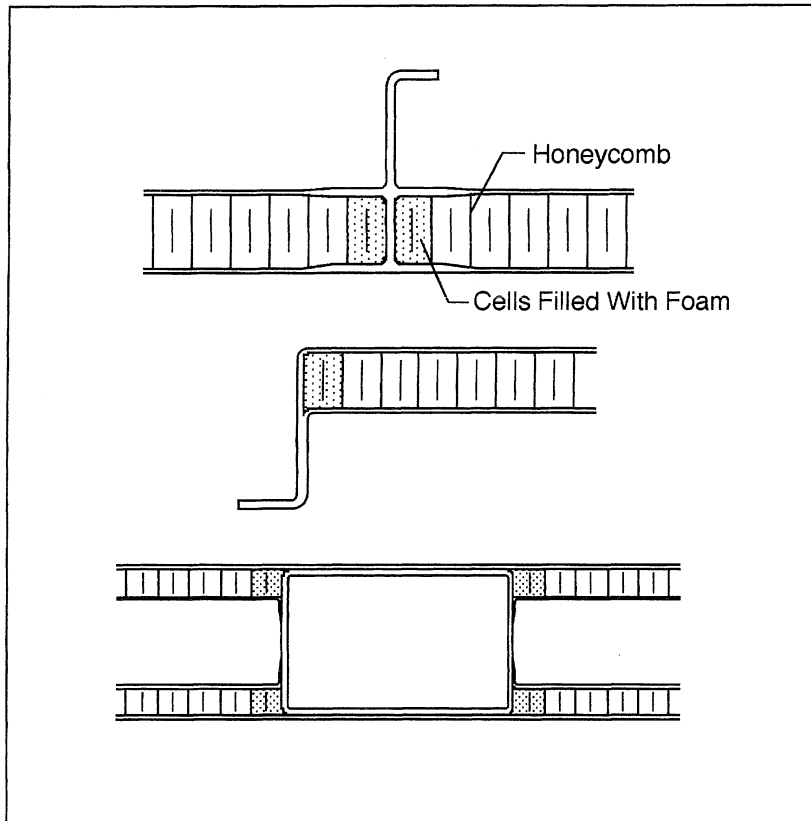


Figure 10.7 Design possibilities using honeycomb core in the resin transfer moulding process.

ing, but will merely highlight a few differences between working with foam and honeycomb.

The target thickness for a honeycomb core would likely be different than for a foam core, especially for low-density materials. Low-density foams are more compressible than is comparable-density honeycomb, and therefore a foam core would be machined thicker to compensate for the compression that would be seen as a result of preform compaction and resin injection pressure.

Tolerances for machining the periphery of honeycomb cores would be less stringent than for foam since the honeycomb acts like a bellows and will compress to fit the cavity in the RTM mould. For this reason the nominal size for the periphery should be slightly larger to ensure the core will never be too small.

Although precise laminate thickness control can be an advantage of RTM the laminate thicknesses for ramps supported by honeycomb (or foam for that matter) may be difficult to control consistently, especially if the ramp angle varies around the periphery.

Honeycomb is more conformable to contour than is rigid foam. Since aerospace panels frequently have a slight contour, and the laminates under the core often contain reinforcing doublers, it may reduce the honeycomb core machining cost to design the honeycomb core to a constant thickness and simply drape it over doublers in the lower skin. For severe three-dimensional contours Flex-Core™ from Hexcel or thermoformed conventional honeycomb may be used.

10.4 BALSA WOOD CORES

Balsa is a tree grown on plantations and along the rivers in Ecuador. It grows very fast and develops a vertically aligned cell structure, a sort of natural compromise between foam and honeycomb. The cells appear to be closed yet allow transport of the tree fluids. This is important because the cells will also transport an RTM resin into the core if it is not sealed. Balsa core has been used in aircraft floor panels for decades.

10.4.1 BALSA SELECTION

End-grain balsa, which has been bonded together from small blocks with the wood grain in the thickness direction, is the form of balsa appropriate for core material. The specific compression strength of end-grain balsa is very high, second only to Nomex™ honeycomb [Figure 10.3(a)]. The specific shear strength is somewhat lower in comparison with other core materials [Figure 10.3(b)]. The high ratio of compression strength to shear strength has caused problems in balsa cored aircraft floor panels where a concentrated load, such as the high heel of a woman's shoe, has pushed a plug of balsa out of the core, delaminating the opposite skin. The specific shear modulus is the highest of the core materials shown in Figure 10.3(c). Balsa performs well in fatigue, is not brittle, exhibits low creep, is resilient and tolerates processing temperatures of 180°C.

One disadvantage of using balsa is that it is available in only a few densities: 150 kg/m³ is the most common, with 100 kg/m³ and 250 kg/m³ harvested in smaller quantities and at higher prices. Each of these densities is an average. A sheet of 150 kg/m³ end-grain balsa could contain small blocks with individual densities from 110 kg/m³ to 210 kg/m³. The mechanical properties of these individual blocks vary dramatically. It is important to understand the sorting and selection criteria for the different grades available. Select grade is recommended for high-performance applications.

The manufacture of a sheet of end-grain balsa that meets high quality standards relies on controlled kiln drying of the cut balsa, accurate sorting, selection and placement of the individual blocks into the array and consistent bonding to form the billet. The balsa is generally shipped in long billet form to be sliced and made into various sheet products by the manufacturer.

10.4.2 PROCESSING CONSIDERATIONS

Balsa can be cut with typical high-speed wood cutting equipment. As mentioned in the introduction to this section, it is necessary to seal the cells on the surface to prevent resin penetration and to improve the bond between the laminate and the balsa. The balsa manufacturers have developed proprietary coatings for this purpose; however, these have been formulated for polyester and vinyl ester resins. Users should test the compatibility between the RTM resin and the sealer by performing flat-wise tensile or peel tests, at elevated temperatures also, before proceeding. It is also recommended to test the sealing ability of the coating at resin injection temperature and pressure. If a balsa sheet manufacturer's sealer is chosen, that same company will probably cut the sheet to final size and shape before they apply the sealer in-house.

Balsa readily absorbs moisture from the atmosphere. To reduce moisture pick-up it is shipped in plastic bags. Should it be necessary, dry the core at 94°C in a convection oven for 90 min for 25 mm thick core, and for 240 min for 50 mm thick core.

Exposure to the high temperatures of the aerospace RTM process is not a problem for balsa. Several hours at 180°C was shown not to degrade the room-temperature compression strength [7].

Many of the processing considerations for foam core apply to balsa.

10.5 BLADDERS

Bladders can solve many common tooling and process problems in RTM. The most obvious use is for the moulding of internal cavities which would trap a solid mandrel because of obstructions or negative draft. A bladder is a flexible membrane that compresses against, and defines the shape of, a surface of the composite being moulded; this surface is often an internal cavity. Usually, compressed air, gas or liquid is the source of the pressure that compresses the composite, but solid fillers have also been used.

A bladder's flexibility allows it to conform to preform surface changes caused by lay-up redesign, ply placement variability, ply drop-offs or contour. Bladders can stretch to alleviate preform loading difficulties, such as the insertion of blade stiffeners into slots in the tool or the

uniform compression of bulky tubular reinforcements that would be pinched by multipiece solid tooling.

Very large RTM parts have been moulded by means of bladder technology, including 8.5 m long wind turbine blades and an 18 m long hollow furling boom for a sailing yacht. The use of bladders for the wind blade and the boom eliminated the need for a press to close the mould. The mould halves were clamped together, and when consolidating pressure was desired the bladder was inflated.

Even for smaller tools, the use of a bladder can lower tooling costs by replacing multiple machined tooling elements, avoiding the sealing problems between each element and reducing the tooling tolerances. This is especially important for prototype and short-run production tooling.

Bladders can solve resin injection problems by giving uniform preform compaction and allowing compaction pressure to be varied throughout the injection phase. The low thermal mass allows faster heat-up and cool-down cycles. Bladders also avoid the problems associated with thermal expansion of metal or solid elastomeric tooling, which can include dry fibres, excessive mould deformation and tooling lock. Bladders can also be used effectively in the preforming process.

10.5.1 TYPES OF BLADDERS

Reusable versus fly-away bladders

The majority of this section discusses reusable bladders made from elastomers. An alternative approach, which has been used successfully in the sporting goods industry, is to make the bladder from thin polymeric sheet and leave it in the part. Nylon film has been employed, as heat-sealed sheet and as lay-flat tubing. High-quality film is critical, with a minimum of impurities; this allows films as thin as 0.12 mm to be used.

The Automotive Composites Consortium patented the blow moulding of a hollow core that remains in the RTM component [8]. If these cores are pressurised with air they would be fly-away bladders.

Reinforced versus unreinforced bladders

Bladders that will be trapped in an internal cavity will need to be deformed and stretched to remove them and will therefore be completely or mostly made of unreinforced elastomer. Thin, unreinforced bladders will be susceptible to shrinkage, wrinkling and improper location. They require that the opposite tooling surface be rigid enough to locate accurately the composite. Thick unreinforced bladders are commonly used

for trapezoidal hat-stiffener mandrels. These have adequate rigidity on which to lay-up fabric plies.

When demoulding difficulties are not an issue, fibre reinforced elastomer may be preferred in a bladder. The advantages include less shrinkage, more accurate placement, better surface finish and definition, and adequate rigidity for moulding with bladders on both sides of a composite. Figure 10.8 shows a reinforced bladder made from Airpad™ supplied by Airtech International Inc.

Bladders pressurised with air or gas

Air pressurised bladders are the most common type of bladder. Each bladder is fitted with pneumatic plumbing which passes through the rigid RTM mould to an external pressure source. The key function of the bladder is to be an impermeable membrane to prevent the gas from passing through it into the preform. This is not as easily accomplished as one might think. Some elastomeric materials do not perform well as gas barriers, even with a thickness of a couple of millimetres. This is especially important in aerospace RTM when a high level of vacuum is applied to the preform during injection.

Gas permeability will be discussed in more detail in section 10.5.3 on bladder materials.

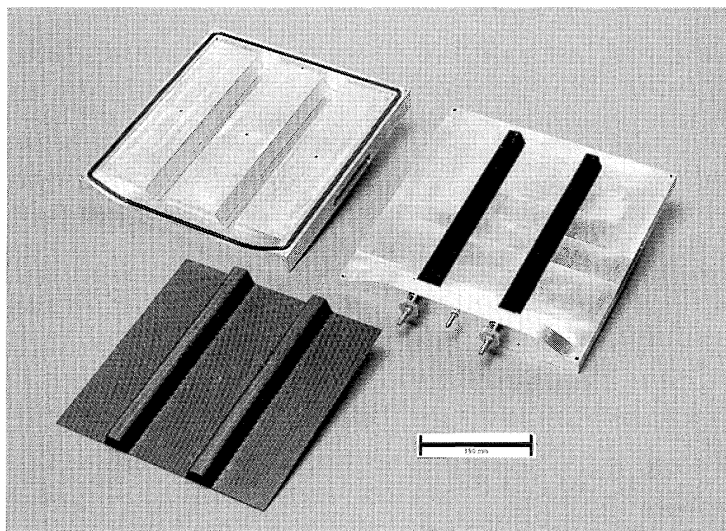


Figure 10.8 Airpad™ bladders and tooling used to mould a stiffened panel. Reproduced courtesy of the Cooperative Research Centre for Advanced Composite Structures, Fishermens Bend, Vic., Australia.

A typical loading operation with bladder tooling may proceed as follows. A preform (or separate plies of fibre reinforcement) is (are) loaded into a rigid RTM mould half. The bladder is inflated to a low pressure to give it shape. Preforms are placed on the bladder and it is set into the RTM mould. Additional preforms are placed in the mould and the second mould half is closed and clamped. The pneumatic fittings are tightened to prevent leaks. The bladder is pressurised for resin injection.

An external bladder can be used for moulding the external surface of a tubular part; an example is shown in Figure 10.9. This may be more useful in the preforming operation to compact a bulky tubular reinforcement without pinching, but it can also be used for moulding. The tubular bladder is mounted inside a can so that vacuum can be drawn between the bladder and the can thereby expanding the bladder diameter enough to insert the fibre reinforcement. The cavity external to the bladder is vented or possibly pressurised and the cavity internal to the bladder, which contains the preform, is brought to a high level of vacuum in preparation for resin injection.

Bladders filled with fluid

There are situations where many repeating bladders are used, for example panels with rows of stiffeners, or a grid of intersecting stiffeners, and the number of plumbing connections becomes excessive. An alternative to gas pressurisation is to fill the bladders with a fluid or a gel and seal them. The source of pressure is mechanical compression when the mould is closed and thermal expansion during the heat-up. Both of these

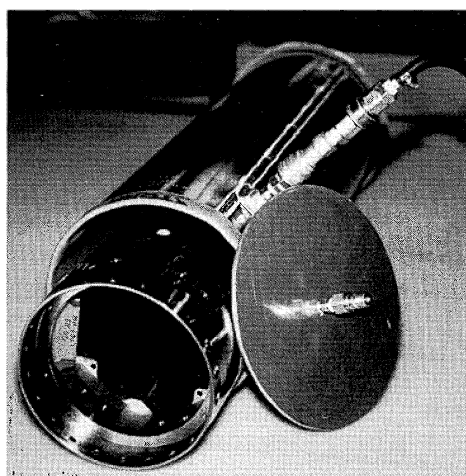


Figure 10.9 External tube bladder expanded by using vacuum, showing mandrel placed inside. Reproduced courtesy of Torr Technologies Inc., Auburn, WA, USA.

methods of generating pressure can result in extremely high pressures and therefore a method of regulating the pressure is needed. Such a bladder must be extracted without collapsing. Owing to the thermal mass of the fluid and the insulating effects of the elastomeric bladder skin this tooling system would require additional time to heat unless the bladder fluid is actively heated.

Bladders filled with solid particles

The most innovative bladder tooling that has recently been introduced is filled with solid particles. Bladders designed and manufactured by International Design Technologies Inc. are filled with solid media and function on the same principal as a vacuum-packed package of ground coffee. When there is a vacuum in the bladder it is rigid for lay-up or moulding against; when the bladder is vented and some of the media removed it becomes flexible and can be collapsed. The procedure for using this product begins with placing the custom-shaped bladder inside its forming mould, applying vacuum between this mould and the bladder and venting the inside of the bladder. This stretches the membrane to the inside shape of the forming mould. The bladder is filled with solid media and vacuum is applied to the interior followed by venting of the exterior cavity and removal of the forming mould. The bladder is now stiff like a package of ground coffee. A two-armed duct mandrel full of solid media is shown in Figure 10.10; the elastomeric portion measures 1.2 m tall. This type of bladder can be used for lay-up or simply be loaded into an RTM mould with preforms. After resin injection the bladder can remain under internal vacuum or it can be pressurised. Following cure, the bladder is vented to make it flexible and, if necessary, media is removed to allow complete collapse for demoulding. The entire bladder and solid media are reusable.

Plastech TT has developed the Smart Core system, which works on a similar principal yet has been refined by the addition of a few features expressly for RTM. The Smart Core was used by Polymarin in The Netherlands to manufacture the 8.5 m wind turbine blade and the 18 m hollow furling boom mentioned in the introductory text of section 10.5. These examples demonstrate that this type of bladder is appropriate, if not preferred, for very large parts. Plastech TT uses a proprietary particle to fill the Smart Core. It is placed in a shape-forming mould which is intentionally smaller than the eventual size of the bladder, gives the bladder resin flow channels on its surface and incorporates an injection lance for distributing large amounts of resin over long distances. During resin injection, the lance provides the highway for the resin; the surface resin flow channels are the arterial routes, and even the preform improves resin flow, being more permeable because of the slightly small

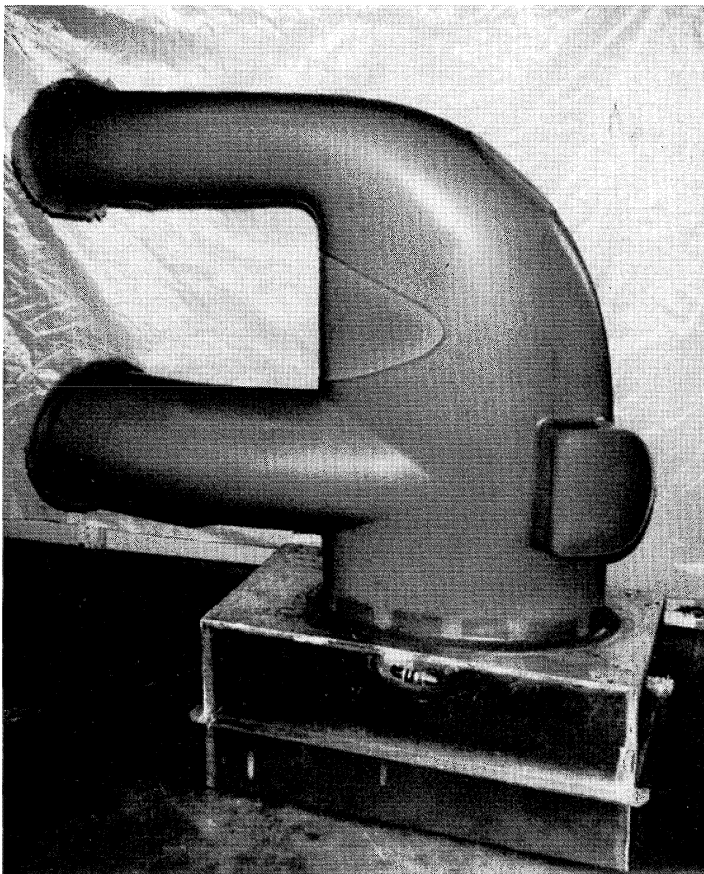


Figure 10.10 Two-armed duct mandrel filled with solid media and rigidised with internal vacuum. Reproduced courtesy of International Design Technologies Inc., Bonney Lake, WA, USA.

core size. After injection, the lance is withdrawn and the Smart Core is pressurised to remove the surface flow channels and enlarge the core which compresses the preforms to their desired thickness [9, 10].

10.5.2 PROCESSING CONSIDERATIONS WHEN USING BLADDERS

The injection of resin into a preform with air pressurised bladders is a pressure balance game. Popular opinion points toward higher pressure in the bladder than in the resin. This pressure differential prevents the resin from collapsing the bladder. This requires that the injection machine has control of the resin pressure so as not to exceed the desired pressure differential. The relationship between elements of the bladder

RTM process has been computer modelled. It has been shown that there is a favourable resin pressure distribution through the preform, a reduced injection time for the bladder process and an increase in the volume of the preform throughout the injection because the net pressure compacting the preform decreases once the resin arrives [11].

Determining the optimum pressure settings is still largely a matter of trial and error. The greater the pressure difference between the bladder and the resin, the more compacted the preform will be and the higher the fibre volume fraction. It is common to inject at a modest resin pressure and low pressure differential, then increase the bladder pressure to compact the preform to the desired fibre volume fraction. The result is that excess resin enters the preform during injection and is squeezed out after the pressure increase. The success of this will depend on the distance the resin must travel to exits, the permeability of the preform and the viscosity of the resin late in the injection cycle.

A tooling feature that would aid this type of process is a vacuum pot for collecting the resin from several exit tubes that doubles as a pressure-pot to provide back pressure on the resin while still allowing it to exit because of the greater bladder pressure. A larger final resin pressure may be needed to achieve better wet-out of the reinforcement or to reduce surface porosity.

When loading a pneumatic bladder into a mould it may be helpful to fill it with enough air to give it shape without significant internal pressure. Glass or carbon prepreg can be incorporated into areas of a bladder that requires stiffness. Sufficient shape and support of a bladder for a lay-up operation can also be obtained by incorporating an internal sub-structure made from sheet metal or composites. The substructure is perforated for uniform bladder pressurisation. Where negative draft is involved, sections of the substructure can be hinged to move out of the way to allow extraction. Demoulding a bladder may be aided by pulling vacuum inside it to cause it to collapse.

Release agents formulated for elastomers will be necessary if the resin is contacting the bladder material. Caution is advised when applying release agent to an elastomer in its relaxed state if it will stretch and expand significantly in processing, as this may expose surface which is not protected by release agent. Solid releasing barriers are preferred where possible. Films of fluorinated ethylene propylene (FEP) can be bonded to some elastomer systems during the fabrication of the bladder. This is especially useful for silicone bladders because the film will prevent the amines in the resin from attacking the silicone.

Bladders can be deformed by the bridging of preforms in corners. The corners of bladders are often built up with additional material to improve corner definition and reduce this deficiency. Preforms must also be compacted with accurate corner geometry and properly placed in the mould.

An interesting option for resin porting exists with a bladder; a resin entrance or exit can be built into the wall of the bladder with the resin tube passing through the internal cavity of the bladder to exit the mould near where the bladder air pressure lines exit. This may solve a difficult resin flow problem.

10.5.3 BLADDER MATERIAL SELECTION

Several elastomeric materials are currently used in the bladder manufacturing industry. Table 10.3 compares several properties to aid in the selection of elastomers for use in RTM. Silicone has generally been preferred for bladders made specifically for aerospace RTM applications, in spite of its undesirably high permeability to gases, marginal resistance to hydrocarbons and susceptibility to attack by amine hardeners. These weaknesses are overcome by increasing the thickness of a silicone bladder wall and by incorporating a release layer of bondable FEP or adhesive-backed Teflon™ tape.

There is an entire industry which fabricates bladders for custom applications. Compression moulding and blow moulding are processes frequently used, and fabric reinforcements can be incorporated into the walls. These companies have extensive experience with most of the elastomers listed in the accompanying table, as well as with plumbing attachments and hardware.

For companies wanting to use their in-house tool-making capability, the decision of which elastomer to select may be influenced by the technical support and completeness of the line of bladder-making products available. For example, Airtech International carries two lines of bladder products: the Arlon™ line of silicone materials and the Airpad® line of flexible acrylic rubber both include cured, uncured, reinforced and unreinforced sheets. In addition, bondable FEP and valve hardware are available. It is recommended that Airpad™ be supported by internal glass reinforcement or with epoxy prepreg since the unreinforced elastomer exhibits high shrinkage after repeated cure cycles.

10.5.4 MAKING INTERNAL BLADDERS

Several methods can be used for building bladders (a list of the manufacturing options appropriate for each bladder material is shown in Table 10.3):

- blow moulding of unreinforced or fabric reinforced elastomer into an external mould – this method has the advantage of not using any internal tooling that can be difficult to remove;
- compression moulding an elastomeric sheet or moulding a compound to shape in a heated matched mould under high pressure;

Table 10.3 Property comparison for bladder materials

	Silicone	Fluoro Silicone	Ethylene Propylene Diene (EPDM)	Nitrile or nitrobutyl rubber NBR or Buna N	Styrene-butadiene (SBR or Buna S)	Fluoro-elastomer (Viton®)	Ethylene Acrylic (Vamac™) (Airpad™)	Flexible Acrylic (Airpad™)	Iso butylene -isoprene (Butyl)	Poly chloro prene (Neoprene)
Permeability to Gases	high 260	medium 230	medium 175	low 150	medium 120	low 210	low 170	low 190	very low 150	medium 105
Maximum Service Temperature (°C)	100–800	200–500	100–700	400–600 fair to good	450–500 fair	180–220 poor	200–300	500 good	300–800 good	100–800 good
Elongation (%)	poor to fair	poor to fair	fair to good	30A–90A 580	30A–100A 700	30A–90A 670	50A–75A	60A–77A	45A 620	30A–100A 580
Tear Resistance	20A–90A 810	40A–90A 810	30A–90A 580							
Hardness (Durometer)										
Volumetric Coefficient of Thermal Expansion $\times 10^{-6}$ (cm/cm°C)	poor	excellent	poor	good	poor	excellent			poor to fair	fair
Resistance to Aromatic Hydrocarbons	Bladder	cast, lay-up, extrusion, spray, rotomold	lay-up, extrusion, blow moulding, cast, rotomold	compression moulding	blow moulding, compression moulding	lay-up, blow moulding	lay-up	blow moulding	blow moulding, com- pression moulding	blow moulding
Manufacturing Options										
Relative Cost	moderate	very high	low	low	low	high	moderate	moderate	low	low

- casting a liquid elastomer into a mould which defines the inner and outer surfaces of the bladder, curing the elastomer and removing the mould;
- extruding a constant section hollow bladder and plugging the ends with liquid elastomer;
- cutting and shaping pieces of cured elastomer sheet and bonding them together with adhesive or uncured sheet;
- laying uncured elastomer sheet into a mould defining the outer surface of the bladder; reinforced elastomer, composite prepreg, and foaming adhesive can also be incorporated to add stiffness or give shape to corners; this lay-up would be consolidated by using an internal nylon bag and cured in an autoclave; the nylon bag may remain inside the bladder;
- laying cured and/or uncured elastomer sheet onto a mould defining the inner surface of the bladder, curing the elastomer, cutting the bladder off the mould and splicing and bonding the bladder back together;
- rotational moulding a hollow bladder by using castable elastomer in a multipiece external mould; this method has the advantage of not using any internal tooling that can be difficult to remove;
- spraying liquid elastomer, thinned in solvent, onto an open mould; silicone can be applied by this method, however, the large amount of volatile gases given off makes this process hazardous and it may not pass emission regulations.

Superior shape definition of the bladder exterior will be necessary when making bladders that will be pressurised with air or fluids, otherwise they will dislocate, bridge corners and thin out. Bladders that will be filled with solid particles will take an accurate exterior shape from the shaping mould during the filling of these bladders and thus do not require a complete shape definition in the elastomer.

The mould for making the bladder can in itself be a challenge. Consider some of the techniques discussed in this chapter for removable inner surface definition tooling, including melt-out and wash-out (section 10.6). One could break out the tool, stretch the bladder off the tool or even leave the tool inside, such as with the internal substructure already discussed (section 10.5.2).

When making a bladder with an elastomer that shrinks appreciably upon repeated cure cycles it is important to post-cure the bladder at 15°C to 25°C above its use temperature, thus pre-shrinking it. Another option is to reinforce the elastomer with glass fabric or composite prepreg to reduce its shrinkage.

Incorporation of solid release films or barriers during the fabrication of the bladder is the preferred way of ensuring consistent release of the

bladder from the moulded part. A film of FEP can be bonded to some elastomer systems during the bladder fabrication process.

10.6 PHASE-CHANGE TOOLING INSERTS

The ability to make hollow parts without large access holes provides a high degree of design flexibility. Phase-change inserts can be removed through a hole less than 0.25 cm where necessary. Rigid mould surfaces on all sides can be valuable for both quality and process considerations, since process parameters and thickness distributions will be more consistent than with flexible mandrels.

Most crystalline and some amorphous materials will undergo a phase change at some temperature. The challenge is finding materials that have both an appropriate melt temperature and suitable physical properties. Such materials can be categorised as follows: melt-out metal alloys, eutectic salts, and waxes. Although technically not a phase change material, soluble mandrels that can be dissolved and removed as a fluid will be discussed here. These are commonly referred to as wash-out or wash-away mandrels. The entire mandrel need not melt; a conglomerate of small particles suspended in or bound together by phase change or soluble materials can still be removed through a small opening. The mandrel can also be broken into pieces that can be removed around restrictions that are not as severe.

A high degree of precision is possible when required, and for most cases phase change inserts can also be quickly and cost-effectively moulded. Many of these materials can also be recycled efficiently with few environmental or safety concerns. Non-porous mandrels can even fracture without causing part rejection. Some of these materials have a high density that can lead to loading problems, but the mandrel could be hollow or filled with a lightweight material. If the melting point of the mandrel is close to the required post-cure temperature, assurance can be gained that all of the laminate has reached the required temperature when most of the material has melted. As with all unheated tooling inserts the part cure schedule must be extended to allow distant areas to heat up.

It is also worth considering these materials to form an outside mould surface of such high complexity that the mould must be destroyed for each part. Preform placement may be a problem for many of these situations, but may be possible in some.

10.6.1 SELECTING MELT-OUT AND SOLUBLE MANDREL MATERIALS

In addition to the important physical properties considered for other insert materials, the melt temperature is of primary concern. The melt

temperature should be higher than the gel temperature but lower than the post cure temperature. When a one-step cure is desired the melt-out must be done after cure but with a temperature that is lower than the glass transition temperature of the RTM resin. The wash-out system does not require that heat be used and is viable for resins that do not require, or cannot withstand, secondary heating.

Compressive strength is not likely to be a factor since the materials in consideration have adequate compressive strength for RTM. For hollow mandrels the flexural strength of the material can be important, and conservative load estimates are advisable. Impact resistance is poor with plasters, a benefit when breaking out a mandrel. Table 10.4 outlines the relative performance of these materials in temperature categories.

10.6.2 EUTECTIC SALTS

Some of the first and still the most commonly used phase change materials are eutectic salts. As the name would imply, they are combinations of metal salts that have a specific melting point; a commonly used version is called Paraplast® (from Hexcel). Some common melt temperatures are 160°C, 210°C and 270°C; the use temperature is about 15% lower. Eutectic salts normally contract less than 1% in volume upon solidification. Both the solid material and the melted material have the appearance of plaster. The liquid properties are similar to a thin plaster mix and have similar hardness and strength when solid. Most eutectic salts will absorb moisture from the air, which will dissolve surface material, making the mandrel slimy after hours of exposure. For this reason these mandrels should be sealed immediately upon demould and raw material should be stored in sealed containers. Mandrels that are to be shelved will last longer if stored under vacuum in a bag. Some salts can be dried, but others will absorb water that cannot be removed with heat. This will increase the melt viscosity of the recycled material and leads to the formation of clumps that will not melt [12].

Eutectic salts have a specific gravity around 2.0, a latent heat of fusion of about 75 kJ/kg and a specific heat of 1.4 kJ/kg °C. Heating any mandrel can require a substantial amount of time, but with eutectic salts melting the mandrel requires as much heat as is required to increase the temperature of the mandrel by over 53°C. Where thick laminates or cores are insulating the mandrel, more time may be required than for the typical cure schedule.

When dissolved in water, often used to clean residual salt from the cavity, the eutectic brine solution is highly alkaline (pH 10–13). PMI foams such as Rohacell™ will become a soft gelatine if wet by this solution for a few hours. Once cured, few aerospace resins would be damaged by this solution, but another reason for sealing is to maintain a

Table 10.4 Comparison of Various Melt-out and Soluble Mandrel Materials

Temperature Range (°C)	Material	Relative Strength (1–10)	Specific Gravity	Coefficient of thermal expansion × 10 ⁶ (cm/cm °C)	Cost	Can be Moulded Hollow?	Latent Heat (kJ/kg)	Toughness
80–150	Wax	1–2	1	200	Medium	Yes	25–40	Fair
130–1000 0–400	Melt-Out Metal Soluble Plasters	10 2–5	7–8 1.5–3	150–240 30–70	High Low	Possibly Yes	50 Not available	Excellent Poor
160–270 0–1000	Eutectic Salts Conglomerates	5–7 1–8	2 1–6	50 0–800	Medium Not available	Yes Possibly	75 Varies	Fair Varies

barrier between the possibly incompatible liquid resin and the eutectic salt mandrel. Since these materials contain nitrates disposal is regulated in some areas.

10.6.3 MELT-OUT METAL ALLOYS

Metal alloys are excellent for small precision mandrel requirements, partially because of low contraction or even expansion upon solidification. The metal has sufficient strength to be used in almost any mandrel application. With a low CTE ($1.5\text{--}2.5 \times 10^{-5}$ per $^{\circ}\text{C}$) when compared with waxes, foams or elastomers ($1.5\text{--}8 \times 10^{-4}$ per $^{\circ}\text{C}$), the mandrel has little effect on the RTM injection process. Melt temperatures can be varied, but 140°C and 180°C are available. Large mandrels will be heavy and will absorb large amounts of heat in the melting process. These limitations on size can be overcome, but economic factors such as high material cost would weigh heavily in favour of another material. The high density and surface tension of metals are useful when re-melting. Foreign materials such as resin chunks will float to the surface as slag. To increase the melting speed and aid removal of contaminants, the mandrels can be heated in an oil bath. This allows nearly a 100% recovery of the metal. Pressure casting can be used when very low porosity and excellent surface finish are required. Automated insert manufacturing machines are available where production volume can justify the investment [13].

10.6.4 WAXES

Wax is a lightweight, non-porous and somewhat flexible material that is suitable for a phase change mandrel. These properties can provide a forgiving combination that lends waxes to many applications. Maximum melting temperatures are about 150°C where low melt viscosity is required. Some waxes have enough flexibility to use the Poisson effect, to debulk side laminates as the mould is closed, without fracturing. Wax can be used alone or with fillers to reduce shrinkage or increase the softening temperature. Combinations of different waxes to provide suitable properties can be specially formulated for specific RTM applications. Wax can be cast to almost any shape accurately, can be repaired easily and requires no special storage or disposal precautions. Most waxes are difficult to dissolve but high-pressure hot water with detergent can help clean out residual material. Owing to a high CTE and a phase change the wax will expand upon heating, which may cause pressure during melt-out if the drain hole is not open. As with most castable materials, pressure casting can be used to reduce porosity. Millions of wax patterns are used to define accurate cavities in the investment casting industry annually. Even though many differences exist

in the applications, much of the investment casting wax technology could be applied to phase change RTM mandrels.

10.6.5 SOLUBLE PLASTERS AND CONGLOMERATES

The use of plaster for both internal and external tooling is common where durability is not required. Most plasters are not water soluble, and some are soluble only after a heat cycle. Other soluble materials include blown or syntactic polymer foams (such as styrene) which are solvent sensitive. As with other materials, plasters are frequently used with inert fillers to alter the process or physical properties. One example is called Easy-Out™, patented by the Easy Out Company. Although not strong in flexure or tension, the material can withstand 7 atm pressure at temperatures up to 400°C. These mandrels will cure in 30 min and must be dried 30 min for each centimetre in thickness at 300°C. The cost is about £1.00 per kilogramme and the material is 20% lighter than white plaster. Once dried, it is water soluble and can be used as a break out mandrel [14]. Plasters must usually be sealed with shellac, silicone/water emulsion, PVC or other suitable polymer resin or film to prevent resin intrusion and to release the mandrel. Usually no toxicity or disposal precautions are required.

Conglomerates of any phase change or soluble materials with inert fillers can provide many properties unavailable with the neat material. Oils, dextrose and many other compounds can also be used as binders if they solidify, dry or are used so as to prevent a contamination threat. Slurries of binders and fillers can also have a low density (specific gravity less than 1.0) when desirable for larger sized mandrels. Many fillers have been used for soluble mandrels from synthetic and natural sources. Perlite, vermiculite and mica can be used as lightweight mineral fillers. Sand, calcium carbonate and diatomaceous earth might weigh more but are inexpensive and suitable as fillers. Polymer foam beads, powders and microballoons are suitable synthetic particles that can be bound together to form lightweight, but possibly porous, mandrels. Moulds and cores of similar composition are made in the metal casting industry, and much of this technology could be borrowed and used in RTM mandrels. The binder need not be soluble initially; in some cases the mandrel only becomes soluble after experiencing cure temperatures. In the extreme case, very little binder is used and, once dissolved, the filler particles can be conveyed from the cavity in an unchanged state.

10.6.6 BREAK-OUT MANDRELS

Break-out mandrels are viable when accessibility to the cavity is good but when undercuts, curves or locating internal metal inserts make ordinary

tooling difficult to extract. Plasters, eutectic salts and other materials can be removed by demolition. One might say that the only difference is that the solvent or heat is replaced by a hammer. Although mandrel breakage may sound crude this has proven to be a very effective method for many applications. Often mandrel breakage is considered as a last resort but should actually be considered prior to the melt-out or wash-out operations. Both dissolving and melting are enhanced by reducing the size of the pieces. When the mandrel is hollow, one blow can do the work of hours of heat or solvent. The trusty hammer should be used with some discretion when the laminates are thin, hot, or only partially cured. Thick laminates are not as likely to be damaged by careful blows but some precautions are advisable. For areas with thin skins over a hollow mandrel a soft mallet is used to break the mandrel through the laminate. This technique is used primarily on ducts and secondary structures but with testing or a special impact tool might be applied to primary structures.

When a solid face of the mandrel is exposed it is best to put a hole in the centre with a star chisel or drill. Then, working a straight chisel or blunt punch from the edge toward the centre, remove pieces as large as possible. A chisel should not be used where it can strike laminate; there should always be mandrel between the side being removed and laminate. Therefore, if the chisel skips off the intended location it will strike only the inside of the mandrel, not the laminate. When the mandrel is hollowed out it may then be possible to cave in the sides. Hollow mandrels are much easier to break out and remove than solid mandrels, which should be avoided for break-out applications.

10.6.7 CREATING THE MANDREL SHAPE

Most mandrel materials considered here are usually cast or moulded to size. This is preferable to machining in most cases, especially when the material contains abrasive particles. Stereolithography techniques may be applied to manufacture polymer mandrels that can be melted or dissolved.

The materials used to make the casting moulds are many and varied. Metal moulds that have been cast or machined are the most durable, as thermal shock and cycling are damaging to composite moulds. Soluble mandrels may not require the use of heat in manufacture, substantially reducing the cost of tooling. Plastic moulds are common for materials where low processing temperatures are used.

Plasters and melt-out mandrels can be cast solid or hollow. In most cases the material must have a low enough viscosity to be self-levelling and smoothly fill the mould. This is best done by using a pressure-pot or head pressure to dispense the material, filling from the bottom with an

extension nozzle. The flow rate is regulated so as not to entrap air from turbulence but also not to allow freezing prior to fill. A simple alternative is to pour the liquid down the side of the mould, like beer into a mug. Air-locked cavities are to be avoided as they will require air venting and possibly an extension to avoid spillage (Figure 10.11). If the molten material is pressurised until solidification or cast under vacuum conditions, the void content of the mandrel will be reduced. A high-pressure casting method uses a heated ram to force the molten material into the cavity. The mould must be rigid and clamped well to resist pressures as high as 100 bar.

Various methods can be used to produce hollow mandrels. If all sides are to be sealed as moulded, rotational moulding techniques can be used. With this system, the mould is closed and connected to a two-axis gimbal. Once filled with the amount of material required for the desired wall thickness it is then plugged and rotated about both axes. The material freezes, or melts then freezes later, on the inside mould surface. This occurs evenly when the revolution rates, mould temperature and melt temperature are correct. The material is added in the liquid or powdered state and the appropriate temperatures are accommodated. Since after cooling a partial vacuum may be left in the cavity it must either be vented or be strong enough to support the pressure of

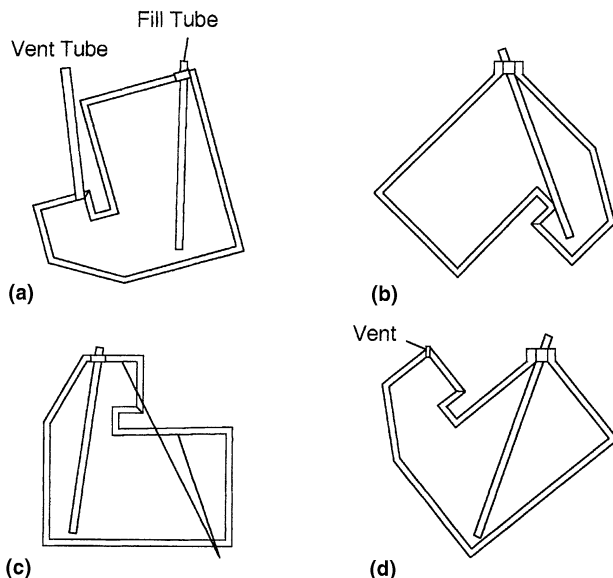


Figure 10.11 Orientation of mandrel mould during the casting process. (a) acceptable, vent tube required; (b) acceptable, fill small cavity first; (c) poor, air entrapment likely; (d) ideal, no vent extension tube, no air entrapment.

atmosphere as well as RTM. Other materials that cure or dry may also be moulded by a similar process.

Ceramics, plasters and other materials can be slip formed by filling the mould with material and allowing time for the walls to gel. Then the remaining material is drained, leaving a shell. This may need to be repeated several times to obtain the desired thickness. This technique will also work with some phase change materials, but heat transfer through the mould determines the wall thickness. The tooling must accommodate the heat and uniformly cool the cavity walls until the balance of the material can be drained through a heated drain. The hole through which extra material is drained must be sealed off against the RTM tooling, be plugged or the entire hollow space filled with another material prior to sealing the mandrel surface.

Other hybrid techniques for making lightweight mandrels could include using lower melt out or soluble mandrels inside of higher melt or more solvent resistant outer material. For example, the mandrel could be metal-coated by using a form of flame spray. This coating could melt out or become a liner for the composite part.

It is also feasible to produce phase change inserts by means of traditional foundry core manufacturing equipment, such as core blowers or screw feed machines, for certain applications, with oil, polymer or inorganic binders. These inserts would be porous and require sealing if used directly or they could be used in a hybrid system.

10.6.8 SEALING THE MANDREL SURFACE

There are a variety of surface sealers available. The most obvious are the materials used to seal wood and other porous surfaces, such as lacquer, silicone, PVC, PVA (polyvinyl acetate) and urethane. The mandrel sealer can transfer and serve an additional role while in service with the part or be removed after the mandrel. The necessity for a sealer depends on the mandrel material and the required surface finish. Experimentation with various sealants on the selected mandrel material will probably be necessary in order to ascertain their effectiveness and limitations. Various release tapes and shrink wrap materials work well where provisions for their removal can be made. The best type of sealer to use depends on many factors; the more obvious factors such as cure temperature and resin compatibility are crucial, but damage tolerance, abrasion resistance, application thickness and other less obvious factors may also be important. Section 10.3.1 on sealing open-cell cores contains other applicable methods. If the sealer bonds to the RTM resin the cavity may have residual mandrel material bonded to the composite and a poor surface finish. The sealer should be treated with a release agent to avoid this unless it provides inherent release or can be dissolved for removal.

10.6.9 PROCESSING CONSIDERATIONS FOR MELT-OUT MANDRELS

All types of melt-out mandrel materials have similarities. In order to be useful they must melt at a temperature that will not damage the matrix resin. They must be able to withstand lay-up, clamping and injection pressures at injection temperature. The material must maintain enough strength to support the preform and resin pressure until gel, which may occur at a higher temperature than the injection. The melting process can occur while still in the mould during post-cure if the mould is equipped with ports to expose the partially cured part. A hole can then be drilled through, or a fitting through the composite opened, to allow the molten material to escape while the part post-cures.

If the resin or component design will allow a free-standing post-cure, the melting process is simplified. The part is nested in a support, as for any oven post-cure, but is orientated such that the molten material can flow out of the cavity and be replaced by air. It may be necessary to revolve the part through various orientations in order to get complete drainage, possibly from multiple holes. Centrifugal force can be used to accelerate the draining process. The heating fluid need not be air; many other fluids can provide more heat as well as other benefits.

Some situations call for a hot fluid blast to move the molten material to the exit. Pressurised fluid that has been heated to the post-cure temperature can be used as an agitator to move molten mandrel material toward the exit (both sharing the same hole perhaps). Another advantage to a heated fluid jet is that it pumps more heat into the melting mandrel (which may be isolated from normal heat sources by the part surrounding it), prevent vapour lock and also keeps the drain clear of floating chunks.

It is beneficial if the melt-out material is also soluble so that any residue can be flushed out thoroughly. The most critical application is where fuel or other liquid that could be contaminated is to be stored in the hollow cavity left by the mandrel. In some cases the surface sealer used on the mandrel can be more difficult to remove than the mandrel. Treating the sealant with a release agent prior to loading will alleviate this.

Once the majority of the mandrel has been drained the rest can be dislodged with high-pressure water or air, even if it is not soluble. Other solvents can be pumped where they are more effective. In the case of soluble mandrels, the 'melting' would be done after the part is demoulded without the necessity for heat (although hot solvent can hold more solute). Impingement velocity is important to help dissolve the material more quickly, especially when insoluble particles are suspended. In some cases, such as for insoluble waxes, detergents may be useful for cleaning residue from the cavity.

When solvents are used it is possible to extract the mandrel in a closed-loop solid extraction process similar to that used for vapour degreasing. The solvent is boiled under the mandrel so that the vapour will condense fresh solvent on the cooler mandrel, dissolving some of it, then the liquid can return to the boiling solution where it leaves the solute, and the cycle repeats. Once the mandrel is in solution the mandrel material can be reclaimed if reusable, as can the solvent by simple distillation with the same equipment. Once the cycle is complete the part can be removed clean and dry. This process need not use dangerous or highly volatile solvents, even water could be used. The advantage is that the closed loop does not require the disposal of large quantities of solvent containing the mandrel material, and the mandrel is returned to the solid phase.

10.6.10 THERMAL CONSIDERATIONS FOR MELT-OUT MANDRELS

The phase change process requires heat (a quantity known as the latent heat of fusion) and can substantially delay a cure schedule when heat must pass through foam cores and other insulating lamina. Many possibilities exist to provide solutions for this problem, including heated fluid baths, embedded heaters, hollow mandrels or air impingement heating.

In order to displace the desired cavity accurately it is necessary that the phase change and thermal shrinkage be properly modelled prior to construction of the mould (or pattern). In order to compensate for the phase change shrinkage (or expansion) a shrink factor must be determined. This procedure may be published by the mandrel material vendor or, for the case of special formulations, must be determined by the user. This can be accomplished by casting coupons in a mould, preferably made from the same material as the mandrel casting mould. The molten material is poured into the preheated cavity and allowed to cool. When the material has cooled to the temperature at which gel is expected to occur the dimension is measured and is divided by the mould dimension at room temperature (assuming the final mould will be sized at room temperature). The ratio (probably less than 1) is then divided into the target dimensions of the mandrel at gel temperature to obtain the dimension of the mould in which to cast the mandrel. Measuring the size of the coupon at gel temperature eliminates the need for CTE compensation, necessary if it is measured at room temperature. An expansometer such as those used for plasters can be used if equipped for temperature measurements [15]. The gel temperature is often difficult to determine when the mould temperature is ramping; however, it can be estimated by experimentation or by studying rheometric charts for the resin system. Slight adjustments in the size of the mandrel can be made by changing the melt temperature of the material, by varying the mould preheat temperature or by adding inert fillers.

10.7 EXTRACTABLE TOOLING INSERTS

The term ‘extractable tooling’ includes tooling elements that define the shape of the composite part which are essentially rigid and are removed intact for reuse. This approach offers the advantages of accurate internal cavity definition, fully reusable tooling without special processing and, often, durable long life. Examples of this type of tooling insert include one-piece pull-out metal internal tooling, extruded silicone mandrels for hat stiffeners, multiple aluminium pieces that fit together like a puzzle and are removed through a small opening, and metal blocks that nest into the external RTM mould.

10.7.1 MATERIAL SELECTION

The same materials that would be considered for the RTM mould are viable candidates for extractable tooling, along with some others. The following list contains the primary and secondary candidates for extractable tooling materials:

- primary material candidates:
 - aluminium,
 - steel,
 - cast iron,
 - electroformed nickel with back-up structure,
 - metal spray with back-up structure,
 - elastomer (silicone, EPDM, etc.),
 - composite laminate;
- secondary material candidates:
 - invar (low CTE, high cost),
 - monolithic graphite (very low CTE, not durable),
 - ceramic (not durable),
 - unfilled polymer (Solid Teflon™, etc.) (high CTE, not durable),
 - filled polymer mass casting (low service temperature).

Several physical properties are important in the choice of material for extractable tooling.

Coefficient of thermal expansion (CTE)

Choose a CTE for the extractable tooling that is higher than the CTE of the composite material; this ensures that the internal tooling shrinks away from the composite when it cools down. Also, choose a CTE for the extractable tooling that is equal to or higher than the CTE of the RTM mould. This prevents the internal tooling and the composite part from becoming locked in place after cool-down. It will be necessary to

undersize the length of the mandrel in order to avoid thin laminates on the ends. Where the mandrels contact the mould on both ends mould damage can occur if insufficient expansion room is provided. These guidelines do not apply to tooling that will be kept at constant temperature during the entire RTM process.

Hardness and toughness

Choose a material with adequate surface hardness and toughness so that it will not be dented, cracked or broken by factory handling or by the sometimes abusive tooling-extraction operation. For mandrels with only a slight draft angle, even a small dent on a radius will prevent its easy extraction from the moulded part.

Density

The weight of a tooling element is important. If the weight exceeds that which a person can safely work with, attachment of a lifting aid may be required. This will complicate the tooling considerably, since all holes, slots or threads for the lifting aid must be plugged to keep resin out, or enclosed with an O-ring. For large tooling elements, hollow construction is an alternative.

Poisson effect

Elastomeric tooling has the advantage of stretching to a smaller cross-section when pulled. This is especially useful with constant section mandrels. An elastomer with faster heat-up and lower CTE is preferred. A tightly trapped elastomer can exert more than 100 bars of pressure on the surrounding mould as a result of thermal expansion.

Repair

The ability to repair nicks and scratches on a piece of extractable tooling is necessary in the typical manufacturing environment. A compartmentalised protective case to hold each piece of extractable tooling is worth considering.

Heat transfer

Large extractable tooling should be actively heated as the primary RTM mould is heated. Small extractable tooling relies on conduction of heat from adjacent mould surfaces, usually through an insulating preform. The temperature of these small tooling elements can lag the rest of the mould significantly.

If the RTM production cycle time needs to be short, choose an extractable tooling material that will heat up quickly. An exception could be made for materials that are somewhat insulating, such as silicone or ceramic. Resin injection can occur before extractable tooling made from these materials has fully heated up; however, be aware of what will happen when they reach maximum temperature and have fully expanded. Provisions for this expansion after injection or even after gelation must be incorporated.

Three material properties have a strong influence on how quickly a volume of material will heat up: thermal conductivity, k , specific heat, c_p , and density, ρ . A ratio of these properties is useful in comparing materials for heat-up time. The time to heat-up is related to:

$$\frac{c_p \rho}{k}$$

This ratio has been computed for the tooling materials listed in Table 10.5. Each value was normalised to set the heat-up time for the fastest material at 1.0. The difference in time to heat-up between aluminium and silicone is surprising. Values for CTE, maximum use temperature and density are also listed.

10.7.2 DESIGN AND PROCESSING CONSIDERATIONS

One could separate the design possibilities into three categories:

- extractable tooling with positive draft – the tooling naturally separates from the moulded part as they are demoulded; this approach is preferred as it will involve the simplest demoulding and fewest individual pieces;
- extractable tooling with zero draft – these are constant section shapes or mandrels that rely on a high CTE, the Poisson effect of an elastomer, very low friction surfaces or a big hammer to demould the part;
- extractable tooling with negative draft – the hole through which the tooling must be extracted is smaller than the tooling package, so the package is separated into pieces which can be removed one at a time.

Regardless of which category best describes the tooling being designed, seven details are important to consider when one is designing extractable tooling.

- Draft – wherever possible, design for a 2° minimum draft angle to facilitate demoulding.
- Accurate location – if the preform or fibre reinforcement can locate the extractable tooling with acceptable accuracy, the tooling can be free-floated in the preform. Pressure imbalances during resin injection can

Table 10.5 Extractable tooling property comparison

Material	Linear Coefficient of Thermal Expansion $\times 10^6$ (cm/cm °C)	Maximum Use Temperature (°C)	Relative Time to Heat-up Compared with Monolithic Graphite	Density (g/cm³)
Aluminum	23.6	>200	2.1	2.77
Steel	14.8	>200	12	7.84
Cast Iron	11.2	>200	17	7.2
Silicone Elastomer	900	260	1,200	1.40
Ethylene propylene diene (EPDM) Elastomer	600	175	730	0.86
Composite Laminate (glass/epoxy)		120-190	180	1.9
Invar	4.5	>200	60	8.14
Monolithic Graphite	1	>300	1	1.88
Ceramic	7	>200	180	4.17
Unfilled Polymer (Solid Teflon® PFA)	190	230	140	2.15
Aluminum-Filled Polymer Mass Casting	40	90-120	5	2.1

move a tooling element out of position. If special location features are needed avoid straight pins with bushings as they will fill with resin. Features with significant draft and no cavities for resin to accumulate are preferred. These include cones and truncated pyramids.

- Gaps between pieces – any gap between rigid tooling will be filled by resin. This in itself may not be a problem; however, these gaps will also be paths for resin to ‘race track’ around the preform and arrive at an exit prematurely or cause resin flow fronts to converge. The resin path through the gap can be blocked by a seal or Teflon™ tape. The problem of resin ‘race tracking’ is not as serious as it sounds and it is much more easily solved by carefully choosing the resin port and vent locations than by incorporating O-ring seals in the extractable tooling.
- Thin flash of resin – the flash of resin that will fill a 0.05 mm gap is difficult to remove; it will break into small pieces and the static charge will cause it to stick to the mould. Clean-up can be facilitated by designing all gaps to be at least 0.25 mm thick in such a way that they do not diminish location accuracy.
- Channels for resin – port and vent channels for the resin can be machined into the sides of an extractable tooling block which does not contact a preform to move resin from the preform to a convenient exit in the RTM mould.
- Threaded holes – it may be necessary to attach a bolt or lifting aid to an extractable tooling insert to remove it. An O-ring can enclose the threaded hole to keep resin out. Alternatively, the threaded holes can be filled with a plastic threaded plug and the Allen key in the plug can in turn be filled with a silicone plug to keep resin out.
- Elastomeric tooling expansion – when an elastomeric extractable tool with a high CTE is trapped in a rigid RTM mould and heated it can exert more than 100 bars of pressure on the surrounding mould. It is difficult to determine the fibre volume of the preform both during injection and after cure when the tooling changes size so dramatically. To make things worse, the elastomer will likely shrink with repeated thermal exposure, changing its size through many production cycles.

An RTM development team at Northrop patented a solution to this problem with a combination of RTM and trapped rubber moulding. They built a cavity mould defining the extractable tooling size and shape at maximum RTM cure temperature. They poured liquid silicone into this cavity mould and cured it immediately at or near the RTM cure temperature. The silicone squeezed out the holes as it expanded and cured. After cool-down, the result was an extractable tool which was quite small during loading, slightly small during resin injection and the correct size and shape at resin gelation with the ability to exert some pressure on the laminate at maximum cure temperature [16].

Another solution to elastomer expansion was also patented: the use of independent temperature control of the metal and elastomeric tooling [17]. When used in conjunction with pressure sensing and closed-loop control the temperature could be varied to obtain a specific compaction pressure cycle on the preform and curing composite. Unlike other methods, this is not sensitive to the gradual shrinking of the elastomer.

References

1. Banuk, R. (1993) Design considerations for foam and honeycomb core structure. *Proceedings of the 38th International SAMPE Symposium*, Society for the Advancement of Material and Process Engineering, 1161 Parkview Drive, Covina, CA 91724-3748, pp. 1751–61.
2. Johannsen, T. (1984) Rigid closed-cell foams as sandwich core materials: properties, design and manufacturing techniques. *Proceedings of the Regional Technical Conference, Society of Plastics Engineers, October 1984*.
3. Stover, D. (1991) Foam and syntactic film give core support to composites. *Advanced Composites* (January/February), 32–8.
4. Ware, M. (1985) Thermal expansion resin transfer molding (TERTM) – a manufacturing process for RP sandwich core structures. *Proceedings of the 40th Annual Conference, Composites Institute, Society of Plastics Industry, January 1985*, Session 18-A, pp. 1–3.
5. Boeing Company (1996) Resin transfer molding in combination with honeycomb core. *US Patent*, 5,567,499, October.
6. Fisher, K. (1995) RTM and core materials offer product advances. *High Performance Composites* (September/October), 23–6.
7. Baltec Corporation (1989) Compressive properties of end-grain balsa vs. thermal aging. Baltek internal memorandum, August 21 Baltec Corporation, PO Box 195, Northvale, NJ 07647, USA.
8. Automotive Composites Consortium (1992) Resin molding process utilizing a blow molded core. *US Patent*, 5,169,590, December 8.
9. (1994) RTM hollow mouldings: from fiction to fact, *Reinforced Plastics* (April), 34–7.
10. Brooks, N. (1995) Hollow RTM becomes a booming business. *Reinforced Plastics* (January), 20–23.
11. Fong, L., Liu, B. and Advani, S.G. (1995) Modeling and simulation of resin transfer molding with flexible mold walls. *Proceedings of the 50th Annual Conference, Composites Institute, Society of Plastics Industry, January 1995*, Session 3-A, pp. 1–5.
12. Hexcel Chemicals (1988) Technical Data Bulletin on Paraplast 8100 ○ 8101 ○ 8102, 200701 Nordhoff St., Chatsworth, CA 91311.

13. Electrovert-MDD (1993) Electrolloy Metal Alloys Data sheet, 1111 W.N. Carrier Pkwy, Grand Prairie, TX 75050.
14. Becker, W. (1988) Evaluation of Easy Out breakaway mandrel system. Institute for Aviation research report, 1845 Fairmount, Wichita, KS 67260-0093.
15. United States Gypsum (1975) Industrial tooling with Hydrocal gypsum cements. Bulletin TAC-165, 101 S. Wacker Dr., Chicago, IL, 6060.
16. Northrop Corporation (1993) Method of making composite laminate parts combining resin transfer molding and a trapped expanding member. *US Patent*, 5,204,042, April 20.
17. Dow Corning Corporation (1989) Fixed-volume trapped rubber molding apparatus. *US Patent*, 4,812,115, March 14.

Manufacturing and tooling cost factors

11

Teresa Kruckenberg

11.1 INTRODUCTION

The need to reduce the cost of composite parts is critical in these economic times. The traditional manufacturing method of prepreg lay-up is labour intensive and requires autoclave curing. Reducing product cost while maintaining quality is imperative. Resin transfer moulding (RTM) is one method that can reduce the cost of composites.

Additionally, RTM designs can compete with metal designs when prepreg designs are not even considered for these applications. The type of structure, complexity, primary structural application and quality requirements of the RTM design allow it to compete with the metal design at a competitive cost.

Some of the benefits and disadvantages of RTM significantly impact the cost, and these factors will be discussed further in this chapter. The benefits of RTM include:

- low-cost materials;
- non-autoclave cure;
- reduced lay-up time;
- improved reproducability;
- excellent surface finish;
- net or near-net shape manufacturing;
- improved laminate quality;
- improved tolerance control;
- integration of parts.

The disadvantages include:

- high tooling costs;
- difficulty of using certified prepreg resins;
- reduced cost benefits for low-volume applications.

Product design teams must assess these cost factors when concurrently designing a product prior to manufacturing. A large percentage of the final cost of a part is determined in the early phases of the product life-cycle [1, 2]. The cost factors for traditional autoclave-cured prepreg manufacturing have been well documented [1, 3]. Since RTM is new in the aerospace industry, the cost factors are not yet well established. This chapter will present the cost factors and attempt to quantify some of the costs involved with RTM.

11.2 RECURRING COST FACTORS

11.2.1 EFFECT OF MANUFACTURING QUANTITY

Manufacturing quantity has a major impact on whether RTM is a cost-competitive process. A new production programme of less than 100 parts may need to be analysed closely to determine if RTM is cost-effective, as usually initial tooling costs are high.

To determine the feasibility of RTM for a low production program (less than 100 parts) the following cost factors should be considered:

- mould costs;
- facility costs;
- qualification costs;
- recurring savings.

When switching an existing autoclave-cured prepreg program to RTM, the pay-off quantity is usually calculated by dividing the non-recurring costs by the cost saving per part. A pay-off quantity of 100 units is normally the acceptable maximum for a 500 unit program.

The learning curve is generally less steep for RTM parts than for prepreg parts. A complex-shaped prepreg part can have a steep learning curve whereas the RTM learning curve is much lower. In the beginning, this is because hand lay-up of prepreg onto complex shapes requires more skill than most RTM preforming techniques. The learning curve beyond 15 to 20 parts has more to do with design changes or system efficiencies. There are usually mould adjustments required, but since RTM is a more automated process the need for system and design changes is usually less than that required for autoclave-cured prepreg parts. The more the RTM system is automated, with a smart injection system, automated preforming and advanced mould assembly and

clamping techniques, the flatter the learning curve. Generally, the learning curve for prepreg parts is the steepest (*c.*75%) for the first 100 parts, less steep (*c.*80%) for the second 100 articles, and from the 200th to 250th article the curve is generally at about 95% because learning has been completed [2]. For RTM parts the learning curve could be expected to be the steepest (*c.*85%) for the first 100 parts, then reach 95% around 100 units, depending on the amount of automation used in the process. However, since RTM is relatively new to the aerospace industry, learning-curve profiles are not well established. Figure 11.1 shows a comparison of an expected learning curve for RTM and a typical learning curve for a prepreg part.

11.2.2 MATERIAL COST FACTORS

RTM has the potential for lower material costs than prepreg. If the fabric is supplied dry and the resin supplied in bulk then material cost is saved by eliminating the prepegging operation. This cost saving may not be realised with some materials because RTM is relatively new to the aerospace market and high volumes of resin and fabric are not being ordered compared with prepreg.

The material costs shown in Table 11.1 have been supplied by Hexcel, 3M, and other resin and fabric suppliers. All costs are in US dollars. The majority of high-temperature epoxy resins cost between \$70 to \$145 per kilogramme. Low-temperature resins are very inexpensive, at \$6 to \$40 per kilogramme; however, these are two-part systems which require

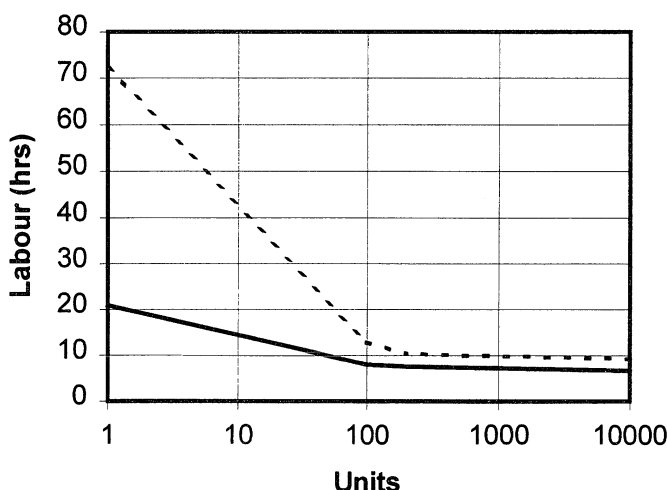


Figure 11.1 Learning curves for resin transfer moulding (solid line) and prepreg (dashed line) in terms of hours of labour per number of units produced.

Table 11.1 Raw material costs

Product	Quantity	Cost (US dollars)
Epoxy Resins:		
one or two part, 177 °C cure	500 kg	70–145 per kilogramme
two part, 120°C cure	500 kg	6–40 per kilogramme
film, 600 gsm, 177 °C cure	500 m ²	40–55 per square metre
Bismaleimides: one part	500 kg	145–165 per kilogramme
Carbon Fabrics:		
carbon	50 000 m ²	25–50 per square metre
tackified carbons	50 000 m ²	26–58 per square metre
Prepreg Fabric:		
epoxy, 177°C cure, carbon fabric	3000 m ²	80–100 per square metre

mixing before injection. Depending on the fibre type, fabric weight and weave style, most carbon fabrics cost in the range of \$25–\$50 per square metre for a quantity of 50 000 m². Fabric with 12 k tows will fall in the low end of this range, and fabric with 3 k tows will fall in the high end. Application of tackifier to the fabric will increase the dry fabric cost by approximately 5% to 15%, depending if the tackifier is applied to one side or both sides of the fabric.

Fibre tow is the least expensive form of fibre material, and if used in robotic winding can significantly reduce the overall part cost. Most carbon fibre tow costs between \$45–\$90 per kilogramme. E-glass roving costs between \$10–\$20 per kilogramme.

Material cost reduction can be significant for RTM. For example, if prepreg for a 120°C cured part costs \$50 per square metre, and the part volume is 600 cm³, then the material cost for this part is \$75. This cost does not include material scrap. If this part can be robotically wound using \$55 per kilogramme fibre and \$25 per kilogramme resin then the material cost for this part is 47% less than the prepreg part. If \$35 per square metre fabric is used instead, then the material cost for this part is 20% less than the prepreg part. See Table 11.2 for a comparison of the costs.

One of the benefits of RTM is that advanced textiles can be used. These textiles may have a high material cost, but the savings realised from reduced labour can be substantial. To determine the real cost savings from using advanced textiles it is desirable to perform a global cost study that includes materials, labour, trimming and inspection operations.

Expendable materials are a significant cost for the autoclave process. These include bagging film, release films, porous release film, bleeder cloth, breather cloth and sealant tape. RTM expendable materials include tubing (\$1–\$2 per metre), fittings (50 cents to \$4), and containers (50 cents to \$2) for mixing and/or heating the resins. These materials can be reduced further by the following techniques:

Table 11.2 Example part material costs: a comparison of prepreg and resin transfer moulding (RTM)

	Prepreg ^a	RTM		RTM	
		Resin ^b	Fibre ^b	Resin ^b	Fabric ^a
Raw Material Cost	\$50	\$25	\$55	\$25	\$35
Part Material Cost (US\$)	\$75	\$40		\$60	

^a Raw material cost in US dollars per square metre.

^b Raw material cost in US dollars per kilogramme.

- modify the fittings to run tubing through the fittings or purchase bored-through fittings – this requires replacing only the olive for each moulding;
- use hose clamps for low-temperature and low-pressure mouldings;
- use polyvinylchloride (PVC) or nylon tubing for low-temperature mouldings;
- use annealed copper tubing for high-temperature mouldings;
- reuse tubing from dispensing equipment to oven wall for some one-part resins (the applicability of this technique depends on the resin chemistry and line temperature);
- manufacture dispensing equipment suited for the application;
- use a pail unloader when working with high-temperature one-part resins already degassed.

11.2.3 MANUFACTURING COST FACTORS

The major manufacturing steps for the RTM process are shown in Figure 11.2.

Preforming

The most significant cost benefit of RTM is the reduction of lay-up time. Lay-up of dry fabric is usually faster than lay-up of prepregged materials

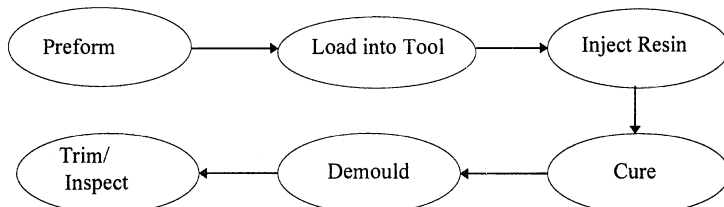


Figure 11.2 Major Manufacturing Steps Required in resin transfer moulding.

because of the hand-consolidation and wrinkle-smoothing time involved with prepreg lay-up. Automated preforming or use of advanced textiles can further reduce this draping time. Advanced textiles include multi-layer non-crimp fabrics, three-dimensional (3D) braids, angle interlock weaves, 3D knits, and woven-to-shape preforms, which all reduce pre-forming time by reducing the number of layers and by fabricating net shape preforms. Automated techniques for making preforms are essential for reducing costs. Automated systems have the potential to increase overall part quality while decreasing human labour content and material scrap [1].

Preforming of dry fabrics and fibres can be automated by using similar techniques to those used for thermoplastic components such as filament (robotic) winding, press (stamp) forming, vacuum forming and dia-phragm forming. The fabric or fibre tow is usually coated with 3%–5% epoxy binder or tackifier. Since the tackifier is normally epoxy that has been b-staged (Appendix A, Glossary) to a point where it is a solid at room temperature but flows again upon heating, the tackifier acts like a thermoplastic. However, there is a limit on the amount of heating the tackifier can be submitted to without curing. The forming temperature is substantially less than that required for high-performance thermoplastics such as polyetheretherketone (PEEK) or polyphenylene sulphide (PPS). Most preforms can be formed at 80°C–100°C for a couple of minutes, which makes the forming equipment substantially less expensive than that required for thermoplastics. The majority of preforming tools can be manufactured with wood or plastic. Inexpensive heat sources such as infra-red lamps, heat blankets, hot-air guns, heated dies and ovens can be used to melt the binder or tackifier for consolidation of the preform.

Some fabric suppliers provide fabric with the tackifier already applied. This normally costs an additional 5%–15%, depending whether the fabric is coated on one or both sides. Resin suppliers may provide RTM resin in a powdered form to be used as a tackifier. In this situation the fabric will require coating by manual application, machine powder coating, spraying of tackifier dissolved in solvent or some other automated method to apply the powder. The powder needs to be distributed and then heated for a short time to ensure that it adheres to the fabric. The cost of producing tackified fabric will need to be assessed in the cost study.

Preform complexity is a significant factor in recurring costs. Inserts, moulded holes, complex shapes and 3D fibre architecture significantly add to the preform complexity. However, the more automation in the preforming process, the less impact on costs. Inserts and moulded holes can be used to minimise subsequent bonding or drilling operations and to improve part quality.

Preform costs can be minimised by using a hybrid preform with high modulus fibres in the principle stress direction and lower cost materials in the secondary stress directions [4]. Stress optimisation programmes can be utilised to design the fibre architecture for placement of fibres where essential. Automated preforming methods such as 3D weaving, or fibre placement, can be used for selected placement of fibres.

Automated preforming or advanced textiles can be used to manufacture net or near-net shape preforms. These preforms are then loaded into a mould for manufacture of a net or near-net shape part. The cost of a trim fixture and the recurring cost of the trimming operation can be eliminated for net shape manufacturing and minimised for near-net shape manufacturing.

Gerber, die or ultrasonic knife cutting of individual plies or ply stacks is essential to an efficient production programme. The cutting process can be optimised to produce tackified fabric with a neat edge for net preforming. In some instances, depending on the shape, it is more cost effective to trim on the preforming tool. Depending on the part geometry and mould configuration, net shape moulding may not be appropriate. Plies that shear in opposite directions around complex contours may be difficult to preform net. For example a sine-wave rib with $0^\circ/90^\circ$ and $\pm 45^\circ$ plies would be difficult to preform net.

Resin Transfer Moulding with Prepreg Resins

Some companies are considering using prepreg resins for RTM to eliminate the cost of a materials allowables programme. However, this strategy introduces its own problems and costs as it can be difficult to use RTM with prepreg resins. Resins designed for use in prepregs generally have a much shorter pot life and a much higher viscosity than RTM resins. However, these difficulties can be overcome for some parts. The trade-off is that the cost of the prepreg resin may be higher than the cost of an RTM resin, so recurring costs may be increased even though the non-recurring allowables cost is eliminated. The out-time for a prepreg resin is short and it is likely to have more costly storage requirements. More material wastage and/or requalification tests of expired shelf-life resin may be expected when one uses a prepreg resin. There is also a higher potential for an increased reject rate with prepreg resins because of the tighter processing window.

Quality

RTM has the benefit of improved reliability. When a matched-metal mould is used, and processing parameters are constant, the parts produced will be dimensionally almost identical. However, adequate and consistent clamping forces must be used for closing the mould. If the

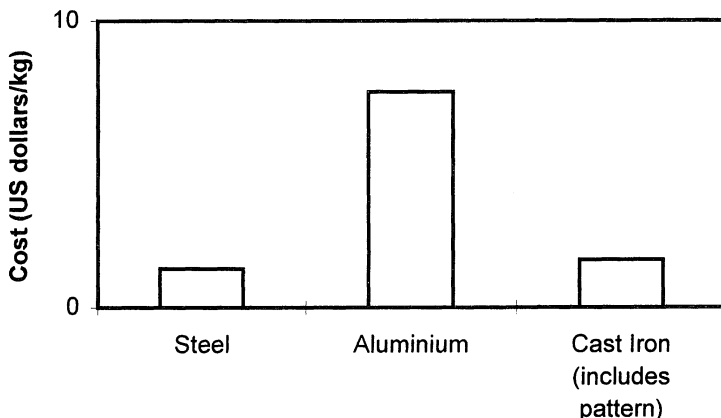


Figure 11.3 Mould Material Cost Comparison.

processing parameters are tightly controlled then the part porosity level will remain constant. This will reduce the scrap rate and rework time involved.



Figure 11.4 Resin transfer moulded F22 sine-wave spars and frames. Reproduced courtesy of DOW-UT, Wallingford, CT.

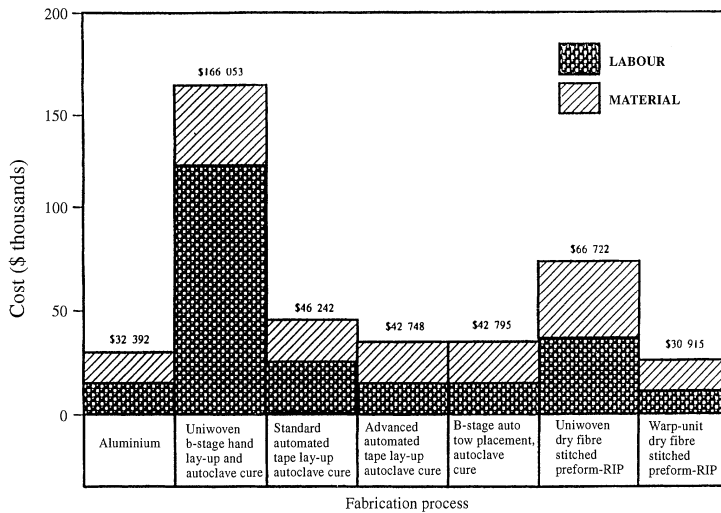


Figure 11.5 Estimated cost summary for 2.4 m × 6.1 m blade-stiffened panels. Reproduced from [7] Copyright © 1990 by McDonnell Douglas Corporation. All rights reserved under the copyright law.

For thin RTM parts almost all significant defects appear to be detectable by visual inspection of the surface. If and when this can be verified it may be possible to reduce non-destructive examination (NDE) costs substantially.

The finish on the mould determines the finish that appears on the part. It is worth the cost to spend more time on mould polishing to eliminate the surface preparation necessary for some prepreg parts to obtain a good surface finish. The initial tooling may be more expensive, but significant recurring cost savings can be realised in this situation. Generally, a good tool produces a good part.

Part Complexity

With increasing part complexity tooling costs rise for all processes. A small cost study of various moulds with increasing complexity is given later in this chapter. However, with RTM, the fabrication cost rise is less steep, and so RTM becomes more cost effective with increasing part complexity. For prepreg parts, the recurring costs will rise more rapidly because of the increased lay-up time and added debulking cycles. The average total recurring part cost for RTM is considered to be 25% less than the total recurring costs for autoclave-cured prepreg for good RTM applications. These savings will rise substantially with increasing part complexity and preform automation. Chapter 1 gives good examples of RTM applications.

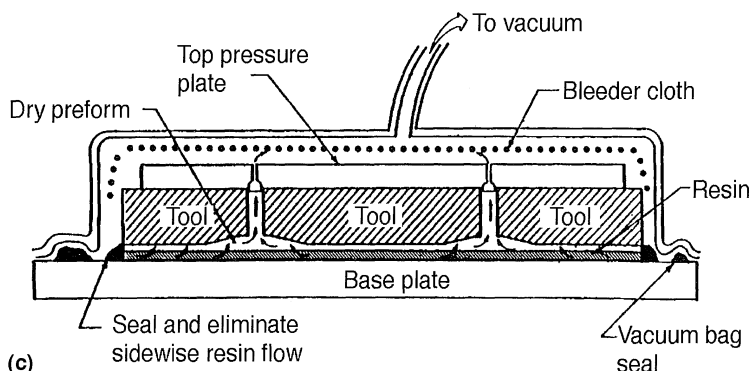
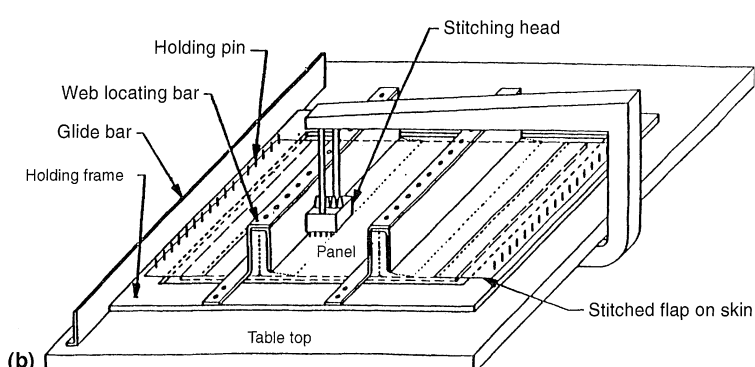
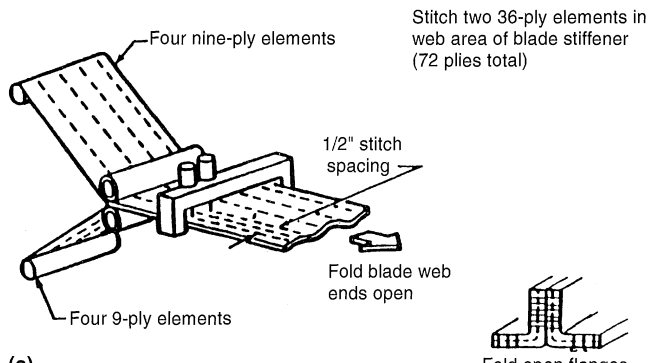


Figure 11.6 (a) Stitching concept for stiffeners; (b) stitching T-flange to skin; (c) vacuum impregnation of stiffened panel. Reproduced from [7] Copyright © 1990 by McDonnell Douglas Corporation. All rights reserved under copyright law.

Cost Studies

There are several methods for modelling the cost of composites. Most companies have their own internal method for estimating costs, based on their experiences of previous programmes. In one method cost data is plotted on a log–log graph versus indicators such as performance, weight, manufacturing method and part complexity: a first-order equation can be fitted to the plot. Another method is to use detailed manufacturing time step estimates. One well known example of this is the Advanced Composites Cost Estimating Manual (ACCEM) developed by Northrop for the US Air Force [3]. The following is a list of detailed manufacturing steps that may be used for estimating RTM recurring labour:

- mould surfaces cleaning;
- preform mandrel cleaning;
- release agent application to surfaces;
- fabric cutting;
- preform lay-up;
- preform assembly onto preform mandrel;
- preform consolidation;
- preform assembly into mould;
- mould assembly and clamping;
- tubing assembly;
- injection equipment assembly;
- vacuum trap assembly;
- thermocouples installation;
- leak check;
- mould preheating;
- resin preheat and degassing;
- resin injection;
- injection completion;
- injection equipment disassembly;
- part curing;
- tubing disassembly;
- mould disassembly;
- part trimming.

To make a global cost model comparing the RTM process with pre-preg, the following factors need to be included [5]:

- capital equipment costs;
- maintenance of equipment, tooling and facilities;
- equipment power consumption;
- quality assurance personnel;
- machine cycle times;
- machine downtime;

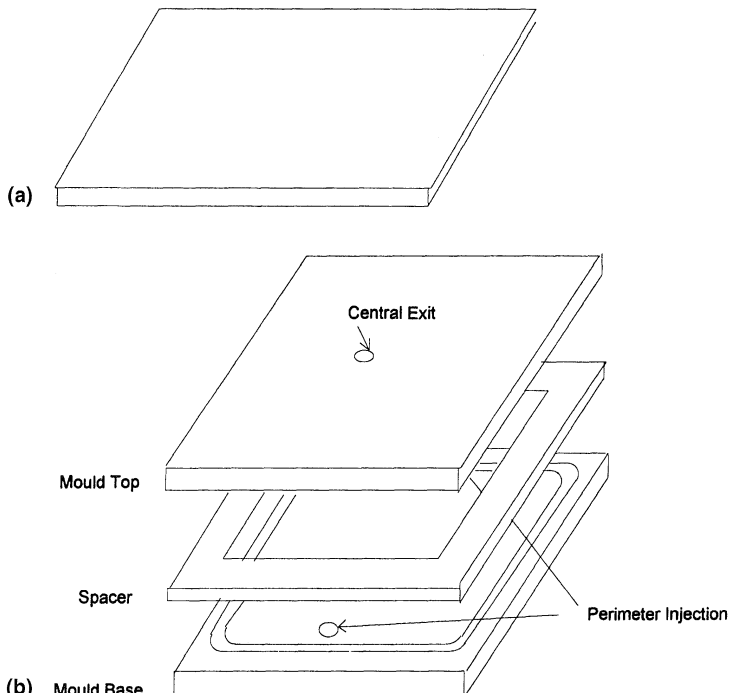


Figure 11.7 Concept 1: (a) flat panel laminate; (b) flat panel mould.

- facilities expenses;
- programming time;
- supervisory labour;
- equipment downtime;
- human cycle times;
- part demoulding and tool cleaning;
- tooling costs;
- process yields;
- scrap;
- rework;
- set-up.

Usually the best approach to model fully the cost of the application is to use the basic manufacturing steps and some global factors. This should include the savings arising from part complexity (elimination of details, and inventory) and subsequent assembly as well as tooling costs of the details and the assembly operation and cost avoidance achieved by close tolerance control (reduced shimming during bonding, or elimination of

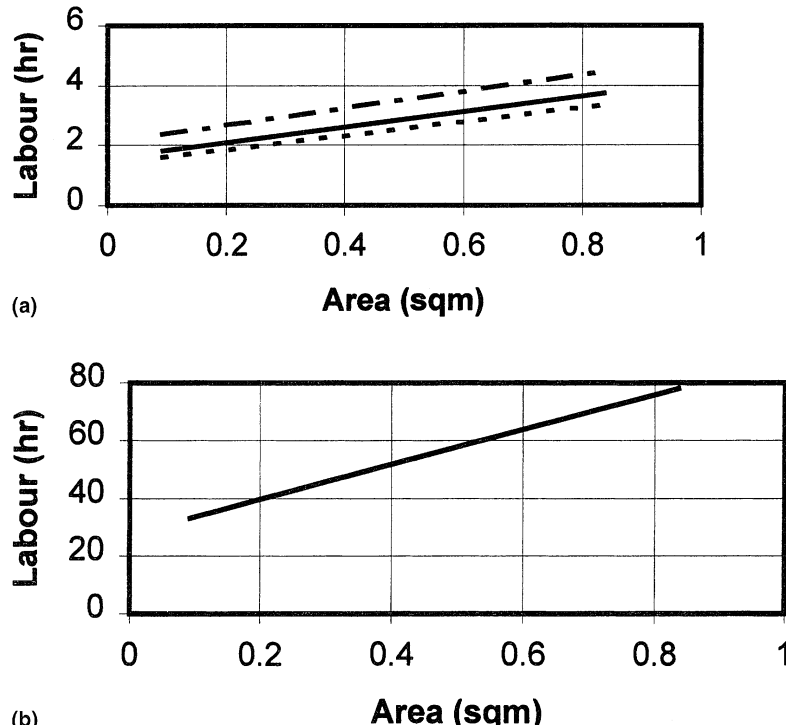


Figure 11.8 Concept 1: (a) manufacturing costs for resin transfer moulding of flat panels - - - = 16-ply; — = 8-ply; - - - = 4-ply); (b) manufacturing costs of flat panel mould.

laminate thickness matching regarding blind fastener grip length). The saving from good, repetitive quality is significant. The cost of rework, standard repairs and scrap, so significant in prepreg manufacturing, is virtually eliminated in RTM. The true potential of RTM is not shown until the cost avoidance and cost savings factors are incorporated into the model (Allen Samuel, DOW-UT, 1996, personal communication).

11.3 NON-RECURRING COST FACTORS

11.3.1 INJECTION EQUIPMENT

Injection equipment can cost from \$200 to \$100 000, depending on what type of system is required. A simple paint pressure-pot can be used for injection of low-temperature resins and will cost approximately \$200 to \$300. A heated pressure-pot will cost between \$3000 and \$7000. A heated pail unloader (typically used with one-part resin systems) will cost between \$10 000 and \$20 000. The more expensive piston injection systems

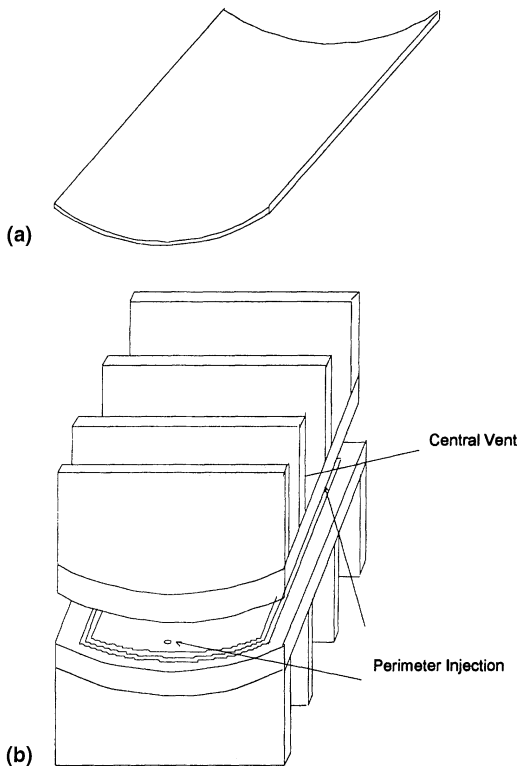


Figure 11.9 Concept 2: (a) curved panel; (b) curved flat panel mould.

include comprehensive data acquisition systems. These systems can record the following data:

- volume injected;
- volume remaining;
- flow rate;
- pressure (in-line and on-tool);
- flow front position;
- degree of cure;
- line temperature;
- pot temperature;
- tool temperatures;
- tool deflection.

The average pneumatic-driven system which contains most of these capabilities will cost around \$40 000 to \$50 000. Electric-driven or hydraulic-driven systems will cost more than a pneumatic-driven system.

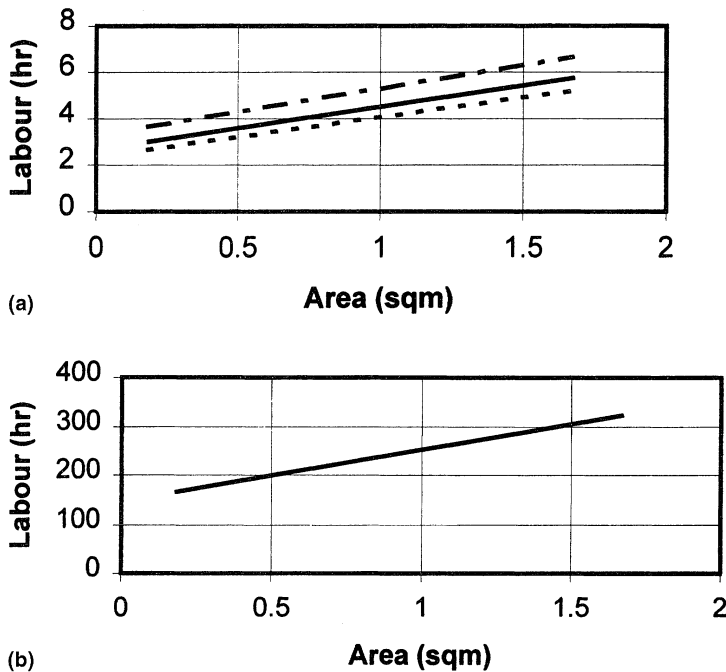


Figure 11.10 Concept 2: manufacturing costs for resin transfer moulding of curved panels (— = 16-ply; — = 8-ply; - - - - = 4-ply); (b) manufacturing costs of curved panel mould.

but will allow the flow rate to be closely controlled. The volume of the injection cylinder will also affect the cost substantially.

Vacuum is used with RTM to increase the injection driving force and to remove air during the flow process. Shop vacuum may not be adequate for air removal, so a vacuum pump may need to be purchased. A double-stage vacuum pump will cost between \$1000 and \$5000, depending on the capacity.

11.3.2 HEAT SOURCE

RTM parts can be cured in an integrally heated mould, in a press or be oven cured. Each of these methods requires less investment and less energy than the traditional autoclave cure approach. An autoclave can cost over 10 times the cost of an efficient oven for the same capacity. When designed properly, integrally heated moulds provide the most energy-efficient heat source. Integrally heated moulds may also reduce the recurring cost by eliminating mould transportation and minimising injection set-up.

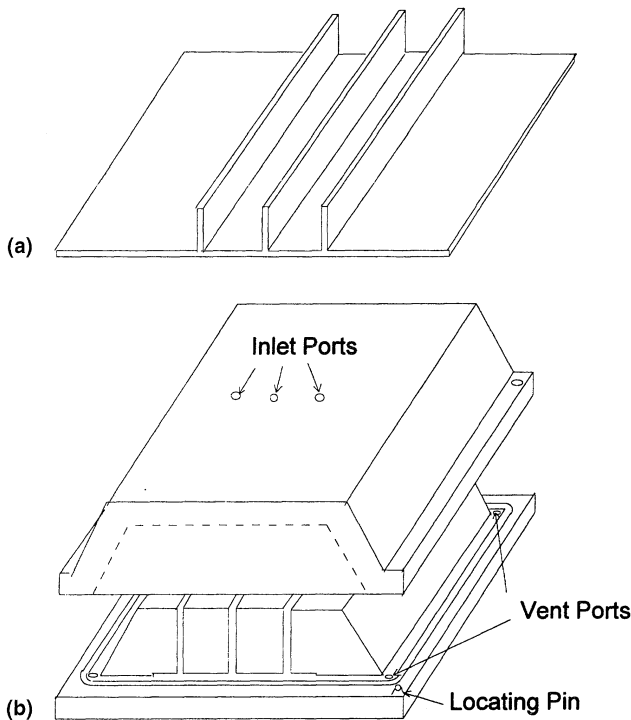


Figure 11.11 Concept 3: (a) stiffened panel; (b) stiffened panel mould.

11.3.3 MOULD COSTS

The moulds for RTM are usually more expensive than tooling used for prepreg. This is because RTM requires a matched mould with a much increased mould stiffness compared with prepreg tooling. This disadvantage may prevent an RTM research and development project from transferring into production, even when the recurring cost saving is substantial. More effort is needed to reduce tooling costs. However, it is important not to sacrifice quality because a poor mould design results in increased recurring costs and decreased part quality.

Almost all RTM moulds are manufactured from metal. Composite tools can be used, but the life of the tool is significantly reduced and any wear on the surface shows on the part. Composite tools may be preferred in some cases because of the similar coefficient of thermal expansion to the part. Generally, well-designed matched-metal moulds should last well over 800 parts and will allow much tighter tolerances than composite moulds. Spheroidal graphite cast iron is a preferred material for a complex-shaped mould. This type of cast iron is durable,

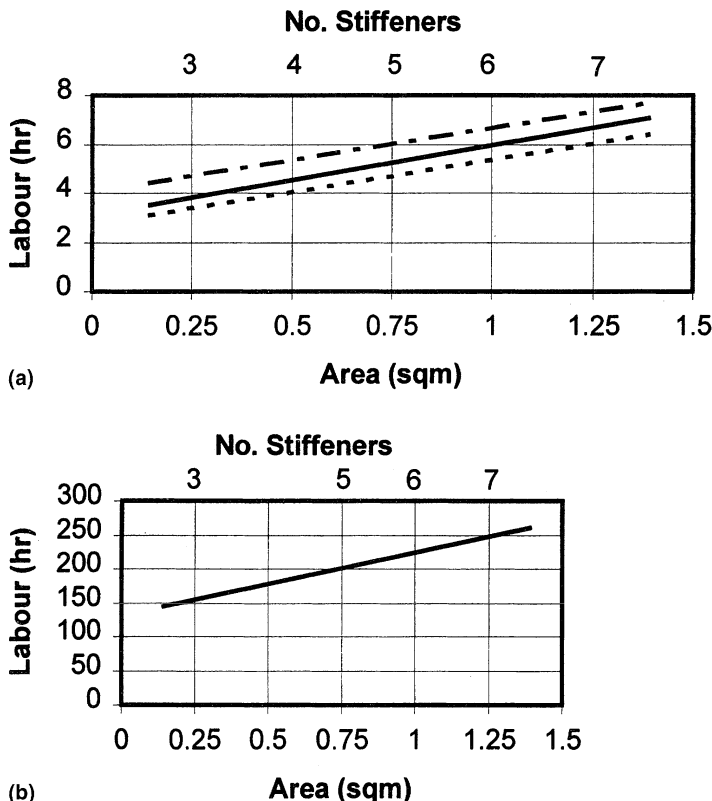


Figure 11.12 Concept 3: manufacturing costs for resin transfer moulding of stiffened panels (--- = 16-ply; — = 8-ply; - - - = 4-ply); (b) manufacturing costs for stiffened panel mould.

and copper tubes may be embedded into the mould for integral heating. The cost of a cast iron mould is usually less than that for steel for a complex shape. A model is fabricated for casting to a rough shape, then less than 1.2 cm is machined away to give the final contour, minimising machining time. Aluminium is often used for inserts to take advantage of its larger thermal expansion. Aluminium is also suitable for prototype moulds because of its lighter weight, but is not usually used for production because it is not as durable. Figure 11.3 illustrates the comparative costs of tooling materials (costs provided by Marand Precision Pty. Ltd, Melbourne, Australia). Aluminium raw material costs are significantly more than those of steel or cast iron; however, final tool costs may be comparable because aluminium is easier to machine.

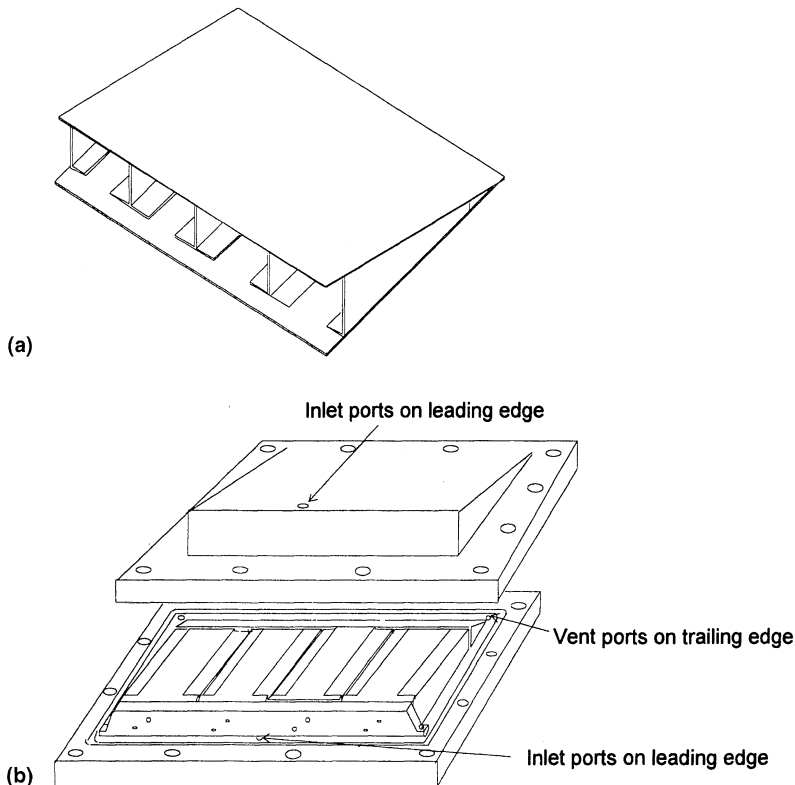


Figure 11.13 Concept 4: (a) flap; (b) flap mould.

11.3.4 CERTIFICATION COST FACTORS

Chapter 14, on certification, addresses some of the issues involved with certification of a new RTM part. In some cases it is more cost-effective to perform a materials allowable programme with limited part structural testing. In others, minimal materials testing and an extensive structural test programme may be a better option.

Materials Allowable Programme

Some companies have developed certified allowables with RTM resins. Typically, a new resin is used with an existing qualified fabric to make specimens for testing. Materials allowable test programmes usually require three batches of resin and three lots of fibre or fabric for testing. There may be over 20 tests to perform at different temperatures and moisture contents. This is an expensive process which can cost over a

million US dollars. However, the approach qualifies the resin for use with this fibre or fabric on other applications, perhaps justifying greater initial certification costs.

11.4 APPLICATIONS

The Airforce F22 fighter programme has over 300 RTM parts which directly replace metal designs. DOW-UT produces 44 detail sine-wave spars (Figure 11.4) for Boeing. The RTM process for making these carbon fibre epoxy sine-wave spars results in a \$250 000 savings per aircraft. Additionally, the process results in greater quality, increased production rates and the capability of manufacturing highly complex parts [6].

McDonnell Douglas Aircraft Company has been evaluating resin infusion for large wing skins [7]. Stitching of dry fabric has been incorporated into the preform to improve damage tolerance. Figure 11.5 shows the cost study comparison of various processing methods for a 2.4 m \times by 6.1 m blade-stiffened panel. These estimated cost numbers do not reflect the total panel cost – only materials and fabrication labour cost are included. The aluminium structure is estimated from large-scale production records. The composite cost estimates are conservative as shown by the use of automated equipment – 50% efficiency factors are added to the processing time. The efficiency of the automated methods would be expected to improve considerably during production, providing a substantial cost saving.

The stitched warp-knit fabric with the resin infusion process is cost competitive with the aluminium design. Nine-ply warp-knit fabric is the baseline material, with the skin consisting of six nine-ply elements stitched together; each stiffener angle consists of four nine-ply elements stitched together. Two of the 36-ply angle elements are stitched together in the web and the flanges are folded open [Figure 11.6(a)]. The stiffeners are then stitched to the skin as shown in Figure 11.6(b). The preform is positioned on top of the resin for infiltration by vacuum under a bag [Figure 11.6(c)]. Traditional RTM is not appropriate for this application as the size and weight of a matched mould would create handling difficulties and the cost would be prohibitive.

11.5 CASE STUDIES

The intent of these studies was to evaluate the effect of size and complexity on the mould and manufacturing cost. Mould cost estimates were provided by Marand Precision Engineering, Melbourne, Australia. The following four part concepts were selected for the study: flat panel, curved panel, stiffened panel and a flap. Mild steel was used for the study since it is preferred over aluminium for high-quantity parts.

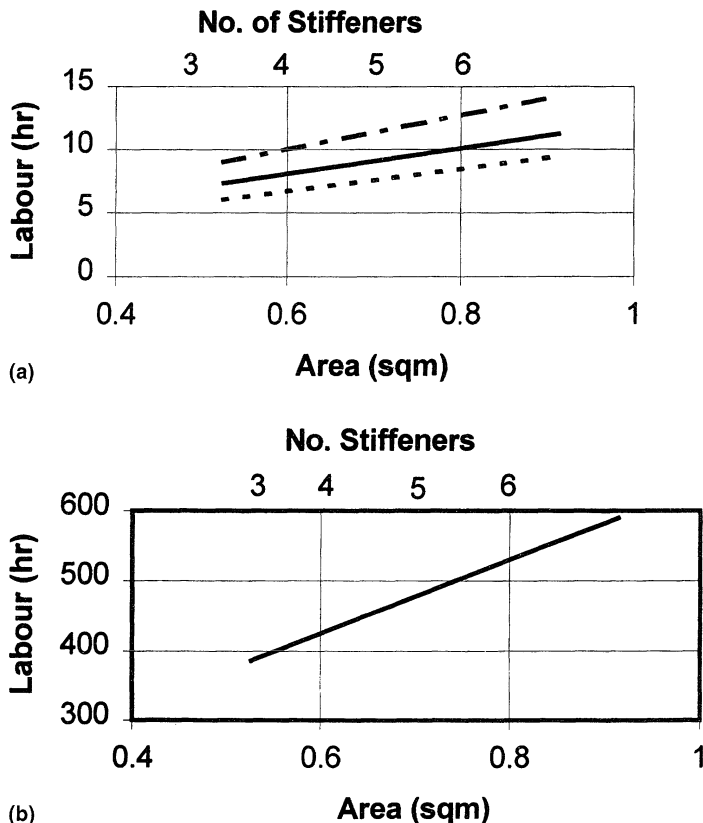


Figure 11.14 Concept 4: (a) manufacturing costs for resin transfer moulding of a flap (--- = 16-ply; —— = 8-ply; - - - = 4-ply); (b) manufacturing costs of the flap mould.

Aluminium inserts were used where their higher coefficient of thermal expansion was of benefit. The recurring costs were estimated using detailed manufacturing time-step estimates excluding cure time. Material costs were not included.

11.5.1 CONCEPT 1: FLAT PANEL

Concept 1 is a flat panel laminate [Figure 11.7(a)]. Figure 11.8(a) shows the recurring cost estimates for the RTM of various thickness laminates. The flat panel mould design is a simple two-piece steel mould with a picture-frame spacer to obtain the desired laminate thickness [Figure 11.7(b)]. The clamping method, using a hollow beam back-up structure with bolts, is not shown. Figure 11.8(b) shows the non-recurring cost of manufacturing the mould.

11.5.2 CONCEPT 2: CURVED PANEL

Concept 2 is for a curved panel and is shown in Figure 11.9(a). Figure 11.10(a) shows the recurring cost estimates for the RTM of various thickness curved panels. The mould design is a two-piece mild steel mould for a curved panel [Figure 11.9(b)]. A press is used to clamp the mould. Figure 11.10(b) shows the non-recurring cost of manufacturing the mould.

11.5.3 CONCEPT 3: STIFFENED PANEL

Concept 3 is for a stiffened panel and is shown in Figure 11.11(a). Figure 11.12(a) shows the recurring cost for resin transfer moulding of various thickness stiffened panels. The stiffened-panel mould is a two-piece mould design with inserts for forming the T-sections [Figure 11.11(b)]. There are three injection ports through the top of the stiffeners, with four vents in the corners. A press or integral bolts can be used for clamping the mould. Figure 11.12(b) shows the non-recurring cost of manufacturing the mould.

11.5.4 CONCEPT 4: FLAP

Concept 4 is for a flap and is shown in Figure 11.13(a). Figure 11.14(a) shows the recurring cost for the RTM of various thickness stiffened panels. The flap mould design is a two-piece steel mould with aluminium inserts used for the ribs [Figure 11.13(b)]. The injection ports are located on the leading edge with a small weir for flow down the length of the edge. The vent ports are located on the corners of the trailing edge. Integral bolts are used for clamping the mould. Figure 11.14(b) shows the non-recurring cost of manufacturing the mould.

11.5.5 SUMMARY

Figure 11.15(a) summarises the manufacturing costs for all concepts. As expected, the graph shows that increasing part complexity increases labour. Figure 11.15(b) compares mould costs for all concepts. Perhaps surprisingly, the stiffened panel mould should be less expensive to manufacture than the curved panel mould.

Figure 11.16 compares the recurring costs for manufacturing an eight-ply flat panel laminate by RTM and by autoclave-cured prepreg. A 5%–11% recurring cost advantage is indicated for RTM over the prepreg option. This slight advantage is primarily a result of the reduction in wrinkle-smoothing time.

Figure 11.17 compares RTM and secondarily bonded prepreg for an eight-ply flap. A recurring cost advantage between 30%–36% is indicated

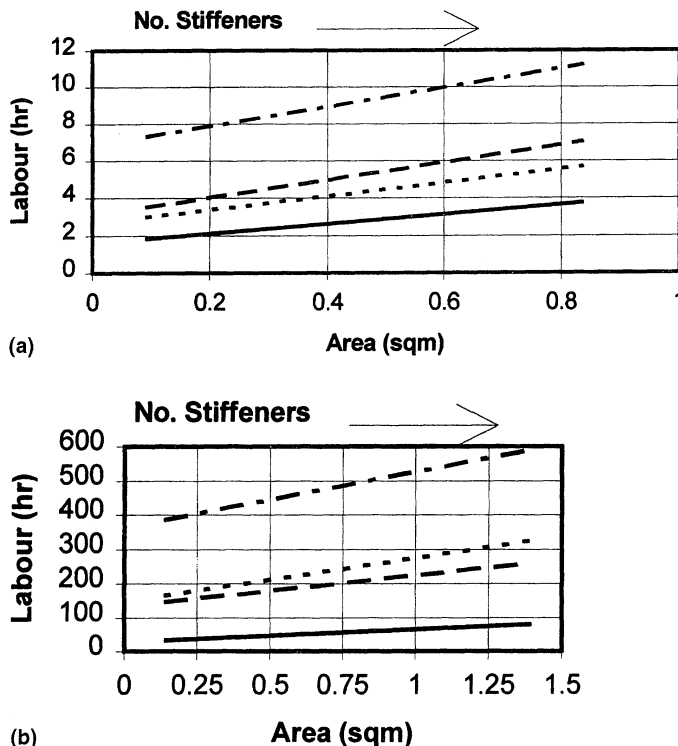


Figure 11.15 Comparison of (a) manufacturing labour for all concepts; (b) mould costs for all concepts. — = concept 1; ---- = concept 2; - - - = concept 3; ----- = concept 4.

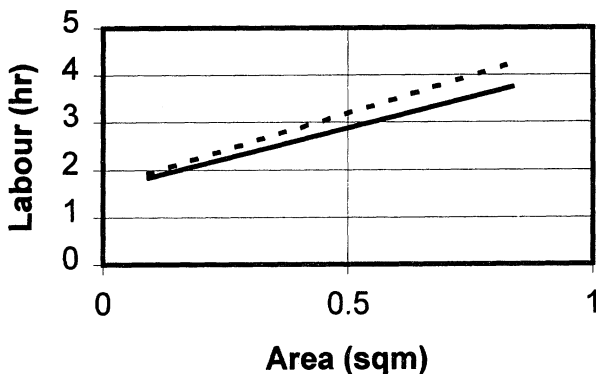


Figure 11.16 Comparison of recurring costs for the flat panel for resin transfer moulding (—) and prepreg (- - -).

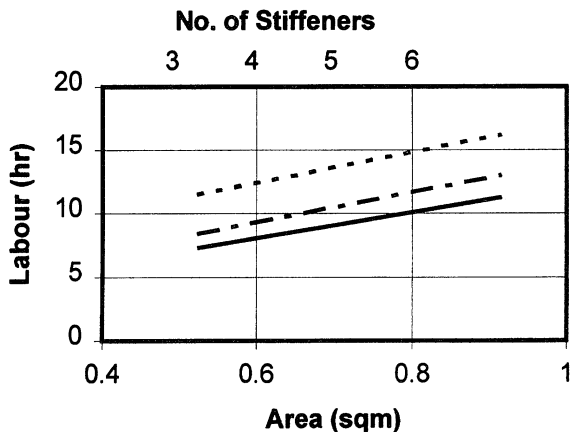


Figure 11.17 Comparison of recurring costs for the flap for resin transfer moulding (—), co-cured prepreg (---) and secondarily bonded prepreg (- - -).

for RTM. This is to be expected because RTM is more likely to be cost effective for complex shapes where significant lay-up time can be reduced and bond time eliminated. Figure 11.17 also compares RTM with a co-cured prepreg flap. The co-cured flap shows a cost advantage of 20% – 26% when compared with the secondarily bonded prepreg flap. However, RTM still indicates a 10% cost advantage over the co-cured flap.

References

1. Foley, M. and Bernardon, E. (1990) Cost estimation techniques for the design of cost effective automated systems for manufacturing thermoplastic composite structures. *35th International SAMPE Symposium*, Society for the Advancement of Material and Process Engineering, 1161 Parkview Drive, Covina, CA 91724-3748, April 2–5, pp. 1321–35.
2. Noton, B. (1987) Cost drivers in design and manufacture of composite structures, in *ASM International Engineered Materials Handbook, Volume 1*, ASM International, Metals Park, OH, pp. 419–24.
3. T. Gutowski, D. Hoult, G. Dillon *et al.* (1994) Development of a theoretical cost model for advanced composite fabrication. *Composites Manufacturing*, 5(4), 231–9.
4. Curtis, P.T. and Browne, M. (1994) Cost-effective high performance composites. *Composites*, 25(4), 273–4.
5. Foley, M. (1990) Techno-economic automated composite manufacturing techniques. *22nd SAMPE International Technical Conference*, Society for the Advancement of Material and Process Engineering, 1161 Parkview Drive, Covina, CA 91724-3748, November 6–8, pp. 764–5.
6. Material News (1996) RTM for aircraft. *Sampe Journal*, 32(4), 21.
7. Palmer, R. (1995) Techno-economic requirements for composite aircraft components. Presented at New Fabric Technologies, New Manufacturing Processes for Advanced Composite Structures Course, 29 March, Cooperative Research Centre for Advanced Composite Structures, Fishermens Bend, Vic., Australia.

Data acquisition: monitoring resin position, reaction advancement and processing properties

12

David E. Kranbuehl and Al Loos

12.1 INTRODUCTION

The resin transfer moulding (RTM) process has been used in the past primarily for the production of lower performance composite structures. These structures typically have low fibre volumes and use relatively low-temperature matrices such as polyester resins. Advanced composite structures constructed with high-temperature resins require high fibre volumes with low void contents to be qualified for aircraft service [1].

The primary problem limiting the use of the RTM process for advanced composite structures is obtaining high fibre volumes when using the high-temperature thermosetting matrix materials. Most thermosetting polymer matrix materials [e.g. epoxies, bismaleimides (BMIs), polyimides] exhibit a higher processing viscosity when formulated for higher temperature service. This increase in viscosity significantly increases the difficulty of RTM with the higher temperature resins typically used in aerospace composite parts. The problem of the viscosity increase is compounded by a decrease in the permeability of the fibre preform to resin flow at higher fibre volumes. The permeability of the preform is cut in half when the fibre volume increases from 56% to 62% [2, 3]. The primary deterrent to successful RTM of advanced composite structures is obtaining adequate flow and a distribution of the resin into the fibre preform without forming voids or porosity [3–5].

In the development of RTM techniques for high-performance aircraft structures, two approaches are used. The first involves conventional RTM using a mould of fixed geometry in which the preform is placed. Once the fabric is positioned and the mould closed to create a known geometry with a known fibre volume fraction of around 60%, the resin is injected. In the second approach, sometimes called resin film infusion (RFI) to distinguish this variation from conventional RTM, a resin film is placed in the bottom of the mould as a rubbery – or, once cooled, glassy – material. The RFI process is similar to conventional RTM except that the heated resin film which becomes liquid is used to infiltrate the dry textile preform through-the-thickness instead of primarily liquid resin in-plane flow. The thickness of the resin film placed on the surface of the base plate depends on the mass of resin required completely to infiltrate and wet-out the preform. The dry preform is placed on top of the resin film and the spacer and fixed and float tools are located in place. An aluminum or carbon pressure plate is placed over the assembly. A vacuum bag is placed over the tool and the entire assembly is placed into an autoclave for infiltration and cure. At some point in the processing cycle, consolidation pressure is applied to the assembly. The vacuum forces resin into the preform and the pressure compacts the fabric preform to the specified fibre volume fraction. The tool assembly is heated according to a prescribed temperature cycle which decreases the resin viscosity, allowing for infusion and fibre wet-out and cure of the resin-saturated preform.

In both types of RTM processing the major objective of attaining complete resin impregnation of the fabric is usually achieved as already described by heating the thermoset resin to reduce the viscosity. For thermosetting resins, heating the resin in turns advances the reaction which in turn causes the viscosity to increase. Hence the conflicting forces of higher temperatures, which not only reduce the initial viscosity but also increase the rate of reaction advancement and viscosity with time, making RTM challenging. For this reason on-line data acquisition – *in situ* sensing of resin position, reaction reach advancement and viscosity – becomes an important tool to assist in the achievement of a high fibre volume fraction, void-free RTM laminate.

In this chapter an understanding of the fundamental science underlying *in situ* dielectric sensing is provided. The use of dielectric sensing to monitor resin infiltration and cure during RTM and RFI fabrication of an epoxy composite part in a manufacturing plant is described. Also present are the results of an expert sensor system to control automatically the RTM fabrication process.

At the heart of dielectric sensing is the ability to detect the presence of the resin and then to monitor the changes in the molecular mobility of ions and the changes in the molecular mobility of dipoles in the presence of a force created by an electric field. These variations in molecular position due to the force created by an electric field are a very sensitive

means of monitoring changes in macroscopic processing and mechanical properties such as viscosity, modulus, glass transition temperature (T_g) and degree of cure. Mechanical properties reflect the change in position on a macroscopic level arising from a mechanical force. The reason why dielectric sensing is so sensitive is rooted in the fact that changes on a macroscopic level originate from changes in force–position relationships on a molecular level. Indeed, it is these molecular changes in force–displacement relationships which the dielectric sensor monitors as the resin cures and which are the origin of the resin’s macroscopic changes in flow, degree of cure and other mechanical properties.

Why is on-line dielectric sensing needed? First, dielectric sensing allows one to monitor or see the actual state of the resin in the tool at all times during the cure process. Temperature and pressure do not provide direct information about the state of the resin. Thus dielectric sensing is one of the few means by which the operator can actually monitor the state of the resin and tell both the stage and position of the resin throughout the entire fabrication process.

Second, by actually monitoring the state of the resin it is possible to control the fabrication process by data rather than a procedure such as a set time–temperature sequence. This means one can have an automated self-correcting intelligent cure process which can adapt to variations in resin age, fabric permeability, tool heat-transfer characteristics and so on.

Third, modelling and individual thinking which leads to a procedure-driven cure cycle is beset with operating difficulties. Most notably, as has been described by George Springer [6], modelling requires extensive material data characterisation of resin properties, as well as preform properties which are time consuming to measure and, most importantly, which will vary from day to day, batch to batch, and lay-up to lay-up. Further, results are limited generally to a particular or a simplified geometry. Fabric preform properties will vary from preform to preform, with lay-up, with bagging, with position within the preform and so on. Heat-transfer characteristics will similarly vary with the tool and the heating method. Thus, given the time and material cost, it is critical to monitor or see what is actually happening and have the sensing ability to detect, verify and even correct the processing properties as the cure proceeds. Hence, both monitoring and modelling are essential.

In summary, in this chapter we discuss how acquisition of dielectric sensing data provides invaluable insight in observing the position of the resin, the state of the resin during the process, verifying and reducing the time in developing a cure process as well as providing an automated self-correcting intelligent control system. Acquisition of dielectric monitoring data has, at the same time, the future potential to provide on-line quality verification of the fabrication process, thereby increasing product reliability and reducing post-fabrication test costs.

12.2 INSTRUMENTATION

The dielectric sensing technique [7–33] has been shown to be effective for monitoring a variety of resin cure processing properties such as reaction onset, viscosity, point of maximum flow, degree of cure, buildup in T_g and reaction completion as well as detecting the variability in processing properties arising from resin age and exposure to moisture. The dielectric sensing technique has been shown to be able to monitor similar processing properties in thermoplastics such as T_g , melting temperature (T_m), recrystallisation and solvent-moisture out-gassing, [7, 28]. The dielectric technique has the particular advantage over other chemical characterisation measurements of being able to monitor these processing properties continuously and *in situ* as the resin changes from a resin of varying viscosity to a cross-linked insoluble solid. Another advantage is that measurements can be made simultaneously on multiple samples or at multiple positions in a complex part. Of particular importance is the ability of dielectric sensing to monitor the changing properties of polymeric materials in composites, films, coatings [29, 30], as adhesives and to detect phase separation in toughened systems [31–33].

In the work reviewed here, dielectric sensing measurements at frequencies from the hertz to megahertz region were taken continuously throughout the entire cure process at regular intervals and converted to the complex permittivity, ε , where

$$\varepsilon = \varepsilon' - i\varepsilon''. \quad (12.1)$$

Measurements were made with a geometry independent DekDyne microsensor system which has been patented and is commercially available. The sensor itself is planar, 2.54 cm × 1.27 cm in area and 5 mm thick. The sensor-bridge microcomputer system is able to make continuous uninterrupted measurements of both ε' and ε'' over 10 decades in magnitude at all frequencies. The sensor is inert and has been used at temperatures exceeding 400°C and over 1000 psi pressure.

Commercially available dielectric sensing systems are available in the United States through DekDyne Inc., Micromet Inc., Radius Engineering Inc. and in Europe through Robit in Norway. (A list of manufacturers and their contact details is given at the end of this chapter.)

12.3 THEORY

Frequency-dependent measurements are made of the sensor material's dielectric impedance, Z , as characterised by its equivalent capacitance, C , and conductance, G , where

$$Z^{-1} = G + i\omega C \quad (12.2)$$

where $\omega = 2\pi f$, and f is the measured frequency. C and G are used to obtain the calculated complex permittivity, ϵ^* . This calculation is possible when using a sensor whose geometry is invariant over all measurement conditions. The real and imaginary parts of ϵ^* are then given by:

$$\epsilon'(\omega) = \frac{C^{\text{mat}}(\omega)}{C_0} \quad (12.3)$$

$$\epsilon''(\omega) = \frac{G(\omega)}{C_0 2\pi f} \quad (12.4)$$

where $C^{\text{mat}}(\omega)$ is the capacitance of the sensor material and C_0 is the air replacement capacitance of the sensor.

The time at which the resin front reaches the positions of the sensor is readily detected by a sudden increase in C and G and similarly a corresponding sharp jump in the values of ϵ' and ϵ'' .

In order to monitor on a more advanced level the extent of reaction advancement, viscosity, and so on the change in the value of the ionic and/or dipolar mobility needs to be determined from the frequency dependence of $\epsilon''(\omega)$ and $\epsilon'(\omega)$ and then correlated from laboratory measurements with the value of the viscosity and reaction advancement.

Both the real and the imaginary parts of ϵ^* can have an ionic and dipolar component:

$$\epsilon' = \epsilon'(\text{ionic}) + \epsilon'(\text{dipolar}) \quad (12.5)$$

$$\epsilon'' = \epsilon''(\text{ionic}) + \epsilon''(\text{dipolar}) \quad (12.6)$$

Plots of the product of frequency, where $\omega = 2\pi f$, multiplied by the imaginary component of the complex permittivity, $\epsilon''(\omega)$, make it relatively easy to determine visually when the low-frequency magnitude of ϵ'' is dominated by the mobility of ions in the resin and when at higher frequencies the rotational mobility of bound charge dominates ϵ'' . Generally, the magnitude of the low-frequency overlapping values of $\omega \epsilon''(\omega)$ monitor the change with time of the ionic mobility. The changing ionic mobility is a molecular probe which quantitatively monitors the viscosity of the resin.

The peaks in $\epsilon''(\text{dipolar})$ (which are usually close to the peaks in ϵ'' as directly measured) can be used to determine the time or point in the cure process when the 'mean' dipolar mobility and its corresponding value of T_g have attained a specific value. Thus, time of occurrence of a given dipolar mobility as measured by a peak in the high-frequency value of $\epsilon''(\omega)$ is a means of monitoring quantitatively the change in the glass transition temperature during processing.

The changing value over time, t , of $(d\epsilon''/dt)/\epsilon''$ is used to monitor *in situ*, during processing, the build-up in degree of cure and related end-use properties such as modulus, hardness and so on during the final stages of cure or post-cure.

12.4 CALIBRATION: MONITORING CURE IN MULTIPLE TIME-TEMPERATURE PROCESSING CYCLES

As a representative example of cure monitoring using a common commercially used aerospace resin and a complex cure cycle, Figure 12.1 displays the output of $\omega \epsilon''(\omega)$ for a two-stage, 121°C and 177°C ramp-hold sequence used to cure a commercial, widely used MY720 aromatic epoxy system [plotted here as $\log \omega \epsilon''(\omega)$]. This resin consists of tetra-glycidyl 4,4' diamino diphenylmethane (TGDDM) and diamino diphenyl sulphone (DDS). A form of this system with catalyst is sold by the Hercules Corporation as 3501-6.

Figure 12.1 shows two peaks of the overlapping $\omega \epsilon''(\omega)$ lines. These indicate the times and magnitude of maximum flow as monitored by the ionic mobility. The first peak, the highest degree of flow, occurs at the beginning of the first hold. The second point of high flow, high ionic mobility, occurs midway up the ramp between the 121°C hold and the 177°C hold. As the temperature rises the fluidity increases until such time as the rate of reaction and thereby the degree of cure, which is also increasing during the temperature ramp, overwhelm the temperature effect on fluidity. At this point the fluidity begins to drop and a peak in $\omega \epsilon''(\omega)$ occurs, indicating the second occurrence of maximum flow.

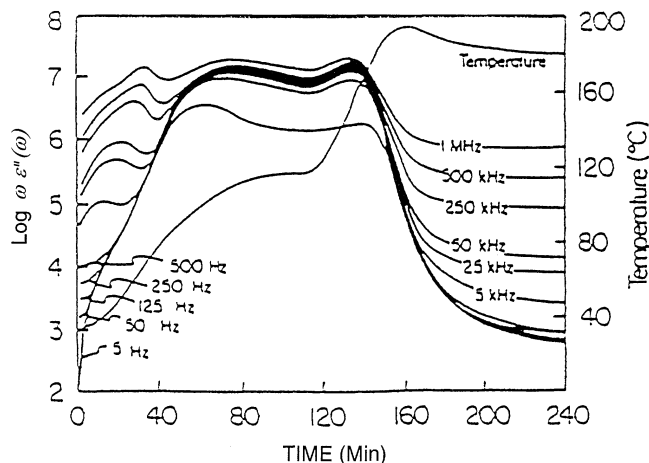


Figure 12.1 Plot of $\log \omega \epsilon''(\omega)$ against time of the sensor output at the 64th ply of the thick... $\omega = 2\pi f$; f = frequency; ϵ'' = the imaginary part of the complex permittivity.

The gradual drop in the magnitude of $\varepsilon''(\omega)$ during the final hold and its rate of change, $d\varepsilon''/dt$, monitor the build-up in modulus. When ε'' attains a constant value the system has reached its final lowest value of dipolar ionic mobility. Thus, when no further changes in mobility can be detected, $(d\varepsilon''/dt) = 0$; the system is fully reacted at that hold temperature. Monitored in this way, the changing values of ε'' are a very sensitive means of detecting the final small changes in degree of cure and the build-up in end-use properties such as T_g , modulus and so on. Figure 12.1 suggests even after a 2 h hold, for this fresh 3501-6 resin the mobility is still decreasing and final cure or end-use properties have not been attained.

Figure 12.2 shows the correlation between the viscosity and the ionic mobility based on isothermal runs for this system as monitored by the value of $\varepsilon''(5\text{ kHz})$. A representative calibration curve relating the dielectric sensor output to degree of cure is shown in Figure 12.3. Unlike viscosity, separate calibration curves for different temperatures must be generated from the isothermal runs because they are temperature-dependent.

The build-up in final curve properties such as degree of cure during the last hold is monitored with a high degree of sensitivity using the value of $(d\varepsilon''/dt)/\varepsilon''$.

Figure 12.4 is the correlation plot of the normalised rate of change in $\varepsilon''(5\text{ kHz})$ [based on numerous differential scanning calorimeter (DSC) runs] of the build-up in the degree of cure compared with model-predicted values.

Figures 12.5 and 12.6 show two important applications of dielectric sensing as applied to quality evaluation and processing of an epoxy

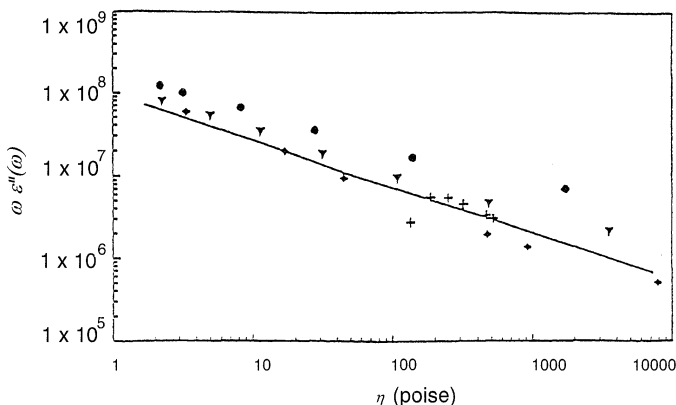


Figure 12.2 $\log \omega \varepsilon''(\omega)$ against $\log(\text{viscosity})$, $\log \eta$, for the TGDDM (tetraglycidyl 4,4' diamino diphenylmethane) epoxy based on four isothermal runs: ● = 149°C; ▽ = 135°C; ● = 121°C; + = 100°C. $\omega = 2\pi f$; f = frequency; ε'' = the imaginary part of the complex permittivity.

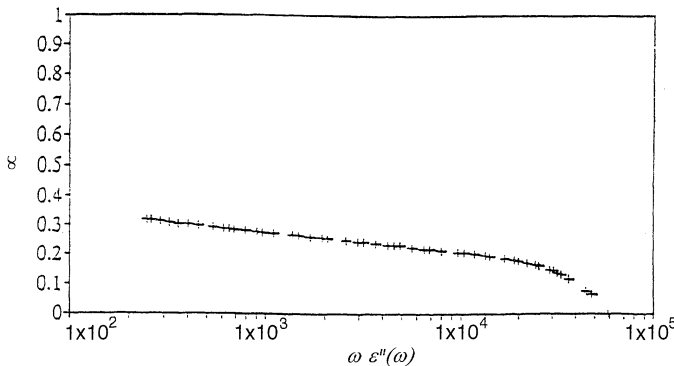


Figure 12.3 Correlation curve relating degree of cure, α , to $\omega \epsilon''(\omega)$ at 135°C. $\omega = 2\pi f$; f = frequency; ϵ'' = the imaginary part of the complex permittivity.

system. Figure 12.5 shows the effect on processing properties as monitored by the value of $\omega \epsilon''(\omega)$ for this system when the first hold temperature drifts 10°C higher, to 131°C. Figure 12.6 shows the output for the original 121°C, 177°C ramp hold sequence but for a batch of 3501-6 epoxy resin after it has been left to age at room temperature for 30 days.

Even without the calibration relations the effect on cure processing properties can be clearly seen from the sensor output. In Figure 12.5, the value of ϵ'' peaks a little higher but drops much more rapidly. The second peak in ϵ'' during the ramp is much lower. Thus the effect of the 131°C hold compared with a 121°C hold is to cause a slightly higher fluidity initially. But the high-fluidity region lasts for a much shorter time.

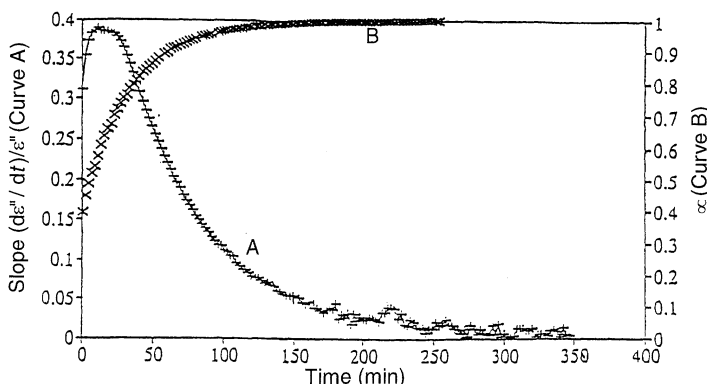


Figure 12.4 Correlation of $(d\epsilon''/dt)/\epsilon''$ (curve A) and degree of cure, α (curve B), with time, t , showing the sensitivity of the normalised rate of change in ϵ'' (the imaginary component of the complex permittivity) to changes in final degree of cure near end reactions.

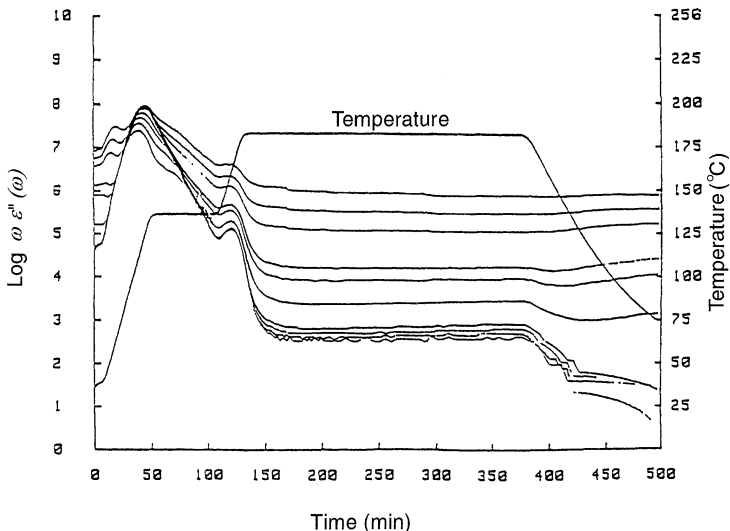


Figure 12.5 TGDDM (tetraglycidyl 4,4' diamino diphenylmethane) epoxy cured in a press with a 135°C, 177°C cure cycle. Values of $\omega\epsilon''(\omega)$ are displayed for frequencies (in order from top to bottom) of 1 MHz, 500 kHz, 250 kHz, 125 kHz, 50 kHz, 5 kHz, 500 Hz, 250 Hz, 125 Hz and 50 Hz. $\omega = 2\pi f$; f = frequency; ϵ'' = the imaginary part of the complex permittivity.

Equally important, one can see that at the second point of high fluidity, which is usually critical for composite-prepreg consolidation, the fluidity is significantly lower. The overall effect of aging is seen in Figure 12.6 as decreasing the level of fluidity throughout the cure procedure. Full cure is achieved much sooner in the final hold for the aged resin as the value of $d\epsilon''/dt$ approaches zero much sooner.

12.5 MONITORING RESIN INFILTRATION IN CONVENTIONAL RESIN TRANSFER MOULDING, AND MODEL VERIFICATION

A schematic diagram of a single side port injection experiment using conventional RTM is shown in Figure 12.7. Resin enters the cavity through a single side port and flows along the 0.32 cm channel around the perimeter of the fabric. Resin then begins to infiltrate through the edges of the preform, saturates the preform and exits through the centre port.

The finite element mesh for the resin infiltration model discussed here consisted of 2707 quad elements and a total of 2816 nodes [34]. The measured E-glass fabric warp and fill direction permeabilities at 43% fibre volume fraction were input for each element [35]. Oil was used as the impregnating fluid.

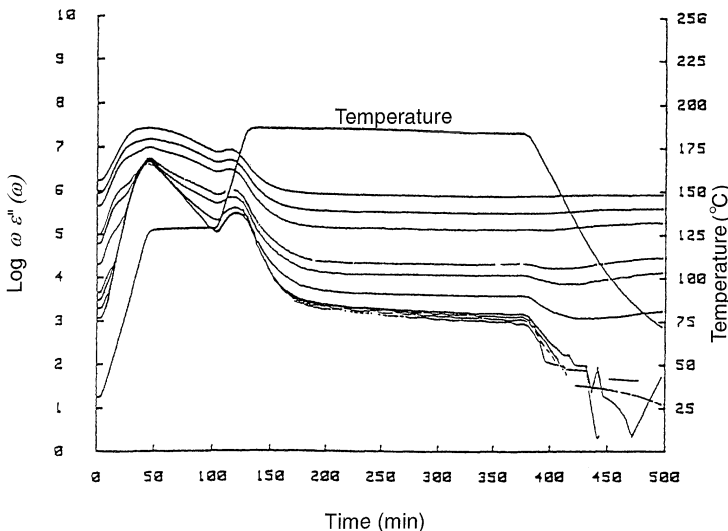


Figure 12.6 TGDDM (tetraglycidyl 4,4' diamino diphenylmethane) epoxy which has been aged at room temperature for 30 days, after which it was cured in a press using a 121°C intermediate hold. $\omega = 2\pi f$; f = frequency; ϵ'' = the imaginary part of the complex permittivity.

The influence of the channel was considered in the model by adjusting the permeability of the elements representing the channel until the model-predicted inlet port and channel pressures matched the measured values. This technique gave a reasonably good representation of the resin channel in the simulation.

Comparisons between the model-predicted and sensor-detected as well as visually recorded flow fronts are shown in Figure 12.8. The time that the visual image was captured on the video tape is denoted on each figure. The dark shaded area is the resin-saturated region of the preform, the whitish area is the dry preform and the solid line represents the model-predicted flow front. The images of the model-predicted flow fronts were taken at times corresponding to the images stored to disk from the video tape. Each model-predicted flow pattern was overlaid on top of the appropriate video image taken from the experiments.

As can be seen from Figures 12.8(a) and 12.8(b) the model matched the measured infiltration times very well. Note that the measured flow front is somewhat wavy during infiltration. This may be a result of the flexibility of the plastic top plate.

A grid showing the positions of the dielectric sensors, which were located underneath the glass fabric, has been overlaid on Figures 12.8(a) and 12.8(b). The grid was helpful in comparing the dielectric sensor

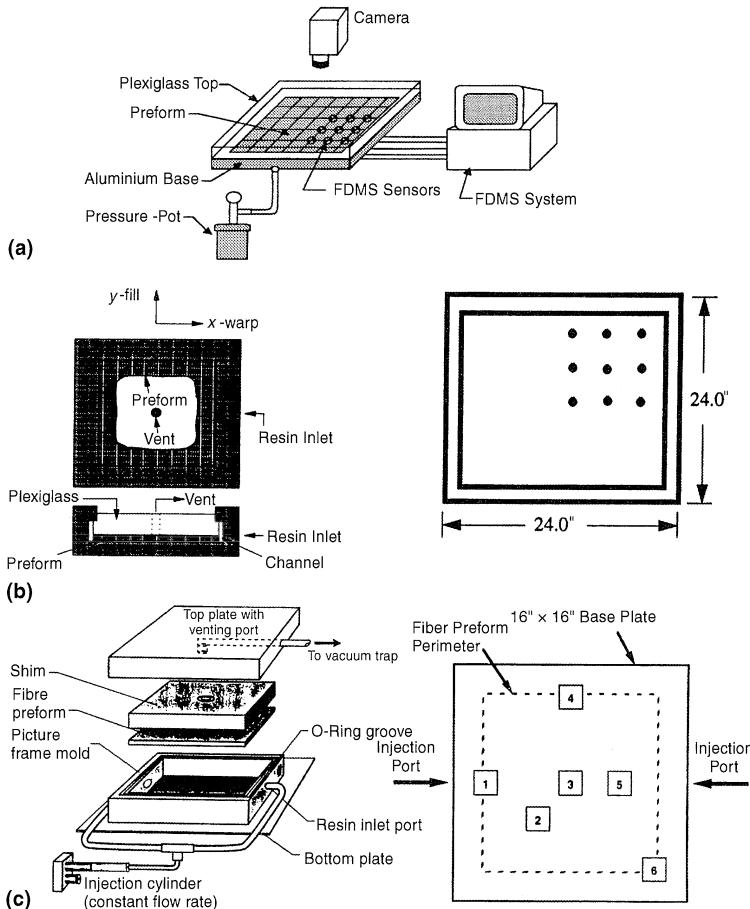


Figure 12.7 Schematic diagrams of (a) flow visualisation apparatus; (b) (i) single side port injection experiment, (ii) location of the frequency dependent electromagnetic sensors (FDEMS) sensors array in the visualisation figure (FDEMS sensors indicated by ●); (c) (i) resin transfer moulding (RTM) assembly, (ii) location of FDEMS sensor array in bottom plate of RTM mould (FDEMS sensors indicated by numbered boxes).

response with the visual and model flow front positions. The sensor locations and measured wet-out times are denoted on each figure. As can be seen from the figures, the dielectric sensors can detect the location of the resin flow front to within 5 s of the visually measured infiltration times. The accuracy of the dielectric sensor measurements can be improved by increasing the scanning rate of the data acquisition system. Clearly the advantage of the sensors is that they can be placed in a steel mould and in a fabrication device such as a press or autoclave.

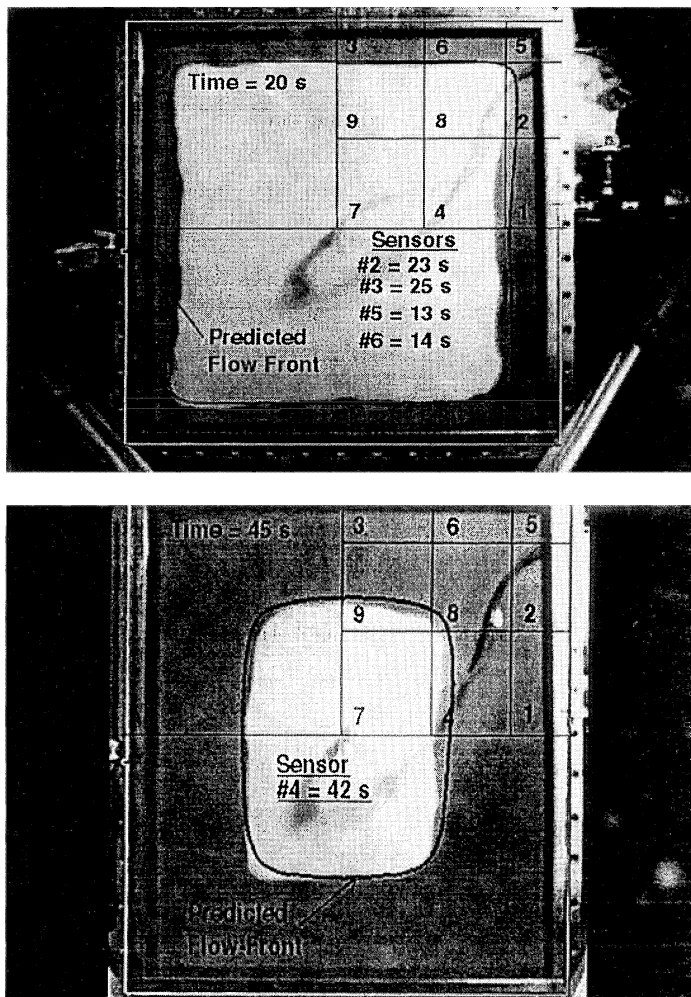


Figure 12.8 Comparison between the model-predicted and recorded flow front at an infiltration time of (a) 20 s; (b) 45 s. Dark shaded area = resin-saturated region of the preform; whitish area = dry preform; solid line = model-predicted flow front; the grid shows the positions of the nine sensors.

Another mould fitting experiment was conducted with Shell 1895/W resin and 1M7/8HS carbon preform at a flow rate of $10 \text{ cm}^3/\text{min}$. The purpose of the experiment was to use the dielectric technology again to monitor resin position as a function of time during the filling process and compare the recorded times with the model-predicted values in the all-steel mould.

The finite element mesh for this resin infiltration model consisted of 620 quad elements and a total of 669 nodes. The measured 1M7/8HS fabric warp and fill direction permeabilities at 60% fibre volume fraction were input for each element [35].

The resin flow patterns during mould filling are shown in Figure 12.9. The locations of the six dielectric sensors and the corresponding wet-out times are denoted on the figure. The wet-out of sensor 1 was used to approximate the beginning of the mould filling process. There is excellent agreement between the measured wet-out times and model predictions for both the internal (sensors 2, 3 and 5) and perimeter (sensors 4 and 6) sensor locations. Note the model predicted a skewed flow pattern resulting from the shifting of the preform during mould closing. By carefully measuring the channel dimensions upon completion of the test, a more accurate prediction of the flow patterns at the beginning of infiltration was obtained.

A comparison between the measured and model-predicted mould inlet pressure is shown in Figure 12.10. Pressure readings were also taken in the channel adjacent to sensor 4 and in the identical location on the other side of the mould. The data indicate that the pressure drop in the channel is quite small, as expected. The model accurately predicts the pressure behaviour as a function of infiltration time. The fluctuations in

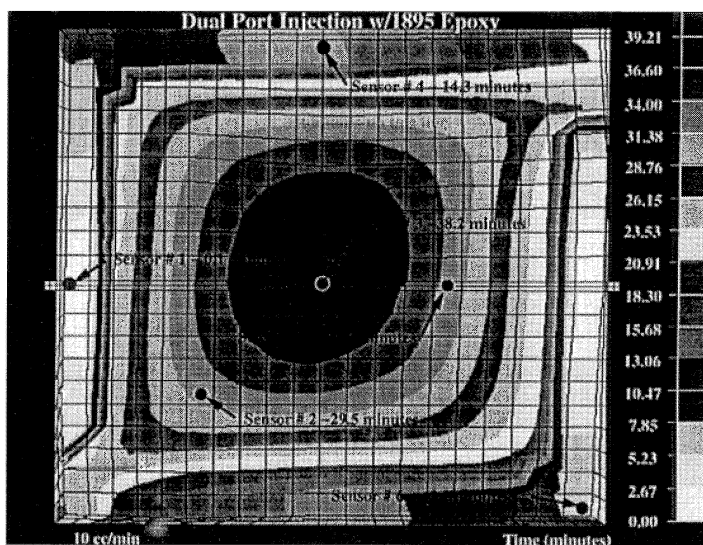


Figure 12.9 Model-predicted flow patterns during mould filling for a flow rate of $10 \text{ cm}^3/\text{min}$. The wet-out time is given by each sensor. The experiment was conducted with Shell 1895/W resin and 1M7/8HS carbon preform.

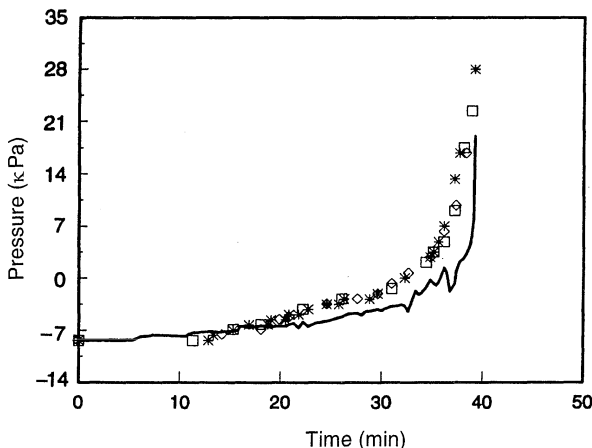


Figure 12.10 Comparison between measured and model-predicted inlet pressure for a flow rate of $10 \text{ cm}^3/\text{min}$. Experimental conditions are described in Figure 12.9. Measurements: * = at inlet; ◇ = at sensor 4; □ = across from sensor 4; — = model-predicted pressure at inlet.

the pressure predictions are a result of variations in the injection pump flow rate.

12.6 IN SITU REAL TIME FLOW SENSING IN RESIN FILM INFUSION AND PROCESS MONITORING

Figure 12.11 is a schematic of a T-stiffened panel with nine sensors. As a representative example of cure monitoring, Figure 12.12 shows the output of $\omega \varepsilon''(\omega)$ from sensor 5 (seen in Figure 12.11) for the MY720 aromatic TGDDM epoxy system commercially sold as 3501-6 by Hercules.

Measurements were taken at 3 min intervals of ε'' during the resin film infusion cure cycle in an autoclave at the Northrup Corporation Los Angeles plant. The T-stiffened carbon preform was furnished by the Douglas Aircraft Company. Temperature holds occurred at approximately 120°C and 177°C . Four frequencies – 250 Hz, 500 Hz, 5000 Hz and 25000 Hz are shown in Figure 12.12. The time the resin front infiltrates to the sensor's location is shown by the large jump in sensor output. The overlapping lines indicate the signal is dominated by ionic mobility until the second hold has been reached. Figure 12.2 showed the correlation between the viscosity, η , and the ionic-mobility-dominated values of ε'' . It showed ε (ionic) $\propto 1/\eta$ for viscosities up to 10^3 poise, at which point the relation between the 'molecular viscosity' governing ionic mobility no longer is directly related to the reciprocal of the macroscopic viscosity as measured on a dynamic mechanical viscometer. In general, this approximate inverse relationship between molecular mobility and viscosity

Ply Drop-off Stitched Preform with 9 FDEMS Sensors

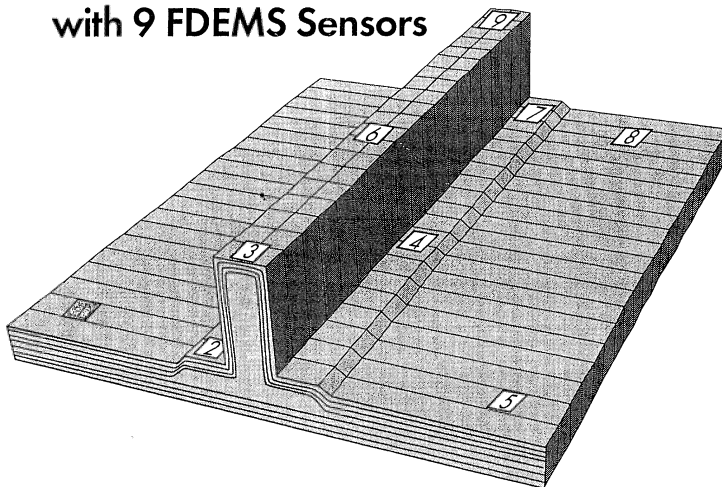


Figure 12.11 Ply drop-off stitched preform with nine FDEMS sensors.

breaks down as the resin begins to cross-link and gel. Thus, dielectric sensing can be used to monitor quantitatively through calibration, such as in Figure 12.2, the viscosity *in situ* during processing. Through correlation with other techniques, dielectric sensor output can be calibrated

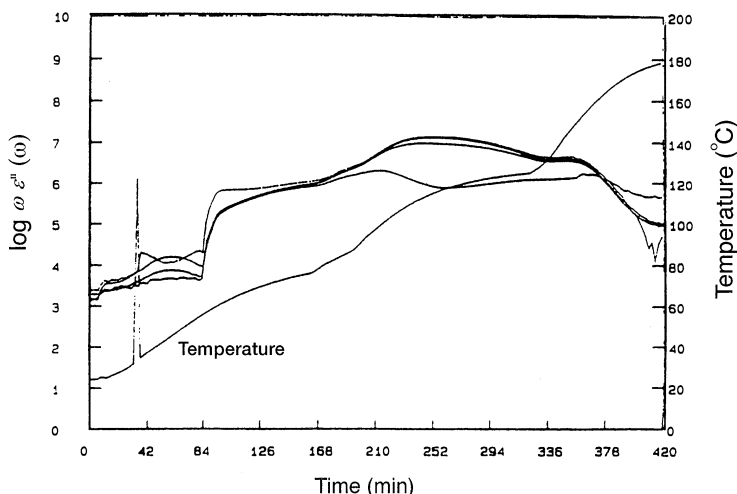


Figure 12.12 FDEMS output of a resin film infusion run carried out at the Northrup Corporation's Los Angeles plant. Four frequencies are shown: 250 Hz, 500 Hz, 5000 Hz, and 25000 Hz (in order from bottom to top)

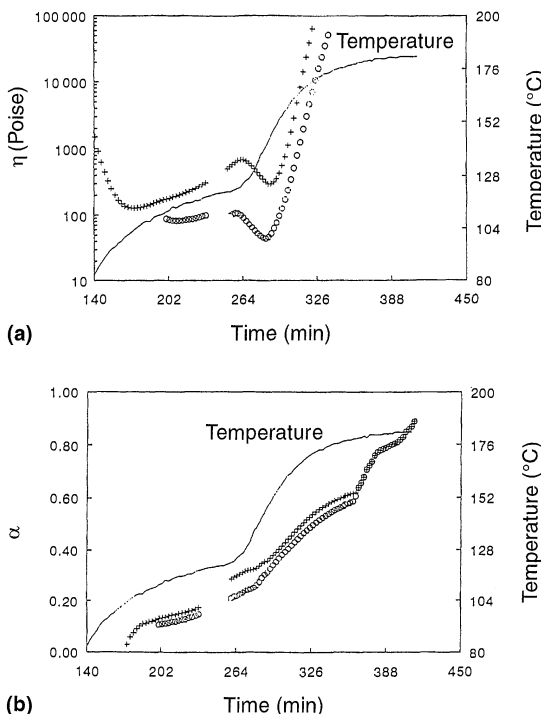


Figure 12.13 (a) Viscosity, η ; (b) degree of cure, α , of two different positions on the preform (Figure 12.11); + = at position 1, on the flat panel; o = position 3, at the top of the T-stiffener.

to detect gel. A calibration curve relating degree of cure, α , and the dielectric sensor output was shown in Figure 12.3. Unlike the viscosity calibration curve, this calibration is temperature-dependent.

The build-up in final cure properties such as degree of cure during the last hold was monitored *in situ* using the frequency dependent electromagnetic sensors (FDEMS) $(d\epsilon''/dt)/\epsilon''$ output and using the correlation plot shown in Figure 12.4 for 3501-6 (Hercules Corporation).

Figures 12.13(a) and 12.13(b) show, respectively, the viscosity and degree of cure at two different positions on the preform – position 1 on the flat panel and position 3 at the top of the T-stiffeners (Figure 12.11). These results are obtained from the dielectric sensor output as shown in Figure

Table 12.1 Sensor Wet-out Times. Experimental details are given in text, section 12.6.

Sensor Location	1	2	3	4	5	6	7	8	9
Wet-out Time (min)	63	104	168	114	97	168	110	100	163

12.12 and using the calibration plots such as shown in Figures 12.2 and 12.3. Wet-out times at the nine sensor locations are shown in table 12.1.

12.7 SMART AUTOMATED CONTROL

A smart artificial intelligence control system is based on monitoring the actual state of the resin, not on a predetermined time-temperature procedure [36–40]. Thus the temperature scheme the fibre-resin part experiences is not based on time but on the achievement of molecular landmarks in the curing process. Because these critical points may not occur at the exact same time for each part being made, time is not wasted holding a part at some stage when the resin can be advanced. The smart, closed-loop process has the flexibility to adjust to variations in resin cure and heat transfer properties. Thus it is much more efficient and reliable than a rigid time-temperature procedure.

An intelligent closed-loop system produces more consistent parts. The resin's advancement to the next stage of cure is based on its achieving a certain molecular state. Consequently, with each part made, wet-out of the fibres is defined by monitoring the position of the resin front. The advancement of the viscosity and degree of cure is monitored. Final cure is defined by a universal degree of cure. This is a more consistent way to produce high-performance composite parts than simply subjecting them to the same time-temperature schedule when batch variations and differences in prefabrication handling are present.

Figure 12.14 is a schematic of the dielectric sensor smart system for monitoring quality and for expert automated process control. The expert system was constructed to optimise and control the achievement of six critical stages during the cure process:

1. achieve a low resin viscosity;
2. maintain a low viscosity until impregnation is complete;
3. advance the resin reaction at an intermediate temperature to a particular degree of cure that avoids an excessive exothermic effect (this value varies with part thickness);

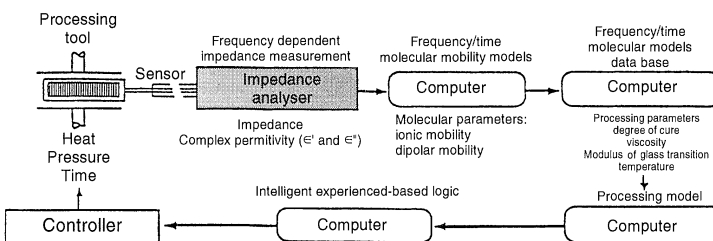


Figure 12.14 Schematic of the FDEMS sensor smart system for monitoring quality and for expert automated process control.

4. ramp to final cure temperature once reaction has advanced;
5. monitor degree of cure during final hold;
6. determine achievement of proper degree of cure, which is related to attainment of ultimate T_g and use properties;
7. turn the process cycle off.

Figure 12.15 shows the sensor output for the smart automated sensor expert system-controlled run. The resin reached the centre sensor at 37 min. The viscosity was advanced during a 121°C hold to a predetermined value of a degree of cure ($\alpha = 0.35$), based on a cure model's predictions of the extent of the exothermic effect. This value of α is clearly dependent on panel thickness. At this point (130 min) the ramp to 177°C was begun. Achievement of an acceptable complete degree of cure was determined by the sensor at 190 min. Then the cure process was shut down.

12.8 CONCLUSIONS

Data acquisition through dielectric sensing has been shown to be an important means for monitoring the position of the resin from and during both conventional RTM and RFI processing. Using the frequency dependence of ϵ' and ϵ'' the sensing technique can be used to monitor viscosity and degree of advancement *in situ* at a specific position in the mould. The sensing technique is useful for verifying RTM models.

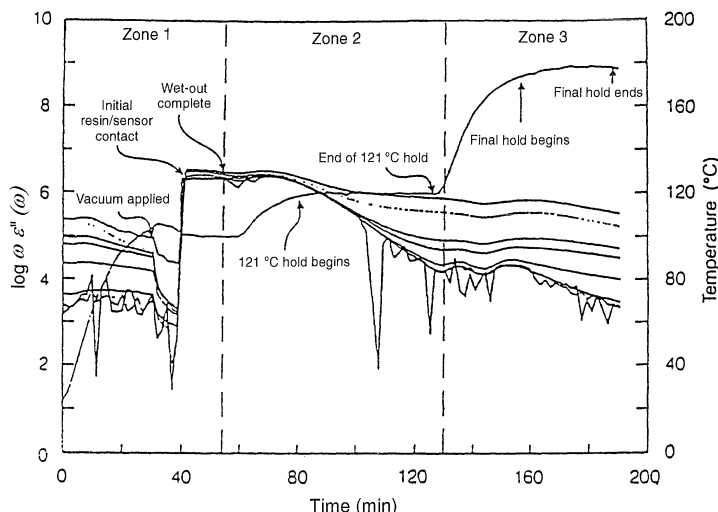


Figure 12.15 Sensor output for the smart automated sensor expert system-controlled run. $\omega = 2\pi f$; f = frequency; ϵ'' = the imaginary part of the complex permittivity.

Use of a 'smart' dielectric sensor control system for monitoring the processing properties *in situ* during the fabrication process of a composite part was demonstrated. The sensor control system can be used to monitor resin properties for quality assurance, to ensure fabric impregnation and to control intelligently and optimise through *in situ* sensor feedback and model predictions the composite fabrication process.

Acknowledgments

The authors appreciate partial support from the NSF Science and Technology Center at Virginia Polytechnic Institute and State University under Contract number DMR91-2004, a NASA Langley grant and support from the Northrup Corporation. Questions regarding the instrumentation should be directed to the author.

References

1. Hasko, G., Dexter, H., Loos, A. and Kranbuehl, D. (1994) Application of science based RTM for fabricating primary aircraft structural elements. *Journal of Advanced Materials*, **26**, 9–15.
2. Gutowski, T. G. (1986) Applications of the resin flow/fiber deformation model. *31st International SAMPE Symposium*, Society for the Advancement of Materials and Process Engineering, 1161 Parkview Drive, Covina, CA 91724-3748, April, p 245–54.
3. Milovich, D. and Nelson, R. (1990) Dielectric resin flow sensing. SME Technical paper, March 6. Society of Manufacturing Engineers, SME Drive, PO Box 930, Dearborn, MI 48121.
4. Stark, E. (1987) New non-MDA epoxy resin systems for resin transfer molding (RTM) and filament winding. *32nd International SAMPE Symposium*, Society for the Advancement of Materials and Process Engineering, 1161 Parkview Drive, Covina, CA 91724-3748, April 1987, pp. 1092–103.
5. Potter, K. (1987) Bismaleimide formulations for resin transfer moulding. *32nd International SAMPE Symposium*, Society for the Advancement of Materials and Process Engineering, 1161 Parkview Drive, Covina, CA 91724-3748, April, pp. 1–12.
6. Cirisciolo, G. Springer (1990) *Smart Autoclave Cure*, Technomic, Lancaster, PA.
7. Kranbuehl, D. (1986) *Developments in Reinforced Plastics*, Vol. 5, Elsevier Applied Science, New York, pp. 181–204.
8. Kranbuehl, D. (1989) *Encyclopedia of Composites*, ed. S. M. Lee, VCH Publishers, New York, pp. 531–43.
9. Senturia, S. and Sheppard, S. (1986) Dielectric properties of bisphenol – A epoxy resins. *Applied Polymer Science*, **80**, 1–48.
10. May, C. (1983) Chemorheology of thermosetting resins. *Polymer Materials Science and Engineering*, ACS Symposium Series 227, American Chemical Society, Washington, DC.
11. Hedvig, P. (1977) *Dielectric Spectroscopy of Polymers*, John Wiley, New York.
12. Mijovic, J., Bellucci, F. and Nicolais, L. (1995) Impedance spectroscopy of reactive polymers, correlations with chemorheology during network formation. *Electrochemical Society*, **142**(4), 1176–82.

13. Mijovic, J. and Yee, C.F.W. (1994) Use of complex impedance to monitor the progress of reactions in epoxy/amine model systems. *Macromolecules*, **27**, 7287–93.
14. Bellucci, F., Valentino, M., Monetta, T. *et al.* (1995) Impedance spectroscopy of reactive polymers, 2. Multifunctional epoxy/amine formulations. *Journal of Polymer Science Part B, Polymer Physics*, **33**, 433–43.
15. Mangion, M.B.M. and Johari, G.P. (1990) Relaxations in thermosets. 7. Dielectric effects during the curing and post curing of an epoxide by mixed amines. *Macromolecules*, **23**, 3687–95.
16. Mangion, M. and Johari, G. (1991) Relaxations in thermosets. IX ionic conductivity and gelation of DGEBA-based thermosets cured with pure and mixed amines. *Journal of Polymer Science B*, **29**, 1117–25.
17. Parthun, M.B. and Johari, G. (1992) Relaxations in thermosets: dielectric studies of curing kinetics of an epoxide with amines of varying chain lengths. *Macromolecules*, **25**, 3254–63.
18. Boiteux, G., Dublineau, P., Feve, M. *et al.* (1993) Irradiation effects of AC conductivity on organic solids. *Polymer Bulletin*, **30**, 441–7.
19. Mathieu, C., Boiteux G., Seytre, G. *et al.* (1994) Microdielectric analysis of the polymerization of an epoxy-amine system. *Journal of Non-Crystalline Solids*, **172–174**, 1012–16.
20. Xu, X. and Galiatsatas, V. (1993) Dielectric cure characterisation of model elastomers: influence of individual components. *SPE Technical Papers (ANTEC '93)*, **39**, 2875.
21. Xu, X. and Galiatsatas, V. (1993) Dielectric cure characterisation of model elastomers. *Macromolecules Symposium*, **76**, 137.
22. Deng, Y. and Martin, G. (1994) Modeling diffusion during thermoset cure: an approach based on dielectric analysis. *Macromolecules*, **27**, 5141–6.
23. Companik, J. and Bidstrup, S. (1994) The viscosity and ion conductivity of polydimethylsiloxane system. 1. Chain length and ion size effecta. *Polymer*, **35**, 4823–40.
24. Tombari, E. and Johari, G.P. (1992) Dielectric relaxation spectroscopy of reaction controlled slowing of molecular diffusion in liquids. *Journal of Chemical Physics*, **97**, 6677–86.
25. Johari, G. P. and Pascheto, W. P. (1995) Molecular kinetics during the growth of the macromolecule poly(di-hydroxy propyl ether of bisphenol-A-*n*-hexyl-amine) studied by dielectric spectroscopy. *Journal of the Chemical Society, Transactions*, **91**, 343–51.
26. MacKinnon, A., Jenkins, S., McGrail, P. and Pethrick, R. (1992) A dielectric, mechanical, rheological, and electron microscopy study of cure and properties of a thermoplastic-modified epoxy resin. *Macromolecules*, **25**, 3492–9.
27. Maistros, G., Black, H., Bucknall, C. and Partridge, I. (1992) Dielectric monitoring of phase separation during cure of blends of epoxy resin with carboxylterminated poly (butadiene-co-acrylonitrile). *Polymer*, **33**, 4470–8.
28. Kranbuehl, D., Delos, S., Hoff, M. *et al.* (1987) Monitoring processing properties of high performance thermoplastics using frequency dependent electromagnetic sensing. *Proceedings of the 32nd International SAMPE Symposium*, Society for the Advancement of Materials and Process Engineering, pp. 338–48.

29. Kranbuehl, D. (1993) In situ measurement of cure latex coalescence and end-use properties in this film coating using frequency dependent impedance sensors. *Polymer Materials Science and Engineering Preprints*, **68**, 224–5.
30. Kranbuehl, D. (1990) Dielectric cure monitoring. *Polymer Materials Science and Engineering Preprints*, **68**, 289–90.
31. Kranbuehl, D., Kim, T., Liptak, S. C. and McGrath, J. E. (1993) In situ monitoring of phase inversion in a thermoplastic toughened thermoset. *Polymer Preprints*, **34**, 488–9.
32. Maistros, G., Black, H., Bucknall, C. and Partridge, I. (1992) Dielectric monitoring of phase separation during cure of blends of epoxy resin with carboxylterminated poly(butadiene-co-acrylonitrile). *Polymer*, **33**, 4470–8.
33. MacKinnon, A., Jenkins, S., McGrail, P. and Pethrick, R. (1992) A dielectric, mechanical, rheological, and electron microscopy study of cure and properties of a thermoplastic-modified epoxy resin. *Macromolecules*, **25**, 3492–9.
34. MacRae, J. D. (1994) Development and verification of a resin film infusion/resin transfer molding simulation model for fabrication of advanced textile composites. MS thesis, Virginia Polytechnic Institute and State University, Blacksburg, VA.
35. Hammond, V. H. (1993) Verification of a two-dimensional infiltration model for the resin transfer molding process. MS thesis, Virginia Polytechnic Institute and State University, Blacksburg, VA.
36. Kranbuehl, D. E., Kingsley, P., Loos, A.C. (1994) Insitu sensor monitoring and intelligent control of the resin transfer molding process. *Polymer Composites*, **15**, 299–305.
37. Kranbuehl, D., Hood, D., Rogozinski, J., et al. (1995) In situ FDEMS sensing for intelligent automated cure in resin transfer molding of advanced architecture textile preforms. *Proceedings of the 40th International SAMPE Symposium*, Society for the Advancement of Materials and Process Engineering, 1161 Parkview Drive, Corvina, CA 91724-3748, pp. 1466–77.
38. Loos, A. C., MacRae, J., Hammond, V. et al. (1993) Analytical modeling and sensor monitoring for optimal processing of advanced textile structural composites by resin transfer molding infiltration. Society of Plastics Engineers, Technical Paper, XXXIX, pp. 3478–80.
39. Kranbuehl, D., Kingsley, P., Hart, S. et al. (1992) Sensor-model prediction, monitoring and in-situ control of liquid RTM advanced fiber architecture composite processing. *Proceedings of the 37th International SAMPE Symposium*, Society for the Advancement of Materials and Process Engineering, 1161 Parkview Drive, Corvina, CA 91724-3748, pp. 907–13.
40. Kranbuehl, D., Kingsley, P., Rhodenizer, H. et al. (1992) *Society of Plastic Engineers*, **38**(2), 2049–51.

MANUFACTURERS

DekDyne Inc., 201 Harrison Avenue, Williamsburg, VA 23185, USA.
 Hercules Corporation, Aerospace Materials, Bacchus Works, Magna, UT 84044.
 Micromet Instruments Inc., 7 Wells Avenue, New Centre, MA 02159, USA.
 Radius Engineering Inc., 3474 South 2300 East, Salt Lake City, UT 84109, USA.
 Robit AS, PO Box 100, N-1361 Billingstad, Norway.

Quality and process control

13

Bernd Räckers, Chris Howe and Teresa Kruckenberg

13.1 INTRODUCTION

A key issue in the success of a new technology such as resin transfer moulding (RTM) is quality and process control. A clear understanding of the process is essential, especially when a new process is being established. Many developments and new projects have failed because of a lack of knowledge about the process variables and limits.

The first applications of RTM occurred in the non-aerospace industry where lower structural requirements and larger processing windows are common. These applications did not require extensive process and quality control measures. Little information could be transferred to RTM for aerospace applications. Therefore, a major task in the development of RTM for aerospace applications was to learn the principles of and to understand RTM. Intensive work was done by the industry to define its characteristics, variables and limits. This work was done by many aerospace companies, research institutions and material suppliers who provided the new resins required for high-performance aerospace applications. This combined work minimised the cost and effort to introduce RTM into aerospace.

What defines a good quality composite laminate? The answer is simplified by identifying the basic characteristics that structures should meet and upon which all laminate properties are dependent [1]:

- void or porosity content – the volume of air bubbles or spaces in a laminate should be less than that allowed by the given structural design;

- level of laminate consolidation – resin content, fibre volume fraction and associated distribution gradient;
- degree of cure – formation of the polymeric resin and structure;
- fibre orientation – conforming to the design requirements;
- interfacial bonding – bonding between the resin and fibre as intended.

The quality of RTM laminates can be assessed by the level of imperfections or defects. Defects reduce the quality of polymer composites. This reduction in quality is in respect to mechanical properties, aesthetics and environmental degradation [2–5]. Defects in polymer composites are outlined in ASTM D2562-94. The most common types of defects in RTM laminates are dry spots, voids and resin-rich areas. This chapter will discuss the type of defects typical to the RTM process and methods for preventing or eliminating these defects.

The laminate consolidation, degree of cure and proper fibre orientation are optimised through process control. Process control is not only a matter of maintaining control of the process during manufacturing but of developing proper control of the key characteristics and tolerances during the development of new RTM parts. The aim is to have reliable control methods at minimum but necessary expense. Process control and quality assurance work together as having well-established control measures, and processing windows will produce RTM parts of reliable quality. This chapter will discuss the basic ideas of process and quality control with different approaches given.

13.2 DEFECTS

A dry spot is defined as a region of preform that has not been filled by resin. A void is a bubble of air or other gas(es) trapped within the laminate. Porosity is defined as a collection of voids within a region. Commonly, a network of porosity is observed at the perimeter of a dry spot, as shown in Figure 13.1. The completely dry region is located on the left-hand side, with the porosity located through the middle to the right-hand side.

This section will characterise voids specific to RTM laminates, investigate the detection techniques for voids, outline the formation of voids and dry spots and determine the effect of porosity on the mechanical properties of RTM laminates.

13.2.1 VOID CHARACTERISATION

Voids can be found in the available free space within reinforcements. Reinforcements more commonly used in RTM laminates are fabrics. A fabric is composed of fibre tows which are either interlaced or loosely

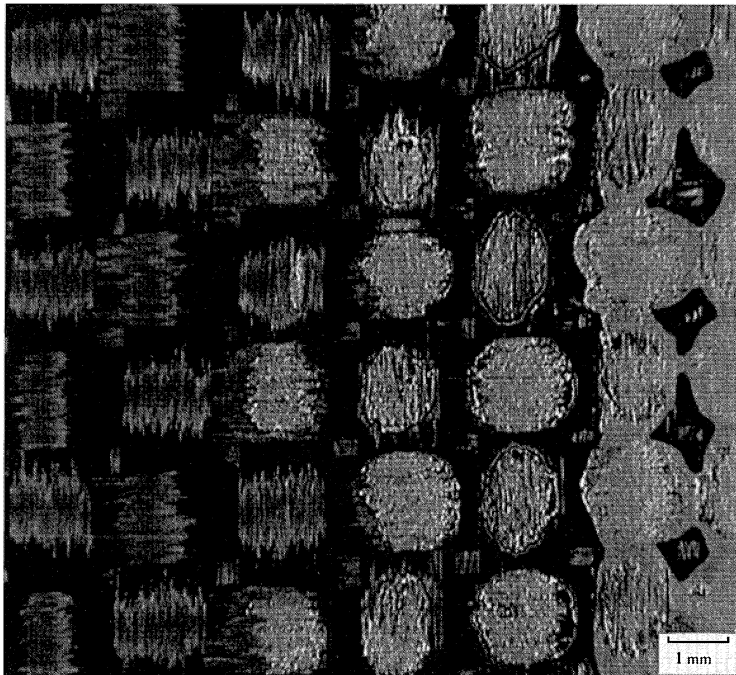


Figure 13.1 A photograph showing defective dry spot region: dry fibres are on the left and partial resin and porosity on the right. Reproduced courtesy of the Cooperative Research Centre for Advanced Composite Structures, Fishermens Bend, Vic., Australia.

held together with a yarn. A fibre tow consists of thousands of individual filaments. For a fabric, the available free space that a bubble can occupy is located either within the fibre tows or between the tows. Lundstrum *et al.* (1994) have shown that voids formed within fibre tows have the shape of cylindrical tubes, whereas voids formed between tows resemble spherical bubbles [6]. Figure 13.2 shows typical voids located within and between fibre tows in RTM laminates.

The size and geometry of the free space located between fibre tows is a function of the fabric design and level of compaction within the preform. This free space influences the morphology of bubbles, which are not always spherical in shape. Howe *et al.* (1997) have shown that in high fibre volume fraction RTM laminates the shape of large voids is confined by the pore space geometry, which is asymmetric for the 5-HS carbon fabric used [7]. Goodwin *et al.* (1997) have shown that RTM laminates manufactured from different fabrics, that is a plain weave and a 5-HS woven carbon fabric, contain different void morphologies [8]. Voids in a plain weave fabric laminate were found to contain large voids with blunt

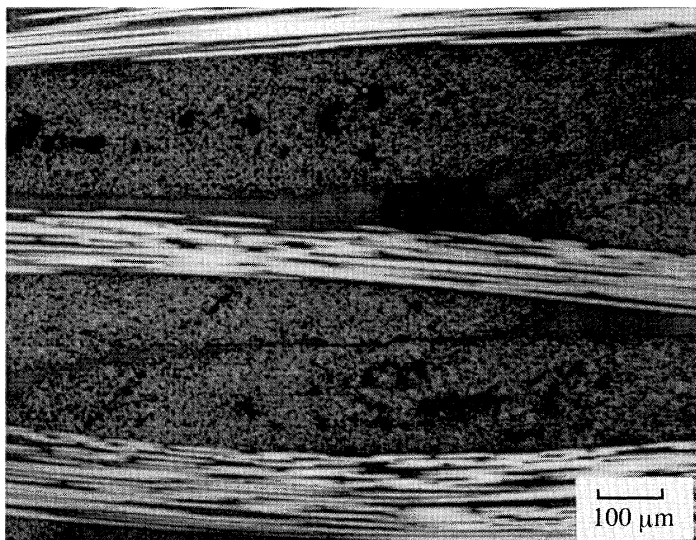


Figure 13.2 Micrograph showing voids located within and between tows. Reproduced courtesy of the Cooperative Research Centre for Advanced Composite Structures, Fishermens Bend, Vic., Australia.

edges, whereas a 5-HS laminate was found to contain a high population of small voids with sharper edges. Therefore, RTM laminates with different reinforcements will have different void shapes and sizes.

A comparison of prepreg with RTM laminates made from the same constituents has shown different void morphologies [7]. The prepreg laminate contained voids with a higher aspect ratio (width:height), and larger voids were more common at lower overall porosity contents than in the RTM laminates.

13.2.2 VOID DETECTION

Voids within polymer composites are assessed quantitatively in terms of void volume fraction and qualitatively in terms of their size, shape and location. Both types of measurement are important. The measurement of void content is required for determining the effect of voids on the mechanical properties of RTM laminates.

The techniques for the measurement of void content are generally classified into two groups: destructive and non-destructive. Destructive techniques involve segmenting a section of laminate from the component. These techniques include optical image analysis (OIA), matrix digestion, burn-off, water buoyancy and density gradient techniques.

For carbon/epoxy laminates it is impossible to see voids within the laminate. The most accurate method for determining void morphology is therefore optical image analysis of polished cross-sections, where the microscope image enables accurate assessment of void shape and size [9]. OIA involves the recording of a finely polished composite surface as a digital image that can be analysed by a computer software program. Analysis capabilities include measurement of void content and void morphology. A typical image analysis system includes an optical microscope, a camera, a frame grabber and a computer.

Matrix digestion of carbon-reinforced laminates and burn-off of fibreglass-reinforced laminates are commonly used for determination of fibre volume fraction. Matrix digestion is discussed in more detail in Chapter 14, section 2.3. Once the fibre weight is known the laminate density can be determined. The void volume fraction can be determined from the actual and theoretical laminate density values. The water buoyancy and density gradient techniques are less commonly used for determining void volume fraction as they do not also determine the fibre volume fraction.

The most common non-destructive technique is ultrasonic C-scan inspection. This technique involves transmitting ultrasonic waves from a probe through a laminate immersed in a bath (or spray) of water. Defects within the laminate cause the transmitted signal to be reflected. The receiver measures the level of signal loss (usually recorded in decibels) from scatter caused by the defects. A map of this signal loss across the entire laminate can illustrate defective regions and be correlated to a volumetric void content. This correlation requires the use of another technique (such as OIA) to calibrate the relationship between decibel loss and void content [3].

13.2.3 DEFECT FORMATION

Voids are primarily caused by the mechanical entrapment of air or volatiles [10–12]. This entrapment often arises from the combination of an irregular resin flow front and obstructions within the reinforcement, such as crimps and stitches [13]. The irregular flow front is caused by the heterogeneous nature of the preform [14]. The preform contains two avenues through which the resin can travel; these are between and within the tows. The driving force to fill each avenue is different. With the very small free space between fibres within the tows the resin fills these mainly by the action of capillary pressure. In the spaces between the tows the resin filling process is controlled by the overall hydrodynamic pressure gradient. Patel *et al.* (1995) have identified that the relative position of the flow front between and within tows is determined by the ratio of viscous and capillary forces, called the modified capillary

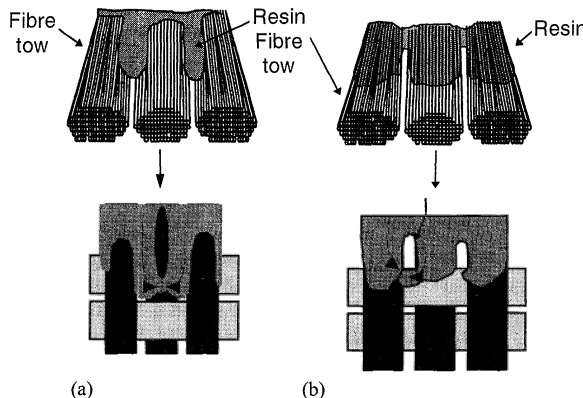


Figure 13.3 Schematic showing how the combination of an irregular flow front and fibre tow interlacing leads to void formation: (a) entrapment of air within fibre tow; (b) entrapment of air between fibre tows.

number [13]. For a high capillary number, flow leads between the tows, whereas flow leads within the tows for a low capillary number. Factors affecting the viscous forces are injection pressure and resin viscosity; for the capillary forces the factors are surface tension of the resin and the wetting contact angle. Figure 13.3 illustrates how voids between tows and within tows can form, based on the irregular flow front and fibre tow interlacing. Figure 13.3(a) shows how flow leading between fibre tows causes the formation of a trapped air pocket within a fibre tow. Conversely, Figure 13.3(b) shows how flow leading within the tows causes the formation of a void between tows. Note that the tow intersection allows for the leading resin paths to meet in both cases, which causes air entrapment. To overcome this problem, mould evacuation is commonly used in RTM. When a void is formed by entrapment, its internal pressure will be close to vacuum rather than at atmospheric pressure. As the level of hydrostatic pressure increases the void must shrink accordingly and may collapse entirely [10].

Other void formation processes include volatilisation of gases and the injection of bubbles into the preform within the resin [6]. Leaks are also a problem in vacuum-assisted RTM, allowing air to displace resin from the impregnated preform and thus creating voids.

Figure 13.4 shows a comparison between voids formed by the different causes identified above [15]. Figure 13.4(a) shows voids caused by the mechanical entrapment of air which are large and confined to the free space between fibre tows. Figure 13.4(b) shows how small bubbles introduced with the injected resin form small spherical voids between tows. Figure 13.4(c) shows similar small voids occupying space between tows. These voids were apparently caused by volatilisation of gases

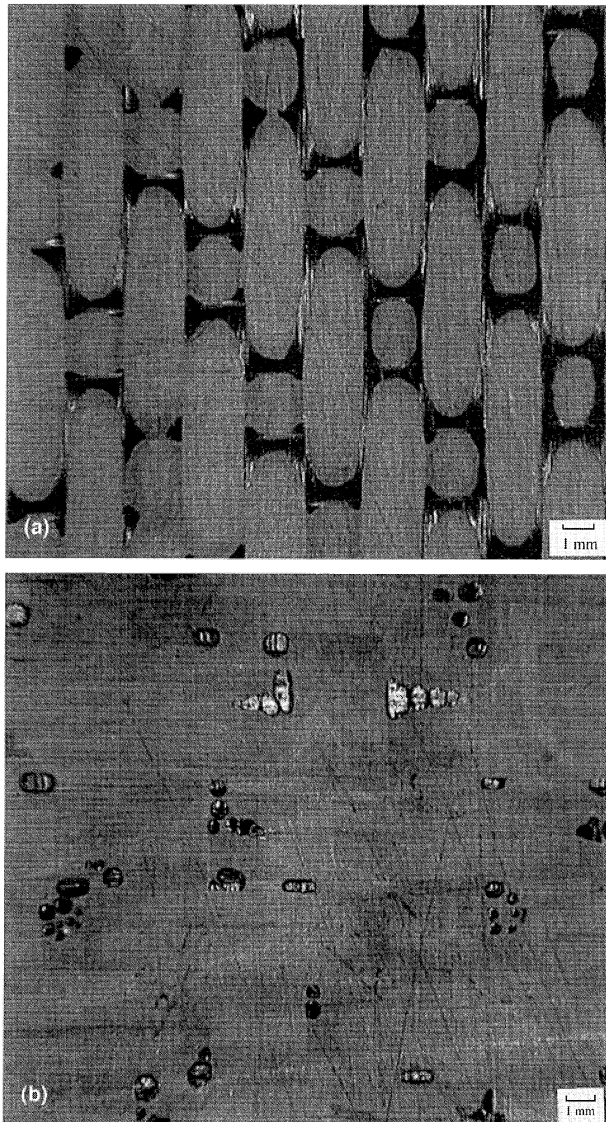


Figure 13.4 Photographs showing (a) voids located at tow intersections; (b) spherical voids caused by air injected with the resin; (c) voids apparently caused by volatilisation of gases during cure; (d) voids caused by air leak from the outlet line. Reproduced courtesy of the Cooperative Research Centre for Advanced Composite Structures, Fishermens Bend, Vic., Australia.

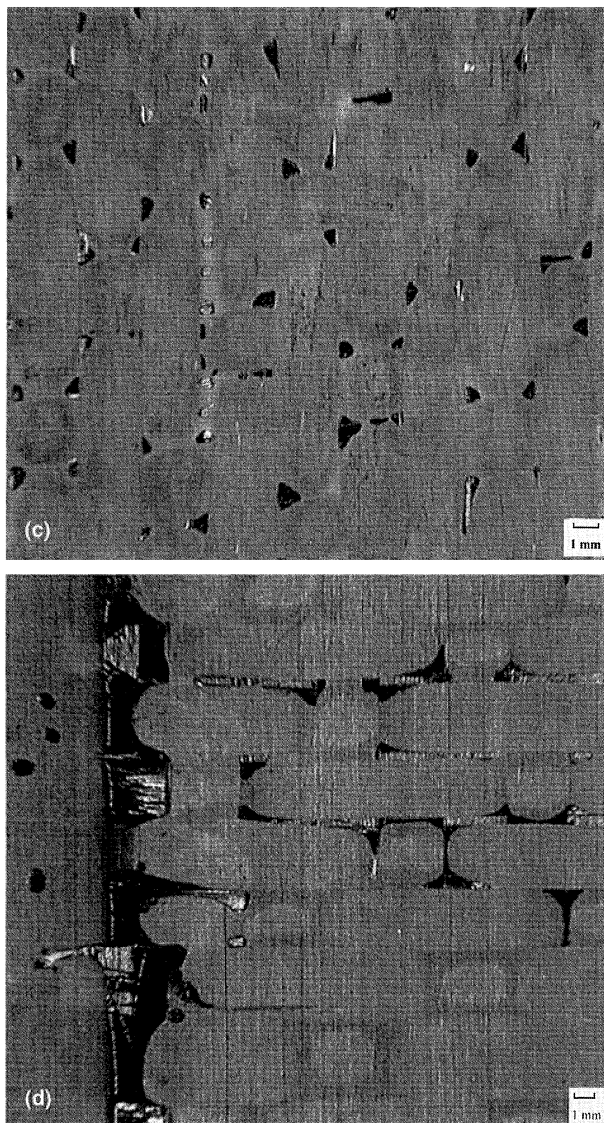


Figure 13.4 c,d

during cure. Figure 13.4(d) shows how an air leak at the outlet line causes the displacement of resin from between fibre tows.

In conjunction with the void formation process the level of bubble transport during mould filling and void stability during cure will determine the distribution and content of voids within the laminate. Patel

et al. (1994) showed that a void, once formed, has the ability to be mobilised, depending on the relative magnitude of the viscous drag forces, the steric hindrance of the preform and the capillary pressure acting on the void [13]. During cure, the concentration of volatile species and hydrostatic pressure influence the growth or shrinkage of bubbles [16, 17].

Dry spots are commonly caused by inappropriately placed inlets and outlets, racetracking, variation of permeability in the fibre preform or premature resin gelation [18]. Figure 13.5 shows schematically how a dry spot is formed by racetracking. The resin initially fills the larger free space at the perimeter of the preform and reaches the exit line before the preform is completely filled. The resin then back-fills, causing the entrapment of a large air pocket within the preform. This air pocket shrinks until its air pressure is balanced by the resin pressure in the saturated region.

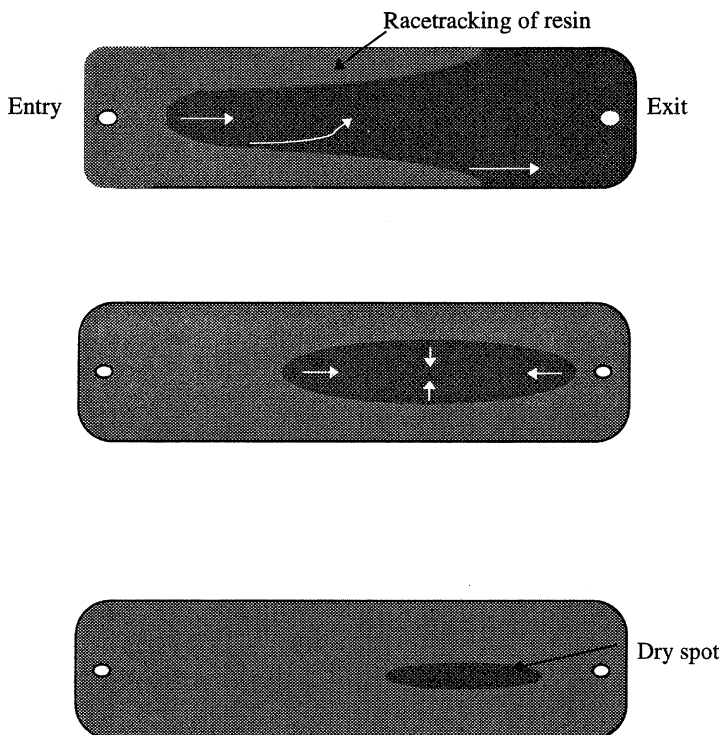


Figure 13.5 Schematic showing dry spot formation caused by racetracking: (a) initial rapid flow front path, showing racetracking of resin; (b) resin reaches the exit port before the preform is completely filled; the trapped off region continues to fill by capillary force, under a slow flow front; (c) dry spot formed.

Han and Lee have shown how dry spots form and how to eliminate dry spots through a packing and bleeding process [19]. Packing (back pressure) involves blocking the exit line while keeping the injection pressure on. The process increases the surrounding pressure acting on the dry spot. This will act to shrink the dry spot and increase the internal dry spot pressure. The bleeding (burping) step is introduced by re-opening the exit line after the packing procedure. The high transient pressure difference between the dry spot and the exit allows the trapped air to move towards the exit.

13.2.4 STRUCTURAL EFFECTS

Voids are particularly detrimental to the compressive strength of composites [4] and to the matrix-dominated properties, such as interlaminar shear strength [2, 4, 5, 20–22]. For a composite to be used in demanding applications the effect of voids on the mechanical properties should be determined. Many researchers use the interlaminar shear strength test (ILSS) to investigate the effect of voids on the strength of a laminate. A comparison of published results shows a significant variation in the apparent decrease in strength caused by void content. Various researchers have shown that void locations, shapes and sizes may influence the values of measured strengths [2, 20–22].

As previously discussed for RTM laminates (section 13.2.1), void morphology is dependent on the fabric and level of compaction, and this difference in void morphology affects the amount of strength reduction [8]. For a five-harness fabric RTM laminate a 7% reduction in ILSS per 1% porosity has been observed, whilst a plain weave fabric laminate has shown a 4% reduction in ILSS per 1% porosity. The difference in the effect of porosity is attributed to the void morphology and distribution. The five-harness fabric contained a higher level of asymmetric voids with corners of lower radii compared with the more symmetrically shaped elliptical voids within the plain weave composite. Voids of lower radii of curvature lead to higher stress concentrations [23].

It is considered important to combine property data on void effects with detailed investigations into the void location, shape and size for specific laminate systems to help determine the mechanism by which voids reduce the ILSS. Post-test optical image analysis studies of defective and non-defective RTM laminate coupons show the types of failure cracks common to the ILSS test and how such cracks interact with voids, as shown in Figure 13.6.

The types of voids observed in RTM laminates are somewhat different from those seen in prepreg laminates, as shown by Howe *et al.* [7]. The prepreg results showed a greater drop in ILSS. The voids in the prepreg

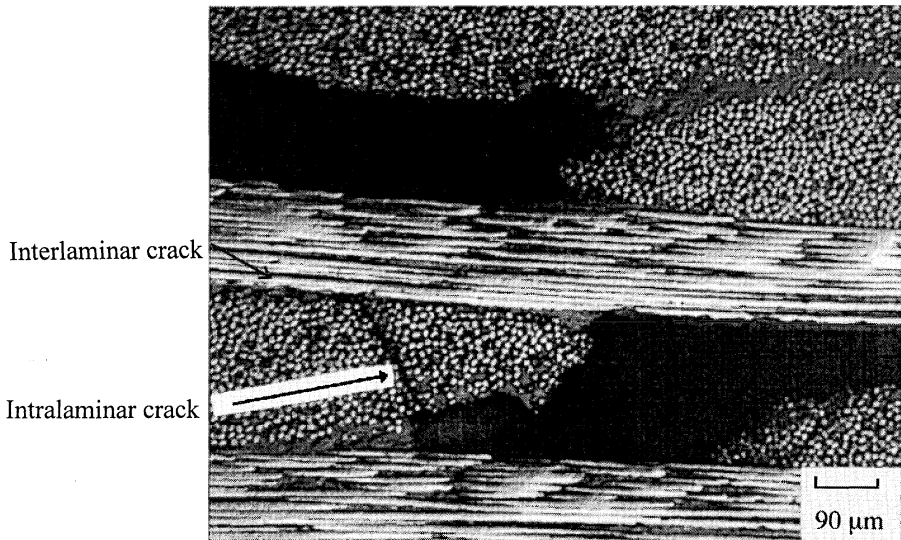


Figure 13.6 Micrograph showing crack propagation with initiation of an intralaminar crack at the void tip and the transformation to an interlaminar crack. Reproduced courtesy of the Cooperative Research Centre for Advanced Composite Structures, Fishermens Bend, Vic., Australia.

laminate coupons have a higher aspect ratio, which explains the greater strength reduction.

13.2.5 DEFECT PREVENTION

Dry spots can be prevented or eliminated by proper gating location and by optimised resin and mould temperatures. If racetracking is causing the dry spot then the application of vacuum during injection, back pressure and subsequent burping may fill the dry spot and drive the entrapped air towards the exit line.

Porosity can be prevented or eliminated by:

- checking the mould for air leaks;
- using a strong vacuum during injection to prevent air entrapment;
- increasing the injection pressure to reduce bubble size;
- degassing the resin to remove air and volatiles from the resin;
- reducing the vacuum if volatiles are given off;
- removing moisture from the reinforcement by application of vacuum.

A surface imperfection which may appear to look like porosity can also be caused by excessive build-up of mould release on the mould surface.

Examination of the mould surface will reveal if this is a problem as the fabric weave will be imprinted on the release build-up.

13.3 PROCESS CONTROL

13.3.1 A COMPARISON BETWEEN THE AUTOCLAVE-CURED PREPREG PROCESS AND RESIN TRANSFER MOULDING

To introduce a new process into aerospace requires knowledge of how it is different from well-known and established processes. In this case, the commonly-used process is autoclave-cured prepreg technology. Many of the relevant subjects on certification of new prepreg parts can be used for RTM parts. Therefore, knowledge of the differences between the two processes may minimise effort and mistakes.

The two processes have much in common, but some things are quite different. The biggest difference concerns the impregnation of the fibre reinforcement with the matrix. Whereas prepreg is made in a continuous process by adding fibre and matrix in an industrial, highly automated process, during RTM the fibres are dry until the mould is closed and the resin is injected. RTM can be divided into two steps: first, the arrangement of the fibres according to the requirements and, second, the injection of the resin into the mould and subsequent cure. However, the resin stage advances upon preheat or mixing of the resin for injection and hence there is a pot-life for injection.

For the first part, the arrangement of fibres for RTM is similar to lay-up of prepreg. In both cases the fibre reinforcement has to be stacked to the required geometry and thickness. Prepreg normally provides sufficient tackiness for keeping the stacked plies together because the resin is already on the fibres. RTM reinforcements are dry and do not stick together. Additional measures such as the application of tackifiers or stitching may have to be taken to bind the plies together. On the other hand, RTM allows the use of various types of advanced fibre reinforcements such as braids, multiaxial fabrics and three-dimensional fabrics that can be impregnated during the RTM injection but not prepregged because of their thickness or shape. The final shape of the part having the actual or near part thickness and geometry is built up with the fibres and is called the preform.

Prepregging is done in a continuous process on high-capacity machines. The resin is already mixed in a separate operation. The fibre-resin ratio is controlled during impregnation. Most of the recent prepreg systems are 'zero-bleed systems', having no (or a very small amount of) excess resin. Owing to the low processing speed and the method of impregnation, that is hot-melt impregnation, costs are high. After manual lay-up, curing takes place in the autoclave, providing temperature for

curing and pressure for consolidation. Apart from consolidation, which actually means thickness adjustment by bleeding voids and excess resin, no resin flow happens.

There are several differences in the RTM process; the resin flows through the preform under a pressure gradient to eliminate voids. The resin can be mixed while being pumped or sucked into the mould, but most aerospace companies use one-component resins that are already premixed by the resin manufacturer. Generally, thickness is controlled by the closed mould. The resin is usually preheated to lower its viscosity for injection. However, a maximum preheat temperature is imposed because the higher the temperature, the shorter the processing time as the resin viscosity increases during resin stage advancement. This will limit the maximum injection length. Large parts are not possible without multiple injection points. The cure is usually accelerated after injection by increasing the mould temperature.

Comparing the standard prepreg with RTM parts after successful manufacture, the performance of both are nearly equivalent if the same fibre reinforcements are used. If a part has been manufactured to a well-defined quality level (negligible porosity) it usually does not matter which process has been used. Different resins may provide slightly different properties such as different glass transition temperatures T_g , or damage tolerance levels, but these are not a result of the selection of the process.

Detailed knowledge of these key issues for the RTM process will help to educate the manufacturing, design and stress authorities who will ultimately approve the RTM process.

13.3.2 RESIN TRANSFER MOULDING PROCESS CONTROL REQUIREMENTS

RTM requires more process control measures than the standard autoclave-cured prepreg process as impregnation as well as the subsequent cure must be controlled. Adequate process control guarantees reliable part quality and lowers reject rates. Therefore, efficient process control is an important means of manufacturing commercially competitive parts.

Process control is not only a function of controlling an established process; the first task is to develop a robust process. For example, a matched mould will provide excellent thickness control without any additional effort.

13.3.3 INFLUENCE OF MATERIALS

Process control may influence the performance of the materials, but normally the aim is to fulfil the requirements for a wide processing

window. Therefore, a very important task for material evaluation and screening is to assess the processability of the material as well as the structural performance.

Key processing characteristics for selection of RTM resin systems are:

- injection temperature;
- cure temperature and time;
- injection temperature in relation to the cure temperature;
- apparent resin minimum viscosity during dynamic test;
- isothermal viscosity profiles;
- shelf-life at storage and shop floor temperatures.

The most important aspect for fibre reinforcements is their permeability. The main influence on permeability is the fibre volume fraction of the component. Although structurally a 60% fibre volume fraction is an optimal compromise between weight gain and shear transfer, a lower fibre volume fraction may have some processing advantages. The permeability will increase and faster injection times or longer flow paths will become possible. The textile industry has developed some other solutions for increasing permeability by weaving fabrics with round-shaped warp yarns. The fabric is woven with every fifth to tenth yarn shaped round to create a flow channel inbetween the yarns.

Apart from conventional fabric, all the other available reinforcements must be checked carefully for permeability. The more complex the shape and the arrangement of the fibres the more difficult the impregnation.

13.3.4 EFFECT OF EQUIPMENT

Equipment for RTM is made up of three types:

- mould;
- injection pump;
- curing device.

All of these may influence the process and must be controlled, if possible by clear specifications during development, to prevent too many and expensive control methods.

Mould design is a primary matter of development. When the design is frozen and the process provides consistent results there is no need for further measures in production. Of course, the mould must be checked regularly for defects and, most importantly in RTM, for leakage.

The injection pumps or pressure-pots are of more concern for the process. Two different resin systems are generally used: one-component or two-component resins. Both types need similar pressure and temperature control measures. Established limits are required to enable

production to control the impregnation. The devices must be equipped with pressure, vacuum, resin-weight (or volume injected) and temperature measurement features. For example, thermocouples should be placed at various points in the resin pot or cylinder, in the injection hose and in the mould. One-component resins need not be checked for the correct mixing ratio, but for two-component resins this is essential. Quality control of the mix ratio is critical, as incorrect ratios will cause a part to be rejected.

The cure may take place at a different facility than the injection process. Conventional ovens, presses, autoclaves or integrally heated moulds may be used. Heat-up rates will vary depending on the thermal capacity of the heating media. Ovens provide the slowest heat-up rate, whereas autoclaves under pressure will provide faster heat-up. A device using direct contact such as a press or an integrally heated mould may allow fast heating, but the higher mass also makes control more difficult.

13.3.5 PROCESS LIMITS AND CONTROLS

Process limits must be established during qualification. This applies to all process-relevant items such as the materials, but also to tooling, equipment and auxiliary materials. All the parameters of the process that influence the performance of the materials and the parts must be controlled during processing.

The most important factor is the knowledge of processability of the materials. As previously mentioned, this is a major task during screening of suitable materials. When a material has been selected the process window must be qualified. Variations in resin mix ratio must be checked, as well as tolerance to processing variations such as resin injection temperature, mould temperature, heat-up rates, injection pressure and so forth.

RTM requires control of some specific features. The first concerns the quality control of neat resin. Regardless of whether a one-component or two-component resin is used, control of the mix ratio and resin chemistry variation is essential. A one-component resin is mixed by the manufacturer on a large scale and with lower variation than is a two-component resin, where the resin mixing is usually done manually in small quantities or during injection by a meter-mix injection system. Therefore, larger variations must be allowed for two-component resins. There are two ways to overcome this: to require a wide process window at a given performance level; to lower the performance requirements to increase the width of the window. A one-component resin can be checked at incoming inspection, whereas two-component resins must be checked before, during and/or after injection. The handling of resins until injection is also subject to control measures. Temperature and time variations may influence both the processing and the part performance. The process

window has to be established relative to the specific equipment used for manufacture. For example, heat may be applied to the resin in various steps. The resin is often preheated to become fluid for injection where it is then pumped through a heated hose and mould. All of these temperatures may be different, with a certain range for each. All the possible combinations of cases must be checked.

Also, storage and shop floor conditions may influence the resin performance and must be checked and qualified as well. Some resins show a 'tolerant' behaviour. However, if allowable storage time is exceeded, processing may not be possible as the resin viscosity increases to a point where it cannot infiltrate the preform.

The second feature concerns the processing of the fibre reinforcements or preforms. Some reinforcements contain tackifier, binder or sizing which may have a limited shelf-life. The subsequent preforming conditions may vary and affect the binder. The fibre orientation position and number of plies during the assembly or manufacture of the preform must be controlled. If mistakes happen here then the mould may not close because there are too many plies or the permeability will be different because there are missing plies.

Mould filling and part performance are influenced by the vacuum applied during injection. As mentioned in sections 12.2.3 and 12.2.5, vacuum is necessary to remove trapped gas during moulding to help prevent the formation of voids. Pressurisation of the mould after injection will also help shrink any voids formed in the part during injection.

All the other aspects of process variations are quite similar to the standard autoclave-cured prepreg process. The cure process can be monitored using dielectric sensing, as discussed in Chapter 12. This system can also be used for monitoring the resin flow front position.

All of the points described earlier in this section must be controlled, in an active way when necessary, for example by temperature control devices. Or, better still, control can be created automatically by the process. For example, thickness control is provided by means of a closed mould. Of course, the equipment for controlling must be able to fulfil the required accuracy.

The key characteristics for controlling the process may be summarised as follows:

- resin mix ratio;
- resin shelf-life;
- tackifier shelf-life;
- preform and tackifier shelf-life;
- fibre orientation, drop-off positions and number of plies;
- preform loading methods;

- resin preheat temperature;
- resin degassing;
- vacuum leak check on mould;
- mould gap check;
- moisture removal from preform;
- injection hose temperature;
- mould temperature during injection;
- injected resin volume or weight
- injection pressure and/or flow rate;
- injection vacuum;
- resin pot-life at temperature;
- mould temperature at cure;
- heat-up rate;
- cure time;
- disassembly methods;
- finishing.

13.3.6 PROCESS CONTROL COUPONS

For a new process it is sometimes necessary to include a test specimen to be manufactured with the part. These specimens are usually manufactured from the trim area of the RTM part. Usually short-beam-shear testing or some other matrix-dominated test method is used. This test may be used at the start of a programme to characterise the process and may be discontinued after a short time.

Process control coupons should be avoided if possible as they incur significant costs to the programme. It is better to perform destructive testing at the start of the programme to verify that the processing window is optimised. This eliminates excess material waste, the labour involved with trimming the part and coupons, and testing.

13.4 QUALITY CONTROL

13.4.1 MATERIAL SPECIFICATIONS

Prepreg material specifications cannot be easily modified for use with the RTM process. Separate materials specifications for the resin and fibre reinforcement are usually required. The neat resin specification will have different resins specified as types. The resin used for tackifying a preform will also be added as a type if it is different from the RTM resin. The resin specification is used for qualification testing and acceptance testing of the neat resin. Qualification testing is used to add a supplier to the material specification qualified supplier list (QPL). Acceptance testing is used to control the quality of the material as received from the supplier

throughout the life of the programme. Qualification testing usually requires three to five batches of material to be tested with the same or more coupon testing than that used in acceptance testing. The following are some common test values required for the resin acceptance: glass transition temperature, maximum DSC (differential scanning calorimeter) exotherm temperature, minimum viscosity and gel point. High-performance liquid chromatography (HPLC) and infra-red spectroscopy are also used.

Several fibre specifications already exist for dry tows or woven reinforcements (such as the Military Specifications). Common tests for acceptance of fibres determine tensile strength, tensile modulus, failure strain, density, sizing content and degree of twist. It may be possible to use one of these existing specifications; however, once the reinforcement is tackified with resin, other control measures are necessary. Thus, a separate specification for tackified reinforcement may be required to control the amount of tackifier applied, the temperature exposure, resulting resin shelf-life and preform storage conditions.

If the part is not structural it may be possible to specify the key requirements on the part drawing. This will eliminate the need for material specifications.

13.4.2 MANUFACTURING SPECIFICATION

The manufacturing specification or process specification will describe the key characteristics of the process. The process window should be left as wide as possible to allow flexibility to the manufacturer. Most likely the manufacturer will have tighter process controls than those specified in the manufacturing specification. The key characteristics mentioned earlier in section 13.3.5 will be given with a tolerance in the manufacturing specification. Besides designation of the key characteristics and their tolerances, the specification will also include process control testing, inspection and safety issues.

To add a supplier to the QPL requires an audit of their facility to ensure conformance to the manufacturing specification. In addition, the supplier is required to have internal process control documentation. Once a supplier is qualified to a specification, any changes to the facility or process will require another qualification effort.

13.4.3 PROCESS QUALITY CONTROL

In-process inspection and quality control during manufacture of RTM parts is critical to meet the structural and dimensional performance reliably. The inspection techniques are usually based on military or federal standards, processing specifications and quality assurance requirements.

The materials used must be identified, and traceability remains with the part. The resin and fabric are usually identified by material type, vendor, lot or batch, and date of manufacture. The fabric may be cut on an automated Gerber or similar machine. With prepreg material it is common to designate the orientation on the backing material. Since dry fabrics do not have backing material, a label with the orientation must be applied before removal from the cutting table. The fibre reinforcement lay-up orientation must be checked with templates or protractors. Usually a reference orientation is scribed in the preform tool to help with the lay-up. The number of plies must be counted or checked during lay-up.

The fibre reinforcement position on the preform tool must be checked before preforming. The preform should be checked for any fibre bridging, wrinkling or slippage of plies outside of requirements. At the beginning of a programme the ply drop-off accuracy can be checked by taking the preform apart one ply at a time. KevlarTM tracers woven into the reinforcement and X-ray inspection can be used to map the fibre deformation during preforming and to detect fibre wash after resin injection. Fibre wash is usually not a problem for high fibre volume fraction (>45%) preforms, and low resin injection pressures (<700 kPa).

Each inspection point must be permanently recorded on a buy-off record. It is common practice to assign some of the responsibility for verifying the inspection to the shop floor supervisor or quality inspector. The determination of this responsibility is usually made in a formal quality system specific to the supplier.

The preforming, cure and post-cure process controls must remain within specified limits; any excursions from specified limits are documented for subsequent disposition and corrective action. Statistical process control charting can be used to ensure the process is within limits and to indicate when something in the process has changed before it exceeds the specified limits.

Equipment must be within specified calibration requirements. In-process test coupons must be fabricated, traced and tested in accordance with specification requirements.

13.4.4 TOOLING

Quality control of the tooling is similar for autoclave-cured prepreg tooling and RTM tooling. Quality control documentation of the tool fabrication process is mostly confined to the tool planning sheet or tool work order [24]. With large or complex moulds a tooling logbook is used in conjunction with the tool planning sheet or work order. The logbook contains the complete history of the tool, including changes that were made after the tool was fabricated.

To qualify a tool, a thorough inspection using either templates, hand-held precision instruments or a coordinate measuring machine is required to show conformance to the tool drawing. When using a coordinate-measuring machine it is important that the tool be validated against the engineering master data (design model or tool model) rather than the cutter path data generated from that master. Once a tool has been qualified to make a given part no significant changes can be made to the tool without requalification.

The RTM mould quality is critical because the parts are well-defined and repeatable using a closed mould. The surface quality seen on the mould will replicate in the part, as well as any mismatches with inserts.

If a pattern is used to fabricate the mould it must be inspected using either templates, hand-held precision instruments or a coordinate-measuring machine. The surface of the pattern should be free of cracks, chips or other surface blemishes. The pattern must contain the latest engineering changes.

13.4.5 NON-DESTRUCTIVE TESTING

A number of non-destructive testing techniques which are used for autoclave-cured prepreg laminates are applicable to RTM laminates. Ultrasonic, radiography, shearography, X-ray, acoustic emission and thermography methods will yield similar results. The reader is referred elsewhere [25] for a review of the various inspection techniques.

Close visual inspection will reveal the majority of the defects common in RTM laminates. Resin richness, resin cracking, preform movement, dry spot formation, porosity and surface blemishes can be found using visual inspection. If there is internal porosity there is usually external porosity visible for thin parts.

13.5 CONCLUSIONS

The intent of this chapter was to give an overview of the types of defects common with the RTM process and methods to prevent or eliminate these defects. Also, a basic understanding of the differences between quality and process control for the RTM process and to the standard autoclave-cured process was given.

The next chapter gives an overview of the certification and qualification process used for the F-22 programme. This will help present a clearer picture of how the quality and process control methods discussed in this chapter are used in actual practice.

References

1. Hinrichs, R. (1987) Quality control, in *Volume 1: Engineered Materials Handbook, Composites*, ASM International, Metals Park, OH, p. 730.
2. Ghiorse, S.R. (1993) Effect of void content on the mechanical properties of carbon/epoxy laminates. *SAMPE Quarterly* (January), 54–9.
3. de Almeida, S.F.M. and Neto, Z.S.N. (1994) Effect of void content on the strength of composite laminates. *Composite Structures*, **28**, 139–48.
4. Suarez, J.C., Molleda, F. and Guemes, A. (1993) Void content in carbon fibre/epoxy resin composites and its effects on compressive properties. *ICCM 9 Composite Properties and Applications*, **6**, 589–96.
5. Bowles, K.J. and Frimpong, S. (1992) Void effects on the interlaminar shear strength of unidirectional graphite-fiber-reinforced composites. *Journal of Composite Materials*, **26**(10), 1487–509.
6. Lundstrom, T.S., Gebart, B.R. and Lundemo, C.Y. (1994) Influence from process parameters on the void formation in resin transfer molding. *Polymer Composites*, **15**(1), 25–33.
7. Howe, C.A., Paton, R.J. and Goodwin, A.A. (1997) A comparison between voids in RTM and prepreg carbon/epoxy laminates. *Eleventh International Conference on Composite Materials (ICCM-II)* 14–18 July, vol IV, 46–57.
8. Goodwin, A.A., Howe, C.A. and Paton, R.J. (1997) The role of voids in reducing the interlaminar shear strength of RTM laminates. *Eleventh International Conference on Composite Materials (ICCM-II)* 14th–18th July, vol. IV, 1–19.
9. Ghiorse, S.R. (1991) A comparison of void measurement methods for carbon/epoxy composites. MTL TR 91-13, US Army Materials Technology Laboratory, Watertown, MA, April.
10. Hayward, J. S. and Harris, B. (1990) Effect of process variables on the quality of RTM mouldings. *SAMPE Journal*, **26**(3), 39–46.
11. Rohatgi, V., Patel, N. and Lee, J.L. (1996) Experimental investigation of flow-induced microvoids during impregnation of unidirectional stitched fiberglass mat. *Polymer Composites*, **17**(2), 161–70.
12. Patel, N., Rohatgi, V. and Lee, J.L. (1995) Micro scale flow behaviour and void formation mechanism during impregnation through a unidirectional stitched fiberglass mat. *Polymer Engineering and Science*, **35**(10), 837–51.

13. Patel, N., Rohatgi, V. and Lee, L. (1994) Void formation and removal in liquid composite molding. *49th Annual Conference, Composite Institute, The Society of the Plastics Industry, Inc.* February 7–9, 1994, Session 10-D.
14. Parnas, R.S. and Phelan, F.R. (1991) The effect of heterogeneous porous media on mold filling in resin transfer molding. *SAMPE Quarterly* (January), 53–60.
15. Howe, C.A. (1996) Defects in RTM laminates. Unpublished report, Department of Materials Engineering, Monash University, Clayton, Vic.
16. Kardos, J.L., Dudukovic, M.P. and Dave, R. (1980) Void growth and resin transport during processing of thermosetting – matrix composites, in *Advances in Polymer Science*, ed. Dušek, K., Springer-Verlag, Berlin Heidelberg, pp. 102–23.
17. Lundstrum, T.S. (1997) Measurement of void collapse during resin transfer moulding. *Composites, Part A*, **28**, 201–14.
18. Wang, T.J., Wu, C.H. and Lee, L.J. (1994) In-plane permeability measurement and analysis in liquid composite moulding. *Composites*, **15**(4), 278–98.
19. Han, K. and Lee, L.J. (1996) Dry spot formation and changes in liquid composite molding: I – experimental. *Journal of Composite Materials*, **30**(13), 1458–74.
20. Oliver, P., Cottu, J.P. and Ferret, B. (1995) Effects of cure cycle pressure and voids on some mechanical properties of carbon/epoxy laminates. *Composites*, **26**(7), 509–15.
21. Wisnom, M.R., Reynolds, T. and Gwilliam, N. (1996) Reduction in interlaminar shear strength by discrete and distributed voids. *Composites Science and Technology*, **56**, 93–101.
22. Hancox, N. L. (1977) The effects of flaws and voids on the shear properties of CFRP. *Journal of Material Science*, **12**, 884–92.
23. Hull, D. (1981) *An Introduction to Composite Materials*, Cambridge University Press, Cambridge.
24. Hanson, S. (1987) Tooling quality control, in *Volume 1: Engineered Materials Handbook, Composites*, ASM International, Metals Park, OH, pp. 738–9.
25. Henneke, E. (1987) Destructive and nondestructive tests, in *Volume 1: Engineered Materials Handbook, Composites*, ASM International, Metals Park, OH, pp. 774–7.

Qualification of resin transfer moulding for aerospace applications

14

Robert William Stratton

14.1 INTRODUCTION

This chapter describes the qualification process of resin transfer moulding (RTM) for military applications. More specifically, the qualification process described is geared for high-performance military aircraft where integrity and minimised weight are a concern. The process described is applicable for composite laminate parts.

The process of qualification of RTM on the F-22 Raptor, Air Dominance Fighter, built by Lockheed Martin and Boeing, will be the model for this chapter and is outlined in Figure 14.1. This chapter will describe a generic qualification plan using some of the techniques developed by the F-22 to qualify several suppliers building over 400 distinct part numbers for engineering, manufacturing and development (EMD) aircraft. Applications and designs must be examined to determine if this type and level of qualification is appropriate. When selecting RTM for manufacture of parts, trade studies should be conducted that take into account the application, mechanical property allowables and any scaling factors that may be required for applications with complex geometries. Many of the same structural and design challenges that face hand laid-up prepreg composite parts are still present with RTM. Final qualification of F-22 RTM components follows a 'building block' approach through full-scale environmentally controlled tests and culminates in the static and fatigue vehicle tests. Qualification for less critical military, or commercial applications may not be as extensive, but the thought process and

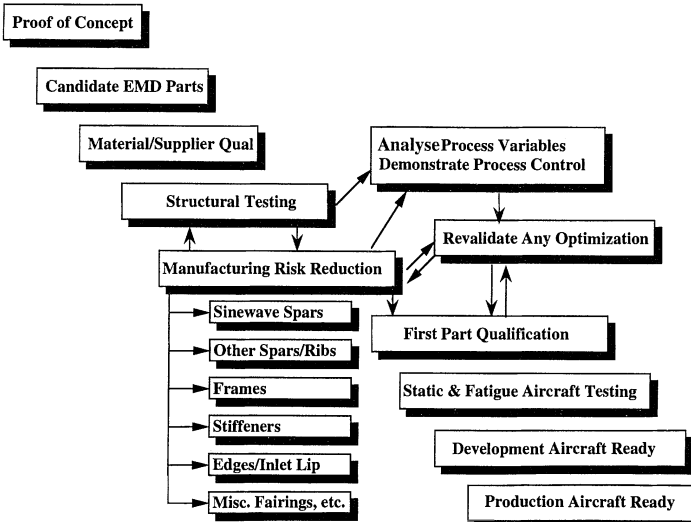


Figure 14.1 F-22 (Lockheed Martin and Boeing) resin transfer moulding qualification plan. EMD = engineering, manufacturing and development; Misc. = miscellaneous.

challenges are the same. RTM designs using advanced textile technology such as braids or stitching are not directly addressed here, but many of the qualification issues are similar.

As the RTM process becomes qualified on more programmes and is more widely accepted throughout the aerospace industry, the qualification process may become less cumbersome. However, for the foreseeable future the burden shall be on the RTM process to prove its structural worthiness, process repeatability and cost advantages compared with other manufacturing methods.

14.2 WHAT IS THE QUALIFICATION PROCESS?

On United States military aircraft programmes materials must be qualified to detailed specifications along with the processes that use the materials. Materials used for primary structure are qualified by controlling the manufacturing method, raw materials and by generating a data base sufficient for statistically derived mechanical allowables. Suppliers must conform to all the specification requirements to be placed on the qualified supplier lists (QPLs).

14.2.1 VARIABLES FOR QUALIFICATION

There are several significant variables that require qualification during one or more of the steps outlined in Figure 14.1: mechanical properties,

fibre volume fraction, fibre orientation (fibre wash), structural details, mechanical property translation from flat panel coupons to complex parts and final part performance. Several of these variables are interconnected, therefore one test element can provide data on several variables. There are many other minor variables, such as processing parameters within the RTM process, but the variables mentioned above are the major issues that structural engineers are concerned with and which will be addressed in this chapter.

14.2.2 ALLOWABLES

Completely characterised mechanical property allowables are required by stress and design engineers in order to design a given RTM structure accurately. It is important to establish not only high mechanical property allowables to minimise the weight of a given part but also to establish low part-to-part variability. Minimal part variability requires resin and fibre constructions that are of consistent quality and made within tight specification requirements. Mechanical tests must be conducted on multiple batches of material to ensure raw material variations and process variations are accounted for in the allowable data base. The details of a mechanical properties test programme will be discussed later, in section 14.3.

14.2.3 FIBRE VOLUME FRACTION

The fibre volume fraction of a given structure is critical in determining the strength. Nominal fibre volume fraction for an aircraft graphite fabric structure should be between 54% and 58%. If the nominal fibre volume fraction is designed to be above 58%, local fibre bunching may occur around a female corner of a complex shape, resulting in local fibre volume fractions above 65%. Data indicate that for fibre volume fractions above 65% mechanical properties begin to decrease from a lack of resin to stabilise the fibres. Also, above 65%, dry areas may become a problem when injecting at lower pressure. Increasing the pressure may eliminate the dry areas but may not produce a structurally sound part. In addition to fibre bunching the fibre areal weight of fabric will vary by several per cent both within a given roll of material and from roll to roll. Variations in fibre areal weight are due to variations in fibre densities, tow anomalies and weaving variables, resulting in higher or lower fibre volume fractions in a controlled cavity. For the above reasons, an ideal fibre volume for aircraft structures designed for minimum weight has been found to be 56% for fabric and 62% for unidirectional architectures. The nominal fibre volume fraction may also be selected to match that of a prepreg system with which the RTM process is being compared and where allowables have already been established.

Fibre volume fractions can be determined in several ways; acid digestion and resin burn-off are considered to be industry standards.

To determine the resin content by acid digestion method the following equation may be used:

$$C^{\text{res}\%} = \frac{W_1 - (W_3 - W_2) \times 100}{W_1} \quad (14.1)$$

where $C^{\text{res}\%}$ is the percentage resin content by weight, W_1 is the specimen weight, W_2 is the weight of the crucible and W_3 is the weight after acid digestion.

To determine the fibre volume fraction the following equation should be used:

$$V_f = \frac{1 - C^{\text{res}}}{\rho_f} \left(\frac{1 - C^{\text{res}}}{\rho_f} + \frac{C^{\text{res}}}{\rho_a} \right)^{-1} \quad (14.2)$$

where V_f is the fibre volume fraction, ρ_f is the fibre density, ρ_a is the resin density and C^{res} is the resin content by weight.

Acid digestion and burn-off have several drawbacks, one of which is that nominal densities are used in the calculation, and typical manufacturing variation in fibre and resin densities (3%–5%) can cause test result variability. These tests also require a piece of the moulded structure to be destroyed; this classifies them as destructive tests and makes them unviable for net moulded parts. In moulded parts to be trimmed, a tag end section can be cut off and tested for fibre volume fraction, glass transition temperature (T_g), and even tension and compression values. These types of tests are very useful for building confidence in the process early on in a programme but are expensive. After confidence has been built up on five parts or so these tests may be eliminated.

Fibre volume fraction can also be calculated non-destructively by measuring the thickness of a part in a given area and applying the following formula:

$$V_f = \frac{nA_w}{t\rho_f} \quad (14.3)$$

where

n is the number of plies;

A_w is the fibre areal weight;

t is the part thickness.

For this calculation to be accurate no fibre bunching must be present, and the fibre areal weight and fibre density are assumed to be nominal. This calculation is most useful for measuring a flat section where ply bunching or thinning is not occurring. This is a simple calculation, but the data are very important to the qualification process. Once the relationship between thickness and fibre volume fraction has been

established, the tracking of thickness with statistical process control (SPC) charts will show when the process is in control and will confirm that the fibre volume fraction, once accurately calculated through the use of destructive tests early in a part run, can then be monitored by simply measuring the part thickness. Although matched metal tooling is being used, thickness in a given area can vary as a result of mandrel and mould assembly. When many mandrels are being assembled to fabricate one part small variations in its assembly can cause significant end part variations. Gaps can be caused by stray fibres trapped between two metal surfaces, misplaced or damaged O-rings or improper pin and bolt assembly. These variables can be controlled by inspecting and recording mandrel gaps by using feeler gauges. Typically, gaps that exceed 0.003" (77 µm) from nominal must be eliminated by reassembling the mandrels. Nominal gaps can be determined by assembling all the tool mandrels without the preform and measuring the as-tooled gaps. This is not the case for prepreg, where resin content and resin bleeding are major variables that affect both the fibre volume fraction and the part thickness. Although nominal fibre volume fractions can be tightly held, part geometries can produce features with significantly reduced or increased local fibre volume fractions. Fibre volume fraction destructive tests should be conducted on parts in all areas of severe geometry, where local bunching and thinning of plies occur. This will give the fibre volume fraction maximums and minimums for a given part and will demonstrate whether the preform building process is repeatable. Mechanical testing should be done across the expected range of fibre volume fractions to ensure that the impact of fibre volume fraction variation is understood and accounted for in the design and analysis, depending on the design and the application.

14.2.4 DESTRUCTIVE TESTING

Valuable destructive tests that are conducted in early production are photomicrograph cross-sections of those areas which are critical or extremely complex. Areas that should be sectioned and examined include joggles in laminates, ply drop-off areas, corners with tight radii and T-filler areas, sometimes known as deltoids. The deltoid is the void area formed by the radii when two C-channels are placed back to back with cap plies on top and bottom. This triangular cross-sectional area must be filled with material such that the fibres around the corner of the C-channel are not distorted. Structural performance is not only dependent on the quality of the preforming in the deltoid area but is also geometry-dependent. A combination of ply distortion (fibre waviness) and complex geometry (such as a sinewave I-beam) may require a strength reduction factor be applied to the design and substantiated by element

and part testing. Ply distortion in this area alone can lead to a reduction in pull-off strength of up to 40% from a predicted analytical model, which assumes no fibre distortion and simple straight constant cross-section. The deltoid fabrication and assembly process must be controlled, along with the forming process of the preform around the radii. Preforms and deltoids should be inspected before moulding to ensure that no wrinkles or extra bulk exists, followed by photomicrograph inspection of the area after moulding. Inspection and acceptance criteria must be defined for this area and inspection techniques be developed and verified. Figure 14.2(a) shows a structurally unacceptable deltoid with fibre waviness, whereas Figure 14.2(b) shows a structurally acceptable deltoid, consistent with its design requirements.

Image analysis is a new destructive test that can be a valuable tool when qualifying RTM parts. Image analysis equipment takes mounted polished cross-sections of a composite and optically scans the section to determine the area of voids compared with the area of the section. By taking a number of samples, or further polishing away more material from a sample and repeating the test, an average can be calculated to represent void volume. The aerospace industry uses various maximum allowable void volumes, but a common maximum value for structural composites is 2% to 3%. A part with less than 2% porosity or void volume should be represented by the allowables data base. Above that level there are knock-down factors that will apply to the part. These knock-down factors are generated by conducting a defect characterisation programme that tests mechanical properties at various defect levels. Ultrasonic inspection is generally used to determine whether parts meet the defect requirements, but image analysis can be used for determining specific levels of defects and to determine how repeatable the process is. An attempt should be made to correlate non-destructive inspection (NDI) techniques with image analysis and the quantifiable effect of porosity/voids on material properties.

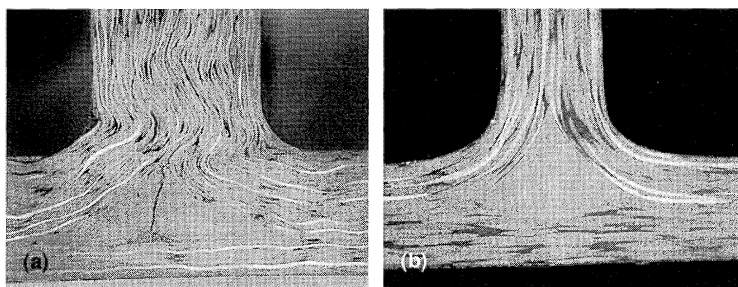


Figure 14.2 (a) Unacceptable deltoid (magnification $\times 6.3$); (b) acceptable deltoid (magnification $\times 10$).

These destructive tests should help determine the types of defects that may be found in the parts and define the acceptance criteria. An effects-of-defects programme would be appropriate to determine the effects of porosity if data are not available for a similar resin/fibre combination. Other parts of an effects-of-defects programme might include, but not be limited to, raw material advancement, fibre waviness or distortion, fibre orientation, high and low resin content and resin-rich areas. Determining what defects and level of defects are acceptable will reduce the cost of fabrication by eliminating expensive processing steps or reducing the number of scrapped parts.

14.2.5 FIBRE ORIENTATION

Fibre orientation is of great concern to stress engineers; their stress analysis assumes that the fibres are in the orientation that is called out on the drawing, and major deviations from those angles can be detrimental to the strength of the part. Typical aerospace composite laminate part designs call out only four ply orientations: 0°, 45°, 90° and 135°. These orientations are given a tolerance of $\pm 2^\circ$ for tape and $\pm 3^\circ$ for fabric. There are several opportunities for the fabric to be distorted out of the orientation tolerance:

1. when the material is tackified;
2. when the material is rolled out to be cut;
3. during removal of plies from the cutting table for stacking;
4. during the preforming process.

The distortion occurs because the fabric (either glass or carbon), used dry or with a small amount of tackifier, is loose and fibres shift easily relative to each other. As fabric is unwound from its roll, tackified, cut or stacked, the warp and fill fibres can pull and shift. The ability of the fabric to distort easily enables RTM to produce complex shapes without cutting and darting. A method for fabric handling and cutting must be demonstrated so that the plies are not distorted before they have been formed. The ply orientation should be checked by using templates or other visual methods before cutting and after stacking. If binder or tackifier is applied to the fabric, uniform pulling and re-rolling of the fabric onto a core is required.

Most military aircraft RTM parts are currently being built using pre-forms, stacked tackified fabric plies that are formed under vacuum and using heat over a tool, usually the male part of the injection tool. The plies are formed from flat stacks into complex curved shapes, such as C-channels. The ply stack must be accurately located on the forming tool. This can be done with locating pins in the tool and with holes precut into

the excess of the preform. The flat areas of the formed preform must be able to meet the $\pm 3^\circ$ orientation tolerance. During this process the plies that form over the complex curved surfaces, or into corners, will distort, bunch and thin, depending on the geometry. Fibre movement is necessary for the RTM process to build complex shapes, but at the same time adequate repeatability of fibre orientation must be demonstrated. Demonstration of the repeatability of the preform forming process is critical to qualifying the RTM process. Fibre distortion is inherent to the processing of complex shapes, but in many cases it is far more desirable to have some fibre distortion than to have cuts and darts in each ply. Cuts and darts may still be required in areas where severe geometry changes are occurring, but, in general, far less are required when compared with hand laid-up prepreg. The stress engineer can account for the fibre distortion and darting of plies when orientation of the distorted ply or plies is known, especially when the new orientation in a given location is repeatable to $\pm 3^\circ$. Orientation can be determined and mapped by building preforms, pulling the plies apart one by one then mapping out the ply orientation of both the warp and fill fibre of each ply in critical locations; this is called a preform tear-down. The preform tear-down can also be used to determine the final location of internal ply drop-offs. Hand lay-up prepreg ply drop-offs can be inspected as each ply is laid down one at a time; this is not generally true for RTM, where stacks of plies with internal drop-offs are formed simultaneously. Drop-off locations will move from their original stacked location during forming. Preform tear-downs should be repeated, changing the ply cutting pattern, until a preform meets drawing requirements, typically within $\pm 0.150''$ (0.381 cm) accuracy.

A non-destructive method of preform inspection is by X-ray. This inspection can be done by building preforms with carbon fabric that is woven with glass tracer fibres spaced evenly [2"-3" (5-8 cm)]. These preforms can be X-rayed, giving a picture of the fibre movement inside the preform. A second benefit of this weave is that after X-raying the preform it can be injected with resin and X-rayed again to show the fibre movement or wash, if any, during the injection process. This fibre wash test can be helpful when injecting with moderate to high viscosity resin, at extremely high injection rates or with low fibre volume fractions. Under these conditions the resin may push fibres around in the direction of the injection or flow fronts. The preforming and injection process repeatability is demonstrated by overlaying the X-ray films from multiple preforms and moulded parts and observing whether the tracer angles are identical. This procedure should show that proper preforming techniques, although distorting the fibre orientation, will do so repeatedly and that the injection process does not move the fibres. These trials should be conducted prior to production of the first part, perhaps as part

of a risk-reduction programme, addressed later, in Section 14.7. This may not be required on every part but should be completed on a part that represents a group or family of parts that are similar in geometry. The lessons learned from the one part should then be applied to the entire part family. Studies into fibre distortion have shown fibre wash is not a concern at fibre volume fractions greater than 45% using resin with injection viscosity below 100 centipoise, injection rates under 150 g/min and injection pressures during flow below 100 psi (689 kPa). Higher injection back pressures, as high as 450 psi (3.1 MPa), usually determined by injection equipment and tooling, should be used only after the initial injection has been completed, to minimise resin shrinkage and void formation. The use of glass tracer fibres in production parts is generally not recommended because the glass tracer fibre is replacing a much stiffer and stronger graphite fibre, causing a reduction in strength approximately equal to the percentage glass by volume used.

14.2.6 PROPERTY TRANSLATION

A constant concern for all composite structures is mechanical property translation from flat panels, used to generate allowables, to complex composite structures. This concern is magnified in many RTM parts because their geometry is usually more complex than traditional hand lay-up parts. To verify property translation it is necessary to test structural elements and/or conduct full-scale structure tests on assembled components. Stress models using mechanical material allowables are used to predict the failure type, location, stress and strain. Many of these models for complex parts will include knock-down factors for cutting and darting as well as fibre distortion. The structural tests will confirm the validity of the knock-down assumptions if any were used. I-beam or T-beam pull-off strength is a good example of a property that can be determined only through subelement pull-off tests. Models exist to predict pull-off strength but these do not account for fibre waviness or fibre distortion caused by severe geometries, as mentioned earlier, in section 14.2.4. These tests are expensive, but provide direct evidence that the design and fabrication of the part or parts meets the structural requirements. Further details of this type of testing are provided later in this chapter, in section 14.3.

14.2.7 CLASSIFICATION OF CANDIDATE PARTS

Composite parts for military aircraft are typically placed in one of three classifications that indicate the criticality of that part to the operation of the aircraft.

-
1. normal controls;
 2. durability critical;
 3. fracture critical.

Normal controls parts are generally easily repairable or replaceable. This category would include structural and non-structural fairings and other easily assessable parts that are not critical to the safe operation of the aircraft. These parts would not require an extensive qualification programme if they were to be fabricated via RTM. Traceability of the materials and processes used is generally provided by material and process standards generated by the material or part fabricator. Many of these parts are sized to minimum gage and may have high factors of safety built in. Qualification of these parts could be as simple as reviewing the manufacturer's specifications and using a resin and fibre purchased to supplier standards. Unfortunately, not many parts fit into this classification; far more are classified as durability critical.

Durability critical parts usually account for over half of the total composite parts on a aircraft. Durability critical parts are sized by durability strength, which is typically the material or parts residual strength after a 4–6 foot pound (5.4–8.1 J) impact and two lifetimes of fatigue, depending on the application and the part requirements. The residual durability strength must be greater than limit load, which is the normal operating load. The relationship between the durability strength and the limit load will be a function of the aircraft's load spectra, controls and environment. The ultimate strength requirement of a part is typically 1.5 times the limit load. When qualifying durability critical parts, demonstration of initial part quality and process repeatability is essential. Statistical process control (SPC) should be used to track the part-to-part variability and to ensure that the RTM process has stayed under control during a production run. Specifications and detailed manufacturing controls should be used to ensure part consistency and avoidance of costly part replacement.

The third type of classification concerns fracture critical parts. Failure of these parts could result in the loss of a critical structure function and consequently the most stringent qualification effort is required. These parts require 100% traceability and record retention for at least seven years. All materials must be certified to specifications and their fabrication controlled by process control documents that specifically indicate how the materials are made and require that no changes can be made without approval of the end user. All data generated during fabrication must be retained, along with test results. For fracture critical parts procedures for meeting specifications should be audited, equipment should be checked for calibration schedules and fabrication should be witnessed by engineers until the process becomes routine. Certified inspectors

should be used to inspect lay-up sequences and cure cycles. First-production fracture critical parts should be destructively tested to ensure fabrication techniques do not generate any internal ply wrinkles or anomalies that cannot be detected with ultrasonic inspection. The NDI techniques must be validated with specific acceptance and rejection criteria. Manufacture of fracture critical parts cannot be treated lightly. All variables must be controlled and monitored because an overlooked problem or mistake can cause a loss of an aircraft and a life.

The classification of the parts to be built will affect the magnitude of the qualification effort, but when many parts are being built parts will fit into all three of the classifications. When all three classifications are represented it is best to treat them all as fracture critical in the manufacturing process and during qualification. This will not only help produce high-quality parts but also will not let the failure of some normal controls parts bring into question the quality of the fracture critical parts. Qualifying and treating parts differently can cause confusion on any shop floor, so it may be best to give the manufacturer the most stringent requirements for all parts and reduce them only when required or when significant cost savings present themselves.

14.3 METHODS OF MECHANICAL PROPERTY QUALIFICATION (STRUCTURAL TESTING)

Design of composite parts requires material property allowables. This is typically conducted using B-basis allowables. Allowables are generated for each combination of fibre, fibre architecture and resin used. Historically, a complete materials allowables programme to generate B-basis allowables can consist of several thousand test coupons generated from at least three different batches of resin and at least two different fibre lots. Testing will range from open hole tension and compression to angle-bend specimens to determine interlaminar tension capability. Approximately 50 different mechanical tests may be conducted with five replicates per batch and tested at -65°F (-18°C) dry, room-temperature dry (RTD), 220°F (104°C) wet and at the maximum service temperature to which the material will be exposed. Materials should be tested for resistance to fuels and solvents, along with being tested in fatigue under various load and environmental conditions. This type of test matrix can cost millions of dollars and take several years to complete. This testing programme is recommended when new materials are being used, when allowables do not already exist or when the applications are broad and design drivers are not the same for all parts. Types of test and amount of testing are driven by designs, applications and structural requirements and will be different for each aircraft.

14.3.1 EQUIVALENCY TECHNIQUE

When cost and/or schedule constraints do not permit B-basis allowables to be generated, and similar materials are being used, an equivalency approach may be appropriate for specific applications of RTM. Equivalency is a more cost-effective method of generating allowables, by demonstrating property equivalence to other existing material data bases, such as proven prepreg resins with similar chemistry. The equivalency technique was developed by the F-22 programme and used to provide allowables for its RTM materials. The F-22 programme showed that the bismaleinide (BMI) resin, 5250-4-RTM, was equivalent to 5250-4 for all properties except for bypass tension, which was approximately 10% lower (the reason for this has not yet been determined). The programme took the idea of showing equivalence one step further and demonstrated that PR500, a RTM resin from 3M, was equivalent to or better than 977-3, a prepreg resin from Fiberite which does not perform well in the RTM process because of its high viscosity. These two epoxies have different chemistries but have very similar properties, and equivalency testing demonstrated that all PR500 properties were equal to or better than those of 977-3. This decreased the qualification time and greatly reduced the cost of qualification. Figure 14.3 illustrates the equivalency building block approach used on the F-22. Final qualification will be 100% complete when the full-scale components and vehicle static and fatigue testing are successfully completed.

By choosing the same fibre and fibre architecture, with a similar resin system, an equivalence matrix may be reduced to approximately 200 coupons from a standard B-basis matrix of 1500 or more. Table 14.1 is an example of a typical equivalency matrix that may be used as a guideline

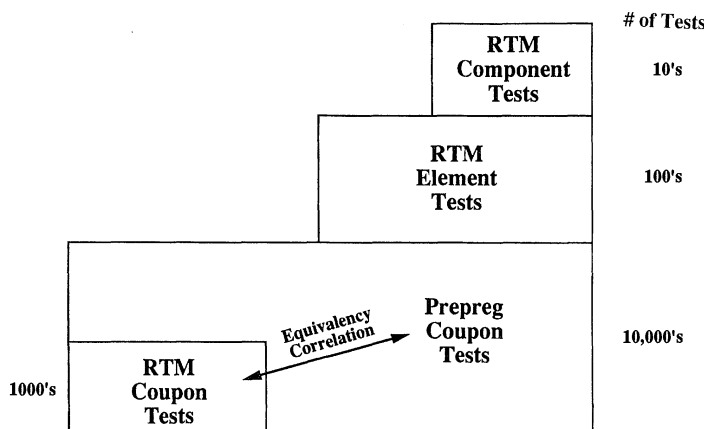


Figure 14.3 Structural building block approach.

Table 14.1 Generic equivalency allowables test matrix

TEST TYPE	LAY-UP	RTA	ETW
LAMINA:			
0/90 TENSION FILL	[0/0/100]	5/5/5	
0/90 COMPRESSION FILL	[0/0/100]	5/5/5	
Laminate:			
UNNOTCHED TENSION	[13/75/13] [25/50/25] [38/25/38]	5/5/5	
UNNOTCHED COMPRESSION	[13/75/13] [25/50/25] [38/25/38]	5/5/5	5
FILLED-HOLE TENSION	[13/75/13] [25/50/25] [38/25/38]	5 5/5/5 5	
FILLED-HOLE COMPRESSION	[13/75/13] [25/50/25] [38/25/38]	5/5/5	
OPEN-HOLE TENSION	[13/75/13] [25/50/25] [38/25/38]	5/5/5	
OPEN-HOLE COMPRESSION	[13/75/13] [25/50/25] [38/25/38]	5 5/5/5 5	5
BEARING WITH TENSION	[13/75/13] [25/50/25] [38/25/38]	5 5/5/5 5	
INTERLAMINAR:			
ANGLE BEND	[25/50/25]	5/5/5	
INTERLAMINAR SHEAR	[25/50/25]	5/5/5	
DADT:			
COMPRESSION AFTER IMPACT	[25/50/25]	12 ^a	
TOTAL		217	

^a Three each at four different impact energy levels.

Note: 5/5/5 = five each from three batches; baseline data are assumed to be available.

DADT = durability and damage tolerance; RTA = room temperature ambient; ETW = elevated temperature wet.

and could easily be altered for specific requirements. The matrix tests three material batches, which include a minimum of two resin batches and two fibre lots. At least two coupons for each test type must be taken from a second test panel, and hot-wet coupons must be taken to 90% complete moisture saturation by weight. Multiple temperatures must be tested such that temperature curves may be generated. The proof of equivalency is from adequate test data that fit the population of the data with which it is being compared.

The equivalence approach may also be used with a modified point allowable approach. When one RTM resin system property (for example,

toughness, as measured by compression after impact) is superior to that of the system with which it is being compared, more extensive testing can be completed on that particular property and replace the lower individual allowable. This may be used for toughened resins where compression after impact properties are the design driver or when service temperatures are different and more testing can be completed at that specific temperature rather than by reading data off the temperature property curve.

If mechanical allowables have been established by one manufacturer and if parts will be built by more than just that one manufacturer, another smaller test matrix can be used to verify equivalency of the second manufacturer's process to the one that generated the allowables. Not all RTM manufacturers use the same equipment, tooling or processing procedures; therefore, each manufacturer's total process must be checked to ensure they can meet the allowables generated. Table 14.2 shows a matrix similar to the one used by the F-22 programme to qualify several manufacturers. This matrix has proven to be very important, because not all manufacturers were able to show equivalence, and on more than one occasion the matrix had to be repeated with new processing parameters. This test matrix can also be used to qualify changes in equipment, processes and manufacturing location as well as changes in the raw materials that always seem to come with a programme that exists for many years.

Table 14.2 A generic part manufacture qualification test matrix

Test type	Material	RTA	ETW ^a
Lamina strength test:			
90 Tension (fill)	[90] ₁₂	5	
90 Compression (fill)	[90] ₁₂	5	
Laminate strength tests:			
Unnotched Tension	[45,0,135,90] _{2s}	6	
Unnotched Compression	[45,0,135,90] _{2s}	6	
Open-Hole Tension	[45,0,135,90] _{2s}	6	
Open-Hole Compression	[45,0,135,90] _{2s}	6	5
Filled-Hole Tension	[45,0,135,90] _{2s}	6	
Filled-Hole Compression	[45,0,135,90] _{2s}	6	5
Double Bearing with Tension	[45,0,135,90] _{2s}	6	5
Compression after impact-Damage	[45,0,135,90] _{3s}	3	
Tolerance		55	15
		Total number of tests = 70	

^a Use same temperature as base line.

Note: three of five replicates can be from one panel; for six replicates, two can be from three unique resin transfer moulding panels.

Once the panels have been built and the test completed the data must be analysed to determine if equivalency exists. Equivalency should be determined on a property-by-property basis. All properties may not show equivalence because of all the variables involved with mechanical testing, and judgment should be used to determine if enough properties are equivalent. In some cases, the RTM system being tested may not be equivalent to the prepreg resin. If the RTM system is better than the system with which it is being compared, allowables from the prepreg resin should be used. If the RTM system is not equivalent, and has lower properties than those of the system with which it is being compared, a knock-down factor may be used to set the RTM material allowables. If large knock-down factors are required and vary from property to property, the equivalency approach can be called into question and a re-evaluation may be required. The method used by the F-22 programme for determining equivalence is described and examples are provided at the end of this chapter.

In many cases RTM resins are reformulated low-viscosity derivatives, with flow inhibitors removed, and a reduction of mixture time at high temperature of prepreg resins on which B-basis allowables have already been completed. Therefore the RTM resins are not identical to the prepreg resins, but the chemistry is similar enough that the mechanical properties should be the same. It is also critical that the fibres and fibre architecture be identical or very similar to the prepreg system. Fibre volume fraction selection should not be taken lightly. The nominal prepreg fibre volume fraction should be duplicated when possible; even though RTM may be capable of producing higher fibre volume fractions than can prepreg, the delta can throw off the data analysis. Normalisation of test data is not straightforward and may cause significant difficulties during data reduction.

14.3.2 STRUCTURAL TESTING

After mechanical allowables have been established, property translation from the coupon level to complex structures must be demonstrated to verify detailed designs. This can be done by mechanically testing the RTM part to failure, demonstrating that the part meets the design requirements. Subsequent parts may be certified in two ways: the first relies on RTM process repeatability for demonstrating requirements, and the second relies on proof loading the parts to show that the design and fabrication requirements are met by every part. This is done by running the part up to limit load, depending on the application.

The two approaches described above are conservative and may be cost-effective when only a few RTM parts are involved, but when a programme has a great quantity of RTM parts, the testing or proof

loading of each part is unrealistic. When many different parts are built it is best to categorise the parts into part families. These part families are determined by size, shape, cross-section and loading condition. The generic F-22 RTM parts list shown in Table 14.3 breaks the parts into part families and lists some geometry features. Once the parts are broken into families, generic structures representing the geometric features of that family can be designed, built and tested under estimated load conditions to determine if design and manufacturing methods meet the requirements. Some basic tests should also be conducted, including T-stiffener pull-off or bending, as shown in Figure 14.4.

Specific designs can be tested as structural subcomponents, such as the F-22 fuel tank test shown in Figure 14.5. This was tested hot-wet through two fatigue lifetimes then taken to ultimate failure to determine failure mode and location. Many of these part-specific tests would be conducted even if the parts were not RTM, but all data gathered gives confidence that the RTM process is under control and that the parts have been built for minimum weight. All of this structural qualification is geared toward demonstrating that the RTM process is simply a manufacturing choice and performs just as prepreg would.

Along with B-basis allowables, structural element and subelement testing should be used to verify the allowables and design assumptions. Generic structures can be designed to represent a family of similar parts. These structures should be used to determine T-stiffener pull-off strengths for different deltoid fill and lay-up configurations. Designs with severe fibre distortion may only be analysed by testing a similar geometry under the expected load conditions. Completion of a structural development test programme prior to final design of parts enables the engineers to reduce or add plies to specific areas as the data dictate. Entire structures may also be tested to show how RTM parts interact with adjacent structure.

14.4 PROOF-OF-CONCEPT PARTS

The building of proof-of-concept parts is where any RTM qualification programme should start and can be completed concurrently with allowables generation; also, many of these demonstration parts can be used for element or structural testing. Parts may be built to determine what shapes and sizes are possible and whether the ribs and integral fittings required can be built into the parts or must be built separately and subassembled later. In general, proof-of-concept parts help determine the range of designs that should be considered for RTM. This also allows individuals and companies to become comfortable with RTM and determine what type of supplier base is available if subcontracting some or all parts. In this phase some initial test data and quality of the

Table 14.3 Examples of F-22 resin transfer moulding parts, with brief description

Parts	Quantity	Description
Forward Fuselage (Lockheed Martin)	12	Shaped I-beam with lightning holes
Fuel Tank Frames	8	Triangular I-beam
Fuel Tank Subframes	24	Long curved panels with beads
Chine Beam Stiffeners	8	Z cross-section fabric/tape
Cockpit Floor Stiffeners; Wing (Boeing Military)	46	I-beams with/window piles and ply drops
Sinewave Wing Spars; Mid Fuselage (Lockheed Martin-Fort Worth)	104	Hybrid hat fabric/tape
Weapon Bay Hat Stiffeners; Vertical and Horizontal Tails (Lockheed Martin)	2	C-channels with ribs and bathtub closeouts
Rear Spars	20	10' I-beams with ply drops
Upper Spars	24	Small C-channels moulded 12 at a time
Hinge Ribs	20	Shorter I-beams
Lower Spars	4	I-beam that transitions into C-channel
Kick ribs	4	I-beam with multiple ribs and closeouts
Root ribs	12	Simple C-channel moulded 6 at a time
Sparlets	12	Close angles, tapered curved C-channels
Closeouts; Aileron, Flaperon and Rudder (Lockheed Martin)	8	C-channel with ribs, local pad-ups
Closeout Spars	6	Long skin with I-beam ribs moulded in C-channel
Fixed Fairings	6	Small V-shaped part with spar
Inlet lip skin and spar	4	Small closed angle I-beams
Driver lip	4	
Aileron and Flaperon Ribs	24	
Miscellaneous	50-60	Small parts (seals, fairings, supports)
Total- approximately 400		

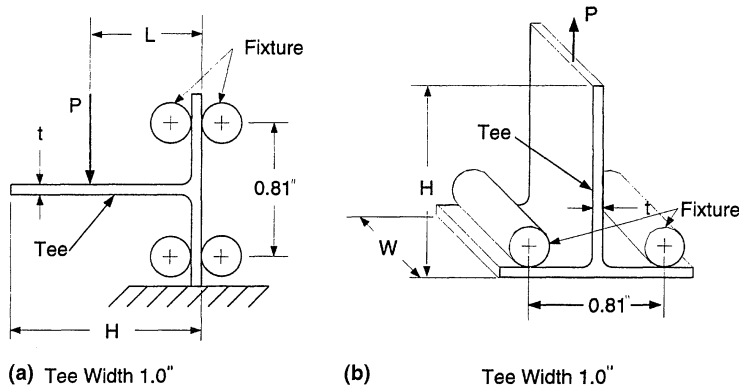


Figure 14.4 (a) T-bend specimen; (b) T pull-off specimen.

demonstration parts built can be used to determine whether to proceed or to pursue other manufacturing techniques. Out of this phase should come a list of candidate parts, a list of RTM manufacturers to work with or a commitment to facilitate internally. Attention must be given at this phase in the programme to whether the facilities to be used are prepared for production or whether they are geared mainly toward research and development (R&D). It is difficult for R&D-type equipment to produce cost-effective, repeatable production parts. Not only is it important to

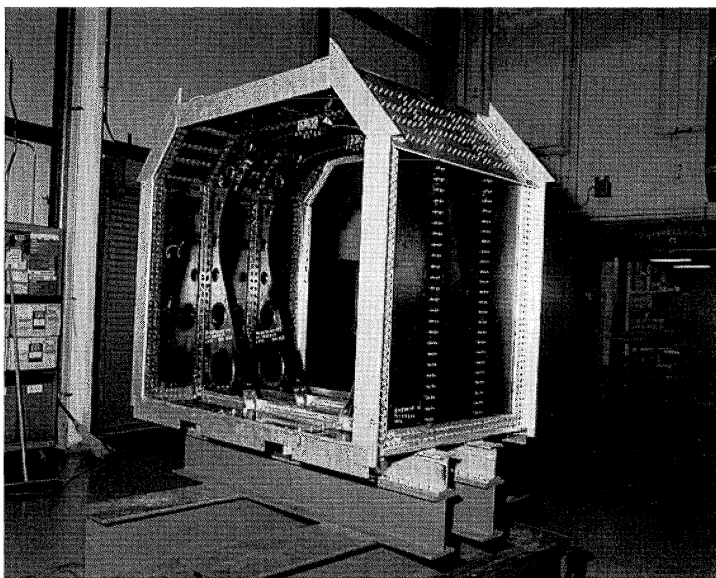


Figure 14.5 Full-scale F-22 fuel tank test.

determine if a demonstration part will meet the requirements but also it is important to determine if the process is repeatable with the equipment and methods used.

14.5 SPECIFICATIONS

Conformance to specification requirements is an important part of the qualification process. By demonstrating conformance to material and process specifications, process repeatability and material property integrity of material allowables is achieved. When more than a couple of RTM parts are being built one should write unique material and process specifications for RTM rather than modifying prepreg specifications, which can prove to be very difficult and costly. Revisions to prepreg sections will cause needless paperwork updates to RTM documentation and can cause havoc on the shop floor. Prepreg material specifications describe requirements for fibre/resin combinations and do not include neat resin, whereas in RTM the fibres and resins are combined in the process specifications not in the material specifications.

14.5.1 MATERIAL SPECIFICATIONS

Fibre and weaving specifications are widely available and probably already exist for the selected fibre material and architecture choices; therefore, only new resin specifications are required. Today, some RTM neat resin material specifications have been written and may be used or modified to fit the desired level of control. Resin should be received from suppliers certified to the specification, with requirements for a minimum viscosity, gel point, glass transition temperature, high-performance liquid chromatography (HPLC) percentage peak area, and maximum differential scanning calorimeter (DSC) exotherm. These data should be tracked with SPC and, after a number of batches have been made, some of these tests can be eliminated to reduce cost. Batch acceptance tests, run after the material has been certified and received, should be utilised to ensure the materials are being tested correctly and accurately by the supplier. Duplication of testing can be expensive and should be avoided if suppliers have demonstrated trustworthiness and accurate testing methods. Material specifications will vary in detail, depending on the use of the parts being built. A material specification should be written for each neat resin system used; in many cases, multiple resin systems may be used on a programme for various applications. If tackified fabric is used in the process, the form of the resin used for tackification should be included in the material specification as a second type, with its own set of requirements.

A material specification may also be written for the tackified fabric. This specification should reference the tackifier resin specification and the fibre and fabric material specifications for the requirements of the raw materials that make up the tackified fabric. When a form of the injection resin is used as a tackifier, only the material uniformity, temperature to which the material is exposed during fabrication, shelf-life and storage conditions need to be specified. The amount of tackifier has not proven to be critical, as long as it is above 2% and less than 10% by weight. If a binder/tackifier other than the injection resin is used tighter control of the amount of binder would be warranted to limit the negative effect on mechanical properties. The minimum amount of that binder/tackifier to produce the desired tack should be determined, and maximum and minimum amounts should be set to the tackification equipment's capabilities. The material specification for tackified fabric may also require that an RTM test panel be constructed and tested (fill tension and compression from each batch of fabric); this provision allows for intermittent checks to ensure the consistency of the materials and process. This requirement is a holdover from traditional prepreg fabrication and can be eliminated after just a few batches, or perhaps never used at all. If open-hole tension and compression tests were conducted these tests could be used to ensure that the allowables are being maintained, because these tests are design drivers on a majority of parts designed. The material specifications should also list all storage and out-time requirements, along with shipping and packaging requirements. Detailed part drawings must call out the materials to build the part, and therefore must call out both the resin and the tackified fabric specifications, or another material specification could be written to group the different resin and fibre combinations in types, 1 through, say, 10. This allows the drawing to call out only one specification and the individual type. This may be necessary, since many drawing release systems will not allow more than one material specification call-out per part detail.

14.5.2 PROCESS SPECIFICATIONS

Process specifications should be written for each resin system and not necessarily for individual parts or applications. The process specifications should require that the fabricator of parts assemble a fabricator process specification (FPS) which details all operating procedures and quality systems that will be used. This allows different fabricators to produce parts to the process specifications while retaining their individual proprietary techniques. Specifications should include requirements for SPC plans, and plans to track key characteristics (KCs) of the process. Detailed manufacturing plans and shop instructions should be written and approved by a materials and processes engineer to ensure

that the methods and procedures used are well documented and not passed on verbally from person to person. Requirements for injection and cure cycles must be listed and temperature records maintained.

Requirements for running temperature control cycles (TCCs) should be placed in the process specifications to ensure that the part has reached the desired temperature during cure. Thermocouples placed in the mould during a simulated injection and cure allow a comparison of actual part temperatures with tool near part thermocouple (NPT) readings. A mould temperature verification run can be accomplished by building a preform and embedding approximately six thermocouples into different parts of the preform and running the wires out through the injection port. A thermal cycle matching the ramp-to-injection and the ramp-to-cure temperature should be run on the tool so that temperature readings of the tool and preform can then be compared. The lag times and the delta between preform and tool reaching the desired temperatures should be added into the injection and cure instructions, thus ensuring the part is seeing the desired temperature for the desired period of time. This can be done on every tool, or just on a few tools within a part family. Parts using the same mould coffin with different internal mandrels generally will not have different thermal profiles from part to part.

In general, process specifications should provide only the mandatory requirements and should let individual fabricator work instructions tighten the processing ranges for specific parts to ensure repeated production of quality parts. There are currently several RTM process specifications being used throughout the industry that can be used as a guide.

14.5.3 NON-DESTRUCTIVE INSPECTION AND ACCEPTANCE SPECIFICATIONS

The NDI and finished part acceptance criteria should be the same for all composite parts, regardless of the manufacturing technique. A few exceptions or additions may be placed in the process specifications to allow for mark-off from multipiece tools and to allow for minor resin richness. Preforms should be inspected so rework or replacement can be done before the part has been moulded. The quality of the preform put into the mould will generally determine the quality of the part coming out. The quality does not generally improve or worsen during injection; therefore, inspection and fixing of problems at the preform level can prevent the need to scrap moulded parts and thus can reduce the overall cost.

14.6 QUALIFICATION AUDITS

A series of audits is required on all material and parts suppliers to ensure that all specification requirements can be and are being met. The first

production batch of material should be audited by materials and process engineers and the supplier's quality assurance organisation to compare the actual manufacturing procedure with what is in their manufacturing instructions and process control document (PCD). The PCD will usually be a proprietary document which details how the material is made; this will include raw materials and their suppliers, mixing instructions, temperature and time ranges and procedures for material batch certification and testing. Any and all changes to PCDs should be reviewed; seemingly minor changes can result in major problems later. Part fabricators should be subjected to prequalification audits which assess each fabricator's equipment capabilities, overall facility and review all quality systems. Not all fabricators will have a facility capable of building all types of parts; some parts may be 20' (6 m) long, and not all RTM houses can handle that length. Additional audits may be required to ensure the process is under control.

14.7 RISK REDUCTION

The purpose of a risk reduction programme is to develop design guidelines for RTM parts prior to design and to demonstrate process capabilities, along with providing additional confidence that RTM parts are as good as or better than their prepreg counterparts from both a quality standpoint and a cost standpoint. Several questions which may still remain unanswered and need to be addressed are as follows.

- Do fibers move in the mould during injection?
- How repeatable are the performing techniques?
- Can $\pm 3^\circ$ be held on fibre orientation on flat areas?
- What type of fibre movement is found in complex areas?
- Can a preform of complexity be built with the techniques developed to date or must new ones be developed for the parts being considered?
- What sort of tooling concepts will work best for the desired tolerances?
- What fibre volume fraction consistency can be achieved?
- Which geometries will require cutting and darting, and which will not?
- What sort of spring-in factor should be used for tooling on I-beams and C-channels?

These questions can be answered by fabricating multiple replicates of the most complex geometries that have been designed. Not all parts may require a specific risk reduction activity, but all part design details should be represented in a risk reduction programme. This can be accomplished by grouping the parts into part families. Parts are placed in families with parts whose geometry, lay-up and structural requirements are similar. Four to six preform replicas of each selected configuration,

representative of a defined family of parts, should be built, and a preform tear-down should be conducted, checking all internal specification and drawing requirements. Multiple parts should also be moulded to demonstrate moulding process control and validation of tooling concepts. These parts when dimensionally examined will help define exact RTM process capabilities and thus help the designer set realistic drawing requirements that will reduce future drawing changes and non-conformance quality paperwork. During risk reduction it is necessary to develop reliable NDI techniques and machining methods; many of these part details will be complex and not amenable to traditional techniques. Once the risk reduction process establishes the necessary data and parameters detailed part design can begin.

14.8 FIRST-ARTICLE QUALIFICATION

Once the materials and RTM process have been qualified it is still necessary to complete some final checks on the production configuration. A preform tear-down, as discussed in section 14.2.5, should be completed on each part family to ensure that scale-up from risk reduction has not introduced any anomalies and that ply drop-offs and cut and dart gaps are as expected and meet drawing requirements.

All shop manufacturing instructions should be reviewed and approved along with all changes made during fabrication to ensure specifications are not being violated or, more likely, misinterpreted. End-to-end checks are necessary to ensure the fabricator is maintaining traceability. NDI standards must be built and approved along with approval of NDI techniques. With some of the odd geometries that the RTM process can build, inspection can be difficult. Special standards and fixtures may be needed.

First-part destructive tests may also be required for at least one part for each part family or for any part that is of particular structural concern. Test specimens are cut from the first production part, and testing may include the following parameters, dependent on the part size, geometry and function:

- tensile strength and tensile modulus [room temperature ambient (RTA)];
- compression strength and compression modulus (RTA);
- T-bend test;
- T pull-off test;
- interlaminar shear;
- interlaminar tension strength;
- resin content and density;
- fibre volume fraction (acid digestion);

- ply thickness;
- ply verification by laminate grind-down;
- glass transition temperature, T_g ;
- sectioning for microphotograph.

These tests are generally run both on prepreg and on RTM parts.

In addition, the first article built for each part number should be 100% ultrasonically and dimensionally inspected. This should include a coordinate measuring machine (CMM) inspection of all dimensions and surfaces to ensure that the part meets loft and other critical dimensions. After the article has been accepted, subsequent parts only require inspection of critical (key) characteristics (KCs), not every dimension. Matched metal moulding repeatability enables a reduction in recurring dimension inspection and is a definite benefit of RTM.

14.9 BRAIDED AND THREE-DIMENSIONAL WOVEN STRUCTURES

Although this chapter was not written with these type of fibre constructions in mind, many of the structural element testing and process verification requirements do apply. The conduction of flat panel testing for allowables is very difficult, leaving part testing and proof loading as the primary qualification options. As industry moves toward these types of structures and away from laminate theory, modelling will have to play a much bigger part in the qualification process.

14.10 CONCLUSIONS

The qualification of RTM parts and of the RTM process are really two separate entities. However, they are very much intertwined, and on the F-22 programme and in this chapter they have been combined into one qualification process. Good structural performance of parts qualifies the process, and a process under control is necessary for good part performance. This chapter lays out a road map to qualify RTM for structural applications, and, although it was geared to large programmes with many parts, sections of the qualification effort could be used to qualify a few parts or just a single part.

The resin transfer moulding process has made some major advances in the past few years that have enabled it to produce structural fracture critical parts for advanced aircraft. With proper thought and planning a qualification process can be created that is not costly, time-consuming or difficult to execute, demonstrating that RTM is nothing more than another manufacturing choice for structural composites.

F-22 PROGRAMME: EQUIVALENCE TESTS

Owing to the small sample sizes involved it is recommended that more than one statistical check be performed.

METHOD 1

The first check is a small sample test concerning the difference between two means. Assumptions:

1. the population variances are unknown but equal;
2. the samples come from normally distributed populations.

The test statistic is determined by using equation (14.4):

$$t = \frac{(\bar{x}_1 - \bar{x}_2) - \delta}{\sigma_{\bar{x}_1 - \bar{x}_2}} \quad (14.4)$$

with degrees of freedom, V given by

$$V = n_1 + n_2 - 2 \quad (14.5)$$

where

n_1 is the sample size of sample 1;

n_2 is the sample size of sample 2;

\bar{x}_1 is the mean of sample 1;

\bar{x}_2 is the mean of sample 2;

$\delta = 0$ if samples are from the same population and

$$\delta_{\bar{x}_1 - \bar{x}_2}^2 = \left(\frac{1}{n_1} + \frac{1}{n_2} \right) \left[(n_1 - 1)s_1^2 + (n_2 - 1)s_2^2 \right] \left(\frac{1}{n_1 + n_2 - 2} \right)$$

s_1 is the standard deviation of sample 1;

s_2 is the standard deviation of sample 2.

This test statistic is a random variable with a Student's t distribution. In another form:

$$t = \frac{(\bar{x}_1 - \bar{x}_2) - \delta}{[(n_1 - 1)s_1^2 + (n_2 - 1)s_2^2]^{1/2}} \quad (14.6)$$

$$v = \left[\frac{n_1 n_2 (n_1 + n_2 - 2)}{n_1 + n_2} \right]^{1/2} \quad (14.7)$$

Example

Sample 1: 8260, 8130, 8350, 8070, 8340;

Sample 2: 7950, 7890, 7900, 8140, 7920, 7840.

1. Null hypothesis; $\delta = 0$; alternative hypothesis, $\delta \neq 0$.
2. Level of significance: $\alpha = 0.01$.

3. Criterion: reject the null hypothesis if $t < -3.250$ or $t > 3.250$, where 3.250 is the value of $t_{0.005}$ for $(5 + 6 - 2)$ degrees of freedom and t is as defined in equation (14.4).
4. Calculation: for this example, $t = 4.19$.
5. Decision: since t (4.19) exceeds 3.250, the null hypothesis must be rejected at level $\alpha = 0.01$.
6. Conclusion: the averages of sample 1 and of sample 2 are not the same. It is recommended that the first assumption in method 1 be confirmed with a test of equality of two variances.

14.11 METHOD 1(a)

Assumption: the samples come from normally distributed populations.
Test statistic:

$$F = s_1^2/s_2^2 \text{ with } n_1 - 1 \text{ and } n_2 - 1 \text{ degrees of freedom.} \quad (14.8)$$

where

- n_1 is the sample size of sample 1;
- n_2 is the sample size of sample 2;
- s_1 is the standard deviation of sample 1;
- s_2 is the standard deviation of sample 2.

This test statistic is a random variable with the F distribution.

Example

Sample 1: 8260, 8130, 8350, 8070, 8340;

Sample 2: 7950, 7890, 7900, 8140, 7920, 7840.

1. Null hypothesis: $\sigma_1^2 = \sigma_2^2$; alternative hypothesis: $\sigma_1^2 \neq \sigma_2^2$.
2. Level of significance: $\alpha = 0.02$.
3. Criterion: reject the null hypothesis if $F > 11.4$, where 11.4 is the value of $F_{0.01}$ for 4 and 5 degrees of freedom.
4. Calculations: $s_1^2 = 15\,750$ and $s_2^2 = 10\,920$. Therefore $F = 1.44$.
5. Decision: since F (1.44) does not exceed 11.4, the null hypothesis cannot be rejected at level $\alpha = 0.02$.
6. Conclusion: there is no reason to doubt the equality of the variances of the two populations.

Appendix A

GLOSSARY

A

a-basis The 'A' mechanical property value above which 99% of the population is expected to fall within 95% confidence. Also called A-allowable. See also B-basis.

absorption The penetration into the mass of one substance by another. The capillary action of an adherand to draw off the liquid film of an adhesive into the substrate. The process where energy is dissipated by a specimen subjected to a radiant energy field.

addition polymerisation A chemical reaction where monomers are linked to each other to form long-chain polymers by chain reaction.

adherand A substrate that is held to another, usually with an adhesive. A detail part for adhesive bonding.

adhesive A material that holds two substrates together by surface attachment.

adhesive film A synthetic resin film, with or without a carrier fabric, used to bond substrates. The resin film is cured under heat and pressure.

advanced composites Continuous fibre reinforced composites with a modulus higher than that of fibreglass fibres. The term also includes metal matrix and ceramic composites, which are outside the scope of this book.

air-bubble void Air entrapped within the composite part, usually located between fibre bundles, spherical in shape, and non-interconnected and usually caused by capillary flow in the fibre bundles or air entrapment in the resin prior to moulding.

amino resins Resins made by polycondensation of a compound containing amino groups, with an aldehyde. With an appropriate catalyst they can be cured at elevated temperatures.

anhydride A compound from which water has been extracted. An oxide of a non-metal which forms an acid when united with water.

anisotropic Material exhibiting different properties along different orientations.

anisotropic laminate Laminate where the properties are different in different orientations along the laminate plane.

aramid A type of fibre manufactured from polyamide (nylon) incorporating aromatic ring structures.

areal weight The weight of a fabric or prepreg per unit area (width × length).

aromatic compound Unsaturated hydrocarbon compound with one or more benzene structures.

autoclave A pressure vessel capable of supplying heat and pressure to a substrate. Usually used for curing laminates and adhesives.

autoclave moulding A process which applies a specific temperature and pressure cycle to cure a composite or adhesive. Usually one-sided tooling with a vacuum bag and breather materials are used in preparing and supporting the specimens.

average molecular weight The molecular weight of the most typical chain in a resin.

B

back pressure Pressure applied or increased at the injection gate especially after the moulding process has been completed.

bagging The application of an impermeable layer of film over a wet resin, prepreg or adhesive lay-up and sealing the edges for the application of vacuum.

bag moulding A process where the consolidation pressure is applied through an impermeable layer of film.

balanced laminate A laminate where the plies are symmetrical about the centre line.

b-basis The 'B' mechanical property value is the value above which at least 90% of the population of values is expected to fall within 95% confidence.

bias fabric Fabric woven with the warp yarns parallel to the length of the fabric and with the weft yarns perpendicular.

binder Plastic or resin used to hold a preform together. Generally considered incompatible with matrix resin as it lowers the glass transition temperature or other properties of the laminate. See tackifier.

bismaleimide (BMI) A type of polyimide that cures by addition reaction rather than by condensation. The glass transition temperature is between that of an epoxy and polyimide.

blank Assembly of fibre mats stacked one on top of the other.

bleed The movement of excess resin out of the laminate during the cure process. A woven or non-woven "bleeder" cloth is positioned to soak up excess resin and allow gas removal during bag moulding.

braiding The weaving of yarns using a braiding machine into circular shapes for two-dimensional braids. Three-dimensional braids are usually done with a cartesian braiding machine and make specific shapes such as T-sections.

breather cloth see **vent cloth**.

b-stage An intermediate stage in the reaction of a thermosetting resin where the resin can still be softened during heating. The resin in an uncured prepreg is b-staged. Binders and tackifiers are usually in a b-stage condition to allow forming of the fabric into a preform.

bulk factor The ratio of the volume of an unconsolidated fibre preform to the final consolidated volume.

bundle A collection of fibres (filaments) in a preferential uniaxial orientation.

burping A process to remove porosity from within the preform during moulding. Usually back pressure is applied with the exit line closed; after a short time the exit line is reopened.

C

capacitance The storage of electricity when a potential difference exists between two conductors. The value is the ratio of the measured charge to the potential difference.

capillary pressure The pressure difference that exists in a capillary across the interface between two immiscible fluids.

carbon fibre Fibre produced by pyrolysis from a precursor such as polyacronitrile (PAN) fibres in an inert environment. Carbon fibre and graphite fibre are sometimes used interchangeably; however carbon and graphite fibres differ. Carbon fibres typically are carbonised at 1315°C and assay at 93%–95% carbon, whereas graphite fibres are carbonised at 1900–2480°C and assay at more than 99% carbon.

cast film A film made by deposition of a heated or solvated resin onto a surface or backing paper.

catalyst A substance that speeds up the rate of reaction of the cure when present in small quantity compared with the other constituents of the resin. It is not or may not be consumed by the reaction.

caul plate Smooth metal or reinforced rubber plate used in lay-up to transmit pressure evenly to the laminate during cure. Also provides a smooth surface to the laminate.

cavity The space inside a mould where the fibre preform is positioned and the resin injected. Some moulds will have multiple cavities and tooling inserts within the cavity.

centre-gated mould A mould where the injection port is located in the centre of the part, and the vents are usually positioned on the edges.

co-bonding The act of curing and bonding a substrate to a precured or metal substrate. Metal or precured inserts may be used when resin transfer moulding.

co-curing The act of curing two substrates simultaneously. b-staged prepreg laminates may be cured simultaneously with the injected resin when resin transfer moulding.

coefficient of thermal expansion (CTE) The change in unit length in a substance per unit change in temperature.

compaction The application of pressure to debulk prepreg or a fabric preform. The process may be carried out at elevated temperature. In prepreg compaction, vacuum is typically used to prevent air entrapment. Preforms are often compacted to the final thickness before positioning into the resin transfer moulding mould.

compatibility The ability of two or more substances to combine to form a homogeneous composition having useful properties. In particular, the ability of one resin (e.g. tackifier) to bond to another resin (e.g. matrix resin) without significant loss of properties at the interface.

composite material The combination of two or more constituents that retain their own identity when combined. For example: resin, fibre and filler. An interface exists between the constituents.

compressive modulus The ratio of compressive stress to strain below the proportional limit.

compressive strength The ability of a material to resist a compressive force to buckle or crush. The value of strength is equal to the failure load divided by the original specimen cross-sectional area.

conditioning The subjection of a material to an environmental or stress condition before testing.

conductivity The electrical or thermal conductance of a unit cube of material. The reciprocal of resistivity.

constituents In composites the constituents are usually the fibre and the resin.

creel A framework that holds the required number of roving balls or supply packages of yarn in a desired position for unwinding during textile processing.

crimp The waviness of a yarn or fabric.

crowfoot A type of weave in which there is a three-by-one interlacing; that is, a filling yarn floats over three warp yarns and then under one. This type of fabric looks different on one side from the other. See four-harness satin.

C-scan The back and forth scanning of composites with ultrasonics. A non-destructive inspection technique for finding voids, delaminations, defects in fibre distribution and so forth.

cure To change the properties of a thermosetting resin irreversibly by chemical reaction. Cure may be accomplished by the addition of curing agents, with or without heat and pressure.

cure cycle The time-temperature-pressure cycle used to cure a composite resin system or prepreg.

cure monitoring Use of an in situ measurement technique, usually electrical impedance measurements to monitor continuously the advancement of the cure process and the change in processing properties.

cure stress A residual internal stress produced during the cure cycle of composites containing reinforcements and/or resins with different thermal coefficients of expansion.

curing agent A catalytic or reactive agent that causes cross-linking. Also called a hardener.

cyanate resins Thermosetting resins that are derived from bisphenols or polyphenols and which are available as monomers, oligomers, blends and solutions. Also known as cyanate esters, cyanic esters, and triazine resins.

D

dam Boundary support or seal used to prevent excessive edge bleeding or resin run-out from a laminate and to prevent crowning of the bag during cure.

damage tolerance A measure of the susceptibility of a structure to damage or in-built defects. Cracks in damage-tolerant designed structures are not permitted to grow.

daylight The distance, in the open position, between the platens of a hydraulic press.

debond A deliberate separation of a bonded joint or interface, usually for repair or rework.

debulking The compaction of the thickness of a layer of prepreg or of a prepreg lay-up by using pressure and/or vacuum to remove most of the air.

deep-draw mould A mould having a core that is appreciably longer than the wall thickness.

degassing The application of vacuum to a resin to remove air and volatiles.

delamination The separation of one or more layers of a laminate.

denier A unit for expressing the weight, in grammes, of 9000 m of a filament, fibre or yarn.

desizing The process of eliminating sizing (generally starch) from fibre or fabrics before applying special finishes. Also the removal of lubricant size following the weaving of a cloth.

desorption A process in which an absorbed material is released from another material. Desorption is the reverse of **absorption**.

diaphragm forming A process of forming a tackified preform or prepreg sheet using a diaphragm (usually rubber), heat and vacuum to form the material onto a mandrel or mould surface. See **vacuum forming**.

die cutting The cutting of shapes from sheet stock by sharply striking it with a shaped knife-edge known as a steel rule die.

dielectric constant (of a material) The ratio of the capacitance of an assembly of two electrodes separated solely by the material concerned to its capacitance when the electrodes are separated by air.

dielectric cure monitoring The use of electrical measurement techniques to monitor changes in electrical properties which result from changes in the mobility of charged and dipolar species during cure and to relate these changes in mobility to changes in macroscopic cure processing properties.

dielectric loss A loss of energy evidenced by the rise in heat of a dielectric arising from the motion of charged and dipolar species in an electric field.

dielectric loss factor The imaginary component of the dielectric permittivity, ϵ''

dielectric loss tangent The quantity $\frac{\epsilon''}{\epsilon'} (= \tan \delta)$ reflecting the ratio of the dielectric loss to the component of the polarisation ϵ' in phase with the electric field.

dielectric permittivity The complex permittivity, $\epsilon^* = \epsilon' - i\epsilon''$, reflecting the components of the polarisation in phase, ϵ' and out of phase, ϵ'' , with the alternating electric field $E_0 e^{i\omega t}$, where $\omega = 2\pi f$, f is the frequency, at $t = \text{time}$.

Differential Pressure Resin Transfer Moulding (DPRTM) Resin transfer moulding with a one-sided tool and vacuum bag or soft tooling. External pressure to the bag is usually applied in an autoclave. Pressure or vacuum within the bag is used to transfer the resin.

Differential Scanning Calorimetry (DSC) A technique to measure the energy absorbed or produced by a material, normally during a temperature ramp. May be applied to detect melting, crystallisation, resin curing, loss of solvents and other processes involving an energy change.

disbond A lack of proper adhesion in a bonded joint. Also, an area of separation between two laminae in the finished laminate. See also **delamination**.

distortion In fabric: the displacement of fill yarn from the original 90° angle relative to the warp yarn. In a laminate: the displacement of the yarns relative to their idealised location owing to motion during lay-up and cure.

draft angle The angle of a taper on a mandrel or mould that facilitates removal of the finished part.

drape The ability of a fabric or prepreg to conform to a contoured surface.

drape forming A method of forming thermoplastic, thermoset or tackified reinforcement sheet in which the sheet is clamped into a movable frame, heated and draped over high points of a male mould. Vacuum is then pulled to complete the forming operation.

dry spot An area of reinforcement apparently not impregnated with resin during a liquid moulding process.

dwell An intermediate step during curing in which the resin matrix is held at a temperature lower than the cure temperature to produce a desired degree of staging or to eliminate porosity.

Dynamic Mechanical Analysis (DMA) A technique in which either the modulus and/or damping of a substance under oscillatory load or displacement is measured as a function of temperature, frequency, time or a combination thereof.

E

E-glass A type of glass fibre with a calcium aluminoborosilicate composition and a maximum alkali content of 2.0%. An inexpensive general-purpose fibre that is most often used in reinforced plastics and which is suitable for electrical laminates because of its high resistivity.

eight-harness satin A type of fabric weave. The fabric has a seven-by-one weave pattern in which a filling yarn floats over seven yarns and then under one. It looks different on one side from the other.

elasticity That property of materials by virtue of which they tend to recover their original size and shape after removal of a force causing deformation.

elastomer A material that substantially recovers its original shape and size after removal of a deforming force.

elastomeric tooling A tooling system that uses the thermal expansion of rubber materials to apply pressure to reinforced plastic or composite parts during cure.

Electric Discharge Machining (EDM) A metal-working process applicable to mould construction in which controlled sparking is used to erode the work piece.

electroformed moulds A mould made by electroplating metal on the reverse pattern of the cavity. A back-up structure is then applied to the mould to increase its strength.

electroplating The electrodeposition of an adherent metallic coating on an electrode for the purpose of forming a surface with properties or dimensions different from those of the basis metal.

elongation Deformation caused by stretching. The fractional increase in length of a material stressed in tension. When expressed as a percentage of the original gauge length it is called percentage elongation.

end A strand of roving consisting of a given number of filaments gathered together. The group of filaments is considered an end, or strand, before twisting, and as a yarn after twist has been applied. An individual warp yarn, thread, fibre or roving.

epichlorohydrin The basic epoxidising resin intermediate in the production of epoxy resins. It contains an epoxy group and is highly reactive with polyhydric phenols such as bisphenol A.

epoxide Compound containing the oxirane structure, a three-member ring containing two carbon atoms and one oxygen atom. The most important members are ethylene oxide and propylene oxide.

epoxy resin A viscous liquid or brittle solid, containing epoxide groups that can be cross-linked into final form by means of a chemical reaction with a variety of setting agents used with or without heat.

eutectic The particular composition within any system of two or more crystalline phases that melts completely at the minimum temperature. Also, the temperature at which such a composition melts.

exotherm The temperature-time curve of a chemical reaction or a phase change giving off heat, particularly the polymerisation of casting resins. The amount of heat given off.

expendable materials Materials that are used in manufacturing a part and are disposed of afterwards.

expendable tooling Tooling materials that are chemically or mechanically removed from a part after manufacture and are disposed of afterwards. Usually used as inserts for undercuts.

F

fabric A material constructed of interlaced yarns, fibres or filaments, usually arranged in a planar structure. Non-woven fabrics are sometimes included in this classification.

fabric deformation The change in shape of a fabric through application of in-plane shear, tensile, compressive and out-of-plane-bending forces. Fabric deformation mechanisms include interfibre shear, interfibre slip, interply slip, fibre buckling and fibre extension.

fatigue The failure or decay of mechanical properties after repeated applications of stress. Fatigue tests give information on the ability of a material to resist the growth of cracks, which eventually bring about failure.

fatigue life The number of cycles of deformation required to bring about failure of a test specimen under a given set of oscillating conditions.

FEP See fluorinated ethylene propylene.

fibre A general term used to refer to filamentary materials. Often, fibre is used synonymously with filament. It is a general term for a filament with a finite length that is at least 100 times its diameter. In most cases it is

prepared by drawing from a molten bath, spinning or depositing on a substrate. Fibres can be continuous or specific short lengths.

fibre bridging Reinforcing fibre material that bridges an inside radius of a part. This condition is caused by faulty layup or insufficient compaction of the reinforcement into the radius.

fibre buckling May occur when the fabric is subjected to local in-plane compression, resulting in the occurrence of wrinkles or folds in the preform. Fibre buckling is more likely to occur when the limit of slip-shear deformation has been reached. Within a fabric drape simulation, this may be anticipated by identifying regions where the interfibre angle has reached the measured fabric locking angle.

fibre diameter The measurement of the diameter of a filament.

fibre direction The orientation of the longitudinal axis of the fibre with respect to a stated reference axis.

fibre extension Extension of fibres, particularly in a fabric during forming. Likely to be negligible for most reinforcements, where the fabric shear stiffness is several orders of magnitude lower than the modulus of the individual fibres.

fibreglass An individual filament made by drawing molten glass. Also the generic name used for composites using glass fibres for reinforcement.

Fibre-reinforced Plastic (FRP) A general term for a polymer matrix reinforced with cloth, mat, strands or other fibre forms.

fibre tow A loose untwisted bundle of continuous fibres. Tow is often used interchangeably with yarn, the twisted version.

fibre volume content The volume fraction or percentage of fibre in a composite.

fibre wash Local movement of reinforcement during filling of a mould with resin. May occur when resin transfer moulding with low fibre volume contents and high injection pressures. May also occur when fibres are carried with high resin bleed during resin film infusion.

filament Fibres, particularly those characterised by extreme length such that there is no filament end within a part except at geometric discontinuities.

filament winding Process for fabricating preforms or composite structures by placing either dry or resin-impregnated fibre reinforcement over a rotating mandrel.

fill Reinforcing yarn woven at right angles to the warp (longitudinal) yarn in a woven fabric.

filler A relatively inert substance added to a plastic to alter its physical, mechanical, thermal, electrical or other properties or to lower cost or density.

film adhesive A synthetic resin adhesive supplied in the form of a film with or without a paper carrier or glass carrier.

finish A material, for treating glass or other filaments. It contains a coupling agent to improve the bond of resin to fibre and usually includes a lubricant to prevent abrasion as well as a binder to promote structural integrity. Usually applied to a fabric. The term is sometimes used interchangeably with sizing. Finish is also used as a term for secondary work on a moulded part such as filing, trimming, buffing, deflashing, tapping, drilling, etc. so that it is ready for use.

flash Excess resin found after moulding at the mould parting line or around inserts.

flexible mould Mould made using a flexible material such as silicone to enable removal of cured pieces with undercuts.

flow The movement of resin under pressure, allowing it to fill the mould.

flow modelling Simulation of the resin flow through a fibre preform in a mould or vacuum bagged tool. Usually uses a finite element mesh to simulate the part.

Fluorinated Ethylene Propylene (FEP) A member of the fluorocarbon family of plastics that is a co-polymer of tetrafluoroethylene and hexafluoropropylene, possessing most of the properties of polytetrafluoroethylene and having a melt viscosity low enough to permit conventional thermoplastic processing. Commonly used as a release ply.

foam tooling Premoulded foam used as a tooling insert for subsequent operations such as preforming and resin transfer moulding.

four-harness satin A satin weave also known as crow-foot satin because the weaving pattern resembles the imprint of a crows foot. The fill yarn interlacing is over three warp yarns, then under one. Satin weave fabrics are easier to form around curvatures. Also called satinet within the textile industry.

G

gate An orifice through which the resin enters or leaves the mould.

gel coat A quick-setting resin applied to the surface of a tool and gelled before lay-up or resin transfer moulding. The gel coat becomes an integral part of the finished laminate and is usually used to improve the surface finish.

gel point The point at which a thermosetting resin attains an infinite value of its average molecular weight. The viscosity at which a liquid begins to exhibit pseudo-elastic properties. This stage can be observed as an inflection point on a viscosity-time plot. Also referred to as gelation.

gel time The amount of time required before a resin sample advances to the gelation point, as defined by a specific test method.

glass cloth Woven glass fibre fabric. See also **scrim**.

glass fibre See **fibreglass**.

glass transition temperature (T_g) The temperature at which increased molecular mobility results in significant changes in the properties of a cured resin system. The glass transition temperature (T_g) can be defined as the inflection point on a plot of modulus against temperature. The properties can decrease significantly before the inflection point. Above this temperature the material behaves more like a rubber; below it, more like glass.

graphite The crystalline, allotropic form of carbon. May be used in bulk form for tooling.

graphite fibres A fibre made from a polyacrylonitrile (PAN) or pitch precursor by an oxidation, carbonisation and graphitisation process.

graphitisation The process of pyrolysis in an inert atmosphere at temperatures in excess of 1925°C, usually as high as 2480°C, converting carbon to its crystalline allotropic form.

green strength The reduced strength of a partially cured part which nevertheless allows it to be removed from the mould and handled without damage or distortion.

grit blasting A surface treatment of a mould or part in which steel grit or sand materials are blown onto the surface.

guide pins Devices that maintain the proper alignment of the mould parts during closure.

H

hand lay-up A manual process of placing (and working) reinforcement or prepreg plies into position on a mould or working surface.

hardener A substance or mixture added to a polymer to promote or control the curing action by taking part in it.

hardness Resistance to deformation; usually measured by indentation. Types of standard tests include the Brinell, Barcol and Rockwell tests.

harness satin A weaving pattern producing a satin appearance. See also **four-harness satin** and **eight-harness satin**.

heat treating Term used for annealing, hardening, tempering and other heat processes.

heterogeneous In materials: consisting of dissimilar constituents separately identifiable: consisting of regions of unlike properties separated by internal boundaries.

hob A master model used to sink the shape of a mould into a soft steel block.

honeycomb Resin-impregnated sheet material or metal foil, formed into hexagonal-cells. Used as a core material in composite sandwich structures.

hybrid A composite laminate containing two or more types of composite systems. Usually only the fibres differ.

hydraulic press A press in which the moulding force is created by the pressure exerted by a fluid.

hydromechanical press A press in which the moulding forces are created partly by a mechanical system and partly by a hydraulic system.

hysteresis Incomplete recovery of strain during the unloading cycle owing to energy consumption. The energy is converted from mechanical to frictional energy (heat).

I

impregnate In composites: to saturate the reinforcement with resin.

impregnated fabric A fabric impregnated with synthetic resin. See also **prepreg**.

inclusion A physical and mechanical discontinuity occurring within a material or part. Usually consisting of a solid, encapsulated foreign material.

infra-red (IR) Pertaining to that part of the electromagnetic spectrum between the visible light range and radar range. Radiant heat is in this range and is often used for preforming. IR analysis is used for identification of polymer constituents.

inhibitor A substance that retards a chemical reaction. Often used to prolong the shelf-life or pot-life of a resin.

initiator Chemical that initiates polymerisation by generating free radicals.

in situ dielectric sensing Use of interdigitated planar electrodes and conventional parallel plate devices to monitor in situ in the mould the changes in the mobility of charged and dipolar species and then to relate these changes in mobility to the changes in the mould of the macroscopic processing properties.

integral composite structure A composite structure in which several of the structural elements are manufactured as a single complex structure (e.g. ribs, spars or skins for an aileron). Resin transfer moulding or co-cure is usually used to manufacture integral structures.

integrally heated Referring to a mould which is self-heated, either by electrical heating or hot oil.

interface The boundary or surface between two different, physically-distinguishable constituents of a composite, such as the contact area between the fibres and the sizing or the reinforcement and the resin.

interfibre angle The smaller angle (less than 90°) between the warp and weft yarns after the fabric has been sheared. Synonymous with interyarn or intertow angle.

interfibre shear Fabrics are sheared as the yarns rotate about their crossover points (stitch or weave centres). The degree of shear is limited by the construction of the fabric, with each material exhibiting an ef-

fective “locking angle” which determines the limit of shear deformation. Synonymous with interyarn or intertow shear.

interfibre slip Some fabrics can deform by slippage at the yarn crossovers so that the fabric is effectively stretched locally. This will usually only be significant when the fabric approaches the limit of shear deformation, although it may be an essential mechanism in the production of complex component geometries. Synonymous with interyarn or intertow slip.

interlaminar Between two adjacent laminae, for example an object (e.g. void), an event (e.g. fracture), or a potential field (e.g. shear stress).

interlaminar shear Shear force tending to produce a relative displacement between two laminae in a laminate along the plane of their interface.

interply hybrid Composite containing two or more different reinforcements combined in discrete layers.

interply slip The slippage of individual plies relative to each other, especially during shaping of fabric or prepreg preforms.

intralaminar Within a single laminae.

intraply hybrid Composites containing reinforcements mixed within a layer, such as alternating yarns in a fabric.

intrinsic viscosity For a polymer, the limiting value, at infinite dilution, of the ratio of the specific viscosity of the polymer solution to its concentration in moles per litre.

isotropic Having uniform properties in all directions. The measured properties of an isotropic material are independent of the axis of testing.

K

Kevlar® An organic polymer composed of aromatic polyamides having a para type orientation (parallel chain with bonds extending from each aromatic nucleus). A registered trademark of E.I. DuPont de Nemours and Company, Inc. Often used as a reinforcing fibre.

knitting A textile method for producing two-dimensional and three-dimensional reinforcement architectures by intermeshing of loops of yarn.

L

lamina A single ply or layer in a laminate made of a series of layers.

laminae Plural of lamina

laminate A product made by bonding together two or more layers or laminae of a material or materials.

laminate orientation The configuration of a cross-plyed composite laminate with regard to the angles of cross-plying, the number of laminae at each angle and the exact sequence of the lamina lay-up.

latent curing agent A curing agent that exhibits long-term stability at room temperature but produces rapid cure at elevated temperatures.

lay-up Assembly of layers of pre-impregnated material or dry fabric per the desired laminate orientation.

learning curve The expected gain in manufacturing efficiency during implementation of a new product using an existing or new manufacturing process. The learning curve is usually represented by a graph depicting the cost per part versus number of parts manufactured.

leno weave A locking-type weave in which two or more warp yarns cross over each other and interlace with one or more filling yarns. It is primarily used to prevent the shifting of yarns in open-weave fabrics.

liquid moulding A general term for processes introducing resin into the reinforcement during manufacture of a composite part. The term includes all variants such as resin transfer moulding (RTM), resin film infusion, vacuum resin infusion, differential pressure RTM and so on.

locking angle The maximum angle at which a fabric will shear without wrinkling.

loop strength The strength required to break a reinforcing yarn by pulling the loop in a prescribed mechanical test.

lot A specific amount of material produced at one time using one process and constant conditions of manufacture and offered for sale as a unit quantity.

M

mandrel A form fixture or mould (usually but not necessarily male) used in the production of a part by lay-up, preforming or filament winding.

mat Fibre bundles held together to form a flat piece of fabric. Usually used to describe a non-woven mat, but sometime used to describe woven layers.

matched mould Matching male and female mould halves used to form a part.

matrix The essentially homogeneous material in which the fibre system of a composite is embedded.

microcrack Tiny cracks formed in composites when local thermal stresses exceed the strength of the matrix. Since most microcracks do not penetrate the reinforcing fibres, microcracks in a laminate made from fabric are usually limited to the thickness of a single ply.

mock leno weave An open weave that resembles a leno and is accomplished by a system of interlacings that draws a group of yarns together and leaves a space between that group and the next. The warp yarns do not actually cross each other as in a real leno. This type of weave is generally used when a high yarn count is required for strength and when the fabric must remain porous.

moisture content The amount of moisture in a material determined under prescribed conditions and expressed as a percentage of the mass of the moist specimen (i.e. the mass of the dry substance plus the moisture).

moisture equilibrium The condition reached by a sample when it no longer takes up moisture from, or gives up moisture to, the surrounding environment.

molecular weight The sum of the atomic weights of all the atoms in a molecule. A measure of the chain length for the molecules that make up a polymer.

monofilament A single fibre or filament of indefinite length that is strong enough to function as a yarn in a textile operation.

monomer A single molecule that can react with like or unlike molecules to form a polymer. The smallest repeating structure of a polymer.

mould A shape, usually rigid, on which a composite part is formed.

moulded edge An edge that is not physically altered after moulding for use in final form.

moulded net Description of moulded part that requires no additional processing to meet dimensional requirements.

mould release agent A lubricant, liquid or powder used to prevent sticking of the moulded articles in the cavity. Facilitates release of the part.

mould surface The side of the part that faces the mould during cure. Resin transfer moulding parts usually have two mould surfaces, whereas resin film infusion parts normally have only one mould surface.

multiaxial fabric A fabric with yarns in orientations other than or in addition to the warp (0°) and weft (90°) directions. Usually a warp-knitted construction.

N

NDE See **non-destructive evaluation**

NDI See **non-destructive inspection**

NDT See **non-destructive testing**

neat resin Resin to which nothing has been added.

nesting The process that occurs during compaction of resin transfer moulding preforms, where prominent yarns in one ply intrude into the 'valleys' of the adjacent ply, and vice versa, reducing the volume of the preform or the necessary compaction pressure.

net-shape part Moulded part that requires no additional processing to meet dimensional requirements.

net-shape preform Preform shaped to final part configuration to enable production of a net-shape part.

newtonian fluid One whose dynamic viscosity is independent of the shear rate

non-crimp fabric A textile fabric produced by binding together layers of yarn with a loose thread. The yarns do not suffer crimping as in woven fabric. The fabric may consist of layers orientated in up to four directions; hence the alternative name, multiaxial fabric. Usually warp-knitted, but can be woven, with care, as uniaxial fabric (uniweave).

non-destructive evaluation (NDE) The analysis of non-destructive inspection (NDI) findings to determine whether the material will be acceptable for its function. Generally considered synonymous with NDI.

non-destructive inspection (NDI) A process or procedure, such as ultrasonic or radiographic inspection, for determining the quality or characteristics of a material, part or assembly without permanently altering the subject or its properties. Used to find internal anomalies in a structure without degrading its properties.

Non-destructive testing (NDT) Generally considered synonymous with non-destructive inspection (NDI).

non-newtonian fluid One whose dynamic viscosity varies with the shear rate

non-recurring cost Costs that occur once in the life of a project (e.g. certification costs, component structural testing costs and material qualification costs).

non-woven fabric In general, a planar textile structure produced by compressing together fibres of engineered orientation (e.g. random, orthotropic) but may contain yarns, rovings and so forth. May be with or without a fabric carrier or substrate. Bonding of the fibres is accomplished by mechanical, chemical, thermal, or solvent means or combinations thereof.

O

oligomer A polymer consisting of only a few monomer units, for example, a dimer, trimer and so forth or their mixtures.

orthotropic Having three mutually perpendicular planes of elastic symmetry.

out time The time a prepreg or resin is exposed to ambient temperature; namely, the cumulative amount of time the prepreg or resin is out of the freezer.

oven dry The condition of a material that has been heated under prescribed conditions of temperature and humidity until there is no further significant change in its mass.

overbraiding Braiding directly over the moulding tool. See also braiding.

oxidation In carbon fibre processing: the step of reacting the precursor polymer with oxygen, resulting in stabilisation of the structure for the hot stretching operation. In general usage: oxidation refers to any chemical reaction in which electrons are transferred.

P

PAN See **polyacrylonitrile**.

parting line A mark on a moulded part surface where two sections of the mould have met in closing.

parting plane The plane which intersects the parting lines.

pay-off quantity The number of manufactured parts required to recover the cost of a manufacturing change. To calculate, the total cost for the change is divided by the savings per part. Profit is realised after this quantity.

peel ply A layer of open-weave material, usually fibreglass or heat set nylon, applied directly to the surface of a prepreg lay-up or preform. The peel ply is removed from the cured laminate immediately before bonding operations, leaving a clean, resin-rich surface that needs no further preparation for bonding other than the application of primer if required.

permeability The ease with which a gas, vapour, liquid or solid can pass through a barrier without physically or chemically affecting it. With resin transfer moulding, permeability of the preform is usually determined experimentally in order to model the flow of resin through the preform.

phenolic Any of several types of synthetic thermosetting resin obtained by the condensation of a phenol or substituted phenols with aldehydes such as formaldehyde.

pinch-off A raised edge around the cavity in the mould which reduces the mould gap and pinches the preform, heavily restricting resin flow and helping to hold the preform in place.

pin-jointed net model A model used to simulate fabric deformation. This approach allows the fabric to be approximated as an orthogonal network of yarns which are connected by pin joints.

pitch A high molecular weight material that is a residue from the destructive distillation of coal and petroleum products. Pitches are used as base materials for the manufacture of certain high-modulus carbon fibres.

plain weave A weaving pattern where the interlacing of the warp and fill yarns alternates (i.e., 'over one, under one'). Both faces of a plain weave are identical. Mechanical properties of laminates containing plain weave fabric are less in magnitude than those of laminates containing fabrics with fewer crossovers.

plastic A material that contains as an essential ingredient an organic polymer of large molecular weight, is solid in its finished state and can be shaped by flow at some point in its processing. The terms plastic, resin and polymer are somewhat synonymous, but the terms resin and polymer most often denote the basic material as polymerised, whereas the

term plastic encompasses compounds containing plasticisers, stabilisers, fillers and other additives.

plasticiser A material incorporated in a plastic to increase its workability, flexibility or distensibility. A material added to a plastic of lower molecular weight to reduce stiffness and brittleness resulting in a lower glass transition temperature.

ply A single layer of prepreg or fabric.

ply wrinkle A condition where one or more of the plies are permanently formed into a ridge, depression or fold.

PMMA See **polymethyl methacrylate**

Poisson's ratio The ratio of the change in lateral width per unit width to the change in axial length per unit length caused by the axial stretching or stressing of a material. The ratio of transverse strain to the corresponding axial strain below the proportional limit.

polar weaving A weaving process that forms cylindrical structures with yarns in the circumferential, radial and axial directions.

polyacrylonitrile (PAN) A polymer used as the base material or precursor in the manufacture of certain carbon fibres.

polymer A high molecular weight organic compound composed of long molecular chains consisting of repeating chemical units.

polymerisation A chemical reaction in which the molecules of monomers are linked together to form polymers.

Polymethyl Methacrylate (PMMA) A thermoplastic polymer synthesised from methyl methacrylate. Sometimes used for cast, integrally-heated resin transfer moulding tooling.

Polytetrafluorethylene (PTFE) Polytetrafluorethylene is a 'TeflonTM' with the highest elevated temperature performance. However, the yield strength is very low. Usually used in coating mould surfaces.

porosity A condition of trapped pockets of air, gas or vacuum within a solid material. Usually expressed as a percentage of the total non-solid volume to the total volume (solid plus non-solid) or a unit quantity of material.

postcure Additional elevated temperature cure to improve the final properties and/or complete the cure. Usually performed free-standing in an oven.

pot-life The length of time that a catalysed thermosetting resin system retains a viscosity low enough to be used in processing.

precursor With respect to carbon or graphite fibre: the rayon, PAN or pitch fibres from which carbon and graphite fibres are derived.

preform A preshaped fibrous reinforcement structure. Usually formed by the application of heat and pressure to a reinforcement stack containing binder or tackifier.

preform binder See **binder**.

preforming Process for shaping the fibre reinforcement into the final part geometry.

preform permeability See **permeability**.

preform tackifier See **tackifier**.

prepreg Fibre cloth, unidirectional fibre or mat impregnated with resin and stored for use. The resin is partially cured to a 'B' stage and supplied to the fabricator ready for lay-up and cure.

pressure intensifier A layer of flexible material (usually a high-temperature rubber) used to ensure that sufficient pressure is applied to a specific location, such as a radius, in a lay-up being cured.

process control During laminate cure, the use of electrical techniques to monitor the cure cycle. Also refers to the overall procedure of recording cure cycle temperatures, vacuum and pressure, plus mechanical testing of a 'process control' panel cured and fabricated along with the part.

promoter Chemical that acts as a catalyst and accelerates the generation of free radicals.

PTFE See polytetrafluoroethylene.

Q

quasi-isotropic A lay-up sequence of the 0°, +45°, -45°, 90° family, with equal amounts of fibre in each direction. With the fibre axes in four directions, laminate properties in the plane of the fibres are nearly isotropic.

R

racetracking Resin flow in a gap or porous area, usually faster than that in other parts of the mould. For example, resin flow between the preform edge and the mould wall.

recurring costs Costs that accrue during manufacturing. For example, raw material costs, and labour costs.

reinforcement A strong material bonded into a matrix to improve its mechanical properties. Reinforcements are usually long fibres, chopped fibres, whiskers, particulates and so forth.

release agent See **mould release agent**.

release film An impermeable layer of film that does not bond to the resin being cured.

residual stress The stress existing in a body at rest, in equilibrium, at uniform temperature and not subjected to external forces. Often caused by the forming and/or curing processes.

resin A polymer (or polymers) and their associated hardeners, catalysts, accelerators, and so on which can be converted to a solid by application of energy, normally in the form of an elevated temperature.

resin content The amount of matrix present in a composite expressed as percentage weight or volume.

Resin Film Infusion (RFI) A process by which resin, initially in the form of a film or sheet, is infused through the thickness of a fibre preform under compaction at an elevated temperature.

resin richness A localised area of excess resin without fibre, usually occurring at radii, steps and edges in moulded parts.

resin-starved Localised area of insufficient resin, usually identified by low gloss, dry spots or fibre showing on the surface.

Resin Transfer Moulding (RTM) A process by which resin is transferred or injected into an enclosed mould in which reinforcement has been placed.

RFI See **Resin Film Infusion**

rheology The study of the flow of materials, particularly the plastic flow of solids and the flow of non-Newtonian liquids. The science treating the deformation and flow of matter.

roving A number of yarns, strands, tows or ends collected into a parallel bundle with little or no twist.

RTM See **Resin Transfer Moulding**

rubber A solid formed from cross-linked polymers which has a glass transition temperature below room temperature and exhibits highly elastic deformation and high elongation.

runner system All the sprues, runners and gates through which the resin flows from the injection system to the mould cavity.

S

sandwich construction A structural panel consisting in its simplest form of two relatively thin, parallel sheets of structural material bonded to and separated by a relatively thick, lightweight core.

satin A warp-faced weave in which the interlacings are arranged with a view to producing a smooth fabric surface, free from twill; each weft yarn makes one and only one interlacing with a warp yarn. The reverse side is called a sateen. The satin weave has the minimum number of interlacings in the weave repeat, making it more easy to shear than a plain weave.

scrim A low-cost reinforcing fabric made from continuous filament yarn in an open mesh configuration. Used as a carrier of adhesive, or in processing of tape or other b-stage material to facilitate handling.

secondary bonding The joining together, by the process of adhesive bonding, of two or more already cured composite parts.

secondary structure In aircraft and aerospace applications, a structure that is not critical to flight safety.

selvage The woven-edge portion of a fabric parallel to the warp.

separator A permeable layer which also acts as a release film. For example a porous TeflonTM coated fibreglass. Often placed between the lay-up and bleeder to facilitate bleeder system removal from laminate after cure.

shear angle The angle is $\alpha - 90^\circ$, where α is the larger angle between the warp and weft yarns after a fabric is sheared. Also, 90° minus the intersection angle.

shelf-life The length of time a material, substance, product or reagent can be stored under specified environmental conditions and continue to meet all applicable specification requirements and/or remain suitable for its intended function.

shell tooling A mould or bonding fixture consisting of a contoured surface shell supported by a substructure to provide dimensional stability.

shore hardness A measure of the resistance of material to indentation by a spring-loaded indenter. The higher the number, the greater the resistance. Normally used for rubber materials.

short beam shear A flexural test of a specimen having a low test span-to-thickness ratio, such that failure is primarily in shear.

short shot The injection of insufficient resin or compound to fill the mould cavity completely.

shot capacity The maximum weight of material an injection machine can provide from one forward motion of the ram, screw or plunger.

shrinkage The relative change in dimension from length measured on the mould when it is cold to the length of the moulded object 24 hours after it has been taken out of the mould.

silicones Plastics based on resins in which the main polymer chain consists of alternating silicon and oxygen atoms, with carbon-containing side groups.

sink mark A depression in the surface of the laminate due to local shrinkage.

sizing Material applied as a very thin coating on fibres to improve their processability and/or to increase the fibre/matrix bond strength in composites.

specific gravity The density (mass per unit volume) of any material divided by that of water at standard temperature.

sprayed metal moulds Moulds made by spraying molten metal onto a master until a shell of predetermined thickness is achieved. The shell is then removed and backed with plaster, cement, casting resin or some other suitable material.

springback Dimensional change that occurs in the preform after the preforming stage and which results in increased thickness and/or angles (for curved preforms). It is the manifestation of the elastic energy stored in the fibres resulting from deformation that occurs during preforming. Springback is sometimes used interchangeably with spring-in for moulded composites.

spring-in Used to describe the reduction of enclosed angle of a moulded composite flange caused by residual stresses.

sprue A single hole through which thermoset resins are injected directly into the mould cavity.

stabiliser Chemical used to control the size of the monomer as in suspension polymerisation, or the molecular weight of the polymer as in stepwise polymerisation.

staging The heating of a premixed resin system, such as in a prepreg, in order to advance the degree of cure, but stopping the reaction before gel point is reached. Staging of resin tackifiers occurs during preforming.

stitching Stitching of a dry fibre preform stack with a fine yarn is usually conducted to improve the laminate damage tolerance or to improve the handling of the preform.

storage life The period of time during which a liquid resin, adhesive or prepreg can be stored under specified temperature conditions and remain suitable for use. See also **shelf-life**.

strand Normally, an untwisted bundle or assembly of continuous filaments used as a unit, including slivers, tows, ends, yarns and so forth. Sometimes a single fibre or filament is called a strand.

stress crack External or internal cracks in a plastic caused by tensile stresses less than its short-time mechanical strength, frequently accelerated by the environment to which the plastic is exposed.

substrate A material upon the surface of which an adhesive-containing substance is spread for any purpose, such as bonding or coating.

surface tension The force existing in a liquid–vapour phase interface that tends to diminish the area of the interface. This force acts at each point on the interface in the plane tangent to that point.

surface treatment A material (size or finish) applied to fibrous material during the forming operation or in subsequent processes.

symmetrical laminate A laminate in which the stacking sequence of plies below its midplane is a mirror image of the stacking sequence above the midplane.

T

tack The stickiness of an adhesive or fibre reinforced prepreg material.

tackifier Resin used to tack a fibre preform together. The resin is usually considered compatible to the resin system: that is, there is no degradation to laminate properties when applied in low concentrations (3%–7%).

teflon™ DuPont trade name for polymers of both tetrafluoroethylene (TFE) and fluorinated ethylene propylene (FEP)

tensile modulus See **Young's modulus**.

tensile strength The maximum load or force per unit cross-sectional area, within the gauge length, of the specimen. The pulling stress required to break a specimen.

tensile stress The normal stress caused by forces directed away from the plane on which they act.

tex A unit for expressing linear density equal to the mass in grammes of 1000 m of filament, fibre, yarn or other textile material.

textile fibres Fibres or filaments that can be processed into yarn or made into a fabric by interlacing in a variety of methods, including weaving, knitting and braiding and other fabric-forming processes. See also **Fibre**.

thermal conductivity The capability of a substance to 'conduct' heat from a hot area to a cooler area. Measured as the quantity of heat conducted per unit time through unit area of a slab of unit thickness having unit temperature difference between its faces.

thermoplastic A plastic that can repeatedly be softened by heating and hardened by cooling through a temperature range characteristic of the plastic and that in the softened stage can be shaped by moulding.

thermoset A plastic that is substantially infusible and insoluble after having been cured by heat or chemical means.

thixotropic With respect to materials: gel-like at rest but fluid when agitated. Having high static shear stress and low dynamic shear stress at the same time. Having the property of losing viscosity under stress.

thread See **yarn**.

thread count The number of threads per centimetre in either the lengthwise (warp) or crosswise (weft) direction of woven fabrics.

three-dimensional fibre architecture Preform or textile with fibres oriented in the *x*, *y* and *z* directions. Usually fabricated with advanced weaving techniques or stitching.

toughness A measure of the ability of a material to absorb energy. Toughness is proportional to the area under the load–elongation curve from the origin to the breaking point.

tow An untwisted bundle of continuous filaments, usually referring to man-made fibres. A tow designated as 3K has 3000 filaments. The term is often used interchangeably with **yarn**.

tracer A fibre, tow or yarn added to a prepreg to aid in verifying fibre alignment and, in the case of woven materials, for distinguishing warp yarns from fill yarns.

twill weave A basic weave characterised by a diagonal rib or twill line. Each end floats over at least two consecutive picks, allowing a greater number of yarns per unit area than in a plain weave, while not losing a great deal of fabric stability.

twist In a yarn or other textile strand: the number of spiral turns about its axis per unit of length. Twist may be expressed as turns per inch (tpi).

The letters S and Z indicate the direction of the twist, in reference to whether the twist direction conforms to the middle-section slope of the particular letter.

U

undercut A protuberance or indentation that impedes the withdrawal of a moulded part from a two-piece mould.

unidirectional laminate A reinforced plastic laminate in which substantially all of the fibres are orientated in the same direction.

uniweave A textile fabric made with 95%–97% of yarns in the warp direction and 3%–5% of the yarns in the weft direction. Often the weft yarns are smaller tex and a different material than the warp yarns as they are used only to bind the yarns together.

unsymmetric laminate A laminate having a stacking sequence without midplane symmetry.

V

Vacuum-Assisted Resin Transfer Moulding (VARTM) A process where vacuum is used to infuse resin through a dry preform. Usually occurs under a vacuum bag, but may use a closed mould.

vacuum bag The plastic or rubber layer used to cover the part for the application of vacuum.

Vacuum Bag Resin Infusion (VBRI) A process where vacuum is used to infuse resin through a dry fibre preform under a vacuum bag.

vacuum forming A method of sheet forming in which the plastic sheet is clamped in a stationary frame, heated and then drawn down by vacuum into a mould. This is a general term which sometimes refers to pre-forming, drape forming and so forth.

vacuum injection moulding A version of resin transfer moulding in which the resin is infused through the reinforcement by the application of vacuum to the mould.

veil A highly permeable, self-wetting, thin fibre mat.

vent An exit port through the mould by which excess resin, air and volatiles are removed during resin transfer moulding.

vent cloth A layer or layers of open-weave cloth used to provide a path for vacuum to ‘reach’ the area over a laminate being cured, so that volatiles and air can be removed. The cloth also allows a pressure differential across the vacuum bag that results in the application of pressure to the part being cured. Also known as breather cloth.

venting In autoclave curing of a part or assembly: the turning off of the vacuum source and venting of the vacuum bag to the atmosphere. The pressure on the part is then the difference between the pressure in the

autoclave and atmospheric pressure. In resin transfer moulding: the turning off of the vacuum source and venting of the mould to atmosphere.

viscoelasticity A property involving a combination of elastic and viscous behaviour. A material having this property is considered to combine the features of a perfectly elastic solid and a perfect fluid. A phenomenon of time-dependent, in addition to elastic, deformation in response to a load.

viscoelastic modulus Measure of energy required to deform a material. It is a vector sum of G' (storage modulus) and G'' (loss modulus).

viscosity The property of resistance to flow exhibited within the body of a material, expressed in terms of the relationship between applied shearing stress and the resulting rate of strain in shear. Viscosity is measured in terms of flow in Pas (10 Poise), with water as the base standard (value of 1.0 Pa s). The higher the number, the less the flow.

void Air or gas that has been trapped and cured into a laminate. Porosity is an aggregation of microvoids. Voids are essentially incapable of transmitting structural stresses or non-radiative energy fields.

void content Volume percentage of voids, usually less than 1% in a properly cured laminate.

volatiles Materials such as water and alcohol in a sizing or resin formulation that are capable of being driven off as a vapour at room temperature or at a slightly elevated temperature.

volume fraction Fraction of a constituent material based on its volume.

W

warp The longitudinally orientated yarn or thread running down the length of a woven fabric. See **Fill** or **Weft**.

warpage Dimensional distortion in a plastic object.

warp beam A cylindrical beam onto which is wound the required length and number of warp yarns. The beam acts as a supply of warp yarn for the weaving process.

water absorption The ratio of weight of water absorbed by a material to the weight of dry material.

water jet Water emitted from a nozzle under very high pressure. Useful for cutting materials.

weave The particular manner in which a fabric is formed by interlacing warp and weft yarns or thread. Usually assigned a style number.

weft The transverse yarns in a woven fabric. Those yarns running perpendicular to the warp. Also called fill.

wet lay-up A method of making a composite by applying the resin system as a liquid as the reinforcement is put in place.

wet-out The condition of an impregnated roving or yarn in which substantially all voids between the sized strands and filaments are filled with resin.

wetting The spreading, and sometimes absorption, of a fluid on or into a surface.

whisker A short fibre or filament. Whisker diameters range from 1–25 µm, with length-to-diameter ratios between 100 to 15000.

wicking Spontaneous imbibition of a liquid into a porous material owing to the influence of capillary pressure.

working life The period of time during which a liquid resin or adhesive, after mixing with catalyst, solvent or other compounding ingredients remains usable. See also **pot-life**.

woven fabric A material constructed by interlacing yarns, fibres or filaments to form such fabric patterns as plain, harness satin, and leno weaves.

woven roving A heavy glass fibre fabric made by weaving roving or yarn bundles.

wrinkle An imperfection in laminated plastics that has the appearance of a crease or fold in one or more sheets of the fabric or reinforcement. Also occurs in vacuum bag moulding when the bag is improperly placed, causing a crease.

Y

yarn An assemblage of twisted or untwisted filaments, fibres or strands, either natural or manufactured, to form a continuous length that is suitable for use in weaving into textile materials. Usually a relatively small cross-section. The term is often used interchangeably with tow, the untwisted larger version.

yarn bundle See **bundle**.

yarn locking The point where a fabric cannot shear anymore without wrinkling and severe deformation.

Young's modulus The ratio of normal stress to corresponding strain for tensile or compressive stress less than the proportional limit of the material.

Z

zero bleed A laminate fabrication procedure which does not allow loss of resin during cure. Also describes prepreg made with the amount of resin desired in the final part, such that no resin has to be removed during cure.

Appendix B

CONVERSION FACTORS

multiply	by	to obtain
atm	1.01325	bar
atm	29.92	inches Hg
atm	14.696	lbf/in ²
bar	1×10^5	Pa
bar	14.5038	lbf/in ²
BTU (British thermal unit)	778.17	ft lbf
BTU	1.055	kJ
BTU/ft h R	1.7298	W/m K
BTU/h	0.2929	W
BTU/lbm	2.326	kJ/kg
BTU/lbm R	4.1868	kJ/kg K
cal	4.184	J
cm	0.3937	in
cm ²	0.155	in ²
cm ³	0.061024	in ³
cp	1	mPa s
cp	0.001	Pa s
ft	0.3048	m
ft ²	0.0929	m ²
ft ³	7.481	gal
ft ³	0.028317	m ³
ft lbf	1.35582	J
gal	0.13368	ft ³
gal/min	0.002228	ft ³ /s
g/cm ³	1000	kg/m ³
g/cm ³	0.03613	lbm/in ³
in	2.54	cm
in ²	6.4516	cm ²
in ³	16.387	cm ³
J	0.239	cal
J	0.73756	ft lbf
kcal/h m K	1.639	W/m K
kcal/kg K	4.184	kJ/kg K
kg	2.20462	lbm
kg/m ³	0.06243	lb/ft ³
kJ	0.9478	BTU
kJ	737.56	ft lbf
kJ/kg	0.42992	BTU/lbm
kJ/kg K	0.239	BTU/lbm R

multiply	by	to obtain
km	3280.8	ft
km/h	0.62137	miles/h
kPa	0.14504	lbf/in ²
kW	737.6	ft lbf/s
l	0.03531	ft ³
l	0.001	m ³
lbf	4.4482	N
lbf/ft ²	6.9444×10^{-3}	lbf/in ²
lbf/in ²	0.06895	bar
lbf/in ²	6894.8	Pa
lbm	0.4536	kg
lbm/in ³	27.6791	g/cm ³
lbm/ft ³	16.018	kg/m ³
m	3.28083	ft
m ²	10.7638	ft ²
m ³	35.3147	ft ³
micron (μm)	1×10^{-6}	m
miles/h	1.6093	km/h
mPa s	1.0	cp
N	0.22481	lbf
Pa	1×10^{-5}	bar
Pa	1.4504×10^{-4}	lbf/in ²
Pa	7.5007×10^{-3}	torr
Pa s	10	Poise
Poise	0.1	Pa s
torr	133.32	Pa
W	3.414	BTU/h
W/m K	0.5781	BTU/ft h R
W/m K	0.85918	kcal/h m K

Index

- A-basis 482
Absorption 482
Acid digestion, *see* Matrix digestion
Addition polymerisation 482
Adherend 482
Adhesive 482
Adhesive film 482
Advanced composites 482
Air bubble – void
 see also Void; Porosity
Airpad® 362, 367
Allowables 458, 466–470
Alloys, *see* Melt-out metal alloys
Aluminium oxide 73
Amine 56–59
Amino resins 482
Anhydride 58–59, 482
Anisotropic 482
Anisotropic laminate 483
Applications, *see* Resin transfer moulding applications
Aramid 70–71, 84, 483
 see also Kevlar™ 49
Areal weight 128, 459, 483
Arlon™ 367
Aromatic compound 483
Arrhenius equation 252
Autoclave 483
Autoclave cured prepreg 1, 2, 12,
 408–409, 445–446
Autoclave moulding 483
Automated strain analysis 131–134
Average molecular weight 483
 see also Molecular weight

Back pressure 36–37, 443, 483
Bag moulding 483
Bagging 483
Balanced laminate 483
Balsa wood 359–360

-properties 342
Basis values, *see* b-basis; a-basis
B-basis 466–470
Bias fabric 483
Bias tensile testing, *see* Fabric, Bias tensile testing
Binder 151–152, 393
 application 155–157
Bismaleimide 64–65, 66, 483
 -suppliers 65, 82
Bladder 360–370
 -materials 367, 368
 -types 361–365
Blank 483
Blanking 157–159
Bleed 483
Blow port 312–313
Boron 71
Braiding 96, 98–102, 155, 483
 -four step 99–101
 -multilayer interlock 101–102
 -overbraiding 152–153
 -three dimensional 6, 8, 99–102
 -two step 99–101
Break-out mandrels 374–375
Bridging 292
B-stage 393, 484
Bulk factor 148, 309, 484
Bundle 484
 see also Roving; Strand; Tow; Yarn
Burn-off 131–132, 437–438, 459–460
Burping 27, 442, 484

C-glass 68
Capacitance 415–417, 484
Capillary number 193, 438–439
Capillary pressure 192–194,
 438–439, 484
Carbon fibre 69–70, 72, 84, 484
 see also Fibre

- Carmen-Kozeny equation, *see* Kozeny-Carmen equation
- Cast film 484
- Catalyst 57–58, 484
- Caul plate 484
- Cavity 484
- Centre-gated mould 484
- Certification 13–14, 20
see also Qualification
- Ceramic 71–73
- Clamp, *see* Mould, Clamping system
- Clamping force, *see* Mould clamping forces
- Closed-cell foam, *see* Foam
- CNC machining 287, 291, 300
- Coating, fibre 74–76
- Co-bonding 19, 484
- Co-curing 1, 410, 485
- Coefficient of thermal expansion (CTE)
- bladder materials 368
 - extractable tooling materials 383
 - differential 313–314, 351, 380–381
 - mould materials 285
 - mould thermal expansion calculation 317
- Compaction 485
- see also* Flow modelling, Transverse compaction, Compressibility curves
- Compaction models 241–242
- Compaction pressure 166, 167
- Compatibility 485
- Composite material 42–43, 485
- Composite tooling, *see* Tooling, Reinforced plastic
- Compressibility curves 166, 167
- Compression-after-impact 54, 89–91, 96
- Compressive strength 485
- Compressive modulus 485
- Computer-aided engineering, reinforcement
- deformation 112–114
- Conditioning 485
- Conductance 415–417
- Conductivity 485
- Constant flow rate injection, *see* Injection equipment, constant flow rate
- Constant pressure injection, *see* Injection equipment, Constant pressure
- Constituents 485
- Contact angle, *see* Wetting contact angle
- Control volume, *see* Flow modelling, Numerical formulations
- Core, *see* Tooling inserts
- Corrosion 23
- Costs 388–411
- advantage 2, 19, 21–22, 108
 - applications 406
 - bladder materials 368
 - case studies 406–410
 - certification 405–406
 - core materials 346
 - heat source 402
 - injection equipment 400–402
 - manufacturing 1–2, 389–390, 392–400
 - material 1, 4, 5, 390–392
 - modelling 398–400
 - mould 403–404
 - mould material 395
 - non-recurring 400–406
 - part complexity 396, 408–409
 - preforming 392–394
 - quality 394–395
 - recurring 389–400
 - RTM with prepeg resins 394
- Creel 91, 485
- Crimp 86, 201, 485
- Cross-linking 50–53
- Crowfoot satin weave 485
- C-scan 485
- see also* Ultrasonic inspection
- Cure 11, 47, 485
- Cure cycle 485
- Cure monitoring 417–420, 486
- Cure stress 486
- Curing agent 55–58, 486
- Cut-and-sew 159
- Cutting 8
- see also* Ultrasonic knife cutting
- Cyanate resin 62–64, 486
- suppliers 64, 82
- Dam 486
- Damage tolerance 23, 103, 486

- Darcy-Weisbach expression 329
 Darcy's law 179–180, 256
 -analysis based on 219–221
 -one dimensional 36–37, 48,
 183–184, 190, 229, 246
 -three-dimensional 207, 229
 -two-dimensional 229
 Data acquisition 412–433
 see also Injection equipment, Data acquisition
 -cure monitoring 417–420
 -resin infiltration monitoring 420–428
 -smart automated control 428–429
 Daylight 486
 Debond 486
 Debulking 159–160, 309–311, 486
 see also Preform compaction
 Deep-draw mould 486
 Defects 435–445
 -effects-of 462
 -formation 438–443
 -prevention 444–445
 Deformation, *see* Fabric and Preform deformation
 Degassing 27, 28–29, 486
 Delamination 486
 Deltoid 460–461, 471
 Denier 486
 Density
 -ceramic fibres 73
 -change during cure 51–53
 -extractable tooling 383
 -one-part epoxy 60
 -one-part bismaleimide 66
 -tooling 381
 Design allowables, *see* Allowables
 Desizing 486
 Desorption 486
 Destructive testing 460–462
 Diaphragm forming 486
 Die cutting 486
 see also Cutting
 Dielectric constant 487
 Dielectric impedance 415–417
 Dielectric loss 487
 Dielectric loss factor 487
 Dielectric loss tangent 487
 Dielectric permittivity 415–417, 487
 see also Cure monitoring
 Dielectric cure monitoring 487
 see also Cure monitoring
 Dielectric sensing
 see also In-situ dielectric sensing
 -instrumentation 415
 -system suppliers 415–433
 -theory 415–417
 Differential pressure RTM 11–12, 487
 Differential scanning calorimetry 487 (DSC)
 Disbond 487
 Dispensing equipment, *see* Injection equipment
 Distortion 487
 Draft angle 382, 487
 see also Mould, Draft
 Drapability, *see* Formability
 Drape 133, 144, 487
 Drape forming 487
 Draping 159–160
 see also fabric drape modelling
 Drape modelling, *see* Fabric drape modelling
 Drape simulation, *see* Fabric drape modelling
 Draping algorithm 124
 Dry Spot 226, 435, 436, 442–443, 444, 487
 Durability critical, *see* Part classification
 Dwell 488
 Dynamic mechanical analysis (DMA) 488
 Easy-Out™ 374
 Edge effects 186–187
 E-glass 68, 72, 488
 Eight harness satin 488
 Elasticity 488
 Elastomer 488
 Elastomeric tooling 384–385, 488
 Electric discharge machining (EDM) 287, 488
 Electroformed moulds 293–294, 488
 Electroplating 488
 Elongation 488
 see also Tensile elongation
 -bladder materials 368
 -resins 53, 58

- Embroidery, *see* Tailored fibre placement
- End 488
- Energy absorption 103
- Epichlorohydrin 488
- Epoxide 489
- Epoxy equivalent weight 57
- Epoxy resin 55–59, 60, 489
-suppliers 55, 59, 82
- Equivalence tests 467–470, 480–481
- Eutectic 489
- Eutectic salts 371–373
- Exotherm 51, 63
- Expendable materials 391–392, 489
- Expendable tooling 489
see also Tooling inserts
- Fabric 489
see also Weaving
-bias ($\pm 45^\circ$) tensile testing 119–120
-drape model examples 124–130
-drape model validation 130–134
-drape modelling 112–148, 238–241, 269–272
-in-plane shear testing 116–119
-out-of-plane bending testing 120–121
- Fabric deformation 114–115, 131–134, 489
see also Preform deformation
- Fabric shear 125–129, 238–239
-effect on mechanical properties 141–145
-stiffness 118
- Fatigue 489
- Fatigue life 23, 489
- FDEM^S 422, 426, 427, 428
- FEP 489
- Fibre 489
see also Filament; Tow; Strand; Reinforcement properties
-orientation 462–464
-preforming, *see* Preforming
-properties 43, 67, 69, 71, 72, 142
-reinforcement 65–76, 148–151
- Fibre bridging 489
- Fibre buckling 115, 489
- Fibre diameter 67, 490
- Fibre direction 490
see also Fibre orientation
- Fibre extension 115, 490
- Fibreglass 67–68, 490
- Fibre-reinforced plastic (FRP) 490
- Fibre volume fraction 3, 43, 458–460
-and shear 125–129, 130–131, 132
-and springback 163–167, 502
- Fibre wash 37, 452, 463–464, 490
- Filament 67, 74, 490
- Filament winding 152–153, 490
- Fill direction 184, 490
- Filler 490
- Film adhesive 490
- Finish, fibre 74–76, 490
- First article, *see* Qualification first article
- Flash 491
- Flexible mould 491
see also Tooling inserts
- Flexural strength
-one-part bismaleimide 66
- Flexural modulus
-one-part bismaleimide 66
- Flow 491
-effect of deformation 234–237
-in-plane deformation 235–236
-in random fabrics 230
-in woven or stitched fabrics 231–233
-and preform architecture 228–234
-racetracking, *see* Race tracking
-transverse 233–234
-transverse compaction 236–237
-unsaturated 233
- Flow modelling 225–281, 491
-case study 267–275, 420–425
-need for 226–228
- Flow modelling governing equations 245–253
-boundary conditions 249–250
-cure kinetics 250–251
-energy equation 248–249
-fill factor 247–248
-heat dispersion 252–253
-isothermal 245–246
-non-newtonian fluids 253
-temperature dependent viscosity 251–252
-two-dimensional 246–247

- Flow modelling, numerical
formulations 253–261
-finite element/control
volume 254–259
-geometry complexity 254
-heat transfer and cure 259–260
-other approaches 260–261
-pure finite element 260
- Flow monitoring, *see* Data acquisition, flow monitoring
- Flow simulation 272–275
see also Flow modelling
- Foam
see also Tooling inserts
-core 9, 339–346
-core material properties 342, 343
-fatigue 340–341
-impact 340
-relative cost of core materials 346
- Foam tooling 491
see also Tooling inserts, Foam core
- Formability 112
- Four harness satin 491
- Fracture critical, *see*
Part classifications
- Gate 491
see also Injection port
- Gelation 47, 50, 63
- Gel coat 491
- Gel point 50, 491
- Gel time 49, 491
- Gerber cutting, *see* Ultrasonic knife cutting
- Glass fibre 84, 491
see also Fibreglass
- Glass cloth 491
- Glass transition temperature (Tg) 46, 50, 491
-binder or tackifier 151
-epoxy values 57, 58, 59, 60
-bismaleimide values 66
- Graphite 491
- Graphite fibre 492
see Carbon fibre
- Graphitisation 492
- Green strength 50, 492
- Grit blasting 492
- Guide pin 306, 309, 492
- Halpin-Tsai equations 141–142
- Hand lay-up 492
- Harness satin 154, 492
see also Four harness satin; Eight harness satin
- Hardener 492
- Hardness 381
-bladder materials 368, 492
-tooling materials 285
- Heater blanket 29, 30–31
- Heat transfer 381–382
- Heat treating 492
- Heterogeneous 492
- Hob 492
- Honeycomb 352–359, 492
see also Nomex™ honeycomb
-core movement 357
-design details 357, 358
-machining 357–359
-mechanical properties 356
-preventing resin from filling cells 353–356
- Hybrid 74, 492
- Hydraulic press 492
- Hydromechanical press 492
- Hysteresis 492
- IML, *see* Tooling IML
- Image analysis, *see* Optical image analysis
- Impregnate 445–446, 492
-definition of impregnated fabric 493
- Inflatable mandrel, *see* Tooling inserts, Bladders
- Infrared 493
- Inhibitor 493
- Initiator 493
- Injection
-port 10–11, 326–328
-sequential 328–329, 332–334
- Injection equipment 25–41
-constant flow rate 32, 36–37
-constant pressure 32, 36, 38
-costs 400–402
-data acquisition 28, 34–36,
-dispense hose 30–31
-manufacturers 25, 26, 32, 37–39, 41
-mix/meter 27–28, 32–33, 34
-pail unloader 30

- pressure pot 29, 32
- production rate 28
- resin feed system 31–32
- resin reservoir 28–30
- Injection time 10
- Injection length 10
- Inserts, *see* Tooling inserts
- In-situ dielectric sensing 35, 413–414, 493
- Integral composite structure 493
- Integrally heated tooling 493
- Interface 493
- Interfibre angle 125–128, 493
- Interfibre shear 114, 159, 235–236, 493
- Interfibre slip 114–115, 235–236, 238–239, 493
- Interlaminar 493
- Interlaminar shear 493
- Interply hybrid 494
- Interply slip 115, 494
- Intralaminar 494
- Intraply hybrid 494
- Intrinsic viscosity 494
- Isothermal viscosity 49
 see also Viscosity
- Isotropic 494
- Kamal and Sourour equation 250–251
- KevlarTM 49, 70–71, 72, 494
- Knitting 102–104, 154–155, 494
 - warp 102–104, 105–107
 - weft 102–104
- Kozeny-Carmen equation 136–137, 180
- Lamina 494
- Laminae 494
- Laminate 494
- Laminate orientation 494
- Latent curing agent 494
- Lay-up 494
- Learning curve 389–390, 494
- Leno weave 494
 - see also* Mock leno weave
- LIBA 7, 105–107
- Liquid moulding 494
- Locking angle 114–115, 116, 144, 239, 495
 - see also* Interfibre shear
- Loom 91
- Loop strength 495
- Lot 495
- Macroflow 228, 233
- Mandrel 495
 - see also* Tooling; Tooling inserts
- Manufacturing specification 451
 - see also* Process specification
- Mass cast resin, *see* Tooling, Mass cast
- Mat forming techniques 153–155
- Material specification 450–451, 474–475
- Materials 42–82
 - see also* Cost, Materials
- Matched mould 495
- Matrix 495
 - see also* Resin
- Matrix digestion 131, 437–438, 459–460
- Maximum service temperature
 - bladder materials 368
 - extractable tooling 383
 - tooling materials 285
- Melt-out and soluble mandrels 370–371, 372
- Melt-out metal alloys 373
- Microcracking 54–55, 65, 495
- Microflow 228, 233
- Mix/meter injection equipment,
 - see* Injection equipment, Mix/meter
- Mock leno weave 154, 495
- Mode I 53, 89
- Mode II 53, 89
- Moisture absorption 45–46
 - see also* Water absorption
 - bismaleimide 66
 - epoxy 58, 59, 60
- Moisture content 495
- Moisture equilibrium 495
- Molecular weight 44, 45, 47, 50, 495
- Monofilament 495
- Monomer 495
- Mould 496
 - see also* Tooling, Injection port; Vent port
 - catastrophic failure 302

- chemical compatibility 301–302
- clamping forces 322
- clamping system 323–326
- costs 403–404
- creating shape 287–288
- deflection in permeability measurement 188, 206
- draft 303–304, 308–309
- durability 300–302
- finish 318–320
- flange 308
- free-floating inserts 311–312
- gap design 303
- guidance 306, 309
- heating 314–317
- materials 284–286, 315–316
- materials cost 395
- parting line, *see* Parting line
- pressure forces 320–323
- repair 320
- resin distribution manifolds 329–330
- sal 306–308
- substructure 322–323
- thermal expansion 317–318
- undercuts 308–309
- wear 301
- Mould release agent 319–320, 496
- Mould surface 301–302, 319, 496
- Moulded edge 496
- Moulded net 302, 496
- Moulding life, *see* Pot life 496
- Multiaxial fabric
 - see* Non-crimp fabric
- Navier-Stokes equation 178
- NDE 496
- NDI 461, 476, 496
- NDT 453, 496
- Neat resin 496
- Nesting 236, 496
- Net-shape part 23, 104, 150–151, 496
- Net-shape preform 92, 150–151, 155, 157, 161–170, 496
- Newtonian fluid 496
 - see also* Darcy's law
- Nextel® 73
 - see also* Aluminium oxide
- Nicalon™ 73
 - see also* Aluminium oxide
- Nickel plating 294–295
- Nomex™ honeycomb 9, 353
 - see also* Honeycomb
- properties 342, 343
- Normal controls, *see* Part classifications
- Non-crimp fabric 6, 7, 105–108, 406, 496
- Non-newtonian fluid 496
- Non-recurring cost 497
 - see also* Costs
- Non-woven fabric 497
- Novolac, *see* Phenolic
- Oligomer 497
- OML, *see* Tooling OML
- Optical image analysis 437–438, 461
- O-ring 306–308, 321–322
- Orthotropic 497
- Out time 497
- Oven dry 497
- Overbraiding 497
 - see also* Braiding, overbraiding
- Oxidation 497
- Pail unloader, *see* Injection equipment, Pail unloader
- PAN 69, 497
- Paraplast® 371
- Part classification 464–466
- Part demoulding 312–314
- Parting line 290–291, 303–305, 308–309, 497
- Parting plane 497
 - see also* Parting line
- Pattern, *see* Tool pattern
- Pay-off quantity 497
- Peel Ply 497
- Permeability 498
 - average, through the thickness 234
 - deformed reinforcement 136–141, 195–198
 - importance of 179–181
 - in-plane 242–245
 - models 242, 268
 - preform 177–224
 - radial flow method 198–206
 - tensor, in-plane 199–202
 - tensor, three-dimensional 207–219

- three-dimensional 206–219
- three-dimensional flow method 218–219
- unidirectional flow method, saturated 181–188
- unidirectional flow method, unsaturated 189–198
- values of glass fabrics, radial flow 201, 205
- values of glass fabrics, unidirectional flow 185
- values of glass fabrics, through-thickness flow 210
- Permittivity, *see* Dielectric permittivity**
- Phenolic** 61–62, 498
 - foam 345
 - novolac 61–62
 - resole 61–62
 - suppliers 61, 81–82
- Phenolic triazine** 63
- Pin-jointed net model** 121, 144, 498
- Pinch-off** 302, 498
- Pitch** 69–70, 498
- Plain weave** 498
- Plastic** 498
- Plasticiser** 62, 498
- Ply** 498
- Ply wrinkle** 498
 - see also Wrinkle*
- Poisson effect** 381
- Poisson's ratio** 142–143, 498
- Polar weaving** 92–93, 498
- Polyester foam** 344
- Polyetherimide (PEI) foam** 345–346
- Polytetrafluorethylene (PTFE)** 30–31, 311, 320, 499
- Polyisocyanurate foam** 344–345
- Polymer** 499
- Polymerisation** 499
- Polymethacrylimide (PMI) foam** 344
- Polymethyl Methacrylate (PMMA)** 499
 - see also Tooling, Mass cast*
- Polyurethane (PUR) foam** 341
- Polyvinylchloride (PVC) foam**
 - cross-linked 343–344
 - linear 343
- Porosity** 434, 435, 444, 499
- Porous media**
 - flow through 177–179
- Port, *see* Injection port;**
 - Vacuum outlet; Vent port
- Postcure** 50, 499
- Pot life** 27, 45, 49, 66, 499
- Powder application** 155–157
- Precursor** 499
- Preform** 499
 - see also Tooling, Perform*
 - compaction 309–311, 320–321
 - debulking 309–311
 - deformation 238
 - design 113–148
 - reinforcements 5
 - storage 172
 - tear-down 463
 - three-dimensional 54
 - tools 170–171, 330–331
- Preforming** 148–176, 499
 - costs 392–394
 - techniques 152–161
 - with foam core 350–352
- Preforming equipment** 171–172
- Preforms** 5–9
- Prepreg** 499
 - applications 4, 22–23
- Press** 326
- Pressure intensifier** 499
- Pressure pot, *see* Injection equipment, Pressure pot**
- Process control** 445–450, 499
 - comparison between autoclave-cured prepreg and RTM 445–446
 - coupons 450
 - document 477
 - effect of equipment 447–448
 - influence of materials 446–447
 - limits 448–450
 - RTM requirements 446
- Process modelling** 261–267
 - inputs 264–267
 - levels of sophistication 263–264
- Process simulation**
 - see also* Process modelling
 - as a design tool 275–276
- Process specification** 475–476
 - see also* Manufacturing specification

- Processing, *see* Resin transfer moulding process
- Promoter 499
- Property translation 464
- PTFE, *see* Polytetrafluorethylene
- Pull-off strength, *see* T-pull-off test
- Qualification 13–14, 456–481
- audits 476–477
 - braided and three-dimensional structures 479
 - F22 RTM qualification plan 457
 - first article 478–479
 - mechanical property 466–471
 - proof-of-concept parts 471–474
 - variables 457–458
 - what is the qualification process? 457–466
- Quality and process control 434–455
- Quality assurance 13–14
- Quality control 450–453
- material specification 450–451
 - manufacturing specification 451
 - non-destructive testing 453
 - process control 451–452
 - tooling 452–453
- Quartz 71
- Quasi-isotropic 500
- Recetracking 237, 384, 442, 444, 500
- Reaction rate 47, 51
- Recurring costs 500
- see also* Costs
- Read 92
- Reinforcement 500
- see also* Fibre reinforcement
 - advanced 83–111
 - properties 75
- Release agent, *see* Mould release agent
- Release film 500
- Repair 381
- Replicated tooling, *see* Tooling, replicated
- Residual stress 500
- Resin 500
- heating 318
 - one-component 5, 46–47, 56, 59, 60
 - pressure 321
 - properties 43, 46, 57–58, 63, 142
 - shrinkage 51–53, 317
 - two-component 5, 55–56, 57
- Resin content 43, 500
- Resin film infusion (RFI) 500
- applications 15–23
 - process 14–15, 413
- Resin port, *see* Injection port
- Resin richness 500
- Resin starved 500
- Resin transfer moulding (RTM) 500
- see also* Process control; tooling examples
 - applications 2–3, 15–23, 472
 - development 12–14
 - process 2–3, 9–11, 14–15, 412–413, 445–446
 - with foam cores 349–352
- Resole, *see* Phenolic
- Rheology 500
- Risk reduction 477–478
- Rohacell® 344, 351–352, 371
- see also* Polymethacrylimide; foam, Core material properties
- Roving 500
- see also* Yarn; Tow
- Rubber 501
- Runner 501
- S-glass 68, 72
- Sandwich construction 501
- Satin weave 501
- see also* Harness satin
- Scrim 501
- Sealing, *see* O-ring
- Secondary bonding 501
- Secondary structure 16, 501
- Selvage 501
- Sensors, *see* Dielectric sensing
- Separator 501
- Shear angle 501
- see also* Fabric shear
- Shelf life 501
- Shell tooling 501
- Shore hardness 501
- Short beam shear 450, 501
- Short shot 501
- Shot capacity 501
- Shur complement 212–213
- Shrinkage 286–287, 502
- see also* Resin shrinkage

- Silicon carbide 73
Silicon nitride 73
Silicone 307–308, 320, 367, 502
Sizing, fibre 74–76, 502
Sleeve-on 160–161
Slip, see Interfibre slip
Soluble plasters 374
Specific gravity 502
 -reinforcements 75
 -tooling materials 285
Specific heat
 -tooling materials 285
Specific modulus
 -reinforcements 75
Specific strength
 -reinforcements 75
Specifications, *see* Manufacturing specification; Material specification; Process specification
Sprayed metal moulds 295, 502
 see also Tooling, metal faced
Springback 502
 -fibre preform 161–170
Spring-in 502
 see also Springback
 -tooling 286–287
Sprue, *see* Injection port
Stabilisers 502
Staging 502
Stitch-bonding 105–107
 see also Non-crimp fabric
Stitching 6, 84–91, 153–154, 397, 406, 502
 see also Non-crimp fabric
 -for joining 91
Stokes equation 178–233
Storage life 502
Strang 74
 see also Tow; Roving
Stress crack 502
Structural testing 470–471
Substrate 503
Surface tension 193, 439, 503
Surface treatment 503
 see also Mould finish
Symmetrical laminate 503

Tack 503
Tackifier 151–152, 393, 475, 503
 -application 155–157
Tailored fibre placement 6, 9, 86–87, 88
Tear resistance, bladder materials 368
Teflon 503
Temperature control cycle 476
Tensile elongation
 -matrix and fibre 43
 -one-part epoxy 60
Tensile modulus 503
 -matrix and fibre 43
 -one-part epoxy 60
 -reinforcement 73, 75
 -tooling materials 285
Tensile strength 503
 -matrix and fibre 43
 -one-part epoxy 60
 -reinforcement 73, 75
 -tooling materials 285
Tensile stress 503
Tex 503
Textile
 -processes 23, 84, 85
 -technology 2–3
Textile fibres 503
 see also Fibres
Thermal conductivity 503
 -tooling materials 285
Thermal expansion, *see* Coefficient of thermal expansion
Thermal stresses 53, 63
Thermoplastic 43–45 503
Thermoplastic polyimide foam 345
Thermoset 43–44, 45–47, 503
Thixotropic 503
Thread 89, 503
 see also Yarn
Thread count 503
Three-dimensional fibre architecture 503
Tolerance 23
Tooling 282–337
 see also Mould; Electronformed mould; Electroplating; Preform tools
 -cast metal 295–298, 332
 -ceramic 298–299
 -cost considerations 299–302
 -effect of precision 300
 -examples 331–336

- fabricated 288–289
- flange design 304–308
- hardness 319
- IML 282–284
- manufacturing rate 299
- mass cast 292–294
- metal faced 293–295
- OML 282–284
- pattern 290–291
- prototype moulds 299
- reinforced plastic 292
- replicated 290–299
- rigid verses semi-rigid 300
- tolerances 286
- Tooling inserts 338–387
 - balsa wood cores, *see* Balsa
 - bladders, *see* Bladders
 - design and processing of extractable tooling 382–385
 - extractable tooling inserts 380–385
 - foam cores, *see* Foam core
 - foaming core shapes 346–349
 - machining foam core shapes 349
 - making internal bladders 367–370
 - making phase change mandrels 375–377
 - phase change 370–379
 - preventing resin from filling honeycomb cells 353–356
 - processing melt-out mandrels 378–379
 - RTM processing with foam cores 349–352
 - RTM processing with balsa wood cores 360
 - RTM processing with bladders 365–367
 - sealing phase change mandrels 377
 - thermal considerations for melt-out mandrels 379
 - types 339
- Toughness 46, 53–55, 88–89, 504
- Tow 67, 74, 231, 504
- T-stiffener pull-off test 461, 471, 473
- Tracer 504
- Triaxial braiding, *see* Braiding
- Tubing 30–31
- Twill weave 504
- Twist 504
- Ultrasonic knife cutting 8, 452
- Ultrasonic inspection 438, 461
- Undercut 504
- Unidirectional laminates 504
- Uniweave 504
- Unsymmetric laminate 504
- Vacuum assisted resin transfer moulding (VARTM) 504
- Vacuum bag 504
- Vacumm bag resin infusion 505
- Vacuum forming 505
- Vacuum injection moulding 505
- Vacuum outlet 10–11
 - see also* Vent port
- Veil 155, 505
- Vent cloth 505
- Vent port 327–328, 330
 - see also* Vacuum outlet
- Venting 505
- Viscoelastic modulus 505
- Viscoelasticity 505
- Viscosity 26–27, 45, 47–49, 57, 505
- Viton® 307
- Void 37, 505
 - see also* Porosity
 - formation 438–442
 - structural effects 443–444
- Void characterisation 435–437
- Void content 434, 505
- Void detection 437–438
- Volatiles 505
- Volume fraction 505
 - see also* Fibre volume fraction; Resin content
- Warp beam 91–92, 506
- Warp yarns 91–92
- Warp direction 184
- Warp knit, *see* Non-crimp
- Warpage 506
- Water absorption 62, 506
 - see also* Moisture absorption
- Water jet cutting 506
- Wax 373–374
- Wear, *see* Mould wear
- Weave 506
- Weaving 5–6, 91–96, 154
 - three dimensional 6, 92–95, 97
 - $\pm 45^\circ$ fabric 83–96

- Weft direction 506
see also Fill direction
- Weft yarns 92
- Weight savings 1, 2, 16, 21–22, 23
- Wet lay-up 506
- Wet-out 506
- Wetting 506
-contact angle 193, 439
- Wicking effects 190–194, 506
- Whiskers 65, 67, 506
- Working life 506
see also Pot life
- Woven fabric **232**, 506
- Woven roving 506
- Wrinkle 115, 144, 238–239, 292, 506
- X-ray inspection, preform 463–464, 452
- Yarn 67, 74, 506
see also Fibre; Tow
- Yarn locking 507
see also Fabric shear
- Young's modulus, resins 43, 46, 57–58, 63, 507
- Zero bleed 507